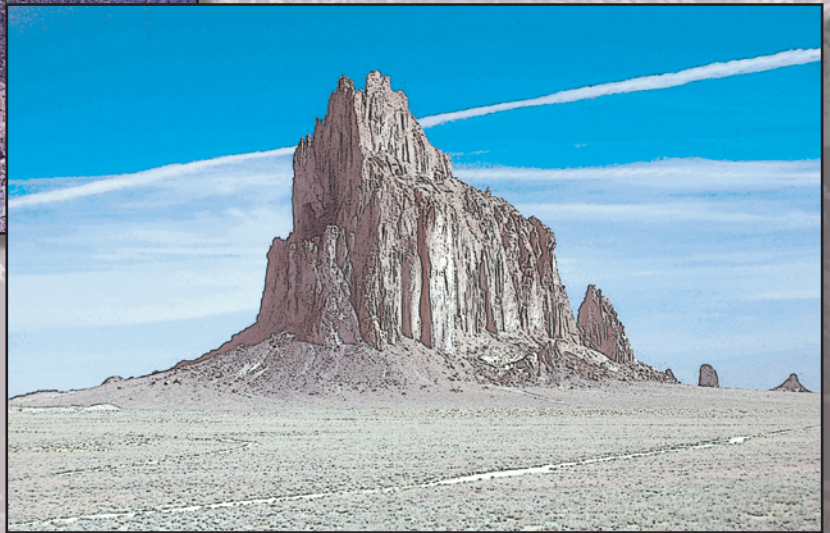
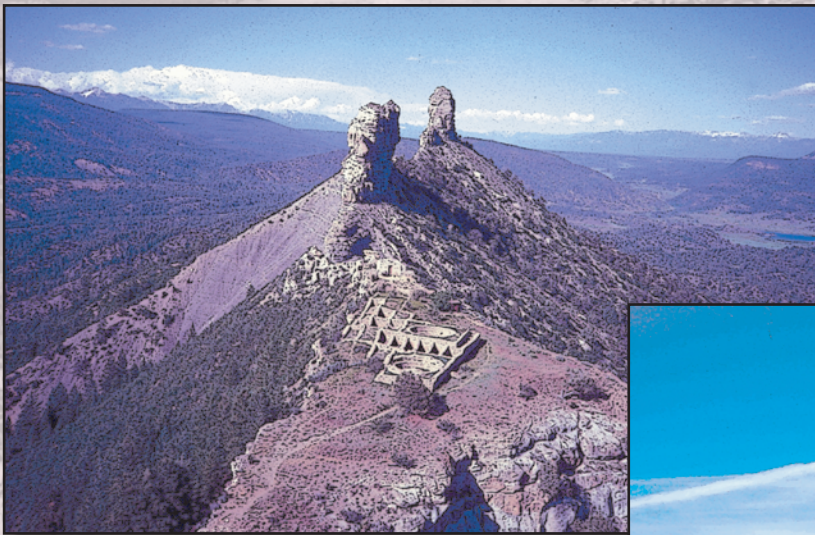


National Assessment of Oil and Gas Project:

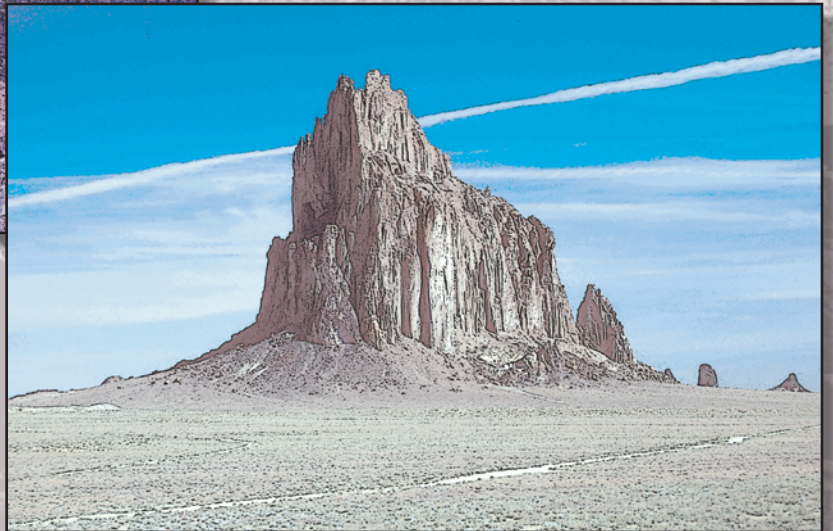
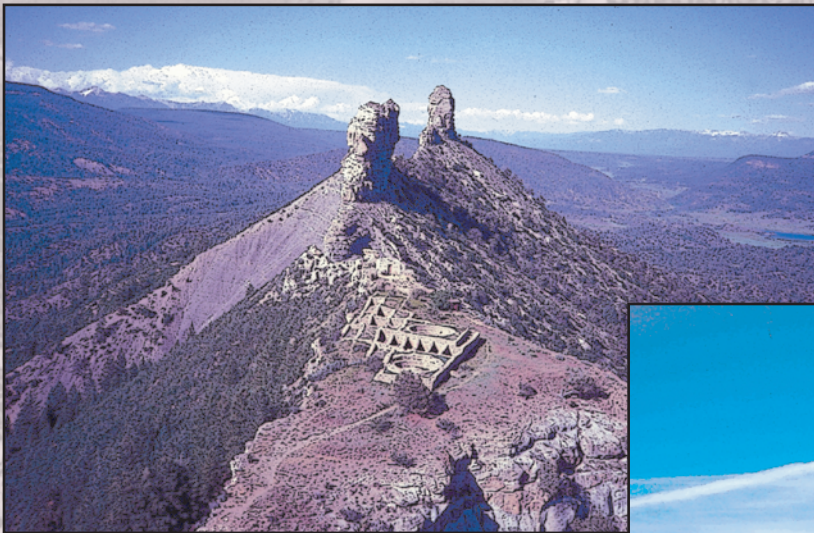
Total Petroleum Systems and Geologic Assessment of Undiscovered Oil and Gas Resources in the San Juan Basin Province, Exclusive of Paleozoic Rocks, New Mexico and Colorado



Digital Data Series 69–F

National Assessment of Oil and Gas Project:

Total Petroleum Systems and Geologic Assessment of Undiscovered Oil and Gas Resources in the San Juan Basin Province, Exclusive of Paleozoic Rocks, New Mexico and Colorado



Main Contents

Assessment Reports

Spacial Data

National Assessment of Oil and Gas Project:

Total Petroleum Systems and Geologic Assessment of Undiscovered Oil and Gas Resources in the San Juan Basin Province, Exclusive of Paleozoic Rocks, New Mexico and Colorado



Click here to return to
Main Contents

Chapter 1

Executive Summary—2002 Assessment of Undiscovered Oil and Gas Resources in the San Juan Basin Province, Exclusive of Paleozoic Rocks, New Mexico and Colorado

By U.S. Geological Survey San Juan Basin Assessment Team

Chapter 2

Introduction to the 2002 Geologic Assessment of Undiscovered Oil and Gas Resources in the San Juan Basin Province, Exclusive of Paleozoic Rocks

By U.S. Geological Survey San Juan Basin Assessment Team

Chapter 3

Geology and Oil and Gas Assessment of the Todilto Total Petroleum System, San Juan Basin Province, New Mexico and Colorado

By J.L. Ridgley and J.R. Hatch

Chapter 4

Geology and Oil and Gas Assessment of the Mancos-Menefee Composite Total Petroleum System, San Juan Basin, New Mexico and Colorado

By J.L. Ridgley, S.M. Condon, and J.R. Hatch

Chapter 5

Geology, Sequence Stratigraphy, and Oil and Gas Assessment of the Lewis Shale Total Petroleum System, San Juan Basin, New Mexico and Colorado

By Russell F. Dubiel

Chapter 6

Geology and Oil and Gas Assessment of the Fruitland Total Petroleum System, San Juan Basin, New Mexico and Colorado

By J.L. Ridgley, S.M. Condon, and J.R. Hatch

Chapter 7

Tabular Data and Graphical Images in Support of the U.S. Geological Survey National Oil and Gas Assessment—San Juan Basin Province (5022)

By T.R. Klett and P.A. Le

Digital Data Series 69—F

U.S. Department of the Interior
U.S. Geological Survey

Plates

1. South-north cross section showing correlation of reservoir units in the Mancos Shale on the east side of the San Juan Basin, New Mexico[included with report]
2. West-east cross section showing correlation of reservoir units in the Mancos Shale in the eastern part of the San Juan Basin, New Mexico[included with report]
3. Reproduction of preliminary structure contour map on the base of the Cretaceous Dakota Sandstone, San Juan Basin of Thaden and Zech (1984)[included with report]

Suggested citation:

U.S. Geological Survey San Juan Basin Assessment Team, 2013, Total petroleum systems and geologic assessment of undiscovered oil and gas resources in the San Juan Basin Province, exclusive of Paleozoic rocks, New Mexico and Colorado: U.S. Geological Survey Digital Data Series 69–F, variously paged.

Conversion Factors

Multiply	By	To obtain
Length		
inch (in.)	2.54	centimeter (cm)
foot (ft)	0.3048	meter (m)
foot (ft)	0.000305	kilometer (km)
foot (ft)	0.000189	mile (mi)
kilometer (km)	3,281	foot (m)
kilometer (km)	0.621	mile (mi)
meter (m)	3.281	foot (ft)
mile (mi)	5,280	foot (ft)
mile (mi)	1.61	kilometer (km)
Area		
sq. kilometer (km ²)	0.386	sq. mile (mi ²)
sq. mile (mi ²)	2.59	sq. kilometer (km ²)
Weight		
metric ton	1.10	ton, short (2,000 lb.)
ton, short (2,000 lb.)	0.907	metric ton
Liquid fuels		
barrel (bbl)	0.159	cubic meter (m ³)
barrel (bbl)	42.0	gallon (gal)
barrel (bbl)	159	liter (L)
cubic meter (m ³)	6.29	barrel (bbl)
gallon (gal)	0.0238	barrel (bbl)
liter (L)	0.00629	barrel (bbl)
Gaseous fuels		
cubic foot (ft ³)	0.0283	cubic meter (m ³)
cubic meter (m ³)	35.3	cubic foot (ft ³)
Coproduct ratios		
cubic feet per barrel (ft ³ /bbl or CF/B)	0.178	cubic meters per cubic meters (m ³ /m ³)
barrel per million cubic feet (bbl/1,000,000 ft ³ or B/MMCF)	5.61	cubic centimeters per cubic meter (cm ³ /m ³)
cubic meters per cubic meters (m ³ /m ³)	5.61	cubic feet per barrel (ft ³ /bbl or CF/B)

Executive Summary—2002 Assessment of Undiscovered Oil and Gas Resources in the San Juan Basin Province, Exclusive of Paleozoic Rocks, New Mexico and Colorado



Click here to return to
Volume Title Page

By U.S. Geological Survey San Juan Basin Assessment Team

Chapter 1 of 7

Total Petroleum Systems and Geologic Assessment of Undiscovered Oil and Gas Resources in the San Juan Basin Province, Exclusive of Paleozoic Rocks, New Mexico and Colorado

Compiled by U.S. Geological Survey San Juan Basin Assessment Team

Digital Data Series 69–F

**U.S. Department of the Interior
U.S. Geological Survey**

U.S. Department of the Interior
KEN SALAZAR, Secretary

U.S. Geological Survey
Marcia K. McNutt, Director

U.S. Geological Survey, Reston, Virginia 2013

For product and ordering information:

World Wide Web: <http://www.usgs.gov/pubprod>

Telephone: 1-888-ASK-USGS

For more information on the USGS—the Federal source for science about the Earth,
its natural and living resources, natural hazards, and the environment:

World Wide Web: <http://www.usgs.gov>

Telephone: 1-888-ASK-USGS

Suggested citation:

U.S. Geological Survey San Juan Basin Assessment Team, 2013, Executive summary—2002 Assessment of undiscovered oil and gas resources in the San Juan Basin Province, exclusive of Paleozoic rocks, New Mexico and Colorado, chap. 1 of U.S. Geological Survey San Juan Basin Assessment Team, Total petroleum systems and geologic assessment of undiscovered oil and gas resources in the San Juan Basin Province, exclusive of Paleozoic rocks, New Mexico and Colorado: U.S. Geological Survey Digital Data Series 69–F, p. 1–4.

Any use of trade, product, or firm names is for descriptive purposes only and does not imply endorsement by the U.S. Government.

Although this report is in the public domain, permission must be secured from the individual copyright owners to reproduce any copyrighted material contained within this report.

Contents

Introduction.....1
Resources Assessed.....2
Resource Summary2
San Juan Basin Assessment Team.....4
Reference Cited.....4

Figure

1. Shaded relief map showing the location and boundary of the San Juan Basin Province (5022).....1

Tables

1. San Juan Basin Province, New Mexico and Colorado, 2002 assessment results3
2. Comparison of undiscovered, oil, gas, and natural gas liquids between the 1995 and 2002 oil and gas assessments of the San Juan Basin Province, New Mexico and Colorado4

Executive Summary—2002 Assessment of Undiscovered Oil and Gas Resources in the San Juan Basin Province, Exclusive of Paleozoic Rocks, New Mexico and Colorado

By U.S. Geological Survey San Juan Basin Assessment Team

Introduction

In 2002, the U.S. Geological Survey (USGS) estimated undiscovered oil and gas resources that have the potential for additions to reserves in the San Juan Basin Province (5022), New Mexico and Colorado (fig. 1). Paleozoic rocks were not appraised. The last oil and gas assessment for the province was in 1995 (Gautier and others, 1996).

There are several important differences between the 1995 and 2002 assessments. The area assessed is smaller than that in the 1995 assessment. This assessment of undiscovered hydrocarbon resources in the San Juan Basin Province also used a slightly different approach in the assessment, and hence a number of the plays defined in the 1995 assessment are addressed differently in this report. After 1995, the USGS has applied a total petroleum system (TPS) concept to oil and gas



Figure 1. Shaded relief map showing the location and boundary of the San Juan Basin Province (5022) (solid red line) assessed in this 2002 National Oil and Gas Assessment; green line circumscribes the Chama Basin.

basin assessments. The TPS approach incorporates knowledge of the source rocks, reservoir rocks, migration pathways, and time of generation and expulsion of hydrocarbons; thus the assessments are geologically based. Each TPS is subdivided into one or more assessment units, usually defined by a unique set of reservoir rocks, but which have in common the same source rock. Four TPSs and 14 assessment units were geologically evaluated, and for 13 units, the undiscovered oil and gas resources were quantitatively assessed.

Resources Assessed

The hydrocarbon commodities quantitatively assessed include oil, gas, and natural gas liquids. Two assessment categories were used, conventional and continuous. Conventional accumulations have high matrix permeabilities, defined seals and traps, defined gas-water or oil-water contacts, and high recovery factors. The assessment methodology for conventional accumulations incorporates a field number and field-size distribution approach, wherein the minimum, median, and maximum numbers of undiscovered accumulations and sizes of undiscovered accumulations are estimated. For inclusion in this study, a discrete accumulation is at least 0.5 million barrels of oil (MMBO) or 3 billion cubic feet of gas (BCFG) in size.

Continuous oil and gas accumulations include those types of accumulations where the source rocks and reservoir rocks are interbedded or are the same; the reservoir rocks are generally characterized by low permeability (except coal-bed methane plays) and may be abnormally pressured. There is no well-defined gas-water or oil-water contact. Included in the continuous category are low-permeability continuous-type accumulations (including basin-centered), shale oil and gas, and coal-bed gas.

Resource Summary

In this assessment, four TPSs were defined (table 1). These are, in ascending order, Todilto, Mancos-Menefee Composite, Lewis Shale, and Fruitland. There were six conventional assessment units (AU) and eight continuous AUs defined (table 1). Three assessment units—the Lewis Continuous Gas AU, Menefee Coalbed Gas AU, and Tertiary Conventional Gas AU—were not previously evaluated in prior USGS oil and gas assessments. The Menefee Coalbed Gas AU is hypothetical because the Menefee Formation has yet to produce coal-bed gas outside of the thermally mature basin center. The Tertiary Conventional Gas AU has production from several Tertiary formations. Several of the 1995 plays have been redefined, based on new thinking about the depositional systems and the geologic controls on oil and gas accumulation. Most of the boundary changes involved assessment units in the Mancos-Menefee Composite TPS or in the Fruitland TPS. These reconfigurations are discussed more fully in the accompanying chapters, and they make direct comparison to the 1995 assessment results difficult.

The assessment results are shown by TPS and AU in table 1. The USGS estimated a mean of 19.10 million barrels of oil, 50.585 trillion cubic feet of gas (TCFG), and 148.37 million barrels of natural gas liquids of undiscovered resources. All of the undiscovered oil resources are in conventional accumulations in the Todilto TPS and Mancos-Menefee Composite TPS. Over 99 percent of the total undiscovered gas resources are estimated to be in continuous accumulations, primarily in the Fruitland TPS, which accounts for 57.9 percent of this estimate. The Fruitland Formation alone accounts for 46.8 percent of the estimated undiscovered gas in continuous accumulations. Over 97 percent of the undiscovered natural gas liquids are in continuous reservoirs in the Mancos-Menefee Composite TPS, Lewis Shale TPS, and Fruitland TPS (table 1). A comparison of total undiscovered resources between the 1995 assessment and this 2002 assessment is shown in table 2.

Table 1. San Juan Basin Province, New Mexico and Colorado, 2002 assessment results.

[MMBO, million barrels of oil; BCFG, billion cubic feet of gas; MMBNGL, million barrels of natural gas liquids. Results shown are fully risked estimates. For gas fields, all liquids are included under the NGL (natural gas liquids) category. F95 denotes a 95 percent chance of at least the amount tabulated. Other fractiles are defined similarly. Fractiles are additive only under the assumption of perfect positive correlation. TPS, Total Petroleum System; AU, Assessment Unit. Gray shading indicates not applicable or not assessed]

	Total Petroleum Systems (TPS) and Assessment Units (AU)	Field type	Total undiscovered resources											
			Oil (MMBO)				Gas (BCFG)				NGL (MMBNGL)			
			F95	F50	F5	Mean	F95	F50	F5	Mean	F95	F50	F5	Mean
Conventional Oil and Gas Resources	Fruitland TPS													
	Tertiary Conventional Gas AU	Gas					25.76	74.40	152.91	79.98	0.23	0.73	1.83	0.84
	Mancos-Menefee Composite TPS													
	Mesaverde Updip Conventional Oil		not quantitatively assessed											
	Gallup Sandstone Conventional Oil and Gas AU	Oil	0.00	1.98	6.29	2.34	0.00	0.29	0.98	0.35	0.00	0.00	0.01	0.00
	Mancos Sandstone Conventional Oil and Gas AU	Oil	5.41	11.33	20.72	11.99	23.34	53.28	106.75	57.57	0.84	2.07	4.52	2.30
	Dakota-Greenhorn Conventional Oil and Gas AU	Oil	0.78	2.26	4.73	2.45	2.53	7.49	17.10	8.34	0.02	0.07	0.16	.08
		Gas					5.59	12.63	22.40	13.35	0.22	0.50	0.96	0.53
	Todilto TPS													
	Entrada Sandstone Conventional Oil	Oil	0.81	2.19	4.18	2.32	1.84	5.15	10.66	5.56	0.07	0.20	0.45	0.22
	Total Conventional Resources		7.00	17.76	35.92	19.10	59.06	153.24	310.80	165.15	1.38	3.57	7.93	3.97
Continuous Oil and Gas Resources	Fruitland TPS													
	Pictured Cliffs Continuous Gas	Gas					3,865.41	5,510.68	7,856.23	5,640.25	9.07	15.95	28.06	16.92
	Fruitland Fairway Coalbed Gas	Gas					3,081.06	3,937.16	5,031.14	3,981.14	0.00	0.00	0.00	0.00
	Basin Fruitland Coalbed Gas	Gas					17,342.26	19,543.12	22,023.27	19,594.74	0.00	0.00	0.00	0.00
	Lewis Shale TPS													
	Lewis Continuous Gas	Gas					8,315.22	10,105.95	12,282.31	10,177.24	18.08	29.25	47.32	30.53
	Mancos-Menefee Composite TPS													
	Mesaverde Central-Basin Continuous Gas	Gas					1,053.32	1,305.62	1,618.35	1,316.79	3.44	5.12	7.60	5.27
	Mancos Sandstone Continuous Gas	Gas					3,980.80	5,062.07	6,437.03	5,116.37	50.64	73.97	108.04	75.96
	Dakota-Greenhorn Continuous Gas	Gas					3,148.66	3,896.17	4,821.14	3,928.98	10.29	15.27	22.66	15.72
Menefee Coalbed Gas	Gas					228.30	569.08	1,418.55	663.94	0.00	0.00	0.00	0.00	
	Total Continuous Resources					41,015.03	49,929.85	61,488.02	50,419.45	91.52	139.56	213.68	144.40	
	Total Undiscovered Oil and Gas Resources		7.00	17.76	35.92	19.10	41,074.09	50,083.09	61,798.82	50,584.60	92.90	143.13	221.61	148.37

Table 2. Comparison of undiscovered, oil, gas, and natural gas liquids between the 1995 and 2002 oil and gas assessments of the San Juan Basin Province, New Mexico and Colorado.

[MMBO, million barrels of oil; TCFG, trillion cubic feet of gas; MMBNGL, million barrels of natural gas liquids].

Total Mean Undiscovered Resources	
2002 USGS Assessment	1995 USGS Assessment
19.10 MMBO	280 MMBO
50.584 TCFG	29.23 TCFG
148.37 MMBNGL	18.51 MMBNGL

San Juan Basin Assessment Team

Members of the team are, in alphabetical order, Ronald R. Charpentier, Steven M. Condon, Troy Cook, Robert Crovelli, Russell F. Dubiel, Joseph R. Hatch, Timothy R. Klett, Jennie L. Ridgley (project chief), and Christopher J. Schenk.

Reference Cited

Gautier, D.L., Dolton, G.L., Takahashi, K.I., and Varnes, K.L., eds., 1996, 1995 National assessment of United States oil and gas resources—Results, methodology, and supporting data: U.S. Geological Survey Digital Data Series 30, Release 2, one CD-ROM.



Click here to return to
Volume Title Page

Introduction to the 2002 Geologic Assessment of Undiscovered Oil and Gas Resources in the San Juan Basin Province, Exclusive of Paleozoic Rocks



Click here to return to
Volume Title Page

By U.S. Geological Survey San Juan Basin Assessment Team

Chapter 2 of 7

Total Petroleum Systems and Geologic Assessment of Undiscovered Oil and Gas Resources in the San Juan Basin Province, Exclusive of Paleozoic Rocks, New Mexico and Colorado

Compiled by U.S. Geological Survey San Juan Basin Assessment Team

Digital Data Series 69–F

U.S. Department of the Interior
U.S. Geological Survey

U.S. Department of the Interior
KEN SALAZAR, Secretary

U.S. Geological Survey
Marcia K. McNutt, Director

U.S. Geological Survey, Reston, Virginia 2013

For product and ordering information:

World Wide Web: <http://www.usgs.gov/pubprod>

Telephone: 1-888-ASK-USGS

For more information on the USGS—the Federal source for science about the Earth, its natural and living resources, natural hazards, and the environment:

World Wide Web: <http://www.usgs.gov>

Telephone: 1-888-ASK-USGS

Suggested citation:

U.S. Geological Survey San Juan Basin Assessment Team, 2013, Introduction to the 2002 geologic assessment of undiscovered oil and gas resources in the San Juan Basin Province, exclusive of Paleozoic rocks, chap. 2 of

U.S. Geological Survey San Juan Basin Assessment Team, Total petroleum systems and geologic assessment of undiscovered oil and gas resources in the San Juan Basin Province, exclusive of Paleozoic rocks, New Mexico and Colorado: U.S. Geological Survey Digital Data Series 69–F, p. 1–8.

Any use of trade, product, or firm names is for descriptive purposes only and does not imply endorsement by the U.S. Government.

Although this report is in the public domain, permission must be secured from the individual copyright owners to reproduce any copyrighted material contained within this report.

Contents

Purpose.....	1
San Juan Basin Province (5022).....	1
Total Petroleum System Approach	1
Commodities Assessed and Assessment Categories	6
Data Sources	6
Assessment Results	6
References Cited.....	7

Figures

1. Shaded relief map showing location and boundary of the San Juan Basin Province (5022).....	3
2. Map showing location of inferred basement structural blocks and other structural elements in the San Juan Basin	4
3. Chart showing regional chronostratigraphic correlations in the San Juan Basin	5

Tables

1. San Juan Basin Province, New Mexico and Colorado, 2002 assessment results	2
2. List of total petroleum systems and their associated assessment units that were defined for the 2002 National Oil and Gas Assessment of the San Juan Basin Province (5022).....	7
3. Comparison of undiscovered, oil, gas, and natural gas liquids between the 1995 and 2002 oil and gas assessment of the San Juan Basin Province (5022), New Mexico and Colorado.....	7

Introduction to the 2002 Geologic Assessment of Undiscovered Oil and Gas Resources in the San Juan Basin Province, Exclusive of Paleozoic Rocks

By U.S. Geological Survey San Juan Basin Assessment Team

Purpose

The U.S. Geological Survey (USGS) periodically conducts assessments of undiscovered oil and gas resources in the United States. The purpose of the U.S. Geological Survey National Oil and Gas Assessment is to develop geologically based hypotheses regarding the potential for additions to oil and gas reserves in priority areas of the United States. The last major USGS assessment of oil and gas of the most important oil and gas provinces in the United States was in 1995 (Gautier and others, 1996). Since then a number of individual assessment provinces have been reappraised using new methodology. This was done particularly for those provinces where new information has become available, where new methodology was expected to reveal more insight to provide a better estimate, where additional geologic investigation was needed, or where continuous accumulations were deemed important. The San Juan Basin was reevaluated because of industry exploitation of new hydrocarbon accumulations that were not previously assessed and because of a change in application of assessment methodology to potential undiscovered hydrocarbon accumulations.

Several changes have been made in this study. The methodology is different from that used in 1995 (Schmoker, 2003; Schmoker and Klett, 2003). In this study the total petroleum system (TPS) approach (Magoon and Dow, 1994) is used rather than the play approach. The Chama Basin is not included. The team of scientists studying the basin is different. The 1995 study focused on conventional accumulations, whereas in this 2002 assessment, it was a priority to assess continuous-type accumulations, including coal-bed gas. Consequently we are presenting here an entirely new study and results for the San Juan Basin Province. The results of this 2002 assessment of undiscovered oil and gas resources in the San Juan Basin Province (5022) are presented in this report within the geologic context of individual TPSs and their assessment units (AU) (table 1). Results are reported as the estimated mean of potential additions to reserves as well as for the 95, 50, and 5 percent fractiles.

San Juan Basin Province (5022)

The 2002 San Juan Basin Province (5022) is located in New Mexico and Colorado between lat 35°1'23" and 37°22'26" N. and long 106°38'23" and 109°3'14" W. (fig. 1). The area assessed, which covers about 16,368 mi², is less than that in the 1995 National Oil and Gas Assessment, where the boundary of the total assessed area followed county lines in many places (Huffman, 1996). Additionally, it was determined that potential source beds in the Chama Basin, located adjacent to the northeast part of the San Juan Basin (fig. 1), never reached the thermal maturity level necessary to generate hydrocarbons. Thus, the Chama Basin, which was included in the 1995 assessment of the San Juan Province, was excluded from this 2002 assessment. The San Juan Basin Province includes not only the central basin where the bulk of the hydrocarbon resources are located but also the surrounding structural features, which consist of all or part of the Chaco slope, Four Corners platform, Hogback monocline, Archuleta arch, Zuni uplift, and Nacimiento uplift (fig. 2).

The San Juan Basin is principally a Laramide structural basin that formed between 75 and 35 million years ago, although rocks as old as Cambrian are present in the basin. The basin has a pronounced northwest-southeast structural grain that appears to have controlled sediment geometry and shoreline positions throughout the Phanerozoic (fig. 3), and hence determined the location of oil and gas resources. This structural grain is probably inherited from Precambrian basement blocks that appear to have formed in the early Paleozoic (Stevenson and Baars, 1986, p. 515; Taylor and Huffman, 1998, 2001; Huffman and Taylor, 2002; fig. 2).

Total Petroleum System Approach

The TPS approach incorporates knowledge of the source rocks, reservoir rocks, migration pathways, and time of generation and expulsion of hydrocarbons. Each TPS is characterized by a single hydrocarbon-source-rock interval or a number of source rocks, in which case, it is called a composite TPS. Within a TPS, there may be one or more assessment units

2 Total Petroleum Systems and Geologic Assessment of Undiscovered Oil and Gas Resources in the San Juan Basin Province

Table 1. San Juan Basin Province, New Mexico and Colorado, 2002 assessment results.

[MMB, million barrels; BCF, billion cubic feet; NGL, natural gas liquids. Results shown are fully risked estimates. For gas fields, all liquids are included under the NGL (natural gas liquids) category. F95 denotes a 95 percent chance of at least the amount tabulated. Other fractiles are defined similarly. Fractiles are additive only under the assumption of perfect positive correlation. Gray shading indicates not applicable or not assessed.]

	Total Petroleum Systems (TPS) and Assessment Units (AU)	Field type	Total undiscovered resources											
			Oil (MMB)				Gas (BCF)				NGL (MMB)			
			F95	F50	F5	Mean	F95	F50	F5	Mean	F95	F50	F5	Mean
Conventional Oil and Gas Resources	Fruitland TPS													
	Tertiary Conventional Gas AU	Gas					25.76	74.40	152.91	79.98	0.23	0.73	1.83	0.84
	Mancos-Menefee Composite TPS													
	Mesaverde Updip Conventional Oil		not quantitatively assessed											
	Gallup Sandstone Conventional Oil and Gas AU	Oil	0.00	1.98	6.29	2.34	0.00	0.29	0.98	0.35	0.00	0.00	0.01	0.00
	Mancos Sandstone Conventional Oil and Gas AU	Oil	5.41	11.33	20.72	11.99	23.34	53.28	106.75	57.57	0.84	2.07	4.52	2.30
	Dakota-Greenhorn Conventional Oil and Gas AU	Oil	0.78	2.26	4.73	2.45	2.53	7.49	17.10	8.34	0.02	0.07	0.16	.08
		Gas					5.59	12.63	22.40	13.35	0.22	0.50	0.96	0.53
	Todilto TPS													
	Entrada Sandstone Conventional Oil	Oil	0.81	2.19	4.18	2.32	1.84	5.15	10.66	5.56	0.07	0.20	0.45	0.22
	Total Conventional Resources		7.00	17.76	35.92	19.10	59.06	153.24	310.80	165.15	1.38	3.57	7.93	3.97
Continuous Oil and Gas Resources	Fruitland TPS													
	Pictured Cliffs Continuous Gas	Gas					3,865.41	5,510.68	7,856.23	5,640.25	9.07	15.95	28.06	16.92
	Fruitland Fairway Coalbed Gas	Gas					3,081.06	3,937.16	5,031.14	3,981.14	0.00	0.00	0.00	0.00
	Basin Fruitland Coalbed Gas	Gas					17,342.26	19,543.12	22,023.27	19,594.74	0.00	0.00	0.00	0.00
	Lewis Shale TPS													
	Lewis Continuous Gas	Gas					8,315.22	10,105.95	12,282.31	10,177.24	18.08	29.25	47.32	30.53
	Mancos-Menefee Composite TPS													
	Mesaverde Central-Basin Continuous Gas	Gas					1,053.32	1,305.62	1,618.35	1,316.79	3.44	5.12	7.60	5.27
	Mancos Sandstone Continuous Gas	Gas					3,980.80	5,062.07	6,437.03	5,116.37	50.64	73.97	108.04	75.96
	Dakota-Greenhorn Continuous Gas	Gas					3,148.66	3,896.17	4,821.14	3,928.98	10.29	15.27	22.66	15.72
Menefee Coalbed Gas	Gas					228.30	569.08	1,418.55	663.94	0.00	0.00	0.00	0.00	
	Total Continuous Resources					41,015.03	49,929.85	61,488.02	50,419.45	91.52	139.56	213.68	144.40	
	Total Undiscovered Oil and Gas Resources		7.00	17.76	35.92	19.10	41,074.09	50,083.09	61,798.82	50,584.60	92.90	143.13	221.61	148.37



Figure 1. Shaded relief map showing the location and boundary of the San Juan Basin Province (5022) (solid red line) assessed in the 2002 National Oil and Gas Assessment (U.S. Geological Survey Assessment Team, 2002); green line circumscribes the Chama Basin.

each of which is defined as a mappable volume of rock that encompasses both discovered and undiscovered accumulations that share similar geologic traits. Additionally, each TPS is characterized by a time of maximum generation and expulsion of hydrocarbons, which is defined by the depositional and thermal history of the basin. For a basin containing multiple TPSs, especially those closely related in time, the time of maximum generation and expulsion of hydrocarbons may be similar for many of the petroleum systems, but the migration pathways may not be the same. Hydrocarbons that have been generated in the more mature parts of the petroleum system source beds and that have migrated away from this area may form discrete, conventional accumulations in stratigraphic and structural traps marginal to the deep basin.

Hydrocarbons that formed within source rocks in the deepest part of the basin and migrated only short distances into interbedded reservoirs and local structural or stratigraphic traps

commonly form continuous-type accumulations. In the San Juan Basin, the continuous accumulations occur over a large area that is gas-charged, although not all wells drilled within the gas-charged area will be economic (Schmoker, 2003). In continuous-type accumulations, exclusive of coal-bed or shale gas accumulations, gas is commonly found in sandstone or sandy reservoirs, and thus, reservoir geometry within the basin setting is an important constraint on where gas might be found. Stratigraphic, unconformity, and structural traps as well as zones of better permeability within reservoirs found within deep central parts of basins may serve as focal points for gas charge. These areas may constitute some of the “sweet spots” within an overall gas-charged system. This 2002 assessment of the San Juan Basin employed the concept of “sweet spot” location when determining the percentage of the gas-charged area that held the potential for additions to reserves of undiscovered resources.

4 Total Petroleum Systems and Geologic Assessment of Undiscovered Oil and Gas Resources in the San Juan Basin Province

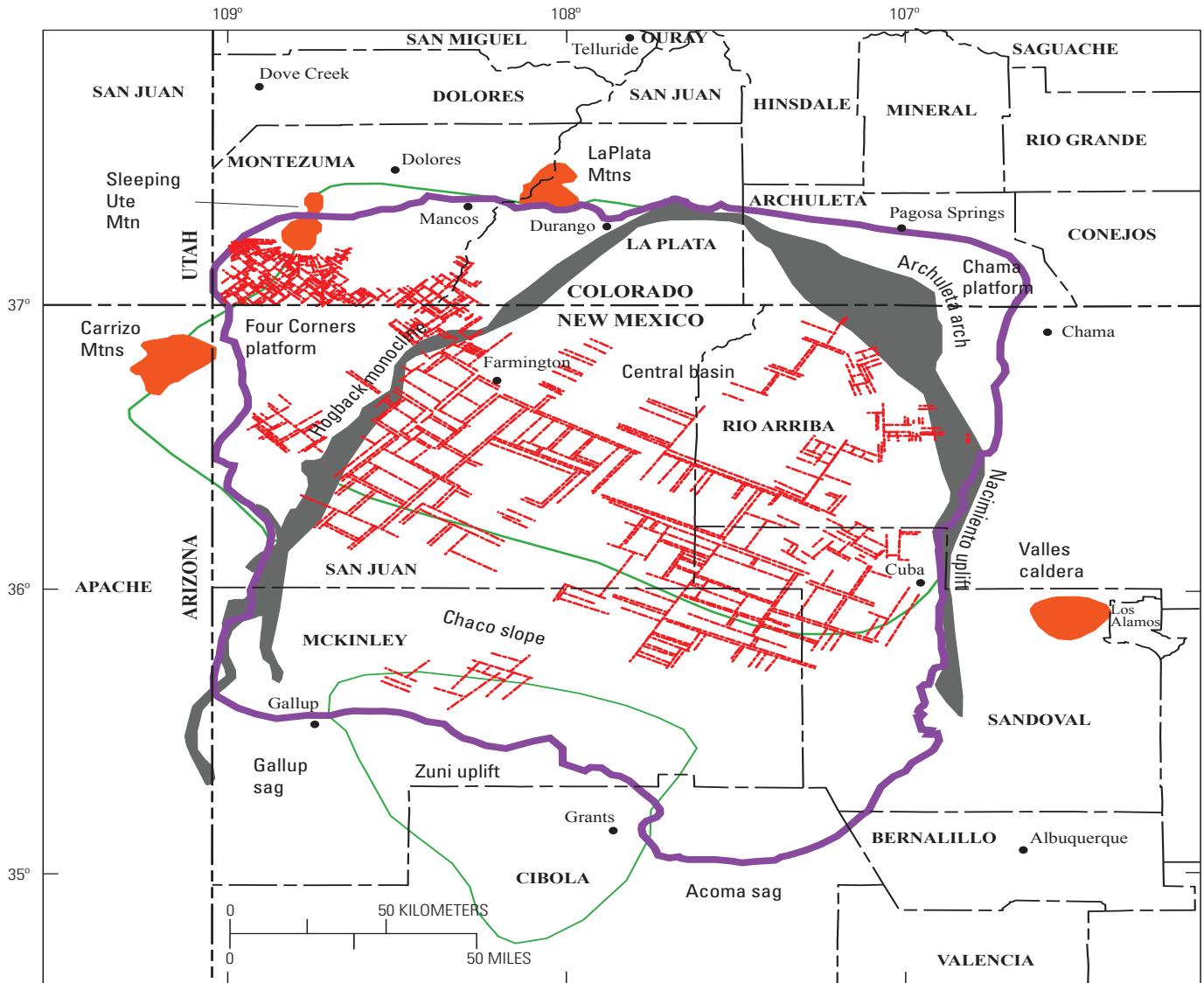


Figure 2. Map showing the location of inferred basement structural blocks (dashed red lines) and other structural elements in the San Juan Basin. Modified from Taylor and Huffman (1998, 2001), Fassett (2000), and Huffman and Taylor (2002). San Juan Basin Province (5022) boundary (purple line). Orange polygons are Late Cretaceous and Tertiary intrusive and extrusive igneous centers; gray polygons are areas of steep dip along monoclines; green line outlines some of the main structural elements.

Commodities Assessed and Assessment Categories

The commodities evaluated in this study include oil, gas, nonhydrocarbon gases, and natural gas liquids, but only oil, gas, and natural gas liquids were quantitatively assessed. There are two accumulation categories used in this assessment, conventional and continuous. Although both of these categories use a different methodology to estimate the potential for additions to reserves, each uses the same evaluation of risk. Risk reflects the uncertainty that hydrocarbons may or may not be present in an area. There are three attributes of risk:

1. charge,
2. reservoir, and
3. trap,

each having a probability of occurrence ranging between zero and one. The definition of each attribute can be found in Klett and Schmoker (2003) for continuous-type accumulations and in Klett and others (2003) for conventional accumulations.

Conventional oil and gas accumulations generally occur in stratigraphic and structural traps within fields; gas-water or gas-oil contacts are common. For inclusion in this study, a field is expected to produce at least 0.5 million barrels of oil (MMBO) or 3 billion cubic feet (BCF) of gas. The assessment methodology for conventional accumulations incorporates a field number and field-size distribution approach, and the minimum, median, and maximum numbers and sizes of undiscovered accumulations are estimated (see Schmoker and Klett, 2003).

Continuous oil and gas accumulations include those types of accumulations where the source rock and reservoir rock are interbedded or the same; the reservoir rocks are characterized by low permeability (except coal-bed methane reservoirs) and abnormal pressures, and there is no well-defined gas-water or gas-oil contact. An important attribute is lateral continuity of an accumulation over a large area (Law, 2002; Schmoker, 2003). Included in the continuous category are tight, low-permeability continuous-type accumulations (including basin-centered), shale gas, and coal-bed gas. Two geologic characteristics of continuous gas accumulations are

1. large volumes of rocks that are pervasively charged with gas or oil, although not all areas may be economic, and
2. lack of dependency upon buoyancy of oil or gas in water for their existence (Schmoker, 2003).

Continuous accumulations have no set minimum production or potential production cutoff like that used in the conventional assessment methodology. Rather, minimum production cutoff is determined for each assessment unit using data from the estimated ultimate recovery (EUR) distribution of wells already drilled, or using analogs from other areas. The continuous assessment methodology uses a cell-based approach to estimate the potential additions to reserves of undiscovered resources. Schmoker (2003) explained the specifics of continuous assessment methodology.

The bulk of the oil and gas resources in the San Juan Basin Province are in rocks of Cretaceous age (fig. 3). Small amounts of oil occur in the Middle Jurassic Entrada Sandstone or in various reservoirs in rocks of Pennsylvanian age. Resources in rocks of Paleozoic age are not included in this San Juan Basin National Oil and Gas Assessment.

Data Sources

Two principal sources of production data were used in the assessment. Data for conventional oil and gas accumulations were obtained from the 2001 Significant Oil and Gas Fields of the United States file (NRG Associates, 2001), a database that is commercially available from NRG Associates. Field data through 2001 were used. Production data for wells from the continuous assessment units were obtained from the PI/Dwights PLUS database, which is commercially available from IHS Energy Group (IHS Energy Group, 2001, 2002, 2003). Background data for the geology used in each description of the total petroleum system as well as the individual assessment units were obtained from published literature, as well as from new scientific efforts at the USGS or existing, unpublished data in USGS geochemistry databases.

Assessment Results

In this assessment, four TPSs were defined. These are, in ascending order, Todilto, Mancos-Menefee Composite, Lewis Shale, and Fruitland (fig. 3). The stratigraphic distribution of the TPSs is shown on the regional chronostratigraphic chart, which excludes formations older than those covered in this report (fig. 3). Each TPS is composed of one or more assessment units, which are principally lithostratigraphic in nature, but are also tied to the primary source interval by migration pathways.

There were six conventional AUs and eight continuous AUs defined (table 2). Three AUs, Lewis Continuous Gas AU, Menefee Coalbed Gas AU, and Tertiary Conventional Gas AU, were defined to include rock units not specifically assessed in 1995. The Menefee Coalbed Gas AU is hypothetical because the Menefee Formation has yet to produce coalbed gas outside of the thermally mature deep basin center. The Tertiary AU has production from several Tertiary formations. Several of the 1995 plays have been redefined, based on new thinking about the depositional systems and the geologic controls on oil and gas accumulation. Most of the boundary changes involved assessment units in the Mancos-Menefee Composite TPS and in the Fruitland TPS. These reconfigurations are discussed more fully in the accompanying geologic reports (see chaps. 4 and 6, this CD-ROM); the changes make direct comparison to the 1995 assessment results difficult.

Table 2. List of total petroleum systems and their associated assessment units that were defined for the 2002 National Oil and Gas Assessment of the San Juan Basin Province (5022).

[N/A, not quantitatively assessed].

Total petroleum system (TPS)	Conventional assessment unit (AU)	Continuous assessment unit (AU)
Fruitland TPS	Tertiary Conventional Gas AU	Fruitland Fairway Coalbed Gas AU Basin Fruitland Coalbed Gas AU Pictured Cliffs Continuous Gas AU
Lewis Shale TPS		Lewis Continuous Gas AU
Mancos-Menefee Composite TPS	Mesaverde Updip Conventional Oil AU (N/A) Mancos Sandstones Conventional Oil AU Gallup Sandstone Conventional Oil and Gas AU Dakota-Greenhorn Conventional Oil and Gas AU	Mesaverde Central-Basin Continuous Gas AU Menefee Coalbed Gas AU Mancos Sandstones Continuous Gas AU Dakota-Greenhorn Continuous Gas AU
Todilto TPS	Entrada Sandstone Conventional Oil AU	

The stratigraphic interval covered by each assessment unit is shown in figure 3. Chapters 3–6 in this CD-ROM contain discussions of geology and geochemistry of specific total petroleum systems in addition to a discussion of each associated assessment unit. Chapter 7 includes companion data used in making assessments of undiscovered petroleum resources for each AU. The relationship between each petroleum system and its associated assessment units is summarized in table 2 and figure 3.

Results of this 2002 assessment are presented in table 1 and in the discussion of each assessment unit. These potential additions to reserves are evaluated regardless of political, economic, or other considerations. The assessment incorporates a more thorough understanding of the geology and geochemistry of the total petroleum systems and “sweet spot” (areas having the highest potential to contain resources) development, and thus, the potential additions to reserves of undiscovered resources is geologically based.

The assessment results are shown by TPS and AU in table 1. The USGS estimated a mean of 19.10 million barrels of oil (MMBO), 50.585 trillion cubic feet of gas (TCFG), and 148.37 million barrels of natural gas liquids (MMBNGL) of undiscovered resources. All of the undiscovered oil resources are in conventional accumulations in the Todilto TPS and in the Mancos-Menefee Composite TPS. Over 99 percent of the total undiscovered gas resources are to be found in continuous accumulations, primarily in the Fruitland TPS, which accounts for 57.9 percent of this estimate. The Fruitland Formation alone accounts for 46.8 percent of the estimated undiscovered gas in continuous accumulations. Over 97 percent of the undiscovered natural gas liquids are in continuous accumulations in the Mancos-Menefee Composite TPS, Lewis Shale TPS, and Fruitland TPS (table 1). A comparison of total undiscovered resources between the 1995 assessment and the 2002 assessment is shown in table 3.

Table 3. Comparison of undiscovered, oil, gas, and natural gas liquids between the 1995 and 2002 oil and gas assessment of the San Juan Basin Province, New Mexico and Colorado.

[MMBO, million barrels of oil; TCFG, trillion cubic feet of gas; MMBNGL, million barrels of natural gas liquids.]

Total Mean Undiscovered Resources	
2002 USGS Assessment	1995 USGS Assessment
19.10 MMBO	280 (91) ¹ MMBO
50.584 TCFG	29.23 TCFG
148.37 MMBNGL	18.51 MMBNGL

¹280 (91) First value included all oil; second value excludes oil from the continuous Mancos Fractured Shale Play 2008.]

References Cited

- Fassett, J.E., 2000, Geology and coal resources of the Upper Cretaceous Fruitland Formation, San Juan Basin, New Mexico and Colorado, chap. Q of Kirschbaum, M.A., Roberts, L.N.R., and Biewick, L.R.H., eds., Geologic assessment of coal in the Colorado Plateau—Arizona, Colorado, New Mexico, and Utah: U.S. Geological Survey Professional Paper 1625–B, p. Q1–Q132.
- Gautier, D.L., Dolton, G.L., Takahashi, K.I., and Varnes, K.L., eds., 1996, 1995 National assessment of United States oil and gas resources—Results, methodology, and supporting data: U.S. Geological Survey Digital Data Series 30, release 2, 1 CD-ROM.

- Huffman, A.C., Jr., 1996, San Juan Basin Province (22), *in* Gautier, D.L., Dolton, G.L., Takahashi, K.I., and Varnes, K.L., eds., 1995 National assessment of United States oil and gas resources—Results, methodology, and supporting data: U.S. Geological Survey Digital Data Series 30, release 2, 1 CD-ROM.
- Huffman, A.C., Jr., and Taylor, D.J., 2002, Fractured shale reservoirs and basement faulting, San Juan Basin, New Mexico and Colorado: American Association of Petroleum Geologists Rocky Mountain Section Meeting, Laramie, Wyo., p. 30.
- IHS Energy Group, 2001, 2002, and 2003, PI/Dwights Plus U.S. well data [includes data current as of September 2001, June 2002, and January 31, 2003, respectively]: Englewood, Colo., IHS Energy Group; database available from IHS Energy Group, 15 Inverness Way East, D205, Englewood, CO 80112, U.S.A.
- Klett, T.R., and Schmoker, J.W., 2003, U.S. Geological Survey input-data form and operational procedure for the assessment of continuous petroleum accumulations, chap. 18 of USGS Uinta-Piceance Assessment Team, Petroleum systems and geologic assessment of oil and gas in the Uinta-Piceance Province, Utah and Colorado: U.S. Geological Survey Digital Data Series 69–B, 8 p. [<http://pubs.usgs.gov/dds/dds-069/dds-069-b/chapters.html>, last accessed 04/2008]
- Klett, T.R., Schmoker, J.W., and Charpentier, R.R., 2003, U.S. Geological Survey input-data form and operational procedure for the assessment of conventional petroleum accumulations, chap. 20 of USGS Uinta-Piceance Assessment Team, Petroleum systems and geologic assessment of oil and gas in the Uinta-Piceance Province, Utah and Colorado: U.S. Geological Survey Digital Data Series 69–B, 7 p. [<http://pubs.usgs.gov/dds/dds-069/dds-069-b/chapters.html>, last accessed 04/2008]
- Law, B.E., 2002, Basin-centered gas systems, *in* Law, B.E., and Curtis, J.B. eds., Unconventional petroleum systems: American Association of Petroleum Geologists Bulletin, v. 86, no. 11, p. 1891–1919.
- Magoon, L.B., and Dow, W.G., 1994, The petroleum system, *in* Magoon, L.B., and Dow, W.G., eds., The petroleum system—From source to trap: American Association of Petroleum Geologists Memoir 60, p. 3–24.
- Molenaar, C.M., 1977, San Juan Basin time-stratigraphic nomenclature chart, *in* Fassett, J.E., James, H.L. and Hodgson, H.E., eds., San Juan Basin III: New Mexico Geological Society Guidebook, p. xii.
- NRG Associates, 2001, The significant oil and gas fields of the United States [includes data current as of December, 31, 2001]: Colorado Springs, Colo., NRG Associates, Inc. [database available from NRG Associates, Inc., P.O. Box 1655, Colorado Springs, CO 80901]
- Schmoker, J.W., 2003, U.S. Geological Survey assessment concepts for continuous petroleum accumulations, chap. 17 of USGS Uinta-Piceance Assessment Team, Petroleum systems and geologic assessment of oil and gas in the Uinta-Piceance Province, Utah and Colorado: U.S. Geological Survey Digital Data Series 69–B, 7 p. [<http://pubs.usgs.gov/dds/dds-069/dds-069-b/chapters.html>, last accessed 04/2008]
- Schmoker, J.W., and Klett, T.R., 2003, U.S. Geological Survey assessment concepts for conventional petroleum accumulations, chap. 19 of USGS Uinta-Piceance Assessment Team, Petroleum systems and geologic assessment of oil and gas in the Uinta-Piceance Province, Utah and Colorado: U.S. Geological Survey Digital Data Series 69–B, 6 p. [<http://pubs.usgs.gov/dds/dds-069/dds-069-b/chapters.html>, last accessed 04/2008]
- Stevenson, G.M., and Baars, D.L., 1986, The Paradox—A pull-apart basin of Pennsylvanian age, *in* Peterson, J.A., ed., Paleotectonics and sedimentation in the Rocky Mountain region, United States: American Association of Petroleum Geologists Memoir 41, p. 513–539.
- Taylor, D.J., and Huffman, A.C., Jr., 1998, Map showing inferred and mapped basement faults, San Juan Basin and vicinity, New Mexico and Colorado: U.S. Geological Survey Geological Investigations Series 2641, scale 1:500,000.
- Taylor, D.J., and Huffman, A.C., Jr., 2001, Seismic evaluation study report: Jicarilla Apache Indian Reservation: U.S. Department of Energy Report DE-AI26-98BC15026R10 (CD-ROM).
- U.S. Geological Survey San Juan Basin Assessment Team, 2002, Assessment of undiscovered oil and gas resources of the San Juan Basin Province of New Mexico and Colorado, 2002: U.S. Geological Survey Fact Sheet 147–02, 2 p.



[Click here to return to
Volume Title Page](#)

Geology and Oil and Gas Assessment of the Todilto Total Petroleum System, San Juan Basin Province, New Mexico and Colorado

By J.L. Ridgley and J.R Hatch



Click here to return to
Volume Title Page

Chapter 3 of 7

Total Petroleum Systems and Geologic Assessment of Undiscovered Oil and Gas Resources in the San Juan Basin Province, Exclusive of Paleozoic Rocks, New Mexico and Colorado

Compiled by U.S. Geological Survey San Juan Basin Assessment Team

Digital Data Series 69–F

U.S. Department of the Interior
U.S. Geological Survey

U.S. Department of the Interior
KEN SALAZAR, Secretary

U.S. Geological Survey
Marcia K. McNutt, Director

U.S. Geological Survey, Reston, Virginia 2013

For product and ordering information:

World Wide Web: <http://www.usgs.gov/pubprod>

Telephone: 1-888-ASK-USGS

For more information on the USGS—the Federal source for science about the Earth,
its natural and living resources, natural hazards, and the environment:

World Wide Web: <http://www.usgs.gov>

Telephone: 1-888-ASK-USGS

Suggested citation:

Ridgley, J.L., and Hatch, J.R., 2013, Geology and oil and gas assessment of the Todilto Total Petroleum System, San Juan Basin Province, New Mexico and Colorado, chap. 3 of U.S. Geological Survey San Juan Basin Assessment Team, Total petroleum systems and geologic assessment of undiscovered oil and gas resources in the San Juan Basin Province, exclusive of Paleozoic rocks, New Mexico and Colorado: U.S. Geological Survey Digital Data Series 69-F, p. 1–29.

Any use of trade, product, or firm names is for descriptive purposes only and does not imply endorsement by the U.S. Government.

Although this report is in the public domain, permission must be secured from the individual copyright owners to reproduce any copyrighted material contained within this report.

Contents

Abstract.....	1
Introduction.....	1
Todilto Total Petroleum System	6
Structural Configuration	6
Hydrocarbon Source Rock.....	6
Todilto Limestone Member of the Wanakah Formation	6
Oil Geochemistry.....	11
Source Rock Maturation	13
Hydrocarbon Migration Summary	13
Hydrocarbon Reservoir Rocks.....	17
Hydrocarbon Traps and Seals	20
Entrada Sandstone Conventional Oil Assessment Unit (50220401)	20
Introduction.....	20
Source.....	20
Maturation.....	20
Migration	20
Reservoirs	21
Traps/Seals	21
Geologic Model.....	21
Assessment Results	23
Acknowledgments	25
References Cited.....	25
Appendix	
A. Input data form used in evaluating the Todilto Total Petroleum System, Entrada Sandstone Conventional Oil Assessment Unit, San Juan Basin Province	28

Figures

1. Map showing boundary of the San Juan Basin Province (5022), Todilto Total Petroleum System, Entrada Sandstone Conventional Oil Assessment Unit, and location of Entrada Sandstone Conventional Oil Assessment Unit oil fields.....	2
2. Chart showing regional chronostratigraphic correlations in the San Juan Basin.....	3
3. Paleogeographic reconstruction showing distribution of rock types and environments of deposition related to deposition of Middle Jurassic Todilto Limestone Member of the Wanakah Formation	4
4. Map showing boundary of the San Juan Basin Province, Todilto Total Petroleum System, and Entrada Sandstone Conventional Oil Assessment Unit.....	5
5. Structure contour map drawn on top of the Todilto Limestone Member of the Wanakah Formation	7
6. Isopach map of Todilto Limestone Member of the Wanakah Formation.....	9
7. Schematic southwest–northeast cross section through the Todilto Limestone Member of the Wanakah Formation in the San Juan Basin	10
8. Burial history curves	14
9. Cross sections.....	18
10. Events chart showing key geologic events for the Entrada Sandstone Conventional Oil Assessment Unit	22
11. Graph showing distribution by halves of grown oil-accumulation size versus rank by size for the Entrada Sandstone Conventional Oil Assessment Unit.....	24
12. Graph showing sizes of grown oil accumulations versus year of discovery for fields in the Entrada Sandstone Conventional Oil Assessment Unit.....	25

Tables

1. Characteristics of Entrada Sandstone reservoir rocks, including oil API gravities	12
2. Assessment results summary for the Todilto Total Petroleum System, San Juan Basin Province, New Mexico and Colorado	23
3. Comparison of estimates from the 2002 Entrada Sandstone Conventional Oil Assessment Unit and the 1995 Entrada Play 2204 assessments of the number, sizes, and volumes of undiscovered oil accumulations	24

Geology and Oil and Gas Assessment of the Todilto Total Petroleum System, San Juan Basin Province, New Mexico and Colorado

By J.L. Ridgley and J.R Hatch

Abstract

Organic-rich, shaly limestone beds, which contain hydrocarbon source beds in the lower part of the Jurassic Todilto Limestone Member of the Wanakah Formation, and sandstone reservoirs in the overlying Jurassic Entrada Sandstone, compose the Todilto Total Petroleum System (TPS). Source rock facies of the Todilto Limestone were deposited in a combined marine-lacustrine depositional setting. Sandstone reservoirs in the Entrada Sandstone were deposited in eolian depositional environments. Oil in Todilto source beds was generated beginning in the middle Paleocene, about 63 million years ago, and maximum generation of oil occurred in the middle Eocene. In the northern part of the San Juan Basin, possible gas and condensate were generated in Todilto Limestone Member source beds until the middle Miocene. The migration distance of oil from the Todilto source beds into the underlying Entrada Sandstone reservoirs was short, probably within the dimensions of a single dune crest. Traps in the Entrada are mainly stratigraphic and diagenetic. Regional tilt of the strata to the northeast has influenced structural trapping of oil, but also allowed for later introduction of water. Subsequent hydrodynamic forces have influenced the repositioning of the oil in some reservoirs and flushing in others. Seals are mostly the anhydrite and limestone facies of the Todilto, which thin to as little as 10 ft over the crests of the dunes.

The TPS contains only one assessment unit, the Entrada Sandstone Conventional Oil Assessment Unit (AU) (50220401). Only four of the eight oil fields producing from the Entrada met the 0.5 million barrels of oil minimum size used for this assessment. The AU was estimated at the mean to have potential additions to reserves of 2.32 million barrels of oil (MMBO), 5.56 billion cubic feet of natural gas (BCFG), and 0.22 million barrels of natural gas liquids (MMBNGL).

Introduction

The boundary of the Middle Jurassic Todilto Total Petroleum System (TPS) was drawn to coincide with the boundary of the San Juan Basin Province except along the northwest and

southwest margins (fig. 1). In these areas, the TPS boundary was drawn basinward from Todilto outcrops because analysis of facies in the Todilto Limestone Member of the Wanakah Formation and the underlying Entrada Sandstone in these areas suggested a lack of source rock potential, insufficient thermal maturity, and unfavorable reservoir geometry. The Todilto TPS is the stratigraphically oldest TPS evaluated in the 2002 National Oil and Gas Assessment of the San Juan Basin Province. The TPS contains only one assessment unit, the Entrada Sandstone Conventional Oil Assessment Unit (AU) (50220401) (fig. 2).

The Todilto TPS comprises two Middle Jurassic rock units:

1. Entrada Sandstone, the reservoir, and
2. the overlying Todilto Limestone Member of the Wanakah Formation, the source and seal (fig. 2).

The Todilto Limestone Member is the source of the oil and small quantities of associated gas found in the Entrada; it is also the seal to migrating hydrocarbons. The Entrada Sandstone is mostly of eolian origin, including large ergs with individual dune thickness ranging from 60 to 330 ft. The ergs are extensive throughout the San Juan Basin and continue into surrounding areas of Utah, Arizona, and Colorado. There is little evidence of basin subsidence on deposition of the upper part of the Entrada Sandstone except near the end of its time of deposition.

Near the close of deposition of the Entrada, an area extending south from central Colorado well into New Mexico subsided. Marine waters from the north flowed south across a sill, located in south-central Colorado, and formed a large bay in the subsided area (Ridgley, 1989) (fig. 3). Rapid flooding in this embayment by marine waters from the north modified the topographic expression of the Entrada dunes, resulting in relict dune topography of variable height. A large inland sea formed within the embayment (Tanner, 1970; Kirkland and others, 1995). This inland sea is characterized by a basal limestone facies, which contains interbedded organic-rich shale, and an overlying anhydrite facies, which alters to gypsum at the surface. These chemical facies make up the Todilto Limestone Member of the Wanakah Formation. Preservation of individual sand dunes overlain by a carbonate unit that serves as both source rock and seal make the Todilto a locally sourced TPS.

2 Total Petroleum Systems and Geologic Assessment of Undiscovered Oil and Gas Resources in the San Juan Basin Province

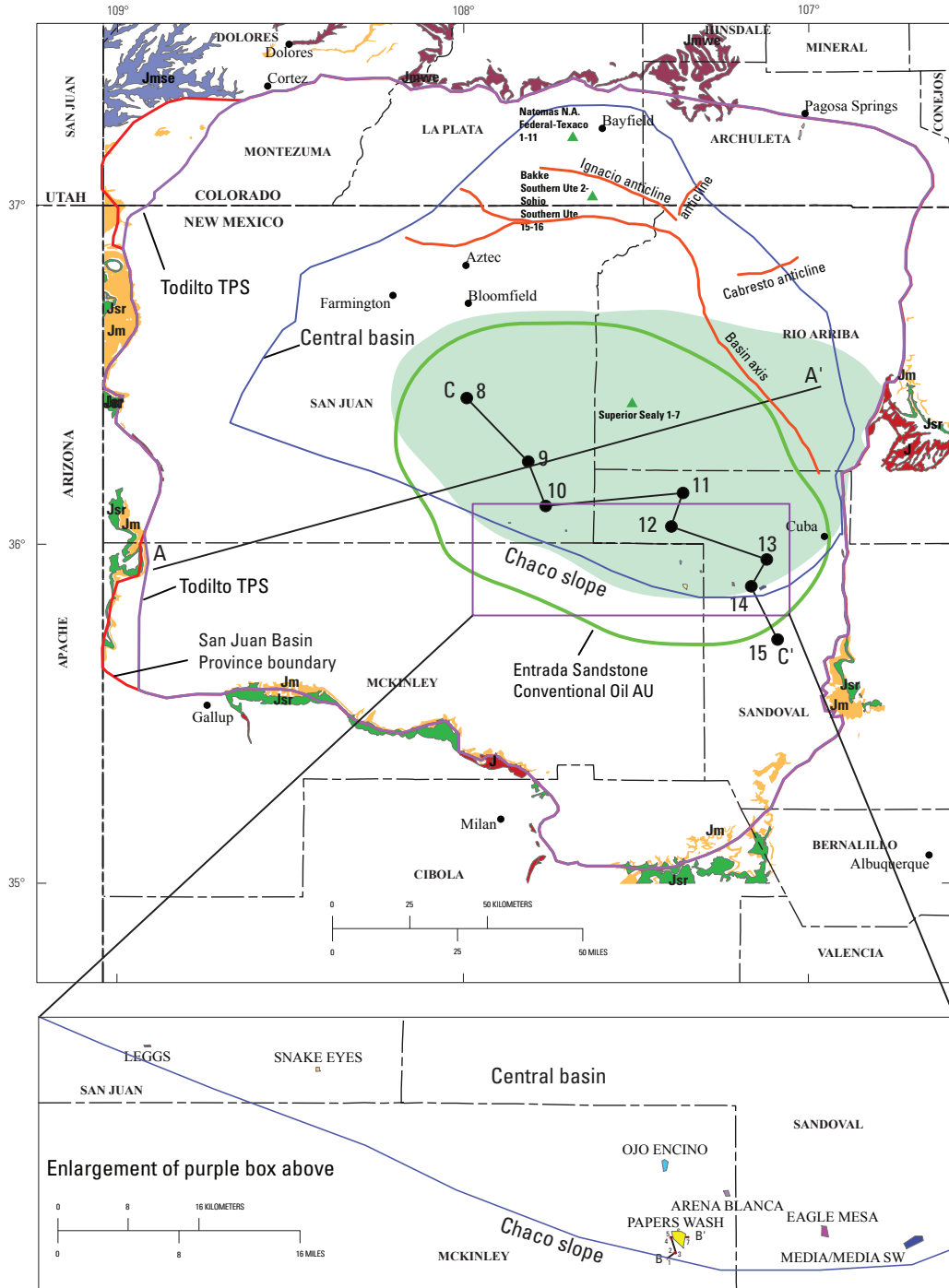


Figure 1. Map showing boundary of the San Juan Basin Province (5022) (red line), Todilto Total Petroleum System (TPS) (purple line), Entrada Sandstone Conventional Oil Assessment Unit (AU) (green line), and location of Entrada Sandstone Conventional Oil AU oil fields (see inset for enlargement and oil field locations). Geologic map from Green (1992) and Green and Jones (1997): J, Jurassic rocks, undivided; Jm, Morrison Formation; Jmse, Morrison and Summerville Formations and Entrada Sandstone; Jmwe, Morrison and Wanakah Formations and Entrada Sandstone; Jsr, San Rafael Group, undivided. Pod of mature oil source rock (solid light-green area) modified from Vincelette and Chittum (1981). Location of cross sections A–A' (fig. 7), B–B' (fig. 9A; see inset) and C–C' (fig. 9B). Also shown are the outline of the central basin area (blue line), location of the Chaco slope, and the location of the three wells (green triangles) for the burial history curves used in this report (figs. 8A–C). Area of the central basin and location of the Chaco slope taken from Fassett (1991).

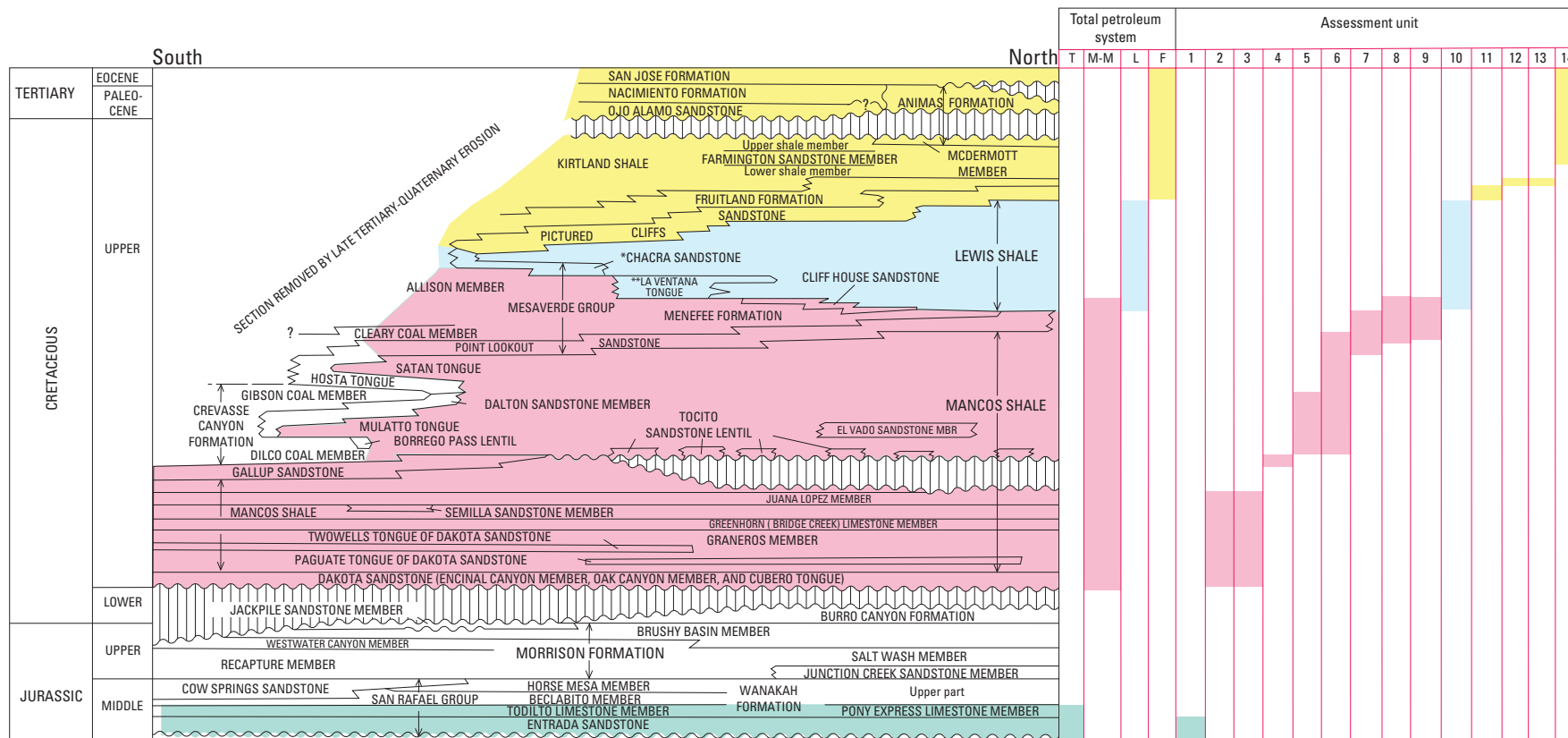


Figure 2. Chart showing regional chronostratigraphic correlations in the San Juan Basin (modified from Molenaar, 1977) to the base of the Jurassic, and the extent of the total petroleum systems and assessment units defined in this 2002 National Oil and Gas Assessment of the San Juan Basin Province (5022), New Mexico and Colorado. Total petroleum systems: F, Fruitland; L, Lewis Shale; M–M, Mancos-Menefee Composite; and T, Todilto. Assessment units: 1, Entrada Sandstone Conventional Oil; 2, Dakota-Greenhorn Conventional Oil and Gas; 3, Dakota-Greenhorn Continuous Gas; 4, Gallup Sandstone Conventional Oil and Gas; 5, Mancos Sandstone Conventional Oil and Gas; 6, Mancos Sandstone Continuous Gas; 7, Mesaverde Updip Conventional Oil; 8, Mesaverde Central-Basin Continuous Gas; 9, Menefee Coalbed Gas; 10, Lewis Continuous Gas; 11, Pictured Cliffs Continuous Gas; 12, Basin Fruitland Coalbed Gas; 13, Fruitland Fairway Coalbed Gas; and 14, Tertiary Conventional Gas. *Chacra sandstone is an informal term used by drillers and geologists in the basin; **La Ventana Tongue of the Cliff House Sandstone. Vertical lines indicate unconformities.

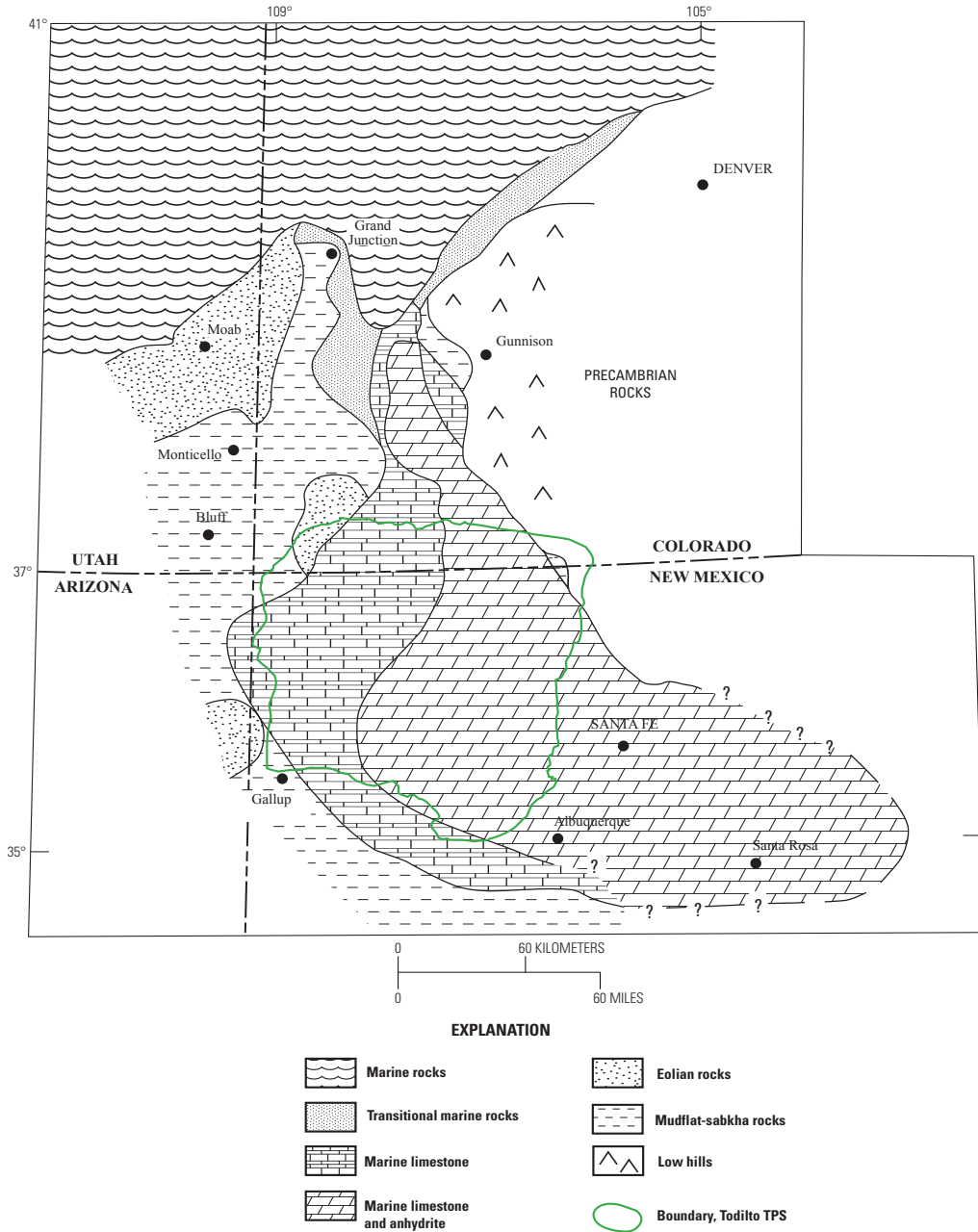


Figure 3. Paleogeographic reconstruction showing distribution of rock types and environments of deposition related to Middle Jurassic Todiito Limestone Member of the Wanakah Formation deposition (from Ridgley, 1989). TPS, Total Petroleum System.

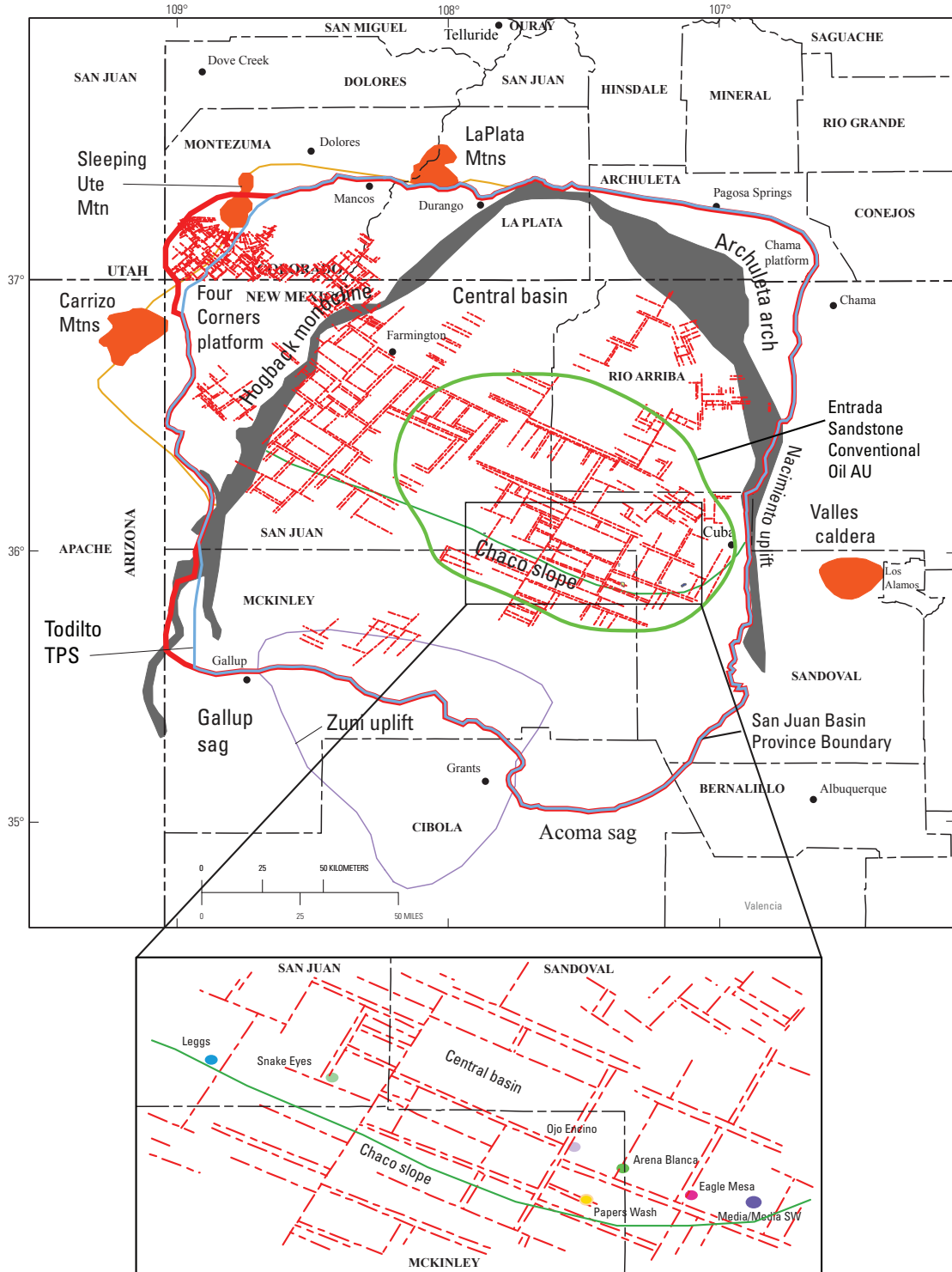


Figure 4. Map showing the boundary of the San Juan Basin Province (5022) (heavy red line), Todilto Total Petroleum System (TPS) (light blue line), Entrada Sandstone Conventional Oil Assessment Unit (AU) (heavy green line), and location of Entrada Sandstone oil fields (inset map). Also shown are the locations of inferred basement structural blocks (dashed red lines) modified from Taylor and Huffman (1998, 2001), and Huffman and Taylor (2002). Names and areal distribution of structural elements modified from Fassett (1991). Orange polygons are Late Cretaceous and Tertiary intrusive and extrusive igneous centers; gray polygons are areas of steep dip along monoclines. Inset map (enlargement) shows the relation of Entrada Sandstone oil fields to inferred basement structural blocks and boundary between the central basin and Chaco slope (light-weight green line).

There are eight oil fields in the Entrada reservoirs:

1. Arena Blanca,
2. Eagle Mesa,
3. Leggs,
4. Media,
5. Media Southwest,
6. Ojo Encino,
7. Papers Wash, and
8. Snakes Eyes (fig. 1),

and several isolated undesignated fields consisting of single wells (see field descriptions in Fassett, 1978a,b, 1983). Approximately 6 MMBO and 124 BCFG have been produced from 44 wells in the Entrada (IHS Energy Group, 2003). Media field, the first Entrada discovery, was found in 1953 (Vincelette and Chittum, 1981) and produced only small quantities of oil until 1969. At that time new exploration concepts were developed, and the field was recognized as primarily a stratigraphic trap and not a structural trap. Once this control on oil accumulation was recognized, subsequent production was increased through the drilling of new wells. After 1969, new drilling for Entrada oil elsewhere in the basin was more successful. Most of the Entrada oil fields were discovered in the early to mid 1970s. The Arena Blanca field was discovered in 1985. Most of the post-1970s discoveries were wildcat wells drilled in the Entrada, and all but the Arena Blanca field consist of single-well production (IHS Energy Group, 2002). Seismic studies have always been an integral part of exploration because the Entrada target (dune crests) is too small to determine from conventional well-log correlation. In the San Juan Basin, fewer than 910 wells penetrate the Entrada.

In the San Juan Basin, a slight break in the regional tilt occurs between the Chaco slope to the south and the central basin to the north (fig. 4). It is near this break in slope in the southern part of the central basin that all the oil fields are found. In fact, the oil fields, although isolated, are aligned northwest-southeast subparallel to the regional structural grain. When these fields are superimposed on the basement blocks (fig. 4), each field occurs within a block near the southern terminus where two blocks intersect. The blocks probably did not control migration of the oil, but rather may have controlled original depositional thickness and preservation of the Entrada. There has been some re-migration of oil out of traps; these sandstone traps are now water wet and some contain residual oil (Vincelette and Chittum, 1981). Flushing of traps probably occurred after the northeast regional tilt was developed, and erosion of rocks along the southern and eastern margin of the basin allowed inclusion of younger meteoric water.

Todilto Total Petroleum System

The Todilto TPS is in many ways similar to the Minnelusa and Leo Total Petroleum Systems in the Powder River Basin (Ahlbrandt and others, 2003). The main difference is that the Entrada is a much more massive sand sea, or erg, with much less source rock potential, and the hydrocarbon accumulations are trapped along the buried topography of the final Entrada dunes that are at the top of the extensive erg system. Key elements that define the Todilto TPS in the San Juan Basin are source rocks of sufficient thermal maturity to generate hydrocarbons, migration pathways that permit the hydrocarbons to move into reservoirs, structural or stratigraphic traps that serve as areas where hydrocarbons accumulate, seals to contain the accumulations, and reservoir rocks to host the accumulations. These key elements are described more fully below.

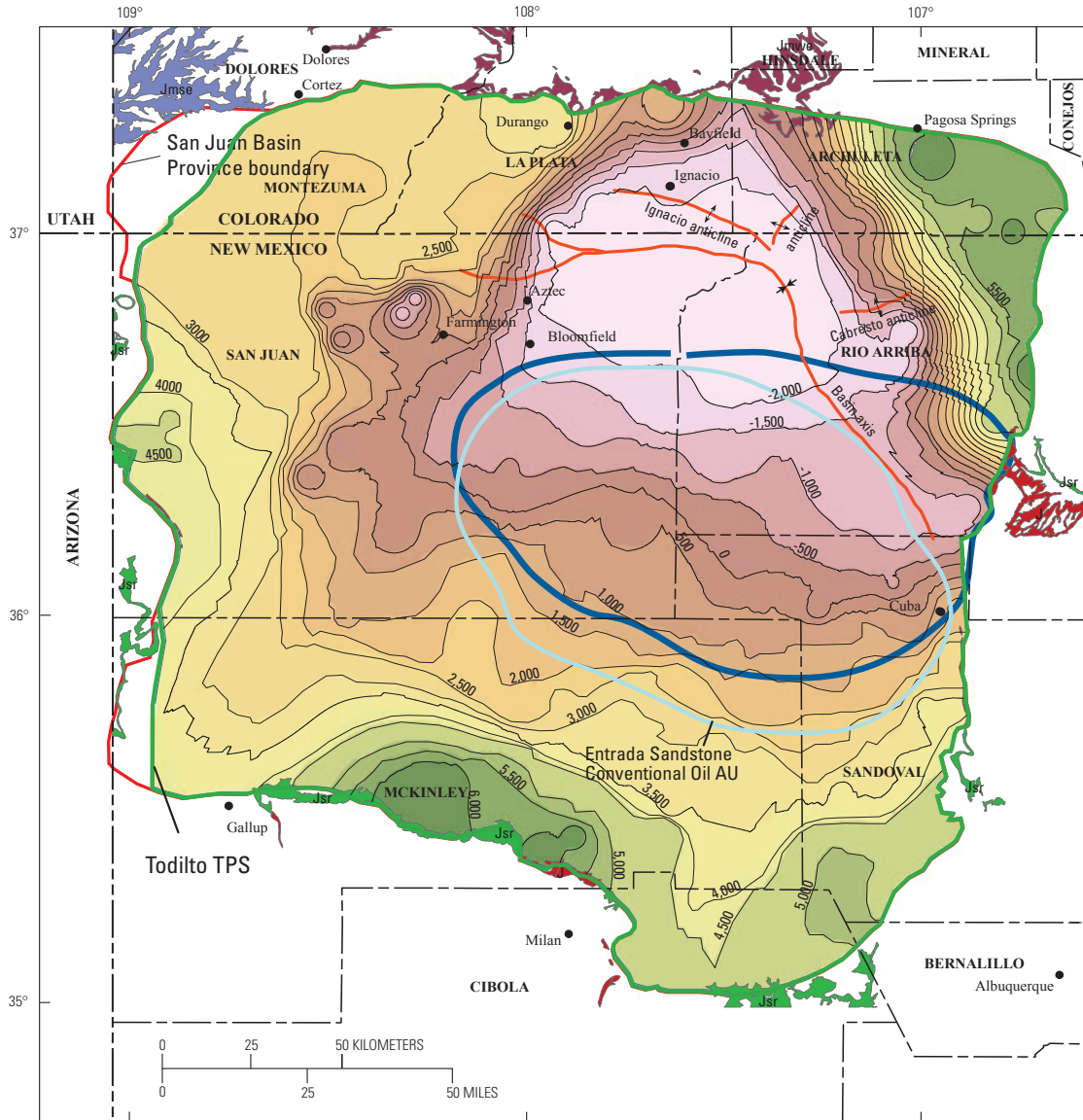
Structural Configuration

Although there was differential tectonic activity during the Paleozoic and Mesozoic, the principal time of formation of the San Juan Basin occurred during the Laramide orogeny, which began in the Paleocene and extended into the Eocene. Structure contours drawn on top of the Todilto Limestone Member (fig. 5) are similar to those drawn on top of the Dakota Sandstone (Thaden and Zech, 1984; plate 1), and both show the present-day configuration of the basin. The basin deepens from south to north (fig. 5); the deepest part of the basin is asymmetrically centered near the Colorado-New Mexico State line. The dip of the structure contours on top of the Todilto rises along the western and northern margins of the basin, coincident with the Hogback monocline, and along the eastern margin, coincident with the Archuleta arch (figs. 4 and 5). Overburden thickness above the Todilto ranges from 0 ft at the outcrop, along the eastern, southern, and western margins of the basin, to more than 9,500 ft in the deeper part of the basin.

Hydrocarbon Source Rock

Todilto Limestone Member of the Wanakah Formation

The Todilto Limestone Member of the Wanakah Formation comprises a basal limestone facies, which contains interbedded organic-rich shale, and an overlying anhydrite facies, which diagenetically alters to gypsum at or near the surface.



EXPLANATION			
●	Cities/towns	Contour interval = 500 feet	
—	Contour lines	-2,500 - -2,000	1-500
—	Todilto TPS	-1,999 - -1,500	501-1,000
—	Area of mature source rocks	-1,499 - -1,000	1,001-1,500
		-999 - -500	1,501-2,000
		-499 - 0	2,001-2,500
			2,501-3,000
			3,001-3,500
			3,501-4,000
			4,001-4,500
			4,501-5,000
			5,001-5,500
			5,501-6,000
			6,000-6,500

Figure 5. Structure contour map, with color shading for depths, drawn on top of the Todilto Limestone Member of the Wanakah Formation (produced from data from IHS Energy Group, 2002); contour interval 500 ft. Geologic map from Green (1992) and Green and Jones (1997). Datum is mean sea level. Pod of mature oil source rock (dark blue line). Also shown is the boundary of the San Juan Basin Province (5022) (red line), Todilto Total Petroleum System (TPS) (dark green line), and Entrada Sandstone Conventional Oil Assessment Unit (AU) (light blue line). See figure 1 for explanations of map symbols.

Throughout most of its areal extent (fig. 3), the limestone facies is laminated, consisting of alternating layers of calcium carbonate and shaly layers rich in organic matter, mostly sapropel (Anderson and Kirkland, 1960). This facies is commonly less than 20 ft thick throughout the depositional extent of the Todilto. The organic matter in the limestone facies appears to be best preserved in the area of the San Juan Basin where the limestone is overlain by anhydrite (Vincelette and Chittum, 1981, their fig. 3). However, preservation of organic matter could extend beyond the anhydrite. The anhydrite facies contains few organic source beds. Along the western and south-western outcrop of the Todilto, the limestone is light gray, contains algal remains, and appears to have been deposited in more oxygenated depositional environments (Tanner, 1970) where organic matter is less well preserved.

Thickness of the Todilto ranges from less than 10 ft along the western margin to over 100 ft in the eastern part of the TPS (fig. 6). The thickness variation directly reflects the amount of topographic relief on the underlying Entrada dunes because the Todilto fills in the topographic relief on top of the dunes as well as covers the crests of the dunes, thus forming potential source rock and seal for underlying Entrada hydrocarbon accumulations. In the central and eastern part of the TPS where there is variable relief on the dunes, the Todilto is thickest, up to 130 ft. Where relief on the Entrada dunes is the greatest and where Todilto overlies the crest of the dunes, it is thinnest, down to 10 ft or less. The area of overall maximum total thickness of the Todilto (fig. 6) also coincides with the areal extent of the anhydrite beds (fig. 3). In the western part of the TPS, the total thickness of the Todilto is generally less than 20 ft and reflects the absence of the anhydrite facies. Isopach thicknesses of the Todilto are only an approximation of the true thickness because there are only about 900 wells drilled into the Entrada and most of these are in the areas of known oil fields.

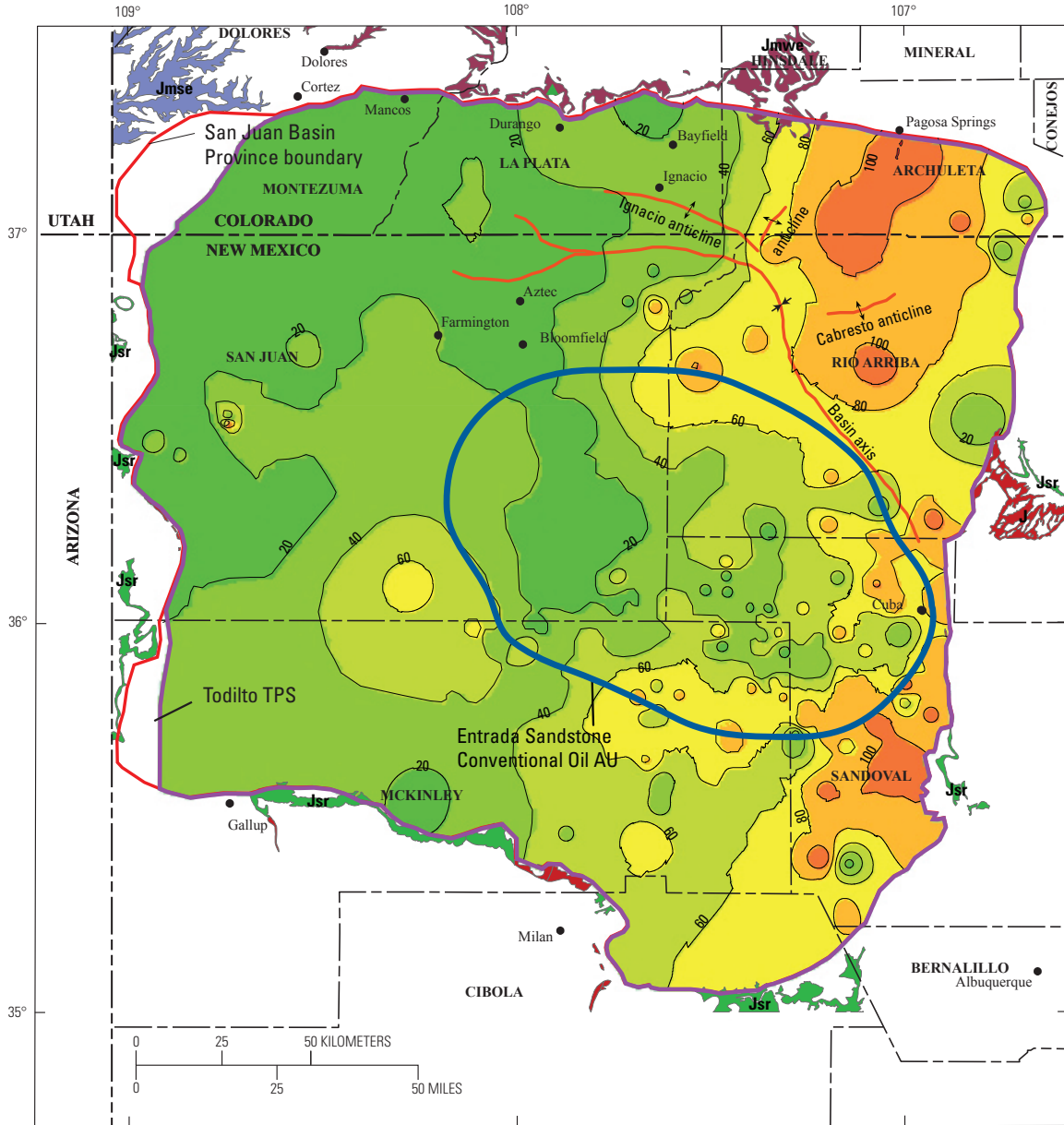
Depths to the top of the Todilto and Entrada are variable, ranging from 120 to more than 10,000 ft ($n = 417$) and from 30 to more than 10,100 ft ($n = 904$), respectively. In the main producing fairway, depths to the top of the producing zone in the Entrada range from 4,600 to 6,000 ft. A structure contour map on top of the Todilto Member shows that the unit is less deeply buried along the western and southern margin of the TPS (fig. 5). If source rocks were at one time present in these areas of the TPS, they may have been oxidized by incursion of post-deposition meteoric groundwater. Indeed, there is evidence from the outcrop along the southern margin of the San Juan Basin that anhydrite once had a greater distribution in the area (Rawson, 1980). Post-depositional groundwater movement has altered the anhydrite to calcium carbonate. Evidence for organic matter once present in the limestone facies along the southern margin of the basin (where the anhydrite has possibly been altered) is inferred from the distribution of uranium deposits—which are associated with isolated organic matter—along the southern margin of the basin at the outcrop or in the near subsurface (Rawson, 1980).

The Todilto Limestone Member can be subdivided sedimentologically into two distinct facies, an outer margin facies (5 to 40 ft thick) and a central basin facies (2 to 120 ft thick) (figs. 1 and 7). The changes in style of deposition and vertical succession of the limestone help to determine the relative position of any location to the original depositional basin geometry and to potential source rocks. Figure 7 shows the interpretation of facies distribution in a schematic cross section through the basin. The outer margin facies can be subdivided into three limestone lithofacies, from base to top:

1. thick, parallel-bedded limestone, where the thickness of individual beds is related to the depth of water in which the calcium carbonate was precipitated;
2. sedimentary boudinage; and
3. massive crossbedded limestone.

Limestones in the thick, parallel-bedded lithofacies are similar in geometry to those considered to represent deposition in “deeper water” (Carrasco-V, 1977; Garrison and Fischer, 1969; Wilson, 1969; Yurewicz, 1977). Overall, this lithofacies consists of couplets of parallel-bedded micritic limestone (2 to 6 in. thick) separated by thin (commonly less than 0.5 in. thick) shaly limestone. The shaly layers are much darker gray than the encasing limestone beds and are probably more organic rich than the thicker limestone beds. The thick, parallel-bedded limestone lithofacies is distributed along the western margin of the central basin facies. It grades laterally landward into and is overlain by the sedimentary boudinage lithofacies (fig. 7). This lithofacies may contain a few potential source beds in the organic-rich shale layers.

The sedimentary boudinage lithofacies is characterized by wavy bedding surfaces, which impart a characteristic sedimentary boudinage or pinch-and-swell appearance (fig. 7). Limestone of this interval is thinner bedded, more micritic, and less sandy than in the overlying massive crossbedded lithofacies. The limestone is darker gray than limestone of the massive crossbedded lithofacies, indicating greater reducing conditions in the depositional environment. Thin silty or sandy, clayey or possibly gypsiferous lenses are commonly intercalated with limestone. The boudinage texture is a result of differential compaction of the limestone lenses into underlying silt, clay, or gypsum lenses while both were still plastic. Similar sedimentary boudinage have been reported from the lower part of the Cambrian and Ordovician Whipple Cave Formation, Nevada (Cook and Taylor, 1977). Wilson (1969, p. 17) and Cook and Taylor (1977, p. 55) suggested that sedimentary boudinage formed in shallow subtidal shelf waters, below wave base but within oxygenated water. Cook and Taylor (1977) also noted that the rocks in the sedimentary boudinage zone of the Whipple Cave Formation were gradational into overlying rocks characteristic of shoaling depositional environments and differed from rocks deposited in deeper water. Potential hydrocarbon source beds probably do not occur in this lithofacies.



EXPLANATION		
●	Cities/towns	
—	Contour lines	Contour interval = 20 feet
—	Todilto TPS	
■		0-20
■		21-40
■		41-60
■		61-80
■		81-100
■		101-120
■		121-140

Figure 6. Isopach map of Todilto Limestone Member of the Wanakah Formation (produced from data from IHS Energy Group, 2002); contour interval 20 ft. Geologic map from Green (1992) and Green and Jones (1997). Also shown is the boundary of the San Juan Basin Province (5022) (red line), Todilto Total Petroleum System (TPS) (magenta line), and Entrada Sandstone Conventional Oil Assessment Unit (AU) (blue line). See figure 1 for explanation of geologic symbols.

The sedimentary boudinage lithofacies is overlain by and grades laterally landward into light-gray to light-purple-brown thick-bedded limestone of the massive crossbedded lithofacies (fig. 7). This limestone is commonly crossbedded and sandy, and locally contains either algal stromatolites or chert pebbles at the top. Crossbedding in the limestone indicates deposition in shallow water depths affected by water currents. The sandier component of the limestone indicates close proximity to the coast where marginal sand could be reworked, during storms or higher water level, into the precipitating limestone. The light-gray color of the rocks and presence of algal stromatolites indicate that the water was well oxygenated, and thus these rocks are poor candidates for preserving high total organic carbon (TOC). These limestones locally contain spherical to irregular masses of sparry calcite that possibly represent replacement of evaporite minerals. Potential hydrocarbon source beds are absent in this lithofacies due to shallow water depositional conditions and presence of oxygenated environments.

The central basin facies occupied the eastern part of the depositional basin, extending from near Gunnison, Colo. to east of Santa Rosa, N. Mex. (fig. 3). It can be divided into two subfacies, A and B, both of which are found throughout this part of the depositional basin and reflect different depositional conditions with respect to buried Entrada Sandstone dune topography (fig. 7). Subfacies A contains only limestone and is confined to the crests of the Entrada dunes. Subfacies B contains limestone overlain by gypsum (anhydrite in the subsurface) and is confined to the flanks and areas where a relict Entrada dune is least thick (fig. 7). Subfacies A can be subdivided into three distinct lithofacies (fig. 7), in ascending order:

1. platy limestone,
2. crinkly limestone, and
3. breccia limestone.

Thin parallel-bedded limestone consisting of thin laminated (only a few millimeters thick) dark-gray, fetid, micrite makes up the platy limestone lithofacies. The limestone has an appearance of papery-thin shale and consists of alternating laminae of micrite and organic matter (sapropel). The best hydrocarbon source beds are found in this lithofacies. At a few locations, thin sandstone beds are intercalated with the basal limestone. The sandstone has limited lateral extent at the outcrop. This platy lithofacies is found in both subfacies A and B (fig. 7) and may serve, in part, as a seal to upward and lateral hydrocarbon migration.

Overlying the basal platy limestone lithofacies is the slightly thicker crinkly lithofacies (fig. 7). This limestone is medium to dark gray and consists of alternating thin laminae of micritic limestone and organic matter that commonly contains clastic grains (Anderson and Kirkland, 1960). The micritic laminae are thicker (up to 10 mm thick) than in the underlying platy limestone lithofacies. Some laminae are light gray or white and represent calcite replacement of bedded gypsum. The clastic-grain laminae are commonly only one grain thick and consist of quartz and lesser amounts of feldspar, clays, and iron minerals. The rhythmic vertical succession of micrite laminae, organic laminae, and clastic laminae in the platy and the crinkly lithofacies imparts the varved appearance so often referred to in the literature. The varved appearance is confined to the central basin facies; individual laminae are believed to be seasonally deposited (Anderson and

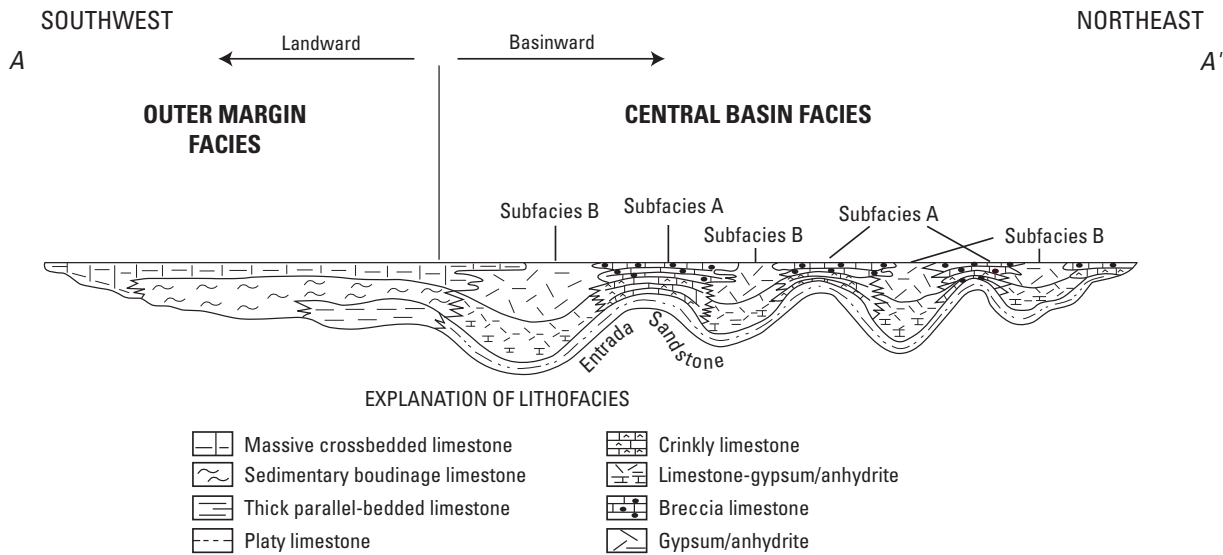


Figure 7. Schematic southwest–northeast cross section (A–A') through the Todilto Limestone Member of the Wanakah Formation in the San Juan Basin, showing interpreted facies distribution between outer margin and central basin. (Approximate location on figure 1.) In the central basin facies, subfacies A, vertical lithofacies distribution over the crest of an Entrada dune; subfacies B, vertical lithofacies distribution between the crests of Entrada dunes.

Kirkland, 1960). Potential hydrocarbon source beds (aggregate up to about 5 ft) are also found in this lithofacies. This lithofacies (5 to 10 ft thick) may also serve, in part, as a seal to upward hydrocarbon migration.

The upper breccia-limestone lithofacies comprises thick, laminated to “brecciated” limestone (fig. 7). This lithofacies (10–30 ft thick) consists dominantly of microcrystalline calcite; however, more sparry calcite is present than in the crinkly lithofacies. This lithofacies is thicker than either of the two underlying lithofacies and commonly has a mound-like shape. The breccia-limestone lithofacies may occur as a single mass or as several laterally continuous masses separated by a bounding surface that represents a paraconformity. The lithofacies is made up of three distinct types of limestone. The first type of limestone consists of sparry calcite that contains fragments of dense micritic limestone similar to that observed in the lower two lithofacies. The sparry calcite is a secondary replacement of authigenic gypsum, and the micrite fragments are not true breccia clasts (Ridgley, 1986). The brecciated fabric is diagenetic and resulted from interstitial growth of gypsum, which ultimately consumed parts of the micrite, leaving remnant patches of micrite that look like breccia clasts. A second type of limestone is similar to the first except that clasts of limestone, similar to that in the lower two lithofacies, are actually clast-supported or are surrounded by calcite. Calcite in this type of breccia is both a true cement and a replacement of authigenic gypsum. This type of limestone may actually represent a true solution breccia. The third type of limestone is wavy-laminated to weakly crossbedded limestone. The limestone is micritic with thin laminae of clastic grains, one grain thick, and is similar to the texture observed in the platy and crinkly subfacies. The clastic grains are quartz, clay minerals, and feldspar. Patches of sparry calcite occur in the micrite. This calcite either replaced individual anhydrite or gypsum grains or clusters of these minerals, or filled in the voids when the evaporite minerals dissolved (Ridgley, 1986). Texturally, the three types of limestone of the breccia-limestone lithofacies indicate the former presence of gypsum. This lithofacies does not contain potential hydrocarbon source beds, nor is it a potential reservoir. However, because of their well-cemented nature, rocks in this lithofacies form a good seal to upward hydrocarbon migration.

Subfacies B can be subdivided into three lithofacies that are lateral equivalents of the three lithofacies of subfacies A (fig. 7). These lithofacies, from base to top, are

1. platy limestone (<5 ft thick),
2. limestone-gypsum/anhydrite (5–20 ft thick), and
3. gypsum/anhydrite (20–100 ft thick).

The platy limestone lithofacies, previously described, is positionally continuous with the platy limestone lithofacies of limestone subfacies A. Source beds with the best hydrocarbon potential are found in this lithofacies. This lithofacies may also serve as a partial seal to vertical and lateral migration of hydrocarbons.

The platy limestone lithofacies is overlain by the limestone-gypsum/anhydrite lithofacies (fig. 7) consisting of thinly laminated limestone that is interbedded with bedded gypsum. The limestone is laminated like that of the underlying platy limestone lithofacies. Generally, within a few feet of the base of this interval, gypsum laminae occur. Initially the gypsum laminae may occur several inches apart. Vertically, more gypsum laminae occur, and they become closer-spaced until proportionally they dominate over limestone laminae. Source bed potential of this lithofacies is minimal because of the amount of gypsum interbeds; the best petroleum source beds are near the base of the lithofacies where the thin laminated limestone beds are most prominent. The upper part of this lithofacies serves as a seal to lateral hydrocarbon migration, focusing the hydrocarbons into the upper part of the Entrada dunes.

Thick beds of gypsum/anhydrite compose the gypsum/anhydrite lithofacies (fig. 7). The gypsum also has a coalescing nodular texture, commonly called “chicken wire,” due to the concentration of insoluble residue along the margins of the gypsum nodules as the nodules grew. The nodular aspect of the gypsum represents diagenetic alteration of originally bedded gypsum. The nodules are not formed by coalescence of large gypsum crystals, such as those described by Warren and Kendall (1985) from coastal salinas of Australia. At many locations the upper massive gypsum also appears to be interbedded with thin discontinuous limestone laminae, especially near the top. This lithofacies does not contain any potential hydrocarbon source beds or reservoirs but does form a seal to lateral migration of hydrocarbons into and out of the upper part of the Entrada dunes.

Oil Geochemistry

There are eight oil fields with Entrada reservoirs:

1. Arena Blanca,
2. Eagle Mesa,
3. Leggs,
4. Media,
5. Media Southwest,
6. Ojo Encino,
7. Papers Wash, and
8. Snakes Eyes (fig. 1),

and several isolated undesignated fields consisting of single wells (see field descriptions in Fassett, 1978a,b, 1983). The Todilto Limestone Member is considered to be the source of oil in the Entrada Sandstone reservoirs (Vincelette and Chittum, 1981). This determination was based on a comparison of oil samples from the Eagle Mesa, Media, and Papers Wash Entrada fields with known Cretaceous and Pennsylvanian oils from the San Juan Basin (Ross, 1980; Vincelette and Chittum, 1981). The Entrada oil sample had a higher boiling point (205°F, 96°C), higher pour point (50° to 90°F, 10° to 32°C), and higher paraffin content compared to Cretaceous or Pennsylvanian oils (Ross, 1980; Vincelette and Chittum,

1981). Entrada oil is characterized by a low pristane/phytane ratio (0.86) and even-carbon predominance index of 0.91, suggesting generation from a carbonate source. API gravities are similar for all fields, ranging from 29.3° at Snake Eyes to 35.5° at Ojo Encino (table 1). These API gravities, which cover a narrow range, are among the heaviest in the basin. Sulfur content is low, ranging from 0.3 to 0.6 percent (Richard Vincelette, written commun., 2003; NRG, 2001).

There is little publicly available organic geochemical data for the Todilto. The range of total organic carbon is unknown; however, one sample from the basal part of the Todilto from the area of the Nacimiento Mountains on the east side of the basin yielded a TOC of 1.24 (Richard Vincelette, written commun., 2003). This sample had a hydrogen index (HI) of 717, which is indicative of type-I organic carbon. Rock-Eval analysis of the sample provided the following information: $T_{max} = 424^{\circ}\text{C}$, $S_1 = 0.32$, $S_2 = 8.89$, and $PI = 0.02$, where S_1 = integral of first peak (existing hydrocarbons volatilized at 250°C for 5 minutes) (in milligrams/gram rock); S_2 = integral of second peak (hydrocarbons produced by pyrolysis of solid organic matter (kerogen) between 250°C and 550°C (in milligrams/gram rock)); and PI, production index ($S_1/(S_1+S_2)$). Although the data indicate that the Todilto in this area is immature, the S_1 and S_2 values indicate sufficient hydrocarbon generative capability under the right thermal maturation conditions.

The most comprehensive published data on the organic geochemistry of the Todilto is on 28 samples from drill cuttings (Vincelette and Chittum, 1981). Although no Rock-Eval analyses were performed on the samples, the samples were

analyzed for kerogen color (for thermal maturation) and subjected to pyrolysis to determine the potential hydrocarbon yield. The high HI value of the single outcrop sample may be indicative of algal organic matter. Unpublished laboratory data for the samples used in the study by Vincelette and Chittum (1981) also support a partly algal source for some of the Todilto source rock samples (Richard Vincelette, written commun., 2003). Residue of some samples had a distinct cellular-type pattern, which might be indicative of colonial-type algae, such as *Botryococcus*. Samples T-2, T-7, T-11, T-13, T-17, and T-23a (see Vincelette and Chittum, 1981, their fig. 9 for locations) were reported to contain some algal-like matter, thereby indicating the presence in the Todilto of type-I organic matter. These samples generally lie outside the zone of maximum oil generation as determined by the color of the kerogen. However, all the samples lie within the area of preserved anhydrite facies, as discussed above, and thus some algal matter must have been present throughout the broader Todilto depositional system and not just confined to the shallow water margins (Tanner, 1970). The presence of algal matter may support a lacustrine or partly lacustrine origin for the Todilto.

Although little Rock-Eval data is available, pyrolysis yields were calculated for 5 samples of the Todilto in New Mexico (Vincelette and Chittum, 1981, their fig. 9). Within the area defined by the central basin facies, pyrolysis yields ranged from 0.6 to 2.4 gal/ton; these values may not reflect potential yield, because the samples are from the part of the basin where the Todilto is thermally mature (Vincelette and Chittum, 1981).

Table 1. Characteristics of Entrada Sandstone reservoir rocks, including oil API gravities, compiled from Vincelette and Chittum (1981) and from field descriptions in Fassett (1978a,b, 1983).

[N/A, not available].

Field	Avg. depth (ft)	Porosity (%)	Permeability (millidarcies)	Water saturation (%)	Oil API gravity (degrees)	Net pay (ft)	Type of drive
Eagle Mesa	5,460	25	430	45	33	23	Water
Leggs	5,400	23.3	N/A	55	31.5	16	N/A
Media	5,250	23	290	58.4	33.5	25	N/A
Media, southwest	5,310	24	360	58.4	33.5	18	Water
Ojo Encino	5,890	22	180	50	35.5	20	Fluid expansion, water drive
Papers Wash	5,170	25	290	53	32.5	29	Fluid expansion, water drive
Snake Eyes	5,600	24	665	50	29.3	23	Fluid expansion, water drive

Source Rock Maturation

The time of thermal maturity of the source-bed facies in the Todilto can be estimated from three burial history curves (Bond, 1984; Law, 1992) (figs. 1, 8A, 8B, and 8C). These curves, taken from the literature, only cover the Cretaceous and Tertiary part of the stratigraphic column. Thus, the time of oil generation in the Todilto can only be extrapolated from these figures as no detailed modeling has been done for this unit. The burial history curves indicate distinct thermal maturation histories for different parts of the basin. Formation of the basin may have begun as late as 90 million years ago during the Sevier orogeny and continued until about 13 million years ago. Only the northernmost burial profile from the Natomas North America Federal-Texaco 1-11 well shows reconstructed temperature profiles. It is inferred that temperature profiles for the composite burial history for the Bakke Southern Ute 2 and Sohio Southern Ute 15-16 wells should be similar to the profiles in the Natomas well because the well also penetrates the deep part of the San Juan Basin. On the other hand, it is inferred that temperature profiles at the Superior Sealy 1-7 well in the southern part of the central San Juan Basin would show lower maximum burial temperature because this well penetrates strata that were never as deeply buried as strata in the Sohio or Natomas wells.

The southernmost burial history curve for the Superior Sealy 1-7 well in Rio Arriba County, N. Mex. (Law, 1992) (figs. 1 and 8A) is located in the northern part of the AU and indicates that this area of the central basin was never as deeply buried as the northern part of the central basin (figs. 4 and 5). Maximum burial for this curve was shown to span a time from 40 to about 12 million years—before uplift and erosion. In contrast, the composite burial curve from the Bakke Southern Ute 2 and Sohio Southern Ute 15-16 wells in the northern part of the central basin in La Plata County, Colo. (Law, 1992) (figs. 1 and 8B), documents a younger, present-day configuration. The northern part of the central basin, in which this northern curve is located, was an area of greater subsidence and accumulation of a thicker section of overburden as represented by Tertiary rocks, when compared to the area of the southern part of the central basin. Any liquid hydrocarbons generated earlier would have cracked to gas. Using the Dakota Sandstone thermal history profile (fig. 8C), the cracking would have started in the late Eocene and continued into the Oligocene.

Maximum hydrocarbon generation for Cretaceous source rocks probably occurred during the mid- to late-Eocene based on the burial reconstructions (fig. 8C) (Bond, 1984; Law, 1992). However, onset of oil generation may have begun as early as mid-Paleocene for source rocks in the Cretaceous Dakota Sandstone–Greenhorn Limestone Member of Mancos Shale interval, which is used here to aid in estimating Todilto maturation throughout the basin (fig. 8C). Oil generation may have continued until the middle Eocene, and in the deeper part of the basin, wet gas and condensate may have been generated until middle Miocene (fig. 8C). The thickness from

the base of the Dakota Sandstone to the top of the Todilto averages about 1,000 ft. This thickness alone would probably not significantly change the overall maturation history of the Todilto source beds, and thus, the maturation history of these Middle Jurassic source beds probably approximates that of the lowest part of the Cretaceous section. Although the onset of hydrocarbon generation may have begun in the late Paleocene, the critical moment for maximum liquid hydrocarbon production was in the Eocene. The critical moment (Magoon and Dow, 1994) that defines the time of maximum hydrocarbon generation, migration, and accumulation will differ throughout the basin. Generation of liquid hydrocarbons ceased in the Pliocene as the basin was uplifted and cooled. Today, bottom-hole temperatures in the producing fields are generally below 60°C.

In their study of source-rock thermal maturity of the Todilto, Vincelette and Chittum (1981) examined the color of the kerogen in 28 samples from outcrop and core. Their results showed the Todilto to be thermally immature along the west, southwest, and extreme northeast parts of the depositional system and to increase in thermal maturity in the central and northern part of the San Juan Basin (Vincelette and Chittum, 1981, their fig. 9). They concluded that potential source beds in the Todilto would be mature enough to produce oil in the central part of the TPS, between the +1,000- and –2,000-ft contour intervals (fig. 5). South and west of this area, the source beds were immature, judged from a few samples. North of the –2,000-ft contour, in the deeper part of the basin, the source beds were considered to be overmature and beyond oil generation. The organic matter from several samples from this part of the basin appeared to be carbonized (overheated), and thus, the expected hydrocarbons would be gas and condensate. The apparent area of maximum oil generation, based on limited data, would be found between 5,000- and 8,000-ft depth, which corresponds to about +1,500- to –2,000-ft structural elevation (Vincelette and Chittum, 1981).

Hydrocarbon Migration Summary

The period of migration and accumulation of oil in the Entrada may have extended from the Eocene through the end of the Miocene. Basin subsidence continued well into the Miocene, and it is this later subsidence that might have aided migration of oil from source to trap. During this period, strata in the southern part of the San Juan Basin were further tilted to the northeast. A slight break in the regional tilt occurs between the Chaco slope to the south and the central basin to the north (fig. 4). All the oil fields are found just north of the Chaco slope in the southern part of the central basin. The oil fields, although isolated, are aligned northwest–southeast subparallel to the regional structural grain and in proximity to the intersection of basement blocks, which have a predominant northwest to southeast orientation (fig. 4). The blocks probably did not control migration of the oil, but rather may have controlled syndepositional thickness and preservation of thick Entrada Sandstone. The migration distance of oil from Todilto

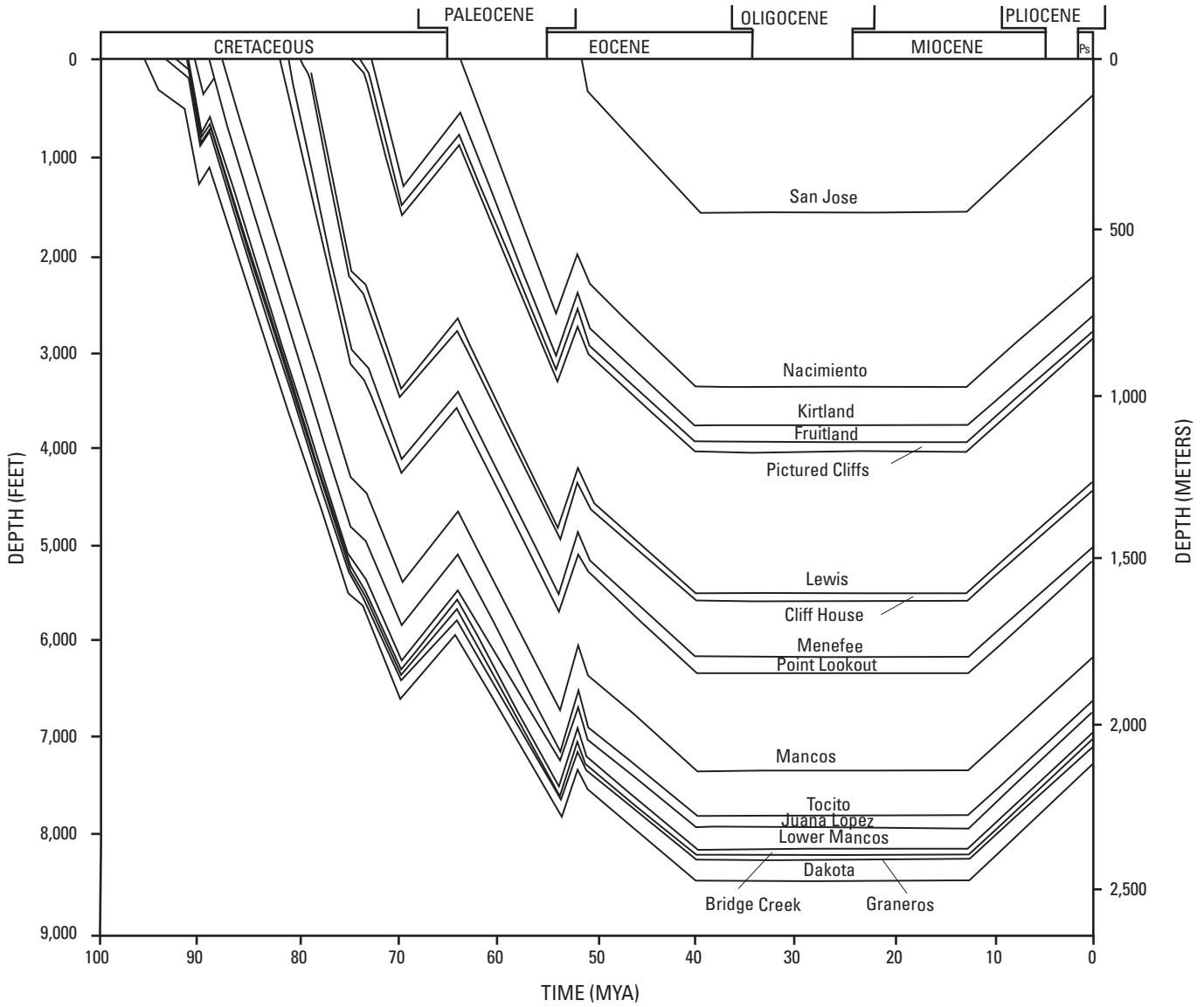


Figure 8A. Burial history curve for the Superior Sealy 1-7 well in the southern part of the central San Juan Basin (modified from Law, 1992). MYA, million years ago; Ps, Pleistocene.

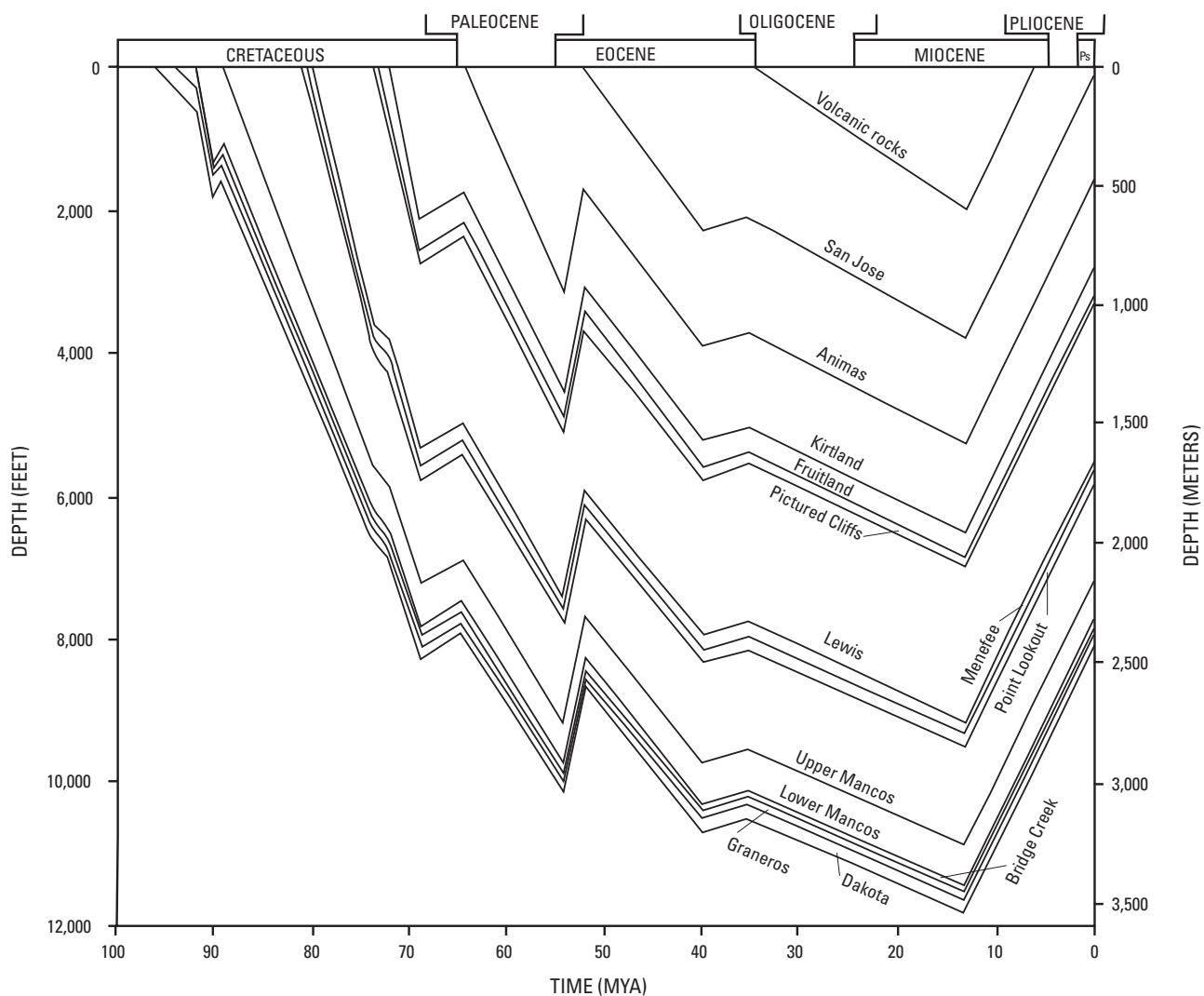


Figure 8B. Composite burial history curve for the Bakke Southern Ute 2 and Sohio Southern Ute 15-16 wells in the northern part of the central San Juan Basin (modified from Law, 1992). MYA, million years ago; Ps, Pleistocene.

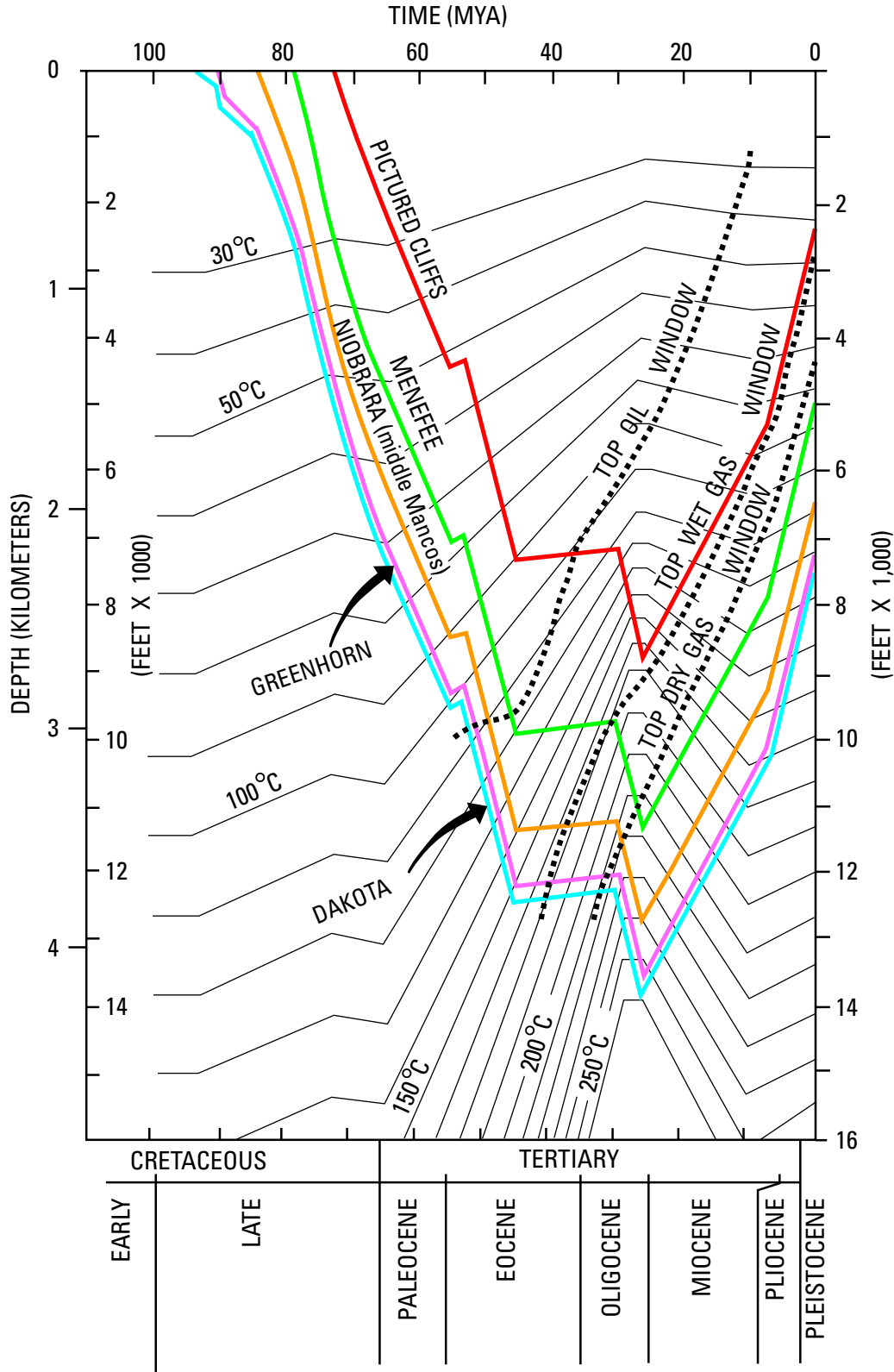


Figure 8C. Burial history curve for the Natomas North America (N.A.) Federal-Texaco 1-11 well in the northern part of the San Juan Basin (modified from Bond, 1984). Geologic time scale is from the Geological Society of America web page <http://www.geosociety.org/science/timescale/timescl.htm>, last accessed 2/1/2008. MYA, million years ago.

source beds into underlying Entrada Sandstone reservoirs was short (less than a few miles), probably within the dimensions of a single dune crest. However, early longer distance migration from the central basin cannot be ruled out. A stratigraphic cross section through the Papers Wash field (fig. 9A) shows the position of the oil. The oil in this field, as well as in others, is confined to the upper part of the dune where the Todilto Limestone Member (both limestone and anhydrite facies) is thinnest and where there is some stratigraphic closure. The oil-water contact (below the oil shown in fig. 9A) in this field appears to occur where the flanks of the dune begin to flatten and dune height and stratigraphic closure is diminished. The position of the oil-water contact may also have been influenced by later hydrodynamic factors and faulting.

The influence of hydrodynamics was documented in the Media and Media Southwest fields (Vincelette and Chittum, 1981). In those fields, oil mostly fills the southernmost parts of the stratigraphic closure. Other wells evaluated in the oil-producing area show evidence of flushing of the original oil accumulation by later hydrodynamic forces, indicating that the oil has remigrated to some other site or has otherwise been lost to the system (Vincelette and Chittum, 1981). Flushing of traps probably occurred after the northeast regional tilt was developed and erosion of rocks along the southern and eastern margin of the basin allowed intrusion of younger meteoric water.

Because the dune topography varies dramatically throughout the central part of the TPS, most of the oil would have been generated fairly locally, as it might have been difficult for the oil to migrate regionally through the laterally adjacent thick anhydrite facies that accumulated in the off-flank position of the dune. The various Entrada fields do not appear to be linked along any regional migration pathway that might suggest movement of hydrocarbons from the deeper part of the central basin along regional faults or through the lower sandstone of the Entrada. All the oil fields appear to occur where the Todilto is sufficiently mature to produce oil within the Entrada Sandstone Conventional Oil AU (fig. 1). These observations suggest that potential Entrada reservoirs are under-filled.

Hydrocarbon Reservoir Rocks

Potential reservoir rocks are confined to the eolian sandstone facies in the Entrada Sandstone. The Entrada Sandstone consists primarily of sandstone deposited in dune and interdune eolian environments. The upper part of the Entrada (generally less than 100 ft thick) shows evidence of having been deposited or reworked in subaqueous conditions related to the incursion of marine waters in which the overlying Todilto Limestone Member was deposited (Reese, 1984; Fryberger, 1986). This water-laid facies is prevalent along the western and southwestern margin of the Todilto depositional system, but also has been reported from outcrops in the Chama Basin to the east (for the location of the Chama Basin, see chap. 2, fig. 1, this CD-ROM) (Tanner, 1970). In the southern part of the basin, the Entrada contains thin beds of reddish-brown siltstone deposited in interdune and inland sabkha environments (Green and

Pierson, 1977). Thin coarse-grained sandstone units have also been reported in the Entrada from the southern part of the San Juan Basin and were probably deposited in ephemeral wadis (Green, 1974). Inland sabkha and wadi deposits are absent to the north and are not found along the eastern margin of the San Juan Basin nor in the Chama Basin; they appear to be confined to the margins of the Todilto depositional system.

The thickness of the Entrada in the San Juan Basin ranges from 60 to 330 ft (Green and Pierson, 1977). The variable thickness reflects, in part, the relict dune topography. Sandstone beds of Entrada generally exhibit three styles of crossbedding that have been observed along the east side of the basin and in the neighboring Chama Basin (Ridgley, 1977; Reese, 1984). In these areas, the basal Entrada consists of large-scale, sweeping wedge and trough cross stratification characteristic of eolian deposition. Parallel laminated beds in the lower part of the Entrada probably represent interdune deposits (Reese, 1984). Sandstones in the interdune deposits are commonly finer grained than in the dune sandstones and where present may be locally interbedded with siltstones and mudstones. The middle part of the Entrada consists of mostly medium-angle planar crossbeds and wavy-laminated sandstone. The wavy laminations were produced by adhesion ripples (Ridgley, 1977; Reese, 1984). The upper part of the Entrada consists of two different styles of deposition (Ridgley, 1977; Reese, 1984). The base of the upper part contains low- to high-angle eolian crossbeds. These beds are overlain by massive, structureless, or parallel laminated beds, in which the lack of well-defined sedimentary structures suggests modification by marine incursion that was associated with early stages of the overlying Todilto transgression. Most of the oil is found in the upper and middle parts of the Entrada.

The relation of Entrada Sandstone reservoirs to overlying source and seal rocks of the Todilto Limestone Member is shown in a regional cross section (fig. 9B) and a cross section through the Papers Wash oil field (fig. 9A). Seismic studies of the Entrada, which is the most effective means of delineating the dune topography (Vincelette and Chittum, 1981; Nestor and Endsley, 1992; Massé and Ray, 1995), are commonly employed in order to delineate potential traps. However, published seismic studies are few. Seismic studies on the east side of the basin indicate that dune crests form ridges that are oriented north-northeast; ridge length may be as long as 15 mi and ridge width may vary from 0.5 to 2 mi (Vincelette and Chittum, 1981). South of these elongate ridges are isolated pods of thicker Entrada, possibly indicating a different dune type or sand sea, or other factors that influenced preservation of dune topography. All the oil fields are found in these thick isolated sand buildups (Vincelette and Chittum, 1981, their fig. 16).

Where the Entrada has been examined at the outcrop, the uppermost sandstones (oil reservoir beds) are fine to medium grained and moderately to well sorted (Ridgley, 1977; Reese, 1984). Quartz is the principal sandstone component, although rock fragments and clays are also present. Quartz grains are well rounded to subangular. Locally, the sandstone beds have been described as silty (Reese, 1984). Porosity in the Entrada changes regionally. In the northern part of the San Juan Basin,

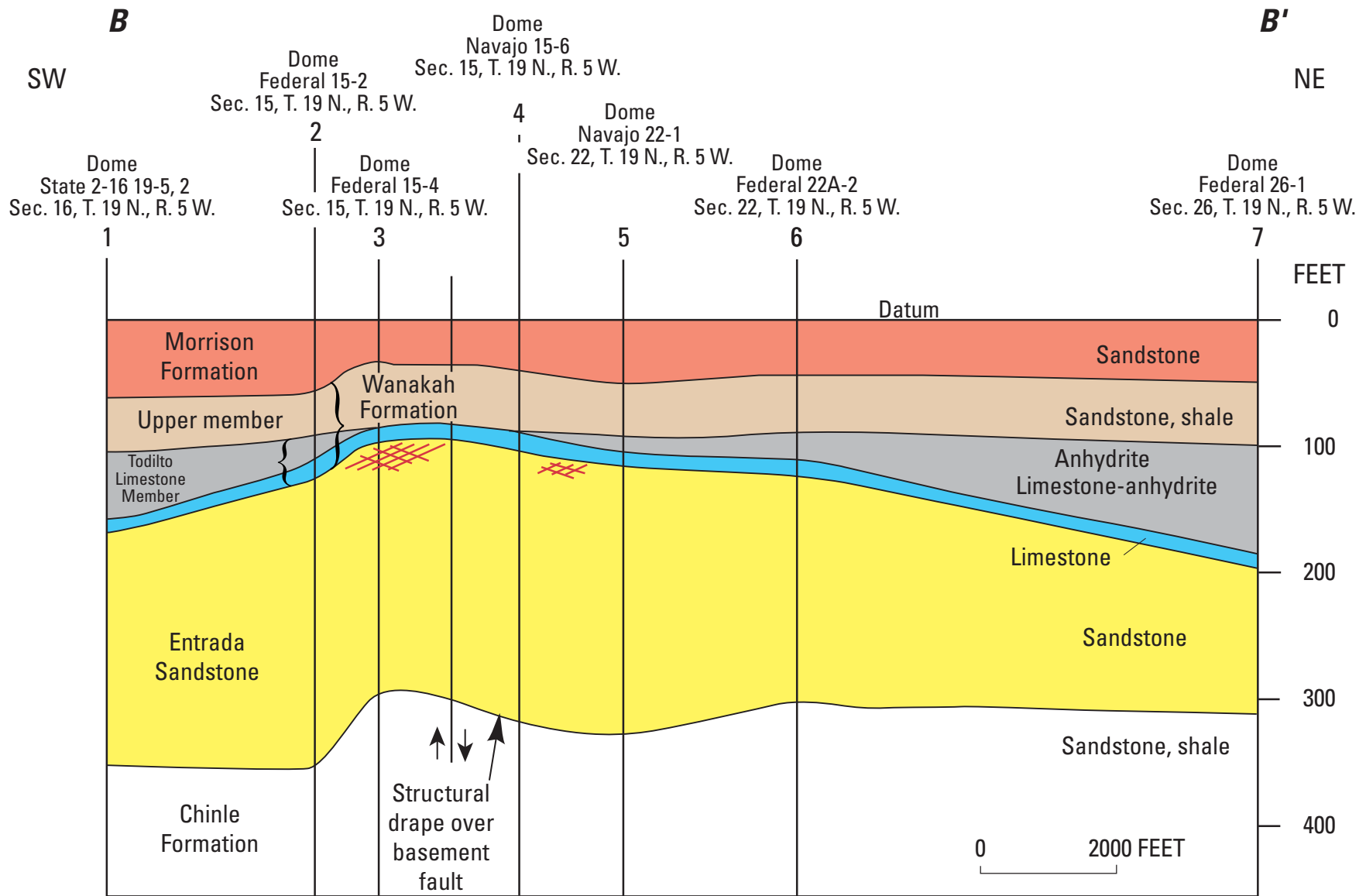


Figure 9A. Cross section B-B' extending from southwest to northeast across the Papers Wash Entrada oil field (modified from Vincelette and Chittum, 1981), showing relation of lithofacies of the Todilto Limestone Member of Wanakah Formation to relief on top of Entrada Sandstone. Datum, top of laterally continuous sandstone in the lower part of the Morrison Formation. Hatched (red), area of oil accumulation. Location of cross section shown on figure 1.

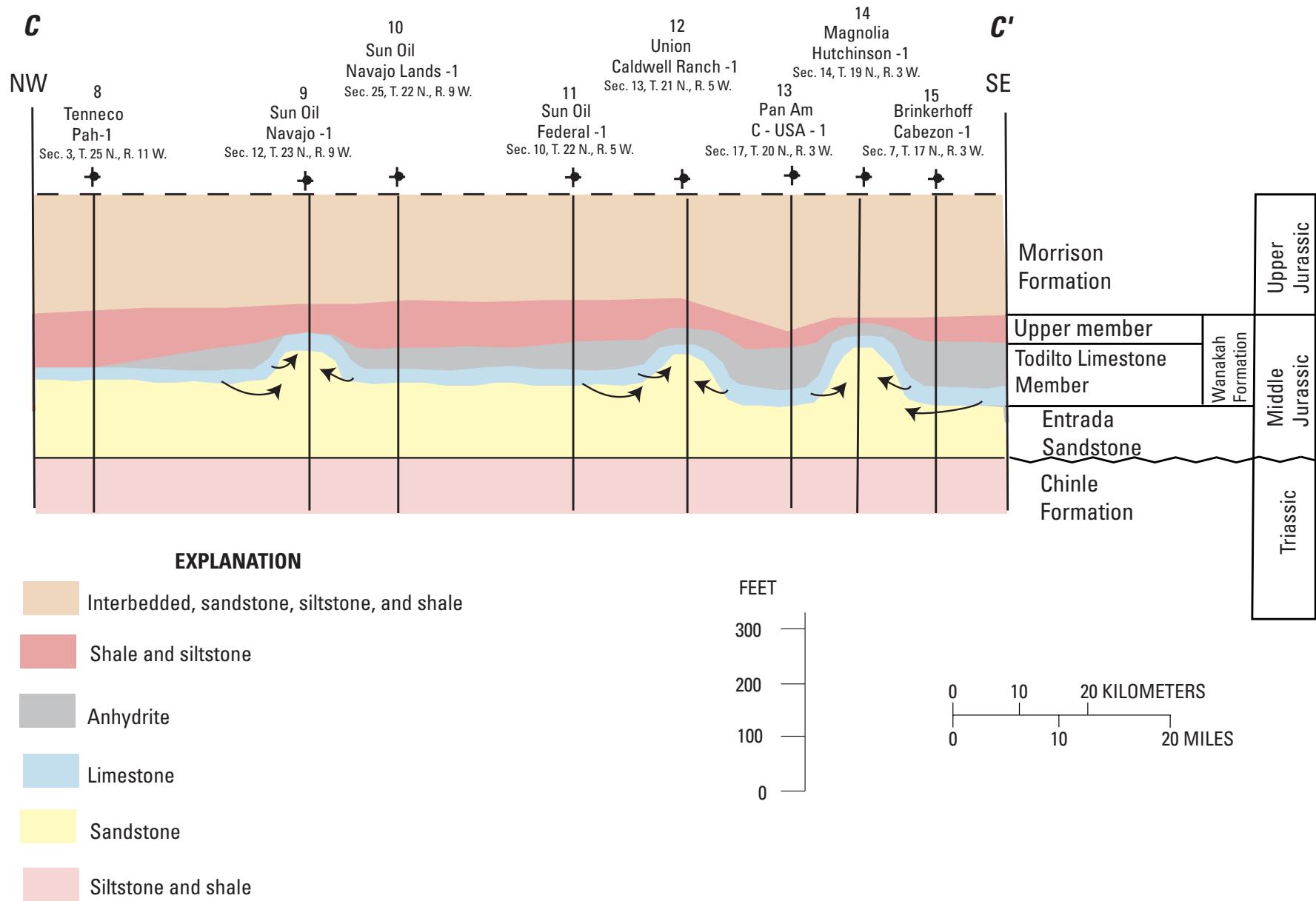


Figure 9B. Regional cross section C–C' extending from northwest to southeast through a part of the Todilto TPS, San Juan Basin (modified from Vincelette and Chittum, 1981). Datum, top of Chinle Formation. Arrows show direction of oil migration from Todilto Limestone Member of Wanakah Formation source beds into the Entrada Sandstone reservoirs. Location of cross section shown on enlargement in figure 1.

below about 9,000 ft in the subsurface, or at about –2,000-ft subsea, the Entrada has been described as extremely tight due to compaction and quartz cementation. On the east side of the basin, some of the pore-filling cements, including quartz, may have formed during migration of fluids during emplacement of Tertiary intrusions (Vincelette and Chittum, 1981). The Entrada in this part of the basin is often used as a disposal interval for waters produced from coal-bed methane production in the Cretaceous Fruitland Formation.

In the area where most of the oil has been found, the Entrada has extremely good porosities, which average about 23 percent, and permeabilities, which average about 300 millidarcies (md). The high permeabilities have allowed introduction of younger water into the Entrada. The age of the post-depositional water is not constrained, but most likely is late Miocene to Holocene, the time period when extensive erosion of rock overlying the Entrada resulted in exposure of the formation along the eastern, southern, and western margins of the San Juan Basin. Recharge waters entering these outcrops may have been responsible for removal or flushing of oil from some potential reservoirs (Vincelette and Chittum, 1981). Table 1 shows characteristics of Entrada reservoir rocks and oil API gravities.

Hydrocarbon Traps and Seals

There are four principal types of traps in the Entrada Sandstone reservoirs:

1. stratigraphic traps related to dune topography with closure of at least 20 ft;
2. structural traps that were influenced by syndepositional movement on basement faults that controlled the geometry, thickness, and possible orientation of individual dunes;
3. northeast regional dip of Todilto–Entrada rocks that tends to limit the area of closure for oil accumulation to the updip southern portions of dune ridges and affects subsequent hydrodynamic repositioning of hydrocarbons; and
4. local and regional porosity changes that help to preserve oil locally or delineate favorable areas for oil accumulation (Vincelette and Chittum, 1981; Nester and Endsley, 1992).

The first two types of traps formed early in the history of deposition of the Entrada. All of the producing Entrada fields are examples of trap type 1 above. Papers Wash field is an example of a combination of types 1 and 2 traps, where preserved dune topography combined with syndepositional structural movement on a basement fault is important in defining the limits of the field boundary. Traps of the third type, controlled by the regional tilt of the strata, began forming in latest Cretaceous time and were enhanced during formation of the basin in Paleocene through Miocene time. The regional dip is estimated at about 1°. Entrada fields influenced by this type of trap include Eagle Mesa and Media fields. The fourth type

of trap formed continuously, from the time of deposition until present day, and reflects the degree of diagenesis and lateral facies changes in the Entrada. Low porosity and permeability zones have been documented for several wells, such as those in the Papers Wash field. These zones tend to inhibit water production and, where oil is present, enhance hydrocarbon recovery (Vincelette and Chittum, 1981).

Thin basal limestone and thick anhydrite beds in the Todilto provide both lateral and vertical seals, preventing migration of oil from underlying Entrada Sandstone reservoirs.

Entrada Sandstone Conventional Oil Assessment Unit (50220401)

Introduction

The boundary of the Entrada Sandstone Conventional Oil Assessment Unit (AU) (050220401) (fig. 1) was drawn to encompass the following areas:

1. those Entrada dunes with enough significant relict topography (at least 20 ft) below the limestone beds of the Todilto Limestone Member of the Wanakah Formation and within the area of the San Juan Basin where anhydrite beds (lateral seal) of the Todilto were deposited (fig. 3),
2. that part of the basin where the Todilto is mature enough to have generated oil, and
3. that part of the basin where Entrada sandstones have good porosity and permeability.

Key parameters of the Entrada Sandstone Conventional AU are discussed below and summarized on figure 10.

Source

The principal source rock for petroleum in the total petroleum system is the Todilto Limestone Member of the Wanakah Formation.

Maturation

Thermal maturation for oil in source rocks of the Todilto Limestone ranges from middle Paleocene to middle Eocene, and until the middle Miocene for gas generation in the area north of the AU.

Migration

The migration distance of oil from the Todilto source beds into the underlying Entrada Sandstone reservoirs was short, probably within the dimensions of a single dune crest. The various Entrada fields do not appear to be linked along any regional migration pathway that might suggest fluid movement

along regional faults or regionally through the Entrada Sandstone. All the oil fields occur where the Todilto is sufficiently mature to produce oil (present depths up to about 8,000 ft) and where isolated pods of thicker Entrada are found. The AU boundary was extended slightly south of the pod of active source rock to incorporate that part of the Chaco slope immediately adjacent to the central basin. In this area, limited well data indicate the presence of thin Todilto and hence probable relict dune topography in the Entrada (figs. 1 and 6). Also, this area would be the most likely to host hydrocarbon accumulations outside the pod of mature source rock because migration distances from the mature source pod to potential reservoirs would be the shortest. The Entrada Sandstone Conventional Oil AU is mostly confined to the pod of active source rock.

Reservoirs

The reservoirs are the upper sandstone facies in the Entrada Sandstone in areas where the Entrada is thick, and relict dune topography is preserved below the overlying limestone and anhydrite sealing facies of the Todilto Limestone Member.

Traps/Seals

Traps in the Entrada are mainly stratigraphic, due to the preservation of dune topography, and diagenetic. Regional tilt of the strata to the northeast has influenced structural trapping of oil, but also allowed for later introduction of water. Subsequent hydrodynamic forces have influenced the repositioning of the oil in some reservoirs and flushing in others. Seals are mostly the anhydrite and the limestone facies of the Todilto, which thin to as little as 10 ft over the crests of the dunes.

Geologic Model

To date, oil in Entrada Sandstone reservoirs has been found at the extreme southern part of the central basin (figs. 1 and 4) near the intersection with the Chaco slope. Although the AU boundary was drawn to encompass the area where relict dune topography of at least 20–30 ft is preserved in the Entrada, oil has yet to be discovered in areas where long linear crests of dunes have been identified (Vincelette and Chittum, 1981). Rather, oil in the Entrada has only been found in some isolated Entrada dunes with 20–30 ft of closure below the limestone facies of the Todilto Limestone Member. Net pay in the fields averages 25 ft, but ranges from 16 ft at the Leggs field to nearly 30 ft at the Papers Wash field (table 1). Oil column height may range up to 45 ft, but not all the oil is moveable (Vincelette and Chittum, 1981). The presence of immovable oil is probably related to partial flushing but also could be related to juxtaposition of local less permeable beds with those having higher permeability. The regional distribution of oil fields suggests that the spill point is rarely reached in the fields.

Traps in the Entrada are principally stratigraphic and are found where relict dune topography is preserved. The traps

formed syndepositionally with the Entrada and were subsequently modified during deposition of the Todilto. The Todilto, source of the oil in the Entrada (Ross, 1980; Vincelette and Chittum, 1981), probably entered the window of oil generation in the middle Paleocene, and oil continued to be generated into the middle Eocene (fig. 10). Oil found in Entrada fields probably formed during this time. In the area north of the AU, oil may have continued to form, but because of the high heat history and greater depth of burial in this area, it would have cracked to gas. The period of generation–migration–accumulation of oil in the Entrada may well have ceased in the middle Eocene, near the end of the Laramide orogeny. However, the basin continued to subside well into the Miocene, and it is this later subsidence that might have aided migration of oil from source to trap.

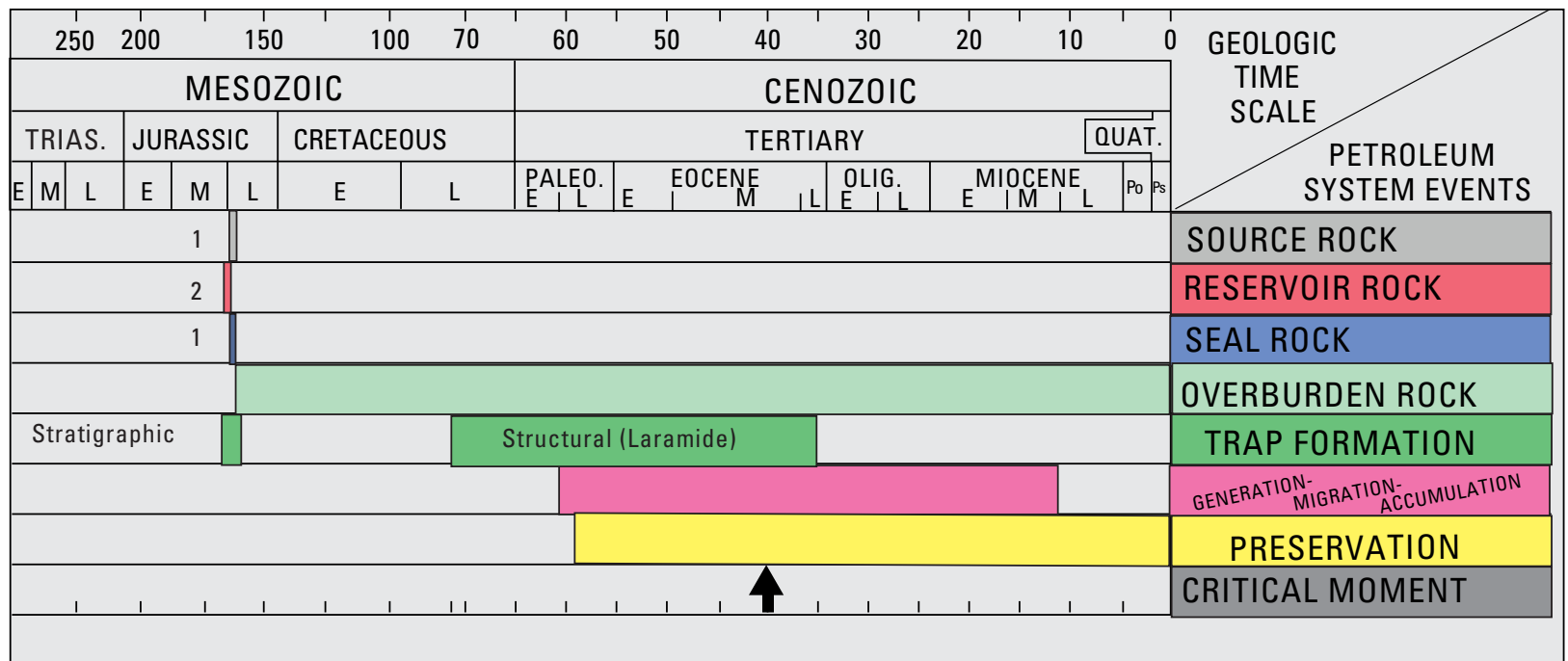
During the Miocene, strata in the southern part of the San Juan Basin were further tilted to the northeast. There is a slight break in the regional tilt between the Chaco slope to the south and the central basin to the north. All the oil fields are found near this break in slope (figs. 1 and 4). The oil fields, although isolated, are aligned northwest–southeast subparallel to the regional structural grain. When these fields are superimposed on the basement blocks (fig. 4), each field occurs within a block near the southern terminus where two blocks intersect. The blocks probably did not control migration of the oil, but rather may have controlled syndepositional thickness and preservation of thick Entrada. There has been some re-migration of oil out of traps; these sandstone traps are now water wet and some contain residual oil (Vincelette and Chittum, 1981). Flushing of traps probably occurred after the northeast regional tilt was developed, and erosion of rocks along the southern and eastern margin of the basin permitted inclusion of younger meteoric water.

Exploration efforts to find oil in the Entrada should focus on areas where

1. relict dune topography of sufficient closure on the top of the Entrada is preserved below the limestone facies of the Todilto Limestone Member of the Wanakah,
2. relict dune facies occurs in conjunction with the anhydrite facies of the Todilto,
3. the Todilto source beds are in the window of oil generation because migration distances from source beds into the sandstone reservoirs are short,
4. the Todilto and Entrada occur between depths of 5,000 and 8,000 ft in the basin (the shallow end of the range would be the most prospective)—depths at which better porosity and permeability in the Entrada are preserved, and
5. the break in the regional slope between the central basin and Chaco slope is located.

Finding oil in the Entrada will be difficult because of the small size of the dune crests, which are best identified by seismic studies. The difficulty of finding new oil plays was demonstrated by Massé and Ray (1995) in a 3-D seismic study of the Entrada Sandstone on the east side of the San Juan Basin. Their study did not define any new Entrada plays, and their results downplayed the potential for new plays in this area.

Entrada Oil Assessment Unit



Rock Units:
 1. Todilto Limestone Member of Wanakah Formation
 2. Entrada Sandstone

Figure 10. Events chart that shows key geologic events for the Entrada Sandstone Conventional Oil Assessment Unit. Black arrow shows critical moment (Magoon and Dow, 1994) for oil generation. Trias., Triassic; Quat., Quaternary; Paleo., Paleocene; Olig., Oligocene; Po, Pliocene; Ps, Pleistocene; E, early; M, middle; L, late. Geologic time scale is from the Geological Society of America web page <http://www.geosociety.org/science/timescale/timescl.htm>, last accessed 2/1/2008, and from Berggren and others (1995).

However, seismic studies have been successful elsewhere, especially in delineating favorable areas for expansion within existing fields (Nestor and Endsley, 1992).

Assessment Results

The Entrada Sandstone Conventional Oil AU (50220401) covers 2,874,000 acres, which is somewhat smaller than the area used in the 1995 USGS assessment Entrada Play 2204 (Huffman, 1996). The AU of this study was restricted to the pod of Todilto source rock, which was mature enough to produce oil, and to where there was sufficient porosity and permeability preserved in the Entrada Sandstone. The AU was estimated at the mean to have potential additions to reserves of 2.32 MMBO, 5.56 BCFG, and 0.22 MMBNGL (table 2). The volumes of undiscovered oil, gas, and natural gas liquids estimated in 2002 for the Entrada Sandstone Conventional Oil AU are shown in Table 3. A summary of the assessment input data of the AU is presented on the data form in appendix A, which for this AU estimates the numbers and sizes of undiscovered accumulations. There are adequate charge, reservoir, traps, seals, access, and timing of generation and migration of hydrocarbons, indicating a geologic probability of 1.0 for finding at least one additional field with a total recovery greater than the stated minimum of 0.5 MMBO (grown) for oil.

This assessment unit produces mostly oil with small quantities of associated gas (IHS Energy Group, 2002). The associated gas was not quantitatively assessed. In estimating undiscovered non-associated gas and the number and sizes

of undiscovered oil accumulations, historical data from NRG Associates (2001) database were used. Only four of the eight Entrada oil fields meet the 0.5 MMBO cutoff. These are Eagle Mesa, Media, Media Southwest, and Papers Wash. No new oil accumulations have been found that meet the minimum accumulation size cutoff since the discovery of the Papers Wash field in 1976. New wildcat discoveries since then have resulted in only single-well fields or a few-well fields—all of which have currently produced below the minimum field-size cutoff, despite having been in production for many years (IHS Energy Group, 2002). Although activity in exploration for new Entrada fields has resulted in only small fields with production below the minimum cutoff, there is still a large area left for exploration. Taking these factors into consideration, it was estimated that a maximum of four oil accumulations meeting the minimum cutoff, could still be discovered. At the median, this value is two undiscovered oil accumulations and at the minimum, one undiscovered oil accumulation.

Figure 11 shows the sizes of grown accumulations for the first and second halves of the discovery period. The accumulations for each half are ranked by size, with rank 1 equating to the largest accumulation and rank 2 equating to the smallest accumulation. Using the discovery information for fields that meet the minimum cutoff, the median grown size of discovered accumulations is 1.38 MMBO for the first half of the discovery period and 2.07 MMBO for the second half (fig. 11), indicating that sizes of accumulations were larger in the second half of the discovery period. The grown size of undiscovered accumulations was estimated from the distribution of discovered accumulation size versus the discovery year (fig. 12). The largest grown

Table 2. Assessment results summary for the Todilto Total Petroleum System, San Juan Basin Province, New Mexico and Colorado.

[MMBO, million barrels of oil; BCFG, billion cubic feet of gas; MMBNGL, million barrels of natural gas liquids. Results shown are fully risked estimates. For gas fields, all liquids are included under the NGL (natural gas liquids) category. F95 denotes a 95 percent chance of at least the amount tabulated. Other fractiles are defined similarly. Fractiles are additive only under the assumption of perfect positive correlation]

Assessment unit	Field type	Total undiscovered resources											
		Oil (MMB)				Gas (BCF)				NGL (MMB)			
		F95	F50	F5	Mean	F95	F50	F5	Mean	F95	F50	F5	Mean
Conventional oil and gas resources													
Entrada Sandstone Conventional Oil	Oil	0.81	2.19	4.18	2.32	1.84	5.15	10.66	5.56	0.07	0.20	0.45	0.22

Table 3. Comparison of estimates from the 2002 Entrada Sandstone Conventional Oil Assessment Unit (50220401) and the 1995 Entrada Play 2204 assessments of the number, sizes, and volumes of undiscovered oil accumulations.

[Sizes, volumes of oil and natural gas liquids, and minimum size considered are in million barrels of oil; volume of associated gas in billion cubic feet. F95 indicates a 95 percent chance of discovering more than the amount tabulated. The F50 and F5 fractiles are similarly defined. 1995 data from Huffman (1996)]

Number of Undiscovered Oil Accumulations				
Assessment year	Minimum	Median	Maximum	Minimum size considered
2002	1	2	4	0.5
1995	5	10	25	1

Sizes of Undiscovered Oil Accumulations				
Assessment year	Minimum	Median	Maximum	Minimum size considered
2002	0.5	1	4	0.5
1995	1	2	4	1

Volume of Undiscovered Oil				
Assessment year	F95	F50	F5	Mean
2002	0.81	2.19	4.18	2.32
1995	2.2	11.10	33.8	21.3

Volume of Undiscovered Associated Gas				
Assessment year	F95	F50	F5	Mean
2002	1.84	5.15	10.66	5.56
1995	0.20	1.00	3.04	1.90

Volume of Undiscovered Natural Gas Liquids				
Assessment year	F95	F50	F5	Mean
2002	0.07	0.20	0.45	0.22
1995	0	0	0	0

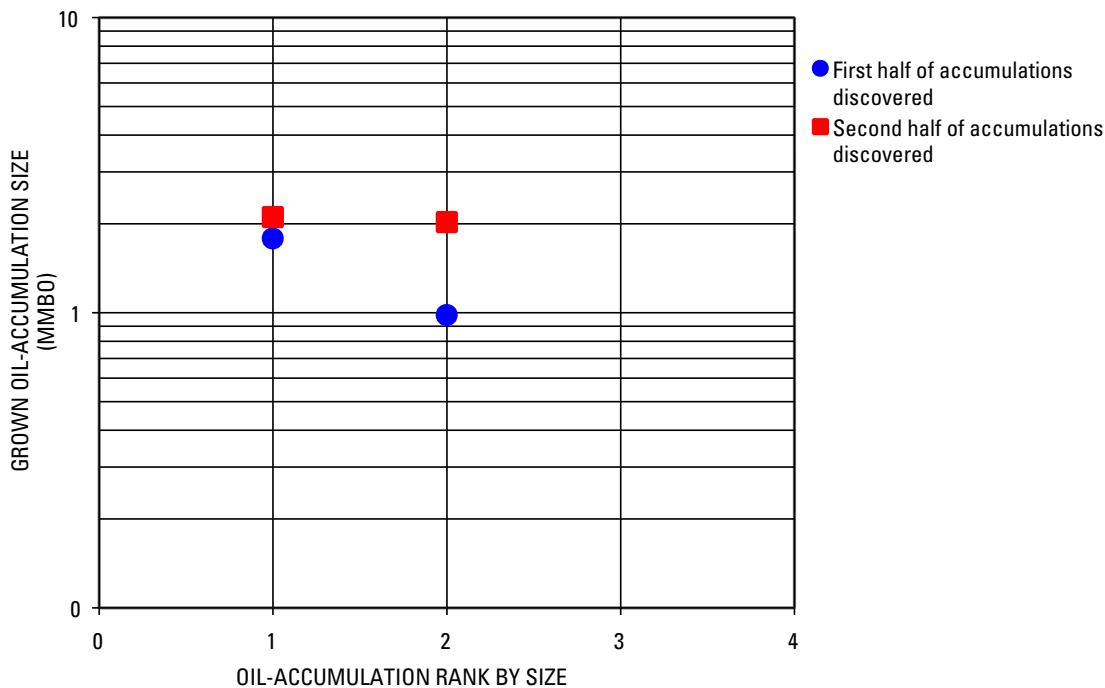


Figure 11. Graph showing distribution by halves of grown oil-accumulation size versus rank by size for the Entrada Sandstone Conventional Oil Assessment Unit (50220401). Data from NRG (2001). MMBO, million barrels of oil.

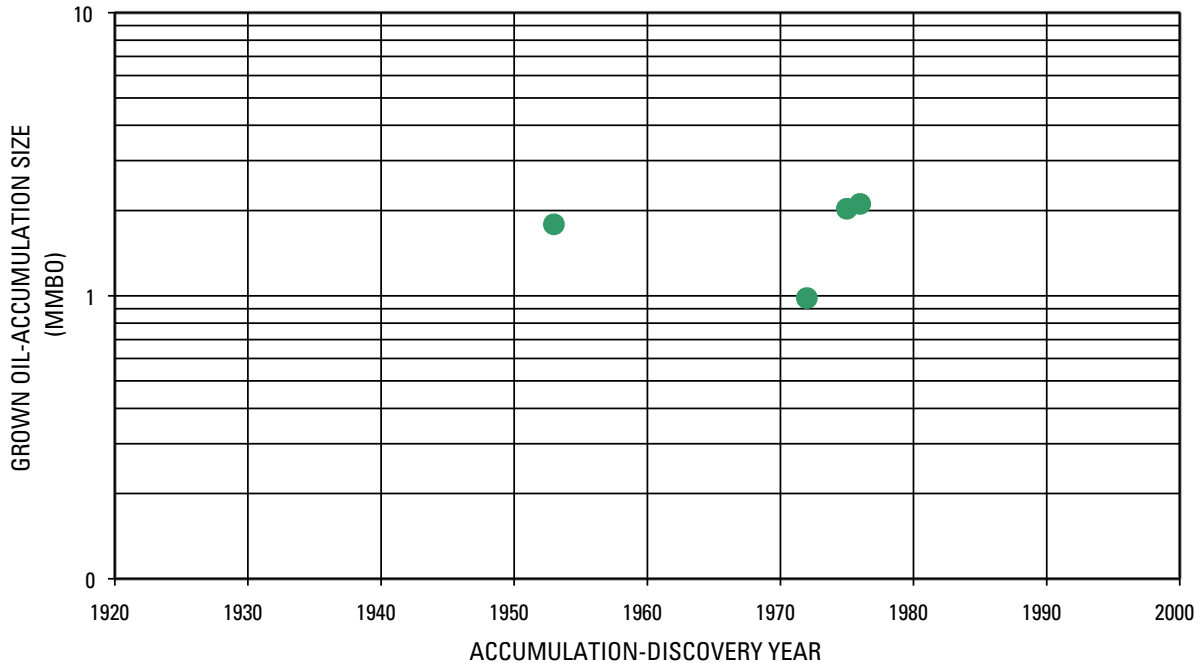


Figure 12. Graph showing sizes of grown oil accumulations versus year of discovery of accumulations (fields) for the Entrada Sandstone Conventional Oil Assessment Unit (50220401). Data from NRG (2001). MMBO, million barrels of oil.

oil field (Papers Wash) is about 2 MMBO. Using these data, the maximum estimated size of undiscovered accumulations is 4 MMBO, the median size is 1 MMBO, and the minimum size is 0.5 MMBO.

The number and sizes of undiscovered oil accumulations in this 2002 assessment are lower than those estimated in 1995 (table 2), even though a smaller minimum size was used in this assessment. This lower estimate reflects the discovery of very small field sizes since 1976, few new productive wildcats, and geologic factors, such as hydrodynamic flushing, which may diminish the occurrence of accumulations whose size at least meets the minimum cutoff. The 2002 estimated undiscovered oil, associated gas, and natural gas liquids for the Entrada Sandstone Conventional Oil AU are, at the mean, 2.32 MMBO, 5.56 BCFG, and 0.22 MMBNGL. These values represent a decrease in undiscovered oil resources, but an increase in associated gas and natural gas liquids resources relative to the 1995 assessment (table 2) (Huffman, 1996).

Acknowledgments

The authors thank T.S. Ahlbrandt and R.B. O’Sullivan for their thoughtful reviews and T.A. Cook and T.R. Klett for interpretations and graphs of production data. Useful discussions and input were also provided by the U.S. Geological Survey, National Oil and Gas Assessment Team, consisting of R.R. Charpentier, T.A. Cook, R.A. Crovelli, T.R. Klett, and C.J. Schenk.

References Cited

Ahlbrandt, T.S., Clayton, J.L., and Schenk, C.J., 2003, Climate controls on petroleum systems—The Pennsylvanian of eastern Wyoming, *in* Cecil, C.B., and Edgar, N.T., eds., *Climate control on stratigraphy: Society for Sedimentary Geology, SEPM Special Publication no. 77*, p. 239–270.

Anderson, R.Y., and Kirkland, D.W., 1960, Origin, varves, and cycles of the Jurassic Todilto Formation, New Mexico: *American Association of Petroleum Geologists Bulletin*, v. 44, p. 37–52.

Berggren, W.A., Kent, D.V., Swisher, C.C., III, and Aubry, M., 1995, A revised Cenozoic geochronology and chronostratigraphy, *in* Berggren, W.A., Kent, D.V., Aubry, M., and Hardenbol, J., eds., *Geochronology, time scales and global stratigraphic correlation: Society for Sedimentary Geology, SEPM Special Publication no. 54*, p. 129–212.

Bond, W.A., 1984, Application of Lopatin’s method to determine burial history, evolution of the geothermal gradient, and timing of hydrocarbon generation in Cretaceous source rocks in the San Juan Basin, northwestern New Mexico and southwestern Colorado, *in* Woodward, J., Meissner, F.F., and Clayton, J.L., eds., *Hydrocarbon source rocks of the greater Rocky Mountain region: Rocky Mountain Association of Geologists Guidebook*, p. 433–447.

- Carrasco-V, B., 1977, Albian sedimentation of submarine autochthonous and allochthonous carbonates, east edge of the Valles-San Luis Potosi platform, Mexico: Society for Sedimentary Geology, SEPM Special Publication no. 25, p. 263–272.
- Cook, H.E., and Taylor, M.E., 1977, Comparison of continental slope and shelf environments in the Upper Cambrian and lowest Ordovician of Nevada: Society for Sedimentary Geology, SEPM Special Publication no. 25, p. 51–81.
- Fassett, J.E., ed., 1978a, Oil and gas fields of the Four Corners area, volume I: Four Corners Geological Society, 368 p.
- Fassett, J.E., ed., 1978b, Oil and gas fields of the Four Corners area, volume II: Four Corners Geological Society, p. 369–727.
- Fassett, J.E., ed., 1983, Oil and gas fields of the Four Corners area, volume III: Four Corners Geological Society, p. 729–1143.
- Fassett, J.E., 1991, Oil and gas resources of the San Juan Basin, New Mexico and Colorado, *in* Gluskoter, H.J., Rice, D.D., and Taylor, R.B., eds., Economic geology: Geological Society of America, The Geology of North America Series, v. P-2, p. 357–372.
- Fryberger, S.G., 1986, Stratigraphic traps for petroleum in wind-laid rocks: American Association of Petroleum Geologists Bulletin, v. 70, no. 12, p. 1765–1776.
- Garrison, R.E., and Fischer, A.G., 1969, Deep-water limestones and radiolarites of the alpine Jurassic: Society for Sedimentary Geology, SEPM Special Publication 14, p. 20–56.
- Green, G.N., 1992, The digital geologic map of Colorado in ARC/INFO Format: U.S. Geological Survey Open-File Report 92–507–A [<http://pubs.er.usgs.gov/usgspubs/ofr/ofr92507A>; last accessed 2/1/2008].
- Green, G.N., and Jones, G.E., 1997, The digital geologic map of New Mexico in ARC/INFO Format: U.S. Geological Survey Open-File Report 97–0052 [<http://pubs.er.usgs.gov/usgspubs/ofr/ofr9752>; last accessed 2/1/2008].
- Green, M.W., 1974, The Iyanbito Member (a new stratigraphic unit) of the Jurassic Entrada Sandstone, Gallup-Grants area, New Mexico: U.S. Geological Survey Bulletin 1395–D, 12 p.
- Green, M.W., and Pierson, C.T., 1977, A summary of the stratigraphy and depositional environments of Jurassic and related rocks in the San Juan Basin, Arizona, Colorado, and New Mexico, *in* Fassett, J.E., James, H.L., and Hodgson, H.E., eds., San Juan Basin III: New Mexico Geological Society Guidebook, p. 147–152.
- Huffman, A.C., Jr., 1996, San Juan Basin Province (22), *in* Gautier, D.L., Dolton, G.L., Takahashi, K.I., and Varnes, K.L., eds., 1995 National assessment of United States oil and gas resources—Results, methodology, and supporting data: U.S. Geological Survey Digital Data Series 30, release 2.
- Huffman, A.C., Jr., and Taylor, D.J., 2002, Fractured shale reservoirs and basement faulting, San Juan Basin, New Mexico and Colorado: American Association of Petroleum Geologists Rocky Mountain Section Meeting, Laramie, Wyo., p. 30.
- IHS Energy Group, 2002, PI/Dwights Plus US Well Data [data current as of June 2002]: Englewood, Colo., IHS Energy Group; database available from IHS Energy Group, 15 Inverness Way East, D205, Englewood, CO 80112, U.S.A.
- IHS Energy Group, 2003, PI/Dwights Plus US Well Data [data current as of January 2003]: Englewood, Colo., IHS Energy Group; database available from IHS Energy Group, 15 Inverness Way East, D205, Englewood, CO 80112, U.S.A.
- Kirkland, D.W., Denison, R.E., and Evans, R., 1995, Middle Jurassic Todilto Formation of northern New Mexico—Marine or nonmarine: New Mexico Bureau of Mines and Mineral Resources Bulletin 147, 37 p.
- Law, B.E., 1992, Thermal maturity patterns of Cretaceous and Tertiary rocks, San Juan Basin, Colorado and New Mexico: Geological Society of America Bulletin, v. 104, p. 192.
- Magoon, L.B., and Dow, W.G., 1994, The petroleum system, *in* Magoon, L.B., and Dow, W.G., eds., The petroleum system—From source to trap: American Association of Petroleum Geologists Memoir 60, p. 3–24.
- Massé, D.J., and Ray, R.R., 1995, 3-D seismic prospecting for Entrada Sandstone reservoirs on the southeastern flank of the San Juan Basin, *in* Ray, R.R., ed., High-definition seismic—2-D, 2-D swath, and 3-D case histories: Rocky Mountain Association of Geologists, p. 143–160.
- Molenaar, C.M., 1977, San Juan Basin time-stratigraphic nomenclature chart, *in* Fassett, J.E., James, H.L., and Hodgson, H.E., eds., San Juan Basin III: New Mexico Geological Society Guidebook, p. xii.
- Nester, D.C., and Endsley, D., 1992, How an independent put inexpensive 3-D seismic to good use in New Mexico: Oil and Gas Journal, v. 90, no. 12, p. 124–126.
- NRG Associates, 2001, The significant oil and gas fields of the United States [data current as of December 31, 2001]: Colorado Springs, Colo., NRG Associates, Inc. [database available from NRG Associates, Inc., P.O. Box 1655, Colorado Springs, CO 80901]
- Rawson, R.R., 1980, Uranium in Todilto Limestone (Jurassic) of New Mexico—Example of a sabkha-like deposit: New Mexico Bureau of Mines and Mineral Resources Memoir 38, p. 304–312.

- Reese, R.R., 1984, Stratigraphy of Entrada Sandstone and Todilto Limestone (Jurassic), north-central New Mexico: Golden, Colorado School of Mines, M.S. thesis, 182 p.
- Ridgley, J.L., 1977, Stratigraphy and depositional environments of Jurassic–Cretaceous sedimentary rocks in the southwest part of the Chama Basin, New Mexico, *in* Fassett, J.E., ed., San Juan Basin III: New Mexico Geological Society Guidebook, p. 153–158.
- Ridgley, J.L., 1986, Diagenesis of the Todilto Limestone Member of the Wanakah Formation, Chama Basin, New Mexico, *in* Mumpton, F.A., ed., Studies in diagenesis: U.S. Geological Survey Bulletin 1578, p. 197–206.
- Ridgley, J.L., 1989, Trace fossils and mollusks from the upper member of the Wanakah Formation, Chama Basin, New Mexico: Evidence for a lacustrine origin: U.S. Geological Survey Bulletin 1808–C, p. C1–C16.
- Ross, L.M., 1980, Geochemical correlation of San Juan Basin oils—A study: *Oil and Gas Journal*, Nov. 3, 1980, p. 102–110.
- Tanner, W.F., 1970, Triassic–Jurassic lakes in New Mexico: *The Mountain Geologist*, v. 7, p. 281–289.
- Taylor, D.J., and Huffman, A.C., Jr., 1998, Map showing inferred and mapped basement faults, San Juan Basin and vicinity, New Mexico and Colorado: U.S. Geological Survey Geological Investigations Series 2641, scale 1:500,000.
- Taylor, D.J., and Huffman, A.C., Jr., 2001, Seismic evaluation study report—Jicarilla Apache Indian Reservation, U.S. Department of Energy Report DE-AI26-98BC15026R10, 1 CD-ROM.
- Thaden, R.E., and Zech, R.S., 1984, Preliminary structure contour map on the base of the Cretaceous Dakota Sandstone in the San Juan Basin and vicinity, New Mexico, Arizona, Colorado, and Utah: U.S. Geological Survey Miscellaneous Field Studies Map 1673, scale 1:500,000.
- Vincelette, R.R., and Chittum, W.E., 1981, Exploration for oil accumulations in Entrada Sandstone, San Juan Basin, New Mexico: *American Association of Petroleum Geologists Bulletin*, v. 65, p. 2546–2570.
- Warren, J.K., and Kendall, C.G. St. C., 1985, Comparison of sequences formed in marine sabkha (subaerial) and salina settings—Modern and ancient: *American Association of Petroleum Geologists Bulletin*, v. 69, no. 6, p. 1013–1023.
- Wilson, J.L., 1969, Microfacies and sedimentary structures in “deeper water” lime mudstones: *Society for Sedimentary Geology, SEPM Special Publication 14*, p. 4–19.
- Yurewicz, D.A., 1977, Sedimentology of Mississippian basin-facies carbonates, New Mexico and west Texas—The Ranchera Formation: *Society for Sedimentary Geology, SEPM Special Publication 25*, p. 203–219.

Appendix A. Input data form used in evaluating the Todilto Total Petroleum System, Entrada Sandstone Conventional Oil Assessment Unit (50220401), San Juan Basin Province. See Klett and Le (this CD-ROM) for a detailed description of the data input form.

**SEVENTH APPROXIMATION
DATA FORM FOR CONVENTIONAL ASSESSMENT UNITS (NOGA, Version 5, 6-30-01)**

IDENTIFICATION INFORMATION

Assessment Geologist:.....	<u>J.L. Ridgley</u>	Date:	<u>9/25/2002</u>
Region:.....	<u>North America</u>	Number:	<u>5</u>
Province:.....	<u>San Juan Basin</u>	Number:	<u>5022</u>
Total Petroleum System:.....	<u>Todilto</u>	Number:	<u>502204</u>
Assessment Unit:.....	<u>Entrada Sandstone Conventional Oil</u>	Number:	<u>50220401</u>
Based on Data as of:.....	<u>PI/Dwights 2001, NRG 2001 (data current through 1999)</u>		
Notes from Assessor:.....	<u></u>		

CHARACTERISTICS OF ASSESSMENT UNIT

Oil (<20,000 cfg/bo overall) **or** Gas (≥20,000 cfg/bo overall):... Oil

What is the minimum accumulation size?..... 0.5 mmoeb grown
(the smallest accumulation that has potential to be added to reserves in the next 30 years)

No. of discovered accumulations exceeding minimum size:.....	Oil:	<u>4</u>	Gas:	<u>0</u>
Established (>13 accums.)	Frontier (1-13 accums.)	<u>X</u>	Hypothetical (no accums.)	<u></u>

Median size (grown) of discovered oil accumulation (mmoeb):			
	1st 3rd	<u>1.38</u>	2nd 3rd <u>2.07</u> 3rd 3rd <u></u>
Median size (grown) of discovered gas accumulations (bcfg):			
	1st 3rd	<u></u>	2nd 3rd <u></u> 3rd 3rd <u></u>

Assessment-Unit Probabilities:

<u>Attribute</u>	<u>Probability of occurrence (0-1.0)</u>
1. CHARGE: Adequate petroleum charge for an undiscovered accum. ≥ minimum size.....	<u>1.0</u>
2. ROCKS: Adequate reservoirs, traps, and seals for an undiscovered accum. ≥ minimum size.....	<u>1.0</u>
3. TIMING OF GEOLOGIC EVENTS: Favorable timing for an undiscovered accum. ≥ minimum size.....	<u>1.0</u>

Assessment-Unit GEOLOGIC Probability (Product of 1, 2, and 3):..... 1.0

4. ACCESSIBILITY: Adequate location to allow exploration for an undiscovered accumulation ≥ minimum size.....	<u>1.0</u>
--	------------

UNDISCOVERED ACCUMULATIONS

No. of Undiscovered Accumulations: How many undiscovered accums. exist that are \geq min. size?:
(uncertainty of fixed but unknown values)

Oil Accumulations:.....min. no. (>0)	<u>1</u>	median no. <u>2</u>	max no. <u>4</u>
Gas Accumulations:.....min. no. (>0)	<u>0</u>	median no. <u>0</u>	max no. <u>0</u>

Sizes of Undiscovered Accumulations: What are the sizes (**grown**) of the above accums?:
(variations in the sizes of undiscovered accumulations)

Oil in Oil Accumulations (mmbo):.....min. size	<u>0.5</u>	median siz <u>1</u>	max. size <u>4</u>
Gas in Gas Accumulations (bcfg):.....min. size	<u> </u>	median size <u> </u>	max. size <u> </u>

AVERAGE RATIOS FOR UNDISCOVERED ACCUMS., TO ASSESS COPRODUCTS
(uncertainty of fixed but unknown values)

<u>Oil Accumulations:</u>	minimum	median	maximum
Gas/oil ratio (cfg/bo).....	<u>1200</u>	<u>2400</u>	<u>3600</u>
NGL/gas ratio (bngl/mmcfg).....	<u>20</u>	<u>40</u>	<u>60</u>
<u>Gas Accumulations:</u>	minimum	median	maximum
Liquids/gas ratio (bliq/mmcfg).....	<u> </u>	<u> </u>	<u> </u>
Oil/gas ratio (bo/mmcfg).....	<u> </u>	<u> </u>	<u> </u>

SELECTED ANCILLARY DATA FOR UNDISCOVERED ACCUMULATIONS
(variations in the properties of undiscovered accumulations)

<u>Oil Accumulations:</u>	minimum	median	maximum
API gravity (degrees).....	<u>30</u>	<u>33</u>	<u>35</u>
Sulfur content of oil (%).....	<u>0.1</u>	<u>0.5</u>	<u>1</u>
Drilling Depth (m)	<u>1400</u>	<u>1600</u>	<u>1800</u>
Depth (m) of water (if applicable).....	<u> </u>	<u> </u>	<u> </u>
<u>Gas Accumulations:</u>	minimum	median	maximum
Inert gas content (%).....	<u> </u>	<u> </u>	<u> </u>
CO ₂ content (%).....	<u> </u>	<u> </u>	<u> </u>
Hydrogen-sulfide content (%).....	<u> </u>	<u> </u>	<u> </u>
Drilling Depth (m).....	<u> </u>	<u> </u>	<u> </u>
Depth (m) of water (if applicable).....	<u> </u>	<u> </u>	<u> </u>



Click here to return to
Volume Title Page

Geology and Oil and Gas Assessment of the Mancos-Menefee Composite Total Petroleum System

By J.L. Ridgley, S.M. Condon, and J.R. Hatch



Click here to return to
[Volume Title Page](#)

Chapter 4 of 7

Total Petroleum Systems and Geologic Assessment of Undiscovered Oil and Gas Resources in the San Juan Basin Province, Exclusive of Paleozoic Rocks, New Mexico and Colorado

Compiled by U.S. Geological Survey San Juan Basin Assessment Team

Digital Data Series 69–F

U.S. Department of the Interior
U.S. Geological Survey

U.S. Department of the Interior
KEN SALAZAR, Secretary

U.S. Geological Survey
Marcia K. McNutt, Director

U.S. Geological Survey, Reston, Virginia 2013

For product and ordering information:

World Wide Web: <http://www.usgs.gov/pubprod>

Telephone: 1-888-ASK-USGS

For more information on the USGS—the Federal source for science about the Earth,
its natural and living resources, natural hazards, and the environment:

World Wide Web: <http://www.usgs.gov>

Telephone: 1-888-ASK-USGS

Suggested citation:

Ridgley, J.L., Condon, S.M., and Hatch, J.R., 2013, Geology and oil and gas assessment of the Mancos-Menefee Composite Total Petroleum System, San Juan Basin, New Mexico and Colorado, chap. 4 of U.S. Geological Survey San Juan Basin Assessment Team, Total petroleum systems and geologic assessment of undiscovered oil and gas resources in the San Juan Basin Province, exclusive of Paleozoic rocks, New Mexico and Colorado: U.S. Geological Survey Digital Data Series 69–F, p. 1–97.

Any use of trade, product, or firm names is for descriptive purposes only and does not imply endorsement by the U.S. Government.

Although this report is in the public domain, permission must be secured from the individual copyright owners to reproduce any copyrighted material contained within this report.

Contents

Abstract.....	1
Introduction.....	1
Mancos-Menefee Composite Total Petroleum System	3
Geologic Framework	3
Stratigraphy	3
Structure.....	8
Hydrocarbon Reservoir Rocks.....	10
Dakota Sandstone	10
Greenhorn Limestone Member of Mancos Shale	11
Gallup Sandstone.....	11
Torrivio Sandstone Member of Gallup Sandstone	13
Semilla Sandstone Member of Mancos Shale	13
Juana Lopez Member of Mancos Shale	13
Sandstone Reservoirs in the Mancos Shale	14
Tocito Sandstone Lentil of Mancos Shale	14
"Gallup" Sandstone of Mancos Shale	14
Sandstone Reservoirs in Upper Part of Mancos Shale.....	15
Mesaverde Group	15
Point Lookout Sandstone	15
Menefee Formation	18
Cliff House Sandstone.....	18
Hydrocarbon Source Rocks	18
Mancos Shale Source Rock Characterization.....	18
Menefee Formation Source Rock Characterization	20
Geochemical Characteristics	22
Mancos Shale	22
Menefee Formation	22
Gas Chemistry	22
Oil Chemistry.....	23
Source Rock Maturation and Thermal History	27
Burial History	27
Vitrinite Reflectance	27
Dakota Sandstone	31
Menefee Formation	31
Hydrocarbon Migration Summary	31
Hydrocarbon Traps and Seals	32
Mancos.....	32
Mesaverde	32
Assessment Unit Definitions	34
Dakota-Greenhorn Conventional Oil and Gas Assessment Unit (50220304)	34
Introduction.....	34
Source.....	34

Maturation.....	34
Migration.....	34
Reservoirs.....	34
Traps/Seals.....	35
Geologic Model.....	35
Assessment Results.....	35
Dakota-Greenhorn Continuous Gas Assessment Unit (50220363).....	41
Introduction.....	41
Source.....	43
Maturation.....	43
Migration.....	43
Reservoirs.....	43
Traps/Seals.....	43
Geologic Model.....	45
Assessment Results.....	45
Gallup Sandstone Conventional Oil and Gas Assessment Unit (50220302).....	48
Introduction.....	48
Source.....	50
Maturation.....	50
Migration.....	50
Reservoirs.....	50
Traps/Seals.....	50
Geologic Model.....	50
Assessment Results.....	53
Mancos Sandstones Conventional Oil Assessment Unit (50220303).....	53
Introduction.....	53
Source.....	54
Maturation.....	54
Migration.....	54
Reservoirs.....	54
Traps/Seals.....	54
Geologic Model.....	54
Assessment Results.....	59
Mancos Sandstones Continuous Gas Assessment Unit (50220362).....	59
Introduction.....	59
Source.....	60
Maturation.....	60
Migration.....	60
Reservoirs.....	63
Traps/Seals.....	63
Geologic Model.....	63
Assessment Results.....	63
Mesaverde Updip Conventional Oil Assessment Unit (50220301).....	65
Introduction.....	65
Source.....	65

Maturation.....	65
Migration.....	65
Reservoirs.....	65
Traps/Seals.....	65
Geologic Model.....	67
Assessment Results.....	67
Mesaverde Central-Basin Continuous Gas Assessment Unit (50220361).....	67
Introduction.....	67
Source.....	67
Maturation.....	67
Migration.....	67
Reservoirs.....	67
Traps/Seals.....	70
Geologic Model.....	70
Assessment Results.....	70
Menefee Coalbed Gas Assessment Unit (50220381).....	70
Introduction.....	70
Source.....	74
Maturation.....	74
Migration.....	74
Reservoirs.....	74
Traps/Seals.....	74
Geologic Model.....	74
Assessment Results.....	74
Summary.....	77
Acknowledgments.....	77
References Cited.....	77
Appendixes	
A. Assessment results summary for the Mancos-Menefee Composite Total Petroleum System, San Juan Basin Province, New Mexico and Colorado.....	83
B–H. Input data form used in evaluating the Mancos-Menefee Composite Total Petroleum System.....	
B. Dakota-Greenhorn Conventional Oil and Gas Assessment Unit (50220304), San Juan Basin Province.....	84
C. Dakota-Greenhorn Continuous Gas Assessment Unit (50220363), San Juan Basin Province.....	86
D. Gallup Sandstone Conventional Oil and Gas Assessment Unit (50220302), San Juan Basin Province.....	88
E. Mancos Sandstones Conventional Oil Assessment Unit (50220303), San Juan Basin Province.....	90
F. Mancos Sandstones Continuous Gas Assessment Unit (50220362), San Juan Basin Province.....	92
G. Mesa Verde Central-Basin Continuous Gas Assessment Unit (50220361), San Juan Basin Province.....	94
H. Menefee Coalbed Gas Assessment Unit (50220304), San Juan Basin Province.....	96

Figures

1. Map showing the boundary of the Mancos-Menefee Composite Total Petroleum System, San Juan Basin, Colorado and New Mexico.....	2
2. Chart showing regional chronostratigraphic correlations in the San Juan Basin from the Tertiary to the base of the Jurassic, and the extent of the total petroleum systems and assessment units defined in the 2002 National Oil and Gas Assessment of the San Juan Basin Province (5022), New Mexico and Colorado	4
3. Time-stratigraphic cross section of Upper Cretaceous and Tertiary rocks in the Zuni and San Juan Basins, Colorado and New Mexico.....	5
4. Map showing the location of inferred basement structural blocks and other structural elements in the San Juan Basin	6
5. Map showing location of shorelines and location of Seboyeta Bay during deposition of the Dakota Sandstone and Mancos Shale.....	7
6. Structure contour map drawn on top of Mancos Shale, San Juan Basin, Colorado and New Mexico using data from IHS Energy Group	8
7. Structure contour map drawn on top of the Menefee Formation using data from IHS Energy Group	9
8. Map of the San Juan Basin showing the position of the Gallup Sandstone A–F shorelines, Borrego Pass Lentil of Crevasse Canyon Formation, and outcrop locations of the Tocito Sandstone Lentil-“Gallup” sandstone interval	12
9. Cross section extending from southwest to northeast across the central part of the San Juan Basin, Colorado and New Mexico	16
10. Isopach map of the Mancos Shale in the San Juan Basin, Colorado and New Mexico, using data from IHS Energy Group.....	19
11. Isopach map of the Menefee Formation in the San Juan Basin, Colorado and New Mexico, using data from IHS Energy Group.....	21
12. Cross plot showing relation between gas methane $\delta^{13}\text{C}$ and gas wetness.....	24
13. Cross plot showing relation between gas methane $\delta^{13}\text{C}$, CO_2 content, and gas wetness	25
14. Cross plots showing relation between gas wetness and present reservoir depth.....	26
15. Burial history curves in the San Juan Basin, Colorado and New Mexico.....	28
16. Time-stratigraphic cross section extending from southwest to northeast from the Zuni Basin through the central part of the San Juan Basin, Colorado and New Mexico, showing the relation between the different source intervals in the Mancos Shale, Graneros Member, and various reservoirs	33
17. Dakota-Greenhorn Conventional Oil and Gas Assessment Unit (AU) (50220304).....	36
18. Map showing distribution of gas-oil ratios from producing reservoirs in the Dakota-Greenhorn Conventional Oil and Gas Assessment Unit and Dakota-Greenhorn Continuous Gas Assessment Unit	38
19. Map showing distribution of oil and gas wells from producing reservoirs in the Dakota-Greenhorn Conventional Oil and Gas Assessment Unit and Dakota-Greenhorn Continuous Gas Assessment Unit	39
20. Events chart showing timing of key geologic events for the Dakota-Greenhorn Conventional Oil and Gas Assessment Unit.....	40
21. Distribution by halves of grown oil-accumulation size versus rank by size for the Dakota-Greenhorn Conventional Oil and Gas Assessment Unit (50220304)	42
22. Distribution of grown oil-accumulation size versus accumulation-discovery year for Dakota-Greenhorn Conventional Oil and Gas Assessment Unit (50220304)	42

23.	Distribution by halves of grown gas-accumulation size versus rank by size for the Dakota-Greenhorn Conventional Oil and Gas Assessment Unit (50220304)	44
24.	Distribution of grown gas-accumulation size versus accumulation-discovery year for Dakota-Greenhorn Conventional Oil and Gas Assessment Unit (50220304)	44
25.	Map showing the Dakota-Greenhorn Continuous Gas Assessment Unit (50220363) boundary in the lower part of the Mancos-Menefee Composite Total Petroleum System, and locations of burial history curves.....	46
26.	Events chart that shows timing of key geologic events for the Dakota-Greenhorn Continuous Gas Assessment Unit.....	47
27.	Graph showing estimated ultimate recoveries of Dakota-Greenhorn Continuous Gas Assessment Unit gas wells divided into three nearly equal periods of production time	49
28.	Graph showing combined distribution of estimated ultimate recoveries of Dakota-Greenhorn Continuous Gas Assessment Unit gas wells	49
29.	Map showing the Gallup Sandstone Conventional Oil and Gas Assessment Unit (50220302) boundary in the lower part of the Mancos-Menefee Composite Total Petroleum System, oil and gas fields, distribution of wells that penetrate the Gallup, and locations of burial history curve.....	51
30.	Events chart showing key geologic events for the Gallup Sandstone Conventional Oil and Gas Assessment Unit.....	52
31–34.	Maps showing	
31.	Mancos Sandstones Conventional Oil Assessment Unit (50220303) in the upper part of the Mancos-Menefee Composite Total Petroleum System, oil and gas fields, and locations of the wells used to construct the burial history curves found in this report	55
32.	Distribution of gas-oil ratios in wells producing from upper Mancos Shale, Tocado Sandstone Lentil, and “Gallup” sandstones in the Mancos Sandstones Conventional Oil Assessment Unit and Mancos Sandstones Continuous Gas Assessment Unit	56
33.	Distribution of producing oil and gas wells in upper Mancos Shale, Tocado Sandstone Lentil, and “Gallup” sandstone reservoirs in the Mancos Sandstones Conventional Oil Assessment Unit and Mancos Sandstones Continuous Gas Assessment Unit.....	57
34.	Distribution of producing oil and gas wells in upper Mancos Shale, Tocado Sandstone Lentil, and “Gallup” sandstone reservoirs in the Mancos Sandstones Conventional Oil Assessment Unit and Mancos Sandstones Continuous Gas Assessment Unit.....	58
35.	Distribution by thirds of grown oil-accumulation size versus rank by size for producing fields greater than 0.5 MMBO (million barrels oil) in the Mancos Sandstones Conventional Oil Assessment Unit (50220303)	61
36.	Distribution of grown oil-accumulation size versus accumulation-discovery year for producing fields greater than 0.5 MMBO (million barrels oil) in the Mancos Sandstones Conventional Oil Assessment Unit (50220303)	61
37.	Map showing the location of the Mancos Sandstones Continuous Gas Assessment Unit (50220362) area and boundary in the middle and upper part of the Mancos-Menefee Composite Total Petroleum System	62
38.	Events chart that shows key geologic events for the Mancos Sandstones Continuous Gas Assessment Unit.....	64

39. Graph showing estimated ultimate recoveries of Mancos Sandstones Continuous Gas Assessment Unit gas wells divided into three equal numbers of wells based on start of production	66
40. Graph showing combined distribution of estimated ultimate recoveries of Mancos Sandstones Continuous Gas Assessment Unit gas wells.....	66
41. Map showing the location of the Mesaverde Updip Conventional Oil and Mesaverde Central-Basin Continuous Gas Assessment Units in the upper part of the Mancos-Menefee Composite Total Petroleum System.....	68
42. Events chart that shows the timing of key geologic events for the Mesaverde Updip Conventional Oil Assessment Unit.....	69
43. Map showing the extent of the Mesaverde Central-Basin Continuous Gas Assessment Unit and its included gas fields in the upper part of the Mancos-Menefee Composite Total Petroleum System	71
44. Events chart that shows the timing of key geologic events for the Mesaverde Central-Basin Continuous Gas Assessment Unit	72
45. Graph showing the estimated ultimate recoveries of the Mesaverde Central-Basin Continuous Gas Assessment Unit gas wells divided into three nearly equal numbers of wells based on start of production.....	73
46. Graph showing the combined distribution of estimated ultimate recoveries of the Mesaverde Central-Basin Continuous Gas Assessment Unit gas wells.....	73
47. Map showing the Menefee Coalbed Gas Assessment Unit in the upper part of the Mancos-Menefee Composite Total Petroleum System	75
48. Events chart that shows the timing of key geologic events for the Menefee Coalbed Gas Assessment Unit.....	76

Plates

1. South-north cross section showing correlation of reservoir units in the Mancos Shale on the east side of the San Juan Basin, New Mexico[\[LINK\]](#)
2. West-east cross section showing correlation of reservoir units in the Mancos Shale in the eastern part of the San Juan Basin, New Mexico.....[\[LINK\]](#)
3. Reproduction of preliminary structure contour map on the base of the Cretaceous Dakota Sandstone, San Juan Basin of Thaden and Zech (1984).....[\[LINK\]](#)

Tables

1. Properties of Dakota Sandstone, Gallup (main) and Gallup (Torrivio Sandstone Member) Sandstone, Tocado Sandstone Lentil, and "Gallup" sandstone oil and gas reservoirs	10
2. Characteristics of Mesaverde Group reservoir rocks and oil and gas data	18
3. Means, standard deviations, ranges, and number of determinations (n) for total organic carbon contents and hydrogen indices of the Mancos Shale and Menefee Formation	22
4. Means, standard deviations, and number of analyses of gas wetness, carbon dioxide content, carbon isotope of methane $\delta^{13}\text{C}_{\text{CH}_4}$ of produced natural gases from reservoirs in the Mancos-Menefee Composite Total Petroleum System, San Juan Basin	23

5. Comparison of 2002 and 1995 estimates of number and sizes of undiscovered oil accumulations in the 2002 Dakota-Greenhorn Conventional Oil and Gas Assessment Unit (50220304) and the 1995 Basin Margin Dakota Oil Play 2205.....43
6. Comparison of 2002 and 1995 estimates of number and sizes of undiscovered gas accumulations in the 2002 Dakota-Greenhorn Conventional Oil and Gas Assessment Unit (50220304) and the 1995 Basin Margin Dakota Oil Play 2205.....45
7. Comparison of 2002 and 1995 estimated undiscovered resources for the 2002 Dakota-Greenhorn Continuous Gas Assessment Unit (50220363) and 1995 Dakota Central Basin Play 2205 and the 2002 Mesaverde Central-Basin Continuous Gas Assessment Unit (50220361) and the 1995 Central Basin Mesaverde Gas Play 2209.....48

Geology and Oil and Gas Assessment of the Mancos-Menefee Composite Total Petroleum System

By J.L. Ridgley, S.M. Condon, and J.R. Hatch

Abstract

The Mancos-Menefee Composite Total Petroleum System (TPS) includes all genetically related hydrocarbons generated from organic-rich shales in the Cretaceous Mancos Shale and from carbonaceous shale, coal beds, and humate in the Cretaceous Menefee Formation of the Mesaverde Group. The system is called a composite total petroleum system because the exact source of the hydrocarbons in some of the reservoirs is not known. Reservoir rocks that contain hydrocarbons generated in Mancos and Menefee source beds are found in the Cretaceous Dakota Sandstone, at the base of the composite TPS, through the lower part of the Cliff House Sandstone of the Mesaverde Group, at the top. Source rocks in both the Mancos Shale and Menefee Formation entered the oil generation window in the late Eocene and continued to generate oil or gas into the late Miocene. Near the end of the Miocene in the San Juan Basin, subsidence ceased, hydrocarbon generation ceased, and the basin was uplifted and differentially eroded. Reservoirs are now underpressured.

Eight assessment units were defined in the Mancos-Menefee Composite TPS. Of the eight assessment units, four were assessed as conventional oil or gas accumulations and four as continuous-type accumulations. The conventional assessment units are Dakota-Greenhorn Conventional Oil and Gas Assessment Unit (AU), Gallup Sandstone Conventional Oil and Gas AU, Mancos Sandstones Conventional Oil AU, and the Mesaverde Updip Conventional Oil AU. Continuous-type assessments are Dakota-Greenhorn Continuous Gas AU, Mancos Sandstones Continuous Gas AU, Mesaverde Central-Basin Continuous Gas AU, and Menefee Coalbed Gas AU. The Mesaverde Updip Conventional AU was not quantitatively assessed for undiscovered oil and gas resources, because the producing oil fields were smaller than the 0.5 million barrel cutoff, and the potential of finding fields above this cutoff was considered to be low.

Total oil resources that have the potential for additions to reserves in the next 30 years are estimated at a mean of 16.78 million barrels. Most of this resource will come from reservoirs in the Mancos Sandstones Oil AU. Gas resources that have the potential for additions to reserves in the next 30 years are estimated at a mean of 11.11 trillion cubic feet of gas (TCFG). Of this amount, 11.03 TCFG will come from

continuous gas accumulations; the remainder will be gas associated with oil in conventional accumulations. Total natural gas liquids (NGL) that have the potential for additions to reserves in the next 30 years are estimated at a mean of 99.86 million barrels. Of this amount, 96.95 million barrels will come from the continuous gas assessment units, and 78.3 percent of this potential resource will come from the Mancos Sandstones Continuous Gas AU.

Introduction

The boundary of the Mancos-Menefee Composite Total Petroleum System (TPS) coincides with the boundary that delimits the San Juan Basin Province for this assessment (fig. 1). The TPS is defined as including all reservoir rocks and potential source beds from the base of the Dakota Sandstone to the top of the Cliff House Sandstone of the Mesaverde Group or the top of the Allison Member of the Menefee Formation of the Mesaverde Group (fig. 2). Within the TPS, there are two principal hydrocarbon source intervals:

1. Mancos Shale and
2. Menefee Formation (fig. 2).

The composite definition was chosen for the TPS because it was impossible to determine exactly which of the two intervals was the source of oil and gas found in each of the various formations that compose the Mesaverde Group. The hydrocarbons probably represent, in some cases, a mixture of the two sources. The boundary of the TPS was drawn to include the known source rocks of the Mancos and Menefee, and known or potential reservoir rocks as shown in figure 2. There are eight assessment units (AU) in this TPS. These are, in ascending order,

1. Dakota-Greenhorn Conventional Oil and Gas AU,
2. Dakota-Greenhorn Continuous Gas AU,
3. Gallup Sandstone Conventional Oil and Gas AU,
4. Mancos Sandstones Conventional Oil AU,
5. Mancos Sandstones Continuous Gas AU,
6. Mesaverde Updip Conventional Oil AU,
7. Mesaverde Central-Basin Continuous Gas AU, and
8. Menefee Coalbed Gas AU (fig. 2).

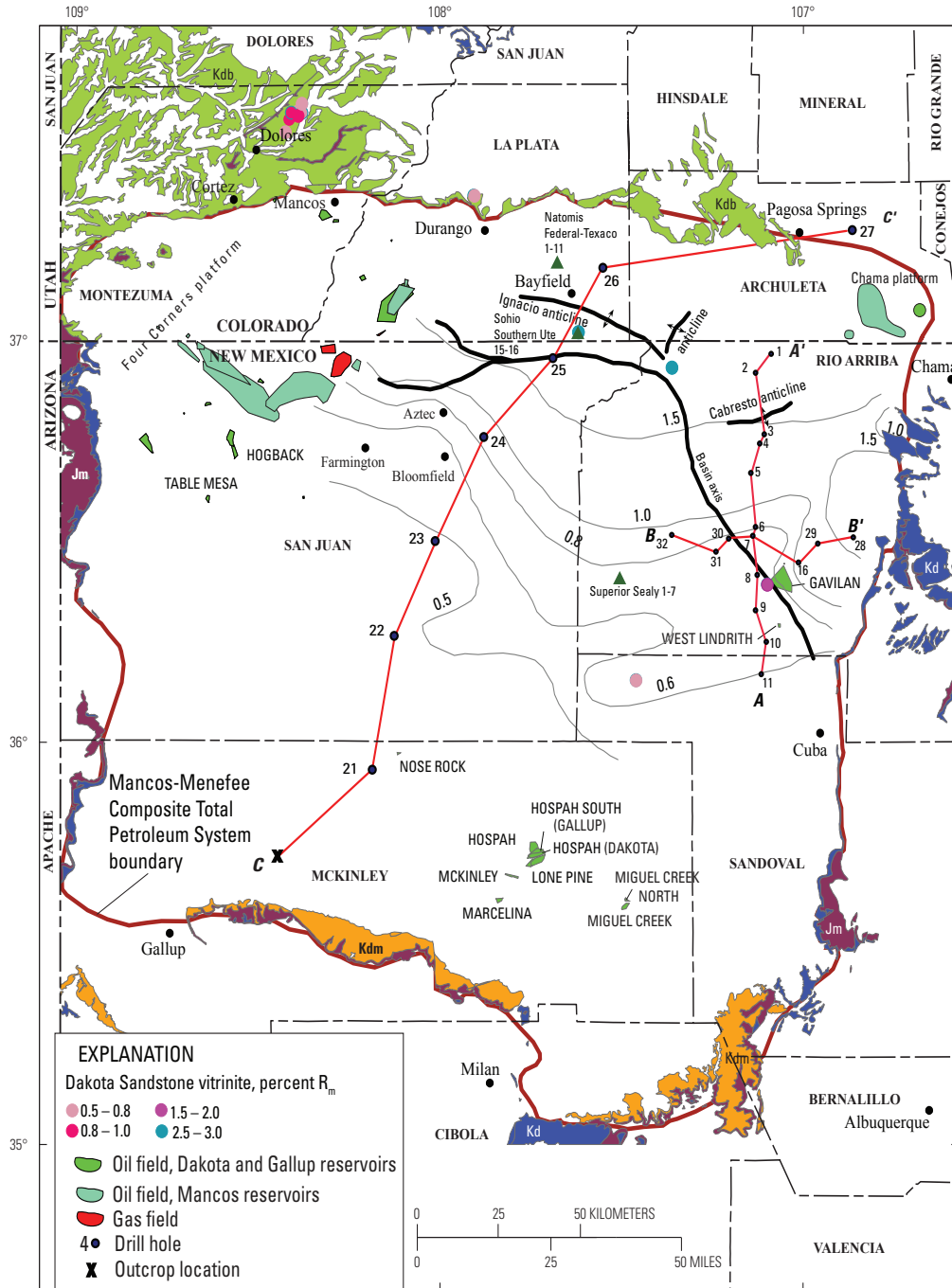


Figure 1. Map showing the boundary (in red) of the Mancos-Menefee Composite Total Petroleum System, San Juan Basin, Colorado and New Mexico. Shown are selected Mancos-sourced oil and gas fields. Menefee maturity contours (in gray) show vitrinite reflectance (R_m) values, in percent, contoured from data in Fassett and Nuccio (1990), Law (1992), and Ridgley (2001b). Isolated R_m vitrinite data from shale or coal in the Dakota Sandstone (colored dots) are from Fassett and Nuccio (1990) and U.S. Geological Survey unpublished data. Also shown are locations of cross sections A–A', B–B' (pls. 1 and 2), and C–C' (fig. 9); principal structures in the basin; and locations of the wells (green triangles) used to construct the burial history curves found in this report (figs. 15A–C). Symbols for geologic map units: Kdm, Dakota Sandstone-Mancos Shale; Kdb, Dakota Sandstone-Burro Canyon Formation; Kd, Dakota Sandstone; Jm, Morrison Formation (Green, 1992; Green and Jones, 1997).

Within the lower part of the Mancos Shale in the TPS, there is a major unconformity that is Coniacian in age (see summary discussion in Ridgley, 2001a). This unconformity separates genetically unrelated (although similar in appearance) strata above and below the unconformity (figs. 2 and 3). The geologic basis for this unconformity has not been identified, but the unconformity is probably tectonically related. The magnitude of erosion below the unconformity increases from south to north across the San Juan Basin (figs. 2 and 3; pls. 1 and 2); at places the unconformity nearly incises into the Juana Lopez Member of the Mancos Shale (Molenaar, 1977b). This unconformity was used to separate the two Dakota-Greenhorn assessment units and the Gallup Sandstone Conventional Oil and Gas AU below the unconformity from the two Mancos sandstone assessment units above the unconformity (fig. 2). Controls on sediment geometry and depositional environments of strata below the unconformity differ from those above it. The Gallup Sandstone Conventional Oil and Gas AU was separated from the Dakota-Greenhorn Conventional Oil and Gas AU because of the very different geometry of the various shorelines and regional distribution of potential reservoir rocks. These differences affect migration pathways for hydrocarbon movement. Seals and traps vary among the five assessment units of the Mancos Shale part of the TPS and are related to

1. facies distributions that reflect variations in depositional environments, and
2. structural control on sandstone-shale geometry and fracture orientation.

The Menefee part of the TPS includes three assessment units from which both oil and gas have been produced, but in different parts of the basin. The lowermost is a conventional oil assessment unit and includes strata in the Menefee Formation and Point Lookout Sandstone. Small amounts of oil have been produced on the updip southern flank of the basin from Menefee and Point Lookout age conventional accumulations. Gas and some condensate are produced from Menefee and Point Lookout reservoirs in the deep, central part of the basin in an accumulation that is considered continuous: Mesaverde Central-Basin Continuous Gas AU. The uppermost assessment unit, Menefee Coalbed Gas AU, is hypothetical and consists of possible coal-bed gas accumulations from thermally immature coal beds within the Menefee.

Key elements that define the Mancos-Menefee TPS are

1. source rocks of sufficient thermal maturity to generate hydrocarbons,
2. reservoir rocks to host the accumulations,
3. migration pathways that allow the hydrocarbons to move into reservoirs,
4. structural or stratigraphic traps in which hydrocarbons could accumulate, and
5. seals to contain the accumulations.

These key elements are described more fully below and in each assessment unit discussion. Methodologies for assessing continuous-type and conventional accumulations are discussed in Schmoker (2003) and Schmoker and Klett (2003).

Mancos-Menefee Composite Total Petroleum System

Geologic Framework

Stratigraphy

Cretaceous rocks, beginning with deposition of the Dakota Sandstone, consist of wedges of marine-to-continental transgressive and regressive strata (fig. 2) that occupy the broader San Juan Basin (as shown in figure 4) (Baltz, 1967; Fassett, 1974, 1977, 2000; Molenaar, 1977b; Owen and Siemers, 1977; Posamentier and others, 1992; Nummedal and Molenaar, 1995; Wright Dunbar, 2001). Figure 3 is a generalized time-stratigraphic cross section through the San Juan Basin and shows the relation of the various reservoir units discussed below. Except for the Dakota Sandstone, shoreline geometry of strata within these wedges generally has a northwest-southeast orientation that may be controlled by basement structural blocks (fig. 4). Shoreline geometry in the Dakota was much more complex and was influenced by a large embayment centered over the southern part of the basin. The Dakota shorelines tend to be oriented west-east to slightly northwest-southeast in Colorado and New Mexico around this embayment (Seboyeta Bay) (fig. 5). Fluvial rocks in the basal part of the Dakota are found throughout the TPS and fill valleys incised into the underlying Jurassic rock. During the Cretaceous, deposition in the basin area was open-ended to the northeast in the direction of deeper marine sedimentation.

The base of the TPS is unconformable with underlying strata throughout the extent of the San Juan Basin Province. The Dakota Sandstone rests unconformably on the Upper Jurassic Morrison Formation throughout the southern part of the San Juan Basin and on the Lower Cretaceous Burro Canyon Formation in the northern part of the basin (Saucier, 1974; Molenaar, 1977b; Owen and Siemers, 1977). Hydrocarbons have been reported from the Morrison Formation (some of these hydrocarbons intervals are in the Burro Canyon Formation based on subsurface analysis of well logs) in a few isolated wells in the northern part of the TPS. These isolated occurrences of hydrocarbons in strata older than those assigned to the TPS may be related to lateral migration of hydrocarbons across faults, where the older rocks have been displaced upward along a fault, thus, juxtaposing them with potential source rock. In this way hydrocarbons may have leaked laterally from the Dakota into the older strata. Alternatively, hydrocarbons may have migrated through channels in the basal Dakota Sandstone that have cut into the Burro Canyon or Morrison Formations, and from there laterally into sandstones of the latter formations.

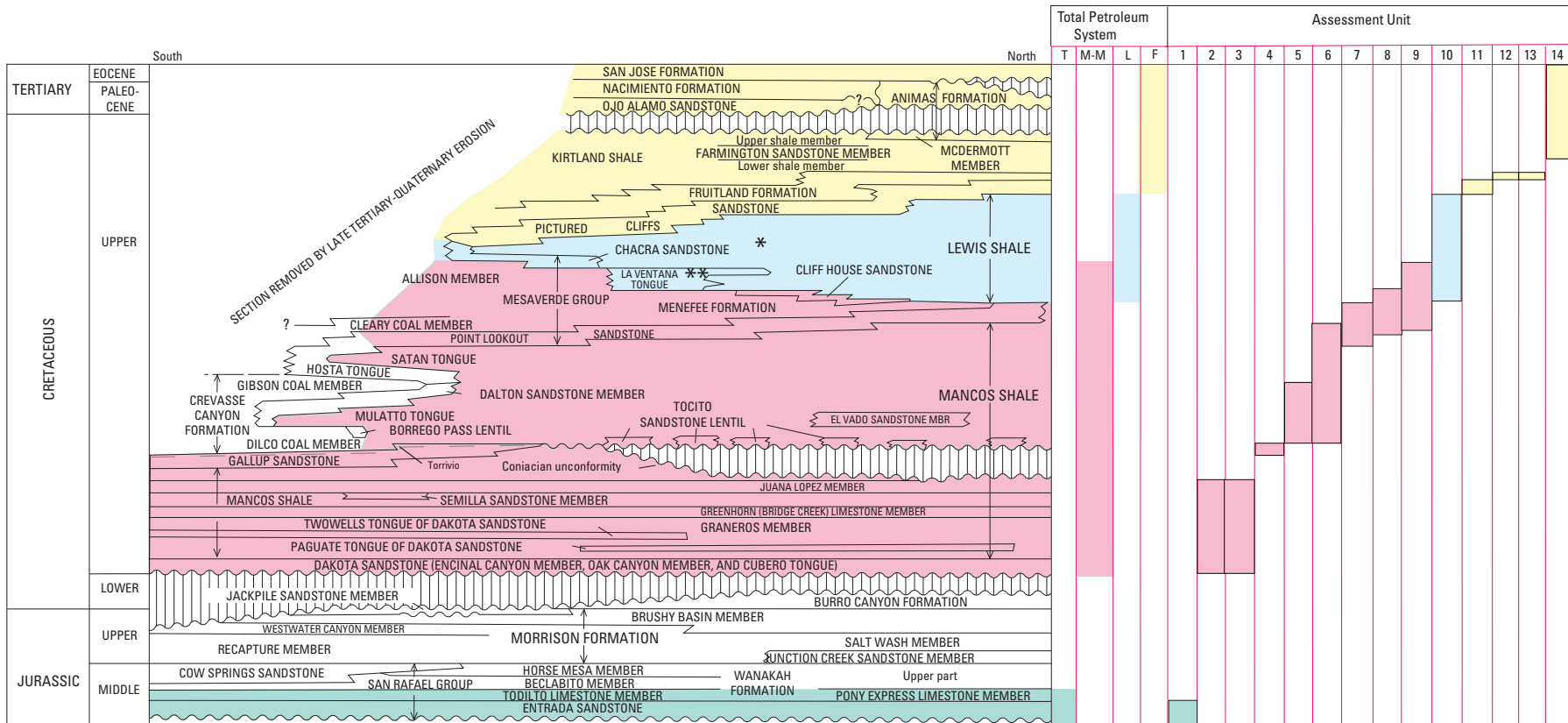


Figure 2. Chart showing regional chronostratigraphic correlations in the San Juan Basin (modified from Molenaar, 1977a) from the Tertiary to the base of the Jurassic, and the extent of the total petroleum systems and assessment units defined in the 2002 National Oil and Gas Assessment of the San Juan Basin Province (5022), New Mexico and Colorado. Total petroleum systems: F, Fruitland; L, Lewis Shale; M-M, Mancos-Menefee composite, and T, Todilto. Assessment units: 1, Entrada Sandstone Conventional Oil; 2, Dakota-Greenhorn Conventional Oil and Gas; 3, Dakota-Greenhorn Continuous Gas; 4, Gallup Sandstone Conventional Oil and Gas; 5, Mancos Sandstones Conventional Oil; 6, Mancos Sandstones Continuous Gas; 7, Mesaverde Updip Conventional Oil; 8, Mesaverde Central-Basin Continuous Gas; 9, Menefee Coalbed Gas; 10, Lewis Continuous Gas; 11, Pictured Cliffs Continuous Gas; 12, Basin Fruitland Coalbed Gas; 13, Fruitland Fairway Coalbed Gas; and 14, Tertiary Conventional Gas. *Chacra sandstone, an informal term used by drillers and geologists in the basin; **La Ventana Tongue of the Cliff House Sandstone. Vertical lines, unconformities.

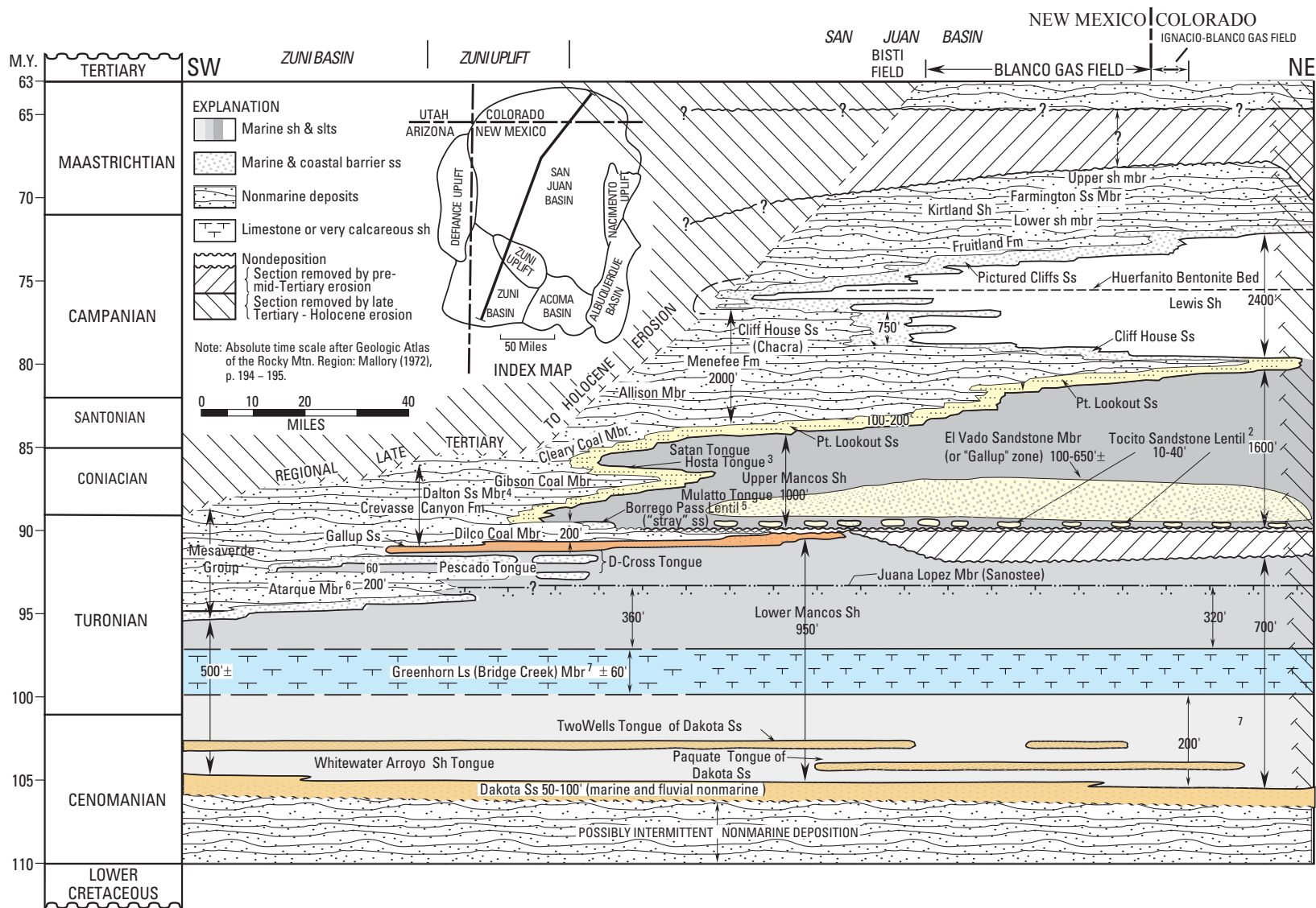


Figure 3. Time-stratigraphic cross section of Upper Cretaceous and Tertiary rocks in the Zuni and San Juan Basins, Colorado and New Mexico. Modified from Pentilla (1964) and Molenaar (1977a). Members shown by footnotes: ¹of Cliff House Sandstone, ²of Mancos Shale, ³of Point Lookout Sandstone, ⁴of Crevasse Canyon Formation, ⁵of Tres Hermanos Formation, ⁶of Mancos Shale, ⁷of Mancos Shale. Shale, sh; siltstone, slts; sandstone, ss; member, mbr; formation, fm.

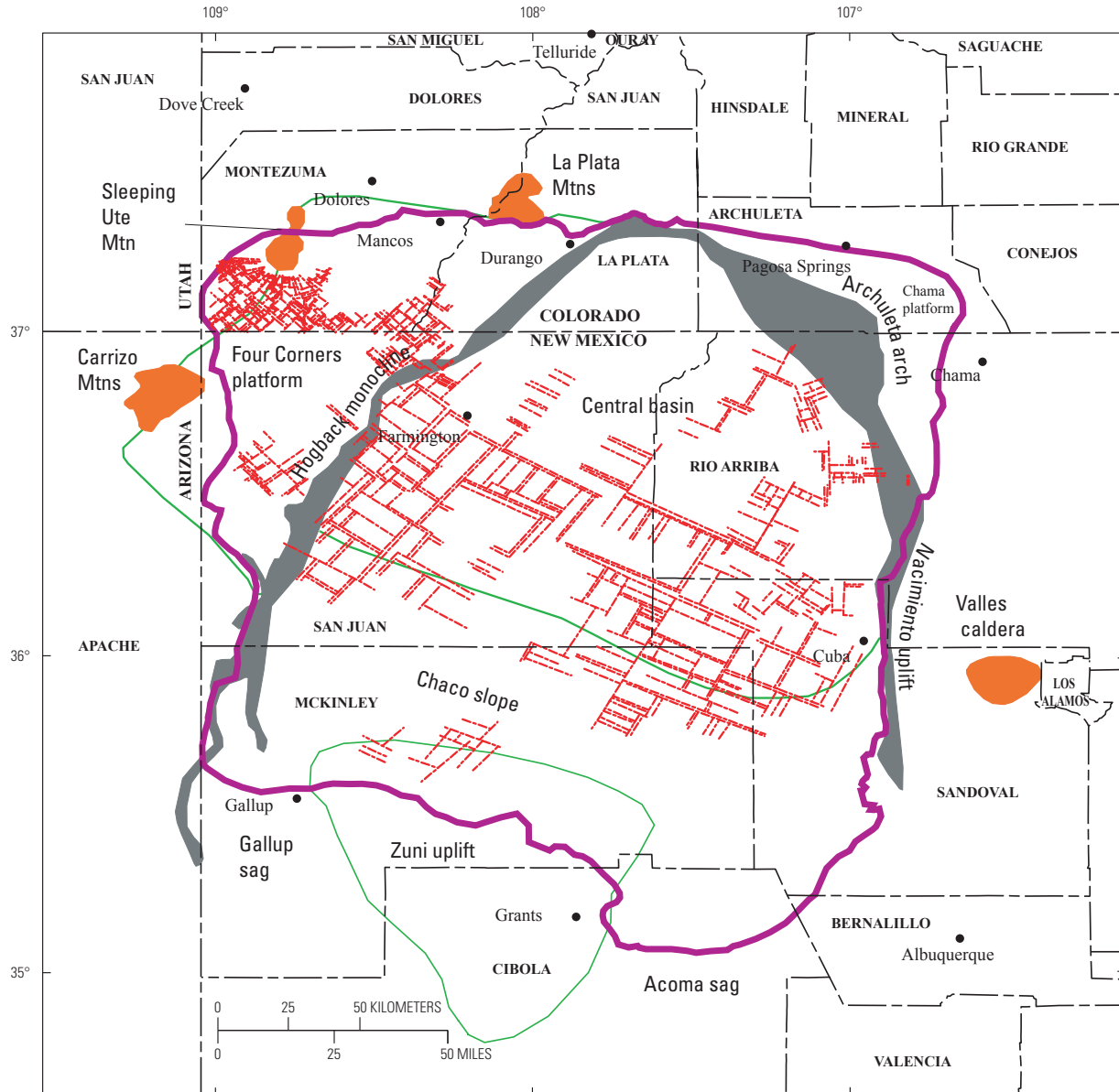


Figure 4. Map showing the location of inferred basement structural blocks (dashed red lines) and other structural elements in the San Juan Basin. Modified from Taylor and Huffman (1998, 2001), Fassett (2000), and Huffman and Taylor (2002). San Juan Basin Province (5022) boundary (purple line). Orange polygons are Late Cretaceous and Tertiary intrusive and extrusive igneous centers; gray polygons are areas of steep dip along monoclines; green line outlines some of the main structural elements.

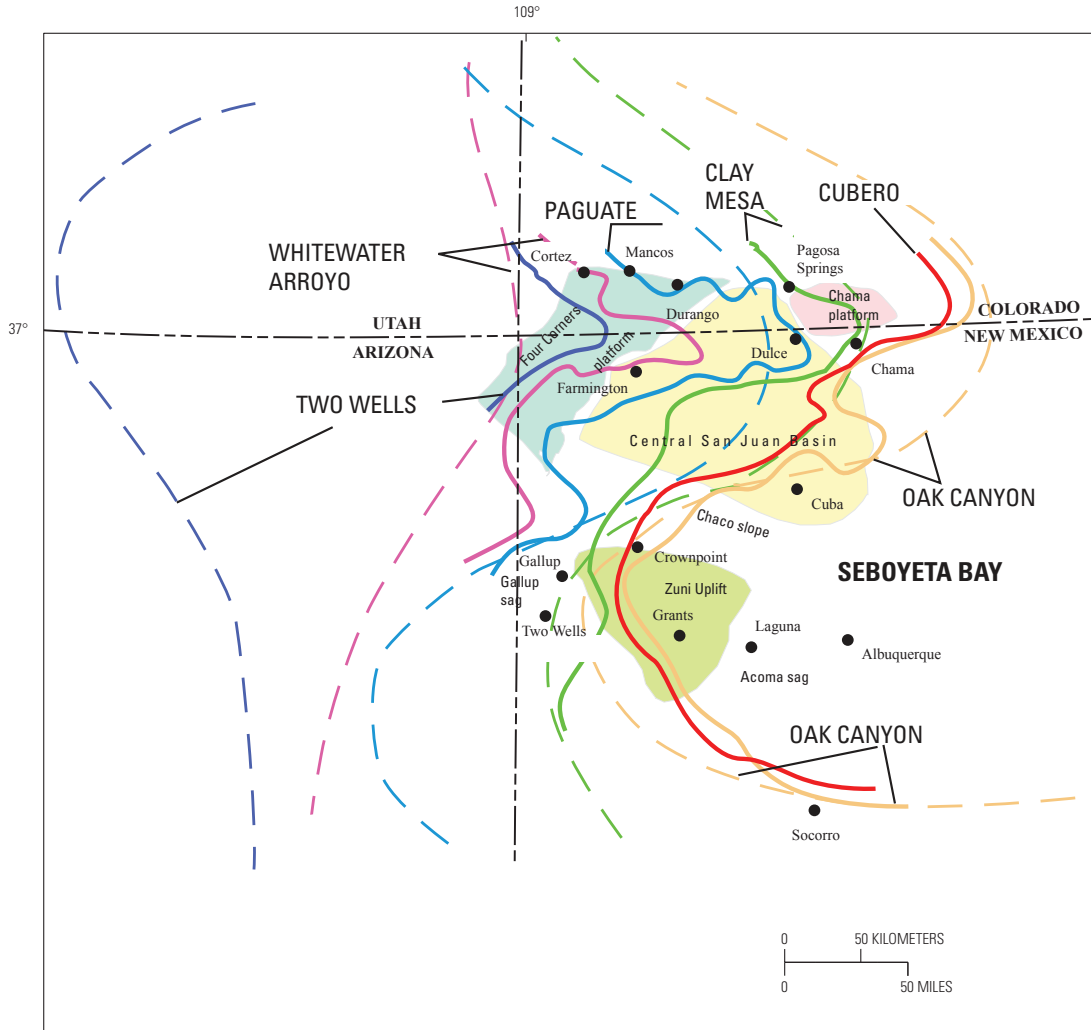


Figure 5. Map showing location of shorelines and location of Seboyeta Bay during deposition of the Dakota Sandstone and Mancos Shale. Members of Dakota and Mancos are, in ascending order: Oak Canyon Member of Dakota, Cubero Sandstone Tongue of Dakota, Clay Mesa Tongue of Mancos, Pagate Tongue of Dakota, Whitewater Arroyo Tongue of Mancos, and Twowells Tongue of Dakota. Dashed lines indicate shorelines based on ammonite data collected from outcrops around the San Juan Basin (Cobban and Hook, 1984). Solid lines are from J.L. Ridgley (unpublished data, 2002).

Structure

A generalized regional structure map, contoured on the top of the Mancos Shale, shows the present-day structural configuration of the San Juan Basin (fig. 6). The Mancos Shale is less than 1,000-ft subsea level in the deeper part of the San Juan Basin; overburden thickness in this area ranges between 6,000 and 7,000 ft. Structure contours on top of the Menefee (fig. 7) also generally parallel structural interpretations of the underlying Dakota Sandstone (Thaden and Zech, 1984; pl. 3) and the overlying Huerfano Bentonite Bed of the Lewis Shale (Fassett, 2000). The top of the Menefee dips gently northward to an elevation of about 1,000 ft above sea level (6,500 ft below the land surface) at the basin axis, and then reverses dip at a steep angle toward the outcrops along

the north basin rim. This northward rise is interrupted by the Ignacio anticline in southern Colorado (fig. 1), which has about 200 ft of closure (Harr, 1988).

Current overburden on the Menefee ranges from 0 to about 6,500 ft (IHS Energy Group, 2001). Overburden shows a gradual thickening from southwest to northeast on the Chaco slope (fig. 4), with maximum overburden along the basin axis. Overburden thicknesses decrease markedly over short distances as the outcrops are approached on the northwest, north, and northeast sides of the basin.

Structure contours drawn on the tops of the Dakota Sandstone (Thaden and Zech, 1984; pl. 3), Mancos Shale (fig. 6), and Menefee Formation (fig. 7) show the gradual northward dip from the Chaco slope (fig. 4) to the basin axis on the north and northeastern sides of the basin (fig. 1). North of the basin

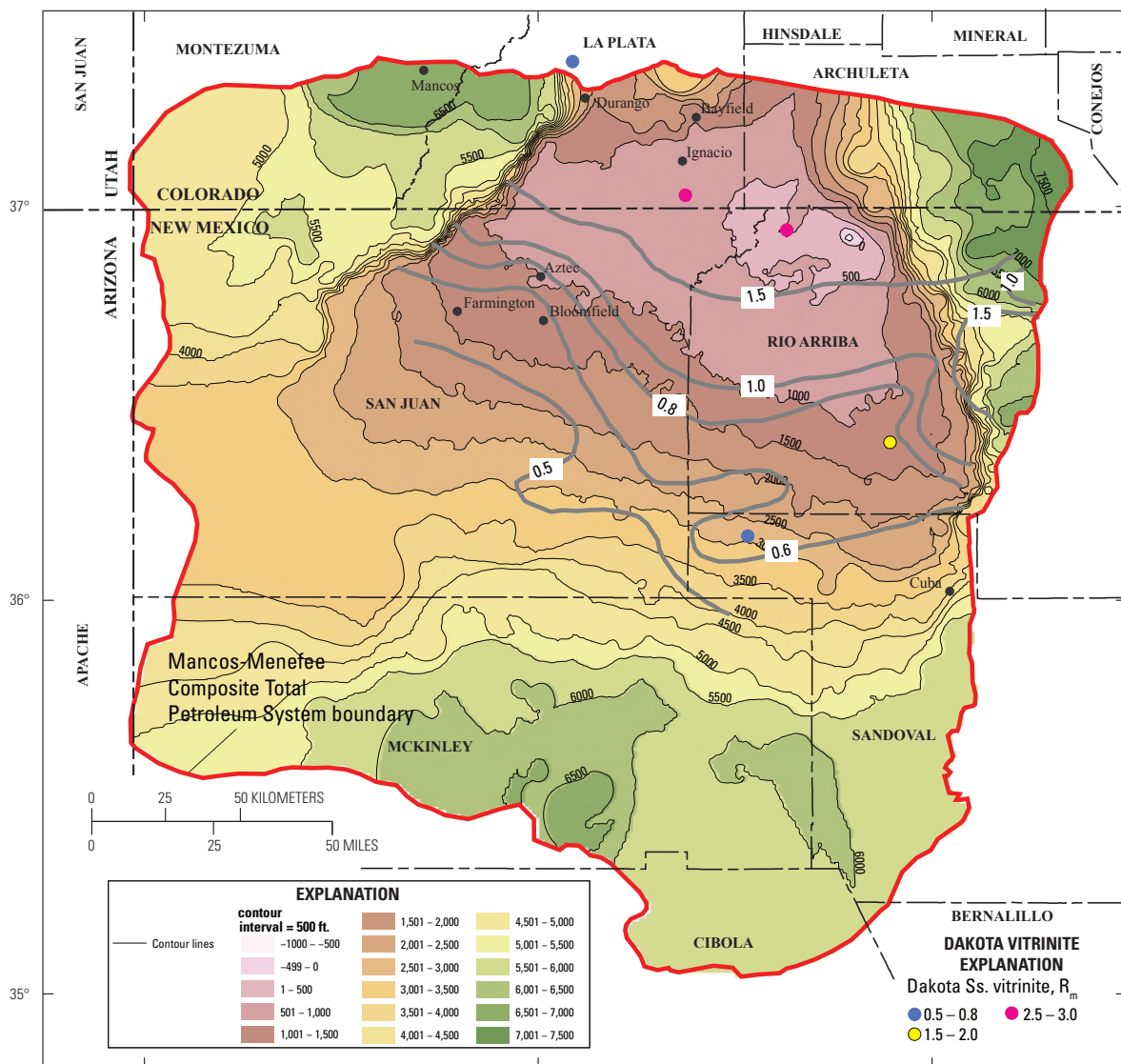


Figure 6. Structure contour map drawn on top of the Mancos Shale, San Juan Basin, Colorado and New Mexico, using data from IHS Energy Group (2002). Contour interval, 500 ft; datum is mean sea level. Menefee maturity contours (in gray) show vitrinite reflectance (R_m) values in percent using data from Fassett and Nuccio (1990), Law (1992), and Ridgley (2001b). Isolated R_m vitrinite data from shale or coal in the Dakota Sandstone (colored dots) are from Fassett and Nuccio (1990) and C. Threlkeld (written commun., 2001).

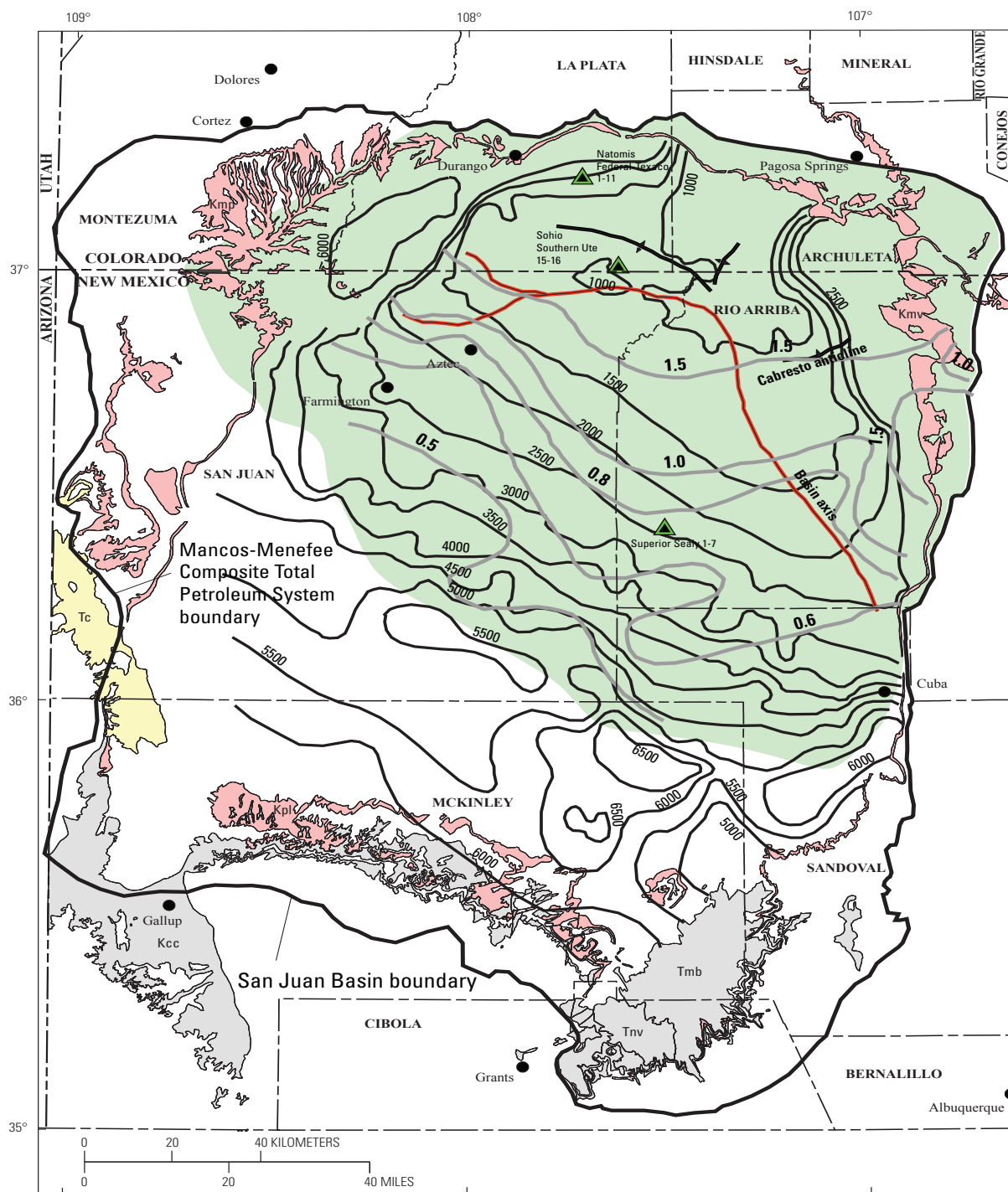


Figure 7. Structure contour map drawn on top of the Menefee Formation using data from IHS Energy Group (2001). Contour interval, 500 ft; datum is mean sea level. Menefee maturity contours (in gray) show vitrinite reflectance values, in percent, using data from Fassett and Nuccio (1990), Law (1992), and Ridgley (2001b). Also shown are locations of the wells (green triangles) used to construct the burial history curves found in this report (figs. 15A–C) and the pod of thermally mature source rocks in the Mancos Shale and Menefee Formation (shaded green). Geologic units are from Green (1992) and Green and Jones (1997): Tc, Tertiary Chuska Sandstone; Tnv, Tertiary Neogene volcanics; Tmb, Tertiary Miocene volcanics; Kcc, Crevasse Canyon Formation; Kmp, Menefee Formation and Point Lookout Sandstone; Kmv, Mesaverde Group; Kpl, Point Lookout Sandstone.

axis, the dip reverses, and the Dakota and other units rise to the surface in southern Colorado. The rise to the north is modified by the Ignacio anticline, just north of the axis, and another unnamed anticline that trends northeastward (fig. 1). The Cabresto anticline (fig. 7), as designated in this study, was determined by contouring the top of the Paleocene Ojo Alamo Sandstone. This small anticline trends east-northeast, perpendicular to the basin axis (fig. 1). The Four Corner platform is a structural bench off the northwest side of the basin (fig. 4). Faults at the level of the Dakota Sandstone are common on the southern and southeastern sides of the basin, but are not identified in most of the central or northern parts (Thaden and Zech, 1984; pl. 3), probably due to a lack of data. Taylor and Huffman (1998, 2001) and Huffman and Taylor (2002) mapped basement faults in parts of the basin (fig. 4), including basin-directed thrust faults underlying the Hogback monocline, at points along the northern and northeastern basin margin, and along the eastern side of the basin at the Nacimiento fault (Baltz, 1967). The various structural elements of the basin have been summarized by Lorenz and Cooper (2001).

Hydrocarbon Reservoir Rocks

Reservoir rocks that have hydrocarbons sourced from the Mancos Shale include the stratigraphic interval bounded by the Dakota at the base and the Lewis Shale at the top (figs. 2 and 3). In the Mancos, isolated limestone or sandstone reservoir units are confined to the lower two-thirds of the formation and are described below. The stratal relations of these reservoir units are shown in plates 1 and 2. Reservoir properties of the main producing reservoirs are shown in table 1.

Dakota Sandstone

The Upper Cretaceous Dakota Sandstone is a complex sequence of fluvial, marginal marine (deltaic and strandplain shoreface sandstones), and marine shelf sandstones (Landis and others, 1973; Owen, 1973; Molenaar, 1977b; Owen and Siemers, 1977; Ridgley, 1977, 1990; Berg, 1979; Aubrey, 1988). The Dakota has been divided into five members, in ascending order:

Table 1. Properties of Dakota Sandstone, Gallup (main) and Gallup (Torrivio Sandstone Member) Sandstone, Toco Sandstone Lentic, and "Gallup" sandstone (Ridgley, 2001a) oil and gas reservoirs in the Dakota-Greenhorn Conventional Oil and Gas, Dakota-Greenhorn Continuous Gas, Gallup Sandstone Conventional Oil and Gas, Mancos Sandstones Conventional Oil, and Mancos Sandstones Continuous Gas Assessment Units. Data summarized from field descriptions in Fassett (1978a,b, 1983a).

[Conv, conventional; cont, continuous; %, percent; md, millidarcy; min, minimum; max, maximum; frac, fracture]

Rock unit	Net pay (ft)	Porosity (%)	Permeability (md)	Water saturation (%)	API gravity (degrees)	Type of accumulation
"Gallup"	min 7 max 278	min 1 max 15	min 0.06 max 22	min 25 max 50	min 34 max 46	Conv oil
"Gallup"	min 11 max 30	16	min ? max frac	40		Conv gas
"Gallup"	min 25 max 400	min 6 max frac	min 0.02 max frac	max 49 unreliable		Cont gas
Tocito	min 5 max 40	min 8 max 20	min 6 max 250	min 23 max 40	min 35 max 51	Conv oil
Tocito	min 6 max 15	min 10 max 15	min 82 max 83	min 31 max 40		Cont gas
Gallup (main)	27	38	110	39	24	Conv oil
Gallup (Torrivio)	min 8 max 35	min 22 max 30	min 10 max 600	min 10 max 50	min 29 max 40	Conv oil
Dakota	min 8 max 100	min 9 max 22	min 0.1 max 700	min 28 max 90	min 35 max 76	Conv oil
Dakota	min 8 max 40	min 14 max 19	min 10 max 83	min 35 max 57		Conv gas
Dakota	min 40 max 65	min 7 max 8	min 0.2 max 0.4	40		Cont gas

1. Encinal Canyon Member,
2. Oak Canyon Member,
3. Cubero Tongue,
4. Paguete Tongue, and
5. Twowells Tongue

(Landis and others, 1973; Owen, 1973; Aubrey, 1988). The Paguete and Twowells are underlain and overlain by tongues of the Mancos Shale. The Dakota rests on a regional unconformity (Aubrey, 1988; Ridgley, 1989) and is conformable with the Mancos Shale with which it intertongues (figs. 2 and 4; pls. 1 and 2). The Dakota was deposited during an overall transgression of the sea into the area of the San Juan Basin. Most of the nearshore and shelf sandstones were deposited as highstand deposits during periods of higher clastic input. Distribution of facies, and hence sandstone reservoirs in the Dakota, were controlled by the positions of the various shorelines that defined the limit of Dakota deposition in the basin (fig. 5). Unlike the northwest–southeast trend to shorelines of the overlying Upper Cretaceous formations, shorelines in the Dakota were arcuate as a result of a major embayment (Seboyeta Bay) in the San Juan Basin (Cobban and Hook, 1984; Ridgley, 1992).

Throughout the basin, the Dakota is of variable thickness, owing to the presence or absence of the Twowells Tongue. The formation is as thick as 500 ft but averages 200–300 ft (Craig, 2001). Sandstones, conglomerates, and thin coal and carbonaceous sandstone of the Encinal Canyon Member fill valleys incised into the underlying Burro Canyon Formation in the northern part of the basin and the Morrison Formation in the southern part. Facies in the overlying Oak Canyon Member were deposited as the sea transgressed over the fluvial facies of the Encinal Canyon. In places, facies of the Oak Canyon comprise a heterolithic sequence of sandstone, siltstone, and carbonaceous sandstone deposited in estuaries and coastal marine environments (Nummedal and Swift, 1987). Sandstones of this member tend to be fine grained, burrowed, and bioturbated. Sandstones of the overlying Cubero, Paguete, and Twowells are fine to medium grained, poor to moderately well sorted, locally burrowed and bioturbated, cross stratified, and contain ripple laminations. Each of these sandstones grade into the underlying shaly unit of the Mancos Shale. They consist of stacked, upward coarsening parasequences of variable thickness. The upper sandstone in each parasequence tends to be cleaner and locally crossbedded (Franklin and Tieh, 1989).

Petrographic studies of the Dakota in the Lone Pine field (Berg, 1979) and West Lindrith field (fig. 1) (Franklin and Tieh, 1989) indicate significant variation in grain size, nature and degree of cementation, porosity, and permeability throughout the formation. Variation was observed within and between discrete sandstone bodies. The cementation history is complex; major cements are quartz, calcite, and clay. Natural fractures are especially prevalent in the West Lindrith field (fig. 1) where they are associated with small-scale folds.

Fractures have been identified elsewhere in the Dakota, from outcrop and core studies, and are important in production (table 1) (Lorenz and others, 1999; Cooper and others, 2000; Jaramillo and others, 2000).

Greenhorn Limestone Member of Mancos Shale

The Greenhorn (Bridge Creek) Limestone Member of the Mancos Shale is found throughout the San Juan Basin (fig. 3; pls. 1 and 2) where it consists of 30 to 70 ft of limestone, silty limestone, and calcareous shale. The member thickens from east to west across the basin; it thins to the southwest and is an excellent subsurface marker unit. The Greenhorn appears to rest conformably on the underlying Graneros Shale Member of the Mancos Shale and is conformably overlain by shale of the lower part of the Mancos Shale (fig. 3; pls. 1 and 2). A persistent bentonite or a low-resistivity shale of undetermined composition marks the base of the unit. The term Greenhorn, rather than Bridge Creek, is used in this report because it is the term used by industry when reporting tops and production. A few wells produce oil from the Greenhorn; most of which are in the Gavilan field (fig. 1). Most production from the Greenhorn is commingled with production from the Dakota. Fracturing of the Greenhorn, especially on the northeast side of the basin where isolated oil production occurs, may be important to production.

Gallup Sandstone

In the San Juan Basin, the Gallup Sandstone (fig. 3) was deposited as a northeast-prograding wedge of conglomerate, sandstone, thin coal, and shale making up a complex intertonguing sequence of sediments deposited in shoreface, estuarine, and fluvial environments (Molenaar, 1973, 1977b; Nummedal and Molenaar, 1995). At the outcrop and in the subsurface where sandstone is the dominant lithology, the Gallup has been subdivided into six principal sandstone units labeled A–F, with F being the oldest (fig. 8) (Molenaar, 1973, 1983; Craig, 2001). Each of the sandstone units prograded slightly more to the northeast than the preceding unit. The northeast pinchout of the A-sandstone unit marks the maximum northeast progradation of thick sandstone in the main Gallup. The northeast limit of each of the sandstone units has been used to define the approximate orientation and position of the various shorelines throughout Gallup deposition (fig. 8). Basinward (to the northeast), each sandstone unit of the Gallup changes facies laterally into a vertically stacked, interbedded sequence of thin sandstone and shale. This thin sandstone and shale sequence changes basinward into predominantly silty shale, and the units in the sequence are referred to as distal Gallup equivalent. These rocks are generally included in the middle unit of the Mancos Shale (pls. 1, and 2) below the Coniacian unconformity (fig. 2).

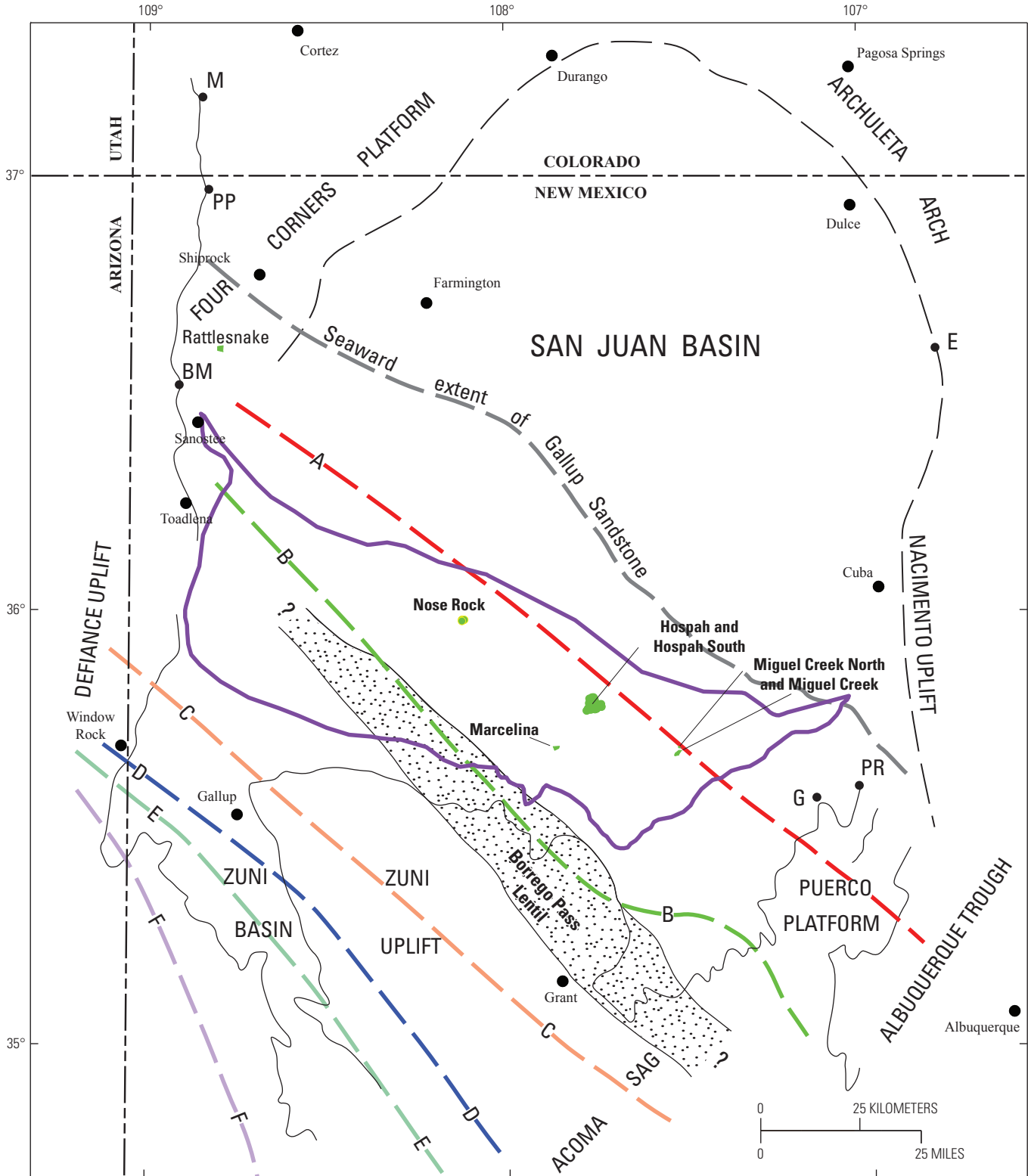


Figure 8. Map of the San Juan Basin showing the position of the Gallup Sandstone A-F shorelines (dashed lines), Borrego Pass Lenticle of Crevasse Canyon Formation (dots), and outcrop locations (single black dots) of the Tocito Sandstone Lenticle—"Gallup" sandstone interval. Outcrop locations are: M, Mounds; PP, Plunge pool; BM, Beautiful Mountain; G, Guadalupe; PR, pipeline road; and E, El Vado Reservoir. Modified from Molenaar (1973, 1983). Also shown is the outline of the Gallup Sandstone Conventional Oil and Gas Assessment Unit (purple) and oil fields that reportedly produce from the Gallup (Hospah) or Gallup Sandstone (green).

In the San Juan Basin, the Gallup is conformable with the underlying lower part of the Mancos Shale and also with members of the overlying Crevasse Canyon Formation (figs. 2 and 3) in the southwest part of the basin. Sandstone facies of the Gallup vary in thickness up to as much as 300 ft and are commonly fine to medium grained and moderately to well sorted (Stone, 1981). Shoreface facies are composed of amalgamated sandstones that coarsen upward. Hummocky cross stratification, horizontal laminations, and rare trough cross beds are the dominant sedimentary structures. Coastal facies, which include estuarine, tidal flats and deltas, and tidal channels, are heterolithic and vary laterally in extent. The sandstones are commonly bioturbated and burrowed; flaser bedding, herringbone cross stratification, and double mud drapes are common sedimentary structures (Nummedal and Molenaar, 1995). The upper part of the Gallup A sandstone and distal Gallup equivalents (included in middle of the Mancos unit below the unconformity on pl. 1) are truncated progressively from southwest to northeast across the San Juan Basin below a regional unconformity of Coniacian age (fig. 3; pl. 1) (Pentilla, 1964; Molenaar, 1977b; Nummedal and Swift, 1987; Craigg, 2001; Ridgley, 2001a). A thick, marine nearshore-bar sandstone of the main Gallup produces oil only in the Hospah South field (fig. 1), where it is called “lower Hospah” (the Hospah sandstone is an informal name used by industry) (Luce, 1978; Struna and Poettmann, 1988). Reservoir properties of the main Gallup sandstone in the Hospah South field are in table 1.

Torrivio Sandstone Member of Gallup Sandstone

In the southern part of the basin, fluvial sandstones that lie landward (to the southwest) of the Gallup sandstones are referred to as the Torrivio Sandstone Member of the Gallup Sandstone (fig. 2) (Molenaar, 1977b,c; Nummedal and Molenaar, 1995, their figs. 4 and 5). The Torrivio was deposited in braided river depositional environments (Molenaar, 1977b,c; Valasek, 1995). From outcrop studies, the Torrivio is conformable, in part, with the different Gallup shorelines and may have been the fluvial feeder system for these strandplain deposits. However, there is also some evidence that the youngest sandstone assigned to the Torrivio overlies a regional erosional surface (Nummedal and Molenaar, 1995; Valasek, 1995). Nummedal and Molenaar (1995) suggested making the Torrivio a member of the Crevasse Canyon Formation. They did not, however, change the stratigraphic position of the Torrivio in relation to the Gallup A–D sandstones. For the purposes of this report, the Torrivio is left in the Gallup because of the way industry has historically identified this sandstone.

The Torrivio Member is described as medium- to fine-grained sandstone that was deposited in continental or marine strandline settings (see field descriptions in Fassett, 1978a; Struna and Poettmann, 1988). Elsewhere, it has been documented as containing mud clasts at the base and characterized by trough cross beds (Nummedal and Swift, 1987). It has been suggested that the Torrivio of the Gallup, N. Mex., area is the

same lithostratigraphic unit as the “upper Hospah” sandstone in the oil-producing Hospah and Hospah South fields (Molenaar, 1977b; Huffman, 1996). In the Hospah South field, the Torrivio is separated from the underlying main Gallup (“lower Hospah”) by a thin coal bed that was deposited during continued regression that produced the Torrivio. The producing Gallup reservoirs in the Marcelina, Miguel Creek, Miguel Creek North, and Nose Rock fields (fig. 1) (see field descriptions in Fassett, 1978a,b, 1983a) are also called “upper Hospah,” and thus correlate with the Torrivio. Using geophysical logs, the Torrivio was correlated between the Hospah and Hospah South, Marcelina, Miguel Creek, Miguel Creek North, McKinley, and Nose Rock fields; in these fields it consists of one or more sandstone beds separated by shale. Reservoir properties of the Torrivio (“upper Hospah”) Sandstone Member are summarized in table 1.

Semilla Sandstone Member of Mancos Shale

Oil has been produced from only one well in the Semilla Sandstone Member of the Mancos Shale, and it was co-produced with oil from the Dakota Sandstone. The member crops out on the east side of the San Juan Basin. At the type section, the Semilla consists of 70 ft (21.3 m) of sandstone deposited as an offshore marine bar (Dane and others, 1968; Molenaar, 1977b), and it is very fine to fine grained, becoming locally medium grained and crossbedded in the upper part. In the subsurface, the Semilla forms elongate northwest- to southeast-trending sandstone bodies that average 10 ft in thickness, but may be as much as 20 ft thick. The Semilla pinches out somewhere between T. 25 and 26 N. (wells 7 and 8, pl. 1). In the subsurface, the Semilla forms a persistent marker bed located 10 to 20 ft below the base of the Juana Lopez Member of the Mancos Shale.

Juana Lopez Member of Mancos Shale

The Juana Lopez Member (often called Sanostee, especially in drilling completion reports) crops out on the east side and is found throughout the San Juan Basin (fig. 3; pls. 1 and 2) where it consists of 90 to 125 ft of dark-gray to very dark gray shale, calcarenite, and thin sandstone (Molenaar, 1977b). The base and top of the member are delineated by beds of hard, very fine grained, orange- to yellow-brown weathering, fossiliferous calcarenite (Landis and Dane, 1967). The Juana Lopez was deposited in marine environments in a shallow sea of low clastic input (Molenaar, 1973). Throughout the subsurface in the study area, the Juana Lopez forms a prominent marker interval characterized by more resistant calcarenite beds at the base and top (pls. 1 and 2). Because of its persistent character, it likely represents a time line over much of the study area and thus is used as the datum in the cross sections (pls. 1 and 2). On the west side of the basin, the Juana Lopez is truncated below the Coniacian age regional unconformity (see Gallup description above). Oil and gas have been

produced from the Juana Lopez in a few wells and production is usually commingled with production from the Dakota.

Sandstone Reservoirs in the Mancos Shale

At the outcrop and in the subsurface, the Mancos Shale above the Coniacian age unconformity and below the Point Lookout Sandstone of the Mesaverde Group consists of, in ascending order:

1. shale with discrete sandstone lenses (Tocito Sandstone Lentil) (the basal Niobrara sandstones of Molenaar, 1977b);
2. interbedded thin sandstone, siltstone, and shale (El Vado Sandstone Member interval of Fassett and Jentgen, 1978); and
3. shale with scattered thin sandstone and siltstone laminae in a gradational sequence with the overlying Point Lookout Sandstone of the Mesaverde Group (fig. 3; pls. 1 and 2).

The Mancos sandstone reservoirs are described below.

Tocito Sandstone Lentil of Mancos Shale

The Tocito sandstones are the primary oil reservoirs in the basin, rest at different positions on the Coniacian unconformity, and become younger from north to south (Molenaar, 1973; Molenaar, 1977a; Nummedal and Molenaar, 1995; Jennette and Jones, 1995; Nummedal and Riley, 1999). Some of the sandstone beds appear to be composites, with upper and lower sandstone separated by an unconformity (Nummedal and Riley, 1999; Valasek, 1995). The depositional history of Tocito sandstones is quite complex and controversial. The sandstones form elongate northwest- to southeast-trending sandstone lenses (pls. 1 and 2) and are found mostly in the central and northern part of the basin east and north of the line that defines the regional truncation of the Gallup Sandstone (fig. 3). They have been interpreted as lowstand sandstones (Hart, 1997), remnants of tidal deltas, transgressive sand ridges (Valasek, 1995; Nummedal and Riley, 1999), and incised valley fill (Jennette and Jones, 1995).

Tocito reservoirs consist of heterolithic facies that may be as much as 45 ft thick in the subsurface. The lowermost lithofacies consist of bioturbated, muddy, glauconitic, fine-grained sandstone; burrowed and bioturbated sandstone; and crossbedded sandstone (Nummedal and Riley, 1999). The uppermost lithofacies comprise burrowed fine-grained sandstone; crossbedded sandstone; ripple-bedded sandstone; and poorly sorted, medium- to coarse-grained, glauconitic, and locally, pebbly sandstone (Tillman, 1985; Jennette and others, 1991; Jennette and Jones, 1995; Nummedal and Riley, 1999). Reservoir properties of Tocito sandstones are summarized in table 1.

“Gallup” Sandstone of Mancos Shale

The interbedded sandstone, siltstone, and shale sequence that overlies the Tocito has been called the El Vado Sandstone

Member of the Mancos Shale by Fassett and Jentgen (1978) and Fassett (1991) and the “Gallup” sandstone by industry; it ranges between 100 and 700 feet thick in the basin. This “Gallup” interval, which lies above the regional Coniacian age unconformity, is not genetically equivalent to the type Gallup Sandstone, which lies below that unconformity. However, industry and IHS Energy (2001) use this term for these beds when reporting formation tops and production data in the basin. The type El Vado, as originally defined on the east side of the San Juan by Landis and Dane (1967), is a more restricted unit than that defined in the subsurface (Fassett and Jentgen, 1978; Fassett, 1991). The El Vado used in this report (pls. 1 and 2) follows the definition of Landis and Dane (1967).

The “Gallup” sequence was reinterpreted to comprise a lower transgressive wedge of sediment that is overlain by a regressive wedge of sediment (fig. 3; pls. 1 and 2) (Ridgley, 2001a). The units within the transgressive wedge were deposited during an overall sea-level rise. Although the stratal relations of the rocks in the transgressive wedge reflect deposition during transgression, the individual genetic packages were deposited during periods of regression as fluviially derived sediment from the south was deposited and redistributed in the marine environment. The overall rise in sea level that accompanied transgression appeared to have been punctuated by periodic stillstands during which greater concentrations of sandstone or sandstone mixed with shale accumulated in neritic environments closer to the shoreline. Therefore, these stillstands can be used to define areas of greater sandstone concentration that might be better reservoirs. In the northeastern part of the San Juan Basin, these sandstone trends are elongate northwest–southeast and subparallel to the inferred paleoshorelines, which overstepped each other in a southerly direction. This overstepping results in a thicker wedge of transgressive sediments in the northern part of the study area and a thinner wedge of transgressive sediments in the southern part of the study area. Cores from the transgressive wedge of sediment show this sequence to consist of stacked parasequences comprising interbedded black shale, silty mudstone, and fine-grained, carbonaceous, very bioturbated, fossiliferous sandstone (Ridgley, 2001a). Locally, “dead” oil coats fossil fragments.

The regressive wedge of sediments includes the El Vado Sandstone Member of the Mancos Shale (pls. 1 and 2) in the lower part and an unnamed sandy and silty sequence above. Sandstones in the type El Vado are fine grained, calcareous, and locally rippled or crossbedded. Sandstone is most prominent in the upper half of the member, whereas siltstone is more abundant in the lower half where it is interbedded with shale. Sandstone beds in the upper half, as observed in core, tend to be thicker compared to those of the underlying transgressive wedge, which are more carbonaceous, and the sedimentary structures are better developed. The increased sand content in the El Vado, compared to that in the underlying transgressive wedge, suggests a closer proximity to the sediment source. The El Vado was deposited as offshore sandstones during

progradation of part of the Dalton Sandstone Member of the Crevasse Canyon Formation (fig. 3) (Ridgley, 2001a).

Overlying the El Vado Member is 300 to 400 ft of thin sandstone and siltstone interbedded with shale, making up the upper part of the subsurface El Vado of Fassett and Jentgen (1978) or “Gallup” of industry. These units lie stratigraphically below the deeper water facies of the marine Satan Tongue of the Mancos Shale (fig. 3). Core from the lower half of this interval shows the Mancos Shale to consist of carbonaceous, wavy to hummocky crossbedded sandstone that is interbedded with thin black shale. This sandstone sequence is similar to the sandstones found in the underlying El Vado Sandstone Member. The pattern of deposition of this sandstone succession indicates deposition in distal marine environments probably during continued regression of the Dalton Sandstone Member. The upper part of the basal 300 to 400 ft contains less sandstone and proportionally more shale. The change from greater sand to less sand marks the turn-around point between the regressive Dalton and the transgressive Hosta Tongue of the Point Lookout Sandstone. This unnamed part of the Mancos produces both oil and gas (pls. 1 and 2) (Ridgley, 2001a). Fractures are important in production of oil and gas in this interval of the Mancos as well as in other “Gallup” units (Gorham and others, 1977; Emmendorfer, 1992). Table 1 contains a summary of reservoir properties of “Gallup” reservoirs.

Sandstone Reservoirs in Upper Part of Mancos Shale

The Mancos Shale above the El Vado ranges in thickness from 700 ft in the southern part of the basin to over 1,100 ft in the northern part (fig. 3). The increase in thickness is related to the stratigraphic rise of the base of the Point Lookout Sandstone of the Mesaverde Group. Regionally, the top of the Mancos Shale is transitional with the overlying Point Lookout Sandstone of the Mesaverde Group, with sandstones gradually increasing in thickness up to the base of the Point Lookout Sandstone described below. This transition interval represents distal equivalents to Point Lookout shoreface sandstones that were deposited farther to the southwest, and could be prospective targets for gas in the deeper part of the basin where the Point Lookout is also productive.

Mesaverde Group

Reservoir rocks that could have had their gas or oil accumulations sourced from the Menefee Formation of the Mesaverde Group include from oldest to youngest, sandstones in the Point Lookout Sandstone, sandstones and coal in the Menefee Formation, and sandstones in the Cliff House Sandstone (figs. 2, 3, and 9), which together compose the Mesaverde Group. The lower half of the Mesaverde Group (Point Lookout and lower part of Menefee) was deposited as a generally progradational package of terrestrial, coastline, and shallow marine sediments that shifted from southwest to

northeast. The upper half of the Mesaverde (upper part of the Menefee and the shallow-marine Cliff House Sandstone) was deposited in a time of overall southwestward transgression.

Although the Cliff House Sandstone interfingers with the Lewis Shale (of the Lewis Shale TPS) (fig. 2), most of the production in the Cliff House is reported (IHS Energy, 2002) as Mesaverde. For this reason, it was impossible to separate Cliff House production from that of other formations of the Mesaverde Group. Therefore, in the 2002 National Oil and Gas Assessment of the San Juan Basin, reservoirs and production in the Cliff House have been included in the Mancos-Menefee TPS. However, production from the Charca sandstone (unit of industry usage that is part of the Cliff House Sandstone) and La Ventana Tongue of the Cliff House Sandstone (figs. 2 and 3) are reported separately (IHS Energy, 2002), and thus, those units were arbitrarily included in the Lewis Shale TPS, even though the units are considered part of the Cliff House Sandstone.

Point Lookout Sandstone

The Point Lookout Sandstone transitionally overlies the Mancos Shale; thin sandstone beds in the transition interval gradually become thicker, coarser grained, and more abundant upward, and the contact is placed where sandstone becomes the dominant lithology. The upper part of the Point Lookout consists of massive, lenticular sandstone beds. A sequence stratigraphic model applied to the Mesaverde has shown that the Point Lookout is composed of a complex assemblage of depositional units, some more favorable than others as hydrocarbon reservoirs (Katzman and Wright-Dunbar, 1992; Wright-Dunbar and others, 1992; Wright Dunbar, 2001). Reservoir quality is thought to be best in shoreface, foreshore, and estuarine sandstones that

1. have the highest original porosity and permeability,
2. pinch out landward into nonmarine mudrocks, and
3. are capped by a sequence boundary (Wright Dunbar, 2001).

The Point Lookout is present across most of the study area, ranging in thickness from about 40 to over 400 ft (Craig, 2001). It is composed of very fine to medium-grained sandstone beds occurring in NW.-SE. aligned lenses 30–50 ft thick, cemented with calcite and iron oxide (Wright Dunbar, 2001). Calcite cement is present in amounts as much as 25 percent (Loomis and Crossey, 1993) and is a major control on porosity. The Point Lookout appears to be absent, either from nondeposition or by post-depositional erosion, in some places, especially in an oblong area extending from T. 33 N., R. 11 W. in Colorado to T. 31 N., R. 6 W. in New Mexico. Cross sections by Molenaar and others (2002) show thickening and thinning of the unit (fig. 9). In general, beds of the Point Lookout Sandstone are thinner, have higher shale content, and are poorer hydrocarbon reservoirs than sandstones of the Cliff House, which are discussed below (Raynolds and Pasternack, 1994).

C
SOUTHWEST ←
Gallup area ←

STAGE	part	MOLLUSCAN FOSSIL-ZONE	STAGE	part	MOLLUSCAN FOSSIL-ZONE	
Maas.	upper	1 <i>Jeletzkyites nebrascensis</i> 2 <i>Hoploscapites nicolleti</i> 3 <i>Hoploscapites birkebeandi</i> 4 <i>Baculites clinolobatus</i> 5 <i>Baculites grandis</i> 6 <i>Baculites baculatus</i> 7 <i>Baculites eliasi</i>	Turonian	lower	38 <i>Prionocyclus germari</i> 40 <i>Scaphites nigricollis</i> 41 <i>Scaphites whitfieldi</i> 42 <i>Scaphites ferronensis</i> 43 <i>Scaphites warreni</i> 44 <i>Prionocyclus macombi</i> 45 <i>Prionocyclus lyatti</i> 46 <i>Prionocyclus praecox</i> 47 <i>Colligoniceras woodguri</i> 48 <i>Monanites nodosoides</i> 49 <i>Vaccoceras birchbyi</i> 50 <i>Pseudosiphoceras flexuosum</i> 51 <i>Wainoceras devonense</i>	
	lower	8 <i>Baculites jenseni</i> 9 <i>Baculites resisideri</i> 10 <i>Baculites canalicatus</i> 11 <i>Baculites compressus</i> 12 <i>Dalymoceras cheyennense</i> 13 <i>Exelhoceras jenneyi</i> 14 <i>Dalymoceras stevensoni</i> 15 <i>Dalymoceras nebrascense</i> 16 <i>Baculites scotti</i> 17 <i>Baculites reducius</i> 18 <i>Baculites gregoryensis</i> 19 <i>Baculites perplexus</i> 20 <i>Baculites</i> sp. (smooth) 21 <i>Baculites asperiformis</i> 22 <i>Baculites nictarini</i> 23 <i>Baculites obtusus</i> 24 <i>Baculites</i> sp. (weak flank ribs) 25 <i>Baculites</i> sp. (smooth)		middle	52 <i>Nigriceras scotti</i> 53 <i>Neocidoceras judithi</i> 54 <i>Burroceras clydensi</i> 55 <i>Euomphaloceras septemseriatum</i> 56 <i>Vaccoceras diartianum</i> 57 <i>Durvegoceras conditum</i> 58 <i>Durvegoceras albertense</i> 59 <i>Durvegoceras problematicum</i> 60 <i>Durvegoceras pondi</i> 61 <i>Plesianthoceras wyomingense</i> 62 <i>Acanthoceras amphitelum</i> 63 <i>Acanthoceras bellense</i> 64 <i>Acanthoceras muldonense</i> 65 <i>Acanthoceras granroense</i> 66 <i>Coninoceras tarantense</i>	
	middle	26 <i>Scaphites hippocrepis</i> III 27 <i>Scaphites hippocrepis</i> II 28 <i>Scaphites hippocrepis</i> I 29 <i>Scaphites</i> sp. III		upper	67 <i>Neogastropiles macdurni</i> 68 <i>Neogastropiles americanus</i> 69 <i>Neogastropiles muelleri</i> 70 <i>Neogastropiles cornutus</i> 71 <i>Neogastropiles huasi</i> 72 <i>Inoceramus boltonensis</i> 73 <i>Inoceramus comancheanus</i>	
	lower	30 <i>Desmocapites hassleri</i> 31 <i>Desmocapites erdmanni</i> 32 <i>Chiocapites chiotanensis</i> 33 <i>Chiocapites variformis</i> 34 <i>Chiocapites siccitanicus</i>		middle	(Gap in biostratigraphic record)	
	Santonian	upper		35 <i>Scaphites depressus</i> 36 <i>Scaphites ventricosus</i> 37 <i>Forresteria alhuadzi</i> 38 <i>Forresteria hobsoni</i>	lower	67 <i>Neogastropiles macdurni</i> 68 <i>Neogastropiles americanus</i> 69 <i>Neogastropiles muelleri</i> 70 <i>Neogastropiles cornutus</i> 71 <i>Neogastropiles huasi</i> 72 <i>Inoceramus boltonensis</i> 73 <i>Inoceramus comancheanus</i>
		middle				
		lower				
Comanchian	upper		upper			
	lower		lower			

[Maas. = Maastrichtian; low. = lower; mid. = middle; up. = upper; pt = part]

- EXPLANATION**
- Formation or member contact
 - Contact that rises (uniformly or abruptly) in stratigraphic position. Queried where uncertain
 - - - Contact, position is uncertain
 - ~?~ Unconformity—Queried where uncertain
 - SP Spontaneous-potential curve
 - GR Gamma-ray curve
 - R Resistivity curve
 - KB Kelly bushing
 - (proj) Projected position of macrofossil from nearest outcrop

Borehole depths shown are in thousands of feet below altitude of Kelly bushing except for boreholes where igneous sills have been removed. Also note that only partial logs of boreholes are shown; upper and lower parts of logs are omitted where they are not applicable to this study.

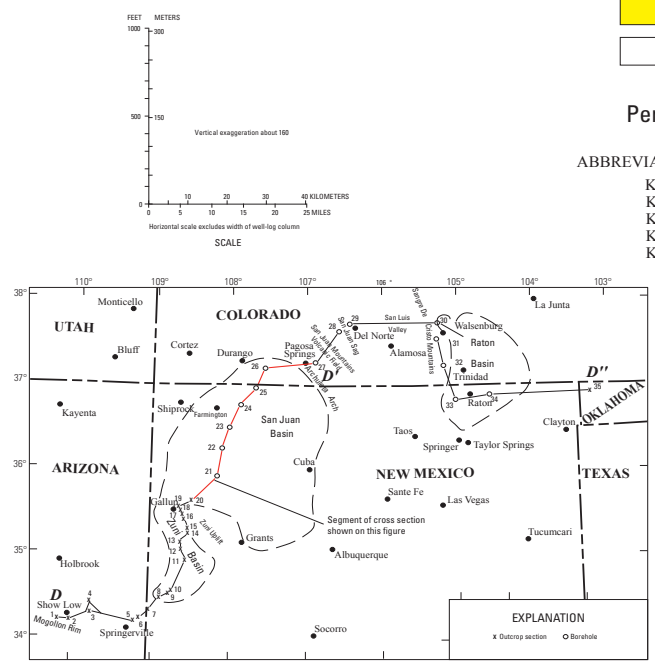
FACIES COLORS FOR CRETACEOUS ROCKS

- Nonmarine strata (various formations)
- Marine and coastal sandstone
- Dominantly marine shale and siltstone

Percent Ro values in red

ABBREVIATIONS FOR STRATIGRAPHIC UNITS

- Kk Kirtland Shale
- Kl Lewis Shale
- Kch Cliff House Sandstone
- Kpl Point Lookout Sandstone
- Km Mancos Shale



INDEX MAP SHOWING LOCATION OF CROSS SECTIONS

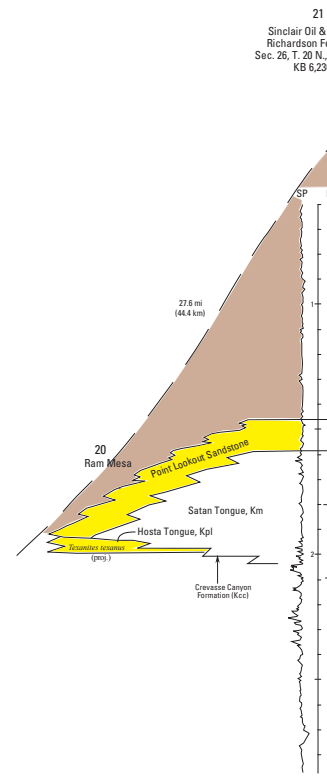
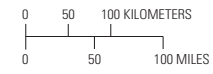
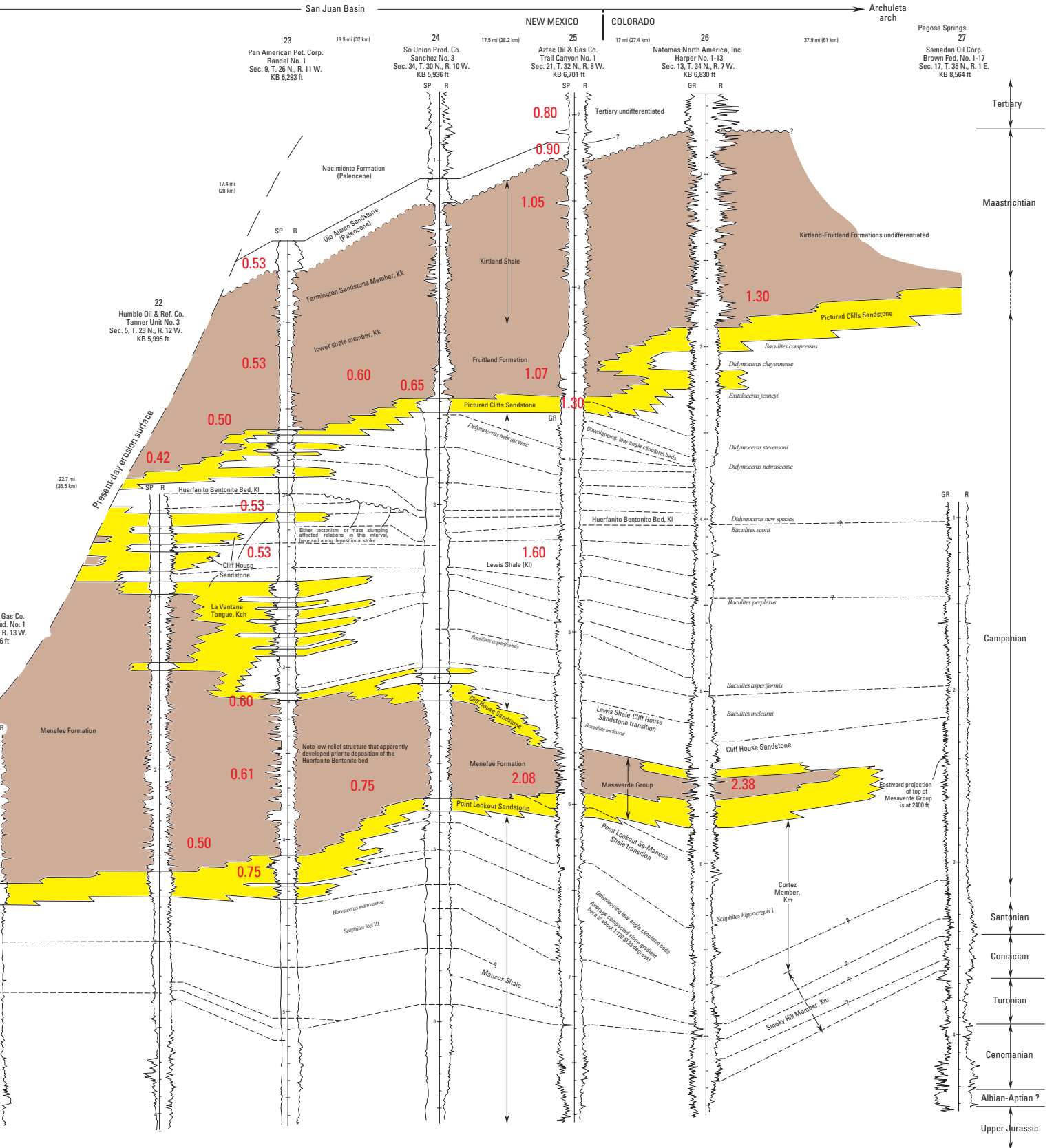


Figure 9. Cross section extending from southwest to northeast across the central part of the San Juan Basin, Colorado and New Mexico (modified from Molenaar and others, 2002).

C
NORTHEAST



Menefee Formation

The Menefee Formation overlies the Point Lookout conformably in places, but in other places this contact is an unconformable sequence boundary (Wright Dunbar, 2001). The Menefee is over 2,000 ft thick (fig. 4) just north of its outcrop belt, and it thins northeastward and pinches out between the Point Lookout and Cliff House Sandstones in the Pagosa Springs area (Zapp, 1949). It was probably originally thicker in some areas in the south part of the basin, but late Cenozoic erosion has removed much of the unit there. The formation crops out around the perimeter of the San Juan Basin, except on the far northeast side, where it pinches out between the Cliff House and Point Lookout Sandstones (Aubrey, 1991). Coal beds and other carbonaceous strata (including humate) in the Menefee acted as source rocks for at least some of the gas in the Mesaverde. Coal may also serve as reservoir rocks. Isolated and amalgamated sandstone beds formed in fluvial channels occur throughout the formation and are also potential reservoir rocks. Some fluvial-channel sandstone units at the base of the Menefee were deposited in back-filled valleys incised into the Point Lookout Sandstone (Wright Dunbar, 2001). Most channels were deposited on alluvial plains in a meandering fluvial system (Siemers and Wadell, 1977); these sandstones are encased in overbank mudrocks. Fluvial channel sandstones are typically fine to coarse grained, have a clay matrix, and are variously cemented with calcite, iron oxide, or silica (Craig, 2001). Channel sandstone thickness ranges from 6–15 ft (Siemers and Wadell, 1977).

Cliff House Sandstone

The Cliff House Sandstone disconformably overlies the Menefee, although some intertonguing has been noted (Fassett, 1977; Beaumont and Hoffman, 1992). The transgressive flooding surface that separates the Menefee and Cliff House is marked by a lag deposit containing sharks' teeth, shells, wood fragments, and rip-up clasts cemented with silica

(Wright Dunbar, 2001). Above the lag deposit, the Cliff House consists of very fine to fine-grained, very well to well-sorted, calcite- or silica-cemented sandstone and common mudrock interbeds (Craig, 2001). The Cliff House is poorly developed in some areas of the basin, especially in the north-central part. Molenaar and others (2002) (see well 25 on figure 9) consider it missing in some wells in the northern part of the basin, and this was verified for this report by examining well logs in that area. Thicknesses as much as 400 ft are reported in Mesaverde National Park (Aubrey, 1991). In much of the New Mexico part of the basin, the Cliff House is well developed. Upper tongues of the Cliff House (La Ventana Tongue and Chacra sandstone of industry usage, fig. 2) are thick units that are included in the assessment of the Lewis Shale TPS. Table 2 shows characteristics of Mesaverde reservoir rocks.

Hydrocarbon Source Rocks

The Mancos-Menefee TPS contains two potential hydrocarbon source rock intervals. These are carbonaceous shale in the Mancos Shale and carbonaceous shale, coal, and humate beds in the Menefee Formation. Carbonaceous shale and coal beds in the Dakota Sandstone may locally contribute to hydrocarbon generation, but these are considered to be of minor importance.

Mancos Shale Source Rock Characterization

The Upper Cretaceous Mancos Shale is the source of most of the oil and gas found in reservoir rocks in the stratigraphic interval bounded by the nonmarine Dakota Sandstone at the base and the Point Lookout Sandstone of the Mesaverde Group at the top (figs. 2 and 3) (Ross, 1980; Rice, 1983). Deposition of the Mancos Shale extended far beyond the area of the San Juan Basin. In this 2002 assessment of the San Juan Basin, the extent of Mancos source beds has been limited to coincide with the San Juan Basin Province boundary

Table 2. Characteristics of Mesaverde Group reservoir rocks and oil and gas data compiled from Prichard (1973) and from field descriptions in Fassett (1978a,b, 1983a) for units assigned to the Mesaverde Updip Conventional Oil Assessment Unit and Mesaverde Central-Basin Continuous Gas Assessment Unit. Reported minimums (min) and maximums (max) are shown; calculated averages (avg) are not shown when there were fewer than five values reported. Fluid pressure gradients were calculated from bottom-hole pressures and bottom-perforated depth.

[%, percent; psi, pounds per square inch; ft, feet; --, not applicable]

		Porosity (%)	Permeability (millidarcies)	Water saturation (%)	Fluid pressure gradient (psi/ft)	Oil API gravity (degrees)	Nitrogen (%)	CO ₂ (%)	Net pay (ft)
Gas-producing sandstones	min	4	0.02	30	0.40	33	0.01	0.6	10
	max	25	6	65	0.45	60	0.5	3	200
	avg	12	2	44	--	--	--	--	63
Oil-producing sandstones	min	15	2.5	40	0.23	29.7	5.11	0.14	5.5
	max	29	400	85	0.43	46	5.9	0.4	30
	avg	22	211	53	0.34	38.7	--	--	13.5

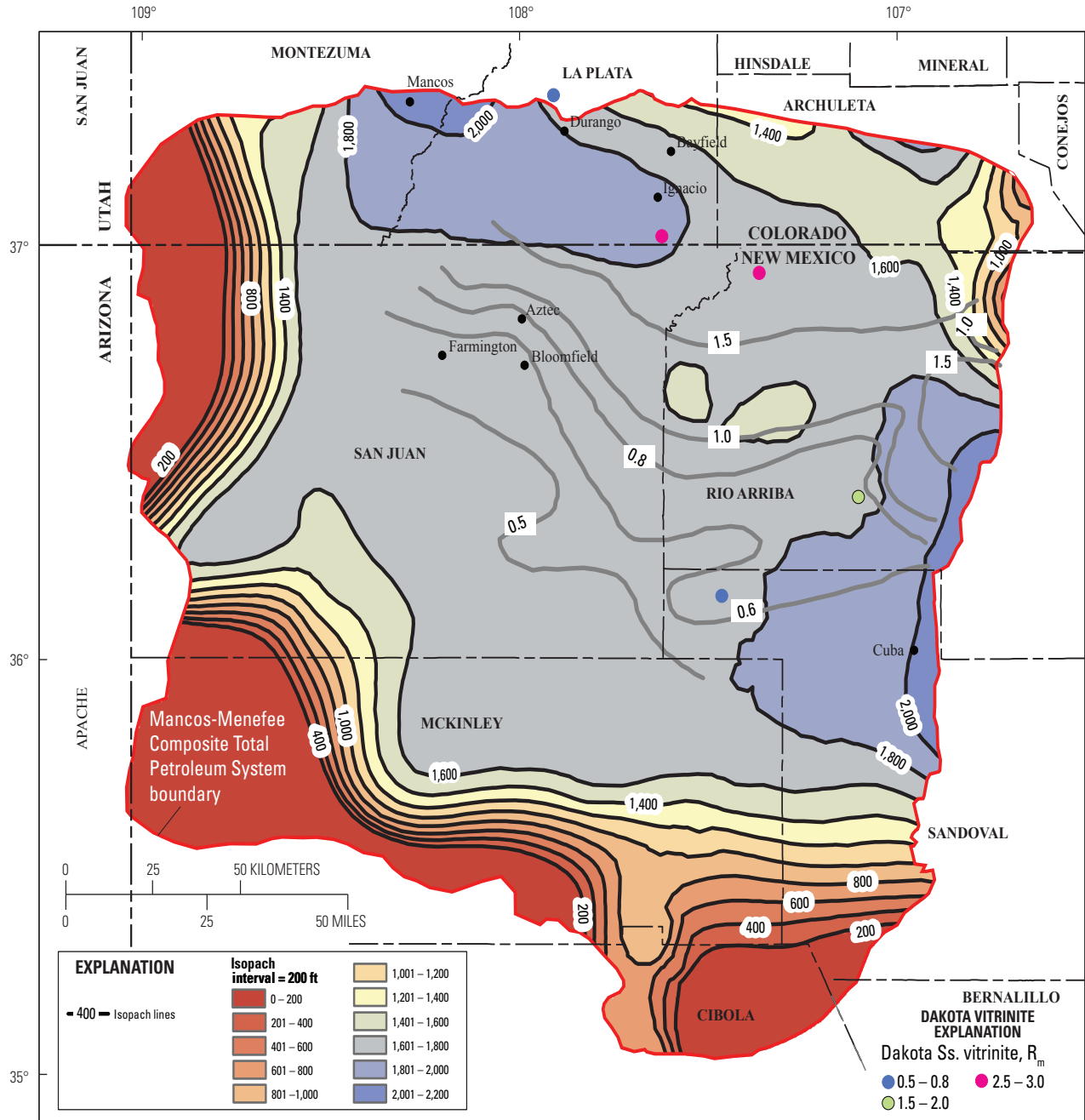


Figure 10. Isopach map of the Mancos Shale in the San Juan Basin, Colorado and New Mexico, using data from IHS Energy Group (2002). Isopach interval, 200 ft. Menefee Formation maturity contours (in gray) show vitrinite reflectance (R_m) values, in percent, using data from Fassett and Nuccio (1990), Law (1992), and Ridgley (2001b). Isolated R_m vitrinite data from shale or coal in the Dakota Sandstone (colored dots) are from Fassett and Nuccio (1990) and C. Threlkeld (written commun., 2001).

(figs. 1 and 4). The Mancos Shale intertongues with thick nearshore marine sequences of the Dakota Sandstone, Gallup Sandstone, and Dalton Sandstone Member of the Crevasse Canyon Formation in the southern and southwestern areas of the San Juan Basin (fig. 3). The shale beds are of marine origin.

A generalized regional isopach map of the Mancos was constructed using the reported top of the Mancos and the top of the Greenhorn (Bridge Creek) Limestone Member of the Mancos Shale (IHS Energy Group, 2001) (fig. 10). The top of the Greenhorn was used because it is well expressed in geophysical logs, and the unit is found throughout the San Juan Basin. The isopach map does not include the Mancos that intertongues with the Dakota and may include, in some areas, sandstone intervals that belong to the Gallup or Dalton. This generalized isopach map can, however, be used to examine relative thickness of potential Mancos source rocks in the TPS. As shown in figure 10, the Mancos ranges in thickness from less than 100 ft to over 2,000 ft. Thin Mancos on the southern and southwestern margin of the TPS is related to intertonguing of the Mancos, Gallup, and Dalton units, whereas thin Mancos in the northwest and northeast parts of the TPS is due to erosion. In the latter areas, the Mancos outcrops and the thickness correspond to erosional remnants. The greater thickness of the Mancos in the northern and eastern parts of the TPS reflects the greater stratigraphic separation between the Greenhorn and the Point Lookout as a result of the stratigraphic rise of the Point Lookout Sandstone during regression. The top of the Mancos is time transgressive.

Menefee Formation Source Rock Characterization

Potential hydrocarbon source beds in the Menefee Formation part of the TPS lie above the Point Lookout Sandstone and below the Cliff House Sandstone of the Mesaverde Group (figs. 2 and 3). The source rocks consist of coal, carbonaceous shale, and humate beds. These beds may be a source of some of the oil and gas produced from reservoirs in the Menefee part of the TPS, although a study (Ross, 1980) of a few oils produced from Menefee reservoirs suggested that the oils were sourced from the Mancos Shale.

The Menefee has been divided into the Cleary Coal Member at the base of the formation and the overlying Allison Member, which also contains thin, lenticular coal beds, especially in its upper part. The Menefee is thickest in the southwest part of the basin, where it is more than 2,000 ft thick in the subsurface and thins to the northeast (fig. 3). Isopach contours, indicating the thickness of the Menefee, are oriented northwest–southeast parallel to the paleoshoreline and regional structural grain (figs. 3 and 11).

Net thickness of coal beds in the basal Cleary Coal Member is generally less than 30 ft. Beds are lenticular making correlation of individual coal beds from one area to another difficult (Hunt, 1936; Whyte and Shomaker, 1977). In the southwestern part of the basin, only remnants of the Cleary Coal Member are preserved (fig. 3), and coals beds are thinner

than 6 ft (Sears, 1934). In the south-central part of the basin, the coal-bearing Cleary interval is about 1,000 ft thick, with as many as nine coal beds vertically stacked in one section; most are less than 3 ft thick. In the southeastern part of the basin, coal beds as thick as 9 ft are present at the base and near the top of the formation. However, most coal beds are 5 ft thick or thinner (Dane, 1936). The Hogback Mountain tongue, an informal unit of the Menefee located at the top of the formation (Whyte and Shomaker, 1977), interfingers with the La Ventana Tongue of the Cliff House Sandstone and contains the most abundant coal in the Menefee. It has from 3 to 18 individual coal beds, which are from 1 to 8 ft thick (Beaumont and Roybal, 1989).

In the northern part of the basin, the Menefee is also characterized by abrupt lateral changes in lithology (Zapp, 1949). As in the south, coal beds in the northern part of the basin are more abundant in the upper and lower parts of the formation, separated by a barren interval. Coal beds attain a maximum observed thickness of 9 ft in this region, but most thicknesses are between 3 and 6 ft (Zapp, 1949). Throughout the basin, Menefee coal beds are interbedded with sandstone beds, fluvial channels and crevasse splays, and overbank mudrocks.

The Menefee was estimated to contain 12 billion tons of coal in beds thicker than 2 feet at depths from 250 to 4,000 ft (Whyte and Shomaker, 1977). Nearly 11.3 billion tons are in the Hogback Mountain tongue, which is also known as the upper coal member (Beaumont and Hoffman, 1992). In a large part of the central basin, coal in the Menefee is deeper than 4,000 ft, which would increase the estimate if coals in this area were included. Coal in the area north of the 0.5-percent R_m vitrinite isoreflectance contour (fig. 11) has probably generated gas (Tissot and Welte, 1978). Heating value ranges from 9,550 to 14,940 BTU per pound, and ash content averages 12 percent (Whyte and Shomaker, 1977). The coal has a low sulfur content, from less than 1 to 3.5 percent, averaging 1.5 percent. The coal rank increases northward in the basin, ranging from subbituminous A in the Standing Rock area (approximately T. 17 N., R. 9 W.) to high-volatile C bituminous in the La Ventana area (T. 19 N., R. 1 W.) (fig. 11), and is probably higher in the deeper part of the basin. The coal along the north rim of the basin is high-volatile A bituminous. At outcrop, these coal beds display good cleat development (Siemers and Wadell, 1977).

A lithology in the Menefee, possibly important to the generation of hydrocarbons, is humate. Humate is found throughout the Menefee, both in association with coal beds and in the so called ‘barren’ parts of the formation (Shomaker and Hiss, 1974; Siemers and Wadell, 1977). Humate is dark-brown to brownish-gray mudstone that contains abundant wood and plant material and was deposited in moderately to poorly drained swamps that received an abundant influx of clay and organic matter (Siemers and Wadell, 1977). It occurs in thin beds, 1–5 ft thick, interbedded with noncarbonaceous mudstone, coal, or sandstone. Humate composes about 8–12 percent of the Menefee in sections measured on the southeast side of the basin (Siemers and Wadell, 1977). Overall, Shomaker and Hiss (1974) estimated that “many millions, probably billions” of tons of humate are in Upper Cretaceous rocks of the San Juan Basin, much of it in the Menefee Formation.

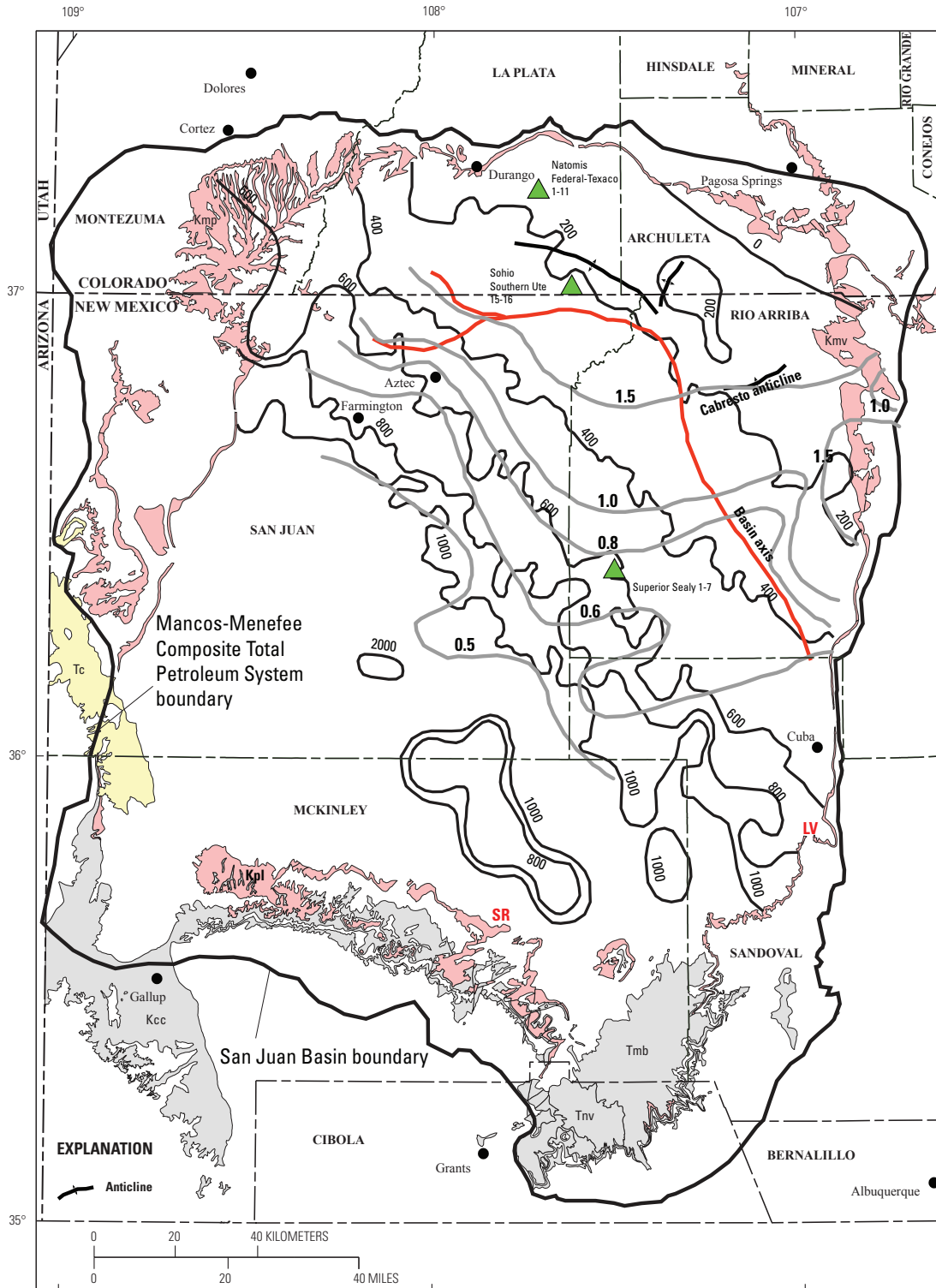


Figure 11. Isopach map of the Menefee Formation in the San Juan Basin, Colorado and New Mexico, using data from IHS Energy Group (2001). Isopach interval, 200 ft. Menefee maturity contours (in gray) show vitrinite reflectance (R_m) values, in percent, contoured using data from Fassett and Nuccio (1990), Law (1992), and Ridgley (2001b). Also shown are locations of the wells (green triangles) used to construct the burial history curves found in this report (figs. 15A–C). Geologic units are from Green (1992) and Green and Jones (1997); Tc, Tertiary Chuska Sandstone; Tnv, Tertiary Neogene volcanics; Tmb, Tertiary Miocene volcanics; Kcc, Crevasse Canyon Formation; Kmp, Menefee Formation and Point Lookout Sandstone; Kmv, Mesaverde Group; Kpl, Point Lookout Sandstone. SR, Standing Rock; LV, La Ventana.

Geochemical Characteristics

The type of organic matter and its thermal maturity in the source rocks, as represented by the hydrogen indices, will determine whether oil, wet gas, or dry gas will be produced (table 3).

Mancos Shale

Geochemical data for the Mancos Shale is limited. The most definitive study of the Mancos has been in the neighboring San Juan sag, located to the northeast of the Chama platform (fig. 4) (Gries and others, 1997). Data from that study indicated that the Mancos Shale is a potential source rock for oil; it contained type-II organic matter in some intervals. Total organic carbon values (TOC) were reported to range from 0.4 to 3.1 weight percent. Similar conclusions were reached by Ridgley (2001a) based on Rock-Eval pyrolysis analysis of 13 samples from the Mancos Shale in the eastern part of the San Juan Basin. In that study, TOC values range from 0.86 to 2.68 weight percent. Both studies showed vertical variation in TOC content. Hydrogen indices for Mancos shales range from 113 to 384 in San Juan Basin samples and from 11 to 486 in San Juan sag samples. Hydrogen indices for intervals of Mancos Shale are higher than for other possible source rocks evaluated in the Menefee Formation, indicating that these intervals are source rocks for oils found primarily in Mesaverde and older Cretaceous reservoirs. Geochemical data from various sources are summarized in table 3.

Menefee Formation

Ridgley (2001b) presented Rock-Eval data from the Menefee Formation on the eastern side of the basin that has a bearing on the hydrocarbon-generating capacity of the Menefee. Analyses of carbonaceous shale from one outcrop and three core samples ranged from 4.2- to 13.0-percent TOC and one coal sample had a TOC of 73.3. These TOC values are within the range conducive to hydrocarbon generation.

The hydrogen index of these samples ranged from 86 to 218, indicative of type-III organic matter, and the coal and shale would be expected to have produced mostly gas, rather than oil. Total organic carbon content of Menefee humate beds is not known, but it can be inferred that the Menefee contains a significant volume of this organic-rich, terrestrial-derived material that contributed an unknown amount of gas and possibly some oil to the Menefee part of the Mancos-Menefee TPS. Table 3 shows generalized geochemical characteristics of samples from the Menefee. Although it may be impossible to type gas in the Mesaverde back to its source, the carbonaceous shale and coal in the Menefee can be expected to produce oil or wet gas and/or dry gas depending on the thermal maturity of the organic matter.

Gas Chemistry

Both associated and nonassociated gas occurs in the Mancos-Menefee TPS. Rice (1983) reported that associated gas was chemically wetter (gas that contains greater than 1-percent ethane and higher molecular weight hydrocarbons) and isotopically lighter than nonassociated gas. These observations were based on gas samples from the Dakota Sandstone, Tooto Sandstone Lenticle of the Mancos Shale, and Mesaverde Group. Natural gas compositions for the major producing reservoir intervals are summarized in table 4. Gas wetness, where wetness (percent) = $100 \times (1 - [\text{mol}\%C_1 / \sum \text{mol}\%C_1 - C_5])$, CO₂ content, and methane $\delta^{13}\text{C}$ composition for the Mesaverde Group and Dakota Sandstone gases are similar. Gases from Gallup Sandstone, Graneros Shale, and Tooto Sandstone Lenticle reservoirs are wetter and contain methane with more negative $\delta^{13}\text{C}$ (table 4).

For most gases from Dakota Sandstone reservoirs, relations exist between gas wetness, methane $\delta^{13}\text{C}$, and CO₂ content. As methane $\delta^{13}\text{C}$ becomes more positive, gas wetness decreases (fig. 12A) and CO₂ content increases (fig. 13A). For Dakota gases, these compositional parameters are related, in part, to present reservoir depth as shown for gas wetness in figure 14A. In figure 14A, the driest gases (wetness <2 percent)

Table 3. Means, standard deviations, ranges, and number of determinations (n) for total organic carbon contents and hydrogen indices of the Mancos Shale and Menefee Formation in the Mancos-Menefee Composite Total Petroleum System, San Juan Basin, New Mexico. Total organic carbon contents and hydrogen indices are summarized from samples with Tmax < 450°C. Data from Rice and others (1989), Pasley and others (1991), Michael and others (1993), Gries and others (1997), and C. Threlkeld (written commun., 2001).

[%, percent; mg/g, milligrams/gram; HC, hydrocarbons; μ , mean; s, standard deviation]

Interval	Total organic carbon (%)	Hydrogen index (mg/g) (Rock-Eval)	Expected types of HC
Menefee Formation coal	range = 30–73.3 (n = 3)	range = 123–290 (n = 3)	Wet and/or dry gas
Mancos Shale	$\mu = 1.9$, s = 1.0 range = 0.8–5.3 (n = 30)	$\mu = 300$, s = 140 range = 86–620 (n = 30)	Wet and/or dry gas, oil

are mostly found at depths greater than 7,000 ft. Similarly, methane $\delta^{13}\text{C}$ and CO_2 content also show changes with present reservoir depth. Methane $\delta^{13}\text{C}$ becomes more positive and CO_2 content increases with depth, although there is some scatter. The significant scatter shown in figure 14A as well as the scatter in methane $\delta^{13}\text{C}$ and CO_2 content with depth is a likely result of the structural reversal of the basin axis throughout geologic time, subsequent differential erosion in the basin, and possibly some gas migration.

Gas composition relations in Mesaverde Group reservoirs are similar to those shown for Dakota Sandstone reservoirs, with gas wetness decreasing (fig. 12B) and CO_2 content increasing (fig. 13B) as methane $\delta^{13}\text{C}$ becomes more positive. These similarities suggest a common hydrocarbon source rock for the gases produced from these two intervals. Mesaverde gas compositions, in contrast to Dakota gases, do not appear to be related to present reservoir depth (fig. 14B). However, methane $\delta^{13}\text{C}$ and CO_2 contents show slight changes with present reservoir depth. Methane $\delta^{13}\text{C}$ becomes more positive and CO_2 content increases with depth, although there is some scatter. The lack of a relation of gas wetness to depth (fig. 14B) and the scatter in methane $\delta^{13}\text{C}$ and CO_2 contents with depth may also result from the structural reversal of the basin axis throughout geologic time and subsequent erosion in the basin.

Although limited to four methane $\delta^{13}\text{C}$ analyses (table 4) for gases from the Gallup Sandstone, Graneros Shale, and Tocito Sandstone Lentil reservoirs, trends in gas compositions appear similar to those shown for the Dakota Sandstone and Mesaverde Group reservoirs.

Oil Chemistry

Two studies (Ross, 1980; Gries and others, 1997) geochemically characterized the oils from the San Juan Basin and adjacent areas and attributed most of the oils to a Mancos source. Van Delinder (1986) analyzed eight Cretaceous oils in McKinley County, N. Mex. from the Dakota, Gallup, and Menefee reservoirs, but did not ascribe a source. He did, however, suggest that many of these oils had a similar

source based on hydrocarbon compounds, and that differences between some of the oils could be due to degrees of biodegradation. Two different oils, "marine" and "nonmarine," are produced from Cretaceous age reservoirs and can be distinguished by their isoprenoid ratios and carbon-isotope compositions. Most of the produced oils in the San Juan Basin belong to the "marine Cretaceous" group of Ross (1980). These "marine Cretaceous" oils have been produced from reservoirs ranging from the Dakota Sandstone near the base of the Cretaceous section through reservoirs in the Farmington Sandstone Member of the Kirtland Shale above the Fruitland Formation (Ross, 1980).

The "nonmarine Cretaceous" oil of Ross (1980) is limited to the Dakota Sandstone in the extreme west side of the Mancos-Menefee TPS. Ross (1980) considered this oil to have been sourced from the Mesaverde-Lewis interval, based in part on the pristine/phytane ratios of 2.5–2.6, which are indicative of a coaly sequence. The Lewis has no coal beds, but coal beds are found in the Menefee Formation of the Mesaverde Group. Oils from the Dakota in that area (see field descriptions in Fassett, 1978a,b) have high API gravities (51°–60°), which are in the condensate range. The area where these oils are found lies outside or along the margin of the 0.5- R_m vitrinite isorefectance contour in the Menefee (fig. 1) and where the Mancos Shale is at the surface. In order to account for the high API gravities, the oil must have migrated to this area from sources deeper in the basin to the east. Alternatively, local heating during emplacement of intrusions in the area may have thermally altered oil previously emplaced or generated locally. The Dakota in this area probably contains carbonaceous shale and thin coals that were deposited during shifts of the Dakota shoreline to the west. Geophysical logs indicate the presence of shale interbedded with sandstone. Local coals in the Dakota, rather than those in the younger Menefee Formation to the east, could have been the source of the observed pristine/phytane ratios in the oils.

Table 4. Means, standard deviations, and number of analyses (n) of gas wetness, carbon dioxide content, carbon isotope of methane ($\delta^{13}\text{C}_{\text{CH}_4}$) of produced natural gases from reservoirs in the Mancos-Menefee Composite Total Petroleum System, San Juan Basin. Data from Rice (1983); Moore and Sigler (1987); Rice and others (1988); Scott and others (1991); and Threlkeld, (written commun., 2001). Wetness (%) = $100 \times (1 - [\text{mol}\% \text{C}_1 / \sum \text{mol}\% \text{C}_1 - \text{C}_5])$.

[%, percent; PDB, Peedee belemnite; Ss, sandstone; Mbr, member; μ , mean; s, standard deviation]

Producing interval	Wetness (%)	CO_2 (%)	$\delta^{13}\text{C}_{\text{CH}_4}$ (per mil PDB)
Mesaverde Group + Point Lookout Sandstone	$\mu = 10.2, s = 7.3$ (n = 86)	$\mu = 1.3, s = 1.1$ (n = 87)	$\mu = -39.8, s = 3.8$ (n = 48)
"Gallup" Ss. + Graneros Shale + Tocito Lentil of Mancos Shale	$\mu = 17.8, s = 10.4$ (n = 30)	$\mu = 1.2, s = 1.5$ (n = 30)	$\mu = -44.4, s = 6.5$ (n = 4)
Dakota Sandstone + Greenhorn Limestone Mbr. of Mancos Shale	$\mu = 9.7, s = 10.5$ (n = 89)	$\mu = 2.0, s = 1.8$ (n = 93)	$\mu = -36.6, s = 4.6$ (n = 47)

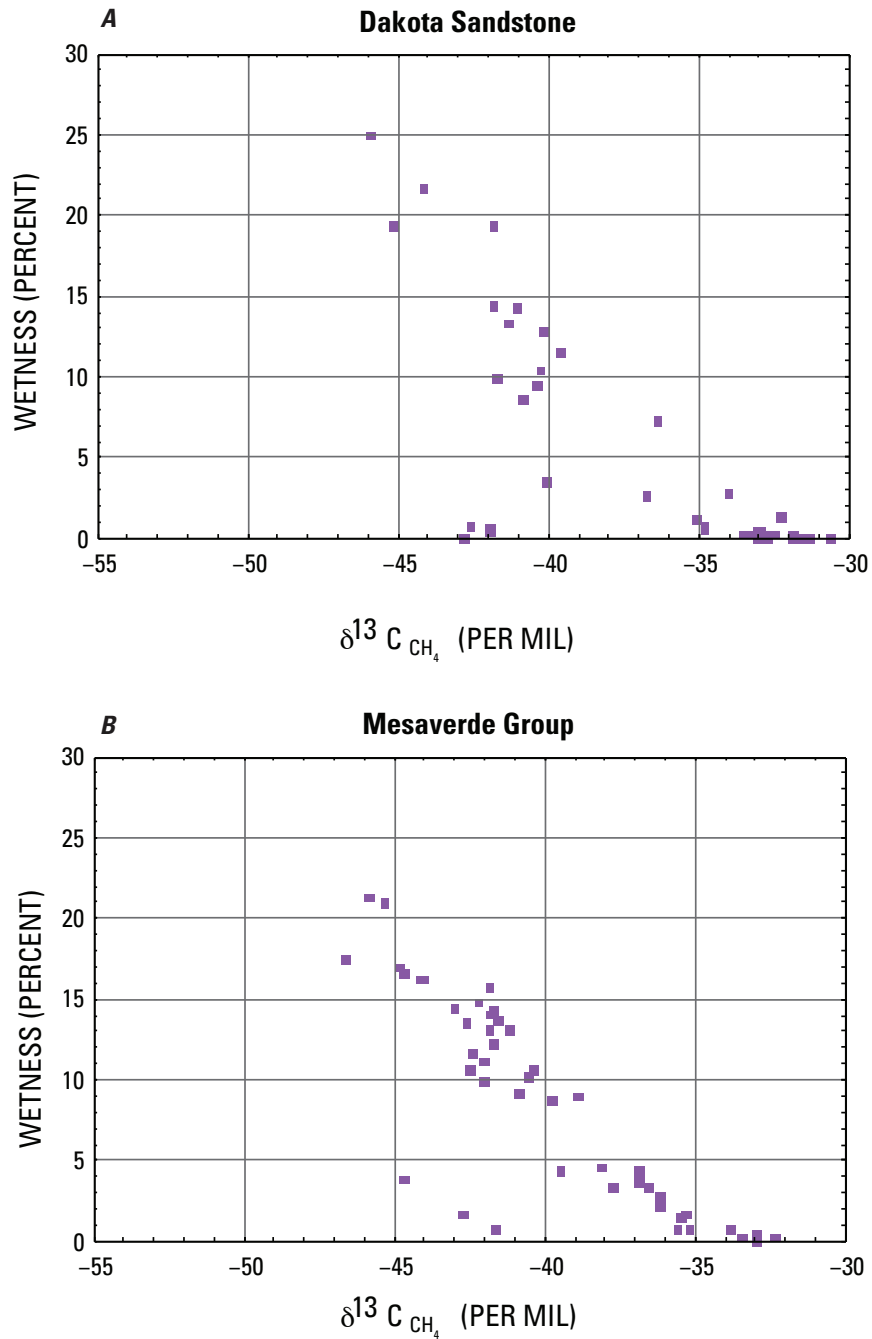


Figure 12. Cross plot showing relation between gas methane $\delta^{13}C$ and gas wetness. Data are from unpublished U.S. Geological Survey Gas Analysis Database (C. Threlkeld, written commun., 2001). (A) Dakota Sandstone, n = 47 samples; (B) Mesaverde Group, n = 48 samples.

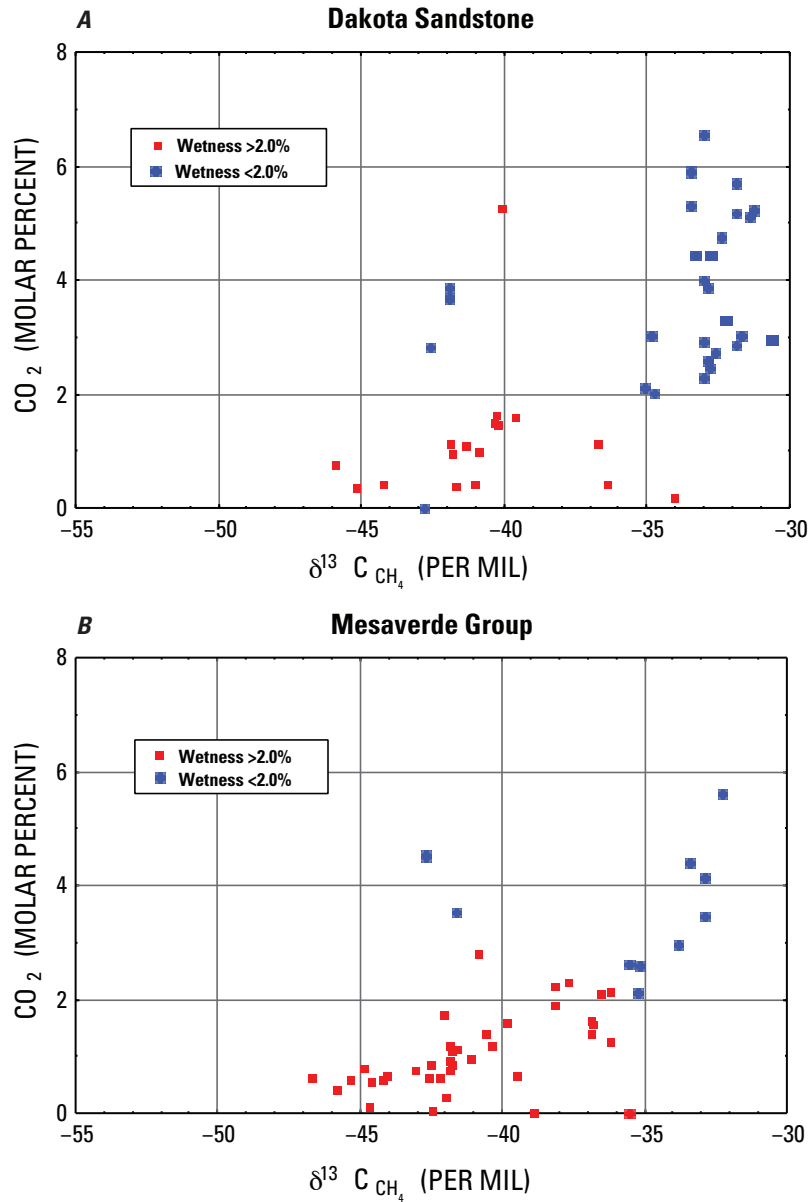


Figure 13. Cross plot showing relation between gas methane $\delta^{13}\text{C}$, CO_2 content, and gas wetness. Data are from unpublished U.S. Geological Survey Gas Analysis Database (C. Threlkeld, written commun., 2001). (A) Dakota Sandstone, $n = 47$ samples; (B) Mesaverde Group, $n = 48$ samples.

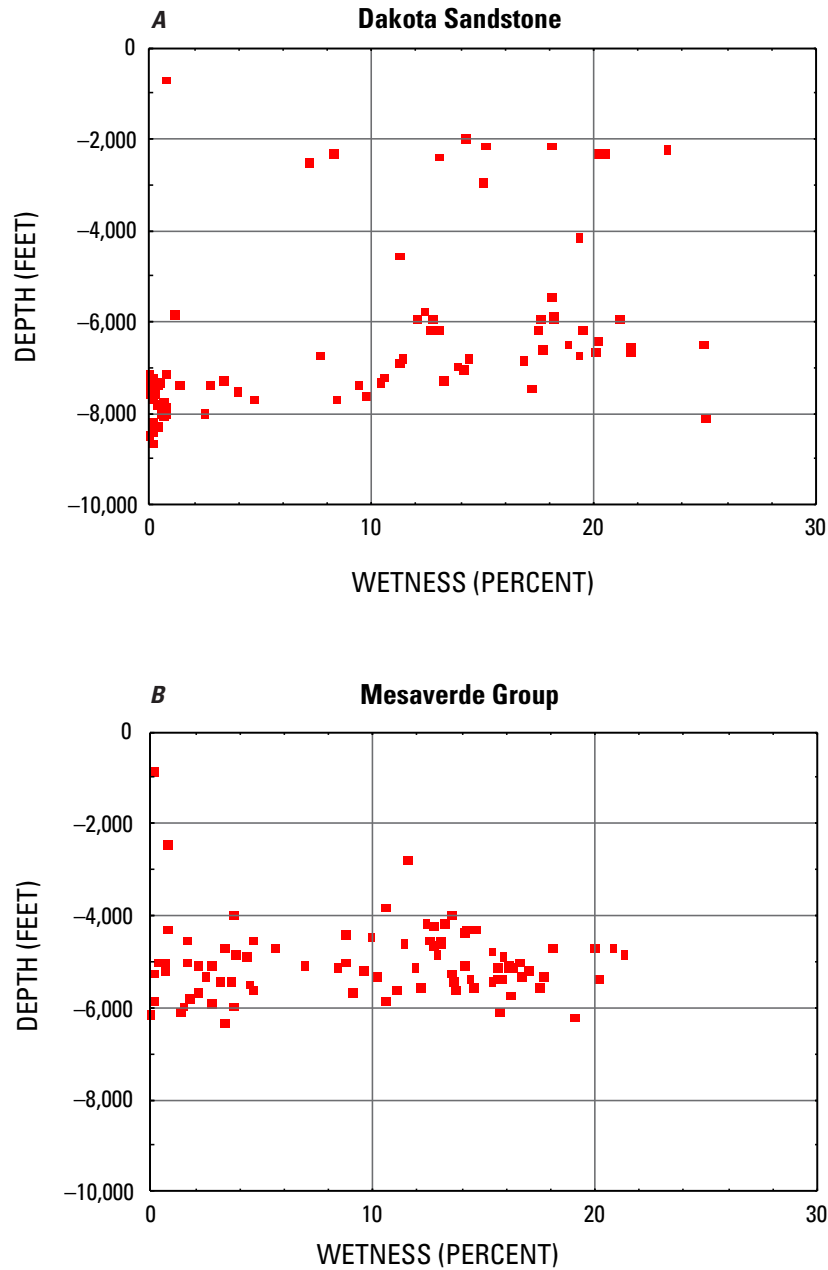


Figure 14. Cross plot showing relation between gas wetness and present reservoir depth. Data are from unpublished U.S. Geological Survey Gas Analysis Database (C. Threlkeld, written commun., 2001). (A) Dakota Sandstone, n = 89 samples; (B) Mesaverde Group, n = 86 samples.

Source Rock Maturation and Thermal History

The thermal history of the Mancos-Menefee TPS source beds is closely linked to the structural evolution of the basin. During the Late Cretaceous (about 90 Ma—millions of years before the present), the central part of the San Juan Basin began to subside slowly. Maximum subsidence in the deepest part of the basin, north of the Colorado-New Mexico State line, occurred during the late Oligocene. During the Miocene, the basin axis shifted to the area south of the Colorado-New Mexico State line. Differential uplift, erosion, and thermal cooling followed basin subsidence. Rocks in the San Juan Basin are generally underpressured.

Burial History

Burial history curves can be used to examine the relation between structural evolution of the basin and thermal maturation of coals for different parts of the basin. Thermal maturation studies (Bond, 1984; Law, 1992) indicate changes in the geothermal gradient in the basin at different periods of geologic time and for different parts of the basin. The highest geothermal gradient was reached in the Oligocene (Bond, 1984). Burial history curves (figs. 15A and 15B) for two distinct parts of the San Juan Basin were presented by Law (1992). The southernmost burial curve is for the Superior Sealy 1-7 well located in Rio Arriba County, N. Mex. (figs. 1 and 15A) (Law, 1992), peripheral to the deep part of the central basin. This curve is representative of the burial history of the southern part of the central basin (fig. 4), which was not buried as deeply as other parts. Temperature profiles through this well have not been constructed; however, maximum temperature in the Dakota Sandstone–Mesaverde Group interval was probably less than temperatures for the northern burial reconstructions (figs. 15B and 15C). The well lies between the 0.7- (extrapolated) and 0.8-percent R_m vitrinite isorefectance contours (fig. 1) in the Menefee Formation.

The curve for the Sohio Southern Ute 15-16 well (figs. 1 and 15B) (Law, 1992) represents burial near the present-day deepest part of the basin and indicates that this area continued to subside from about 90 Ma until the late Miocene (13 Ma). Basin deepening was interrupted by brief periods of uplift and erosion. Maximum burial in this area was in the late Miocene (~ 13 Ma), and at this time the Dakota Sandstone was buried to nearly 12,000 ft. Although temperature profiles through this well have not been constructed, maximum temperature in the Dakota Sandstone–Mesaverde Group interval was probably slightly less than those for the northern burial reconstruction. The duration of maximum temperature would have been less than for the northern well because maximum burial occurred about 12 million years later. A vitrinite reflectance value of 2.5–3.0 percent R_m was measured in the Dakota Sandstone in a nearby well, which lies north of the 1.5-percent R_m vitrinite isorefectance contour in the Menefee Formation (fig. 1).

The northernmost burial history curve on which isotherms have been superimposed is for the Natomas 1-11 Federal well

(figs. 1 and 15C) (Bond, 1984); it indicates that maximum subsidence of the basin in this area ceased in the late Oligocene and that uplift and erosion followed. Further, this burial history curve indicates that maximum burial occurred in the late Oligocene in this area of the basin, whereas to the south (fig. 15B), maximum burial was in the late Miocene. These relations indicate a shift in the basin axis from north to south concurrent with uplift of the northern margin of the basin.

The burial curve and isotherms for the Natomas 1-11 Federal well (fig. 15C) show the Dakota (and thus the lowermost Mancos) entering the oil generation zone in early Eocene (about 53 Ma) and the top of the Niobrara Member of the Mancos Shale entering the zone of oil generation a few million years later. The Dakota was shown to enter the wet gas zone of generation in the middle Eocene and the dry gas zone in the early Oligocene (33 Ma). The Niobrara entered these zones a few million years later. Thus the time of significant maturation of the Mancos Shale spans about 20 m.y. (million years) (Eocene to Oligocene) with the basal part of the formation maturing earlier than the top. Using the curve for the Sohio Southern Ute 15-16 well near the present-day structural axis of the basin (fig. 15B), the Mancos should have continued to mature and generate hydrocarbons well into the Miocene. Maximum depth of burial for the Dakota in the Natomas 1-11 Federal well was projected to exceed 14,000 ft and for the top of the Niobrara to be near 13,000 ft. The burial curve and isotherms (fig. 15C) for the Natomas 1-11 Federal well shows the Menefee entering the zone of oil generation in the mid-Eocene (45 Ma) at a depth of approximately 9,800 ft, entering the wet gas zone in the early Oligocene, and the dry gas zone in the late Oligocene (27 Ma) (Bond, 1984).

Vitrinite Reflectance

Vitrinite reflectance has been extensively studied in Fruitland Formation coals; however, far fewer vitrinite reflectance data exist from the Mancos-Menefee TPS. The top of the zone of oil generation is generally accepted to be at a mean vitrinite reflectance value of 0.5-percent R_m (Tissot and Welte, 1978). The onset of intense thermogenic gas generation is considered to occur between vitrinite reflectance values 0.8–1.0 percent R_m and wet gas generation between 0.5–0.8 percent R_m (Tissot and Welte, 1978). Cracking of oil (condensate) to methane is thought to occur between vitrinite reflectance values 1.0–1.35 percent R_m and maximum generation of thermogenic methane between vitrinite reflectance values 1.20–2.0 percent R_m (Tissot and Welte, 1978).

The pod of active source rock for both the Mancos Shale and Menefee Formation lies near the 0.50-percent R_m vitrinite isorefectance contour line in the Menefee, encompassing much of the northern half of the basin (fig. 7). Most of the nonassociated gas in the Dakota, Mancos, and Mesaverde reservoirs generally is found north of the 0.8-percent R_m vitrinite isorefectance contour (fig. 1) in the Menefee, and associated gas and oil in the Dakota, Mancos, and Mesaverde reservoirs are found south of that contour.

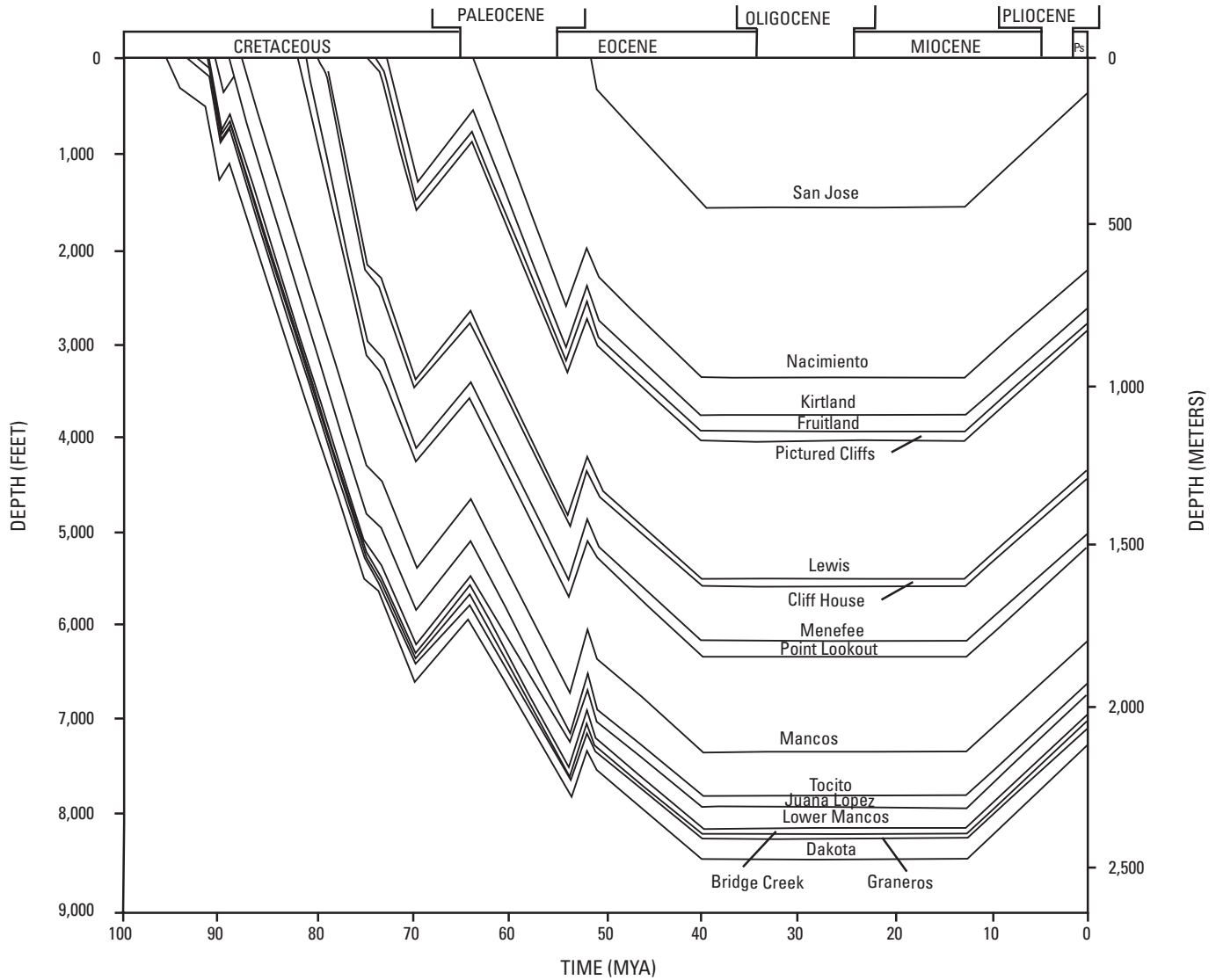


Figure 15A. Burial history curve for the Superior Sealy 1-7 well in the southern part of the central San Juan Basin, Colorado and New Mexico (modified from Law, 1992). Geologic time scale is from the Geological Society of America web page <http://www.geosociety.org/science/timescale/timescl.htm>, last accessed 2/1/2008. MYA, millions of years ago; Ps, Pleistocene.

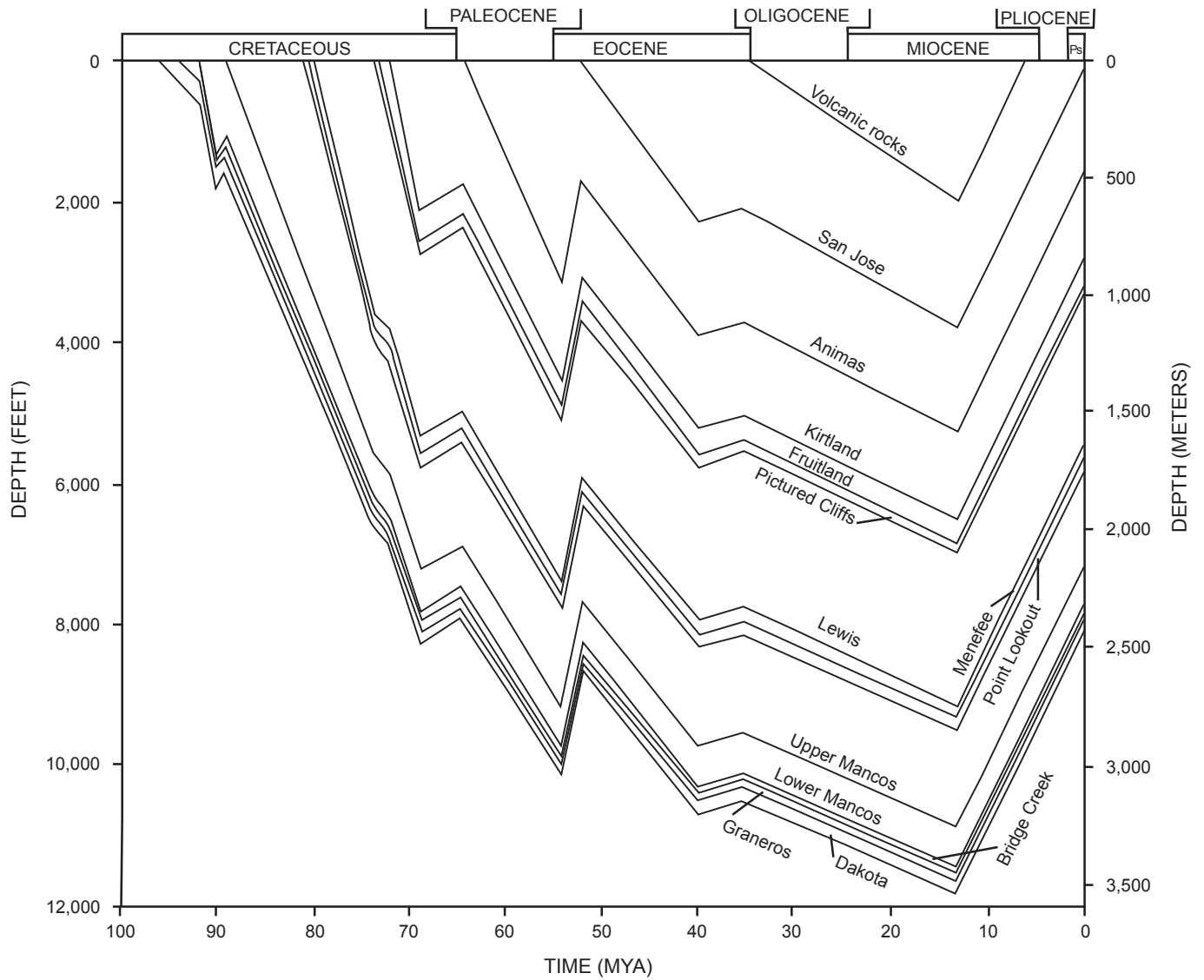


Figure 15B. Burial history curve for the Sohio Southern Ute 15-16 well in the northern part of the central San Juan Basin, Colorado and New Mexico (modified from Law, 1992). Geologic time scale is from the Geological Society of America web page <http://www.geosociety.org/science/timescale/timescl.htm>, last accessed 2/1/2008. MYA, millions of years ago; Ps, Pleistocene.

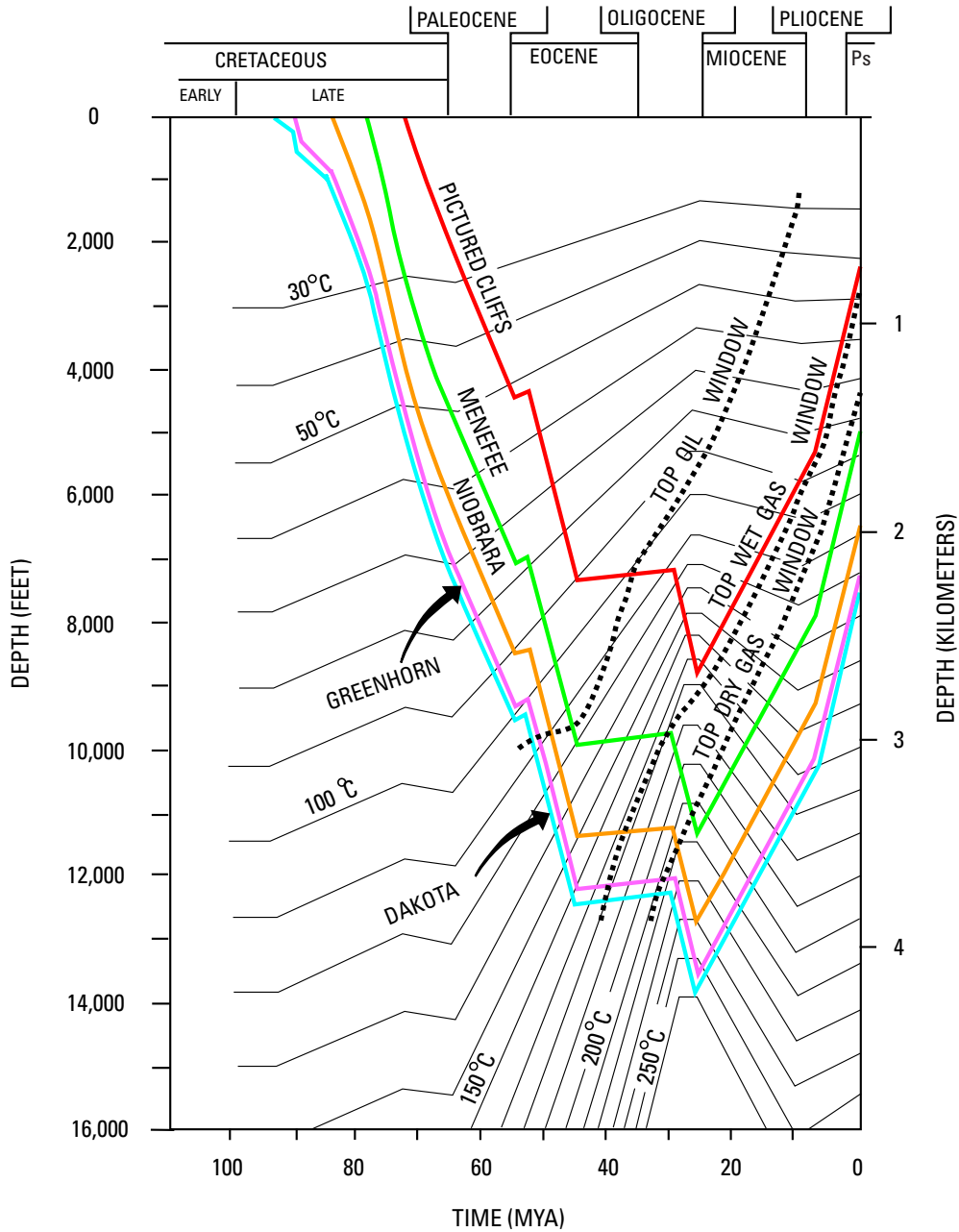


Figure 15C. Burial history curve and isotherms for the Natomas 1-11 Federal well in the northern part of the San Juan Basin, Colorado and New Mexico (modified from Bond, 1984). Geologic time scale is from the Geological Society of America web page <http://www.geosociety.org/science/timescale/timescl.htm>, last accessed 2/1/2008. MYA, millions of years ago; Ps, Pleistocene.

Dakota Sandstone

Few vitrinite reflectance values are available from coals in the Dakota Sandstone and most are from the area of the central basin (fig. 1) (Fassett and Nuccio, 1990; C. Threlkeld, U.S Geological Survey, written commun., 2001). These data indicate that the Dakota–lower Mancos and Menefee strata had a similar thermal history in the southern part of the central basin, but a higher thermal history for the Dakota–lower Mancos relative to the Menefee north of this area (Rice, 1983). Vitrinite reflectance values from coals in the northern outcrop belt of the Dakota are lower (0.5–1.0 percent R_m) than those in the northern part of the central basin (fig. 1). This decrease in the vitrinite reflectance values is similar to that observed for the Fruitland (Fassett, 2000) and reflects the effect of uplift of the northern basin margin as the basin continued to subside to the south. South of the 0.5-percent R_m vitrinite isoreffectance contour in the Menefee, no vitrinite reflectance data from the Mancos or from coals in the underlying Dakota Sandstone exists. Thus, the southern boundary within the Mancos Shale that is thermally mature enough to generate hydrocarbons is not well defined.

The Mancos Shale was probably in the zone of oil generation north of the central basin along the outcrop belt. In the central basin, Mancos sandstone reservoirs contain mainly gas north of the extrapolated 0.75-percent R_m vitrinite isoreffectance contour in the Menefee Formation, whereas oil is found mainly south of this contour. In the northern part of the San Juan Basin, vitrinite reflectance contours in the overlying Menefee Formation range from 1.0-percent to greater than 1.5-percent R_m , and two vitrinite reflectance values in the Dakota Sandstone are between 2.5- and 3.0-percent R_m (fig. 1). The combination of high thermal maturity and present (and past) overburden thickness of the Mancos in the deep part of the basin would influence the type of hydrocarbons produced in the Mancos, which would likely be gas or previously generated oil that would begin to crack to gas.

Menefee Formation

Thermal maturity data (R_m) from Fassett and Nuccio (1990), Law (1992), and Ridgley (2001b), as well as samples analyzed for this study, were used to construct vitrinite isoreffectance contours for the Menefee Formation (fig. 1), which roughly correspond to the structure contour lines that define the shape of the basin. Isoreffectance contours indicate progressively greater thermal maturity of the coals from southwest to northeast across the TPS (fig. 1), similar to the pattern of the Fruitland Formation (Fassett, 2000). The position of the 0.5-percent R_m contour is not well constrained; however, it does indicate that Menefee source beds, which lie north of this contour, would be in the zone of oil or gas generation.

Hydrocarbon Migration Summary

Hydrocarbon migration from Mancos Shale source beds took several routes. In the southern part of the San Juan Basin (fig. 1), oil is found in Dakota Sandstone reservoirs as well as in various genetically unrelated sandstone beds in the upper Gallup Sandstone (Hospah of industry). Although no thermal maturity data have been derived from the Mancos Shale in the southern part of the basin, it is not likely that the oil was locally sourced, because the Mancos Shale is considered to be thermally immature in this area. Oils in the Dakota at Lone Pine field and producing sandstones of the Hospah field are similar; oil-source correlations indicate the Mancos is the source (Ross, 1980). Migration routes of the oil are not known, but it must have migrated from north to south out of the deeper part of the basin where the Mancos Shale is thermally more mature. Inferred migration pathways are shown on figure 16.

Migration may have been along faults. Although few faults have been mapped in the Dakota in the central part of the basin (Thaden and Zech, 1984; pl. 3), a series of interconnected basement faults have been identified (fig. 4), and some of these might extend into the Mancos Shale. Alternatively, basal fluvial Dakota sandstones, which are the most laterally continuous sandstones in the Dakota, may have served as the conduits. Oil in the Hospah field may have migrated vertically upward from the Dakota along faults that cut the sandstones of the Dakota, Gallup, and Torrivio in areas of oil production. Because of the regional orientation of the Gallup sandstones (northwest–southeast), the sandstones could not have served as direct conduits to funnel oil from the deeper part of the basin toward the south. However, oil in Gallup fields and seeps in McKinley County may have migrated through the Gallup from the area where distal Gallup facies (thin sandstone, siltstone, and shale) (fig. 8) underlies Tocito sandstones (Molenaar, 1977b). In this area, which would lie within the pod of mature source rock, there may be sufficient fractures or faults to serve as conduits for oil migration into the main Gallup or Torrivio to the south. The Coniacian unconformity may also have served as a migration path with oil migrating along the unconformity and then into sandstones of the Gallup.

Oil is found in Dakota Sandstone and Mancos Shale reservoirs west of the central basin on the Four Corners platform and east of the central basin on the Chama platform (figs. 1 and 4). In both of these areas, the fields are areally small. Some of the oil, such as that found in Dakota reservoirs at the Hogback and Table Mesa fields (fig. 1) (see field descriptions in Fassett, 1978a,b), may have been locally generated due to high temperatures from local intrusions. The remaining oil probably migrated via faults and fractures from the pod of active source rock in the Mancos Shale (fig. 7). The source rock maturity of the Mancos on the Chama platform (fig. 1) is unknown. However, because the basin was once areally larger than its current configuration, the oil could have been locally sourced, based on vitrinite reflectance in the overlying Menefee Formation and probable extent of mature source rocks in

the Mancos Shale (fig. 7). Oil in Tocito and “Gallup” (drillers’ term; see discussion in reservoir rock section) sandstones was locally sourced and migration pathways were short, essentially from source beds into adjacent sandstone reservoirs (fig. 16). All the oil and gas producing reservoirs in the Tocito and “Gallup” lie within the proposed extent of mature source rocks in the Mancos (fig. 7). Faults and fractures in these reservoirs, as well as in the surrounding Mancos Shale, may also have served as migration pathways.

Some reservoirs in the Dakota, “Gallup,” and Mesaverde contain basin-centered gas accumulations. Here gas accumulated locally either from thermocatalytic conversion of kerogen to gas in closely associated source rocks or from thermal cracking of earlier formed oil. Migration distances are short (fig. 16) if the former is important and nonexistent if the latter is important because the gas would be generated in place.

Gas generated from the Menefee could have

1. remained in place in coal beds or other carbonaceous beds,
2. migrated to nearby fluvial sandstone reservoir rocks, or
3. migrated to the underlying Point Lookout or overlying Cliff House Sandstones, probably via fracture zones (fig. 9).

Coal in the Menefee is mainly in the upper and lower one-quarter to one-third of the formation, so migration distances to the Point Lookout or Cliff House would have been minimal.

Faults and natural fractures are the two most important pathways for vertical migration of hydrocarbons. Faults are common on the south and southeast sides of the basin (Thaden and Zech, 1984; pl. 3), including the area of oil production in the Mesaverde. Ross (1980) noted a close correlation between Mancos bitumen and marine Cretaceous oils, including oil sampled from Mesaverde reservoirs in several fields. This implies that Mancos oil moved upward along faults into Menefee and Point Lookout reservoirs.

Lorenz and Cooper (2001) summarized outcrop and core studies of fractures in Mesaverde rocks in the San Juan Basin. They noted that outcropping Mesaverde sandstones have vertical, relatively long, irregular extension fractures that are not as well-formed as fractures in the quartz-cemented Dakota Sandstone. Moreover, most fractures in both units are limited to sandstone beds and do not cross mudrock interbeds. The fractures mapped from outcrops trend generally north-northeast, with orthogonal secondary fractures related to uplift and erosion at the outcrop. Fractures described from core in the subsurface of the basin were interpreted to have the same NNE.–SSW. orientation as those observed at the outcrop (Lorenz and Cooper, 2001), but cores lacked the secondary cross fractures. Fractures in Mesaverde cores were filled to partially filled with calcite and quartz. Fault zones increased the fracture intensity. Spacing of fractures in both outcrops and core are at or less than the thickness of the beds in which they formed. Fracture intensity is greater in areas of higher productivity, including zones where fractures are closely spaced.

Hydrocarbon Traps and Seals

Mancos

Hydrocarbon traps in Mancos reservoirs vary regionally. In the southern part of the San Juan Basin, traps in the Dakota, Gallup, and Torrivio are combined structural and stratigraphic traps (see field descriptions in Fassett, 1978a,b, 1983a; Berg, 1979). Discontinuous sandstones of marginal marine origin are juxtaposed with faults that not only compartmentalize the fields, but also may have served as pathways for local vertical migration of oil. Local porosity and permeability variations in the Dakota, a result of diagenesis and bioturbation, were also considered to be important controls on trapping and retaining oil in the Dakota at the Lone Pine field (Berg, 1979). Oil in Dakota reservoirs on the Four Corners platform and Chama platform (fig. 1) is in anticlines, some of which may have associated faults. In these areas, the trapping mechanism is combined structural and stratigraphic.

Oil accumulations in the Mancos sandstone reservoirs on the Four Corners and Chama platforms (fig. 4) are in very fine grained sandy, silty, and shaly facies, associated with faults. The fine-grained heterolithic lithology and low permeability of these facies are the principal trapping mechanisms. Oil in Tocito reservoirs is stratigraphically trapped. Oil in “Gallup” reservoirs is primarily trapped by the low permeability of the facies. Some of the “Gallup” fields are associated with small folds, where faulting and fracturing may have assisted not only with local hydrocarbon migration but also with trapping (Emmendorfer, 1992; see field discussions in Fassett, 1978a,b, 1983a; Gorham and others, 1977; Ridgley, 2001a).

Nonassociated gas in Dakota, Tocito, “Gallup,” and Point Lookout reservoirs occurs in basin-centered accumulations in the central basin (fig. 4). Here the principal trapping mechanisms are stratigraphic resulting from laterally discontinuous facies and high capillary pressures due to low permeability in the facies. Structures may be locally important traps.

Mesaverde

Hydrocarbon traps in the Mesaverde are stratigraphic for gas accumulations and are combination stratigraphic and structural for oil accumulations. Although gas production is normally reported as “Mesaverde” and is not identified by formation (IHS Energy Group, 2001), the trends of highest cumulative gas are associated with two linear zones of Cliff House Sandstone—one 125–300 ft thick and the other 300–500 ft thick—that are oriented northwest–southeast across the producing area. Less-productive gas wells are in areas where the Cliff House is generally less than 125 ft thick. A similar correlation between higher cumulative gas production and zones of relatively thick Point Lookout Sandstone was not observed. Gas is trapped within the marginal marine sandstones and within fluvial sandstones where those units pinch out into paludal or marine shales, or overbank mudrocks, respectively.

Oil accumulations in the Menefee on the southwest side of the basin are associated with fluvial channels and commonly with small anticlines or domes. Many of the accumulations also seem to be associated with faults, which could have provided migration paths from the underlying Mancos Shale.

Regional seals in the TPS consist of marine shales (Mancos Shale below and Lewis Shale above). Locally, seals in Dakota and Torrivio (Hospah) reservoirs may be a combination of shale facies into which marine and marginal marine sandstone facies pinch out and changes in permeability within the sandstone units. Seals for Tocado reservoirs are interbedded Mancos Shale, whereas for “Gallup” and other Dakota reservoirs, seals are a combination of interbedded shales and low permeability in the reservoirs. Additional seals are nearshore paludal shales and coal-bearing rocks in the Menefee and fluvial overbank mudrocks of the Menefee Formation.

Assessment Unit Definitions

Dakota-Greenhorn Conventional Oil and Gas Assessment Unit (50220304)

Introduction

The Dakota-Greenhorn Conventional Oil and Gas Assessment Unit (AU) (50220304) covers nearly all but the central basin part of the TPS (fig. 17A). The area of this AU extends from the outcrop of the Dakota Sandstone (Green, 1992; Green and Jones, 1997) to the boundary of the Dakota-Greenhorn Continuous Gas Assessment Unit, discussed below. This AU includes wells that have a calculated gas-oil ratio (GOR) of less than 5,000 cubic feet of gas per barrel of oil (cfg/bo) (fig. 18) and are classified as oil wells (IHS Energy, 2002) (fig. 19). A GOR of 20,000 cfg/bo or greater seems to best define the low permeability gas zone of the central basin and is the cutoff used by the USGS to define a gas accumulation. Of the over 5,700 wells that produce from the Dakota Sandstone in the basin, 120 have a GOR between 5,000 and 20,000 cfg/bo. Wells in this GOR range are found mostly, but not entirely, in the Dakota-Greenhorn Continuous Gas AU (fig. 18) and tend to be surrounded by wells with a GOR greater than 20,000 cfg/bo. These wells have been included in the Dakota-Greenhorn Continuous Gas AU.

Gas was first discovered in the Dakota Sandstone in 1921 on Ute Dome and oil was discovered the following year on the Hogback dome (fig. 17B) (Matheny and Ulrich, 1983); both are on the Four Corners platform (fig. 17A). In 1924, oil was discovered in the Dakota on Rattlesnake dome and gas in the Red Mesa field (fig. 17B). Gas was discovered in the Dakota on Barker dome and oil was discovered in the Dakota on Table Mesa anticline in 1925 (fig. 17B). In the approximately twenty years that followed, additional oil and gas fields were discovered; all were in structural traps, mostly anticlines, marginal to the central basin (figs. 4 and 17A). Here gas is associated with

oil accumulations. The prevailing philosophy of that era was to locate surface structures and drill them.

There were 27 fields producing oil and associated gas in 1983; production was also reported from five additional wells not assigned to any field (Fassett, 1983b). Only three new fields, Hay Gulch, Sierra, and Rio Arriba (figs. 17A and 17B) have been discovered since 1983; each of these is small and only produced for a few years. The easily identified targets for conventional oil and gas in the Dakota have been drilled. New targets will require a thorough understanding of the depositional patterns in the Dakota, the identification of buried structures through seismic analysis, and identification with more certainty the migration pathways into the Dakota from the area of sufficiently mature Mancos Shale (fig. 7). Key parameters of the AU and their timing are listed below and summarized in the events chart (fig. 20).

Source

The primary petroleum source rock for this assessment unit is interpreted to be the Mancos Shale.

Maturation

Thermal maturation for oil and associated gas is interpreted to range from early to late Eocene.

Migration

Oil from the mature pod of the Mancos Shale, located north of the Chaco slope (figs. 4 and 7), migrated into Dakota Sandstone reservoirs in the western, southern, and eastern parts of the AU (figs. 17A and 17B). Migration may have been along faults or through basal channel sandstones that filled valleys incised into the underlying Morrison Formation. In this AU, oil occurs in the updip or flank parts of anticlines or domes in most fields on the Four Corners or Chama platforms (fig. 17A) that formed during the Laramide orogeny, and migration of oil was probably coincident with formation of the structural traps. Within any specific field, migration may have been upward through permeable beds draped on structures or along faults into the upper laterally discontinuous marine and shelf sandstones.

Reservoirs

Reservoirs in the Dakota Sandstone are mostly marginal marine and marine shelf sandstones that are lenticular in shape and are interbedded with shale (see field descriptions and geophysical logs in Fassett, 1978a,b, 1983a). These sandstones tend to be finer grained than the basal fluvial sandstones. In many of the oil fields, the basal fluvial sandstones are water wet. Some oil has been produced from fluvial sandstones deposited on the lower delta plain as well as those that occupy incised valleys. The basal sandstones that are part of the lower incised valley fill tend to be coarser grained and water wet.

Oil and associated gas have also been produced from fractured limestone in the Greenhorn (Bridge Creek) Limestone Member, from sandstone in the Semilla Sandstone Member of the Mancos Shale, and from calcarenites from the Jauna Lopez Member of the Mancos Shale in a few isolated wells.

Traps/Seals

Traps are either stratigraphic, structural, diagenetic, or a combination of these. Stratigraphic traps occur where laterally discontinuous marine sandstone lenses pinch out in marine shales of the Mancos. Structural traps consist of folds, many of which are faulted. Draping of lenticular marine sandstone bodies over folds provides combined stratigraphic-structural traps commonly with an associated gas cap. In such traps, natural fracturing associated with fold development has aided production. Seals are primarily shale beds within the Dakota, regional shale tongues in the Mancos Shale, and local faults.

Geologic Model

Oil fields in the Dakota, except for those that occur in the southern part of the AU, form a rim around the central basin, basin-centered gas accumulation (Dakota-Greenhorn Continuous Gas AU) (fig. 17A). Oil in this conventional AU was generated from marine carbonaceous shale in the Mancos from early to late Eocene (figs. 15C and 20). Along the western, northwestern, and northeastern margins of the AU where the Dakota oil fields are closer to the mature pod of source beds (fig. 7), oil was expelled from the source beds and migrated relatively short distances into marginal marine sandstones of the Dakota (such as in the Hogback, Price Gramps, Rattlesnake, Red Mesa, and Shiprock fields; figs. 17A and 17B). Traps in these areas are structural, stratigraphic, or a combination of both; fractures are important for production (Lauth, 1983). Gas fields in this AU, such as Alkali Gulch, Ute Dome, Barker Creek, and Straight Canyon (fig. 17B) (Fassett, 1983b, 1991), may consist of migrated associated gas because the gas tends to be wet, and gas-water contacts have been identified for most of the fields. Oil in the Price Gramps and Red Mesa fields (figs. 17A and 17B) have low API gravities (31°–33°) (see discussion in Fassett, 1978a, 1983a) and may be biodegraded because the accumulations occur at depths generally less than 1,000 ft. These API gravities are much less when compared to API gravities (>50°) of oil in the Hogback, Rattlesnake, and Shiprock fields (fig. 17B). In the latter fields, oil may have been generated locally in the vicinity of intrusions. Oil production on the Four Corners and Chama platforms has been small, probably due to the shallow depths of the reservoirs, which are within a few hundred feet of the surface, and to water encroachment.

Oil in the southern part of the AU must have migrated to the reservoirs from the pod of mature source rock to the north because the fields lie well beyond mature Mancos source beds, as defined in this report. Inferred migration pathways are shown in figure 16. The oil is hypothesized to have migrated

updip into the reservoirs either along regional faults or through the basal fluvial channel sandstones in the Dakota (fig. 16) into overlying marginal marine sandstones, which form stratigraphic traps. The marine sandstones have a lenticular geometry and pinch out laterally into shales of the Dakota and Mancos.

API gravities of oils from Chacon, Gallo, Lindrith South, Lindrith West, Lybrook, Ojito, and Rio Arriba fields (fig. 17A) (Fassett, 1991) range from 38°–43°, higher than those on the Four Corners and Chama platforms and lower than those from Dakota reservoirs in the southern part of the AU. The oil probably migrated short distances into these reservoirs during the latter part of the Laramide orogeny (Eocene). Most of the oil is stratigraphically trapped, although small structures may have aided in early trapping. Reservoirs have been described as tight, with low permeability (around 0.05 millidarcy) and porosity (<9 percent); natural and induced fractures are needed for economic production (see field discussions in Fassett, 1978b, 1983a). These reservoir properties are similar to those observed in the Dakota basin-centered gas accumulation and point out the need to better understand the time of hydrocarbon generation (oil and gas) relative to the time of loss of effective permeability. Although the fields have some characteristics of continuous accumulations, it is possible that there was initially sufficient permeability in the reservoirs to trap the oil early, but over time, loss of effective permeability (diagenesis) prevented updip migration of the oil. This would then result in an updip permeability barrier to hydrocarbons moving out of the central basin (and water moving in) as downwarping of the central basin continued into the Miocene. Rice (1983) also noted the low permeability barrier between the oil and basin-centered gas accumulation, but did not address the timing loss of effective permeability.

Assessment Results

The Dakota-Greenhorn Conventional Oil and Gas Assessment Unit (50220304) covers 5,811,310.79 acres. The AU was estimated at the mean to have potential additions to reserves of 2.45 million barrels of oil (MMBO), 21.69 billion cubic feet of gas (BCFG), and 0.61 million barrels of natural gas liquids (MMBNGL). The volumes of undiscovered oil, gas, and natural gas liquids estimated in 2002 for the Dakota-Greenhorn Conventional Oil and Gas AU are shown in appendix A. A summary of the assessment input data of the AU is presented on the data form in appendix B, which for this AU estimates the numbers and sizes of undiscovered accumulations. There is adequate charge, reservoir, traps, seals, access, and timing of generation and migration of hydrocarbons, indicating a geologic probability of 1.0 for finding at least one additional field with a total recovery greater than the stated minimum of 0.5 MMBO (grown) for oil or 3 BCF gas (grown).

This assessment unit produces both oil and associated gas (IHS Energy Group, 2002). In estimating the number and sizes of undiscovered oil and gas accumulations, historical data from NRG (2001) database were used. Seven Dakota oil fields meet

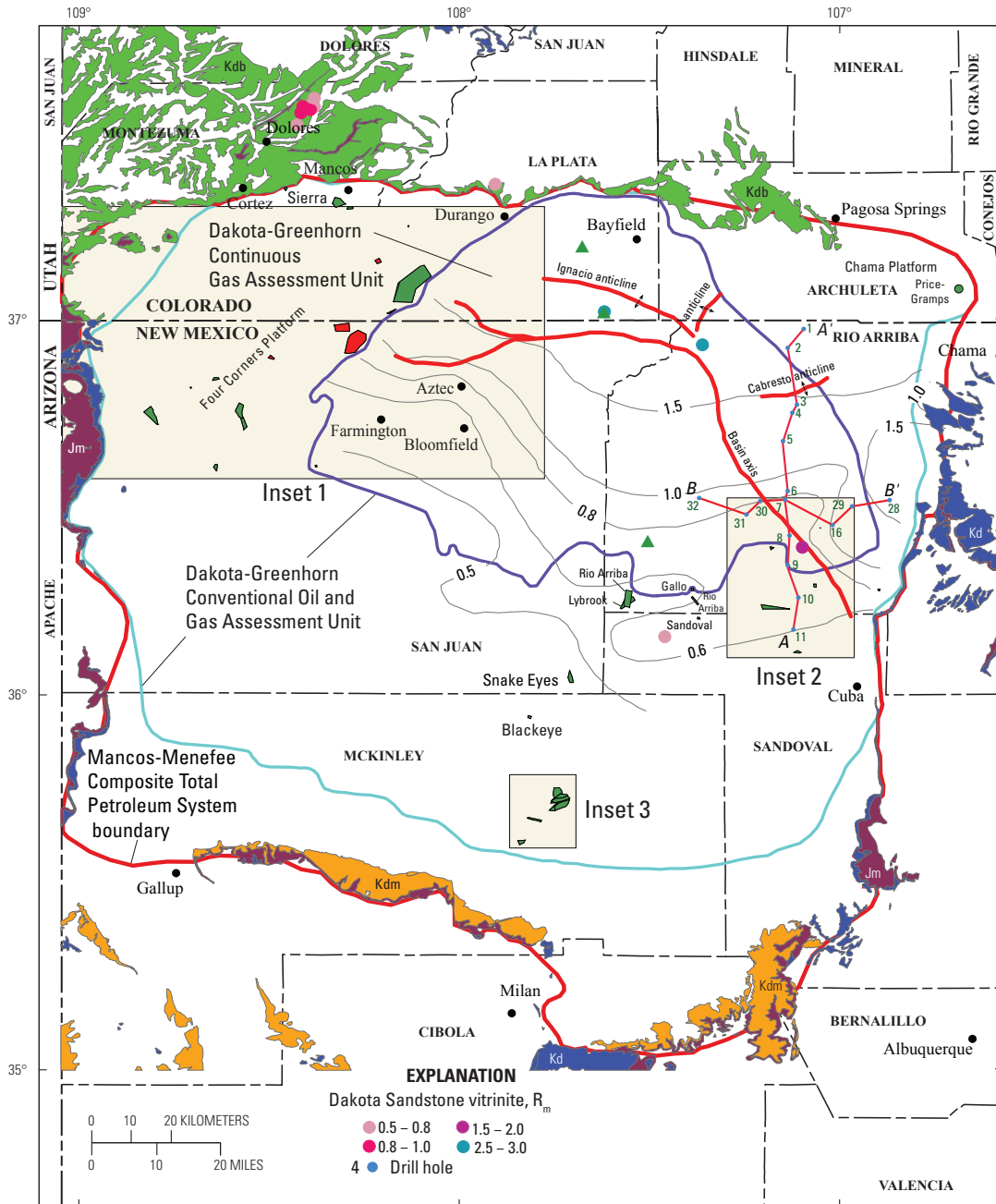
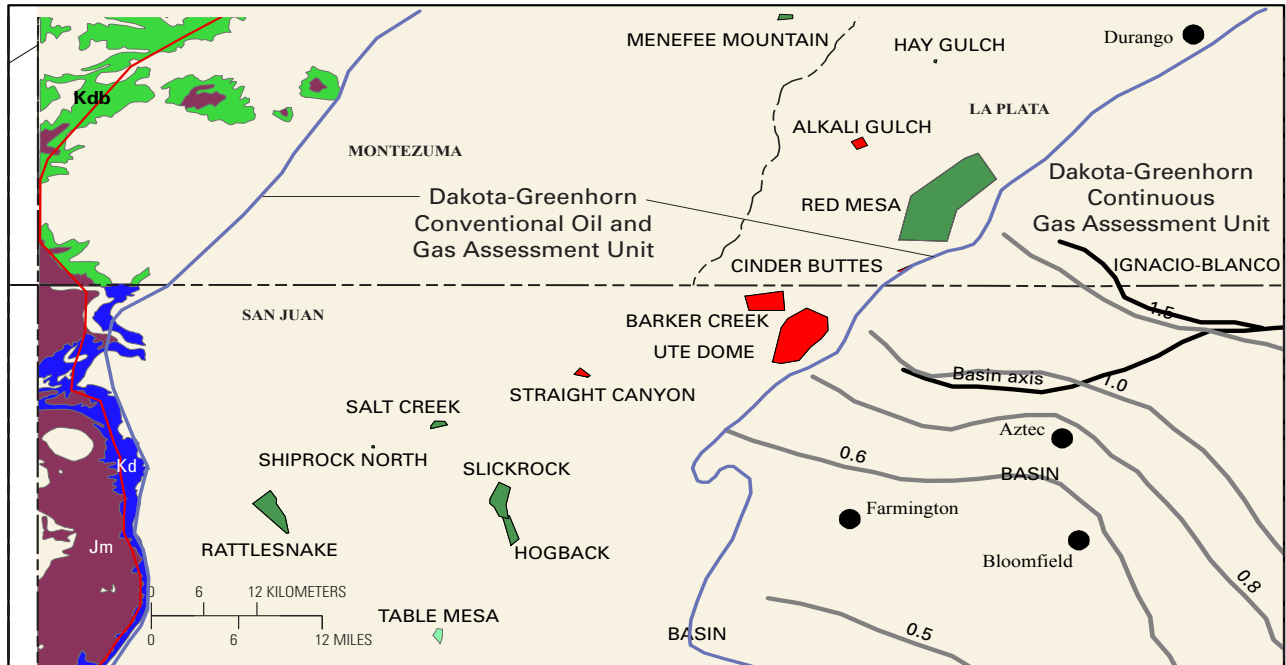
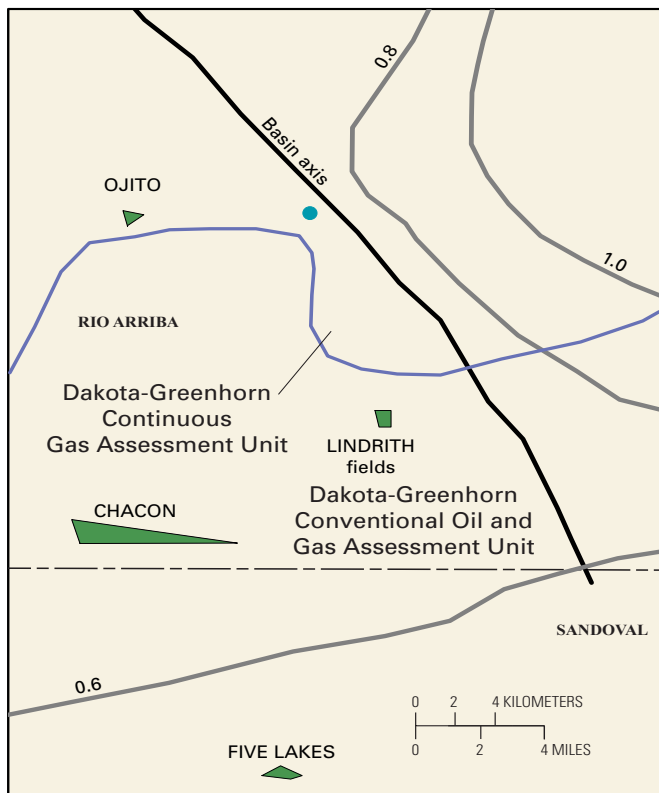


Figure 17A. Map showing the Dakota-Greenhorn Conventional Oil and Gas Assessment Unit (AU) (50220304) boundary (purple), oil (green polygons) and gas (red polygons) fields in the AU, and locations of the wells (green triangles) used to construct the burial history curves found in this report (figs. 15A–C). Also shown are locations of cross sections A–A’ and B–B’ (pls. 1 and 2). Thermal maturity contours (gray) are in the Menefee Formation (Fassett and Nuccio, 1990; Law, 1992; and Ridgley, 2001b); vitrinite data for the Dakota Sandstone (colored dots) are from Fassett and Nuccio (1990) and C. Threlkeld (written commun., 2001). Enlargement of areas of insets 1–3 are shown in figure 17B. Field boundaries are extrapolated from data in IHS Energy Group (2002). Symbols for geologic map units: Kdm, Dakota Sandstone-Mancos Shale; Kdb, Dakota Sandstone-Burro Canyon Formation; Kd, Dakota Sandstone; Jm, Morrison Formation (Green, 1992; Green and Jones, 1997).



Inset 1

Inset 2



Inset 3

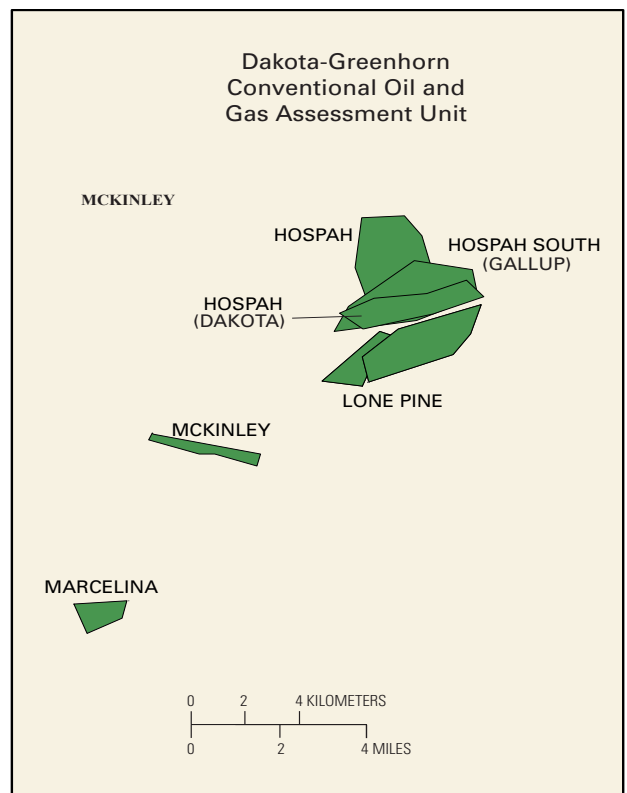


Figure 17B. Selected oil (green) and gas (red) fields in the Dakota Sandstone-Juana Lopez Member of the Mancos Shale interval in insets 1–3 from figure 17A.

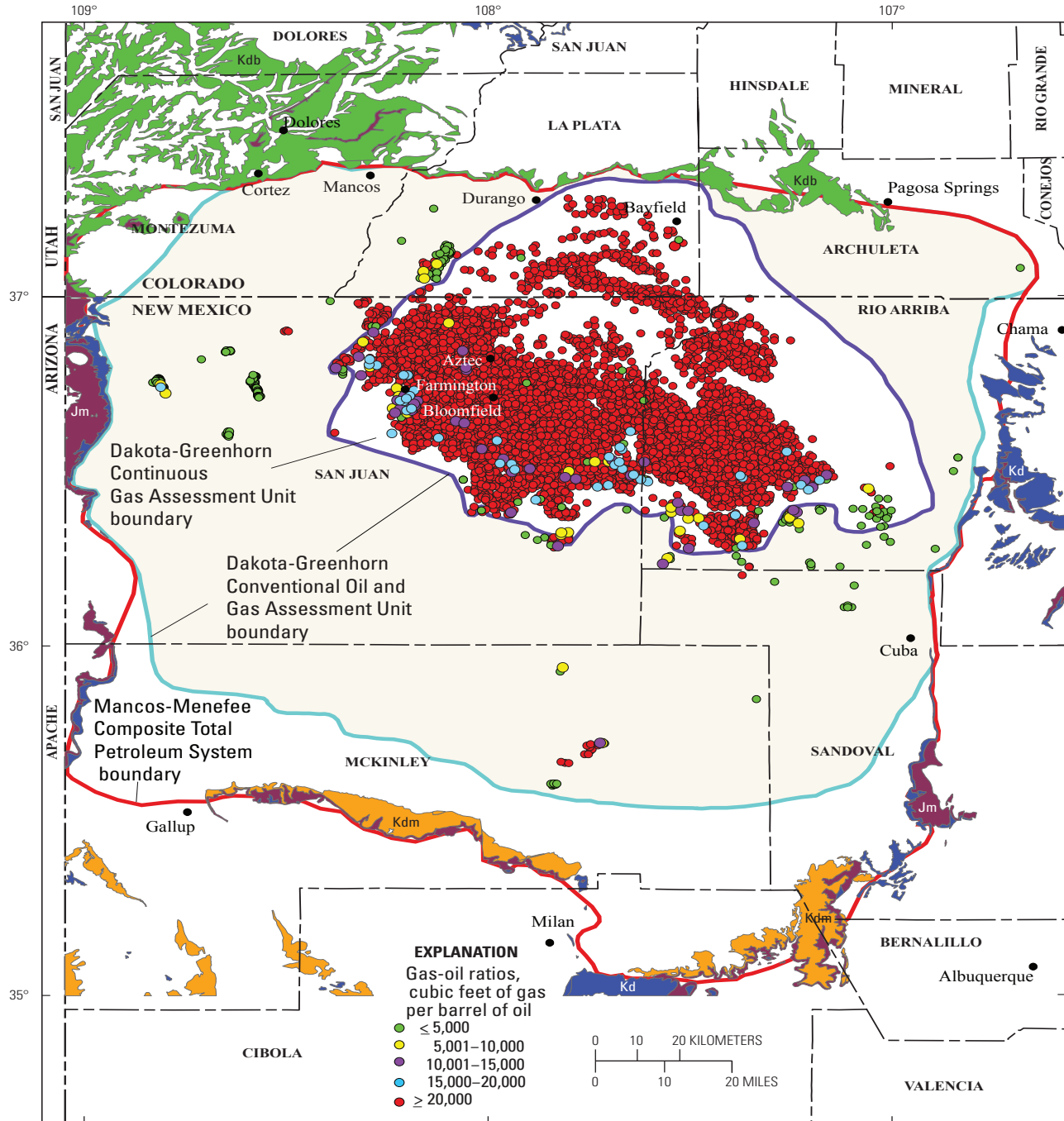


Figure 18. Map showing distribution of gas-oil ratios from producing reservoirs in the Dakota-Greenhorn Conventional Oil and Gas Assessment Unit (tan) and Dakota-Greenhorn Continuous Gas Assessment Unit (white with purple boundary). Symbols for geologic map units: Kdm, Dakota Sandstone-Mancos Shale; Kdb, Dakota Sandstone-Burro Canyon Formation; Kd, Dakota Sandstone; Jm, Morrison Formation from Green (1992) and Green and Jones (1997).

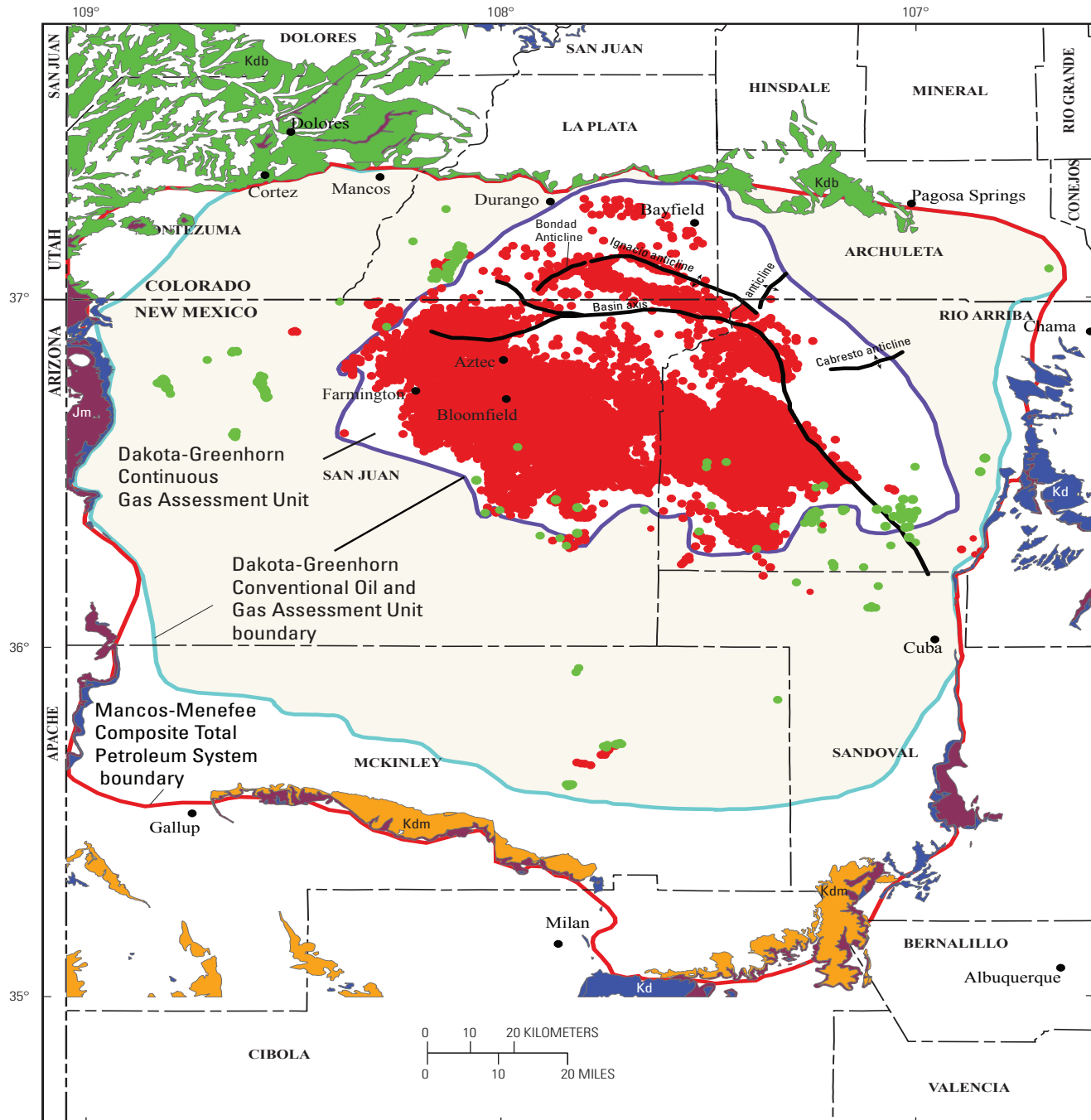
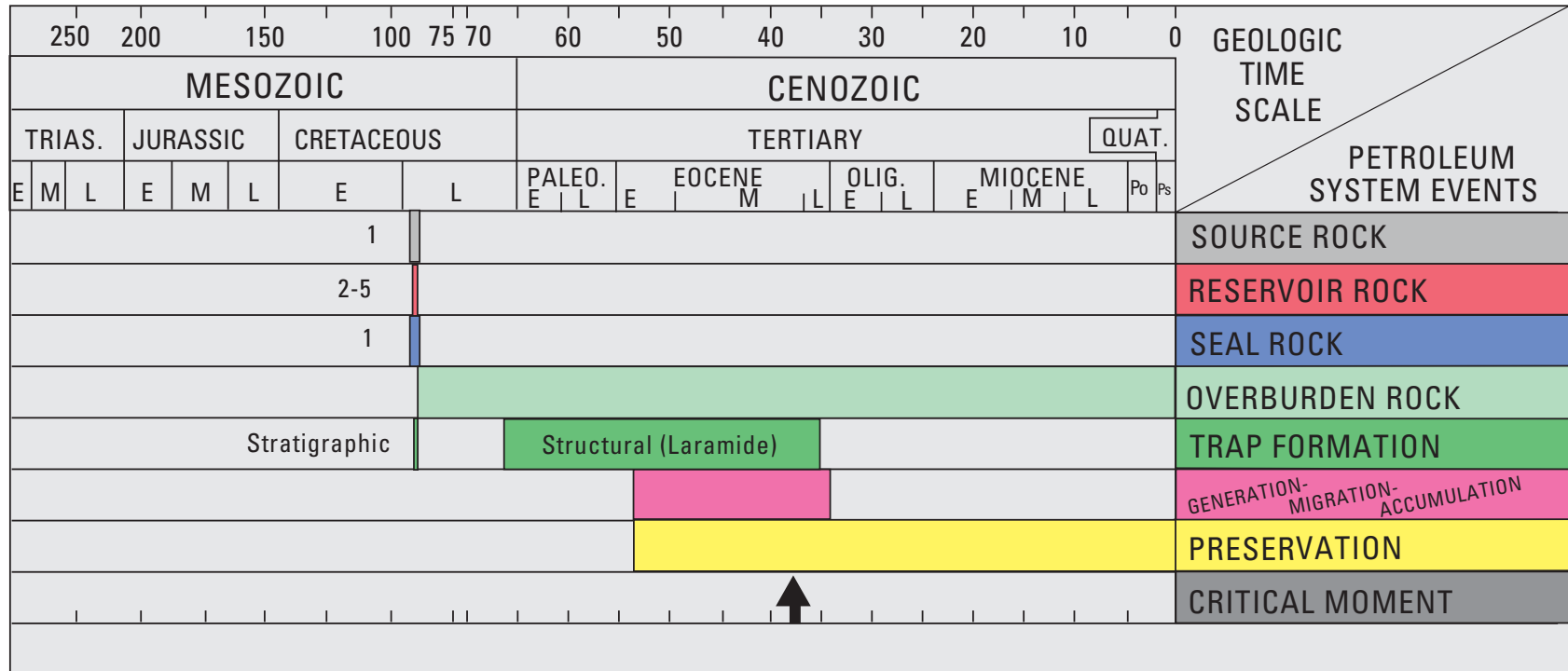


Figure 19. Map showing distribution of oil (green dots) and gas wells (red dots) from producing reservoirs in the Dakota-Greenhorn Conventional Oil and Gas Assessment Unit (tan) and Dakota-Greenhorn Continuous Gas Assessment Unit (white with purple boundary). Some wells also produce from the Morrison or Burro Canyon Formations. Data from IHS Energy Group (2002). Symbols for geologic map units: Kdm, Dakota Sandstone-Mancos Shale; Kdb, Dakota Sandstone-Burro Canyon Formation; Kd, Dakota Sandstone; Jm, Morrison Formation from Green (1992) and Green and Jones (1997).



Rock Units:

1. Mancos Shale
2. Dakota Sandstone
3. Greenhorn (Bridge Creek) Limestone Member of Mancos Shale
4. Semilla Sandstone Member of Mancos Shale
5. Juana Lopez Member of Mancos Shale

Figure 20. Events chart showing timing of key geologic events for the Dakota-Greenhorn Conventional Oil and Gas Assessment Unit. Black arrow, critical moment for oil and gas generation. Events chart format is modified from Magoon and Dow (1994). Geologic time scale is from the Geological Society of America web page <http://www.geosociety.org/science/timescale/timescl.htm>, last accessed 2/1/2008, and from Berggren and others (1995). Trias., Triassic; Quat., Quaternary; Po, Pliocene; Ps, Pleistocene; E, early; M, middle; L, late.

the 0.5 MMBO cutoff: Hogback, Lone Pine, Price Gramps, Rattlesnake, Red Mesa Dakota, Slick Rock, and Table Mesa (figs. 17A and 17B). There have been no new oil fields that have met the minimum field-size cutoff since the discovery of the Lone Pine oil field in 1970.

Although the detailed geology of Dakota reservoirs is unknown for large portions of this AU, the general geology and location of major sandstone bodies is known and allows for an abundance of sedimentary traps. Small structures are probably present but remain unmapped. However, our understanding of migration pathways—from the area where the Mancos is sufficiently mature to produce oil, to the southern part of the AU—is poor. Most of the oil fields are found in close proximity to, and border, the mature source area of the central basin, suggesting that either the charge to the reservoirs was local or the traps efficiently captured most migrating oil. The Lone Pine field, however, is some distance from the central basin. Taking these factors into consideration, it was estimated that a maximum of four undiscovered oil accumulations meeting the minimum cutoff still exist. At the median, this value is estimated at two, and at the minimum, one undiscovered oil accumulation.

Using the discovery information for known fields that meet the minimum cutoff, the median grown size of discovered accumulations is 5.98 MMBO for the first half of the discovery period and 1.69 MMBO for the second half (fig. 21). Four fields meet the minimum cutoff in the first half of the discovery period and three in the second half. Figure 21 also shows the ranking of these fields, by size, for the two discovery periods, and that the three fields in the first half are larger than those in the second half. The size of the undiscovered fields was estimated from the distribution of the discovered field sizes versus the discovery year (fig. 22), where the grown size of an accumulation is determined by adjusting upward the known petroleum volume to account for future reserve growth. The sizes of discovered fields have decreased over the years. The largest grown oil field is about 8 MMBO. Using these data, the maximum estimated size of undiscovered accumulations is 6 MMBO, the median size is 1 MMBO, and the minimum size is 0.5 MMBO. The number and sizes of undiscovered oil accumulations in the 2002 assessment are lower than those estimated in 1995 (table 5) (Huffman, 1996), even though a smaller minimum size was used in this assessment. This lower estimate reflects the lack of discovery of new fields since 1970.

Three gas fields in this AU, Barker Creek Dome, Ute Dome, and Lindrith (fig. 17B), meet the minimum field-size cutoff of 3 BCF gas; no new gas fields that have met the minimum field-size cutoff have been found since the discovery of the Lindrith field in 1973. A maximum of three undiscovered gas accumulations meeting the minimum cutoff is estimated to exist. At the median, this value would be two and at the minimum, one undiscovered gas accumulation.

Using the discovery information for fields that meet the minimum cutoff, the median grown size of discovered gas accumulations is 31.02 BCFG for the first half of the discovery period and 11.4 BCFG for the second half (fig. 23). Two fields meet the minimum cutoff in the first half of the discovery

period and one in the second half. Figure 23 also shows the ranking of these fields, by size, for the two discovery periods. The size of the undiscovered fields was estimated from the distribution of the discovered field sizes versus the discovery year (fig. 24), where the grown size of an accumulation is determined by adjusting upward the known petroleum volume to account for future reserve growth. The sizes of discovered fields have decreased over the years. The largest grown gas accumulation is about 36.5 BCFG. Using these data, the maximum estimated size of undiscovered accumulations is 25 BCFG, the median size is 6 BCFG, and the minimum size is 3 BCFG. The number and sizes of undiscovered gas accumulations in the 2002 assessment are somewhat lower than those estimated in 1995 (table 6) (Huffman, 1996), even though a smaller minimum size was used in this assessment. This lower estimate reflects the lack of discovery of new fields since 1973.

Dakota-Greenhorn Continuous Gas Assessment Unit (50220363)

Introduction

The Dakota-Greenhorn Continuous Gas Assessment Unit (50220363) covers the central part of the TPS (fig. 25). The boundary of this AU was drawn to include

1. the Dakota Sandstone that is surrounded by the Dakota-Greenhorn Conventional Oil and Gas AU, discussed above (fig. 1A); and
2. wells that have a calculated gas-oil ratio (GOR) of greater than 20,000 cubic feet of gas per barrel of oil (cfg/bo) (fig. 18) and are classified as gas wells (IHS Energy, 2002) (fig. 19).

A GOR of 20,000 or greater seems to best define the low permeability gas zone of the basin and is the cutoff used here to define a gas accumulation. However, this AU includes some wells with a GOR between 5,000 and 20,000 because they are totally surrounded by wells with a GOR >20,000 (fig. 18). This gas assessment unit is typical of basin-centered accumulation, in that the gas occupies the central part of a basin and water is found updip from the gas (Schmoker, 1996), although the updip water is not a control on the location of the gas accumulation.

The Dakota-Greenhorn Continuous Gas AU consists of two principal gas fields, Ignacio Blanco (Dakota) in Colorado and Basin in New Mexico (fig. 25). Both the Ignacio Blanco (Dakota) and Basin fields are composites of a number of small fields, the first of which were found in the 1940s (Matheny and Ulrich, 1983). When the Basin pool was established in 1961, many individual field names were abandoned. Most of the wells in this AU have now been drilled on 160-acre spacing in New Mexico; the original spacing was 320 acres. The original approved spacing of wells in the Ignacio Blanco (Dakota) was 640 acres (Bowman, 1978), but over the years as infill drilling has been approved, this spacing has decreased to 160 acres (Matheny and Ulrich, 1983).

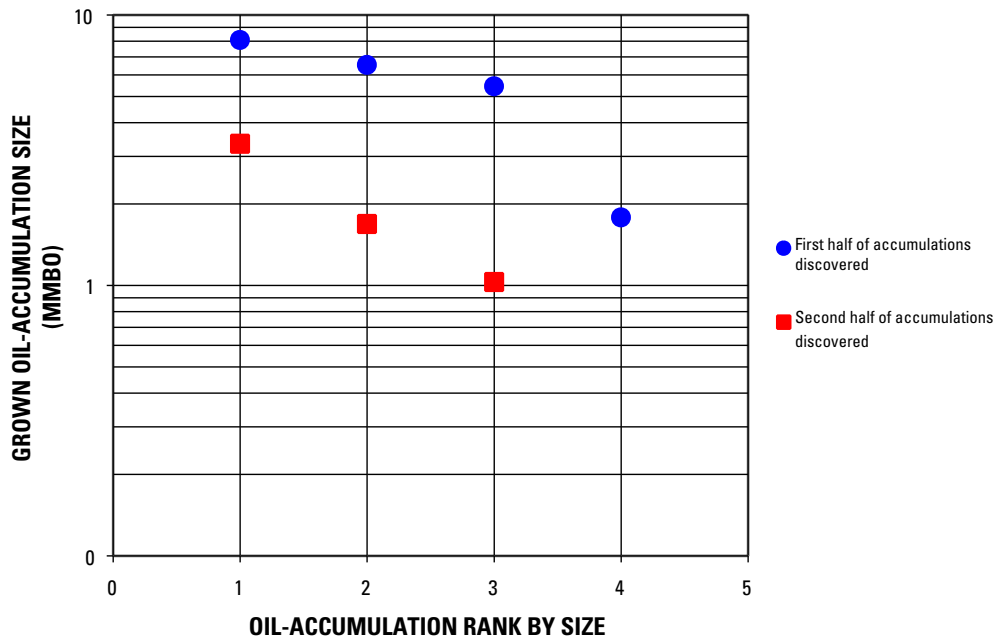


Figure 21. Distribution by halves of grown oil-accumulation size versus rank by size for the Dakota-Greenhorn Conventional Oil and Gas Assessment Unit (50220304). Data from NRG (2001). Only fields exceeding the minimum size of 0.5 MMBO (million barrels oil) are shown.

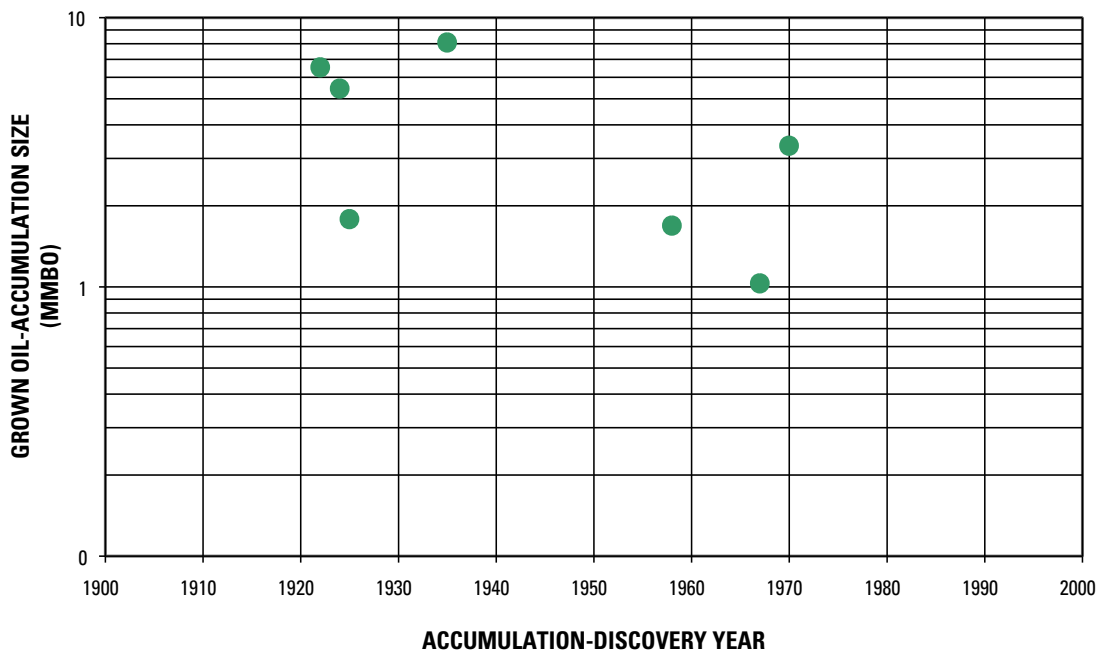


Figure 22. Distribution of grown oil-accumulation size versus accumulation-discovery year for Dakota-Greenhorn Conventional Oil and Gas Assessment Unit (50220304). Data from NRG (2001). Only fields expected to exceed the minimum size of 0.5 MMBO (million barrels oil) are shown.

Table 5. Comparison of 2002 and 1995 estimates of number and sizes of undiscovered oil accumulations in the 2002 Dakota-Greenhorn Conventional Oil and Gas Assessment Unit (50220304) and the 1995 Basin Margin Dakota Oil Play 2205. Sizes and minimum size are in million barrels of oil. Minimum size, minimum size of assessed field. 1995 data from Huffman (1996).

Assessment year	Minimum	Median	Maximum	Minimum size
Number of undiscovered oil accumulations				
2002	1	2	4	0.5
1995	5	10	20	1
Sizes of undiscovered oil accumulations				
2002	0.5	1	6	0.5
1995	1	2	10	1

Gas production in this AU is from a variety of sandstone facies in the Dakota Sandstone that reflect deposition in fluvial, crevasse splay, coastal marine, and shelf environments. These sandstones are now characterized by low porosity and very low permeability (table 1), and the stratigraphic interval from the Dakota Sandstone to the Coniacian unconformity (fig. 2) is underpressured, as is most of the basin. Generally, the fluvial facies that occupy the lowermost part of the incised-valley fill are not gas productive and tend to be water wet (Hoppe, 1978). Although it has been suggested that the gas is being held in place by the updip water (Berry, 1959; Cumella, 1981), Fassett (1991) suggested that the presence of updip water was irrelevant, and that the principal trapping mechanism for holding the gas in place was some type of permeability barrier. It is suggested that high capillary pressure along with low permeability (less than a few millidarcies) barriers due to diagenesis and lateral facies changes are the principal trapping mechanisms. Thus, basin-wide connectivity of permeable beds is absent. Natural fractures are needed to enhance production.

Most of the production comes from the western and southern two-thirds of the AU; the arcuate band of gas production in the northern part of the AU is on the Ignacio-Blanco anticline (fig. 19). South of this anticline is an area where there is little or no production from the Dakota. Part of this latter area coincides with the present-day axis of the basin. The Dakota is reported to be very tight here. In the eastern third of the AU, the uppermost shelf sandstone facies equivalent to the Twowells Tongue (fig. 3, pl. 2) is not well developed and may be absent over large areas. The absence of this unit may have precluded a higher density of exploratory or infill drilling in this part of the AU. New production in the Dakota from this AU may come from

1. additional wells in the eastern third of the AU,
2. infill drilling at less than 160-acre spacing, and
3. recompletion in bypassed sandstone beds in wells that already produced from some Dakota Sandstone beds.

Key parameters of the AU are listed below and are summarized on figure 26.

Source

The primary petroleum source rock for this assessment unit is interpreted to be the Mancos Shale.

Maturation

Thermal maturation for oil and gas is interpreted to range from early Eocene to late Miocene.

Migration

Gas produced in the Mancos Shale or interbedded carbonaceous shale beds in the Dakota migrated short distances into interbedded Dakota Sandstone reservoirs. If the Dakota was originally oil-bearing in this AU and the oil cracked to gas as a result of prolonged heating of the stratigraphic section during the Oligocene and Miocene, migration was nonexistent and the gas was generated in place.

Reservoirs

Reservoirs in the Dakota Sandstone are marginal marine and marine shelf sandstones that are lenticular in shape and interbedded with shale (Bowman, 1978; Hoppe, 1978; Ridgley, 1990; Fassett, 1991) and tend to be finer grained than the basal fluvial sandstones. In the AU, the basal fluvial sandstones are commonly water wet. Reservoirs in the Greenhorn are fractured limestone and in the Juana Lopez, calcarenites.

Traps/Seals

The principal trapping mechanisms are controlled by low permeability of the sandstone and capillary pressure. These factors are augmented by the laterally discontinuous geometry of the sandstone beds, which pinch out into marine shales and paludal mudstones. Local faulting may also be important in compartmentalization of production (Ridgley, 1995). Many of these faults formed syndepositionally, and thus were instrumental in controlling the spatial geometry of sandstone-shale

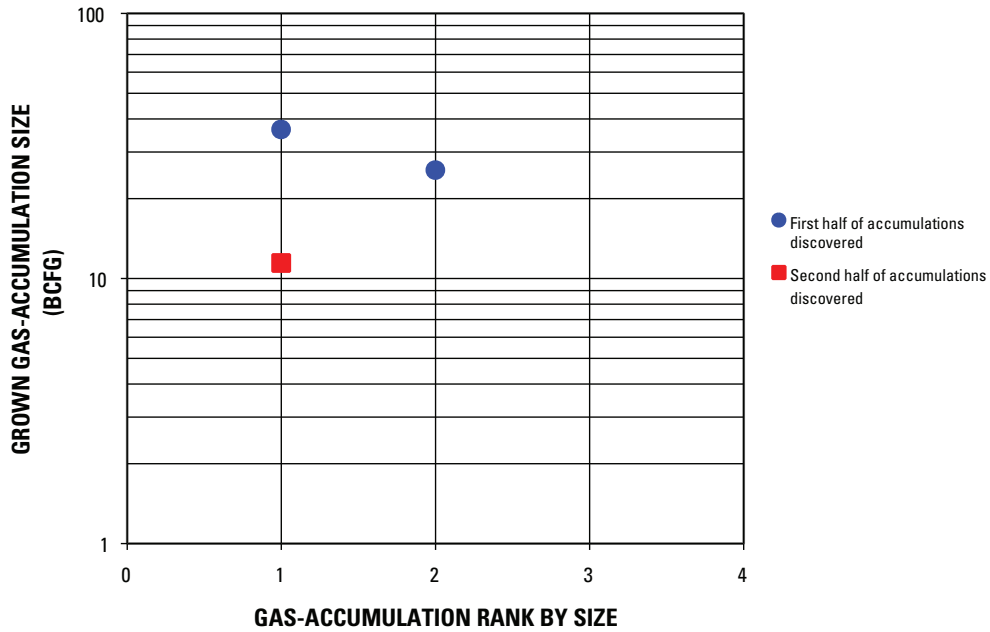


Figure 23. Distribution by halves of grown gas-accumulation size versus rank by size for the Dakota-Greenhorn Conventional Oil and Gas Assessment Unit (50220304). Data from NRG (2001). Only fields exceeding the minimum size of 3 BCFG (billion cubic feet gas) are shown.

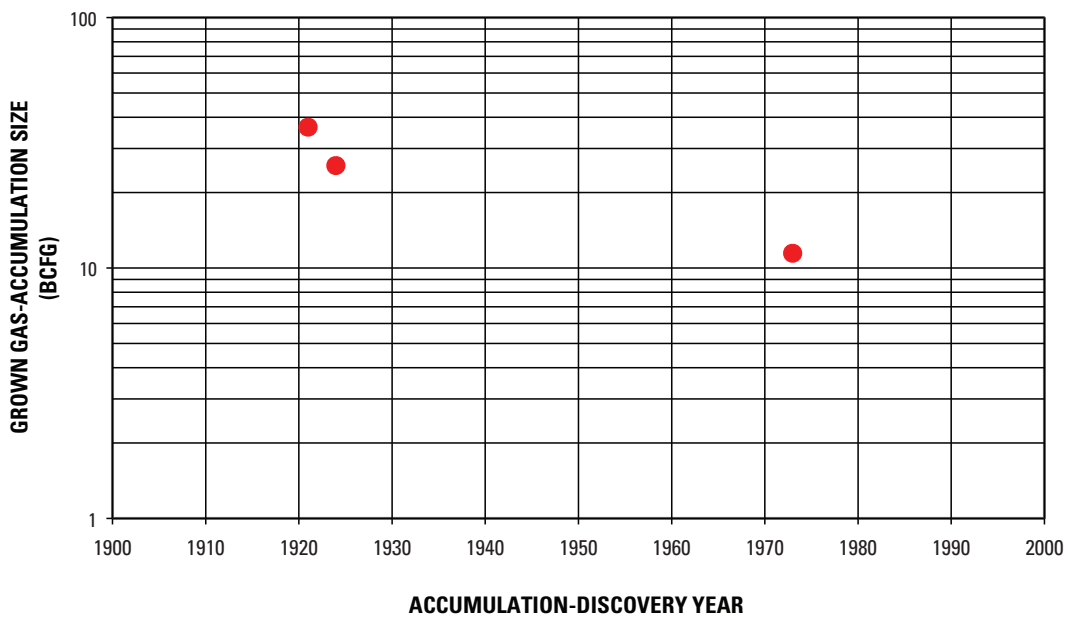


Figure 24. Distribution of grown gas-accumulation size versus accumulation-discovery year for Dakota-Greenhorn Conventional Oil and Gas Assessment Unit (50220304). Data from NRG (2001). Only fields expected to exceed the minimum size of 3 BCFG (billion cubic feet gas) are shown.

Table 6. Comparison of 2002 and 1995 estimates of number and sizes of undiscovered gas accumulations in the 2002 Dakota-Greenhorn Conventional Oil and Gas Assessment Unit (50220304) and the 1995 Basin Margin Dakota Oil Play 2205. Sizes and minimum size gas accumulation are in billion cubic feet of gas. Minimum size, minimum size of assessed field. 1995 data from Huffman (1996).

Assessment year	Minimum	Median	Maximum	Minimum size
Number of undiscovered gas accumulations				
2002	1	2	3	3
1995	1	2	5	6
Size of undiscovered gas accumulations				
2002	3	6	25	3
1995	6	10	25	6

units (Ridgley, 1989). Structures, such as the Ignacio Blanco anticline (fig. 25) and Bondad anticline (fig. 19), are gas bearing. These structures may be important early traps for gas or oil that subsequently cracked to gas. Seals are the various shale beds.

Geologic Model

Gas in this AU occurs within the central part of the San Juan Basin and was generated locally. Gas generated in shale beds in the Mancos Shale or interbedded carbonaceous shale beds of the Dakota as a result of thermocatalytic conversion of kerogen migrated short distances into interbedded sandstone reservoirs of the Dakota. If the Dakota originally contained oil in this AU as suggested by Rice (1983) and the oil cracked to gas as a result of prolonged heating during the Oligocene and Miocene, migration was nonexistent. Facies that host both conventional oil and gas and the continuous basin-centered gas accumulations in the Dakota are the same, stratigraphically, but differ in effective permeability and porosity (table 1). Trapping of the gas in this AU is due to the combination of facies changes, low permeability of the reservoirs, and capillary pressure. The low permeability must have developed in part as well as concurrent with oil and gas generation, thus creating a self-sealing system that did not permit effective updip migration of the late-generated oil and gas. Subtle structures and fractures in addition to lateral pinchout of sandstone reservoirs into enclosing shale may enhance trapping and production, and thus can be used to help define the “sweet” spots within the overall gas-charged AU.

Assessment Results

The Dakota-Greenhorn Continuous Gas Assessment Unit (50220363) was assessed to have potential additions to reserves of 3.93 trillion cubic feet of gas (TCFG) and 15.72 MMBNGL at the mean. The volumes of undiscovered oil, gas, and natural gas liquids estimated in 2002 for the Dakota-Greenhorn Continuous Gas AU are shown in appendix A. These values (table 7) are lower for gas and higher for natural gas liquids compared to the 1995 USGS assessment (Huffman, 1996). The

Ignacio-Blanco and Basin fields have produced over 6 TCFG (IHS Energy Group, 2003). Of this total, slightly more than 211 BCFG (IHS Energy Group, 2002) has been produced from new wells since the last USGS assessment in 1995. A summary of the results, characteristics, and evaluation of the AU is presented on the data form in appendix C.

This AU encompasses an area of 2,513,000 acres at the median, 2,412,000 acres at the minimum, and 2,563,000 acres at the maximum extent of the AU. It contains 5,823 tested cells; for this assessment tested cells are wells that have produced or had some other production test, such as initial production test, drill stem test, or core analysis. A 0.02 BCFG minimum recovery was used for each cell. Applying this cutoff, 5,262 tested cells equaled or exceeded this cutoff. Adequate charge, favorable reservoirs, traps, seals, and favorable timing for charging the reservoirs with greater than the minimum recovery of 0.02 BCFG are present. If the production history of the Dakota-Greenhorn Continuous Gas AU is divided into nearly three equal discovery time periods, plots of the estimated ultimate recoveries (EUR) indicate that the early time period has the best EUR distribution, overall, and the best median total recovery (1.4 BCFG) per cell (fig. 27). Production has generally declined for the remaining two time periods. Part of this apparent decline is due to the fact that wells drilled during the first time block were located in the southern part of the AU, where thicker (stacked) reservoirs are found. Dividing the total production into three nearly equal time periods provides some indication of the maturity of the assessment unit and aids in the estimation of future resources. The EUR distribution for all producing wells in the Dakota-Greenhorn Continuous Gas AU (fig. 28) shows a median total recovery per cell of 0.85 BCFG.

Despite the density of drilling, over 50 percent of the AU remains untested. The subsurface geology is still poorly understood in the eastern part of the AU. Unlike the western half of the AU, the eastern half has much thicker Mancos Shale that overlies overall thinner Dakota Sandstone. Thickness of sandstones of the Dakota, and hence, reservoir facies, is directly related to the various positions of the Dakota shorelines. Positions of these shorelines shifted throughout Dakota deposition, were arcuate in geometry, and thus lacked the strong northwest-southeast geometry of subsequent Cretaceous

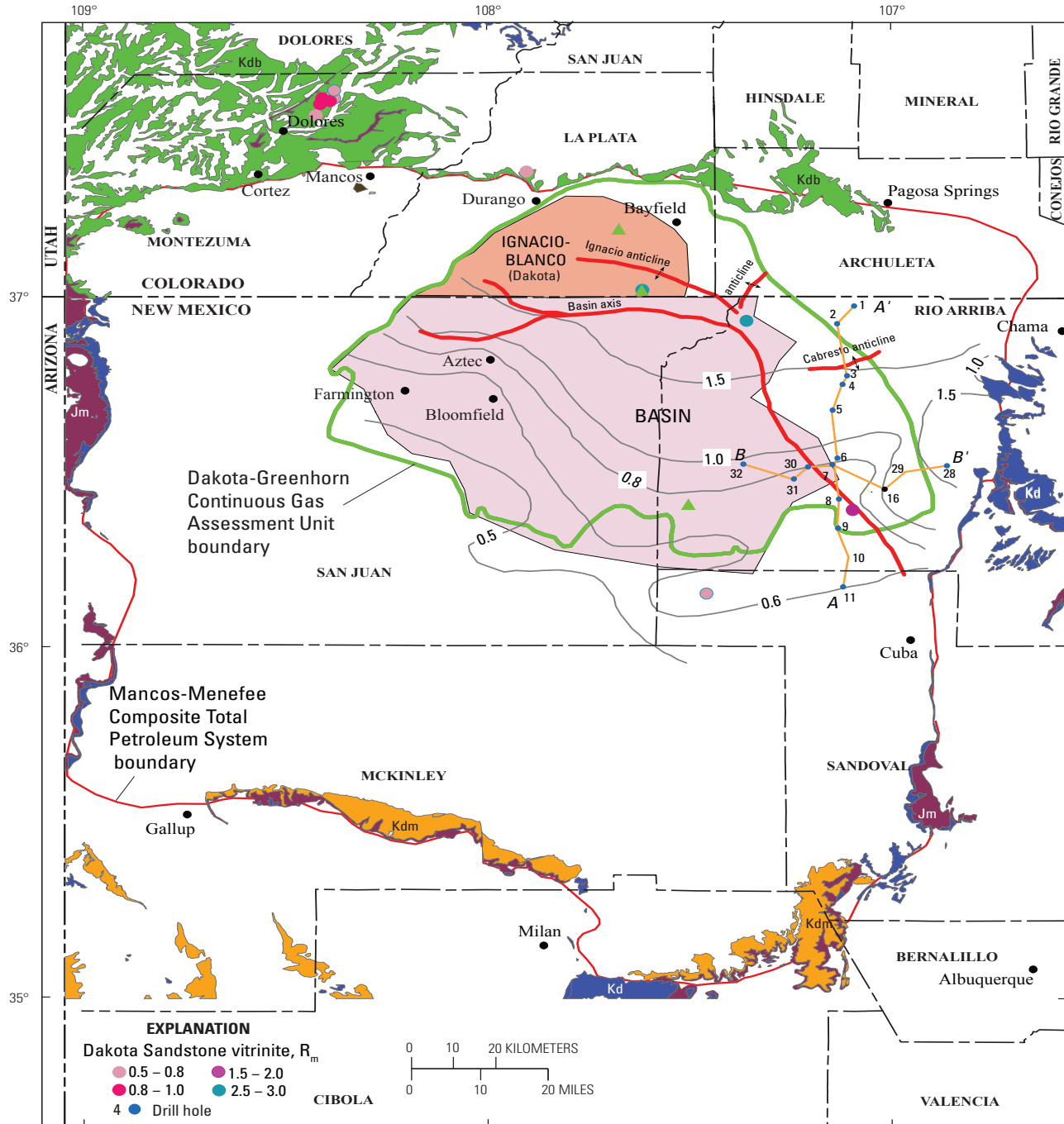
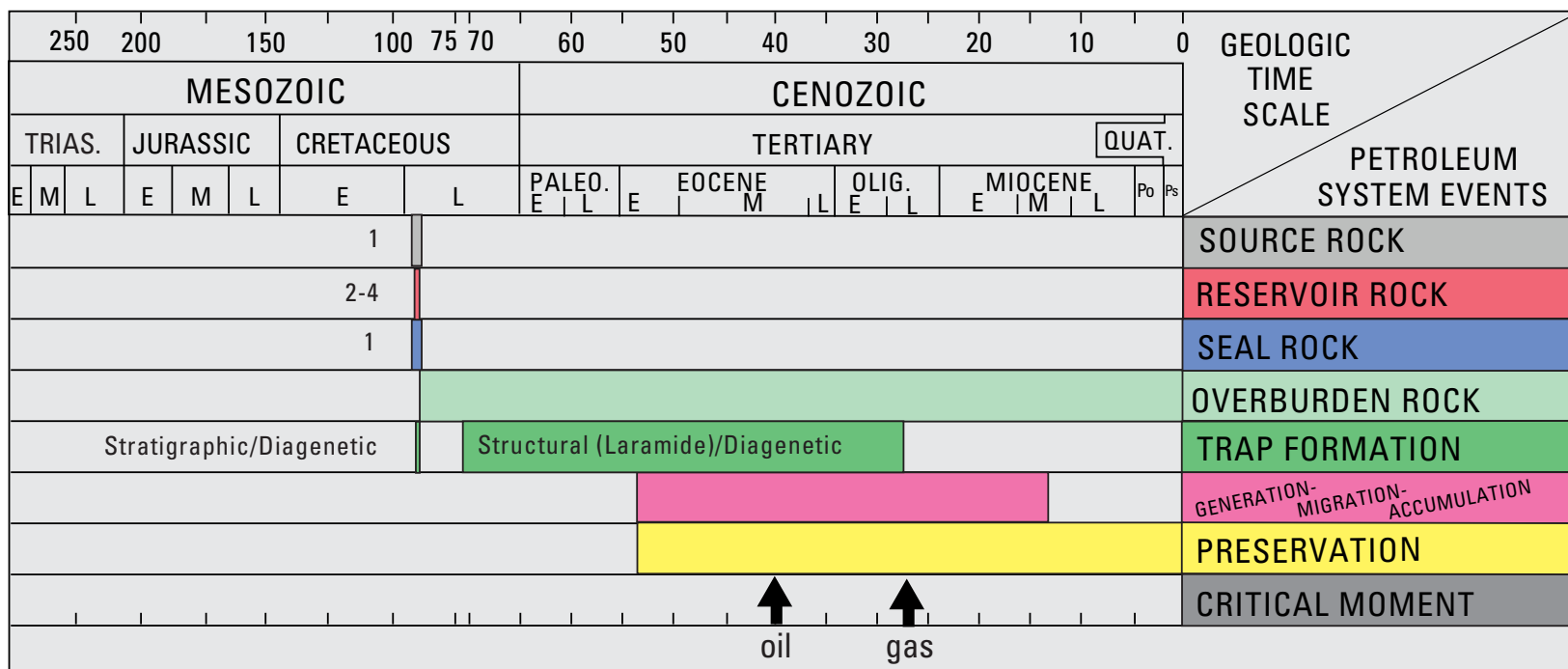


Figure 25. Map showing the Dakota-Greenhorn Continuous Gas Assessment Unit (50220363) boundary (green) in the lower part of the Mancos-Menefee Composite Total Petroleum System, and locations of burial history curves (green triangles) (figs. 15A–C). Symbols for geologic map units: Kdm, Dakota Sandstone-Mancos Shale; Kdb, Dakota Sandstone-Burro Canyon Formation; Kd, Dakota Sandstone; Jm, Morrison Formation (Green, 1992; Green and Jones, 1997). Also shown are locations of cross sections A–A’ and B–B’ (pls. 1 and 2). Thermal maturity contours (gray) are in the Menefee Formation (Fassett and Nuccio, 1990; Law, 1992; Ridgley, 2001b), and vitrinite data for the Dakota Sandstone (colored dots) are from Fassett and Nuccio (1990) and C. Threlkeld (written commun., 2001). Basin gas field (pink polygon) and Ignacio-Blanco gas field (orange polygon) areas are generalized from data in IHS Energy Group (2002).



Rock Units:

1. Mancos Shale
2. Dakota Sandstone
3. Greenhorn (Bridge Creek) Limestone Member of Mancos Shale
4. Juana Lopez Member of Mancos Shale

Figure 26. Events chart that shows timing of key geologic events for the Dakota-Greenhorn Continuous Gas Assessment Unit. Black arrows, critical moments for oil and gas generation. Events chart format is modified from Magoon and Dow (1994). Geologic time scale is from the Geological Society of America web page <http://www.geosociety.org/science/timescale/timescl.htm>, last accessed 2/1/2008, and from Berggren and others (1995). Trias., Triassic; Quat., Quaternary; Po, Pliocene; Ps, Pleistocene; E, early; M, middle; L, late.

shorelines (fig. 5). Drilling for Dakota reservoirs should take into account this different depositional style.

Taking our current knowledge of these constraints into consideration, the entire untested area was not considered to be favorable for having potential additions to reserves in the next 30 years. At the minimum, we estimate 46 percent of the untested area to have potential additions to reserve; at the median, this value is 55 percent of the untested area, and at the maximum, this value is 76 percent. These values were obtained by multiplying the various percentages of untested area deemed favorable by different success ratios. New discoveries will come from infill drilling on closer spacing, step-out drilling from existing fields, and new field discoveries. Total gas recovery per cell for these untested cells is estimated at 0.02 BCFG at the minimum (the cutoff used), 0.4 BCFG at the median, and 8 BCFG at the maximum. The maximum value of 8 BCFG was based on isolated occurrences of high-producing wells (fig. 27).

Gallup Sandstone Conventional Oil and Gas Assessment Unit (50220302)

Introduction

The Gallup Sandstone Conventional Oil and Gas Assessment Unit (50220302) is located in the western and southern part of the TPS (fig. 29). The boundary of this AU was drawn to

1. include the area that lies basinward of the outcrop of the Gallup Sandstone (Green, 1992; Green and Jones, 1997) and roughly the most seaward position of the Gallup A sandstone (fig. 8) (Molenaar, 1983; Nummedal and Molenaar, 1995),
2. include the area of wells that have penetrated the Gallup, and
3. exclude other sandstone reservoirs in the Mancos that occur above the regional unconformity of Coniacian age and thus are genetically unrelated to the Gallup.

Oil with small quantities of associated gas is produced from the Gallup Sandstone.

Almost all of the oil produced from Gallup reservoirs has been from Hospah and Hospah South fields (fig. 8) on the Hospah dome, a north–south trending structure located on the southern flank of the San Juan Basin in the southern part of the AU (fig. 29). Two northeast-trending parallel faults bisect the dome. Production is from two distinct Gallup reservoirs informally called the “upper Hospah” sand (Torrivio Sandstone Member of Molenaar, 1977b) and “lower Hospah” sand (main Gallup Sandstone). Production from the upper sandstone occurs both within the fault-bounded block as well as north of the faulted zone. Production from the “lower Hospah” sand occurs only within the fault-bounded block that defines the Hospah South field. The Hospah structure was identified in 1924, and oil was first produced in 1927 (Bircher, 1978) from the upper Hospah sand. The upper and lower Hospah sand in the Hospah South field (within the fault block) were brought online in the mid-1960s. Oil produced from the Hospah fields is heavy; API gravities range from 24° to 30° and may be biodegraded (Van Delinder, 1986).

Additional oil production has come from the Nose Rock field (figs. 8 and 29), reportedly in a fluvial channel of the Torrivio (Fassett, 1991), although no detailed description is available on this field. The field was discovered in 1986 and produced for less than 12 years (IHS Energy, 2001). A small quantity of oil (243 barrels of oil) was reportedly produced from Gallup reservoirs in one well in the Marcelina field (Edmister, 1983; Fassett, 1991). The Marcelina field (fig. 29) occurs at the north end of a faulted anticline, which has only subtle surface expression. This field was discovered in 1977 and only produced oil from 1980 to 1981 before being abandoned (Edmister, 1983). The oil was reported to have API gravity around 40°. Oil has also been produced from “upper Hospah” or Torrivio in the Miguel Creek and Miguel Creek North fields (fig. 29) in sandstones above the main Gallup. This oil has a reported API gravity of 31°. The small Rattlesnake field (Matheny, 1983) is located outside the AU boundary (fig. 29), and production from the Gallup appears to be localized. Like oil in the underlying Dakota at the Rattlesnake field, oil in Gallup reservoirs is light, between 58° and 60° API

Table 7. Comparison of 2002 and 1995 estimated undiscovered resources for the 2002 Dakota-Greenhorn Continuous Gas Assessment Unit (50220363) and 1995 Dakota Central Basin Play 2205, and the 2002 Mesaverde Central-Basin Continuous Gas Assessment Unit (50220361) and the 1995 Central Basin Mesaverde Gas Play 2209. Gas values are in trillion cubic feet and natural gas liquids in millions of barrels. 1995 data from Huffman (1996)

Commodity	1995 assessment results	2002 assessment results
Dakota-Greenhorn Continuous Gas Assessment Unit		
Gas	8.211	3.929
Natural gas liquids	0.33	15.72
Mesaverde Central-Basin Continuous Gas Assessment Unit		
Gas	9.584	1.317
Natural gas liquids	0.48	5.27

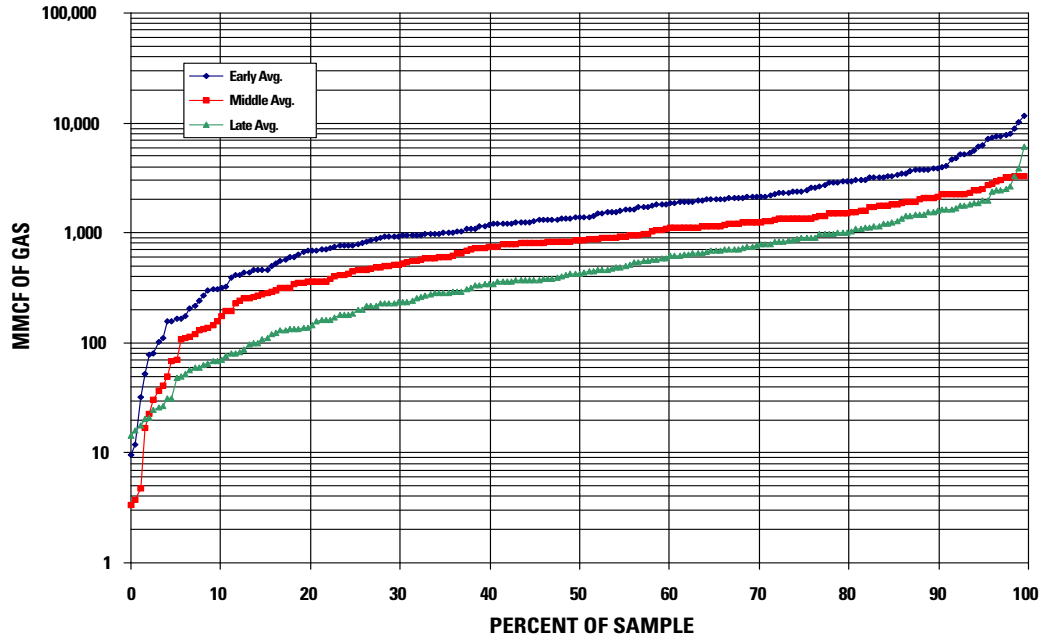


Figure 27. Graph showing estimated ultimate recoveries (EUR) of Dakota-Greenhorn Continuous Gas Assessment Unit gas wells divided into three nearly equal periods of production time. EURs calculated using data from IHS Energy Group (2002). MMCF, million cubic feet. Data provided by T. Cook (2002). MMCF, million cubic feet.

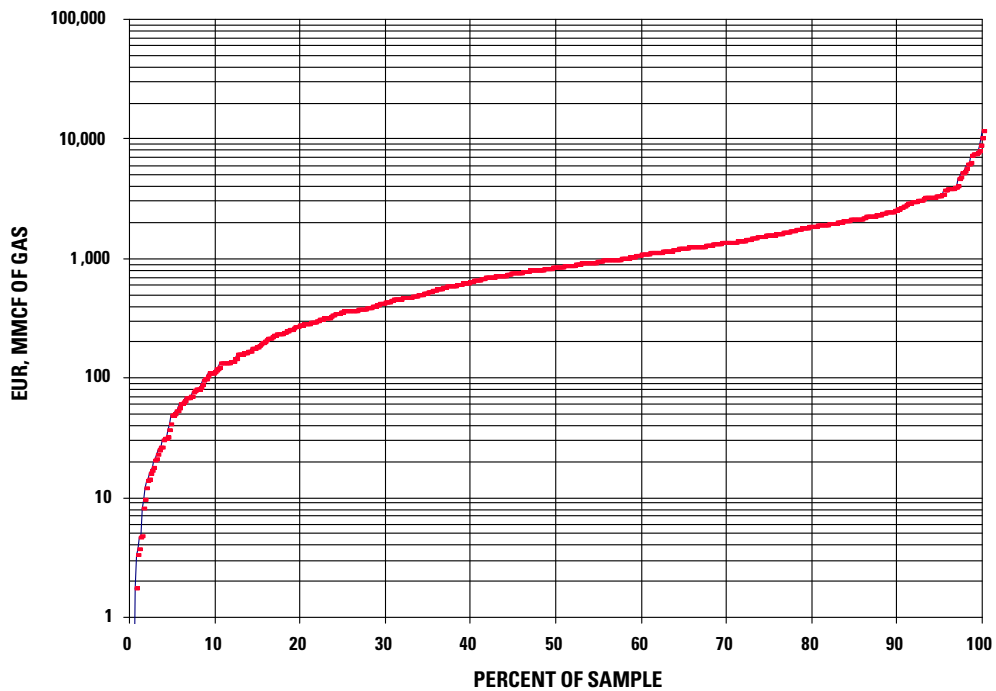


Figure 28. Graph showing combined distribution of estimated ultimate recoveries (EUR) of Dakota-Greenhorn Continuous Gas Assessment Unit gas wells. EURs calculated using data from IHS Energy Group (2002). Data provided by T. Cook (written commun., 2002). MMCF, million cubic feet.

gravity. It was felt that no additional productive areas in the Gallup Sandstone would be found between the Rattlesnake field and the AU, and thus the AU boundary was not extended to include the field.

Oil staining and seeps have been found in the Torrivio Sandstone Member of the Gallup in the outcrop area near Pinedale, N. Mex. (fig. 29) (Molenaar, 1977c; Nummedal and Molenaar, 1995, their figs. 11 and 11G). The stains and seeps occur in several stratigraphic traps in a braided channel system and have been interpreted to be a remnant of a previously formed oil accumulation. The location of oil seeps in the Pinedale area (fig. 29), which is southwest of the Hospah and Marcelina fields, indicates that oil may have moved through a much broader area of the Gallup system. Key parameters of the AU are listed below and are summarized on figure 30.

Source

The primary petroleum source rock for this assessment unit is interpreted to be the Mancos Shale.

Maturation

Thermal maturation is interpreted to range from early to late Eocene.

Migration

Migration distances were longest in the reservoirs in the southern part of the AU (Hospah, Marcelina, Miguel Creek and Miguel Creek North, and Nose Rock fields and Pinedale outcrop). These fields and outcrop lie outside the area of the mature pod of source rock in the Mancos (fig. 7) as previously defined. In the area of the Hospah, Nose Rock, and Marcelina fields, the Gallup shorelines have a northwest–southeast orientation and sandstones in the fluvial Torrivio Sandstone Member are oriented perpendicular or oblique to this. With these orientations, the Gallup sandstones may not be conducive to serving as direct conduits for long distance migration from the pod of mature Mancos Shale to the northeast because the last major sandstone (Gallup A) shoreline lies south of the main oil producing sandstones in the Tocito. However, Molenaar (1977b) suggests that oil in Gallup fields and seeps in McKinley County migrated through the Gallup from the area where distal Gallup facies (thin sandstone, siltstone, and shale) (fig. 8) underlies Tocito sandstones. It is possible that in this area, which would lie within the pod of mature source rock, there are sufficient fractures or faults to serve as conduits for oil migration into the main Gallup or Torrivio to the south. The Coniacian unconformity may also have served as a migration path with oil migrating along the unconformity and then into sandstones of the Gallup. Oil originally from the mature pod of the Mancos Shale, located north of the Chaco slope (figs. 4 and 7), may also have migrated into the underlying Dakota Sandstone at the Hospah and Marcelina fields (fig. 29) and from there updip

along faults into reservoirs of the Gallup Sandstone. Expulsion and migration of oil was probably enhanced by tectonic activity during the Laramide orogeny.

Reservoirs

Reservoirs in the Gallup Sandstone are mostly fluvial sandstones of the Torrivio Sandstone Member in the Hospah or Nose Rock fields; lenticular marine sandstones of the main Gallup at Hospah South field and Torrivio Sandstone Member at Marcelina, Miguel Creek, and Miguel Creek North fields; and possibly marginal marine sandstones of the Gallup in the Rattlesnake field. The reservoir sandstones are interbedded with shale.

Traps/Seals

Traps in the Gallup Sandstone are combination stratigraphic and structural. Stratigraphic traps occur where laterally discontinuous fluvial and marginal marine sandstone lenses pinch out into continental carbonaceous shales of the Gallup or marine shales of the Mancos. Structural traps consist of folds, many of which are faulted. Draping of lenticular fluvial or marine sandstone bodies over folds provide combined stratigraphic-structural traps. Seals are primarily shale beds within the Gallup, regional shale tongues in the Mancos Shale, and local faults.

Geologic Model

In this AU, all the reported oil accumulations lie outside the pod of mature source beds in the Mancos Shale (fig. 7). The oil was generated from marine carbonaceous shale in the Mancos from early to late Eocene. A model to explain the presence of oil in Gallup reservoirs in the southern part of the AU is speculative because of the lack of data to clearly define the migration pathways. In this area, oil API gravities in Hospah fields are very low (24°–32°). However, these oils could be biodegraded (Van Delinder, 1986) because oil from the nearby Marcelina field was reported to have API gravity near 40°. This value (table 1) is close to that reported for most Mancos-sourced oils in fields near the pod of mature source rock. The presence of oil in the Hospah, Marcelina, Miguel Creek, Miguel Creek North, and Nose Rock fields and in outcrops near Pinedale (fig. 29) to the southwest suggests that oil once occurred throughout a large area but has either been removed by erosion or through later meteoric water encroachment (Molenaar, 1977c; Struna and Poettmann, 1988). Traps in this area are structural, stratigraphic, or a combination of both. In the Hospah and Marcelina fields, faults that extend into the underlying Dakota may have served as conduits for upward migration of oil from the Dakota to the Gallup reservoirs. The traps at Nose Rock and Pinedale are both stratigraphic and occur where fluvial sandstone of the Torrivio pinches out laterally into enclosing mudstones.

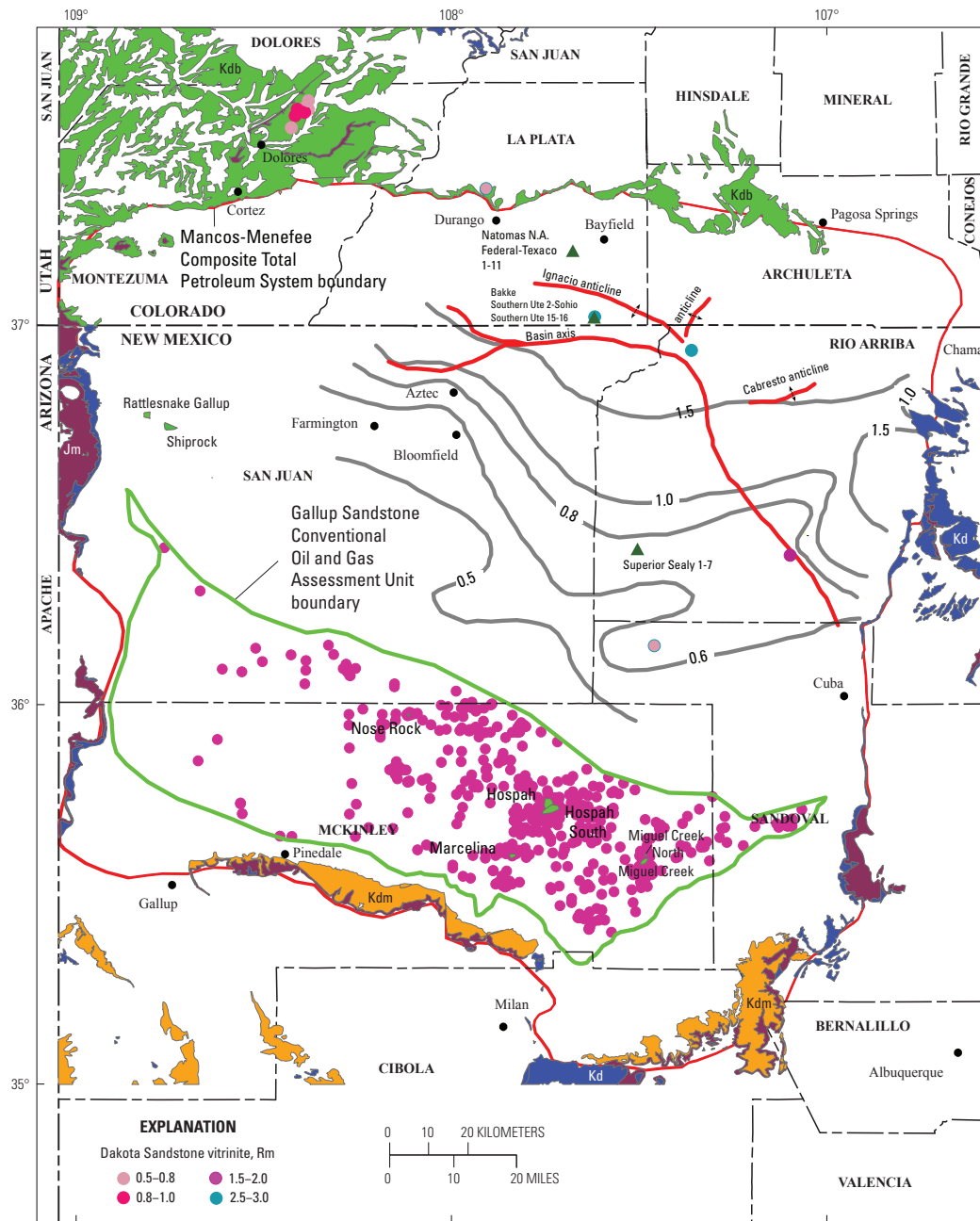
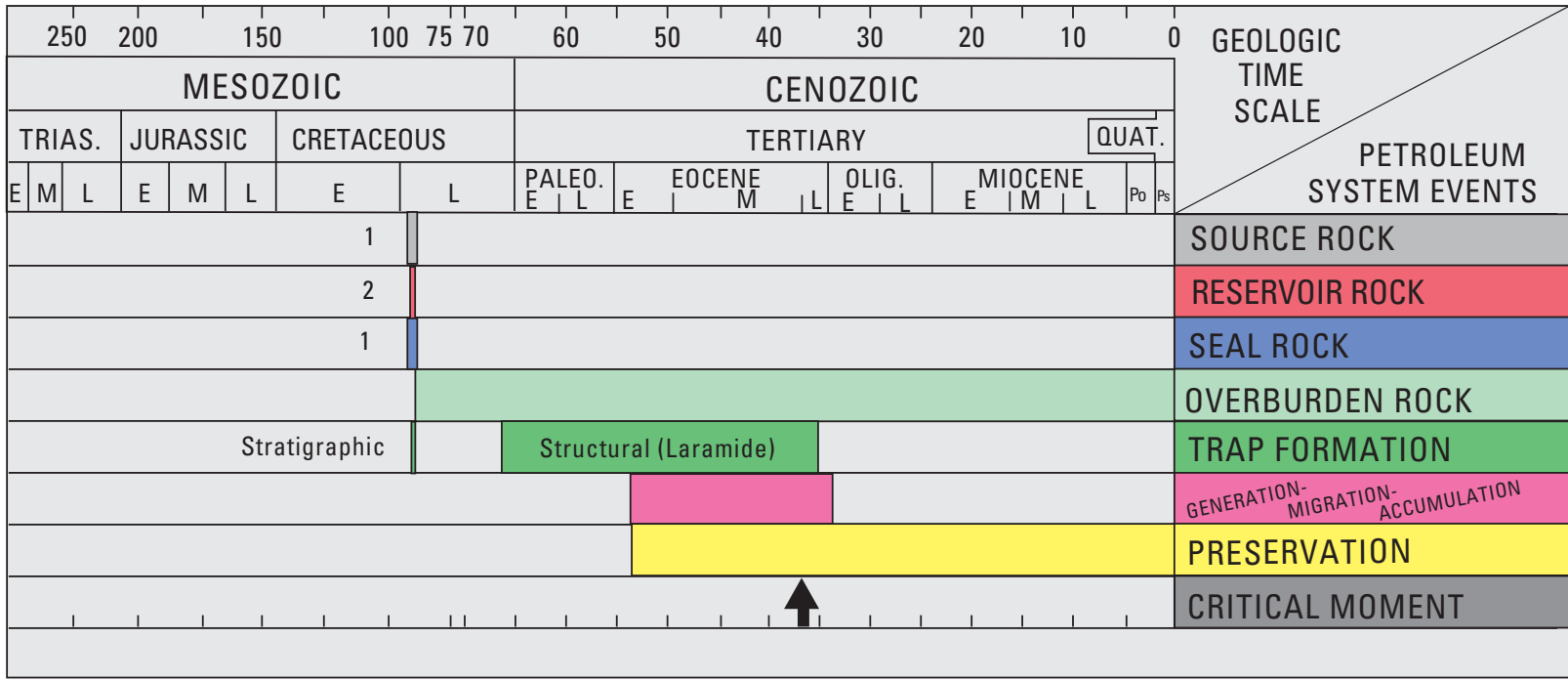


Figure 29. Map showing the Gallup Sandstone Conventional Oil and Gas Assessment Unit (AU) (50220302) boundary (green) in the lower part of the Mancos-Menefee Composite Total Petroleum System, oil and gas fields, distribution of wells that penetrate the Gallup (pink dots) (data from IHS Energy Group, 2002), and locations of burial history curve (green triangles) (figs. 15A–C). Oil field (green) and gas field (red) boundaries are extrapolated from IHS Energy Group (2002). Thermal maturity contours (gray) are in the Menefee Formation (Fassett and Nuccio, 1990; Law, 1992; and Ridgley, 2001b), and vitrinite data for the Dakota Sandstone (colored dots) are from Fassett and Nuccio (1990) and C. Threlkeld (written commun., 2001). Symbols for geologic map units: Kdm, Dakota Sandstone-Mancos Shale; Kdb, Dakota Sandstone-Burro Canyon Formation; Kd, Dakota Sandstone; Jm, Morrison Formation from Green (1992) and Green and Jones (1997).



Rock Units:
 1. Mancos Shale
 2. Gallup Sandstone, Torrivio Sandstone Member

Figure 30. Events chart showing key geologic events for the Gallup Sandstone Conventional Oil and Gas Assessment Unit. Black arrow shows the critical moment for oil generation. Events chart format is modified from Magoon and Dow (1994). Geologic time scale is from the Geological Society of America web page <http://www.geosociety.org/science/timescale/timescl.htm>, last accessed 2/1/2008, and from Berggren and others, (1995). Trias., Triassic; Quat., Quaternary; Po, Pliocene; Ps, Pleistocene; E, early; M, middle; L, late.

Assessment Results

The Gallup Conventional Oil and Gas Assessment Unit (50220302) covers about 2,079,044 acres and was estimated at the mean to have potential additions to reserves of 2.34 MMBO, 0.35 BCFG, and 0 barrels of natural gas liquids. The volumes of undiscovered oil, gas, and natural gas liquids estimated in 2002 for the Gallup Conventional Oil and Gas AU are shown in appendix A. A summary of the results, characteristics, and evaluation of the AU is presented on the data form in appendix D, which in this case evaluates the size and distribution of producing fields in the area. This AU was included in the Tocito-Gallup Play 2207 in the 1995 USGS assessment (Huffman, 1996). There is less than adequate charge (probability 0.8) but adequate reservoirs, traps, seals, access, and timing of generation and migration of hydrocarbons (probabilities of 1.0 each) for finding at least one additional field with a total recovery greater than the stated minimum of 0.5 MMBO (grown). The lower charge probability reflects our inadequate knowledge of charge of these reservoirs.

This assessment unit produces mainly oil with minor associated gas (IHS Energy Group, 2002). No non-associated gas accumulations were estimated. Historical data from the NRG (2001) database were used to estimate the number and sizes of undiscovered oil accumulations. Currently only two oil fields producing from the Gallup Sandstone, Hospah and Hospah South, meet the minimum cutoff. There have been no new oil fields that have met the minimum field-size cutoff of 0.5 MMBO since the discovery of the Hospah South field in 1965. Although many outcrop studies of the Gallup Sandstone describe the relation of the Gallup to the Torrivio (a principal reservoir at the Hospah fields) (Molenaar, 1977b,c, 1983; Nummedal and Molenaar, 1995), the subsurface expression of these relations is poorly known, and no regional studies have been published. Most of the wells drilled through the Gallup are in the eastern half of the AU (fig. 29), and thus the western half of the AU is geologically less well known. Migration pathways from the area where the Mancos is thermally mature enough to produce oil to reservoirs in the AU are poorly understood. These migration pathways are further complicated by the unconformity that progressively cuts into and eventually removes the Gallup to the northeast. We estimated that a maximum of four oil, a median of two, and a minimum of one accumulation, meeting the minimum cutoff, could still be discovered.

Hospah field was discovered in 1926 and Hospah South field in 1965. About 8.3 MMBO have been produced from the Gallup at Hospah and 14.3 MMBO from the Gallup at Hospah South (IHS Energy Group, 2002). Using these data the maximum estimated size of undiscovered accumulations is 15 MMBO, the median size 1 MMBO, and the minimum size 0.5 MMBO.

Mancos Sandstones Conventional Oil Assessment Unit (50220303)

Introduction

The Mancos Sandstones Conventional Oil Assessment Unit (50220303) covers all but the central part of the TPS (fig. 31). The boundary of this AU was drawn to include

1. the area within the TPS boundary of the Mancos Shale that lies basinward of the Mancos outcrop (Green, 1992; Green and Jones, 1997) in the north and lies north of the Gallup Sandstone Conventional Oil and Gas AU,
2. the area outside the boundary of the Mancos Sandstones Continuous Gas Assessment Unit,
3. that part of the Mancos Shale that lies above the Coniacian unconformity and below the Point Lookout Sandstone of the Mesaverde Group, and
4. most wells in these strata that have a calculated gas-oil ratio (GOR) of less than 20,000 cubic feet of gas per barrel of oil (cfg/bo) (fig. 32).

Over 3,800 wells produce from the Mancos Shale Tocito Sandstone Lentil, and "Gallup" (see prior discussion) sandstone reservoirs. Wells with a GOR $\geq 20,000$ are found in the Mancos Sandstones Conventional Oil AU as well as in the Mancos Sandstones Continuous Gas AU described in the following pages. Where they occur in the conventional AU, the wells with a GOR $> 20,000$ are located mostly in gas caps (fig. 32), especially in "Gallup" sandstone reservoirs in the eastern part of the AU. Most wells with a GOR $\leq 20,000$ have been included in the conventional AU. This approach differs from that used in differentiating the Dakota-Greenhorn Conventional Oil and Gas AU from the Dakota-Greenhorn Continuous AU where wells with a GOR between 5,000 and 20,000 were placed in the Dakota-Greenhorn Continuous Gas AU because they were surrounded by wells with a GOR $\geq 20,000$. A different approach was needed because here the GOR changes gradually both between fields and in a basinward direction, especially in the "Gallup" fields in the southeast part of the AU near the boundary with the Mancos Sandstones Continuous Gas AU (fig. 32).

Oil in this AU is primarily produced from two intervals, the Tocito Sandstone Lentil and "Gallup" sandstone; however, production from Tocito reservoirs is reported as "Gallup" in both Colorado and New Mexico (IHS Energy, 2002), making it difficult to differentiate the volume of oil produced from Tocito reservoirs from that produced from the overlying "Gallup." Volumetric analysis must be completed on a field-by-field basis and in some fields production from the Tocito and overlying "Gallup" is commingled. This requires the examination of well logs to determine the producing interval in each field. In 1991, the last time such a breakout of production was reported, Fassett (1991) reported 30 fields completed in the Tocito and 39 in the overlying "Gallup." At that time, Tocito production was nearly two and one-half times that of the "Gallup." The

difference in production can be attributed to the better reservoir properties of the Tocito sandstones (table 1). Also, Tocito reservoirs produce little if any water, unlike most conventional accumulations, and this has led to more produced oil because of the lack of regional water encroachment. Production in the “Gallup” interval is enhanced by the presence of natural fractures, especially in the area of small structures (Gorham and others, 1977; Emmendorfer, 1992). The fractures were reported to be tectonically induced, and thus probably formed during the Laramide orogeny in the Late Cretaceous through Eocene. The best production is reported to come from wells containing open fractures that appear to be filled with oil (see various field descriptions in Fassett, 1978a, b, 1983a).

Earliest oil production from Mancos sandy shale reservoirs was in 1924 at the Red Mesa field (fig. 31), on the west side of the Hogback monocline (fig. 4). Production is reported to be in shale reservoirs of the Mancos and mostly from fractures (Lauth, 1983). In 1927 oil was discovered in the Mancos Shale (below the Juana Lopez and above the Greenhorn Members) in the Mancos River field (fig. 31) on an anticlinal structure on the Mancos Creek monocline; production has been small, less than the 0.5 MMBO cutoff used in this assessment (Emmendorfer, 1983). The oil has an API gravity of 33°. The first Tocito fields were discovered in 1951 and are now combined to form the Blanco Tocito South field (see fig. 37 for location under Mancos Sandstones Continuous Gas Assessment Unit). The next Mancos oil fields were discovered in 1955; production was from Tocito sands in the Bisti field and the silty, sandy zones in the overlying “Gallup” section in the Verde field (fig. 31). Additional fields were discovered in the Tocito and overlying “Gallup” interval in the late 1950s, early 1960s, late 1960s, and sporadically throughout the 1970s (Matheny and Ulrich, 1983). Ten of the 30 fields with oil production from the Tocito (Fassett, 1991) were discovered in 1981 (Matheny and Ulrich, 1983). No major oil field discoveries in the Tocito or “Gallup” have been found since 1984.

Oil in Tocito fields (Fassett, 1991) is from a series of elongate northwest- to southeast-trending reservoirs that are found principally in San Juan County, N. Mex. (figs. 31 and 33). Most of the oil production from the “Gallup” is in Rio Arriba County, although a few oil fields do produce from the “Gallup” in San Juan County (fig. 33) (Fassett, 1991, his fig. 5). The lack of oil production from Tocito reservoirs in Rio Arriba County is due to the fact that most of the Tocito-like sandstones, except for Blanco Tocito South field (see fig. 37 under Mancos Sandstones Continuous Gas Assessment Unit) that are found north of the main oil-producing area, should be gas bearing (Ridgley, 2001a) and thus are found in the Mancos Continuous Gas AU. Key parameters of the AU are listed below and are summarized on figure 34.

Source

The primary petroleum source rock for this assessment unit is interpreted to be the Mancos Shale.

Maturation

Thermal maturation is interpreted to range from early Eocene to early Oligocene.

Migration

Oil in the Tocito reservoirs bordering the western and southern margin of the basin-centered gas accumulation (Mancos Sandstones Continuous Gas AU described below) migrated short distances from the mature Mancos source beds into the sandstone reservoirs where it was stratigraphically trapped. Oil produced from the other “Gallup” reservoirs also migrated short distances from the Mancos source beds and was also stratigraphically trapped in the fine-grained, heterolithic facies.

Reservoirs

Reservoirs included in this AU are

1. lenticular Tocito sandstones, which overlie the Coniacian unconformity, and
2. the “Gallup” sandstones of industry, which includes the transgressive El Vado Sandstone Member of the Mancos Shale, and the regressive wedge of rocks that overlie the Tocito (pls. 1 and 2) (Ridgley, 2001a).

Traps/Seals

The principal traps in the Tocito are stratigraphic; the lenticular sandstones pinch out in all directions into the surrounding marine shales of the Mancos. The principal traps in the overlying “Gallup” sequence are also stratigraphic and enhanced by the low permeability of the sandstone as well as by capillary pressure. These factors are augmented by the laterally discontinuous geometry of the marine sandstone beds, which pinch out into marine shales and neritic mudstones. Structures are locally important in trapping early generated oil. Seals are interbeds of shale.

Geologic Model

Oil in this AU was generated from the mature pod (fig. 7) of marine carbonaceous shale in the Mancos. Initial oil expulsion occurred during the Eocene in the latter part of the Laramide orogeny and may have continued into early Oligocene. During this period, the oil migrated into Tocito and “Gallup” reservoirs in the western, southern, and eastern parts of the AU. Migration distances were short to these reservoirs, essentially from shale source beds to enclosed sandstone reservoirs. All the producing fields lie within the mature part of the Mancos Shale. The Tocito reservoirs are stratigraphic

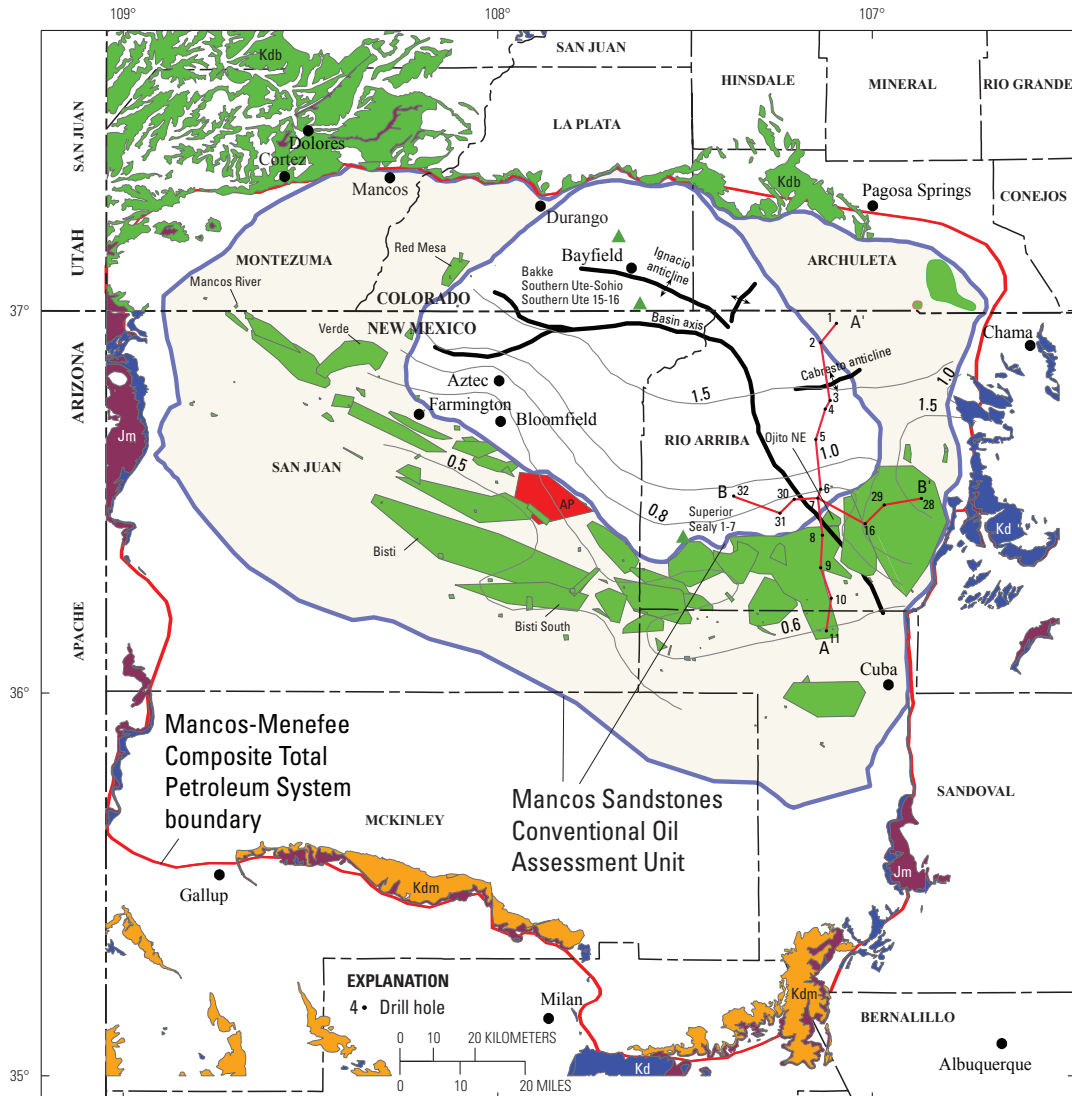


Figure 31. Map showing the Mancos Sandstones Conventional Oil Assessment Unit (50220303) (light tan) in the upper part of the Mancos-Menefee Composite Total Petroleum System, oil (green) and gas (red) fields, and locations of the wells (green triangles) used to construct the burial history curves found in this report (figs. 15A–C). Also shown are locations of cross sections A–A' and B–B' (pls. 1 and 2). Thermal maturity contours are in the Menefee Formation (Fassett and Nuccio, 1990; Law, 1992; and Ridgley, 2001b) and vitrinite data for the Dakota Sandstone (colored dots) are from Fassett and Nuccio (1990) and Threlkeld (written commun., 2001). Field boundaries are extrapolated from data in IHS Energy Group (2002). Symbols for geologic map units: Kdm, Dakota Sandstone-Mancos Shale; Kdb, Dakota Sandstone-Burro Canyon Formation; Kd, Dakota Sandstone; Jm, Morrison Formation from Green (1992) and Green and Jones (1997). AP, Angel's Peak field.

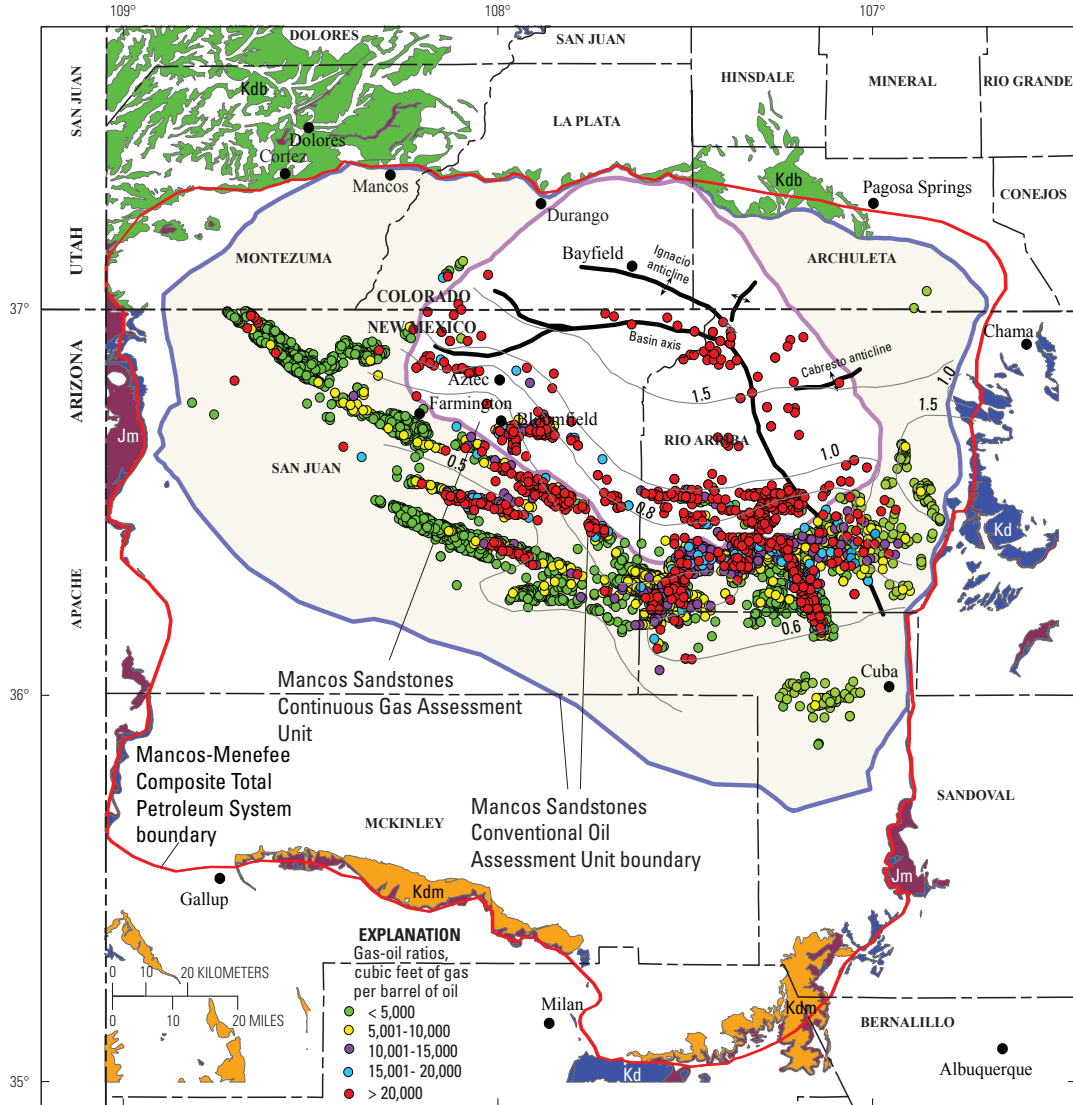
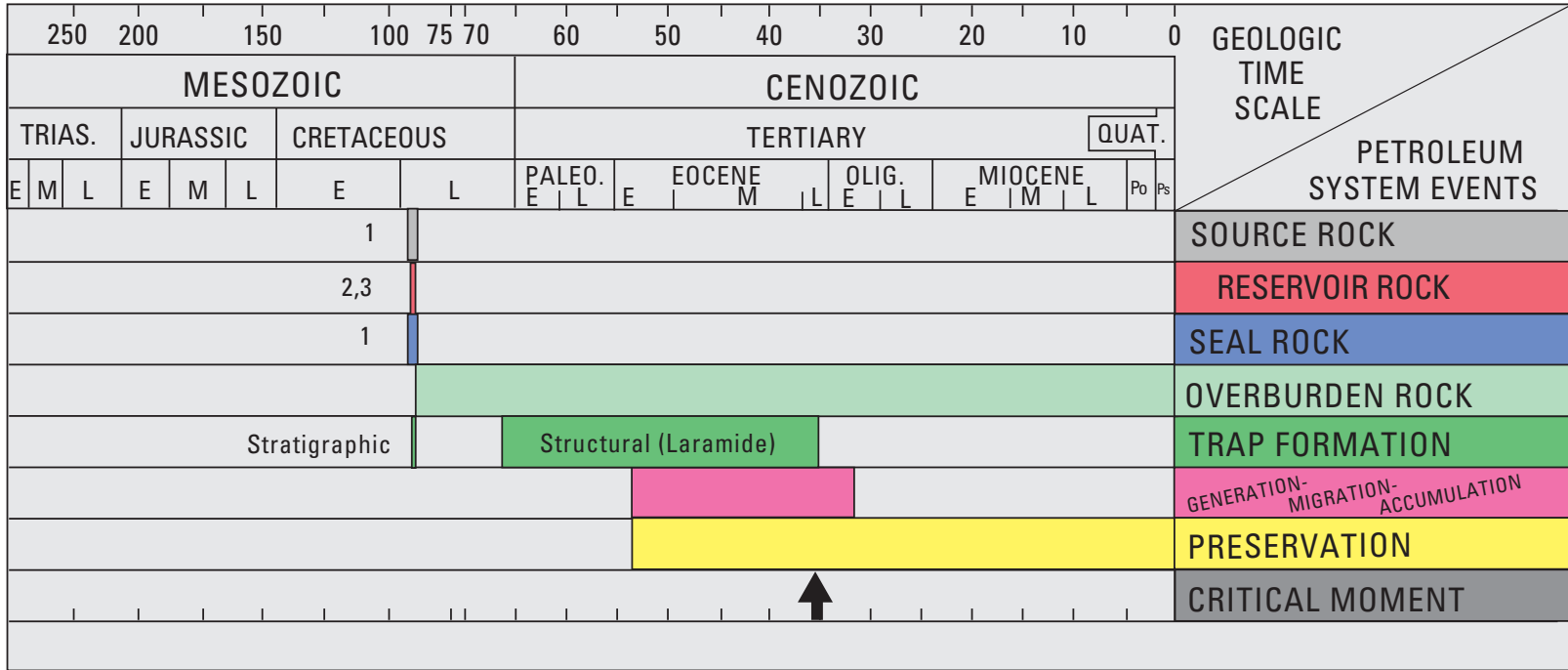


Figure 32. Map showing distribution of gas-oil ratios (in cubic ft of gas per barrel of oil) in wells producing from upper Mancos Shale, Tocito Sandstone Lenticle, and "Gallup" sandstones in the Mancos Sandstones Conventional Oil Assessment Unit (shaded light tan with purple boundary) and Mancos Sandstones Continuous Gas Assessment Unit (white with mauve boundary). Data from IHS Energy Group (2002). Thermal maturity contours are in the Menefee Formation (Fassett and Nuccio, 1990; Law, 1992; and Ridgley, 2001b). Symbols for geologic map units: Kdm, Dakota Sandstone-Mancos Shale; Kdb, Dakota Sandstone-Burro Canyon Formation; Kd, Dakota Sandstone; Jm, Morrison Formation from Green (1992) and Green and Jones (1997).



- Rock Units:
1. Mancos Shale
 2. Tocito Sandstone Lentil of Mancos Shale
 3. "Gallup" sandstone (El Vado Sandstone Member of Mancos Shale)

Figure 34. Events chart that shows key geologic events for the Mancos Sandstones Conventional Oil Assessment Unit. Black arrow shows critical moment for oil and gas generation. Events chart format is modified from Magoon and Dow (1994). Geologic time scale is from the Geological Society of America web page <http://www.geosociety.org/science/timescale/timescl.htm>, last accessed 2/1/2008, and from Berggren and others, (1995). Trias., Triassic; Quat., Quaternary; Po, Pliocene; Ps, Pleistocene; E, early; M, middle; L, late.

traps; the sandstone reservoirs are encased in mudstone. The “Gallup” reservoirs are very fine grained and extremely heterolithic; both these properties would inhibit long distance migration, and any oil generated may have developed relatively in place (Ridgley, 2001a). Production from the “Gallup” reservoirs is enhanced by fractures, especially those associated with the development of small structures (Gorham and others, 1977; Emmendorfer, 1992).

Assessment Results

The Mancos Sandstones Conventional Oil Assessment Unit (50220303) covers about 4,412,500 acres. This AU incorporates part of the Tocito-Gallup Play 2207 and the Mancos Fractured Shale Play 2208 from the 1995 USGS assessment (Huffman, 1996). The AU was estimated at the mean to have potential additions to reserves of 11.99 MMBO, 57.57 BCFG, and 2.3 MMBNGL. The volumes of undiscovered oil, gas, and natural gas liquids estimated in 2002 for the Mancos Sandstones Conventional Oil AU are shown in appendix A. A summary of the assessment input data for the AU is presented on the data form in appendix E, which for this AU estimates the numbers and sizes of undiscovered accumulations. This approach differs from that used in the 1995 National Oil and Gas Assessment of these rocks (Huffman, 1996). In the 1995 assessment, most of the area in this AU and in the Mancos Sandstones Continuous Gas AU were assessed as containing continuous oil and gas accumulations and used a cell-based methodology to assess undiscovered resources (Schmoker, 1996). There is adequate charge, reservoir, traps, seals, access, and timing of generation and migration of hydrocarbons, indicating a geologic probability of 1.0 for the presence of at least one additional field with a total recovery greater than the stated minimum of 0.5 MMBO (grown) or 3 BCFG (grown).

Although the oil was probably generated locally and thus may constitute a continuous oil system (Ridgley, 2001a), most of the oil production is in somewhat defined areas, characterized by sandstone distribution or structure. Areas between the fields do not appear to host oil accumulations. It was therefore decided in this 2002 assessment to assess the oil and associated gas in this AU in terms of conventional accumulations. Most of the gas in Tocito or “Gallup” reservoirs occurs as continuous accumulations, and these accumulations were assigned to the Mancos Sandstones Continuous Gas AU, described below. The change in resource methodology affected the assessment results, and in this case the numbers for oil were reduced and the numbers for gas increased compared to those presented in the 1995 assessment.

This assessment unit produces oil and small quantities of associated gas. There are 29 oil fields in this AU that meet the 0.5 MMBO minimum cutoff and one gas field that meets the minimum 3 BCFG cutoff. Production comes from the Tocito and overlying “Gallup” reservoirs. There have been no new oil fields that have met the minimum field-size cutoff since the discovery of the Ojito Northeast and Bisti South oil

fields in 1984 (fig. 31). Most of the oil fields are found in the southern part of the central basin. The trend of Tocito sandstones is defined by the elongate northwest–southeast areas of oil production, mostly in San Juan County, New Mexico (fig. 33). Within the general exploration area of the AU, the Tocito sandstones are probably well delineated, and any new oil-bearing Tocito sandstones are likely to be found to the southeast in the direction of extension of the Tocito sandstone trend. We estimate that a maximum of 10 undiscovered oil accumulations, a median of 5, and a minimum of 2 meeting the minimum cutoff, could still be discovered.

Using the discovery information for fields that meet the minimum cutoff, the median grown size of discovered oil accumulations is 5.84 MMBO for the first third of the discovery period, 1.84 MMBO for the second third, and 2.9 MMBO for the last third (fig. 35). Figure 35 also shows the ranking of these fields, by size, for the three discovery periods. Grown sizes of oil accumulations are, except for two fields, larger in the first third reflecting discovery of the major Tocito fields. Later production is commingled from the Tocito and “Gallup” interval, or from the “Gallup.” The size of the undiscovered fields is estimated from the distribution of the discovered field sizes versus the discovery year (fig. 36), where the grown size of an accumulation is determined by adjusting upward the known petroleum volume to account for future reserve growth. Later grown accumulations generally show decline from the first third. The largest grown oil field is about 50.9 MMBO. Using these data, the maximum estimated size of undiscovered accumulations is 10 MMBO, the median size is 2 MMBO, and the minimum size is 0.5 MMBO.

There is only one gas field in this AU (NRG, 2001), the Angel’s Peak field (fig. 31), which was discovered in 1958. This field produces both associated gas and oil, although gas exceeds oil production (IHS Energy Group, 2002). There may be small gas accumulations in this AU, but if they exist, they would be less than the minimum 3 BCFG cutoff used in this assessment. No non-associated gas fields exceeding the minimum cutoff are estimated to exist.

Mancos Sandstones Continuous Gas Assessment Unit (50220362)

Introduction

The Mancos Sandstones Continuous Gas Assessment Unit (50220362) covers the central part of the TPS (figs. 4 and 37). The boundary includes

1. the area basinward of the outcrop of the Mancos Shale (Green, 1992; Green and Jones, 1997) that is central to and excluded from the Mancos Sandstones Conventional Oil AU, previously discussed (fig. 31);
2. that part of the Mancos Shale that lies above the Coniacian unconformity and below the Point Lookout Sandstone of the Mesaverde Group; and

- most wells that have a calculated gas-oil ratio (GOR) of greater than 20,000 cubic feet of gas per barrel of oil (cfg/bo) (fig. 32) and thus are primarily reported as gas wells (IHS Energy, 2002) (fig. 33).

A GOR of greater than 20,000 seems to best define the low permeability gas zone of the central part of the basin. Outside that zone, there are wells that have a GOR between 5,000 and 20,000. Most wells in this GOR range have been included in the conventional category. This gas assessment unit is typical of those called basin-centered, in that the gas occupies the central part of a basin (Schmoker, 1996).

Gas is primarily produced from two intervals, the Tocito Sandstone Lentil and “Gallup” in this AU. Production from Tocito reservoirs is reported as “Gallup” in both Colorado and New Mexico. The only production reported as Tocito is from the Blanco Tocito South field, which is an oil field (Fassett and Jentgen, 1978; IHS Energy, 2002) (fig. 37). This makes it difficult to differentiate the volume of gas produced from Tocito sandstones from that produced from the fine-grained facies of the overlying “Gallup.” However, based on the regional distribution of fields producing from the Tocito and “Gallup” (fig. 37), most gas produced to date has come from the “Gallup” interval and nearly all has been from wells in New Mexico. More than 7 MMBO and 174 BCFG have been produced from reservoirs in this AU (IHS Energy Group, 2003).

Currently 31 fields produce gas from the Tocito and “Gallup” in this AU; many of these are small and only the large fields are labeled (fig. 37). In addition there are a number of undesignated fields and wildcat wells that produce from these reservoirs. Based on field descriptions (Fassett, 1978a,b, 1983a), gas is produced from Tocito sandstones in the Blanco Tocito South, BS Mesa, Flora Vista, Largo, and Wild Horse fields (fig. 37), all discovered between 1951 and 1964. The gas is stratigraphically trapped in the lenticular sandstones that lie on or not far above the Coniacian regional unconformity (pls. 1 and 2). These sandstones have good porosity and permeability, although the permeability is less than that found in the oil-producing Tocito sandstones (table 1). Gas is produced from silty and sandy beds at various stratigraphic intervals in the “Gallup” in many fields. Many of the fields consist of one or two wells. Natural fractures are important for production and may have developed in the brittle, tightly cemented rocks concurrent with folding during the Laramide orogeny. A number of the fields are associated with small structures.

Several of the fields included in this AU produce both oil and gas and have wells with a GOR between 5,000 and 20,000. The principal fields that fit these criteria are Armenta, Blanco Tocito South, Baca, Lindrith West, and Tapacito (fig. 37). All are located in the southern part of the AU and point to the difficulty of drawing the boundary between a continuous-type accumulation and conventional accumulations, especially if the reservoirs were once charged with oil and some of that oil has cracked to gas. The Blanco Tocito South field (fig. 37) has produced over 4 MMBO and 12 BCFG (IHS Energy Group, 2002), yet the neighboring Largo and

BS Mesa fields produce only gas. All these fields underlie the 0.8- and 1.0-percent R_m vitrinite isorefectance contours in the Menefee Formation (fig. 37). These fields, with the exception of part of the Armenta field, lie stratigraphically below wells that produce only gas in the overlying Mesaverde Central-Basin Continuous Gas AU and stratigraphically above gas-bearing sandstones in the underlying Dakota-Greenhorn Continuous Gas AU (fig. 19).

Most of the Tocito and “Gallup” reservoirs in this AU have not been adequately tested for gas, and fracture stimulation may be required in order to test for the presence of gas. Because of the low permeability of the reservoirs, gas zones go undetected on conventional log suites. Our uncertainty in evaluating the presence or absence of reservoir facies in this AU lies in the poor understanding of the depositional system and the identification of subtle structures where fractures may have formed. Additionally, it is important to have a better understanding of the origin of the gas. If the gas cracked from oil, most of the reservoirs should be charged with gas, although they may not all be economic. If the gas formed after loss of effective permeability in the “Gallup” reservoirs, production may well be found only in association with fractures.

Potential sandstone and siltstone reservoirs in the Mancos that are transitional with the overlying Point Lookout Sandstone of the Mesaverde Group constitute a hypothetical target to host gas in this AU. These units are the distal marine facies of the prograding Point Lookout shoreface. There is no reported production from these reservoirs, yet the overlying Point Lookout does produce gas in places where it overlies this AU. Key parameters of the AU are listed below and are summarized on figure 38.

Source

The primary petroleum source rock for this assessment unit is interpreted to be the Mancos Shale.

Maturation

Thermal maturation is interpreted to range from early Eocene to late Miocene.

Migration

Migration distances from Mancos source beds into the adjacent sandy reservoirs were short for both early generated oil and late generated gas from the thermocatalytic conversion of kerogen in the marine shales. It is hypothesized that much of the gas now found in the various sandy reservoirs of the Mancos Shale cracked from oil within the reservoirs as a result of prolonged heating induced by greater depths of burial in this AU. As such, this gas was generated in place.

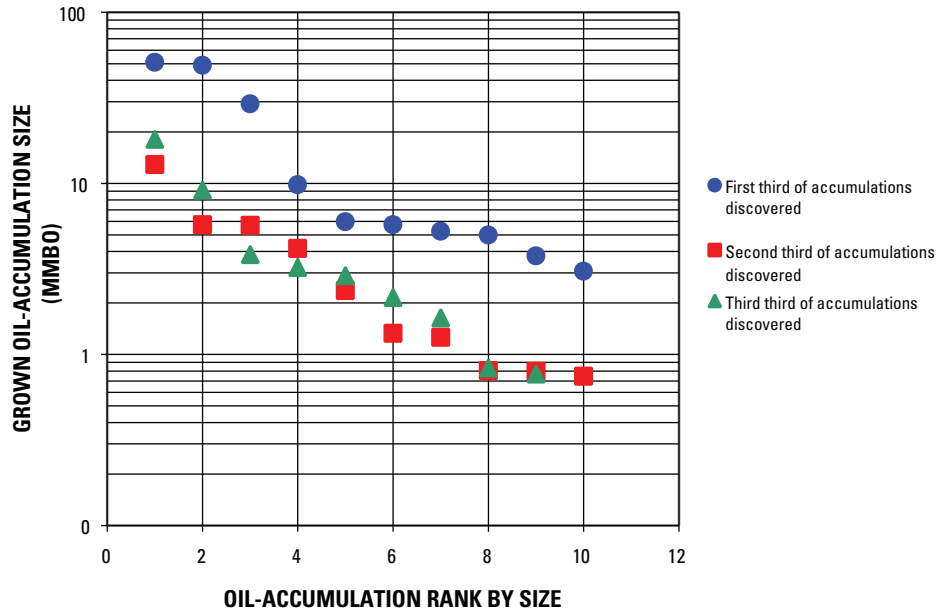


Figure 35. Distribution by thirds of grown oil-accumulation size versus rank by size for producing fields greater than 0.5 MMBO (million barrels oil) in the Mancos Sandstones Conventional Oil Assessment Unit (50220303). Data is from NRG (2001).

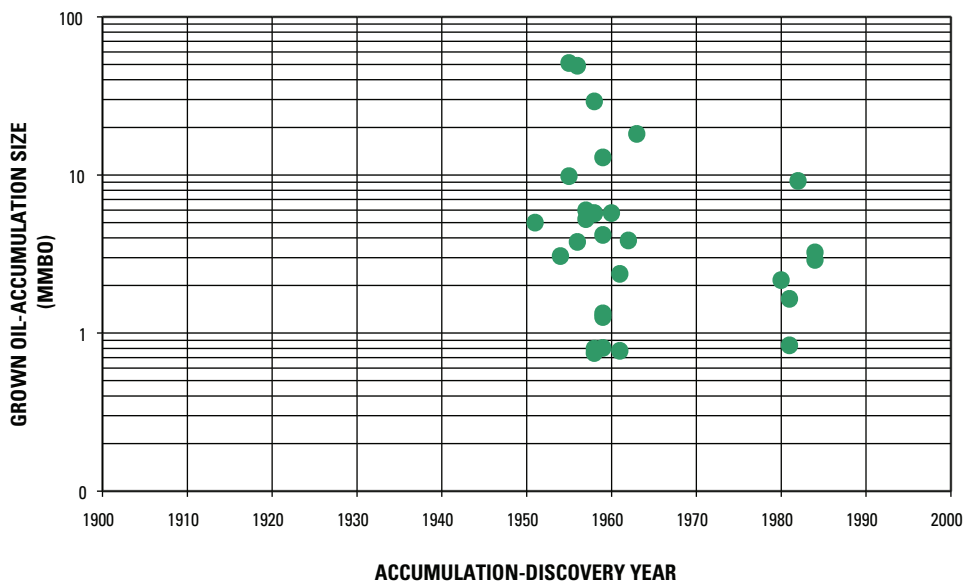


Figure 36. Distribution of grown oil-accumulation size versus accumulation-discovery year for producing fields greater than 0.5 MMBO (million barrels oil) in the Mancos Sandstones Conventional Oil Assessment Unit (50220303). Data is from NRG (2001).

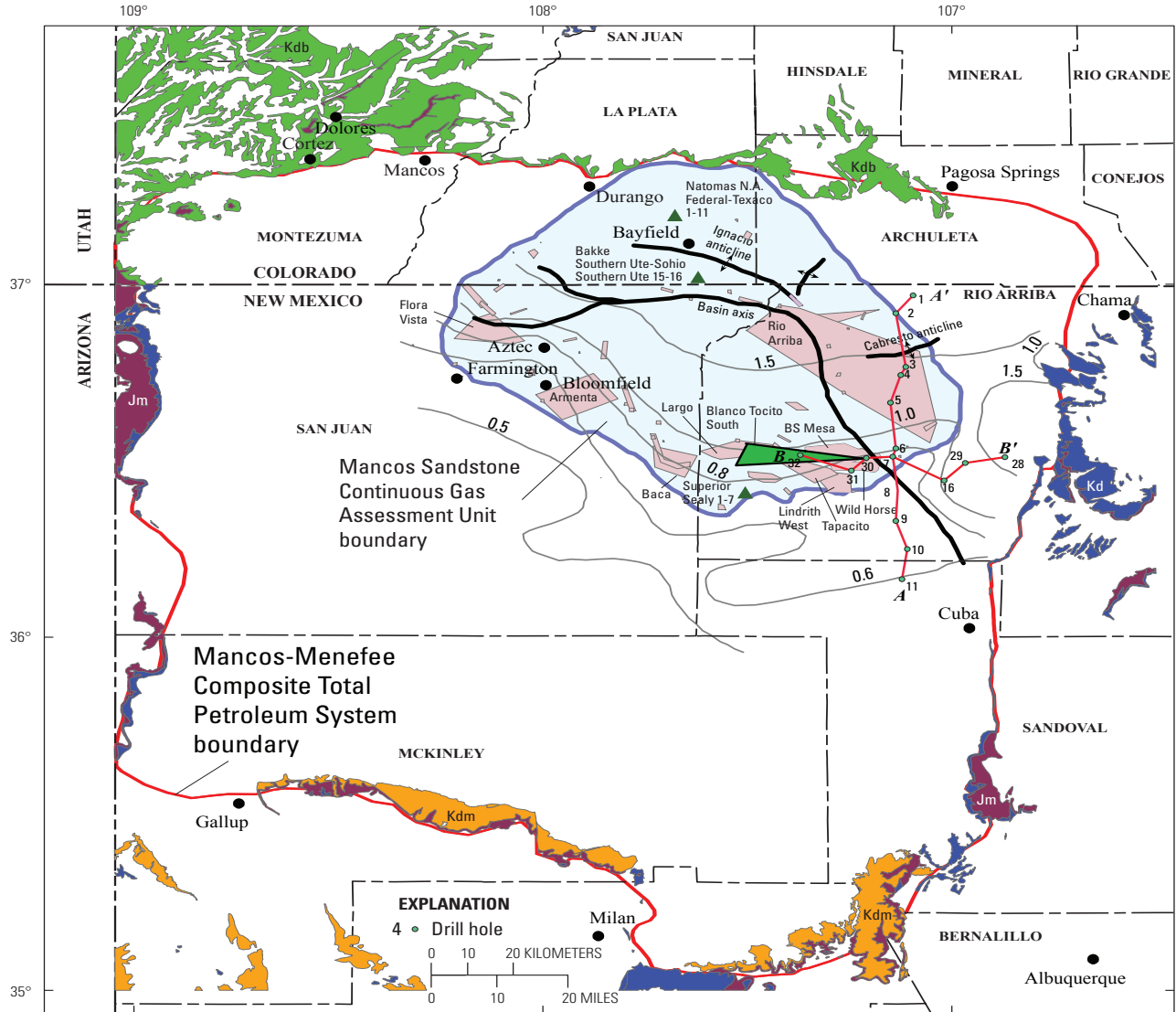


Figure 37. Map showing the location of the Mancos Sandstones Continuous Gas Assessment Unit (50220362) area (light blue) and boundary (light purple) in the middle and upper part of the Mancos-Menefee Composite Total Petroleum System. Also shown are the locations of the wells (green triangles) used to construct the burial history curves found in this report (figs. 15A–C), oil fields (green), and gas fields (pink) in the assessment unit. All gas fields are in the “Gallup” interval, except for the Blanco Tocito South field, which is in the Tocito Sandstone Lentil. Only fields discussed in the text are labeled. Thermal maturity contours (gray) are in the Menefee Formation (Fassett and Nuccio, 1990; Law, 1992; and Ridgley, 2001b). Field boundaries are extrapolated from data in IHS Energy Group (2002). Also shown are the locations of cross sections A–A’ and B–B’ (pls. 1 and 2). Symbols for geologic map units: Kdm, Dakota Sandstone-Mancos Shale; Kdb, Dakota Sandstone-Burro Canyon Formation; Kd, Dakota Sandstone; Jm, Morrison Formation from Green (1992) and Green and Jones (1997).

Reservoirs

The reservoirs in this AU, as in the Mancos Shale Conventional Oil AU, are the sandstone, siltstone, and sandy mudstone units variously called Tocito, “Gallup” (by industry), and basal Niobrara sands by Molenaar (1977b). Included in this group are

1. lenticular Tocito sandstones or basal Niobrara sands of Molenaar (1977b), which overlie the Coniacian unconformity;
2. the “Gallup,” which includes the transgressive El Vado Sandstone Member of the Mancos Shale and regressive wedges of rocks that overlie the Tocito; and
3. sandstone and siltstone reservoirs in the Mancos that are transitional into the overlying Point Lookout Sandstone of the Mesaverde Group (pls. 1 and 2).

Traps/Seals

The principal traps are local structures, low permeability sandstone, and capillary pressure. These factors are augmented by the laterally discontinuous geometry of the marine sandstone beds, which pinch out into marine shales and neritic mudstones. Seals are the various shale beds. Local faulting and fracturing may also be important in compartmentalization of production, as well as in enhancing production (Gorham and others, 1977; Emmendorfer, 1992).

Geologic Model

Gas in this AU occurs in the central part of the San Juan Basin and was generated locally. Gas produced in shale beds of the Mancos Shale as a result of thermocatalytic conversion of kerogen migrated short distances into interbedded sandstone reservoirs of the Tocito and Mancos. Any early generated oil in Tocito or Mancos reservoirs in this AU cracked to gas as a result of prolonged heating during Oligocene and Miocene time, and migration of the gas was nonexistent. Facies that host conventional oil and gas accumulations and continuous basin-centered gas in the Tocito and Mancos are the same. The principal differences between the two types of accumulations are lower permeability and a reduction in porosity in this AU (table 1). Trapping of the gas in this AU is due to the combination of small structures, low permeability of the reservoirs, and capillary pressure, coupled with underpressuring of the reservoirs. The low permeability must have developed, in part, prior to oil generation as well as concurrent with oil and gas generation, thus creating a self-sealing system that did not permit effective updip migration of late generated oil and gas. Subtle structures and fractures in addition to lateral pinchout of sandstone reservoirs into enclosing shale may enhance production, and thus can be used to define the “sweet” spots within the overall gas-charged AU.

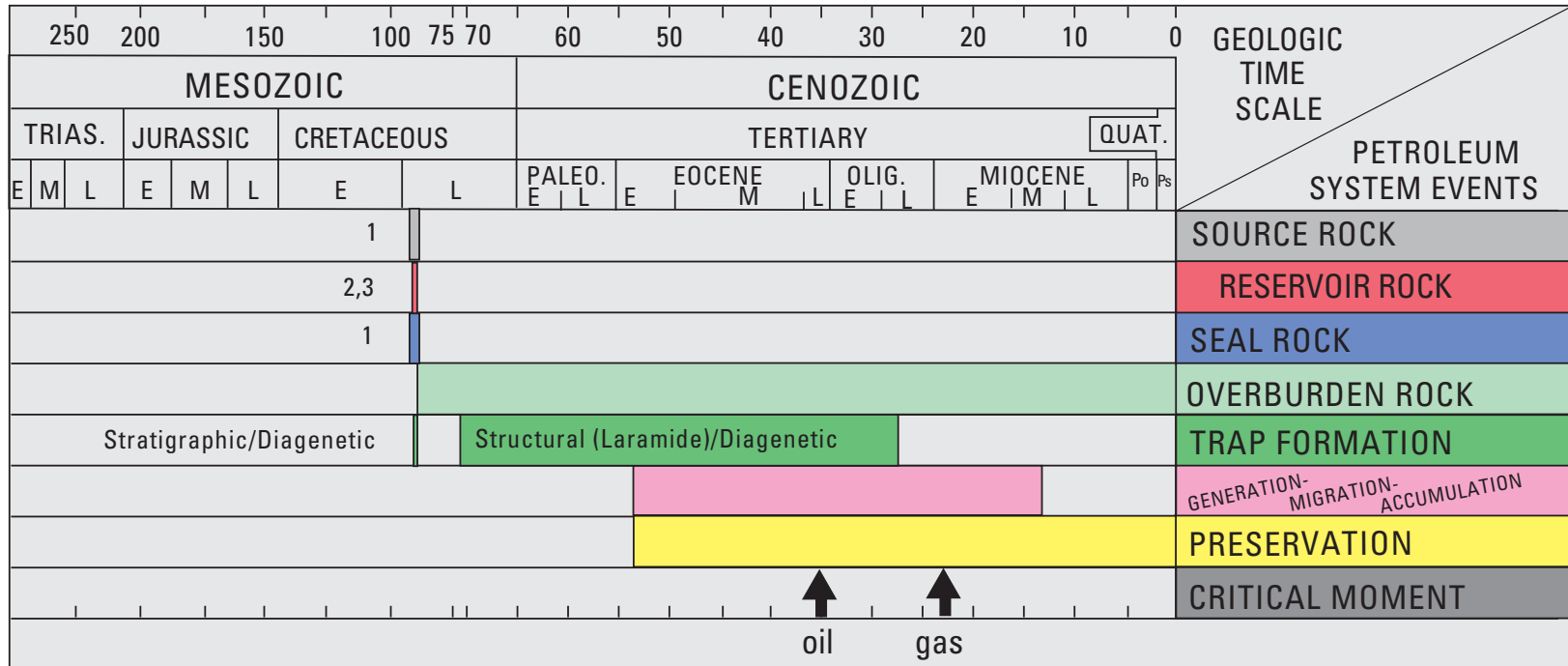
Assessment Results

The Mancos Sandstones Continuous Gas AU (50220362) was assessed to have potential additions to reserves of 5,116.37 BCFG and 75.96 MMBNGL at the mean. The volumes of undiscovered oil, gas, and natural gas liquids estimated in 2002 for the Mancos Sandstones Continuous Gas AU are shown in appendix A. This AU encompasses an area of 1,884,000 acres at the median, 1,845,000 acres at the minimum, and 1,942,000 acres at the maximum. A summary of the assessment input data are presented in the data form in appendix F.

There were 513 tested cells; tested cells include wells that have produced or had some other production test, such as initial production test, drill stem test, or core analysis. A 0.02 BCFG minimum recovery was used for each cell. Applying this cutoff, 460 tested cells equaled or exceeded this cutoff. There is adequate charge, reservoir, traps, seals, access, and timing of generation and migration of hydrocarbons, indicating a geologic probability of 1.0 for finding at least one additional field with a total recovery greater than the stated minimum recovery of 0.02 BCFG per cell. If the production history of the Mancos Sandstones Continuous Gas AU is divided into nearly three equal time periods by discovery date, plots of the estimated ultimate recoveries (EUR) indicate that the earliest time period has resulted in the best EUR distribution overall, and the best median total recovery of 0.53 BCFG per cell (fig. 39). Production has shown a general decline for the remaining two time periods. Part of this apparent decline is due to the fact that wells in this AU drilled during the first time period were located closer to the oil fields in the Mancos Sandstone Conventional Oil AU and were drilled based on step-out drilling from areas of known production. The EUR distribution for the Mancos Sandstones Continuous Gas AU (fig. 40) shows a median total recovery per cell of 0.25 BCFG.

The bulk of the AU remains untested (median is 97.1 percent), and the subsurface geology is poorly defined especially in the northern and western parts. The geologic depositional model predicts that Tocito-like sandstones, where they occur, lie on the unconformity near the base of the Mancos Shale, just above the Juana Lopez Member. Because these sandstones have a linear geometry, elongated northwest–southeast, they should trend throughout most of the AU. They have been identified in the subsurface on the east side of the AU (Ridgley, 2001a) where some of these sandstones are gas bearing (pls. 1 and 2). These sandstones are not present everywhere and, even if gas-bearing, would probably not provide the bulk of the potential resources in this AU, because the sandstones are typically less than 20 ft thick and are laterally discontinuous in all directions.

The transgressive-regressive wedge of sediments of the “Gallup” that overlies the Tocito-like sandstones does produce gas in this AU (wells 2 and 5, pl. 1; wells 16, 28, and 30, pl. 2) and may be several hundred feet thick. However, the distribution of local sandstone buildups, some of which are associated with various shoreline positions, is poorly defined.



Rock Units:

1. Mancos Shale
2. Tocito Sandstone Lentil of Mancos Shale
3. "Gallup" sandstone (El Vado Sandstone Member of Mancos Shale)

Figure 38. Events chart that shows key geologic events for the Mancos Sandstones Continuous Gas Assessment Unit. Black arrows show critical moments for oil and gas generation. Events chart format is modified from Magoon and Dow (1994). Geologic time scale is from the Geological Society of America web page <http://www.geosociety.org/science/timescale/timescl.htm>, last accessed 2/1/2008, and from Berggren and others, (1995). Trias., Triassic; Quat., Quaternary; Po, Pliocene; Ps, Pleistocene; E, early; M, middle; L, late.

These slightly sandier intervals might provide better reservoirs and stratigraphic traps in overall low permeability rocks. There are also poorly defined small-scale structures that might define areas of either initial traps or sites of later fractures. Intervals consisting entirely or mostly of shale, although not now productive, should be examined for their shale-gas potential, especially considering whether early oil, produced in the source beds, was retained and subsequently cracked to gas. Silty and thinly bedded sandstones might be productive (similar to the Lewis Continuous Gas AU, in Dubiel, chap. 5, this CD-ROM), but probably would require fracture stimulation for testing and production.

Taking our current knowledge and the level of uncertainty into consideration, the entire untested area is not considered to be favorable for having potential additions to reserves. We estimate 35 percent of the untested area to have potential additions to reserves at the minimum, 60 percent at the median, and 75 percent at the maximum. These values were obtained by multiplying the various percentages of untested area deemed favorable by different success ratios. New drilling will essentially be infill drilling on closer spacing, step-out drilling from existing fields, and new field discoveries from wildcat drilling. Total gas recovery per cell for untested cells is estimated at 0.02 BCFG at the minimum, 0.35 BCFG at the median, and 5 BCFG at the maximum, which was based on isolated occurrences of high-producing wells (fig. 39).

Mesaverde Updip Conventional Oil Assessment Unit (50220301)

Introduction

The unassessed Mesaverde Updip Conventional Oil AU boundary (fig. 41) includes

1. the area within the outcrop of the Mesaverde Group that lies outside the boundary of the Mesaverde Central-Basin Continuous Gas AU (fig. 41), discussed below; and
2. wells that primarily have a calculated gas-oil ratio (GOR) of less than or equal to 5,000 cubic feet of gas per barrel of oil (cfg/bo).

The main exception to this second parameter is the Red Mesa field on the northwestern side of the basin (fig. 41), which produces only gas in the Mesaverde. The Mesaverde Updip Conventional Oil AU includes areas of potential oil production that are in the structurally shallower and less thermally mature parts of the basin, including the Four Corners platform on the west, the Archuleta arch on the east, and the Chaco slope on the south (fig. 4). The outer boundary of the AU was drawn at the top of the outcropping Point Lookout Sandstone, or where the Point Lookout is not differentiated from the Mesaverde, at about midpoint of the Mesaverde Group.

Oil production from the Menefee Formation in this AU includes the Seven Lakes field in McKinley County, N. Mex. (fig. 41), which produced the first oil in New Mexico in 1911.

Nearly all of the other fields were discovered between 1950 and 1975. Only one oil field (Franciscan Lake) (fig. 41) has had production above the minimum cutoff size of 0.5 MMBO used in the present assessment, and thus this AU was not quantitatively assessed. Production from this assessment unit, as of January 2003, was approximately 6.8 MMBO and 33.5 BCFG (IHS Energy Group, 2003). The possibility of future oil or gas discoveries above the minimum size is estimated to be very low. Any future discoveries will probably be near places where oil has already been found in the southern part of the basin. Key parameters of the AU are listed below and are summarized on figure 42.

Source

The primary petroleum source rock for this assessment unit is interpreted to be the Mancos Shale.

Maturation

Thermal maturation is interpreted to have begun in early Eocene time.

Migration

Oil has migrated upward from the Mancos Shale into Point Lookout Sandstone and sandstones of the Menefee Formation. Many of the small oil fields are associated with faults, which are likely migration routes into reservoir sandstone beds.

Reservoirs

Most production has been from fluvial channels in the Menefee Formation. Two fields, Cuervo and Devils Fork (fig. 41), produce oil from the marginal marine Point Lookout Sandstone.

Traps/Seals

Traps in the Menefee are a combination of stratigraphic and structural. Many fields produce from fluvial channel sandstones that pinch out laterally into overbank mudrocks. Additionally, many of the fields are draped over small anticlines or domes, some of which are faulted. Seals are paludal and overbank mudrocks in the Menefee Formation. Traps in the Point Lookout are stratigraphic pinchouts of marginal marine sandstone into paludal shales in the lower part of the Menefee. Shales in the lower part of the Menefee and in the Mancos are seals for these traps.

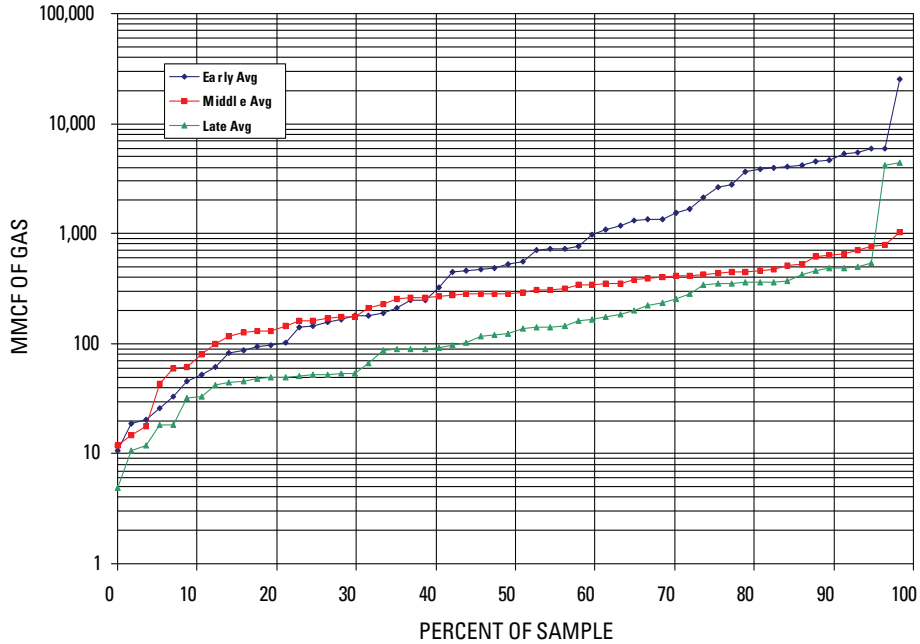


Figure 39. Graph showing estimated ultimate recoveries (EUR) of Mancos Sandstones Continuous Gas Assessment Unit gas wells divided into three equal numbers of wells based on start of production. EURs were calculated using data from IHS Energy Group (2002). Data provided by T. Cook (written commun., 2002). MMCF, million cubic feet.

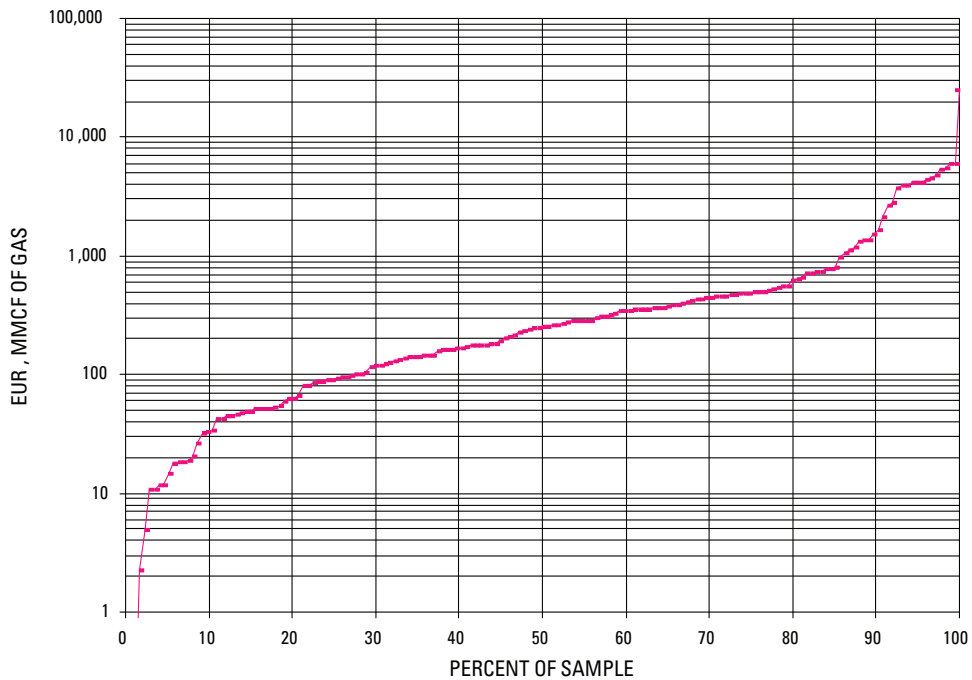


Figure 40. Graph showing combined distribution of estimated ultimate recoveries (EUR) of Mancos Sandstones Continuous Gas Assessment Unit gas wells. EURs were calculated using data from IHS Energy Group (2002). Data provided by T. Cook (written commun., 2002). MMCF, million cubic feet.

Geologic Model

Based on geochemical studies, Ross (1980) indicated that the source of the oil in the Mesaverde is the Mancos Shale. Coal or other carbonaceous beds within the Menefee Formation are not thought to have contributed to the Menefee reservoirs. The Mancos (as defined by the top of the Dakota in fig. 15C) entered the zone of oil generation in the early Eocene and the zone of wet gas in the middle Eocene (fig. 15C). Mancos-generated oil likely migrated upward along faults to reservoirs in the Point Lookout and Menefee. Fluvial channel reservoirs are isolated, sinuous, and scattered through the Menefee, presenting limited targets for exploration. In addition, many of the known producing areas are in association with faults and/or small structures, thus limiting the potential of the AU for further drilling success.

Assessment Results

This AU was not quantitatively assessed as there was significant risk on the existence of a field of minimum size.

Mesaverde Central-Basin Continuous Gas Assessment Unit (50220361)

Introduction

The Mesaverde Central-Basin Continuous Gas Assessment Unit boundary was drawn to include gas accumulations in the deeper part of the central San Juan Basin (fig. 43). The structure contour map drawn on the base of the Dakota Sandstone (Thaden and Zech, 1984; pl. 1) was used as a general guide for locating the boundary on the western and eastern sides of the AU where it is placed along the upper limb of the monocline that borders the basin. The boundary along the northern side of the AU is at the top of the steeply dipping Mesaverde Group contact on the digital geologic map of Colorado (Green, 1992).

The boundary along the southwestern side of the AU includes most wells that produce gas and excludes most wells that produce oil from the Mesaverde, which are included in the Mesaverde Updip Conventional Oil AU. Gas-oil ratios (GOR) were calculated for all producing wells for which data were available. Wells with GOR >20,000 cfg/bo are included in the Mesaverde Central-Basin Continuous Gas AU. Wells with GOR values of <5,000 cfg/bo are excluded from the AU in most cases. Most wells with the GOR range between 5,000 and 20,000 are included in this AU because these wells are surrounded by wells with GOR ratios >20,000.

There have been few divisions of Mesaverde production into separate fields in the AU (fig. 43). The largest Mesaverde field is the Blanco field in New Mexico, whose discovery well was completed in 1927. The Ignacio-Blanco field in Colorado was discovered in 1952. Two small Mesaverde fields just west of the Blanco field, Crouch Mesa and Flora Vista (fig. 43),

were discovered in 1961. Development of the Mesaverde gas fields has been somewhat cyclic. The first big surge of development was from about 1952 to 1962, with peak drilling in 1957 (IHS Energy Group, 2001). Prichard (1973) and Fassett (1991) noted that major development of the Mesaverde (and other units) followed completion of a gas pipeline from the San Juan Basin to California in 1951. Prior to that time much of the produced gas was used locally. A second round of development peaked between 1978 and 1982, and a third cycle of active drilling was between 1987 and 1992. Drilling again increased from 1997 through 2000. Production from this assessment unit as of January 2003 was about 13 TCFG and 54.9 MMBO (IHS Energy Group, 2003).

Drilling is currently permitted on 160-acre spacing. Produced water increases somewhat at the margins of the area of production, and the water to gas ratio (barrels of water to thousand cubic feet of gas) shows marked increases along the entire southern boundary of the AU and in the center of the northeast margin. Future development may be focused more on infill than on discoveries in new areas. Key parameters of the Mesaverde Central-Basin Continuous Gas AU are listed below and are summarized on figure 44.

Source

Mancos Shale and Menefee Formation provide the source. Carbon isotope data suggests a mixed marine and continental source. The Menefee contains abundant volumes of coal, carbonaceous shale, and humate of terrestrial origin, which are all gas prone. Some contribution to Cliff House Sandstone gas may have come from the overlying Lewis Shale.

Maturation

Thermal maturation for oil and associated gas is interpreted to range from middle Eocene to late Oligocene time.

Migration

Migration consists of upward migration of gas from the Mancos Shale into permeable sandstones of the Point Lookout Sandstone; internal lateral migration from coal, carbonaceous shale, and humate beds in the Menefee Formation to sandstone beds in the Menefee; and downward or lateral migration from the Lewis Shale into the Cliff House Sandstone.

Reservoirs

Reservoirs include shoreface and foreshore marginal-marine sandstones of the Point Lookout and Cliff House Sandstones and fluvial channels in the Menefee Formation. In an oblong area that straddles the State line in the northern part of the basin, reservoir rocks in the Mesaverde are poorly developed. The highest gas production is near the center of Blanco

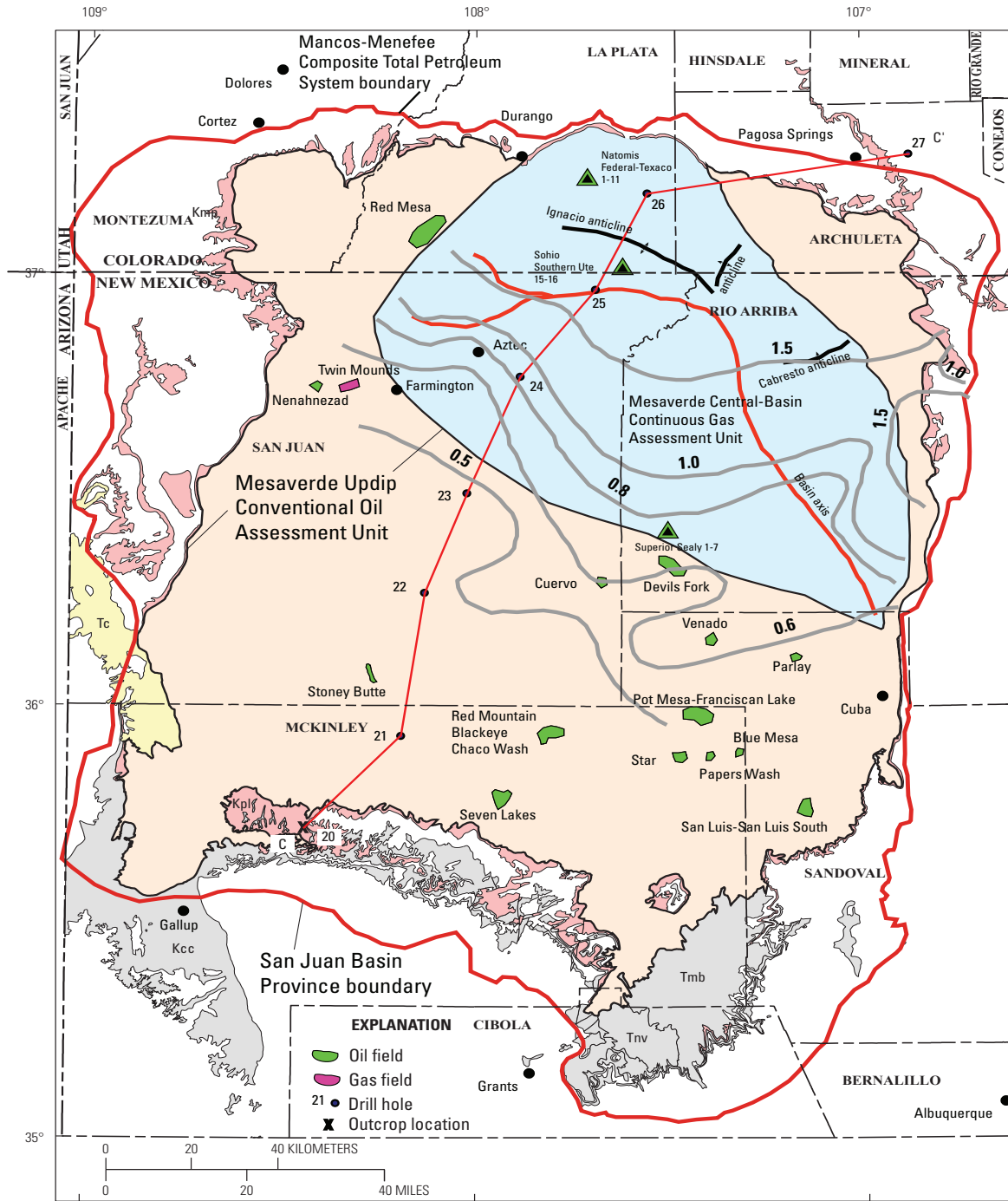
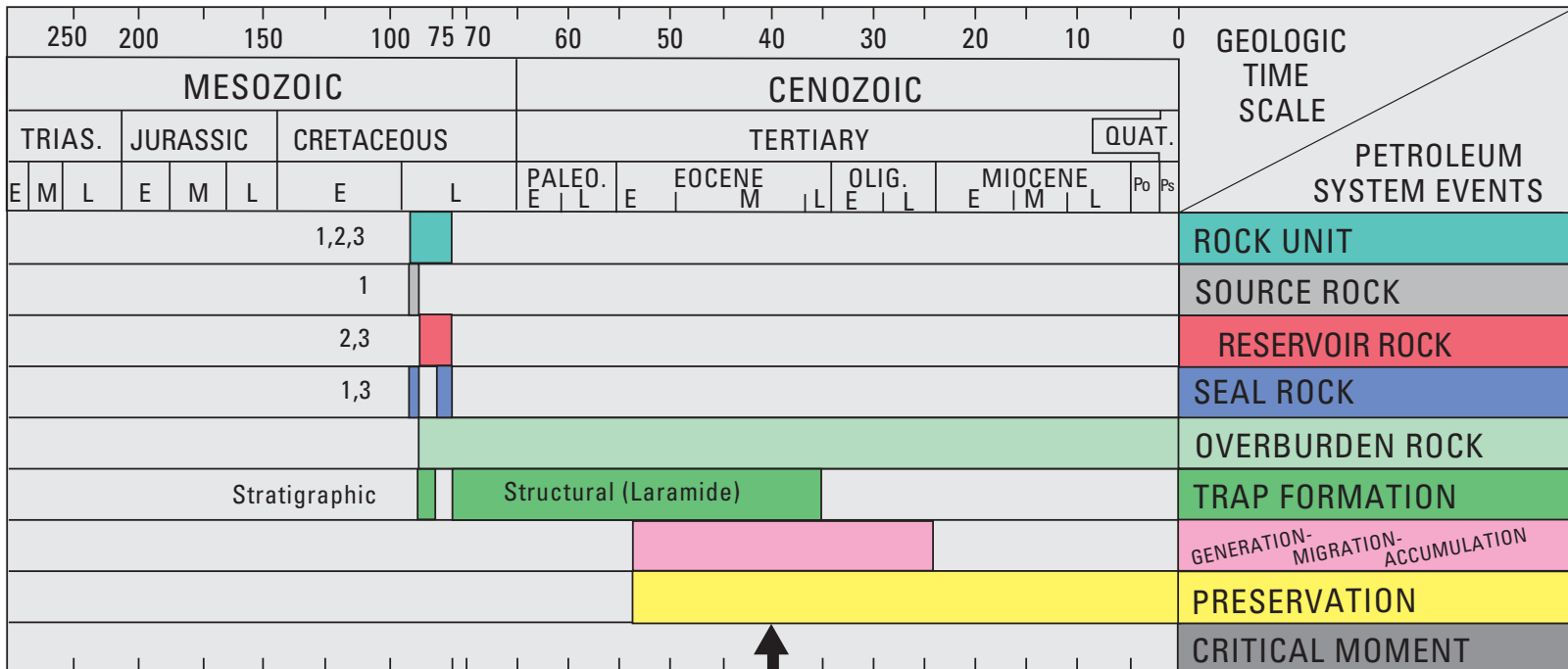


Figure 41. Map showing the location of the Mesaverde Updip Conventional Oil (light tan) and Mesaverde Central-Basin Continuous Gas (light blue) Assessment Units in the upper part of the Mancos-Menefee Composite Total Petroleum System. Menefee maturity contours (in gray) show vitrinite reflectance (R_m) values in percent, contoured from data in Fassett and Nuccio (1990), Law (1992), and Ridgley (2001b). Also shown are the locations of the wells (green and black triangles) used to construct the burial history curves found in this report (figs. 15A–C) and the regional cross section C–C' (fig. 9). Geologic units are from Green (1992) and Green and Jones (1997): Tc, Tertiary Chuska Sandstone; Tnv, Tertiary Neogene volcanics; Tmb, Tertiary Miocene volcanics; Kcc, Crevasse Canyon Formation; Kmp, Menefee Formation and Point Lookout Sandstone; Kmv, Mesaverde Group; Kpl, Point Lookout Sandstone.



Rock Units:
 1. Mancos Shale
 2. Point Lookout Sandstone
 3. Menefee Formation

Figure 42. Events chart that shows the timing of key geologic events for the Mesaverde Updip Conventional Oil Assessment Unit. Black arrow shows critical moment for oil generation. Events chart format is modified from Magoon and Dow (1994). Geologic time scale is from the Geological Society of America web page <http://www.geosociety.org/science/timescale/timescl.htm>, last accessed 2/1/2008, and from Berggren and others, (1995). Trias., Triassic; Quat., Quaternary; Po, Pliocene; Ps, Pleistocene; E, early; M, middle; L, late.

field, and decreases outward toward the margins of the field. Higher gas production is probably associated with a greater degree of fracturing (Teufel and Herrin, 2003).

Traps/Seals

Pinchouts of marine sandstone (Point Lookout and Cliff House Sandstones) into marine or paludal shales, and pinchouts of fluvial sandstones of the Menefee into overbank mudrocks form traps/seals.

Geologic Model

In this AU, gas was generated from the overlying and underlying Lewis and Mancos Shales, and from coal beds and other carbonaceous beds within the Menefee Formation from the middle Eocene to the late Oligocene. Gas was expelled from the source beds and migrated into Point Lookout and Cliff House marginal marine sandstones and into fluvial Menefee sandstones. Gas was trapped stratigraphically where marginal marine rocks pinch out into marine or paludal shales, and also where fluvial channels in the Menefee pinch out laterally into overbank mudrocks. Water saturation is also an important control, preventing gas from migrating updip to the south or north (Masters, 1979). The development of tightly cemented zones within the reservoirs probably also plays an important role in preventing the gas from migrating out of the reservoirs. Natural fracturing enhances production, and induced fracturing is an integral part of well completions.

Assessment Results

The Mesaverde Central-Basin Continuous Gas Assessment Unit (50220361) was assessed to have potential additions to reserves of 1,316.79 (BCFG) and 5.27 (MMBNGL) at the mean. The volumes of undiscovered oil, gas, and natural gas liquids estimated in 2002 for the Mesaverde Central-Basin Continuous Gas AU are shown in appendix A. These values are lower for gas and higher for natural gas liquids compared to the 1995 USGS assessment (Huffman, 1996) (table 7). A summary of the input data for the AU is presented on the data form in appendix G.

This AU encompasses an area of 2,348,000 acres at the median, 2,231,000 acres at the minimum, and 2,583,000 acres at the maximum. There were 6,667 tested cells; tested cells include wells that have produced or had some other production test, such as initial production test, drill stem test, or core analysis. A 0.02 BCFG minimum recovery cutoff was used per cell. Applying this cutoff, 6,478 tested cells equaled or exceeded this cutoff. There was deemed to be adequate charge, favorable reservoirs, traps, and seals over most of the area and favorable timing for charging the reservoirs with greater than the minimum recovery. If the production history of the Mesaverde Central-Basin Continuous Gas AU is divided into three nearly equal time periods, plots of the estimated ultimate

recoveries (EUR) indicate that the first third of production history had the highest median recovery per cell, 2.1 BCFG (fig. 45). The second period of time had lower recovery, at 1.6 BCFG per cell, and the last period of time recovery dropped to 0.5 BCFG per cell. The EUR distribution for the Mesaverde Central-Basin Continuous Gas AU (fig. 46) shows a median total recovery per cell of 1.4 BCFG.

Even with a large part assigned to established fields, the median untested area is 57 percent of the total median AU area. The untested areas are mainly

1. south of the producing area to the Mesaverde outcrops, where the Mesaverde has increasing water/gas ratios;
2. northeast of established producing areas, where the Mesaverde is tightly cemented and also has higher than average water/gas ratios; and
3. areas within producing fields that remain undrilled, either because of State minimum spacing requirements or because of diminishing production trends in areas of established drilling due to lack of reservoir facies, poor fracture development, or water saturation.

With these considerations, the entire untested area was not considered to be favorable. Geologically unfavorable areas were considered to have higher water saturation mainly to the northeast and southeast of the producing fields. Additionally, an oblong area extending northwest to southeast from Colorado to New Mexico was found to have poorly developed sandy reservoirs in the Mesaverde. This area and areas of high water saturation were subtracted from the untested area because they were not considered to be areas favorable for potential additions to reserves. At the minimum, we estimate 15 percent of the untested area to have potential additions to reserves in the next 30 years; at the median, this value is 22 percent of the untested area; and at the maximum, the value is 26 percent. New drilling will consist of infill drilling on closer spacing, step-out drilling from existing fields, and new field discoveries from wildcat drilling. The minimum cutoff of 0.02 BCFG would apply to the percentage of untested cells considered to have potential additions to reserves. Total gas recovery per cell of untested cells considered to have potential additions to reserves is estimated at 0.02 BCFG at the minimum, 0.5 BCFG at the median, and 6.0 BCFG at the maximum. The maximum of 6.0 BCFG is based on the isolated occurrences of high-producing wells (fig. 46).

Menefee Coalbed Gas Assessment Unit (50220381)

Introduction

The Menefee Coalbed Gas AU boundary (fig. 47) coincides with the boundary of the Mesaverde Updip Conventional Oil AU (fig. 41), except in the far northeast part of the basin where the Menefee Formation pinches out between the

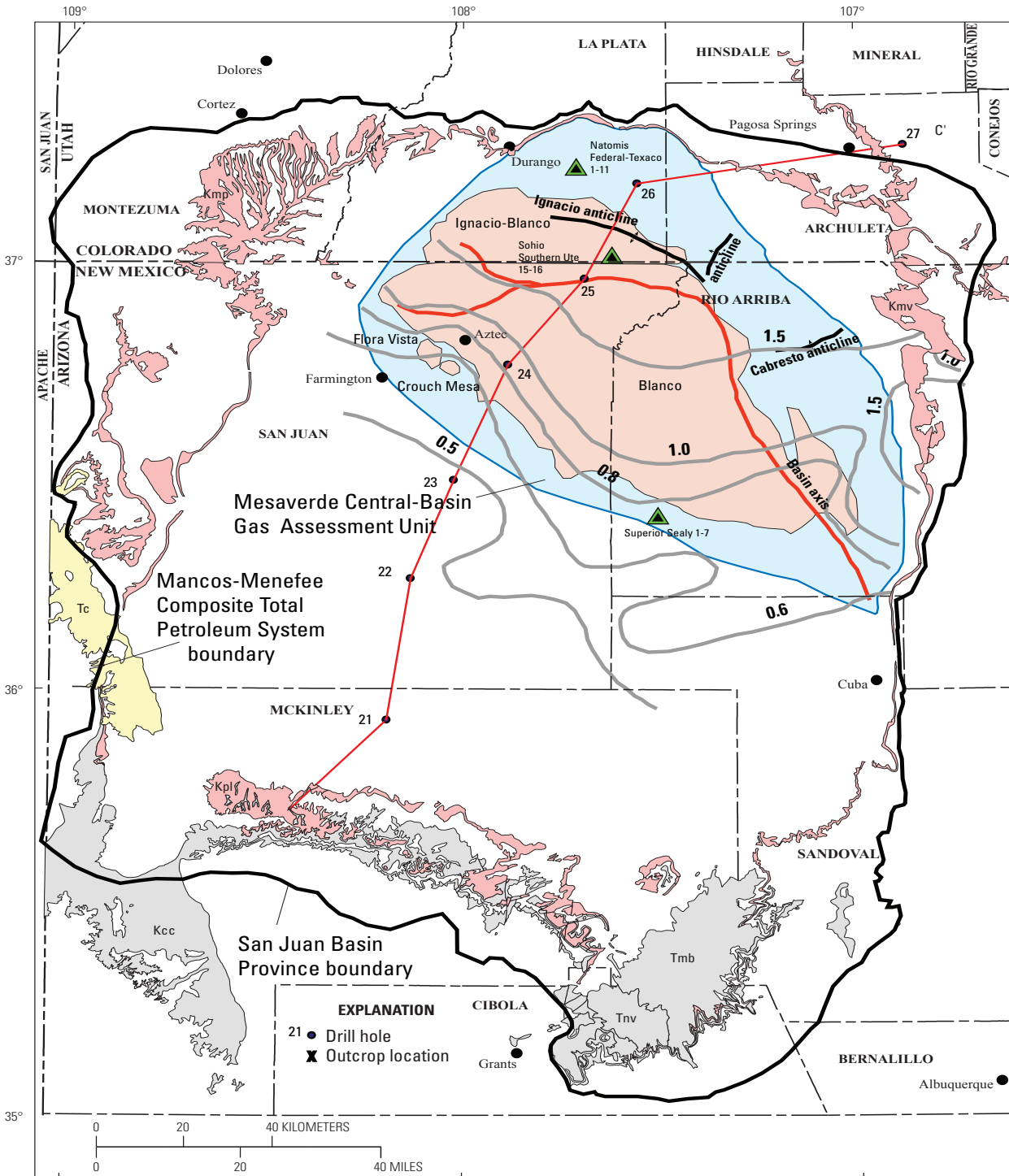


Figure 43. Map showing the extent of the Mesaverde Central-Basin Continuous Gas Assessment Unit (blue) and its included gas fields (light tan) in the upper part of the Mancos-Menefee Composite Total Petroleum System. Menefee maturity contours (in gray) show vitrinite reflectance (R_m) values in percent, contoured from data in Fassett and Nuccio (1990), Law (1992), and Ridgley (2001b). Also shown are the locations of the wells (green and black triangles) used to construct the burial history curves found in this report (figs. 15A–C) and the regional cross section C–C’ (fig. 9). Geologic units are from Green (1992) and Green and Jones (1997): Tc, Tertiary Chuska Sandstone; Tnv, Tertiary Neogene volcanics; Tmb, Tertiary Miocene volcanics; Kcc, Crevasse Canyon Formation; Kmp, Menefee Formation and Point Lookout Sandstone; Kmv, Mesaverde Group; Kpl, Point Lookout Sandstone.

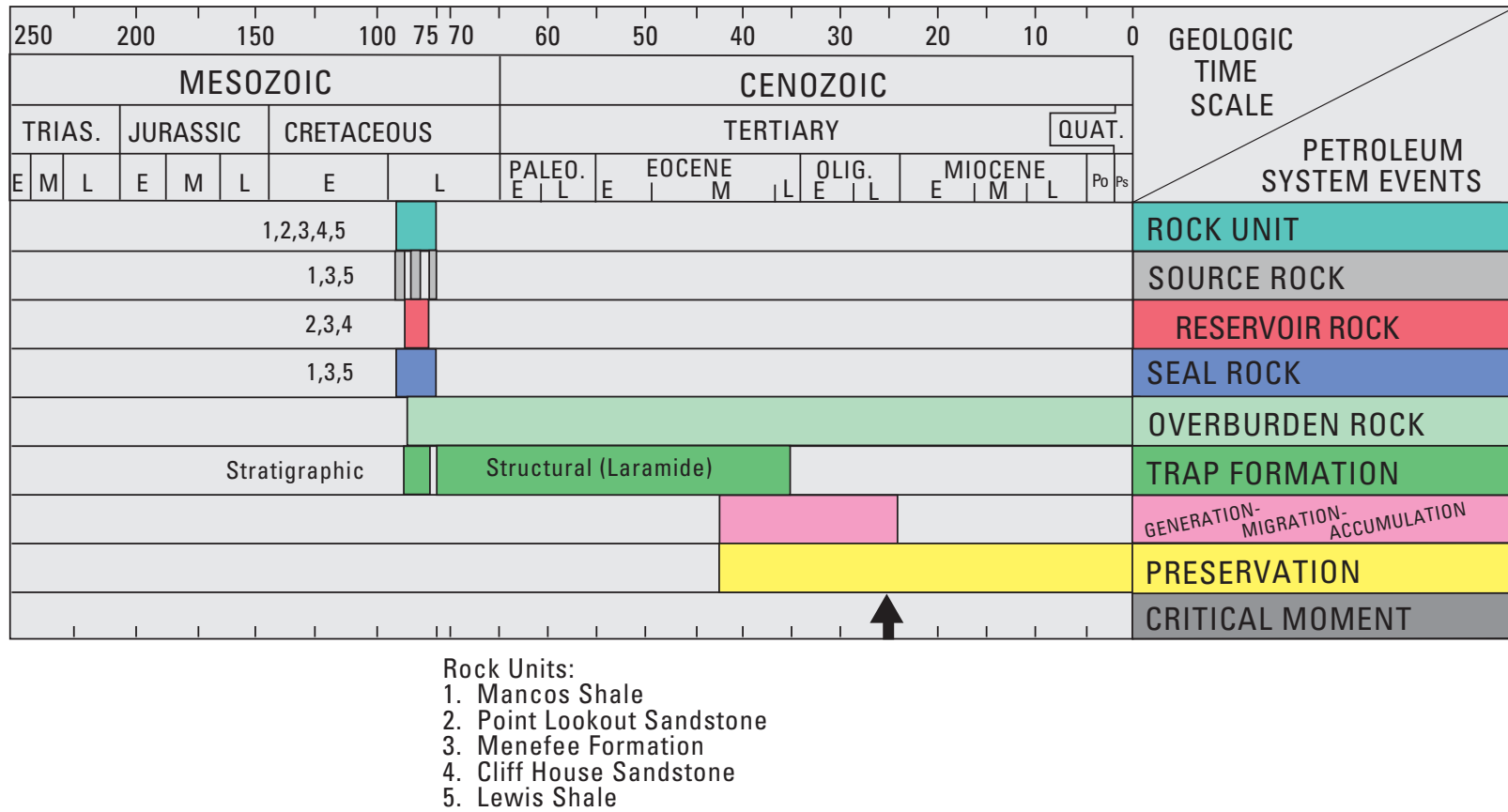


Figure 44. Events chart that shows the timing of key geologic events for the Mesaverde Central-Basin Continuous Gas Assessment Unit. Black arrow shows the critical moment for gas generation. Events chart format is modified from Magoon and Dow (1994). Geologic time scale is from the Geological Society of America web page <http://www.geosociety.org/science/timescale/timescl.htm>, last accessed 2/1/2008, and from Berggren and others, (1995). Trias., Triassic; Quat., Quaternary; Po, Pliocene; Ps, Pleistocene; E, early; M, middle; L, late.

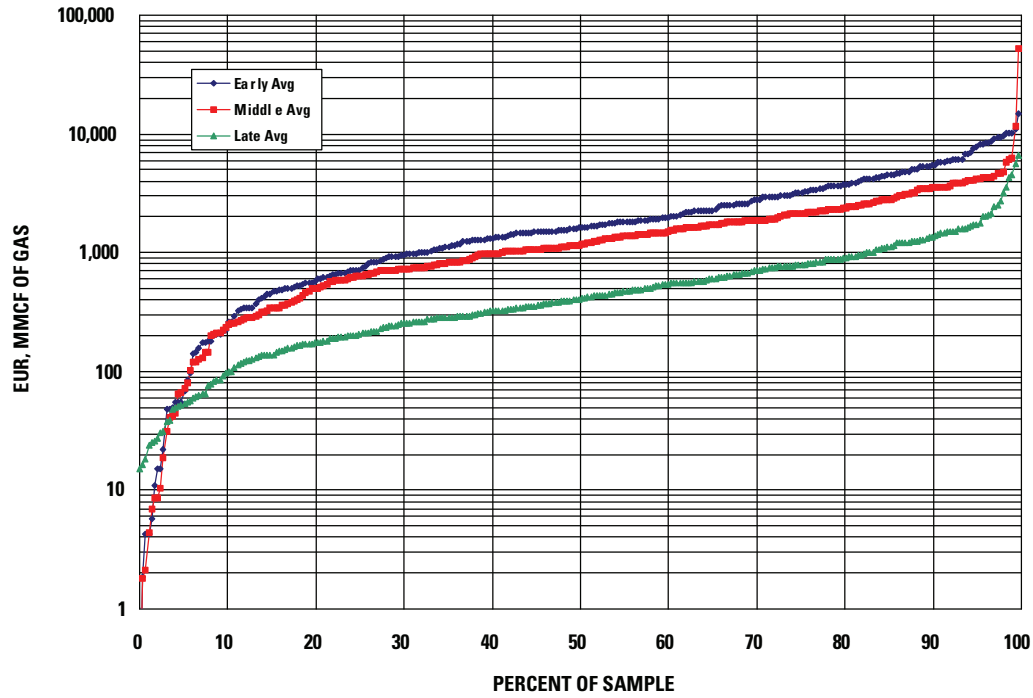


Figure 45. Graph showing the estimated ultimate recoveries (EUR) of the Mesaverde Central-Basin Continuous Gas Assessment Unit gas wells divided into three nearly equal numbers of wells based on start of production. EURs were calculated using data from IHS Energy Group (2002). Data provided by T. Cook (written commun., 2002). MMCF, million cubic feet.

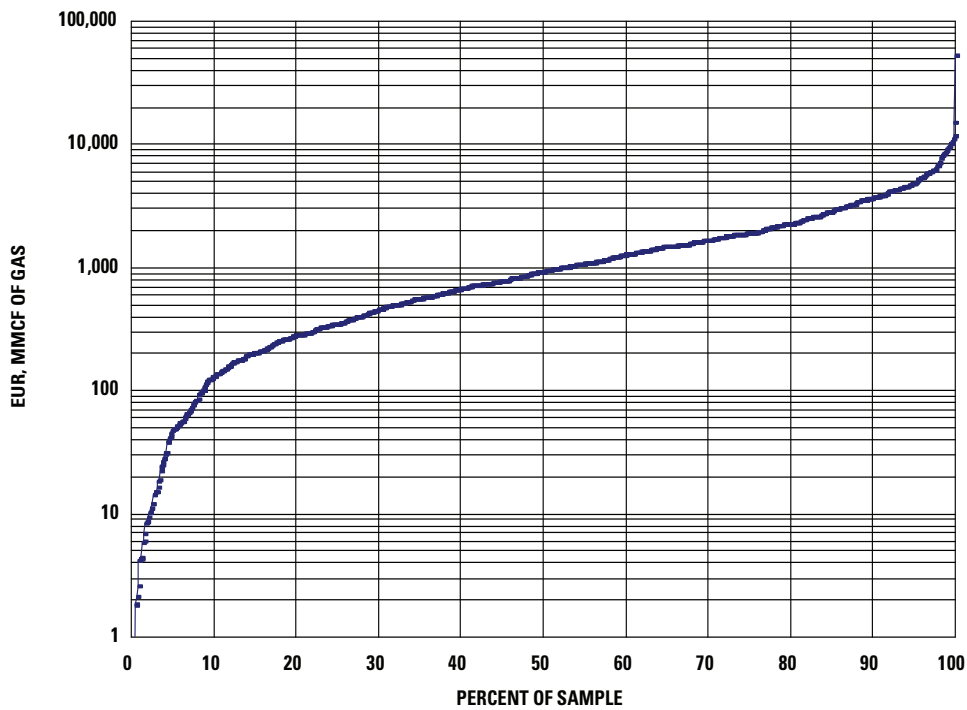


Figure 46. Graph showing the combined distribution of estimated ultimate recoveries (EUR) of the Mesaverde Central-Basin Continuous Gas Assessment Unit gas wells. EURs were calculated using data from IHS Energy Group (2002). Data provided by T. Cook (written commun., 2002). MMCF, million cubic feet.

Cliff House Sandstone and the Point Lookout Sandstone. The Mesaverde Coalbed Gas AU occupies the structurally shallower parts of the basin where the Menefee has been recognized. The AU adjoins the Mesaverde Central-Basin Continuous Gas AU in the deeper parts of the basin, and the top of the Point Lookout Sandstone delimits the AU boundary in the southern part of the basin (Green and Jones, 1997).

To date there has been no gas production from targeted Menefee coals. Three coal-bed wells have been drilled in the southeastern part of the basin, but these have not been productive. Mesaverde coal beds have certainly produced gas in some parts of the basin, but Menefee production is not commonly reported separately from Mesaverde production, making the relative contribution of gas from Menefee coal beds unknown. Bowman (1978) thought that the Menefee contributed only about 10 percent of the total Mesaverde gas production in the Ignacio-Blanco field (fig. 43) in southern Colorado. Possibilities for future discoveries of coal-bed gas may be best in the southern part of the basin where the most coal occurs in the upper part of the Menefee (Siemers and Wadell, 1977), although the coal in this area is of low maturity. Although microbial gas has been produced from low thermal maturity coals in the Powder River Basin (Hobbs, 1978; Law and others, 1991), microbial generation of either early or late coal-bed gas in the Menefee has not been documented. Key parameters of the Menefee Coalbed Gas AU are listed below and are summarized on figure 48.

Source

The primary petroleum source rocks for this assessment unit are interpreted to be coals, carbonaceous shales, and humate beds in the Menefee Formation.

Maturation

Thermal maturation is interpreted to range from early to late Oligocene for thermogenic gas. A contribution from microbial gas is possible.

Migration

Gas is generated and retained in coal beds or shales with little migration.

Reservoirs

Reservoirs are Menefee coal beds, which are thin and discontinuous in most places. Net coal thickness in the Hogback Mountain tongue (an informal unit), in the upper part of the Menefee, is 30 ft; in the basal Cleary Coal Member, it is also about 30 ft. Coal beds, which are thinner and discontinuous in the north part of the basin, are more thermally mature than those in the south part.

Traps/Seals

Deltaic and fluvial overbank mudrocks within the Menefee Formation

Geologic Model

The Hogback Mountain tongue (or upper coal member) of the Menefee is estimated to contain 94 percent of the total amount of coal in the Menefee Formation in beds greater than 2 ft thick and at depths of from 250 to 4,000 ft (Siemers and Wadell, 1977). Coals in this tongue are present in a zone 92 mi long and 12 mi wide, trending northwest-southeast, approximately parallel to and just north of the upper Menefee outcrop contact. Coals occur in an interval of about 450 ft in the upper Menefee and at the base of the Menefee in the Cleary Coal Member. The main coal-bearing belt is south of the 0.60-percent R_m maturity contour of coals in the Menefee, and much of it is outside the 0.50-percent R_m vitrinite isorelectance contour, suggesting that the coal beds were not buried deeply enough to have generated much thermal gas. In one area where the Hogback Mountain tongue occurs, the overlying Fruitland Formation produces coal-bed gas, suggesting that either the Fruitland, and by inference, the Menefee has a high enough thermal maturity to produce gas, or that the Fruitland, and possibly the Menefee, may contain gas generated through microbial processes. Gas samples from the Fruitland in this area have isotopes indicative of biogenic or mixed biogenic-thermogenic gas (Rice and others, 1989; Ridgley and others, chap. 6, this CD-ROM).

Assessment Results

Because there has been no reported coal-bed gas production from the Menefee, an analog was used for EUR distributions. Similarities in the geology of coal beds, and some established coal-bed gas production, led to using the Mesaverde Group of the Uinta-Piceance Province (Johnson and Roberts, 2003) as an analog for the Menefee in the San Juan Basin. The mean assessed undiscovered resources in this AU are 663.94 BCFG at the mean (appendix A). A summary of the input data are presented in the data form in appendix H. The total AU area is 4,797,000 acres, of which 9 percent, or 431,730 acres is considered to have potential for additions to reserves at the median. This area was calculated by adding the area underlain by the Hogback Mountain tongue in New Mexico with an area surrounding the Red Mesa field in Colorado (Lauth, 1983) (where production from coal has been noted in the literature), and multiplying the sum by a success ratio of 70 percent.

The minimum untested area with potential for additions to reserves of thermogenic or microbial coal-bed gas was determined to be only 1 percent of the total AU area, or 47,970 acres. This minimum area takes into account the low thermal maturity of most of the coal in the Hogback Mountain tongue. Only a small area, where there is currently production

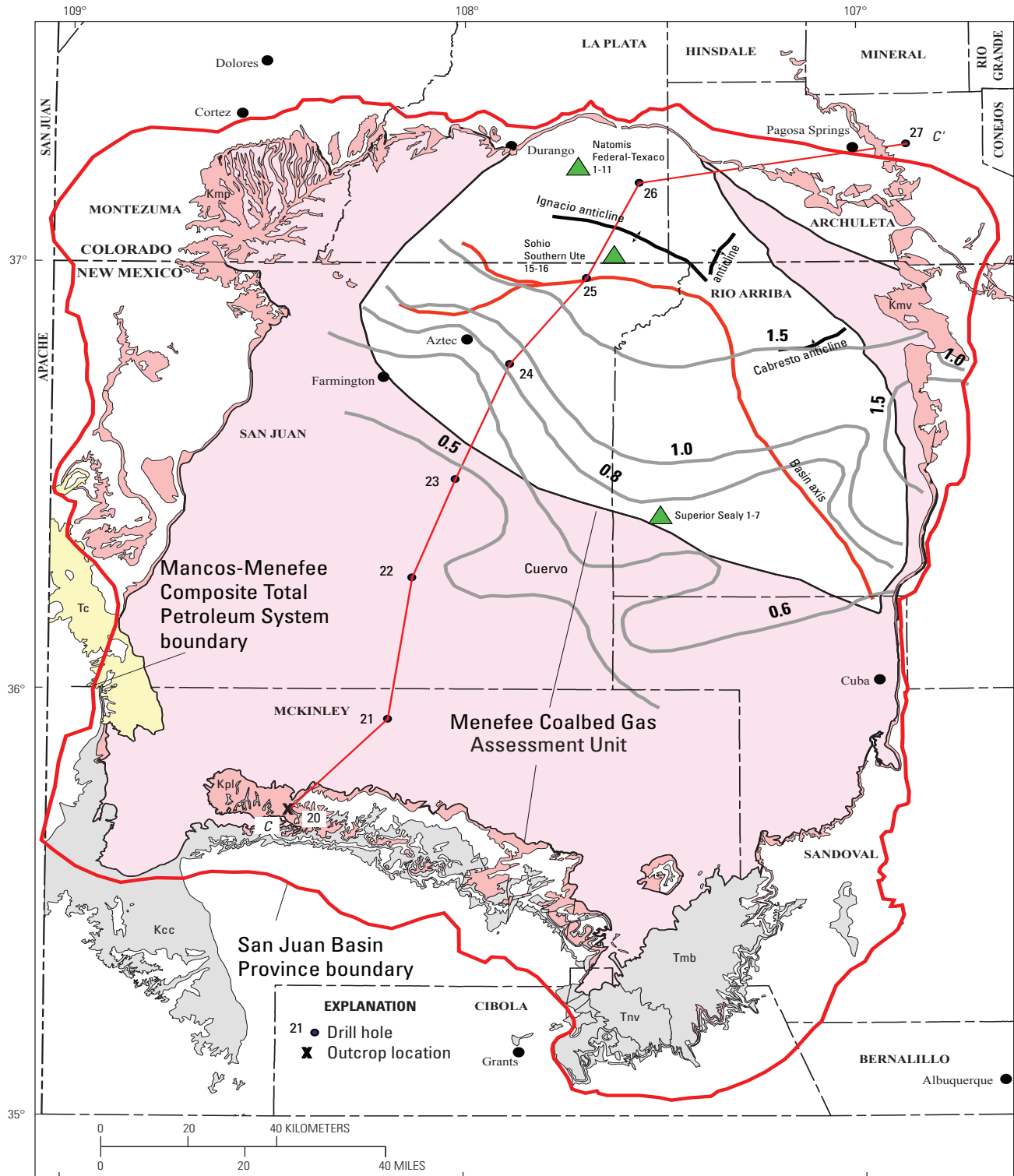


Figure 47. Map showing the Menefee Coalbed Gas Assessment Unit (pink) in the upper part of the Mancos-Menefee Composite Total Petroleum System. Menefee maturity contours (in gray) show vitrinite reflectance (R_m) values in percent, contoured from data in Fassett and Nuccio (1990), Law (1992), and Ridgley (2001b). Also shown are the locations of the wells (green triangles) used to construct the burial history curves found in this report (figs. 15A–C) and the regional cross section C–C’ (fig. 9). Geologic units are from Green (1992) and Green and Jones (1997): Tc, Tertiary Chuska Sandstone; Tnv, Tertiary Neogene volcanics; Tmb, Tertiary Miocene volcanics; Kcc, Crevasse Canyon Formation; Kmp, Menefee Formation and Point Lookout Sandstone; Kmv, Mesaverde Group; Kpl, Point Lookout Sandstone.

from coal in the Fruitland Formation, was considered to be a potential sweet spot in the Hogback Mountain tongue. The area of the Red Mesa field was added to this, and a success ratio of 90 percent was factored in. The maximum untested area with potential for additions to reserves of thermogenic or microbial coal-bed gas was calculated at 27 percent of the AU, or 1,295,190 acres. This area was calculated by first eliminating areas where the Menefee Formation crops out and then reducing the area further by factoring in a 50 percent success ratio.

Summary

The Mancos-Menefee Composite TPS includes all genetically related hydrocarbons generated from organic-rich shales in the Cretaceous Mancos Shale and from carbonaceous shale, coal beds, and humate in the Cretaceous Menefee Formation of the Mesaverde Group. Eight AUs were defined in the Mancos-Menefee Composite TPS. Of the eight AUs, four were assessed as conventional oil or gas accumulations and four as continuous-type accumulations. The conventional AUs are Dakota-Greenhorn Conventional Oil and Gas AU, Gallup Sandstone Conventional Oil and Gas AU, Mancos Sandstones Conventional Oil AU, and the Mesaverde Updip Conventional Oil AU. Continuous-type AUs are Dakota-Greenhorn Continuous Gas AU, Mancos Sandstones Continuous Gas AU, Mesaverde Central-Basin Continuous Gas AU, and Menefee Coalbed Gas AU. Total oil resources that have the potential for additions to reserves are estimated at a mean of 16.78 MMBO and gas resources that are estimated at a mean of 11.11 TCFG for this petroleum system.

Acknowledgments

The authors thank D.J. Taylor and S.B. Roberts for their thoughtful reviews and T.A. Cook and T.R. Klett for interpretations and graphs of production data. Useful discussions and input were also provided by the U.S. Geological Survey National Oil and Gas Assessment Team, consisting of R.R. Charpentier, T.A. Cook, R.A. Crovelli, T.R. Klett, and C.J. Schenk.

References Cited

- Aubrey, W.M., 1988, The Encinal Canyon Member—A new member of the Upper Cretaceous Dakota Sandstone in the southern and eastern San Juan Basin, New Mexico, part 3 of Revisions to stratigraphic nomenclature of Jurassic and Cretaceous rocks of the Colorado Plateau: U.S. Geological Survey Bulletin 1633-C, p. 59–69.
- Aubrey, W.M., 1991, Geologic framework of Cretaceous and Tertiary rocks in the Southern Ute Indian Reservation and adjacent areas in the northern San Juan Basin, southwestern Colorado: U.S. Geological Survey Professional Paper 1505-B, p. B1–B24.
- Baltz, E.H., 1967, Stratigraphy and regional tectonic implications of part of Upper Cretaceous and Tertiary rocks, east-central San Juan Basin, New Mexico: U.S. Geological Survey Professional Paper 552, 101 p.
- Beaumont, E.C., and Hoffman, G.K., 1992, Interrelationships between the upper coal member of the Menefee Formation, the La Ventana Tongue, and the Lewis Shale in the southeastern San Juan Basin, New Mexico, *in* Lucas, S.G., Kues, B.S., Williamson, T.E., and Hunt, A.P., eds., San Juan Basin IV: New Mexico Geological Society Guidebook, p. 207–216.
- Beaumont, E.C., and Roybal, G.H., 1989, Potential for economic coal development in upper coal member of Menefee Formation, Torreon Wash area, Sandoval County, New Mexico [abs.]: American Association of Petroleum Geologists Bulletin, vol. 73, no. 9, p. 1147.
- Berg, R.R., 1979, Oil and gas in delta-margin facies of Dakota Sandstone, Lone Pine field, New Mexico: American Association of Petroleum Geologists Bulletin, v. 63, no. 6, p. 886–904.
- Berggren, W.A., Kent, D.V., Swisher, C.C., III, and Aubry, M., 1995, A revised Cenozoic geochronology and chronostratigraphy, *in* Berggren, W.A., Kent, D.V., Aubry, M., and Hardenbol, J., eds., Geochronology, time scales and global stratigraphic correlation: Society for Sedimentary Geology Special Publication No. 54, p. 129–212.
- Berry, F.A.F., 1959, Hydrodynamics and geochemistry of the Jurassic and Cretaceous Systems in the San Juan Basin, northwestern New Mexico and southwestern Colorado: Stanford, Calif., Stanford University, Ph. D. dissertation, 192 p.
- Bircher, J.E., 1978, Hospah upper sand, *in* Fassett, J.E., ed., Oil and gas fields of the Four Corners area, volume I: Four Corners Geological Society, p. 344–346.
- Bond, W.A., 1984, Application of Lopatin's method to determine burial history, evolution of the geothermal gradient, and timing of hydrocarbon generation in Cretaceous source rocks in the San Juan Basin, northwestern New Mexico and southwestern Colorado, *in* Woodward, J., Meissner, F.F., and Clayton, J.L., eds., Hydrocarbon source rocks of the greater Rocky Mountain Region: Rocky Mountain Association of Geologists Guidebook, p. 433–447.
- Bowman, K.C., 1978, Ignacio Blanco Mesaverde, *in* Fassett, J.E., ed., Oil and gas fields of the Four Corners area, volume I: Four Corners Geological Society, p. 137–139.

- Cobban, W.A., and Hook, S.C., 1984, Mid-Cretaceous molluscan biostratigraphy and paleogeography of southwestern part of Western Interior, United States, *in* Westerman, G.E., ed., Jurassic–Cretaceous biochronology and paleogeography of North America: Geological Association of Canada Special Paper 27, p. 257–271.
- Cooper, S.P., Lorenz, J.C., and Goodwin, L.B., 2000, Controls on fracture orientation and type within the San Juan Basin, New Mexico and Colorado [abs.]: American Association of Petroleum Geologists Bulletin, v. 84, no. 8, p. 1237.
- Craig, S.D., 2001, Geologic framework of the San Juan structural basin of New Mexico, Colorado, Arizona, and Utah, with emphasis on Triassic through Tertiary rocks: U.S. Geological Survey Professional Paper 1420, 70 p.
- Cumella, S.P., 1981, Sedimentary history and diagenesis of the Pictured Cliffs Sandstone, San Juan Basin, New Mexico and Colorado: Texas Petroleum Research Committee Report UT 81–1, 219 p.
- Dane, C.H., 1936, Geology and fuel resources of the southern part of the San Juan Basin; Part 3—The La Ventana-Chacra Mesa coal field: U.S. Geological Survey Bulletin 860 C, p. 1–161.
- Dane, C.H., Kauffman, E.G., and Cobban, W.A., 1968, Semilla Sandstone, a new member of the Mancos Shale in the southeastern part of the San Juan Basin, New Mexico: U.S. Geological Survey Bulletin 1254 –F, 21 p.
- Edmister, J.A., 1983, Marcelina Gallup, *in* Fassett, J.E., ed., Oil and gas fields of the Four Corners area, volume III: Four Corners Geological Society, p. 987–988.
- Emmendorfer, A.P., 1983, Mancos River, *in* Fassett, J.E., ed., Oil and gas fields of the Four Corners area, volume III: Four Corners Geological Society, p. 881–883.
- Emmendorfer, A.P., 1992, Tectonic dolomitization in the Gavilan Mancos oil pool, Rio Arriba County, New Mexico, *in* Lucas, S.G., Kues, B.S., Williamson, T.E., Hunt, A.P., eds., San Juan Basin IV: New Mexico Geological Society Guidebook, 43rd Annual Field Conference, p. 123–132.
- Fassett, J.E., 1974, Cretaceous and Tertiary rocks of the eastern San Juan Basin, *in* Siemers, C.T., ed., Ghost Ranch, north-central New Mexico: New Mexico Geological Society Guidebook, p. 225–230.
- Fassett, J.E., 1977, Geology of the Point Lookout, Cliff House and Pictured Cliffs Sandstones of the San Juan Basin, New Mexico and Colorado, *in* Fassett, J.E., ed., San Juan Basin III: New Mexico Geological Society Guidebook, p. 193–197.
- Fassett, J.E., ed., 1978a, Oil and gas fields of the Four Corners area, volume I: Four Corners Geological Society, 368 p.
- Fassett, J.E., ed., 1978b, Oil and gas fields of the Four Corners area, volume II: Four Corners Geological Society, p. 369–727.
- Fassett, J.E., ed., 1983a, Oil and gas fields of the Four Corners area, volume III: Four Corners Geological Society, p. 729–1143.
- Fassett, J.E., 1983b, Stratigraphy and oil and gas production of northwest New Mexico updated through 1983, *in* Fassett, J.E., ed., Oil and gas fields of the Four Corners area, volume III: Four Corners Geological Society, p. 849–863.
- Fassett, J.E., 1991, Oil and gas resources of the San Juan Basin, New Mexico and Colorado, *in* Gluskoter, H.J., Rice, D.D., and Taylor, R.B., eds., Economic Geology, U.S.: Geological Society of America, The Geology of North America, Boulder, Colo., v. P–2, p. 357–372.
- Fassett, J.E., 2000, Geology and coal resources of the Upper Cretaceous Fruitland Formation, San Juan Basin, New Mexico and Colorado, chap. Q, *of* Kirschbaum, M.A., Roberts, L.N.R., and Biewick, L.R.H., eds., Geologic assessment of coal in the Colorado Plateau: Arizona, Colorado, New Mexico, and Utah: U.S. Geological Survey Professional Paper 1625–B, p. Q1–Q132.
- Fassett, J.E., and Jentgen, R.W., 1978, Blanco Tocito, South, *in* Fassett, J.E., ed., Oil and gas fields of the Four Corners area: Four Corners Geological Society, volume 1, p. 233–240.
- Fassett, J.E., and Nuccio, V.F., 1990, Vitrinite reflectance values of coal from drill-hole cuttings from the Fruitland and Menefee Formations, San Juan Basin, New Mexico: U.S. Geological Survey Open-File Report 90–290, 21 p.
- Franklin, S.P., and Tieh, T.T., 1989, Petrography, diagenesis, and reservoir properties of the Dakota Sandstone of West Lindrith field, Rio Arriba County, New Mexico, *in* Coalson, E.B., Kaplan, S.S., Keighin, C.W., and Oglesby, C.A., eds., Petrogenesis and petrophysics of selected sandstone reservoirs of the Rocky Mountain Region: Rocky Mountain Association of Geologists, p. 117–134.
- Gorham, F.D., Jr., Woodward, L.A., Callendar, J.F., and Greer, A.R., 1977, Fracture permeability in Cretaceous rocks of the San Juan Basin, *in* Fassett, J.E., ed., New Mexico Geological Society Guidebook, 28th Field Conference, San Juan Basin III, p. 235–241.
- Green, G.N., 1992, The digital geologic map of Colorado in ARC/INFO format: U.S. Geological Survey Open-File Report 92–507, <http://pubs.er.usgs.gov/usgspubs/ofr/ofr92507A>; last accessed 2/1/2008.
- Green, G.N., and Jones, G.E., 1997, The digital geologic map of New Mexico in ARC/INFO format: U.S. Geological Survey Open-File Report 97–0052, <http://pubs.er.usgs.gov/usgspubs/ofr/ofr9752>; last accessed 2/1/2008.

- Gries, R.R., Clayton, J.L., and Leonard, C., 1997, Geology, thermal maturation, and source rock geochemistry in a volcanic covered basin: San Juan sag, south-central Colorado: American Association of Petroleum Geologists Bulletin, v. 81, no. 7, p. 1133–1160.
- Harr, C.L., 1988, The Ignacio Blanco gas field, northern San Juan Basin, Colorado, *in* Fassett, J.E., ed., Geology and coal-bed methane resources of the northern San Juan Basin, Colorado and New Mexico: Denver, Colo., Rocky Mountain Association of Geologists Guidebook, p. 205–219.
- Hart, B.S., 1997, The Tocito Sandstones: valley-fills, offshore bars or lowstand shorefaces, *in* Mesozoic geology and paleontology of the Four Corners region: New Mexico Geological Society Guidebook, 48th Field Conference, p. 50–51.
- Hobbs, R.G., 1978, Methane occurrence, hazards, and potential resources, Recluse geologic area, northern Campbell County, Wyoming: U.S. Geological Survey Open-File Report 78–401, 18 p.
- Hoppe, W.F., 1978, Basin Dakota, *in* Fassett, J.E., ed., Oil and gas fields of the Four Corners area, volume III: Four Corners Geological Society, p. 204–206.
- Huffman, A.C., Jr., 1996, San Juan Basin Province (22), *in* Gautier, D.L., Dolton, G.L., Takahashi, K.I., and Varnes, K.L., eds., 1995 National Assessment of United States Oil and Gas Resources—Results, methodology, and supporting data: U.S. Geological Survey Digital Data Series 30, release 2.
- Huffman, A.C., Jr., and Taylor, D.J., 2002, Fractured shale reservoirs and basement faulting, San Juan Basin, New Mexico and Colorado: American Association of Petroleum Geologists Rocky Mountain Section Meeting, Laramie, Wyo., p. 30.
- Hunt, C.B., 1936, Geology and fuel resources of the southern part of the San Juan Basin, New Mexico; Part 2. The Mount Taylor coal field: U.S. Geological Survey Bulletin 860–B, p. 1–80.
- IHS Energy Group, 2001, 2002, and 2003, PI/Dwights Plus U.S. Well Data [includes data current as of September 2001, June 2002, and January 31, 2003, respectively]: Englewood, Colo., IHS Energy Group; database available from IHS Energy Group, 15 Inverness Way East, D205, Englewood, CO 80112, U.S.A.
- Jaramillo, M., Medford, D., Engler, T., 2000, An integrated study of a fractured, low-permeability gas sand [abs.]: American Association of Petroleum Geologists Bulletin, v. 84, no. 8, p. 1240–1241.
- Jennette, D.C., and Jones, C.R., 1995, Sequence stratigraphy of the Upper Cretaceous Tocito Sandstone—A model for tidally influenced incised valleys, San Juan Basin, New Mexico, *in* Van Wagoner, J.C., and Bertram, G.T., eds., Sequence stratigraphy of foreland basin deposits: American Association of Petroleum Geologists Memoir 64, p. 311–348.
- Jennette, D.C., Jones, C.R., Van Wagoner, J.C., and Larsen, J.E., 1991, High-resolution sequence stratigraphy of the Upper Cretaceous Tocito Sandstone—The relationship between incised valleys and hydrocarbon accumulation, San Juan Basin, New Mexico, *in* Van Wagoner, J.C., Nummedal, D., Jones, C.R., Taylor, D.R., Jennette, D.C., and Riley, G.W., eds., Sequence applications to shelf sandstone reservoirs—Outcrop to subsurface examples: American Association of Petroleum Geologists Field Conference Guidebook. Not consecutively paginated.
- Johnson, R.C., and Roberts, S.B., 2003, The Mesaverde Total Petroleum System, Uinta-Piceance Province, Utah and Colorado: U.S. Geological Survey Digital Data Series 69–B, chap.7, 63 p.
- Katzman, D., and Wright-Dunbar, R., 1992, Parasequence geometry and facies architecture in the Upper Cretaceous Point Lookout Sandstone, Four Corners platform, southwestern Colorado, *in* Lucas, S.G., Kues, B.S., Williamson, T.E., and Hunt, A.P., eds., San Juan Basin IV: New Mexico Geological Society Guidebook, p. 187–197.
- Landis, E.R., and Dane, C.H., 1967, Geologic map of the Tierra Amarilla quadrangle, Rio Arriba County, New Mexico: New Mexico Bureau of Mines and Mineral Resources Geologic Map 19, scale 1:62,500, incl. pamphlet, 15 p.
- Landis, E.R., Dane, C.H., and Cobban, W.A., 1973, Stratigraphic terminology of the Dakota Sandstone and Mancos Shale, west-central New Mexico: U.S. Geological Survey Bulletin 1372–J, 44 p.
- Lauth, R.E., 1983, Red Mesa, *in* Fassett, J.E., ed., Oil and gas fields of the Four Corners area, volume III: Four Corners Geological Society, p. 899–900.
- Law, B.E., 1992, Thermal maturity patterns of Cretaceous and Tertiary rocks, San Juan Basin, Colorado and New Mexico: Geological Society of America Bulletin, v. 104, p. 192–207.
- Law, B.E., Rice, D.D., and Flores, R.M., 1991, Coalbed gas accumulations in the Paleocene Fort Union Formation, Powder River Basin, Wyoming, *in* Schwochow, S.D., Murray, D.K., and Fahy, M.F., eds., Coalbed methane of western North America: Rocky Mountain Association of Geologists 1991, p. 179–190.
- Loomis, J.L., and Crossey, L.J., 1993, Diagenesis in a cyclic, siliciclastic regressive sequence—The Point Lookout Sandstone, San Juan Basin, New Mexico and Colorado [abs.]: American Association of Petroleum Geologists Bulletin, v. 77, no. 13, p. 140.
- Lorenz, J.C., Basinski, P.M., Head, C.F., and Peabody, W.W., 1999, Complex natural fracture patterns in Dakota Sandstone reservoirs of the San Juan Basin [abs.]: American Association of Petroleum Geologists, Annual Meeting, p. A83.

- Lorenz, J.C., and Cooper, S.P., 2001, Tectonic setting and characteristics of natural fractures in Mesaverde and Dakota reservoirs of the San Juan Basin, New Mexico and Colorado: Sandia National Laboratories, Sandia Report SAND2001-0054, 77 p.
- Luce, R.M., 1978, Hospah lower sand, south, *in* Fassett, J.E., ed., Oil and gas fields of the Four Corners area, volume II: Four Corners Geological Society, p. 341-342.
- Magoon, L.B., and Dow, W.G., 1994, The petroleum system, *in* Magoon, L.B., and Dow, W.G., eds., The petroleum system—From source to trap: American Association of Petroleum Geologists Memoir 60, p. 3-24.
- Masters, J.A., 1979, Deep basin gas trap, Western Canada: American Association of Petroleum Geologists Bulletin, v. 63, no. 2, p. 152-181.
- Matheny, M.L., 1983, Rattlesnake Gallup, *in* Fassett, J.E., ed., Oil and gas fields of the Four Corners area, volume III: Four Corners Geological Society, p. 1002-1005.
- Matheny, M.L., and Ulrich, R.A., 1983, A history of the petroleum industry in the Four Corners area, *in* Fassett, J.E., ed., Oil and gas fields of the Four Corners area, volume III: Four Corners Geological Society, p. 804-810.
- Michael, G.E., Anders, D.E., and Law, B.E., 1993, Geochemical evaluation of Upper Cretaceous Fruitland Formation coals, San Juan Basin, New Mexico and Colorado: Organic Geochemistry, v. 20, p. 475-498.
- Molenaar, C.M., 1973, Sedimentary facies and correlation of the Gallup Sandstone and associated formations, northwestern New Mexico, *in* Fassett, J.E., ed., Cretaceous and Tertiary rocks of the Colorado Plateau: Four Corners Geological Society Memoir, p. 85-110.
- Molenaar, C.M., 1977a, San Juan Basin time-stratigraphic nomenclature chart, *in* Fassett, J.E., ed., San Juan Basin III: New Mexico Geological Society Guidebook, p. xii.
- Molenaar, C.M., 1977b, Stratigraphy and depositional history of Upper Cretaceous rocks of the San Juan Basin area, New Mexico and Colorado, with a note on economic resources, *in* Fassett, J.E., ed., San Juan Basin III: New Mexico Geological Society Guidebook, 28th Field Conference, p. 159-166.
- Molenaar, C.M., 1977c, The Pinedale oil seep—An exhumed stratigraphic trap in the southwestern San Juan Basin, *in* Fassett, J.E., ed., San Juan Basin III, New Mexico Geological Society Guidebook, 28th Field Conference, p. 243-246.
- Molenaar, C.M., 1983, Principal reference section and correlation of Gallup Sandstone, northwestern New Mexico, *in* Hook, S.C., comp., Contributions to mid-Cretaceous paleontology and stratigraphy of New Mexico: New Mexico Bureau of Mines and Mineral Resources Circular 185, p. 29-40.
- Molenaar, C.M., Cobban, W.A., Merewether, E.A., Pillmore, C.L., Wolfe, D.G., and Holbrook, J.M., 2002, Regional stratigraphic cross sections of Cretaceous rocks from east-central Arizona to the Oklahoma Panhandle: U.S. Geological Survey Miscellaneous Field Studies Map 2382.
- Moore, B.J., and Sigler, Stella, 1987, Analyses of natural gases, 1917-85: U.S. Bureau of Mines Information Circular 9129, 1, 197 p.
- NRG Associates, 2001, The significant oil and gas fields of the United States [data current as of December 31, 2001]: Colorado Springs, Colo., NRG Associates, Inc. [database available from NRG Associates, Inc., P.O. Box 1655, Colorado Springs, CO 80901].
- Nummedal, D., and Molenaar, C.M., 1995, Sequence stratigraphy of ramp-setting strand plain successions—The Gallup Sandstone, New Mexico, *in* Van Wagoner, J.C., and Bertram, G.T., eds., Sequence stratigraphy of foreland basin deposits: American Association of Petroleum Geologists Memoir 64, p. 277-310.
- Nummedal, D., and Riley, G.W., 1999, The origin of the Tocito Sandstone and its sequence stratigraphic lessons, *in* Bergman, K., and Snedden, J.W., eds., Isolated shallow marine sand bodies—Sequence stratigraphic analysis and sedimentologic interpretation: Society for Sedimentary Geology, no. 64, p. 227-254.
- Nummedal, D., and Swift, D.J.P., 1987, Transgressive stratigraphy at sequence-bounding unconformities—Some principles derived from Holocene and Cretaceous examples, *in* Nummedal, D., Pilkey, O.H., and Howard, J.D., eds., Sea-level fluctuation and coastal evolution: Society of Economic Paleontologists and Mineralogists Special Publication 41, p. 241-260.
- Owen, D.E., 1973, Depositional history of the Dakota Sandstone, San Juan Basin area, New Mexico, *in* Fassett, J.E., ed., Cretaceous and Tertiary rocks of the southern Colorado Plateau: Four Corners Geological Society Memoir, p. 37-51.

- Owen, D.E., and Siemers, C.T., 1977, Lithologic correlation of the Dakota Sandstone and adjacent units along the eastern flank of the San Juan Basin, New Mexico, *in* Fassett, J.E., ed., San Juan Basin III: New Mexico Geological Society Guidebook, p. 179–183.
- Pasley, M.A., Gregory, W.A., and Hart, G.F., 1991, Organic matter variations in transgressive and regressive shales: *Organic Geochemistry*, v. 17, p. 483–509.
- Pentilla, W.C., 1964, Evidence for the pre-Niobrara unconformity in the northwestern part of the San Juan Basin: *The Mountain Geologist*, v. 1, no. 1, p. 3–14.
- Posamentier, H.W., Allen, G.P., James, D.P., and Tesson, M., 1992, Forced regressions in a sequence stratigraphic framework; concepts, examples, and exploration significance: *American Association of Petroleum Geologists Bulletin*, v. 76, p. 1687–1709.
- Prichard, R.L., 1973, History of Mesaverde development in the San Juan Basin, *in* Fassett, J.E., ed., Cretaceous and Tertiary rocks of the southern Colorado Plateau: Four Corners Geological Society Guidebook, p. 174–177.
- Raynolds, R.G., and Pasternack, I., 1994, Mesaverde Group sandstone reservoir characteristics, San Juan Basin, New Mexico and Colorado [abs.]: *American Association of Petroleum Geologists Bulletin*, v. 78, no. 13, p. 242.
- Rice, D.D., 1983, Relation of natural gas composition to thermal maturity and source rock type in San Juan Basin, northwestern New Mexico and southwestern Colorado: *American Association of Petroleum Geologists Bulletin*, v. 67, no. 8, p. 1199–1218.
- Rice, D.D., Clayton, J.L., and Pawlewicz, M.J., 1989, Characterization of coal-derived hydrocarbons and source-rock potential of coal beds, San Juan Basin, New Mexico and Colorado, U.S.A.: *International Journal of Coal Geology*, v. 13, p. 597–626.
- Rice, D.D., Threlkeld, C.N., Vuletich, A.K., and Pawlewicz, M.J., 1988, Identification and significance of coal-bed gas, San Juan Basin, northwestern New Mexico and southwestern Colorado, *in* Fassett, J.E., ed., Geology and coal bed methane resources of the northern San Juan Basin, Colorado and New Mexico: *Rocky Mountain Association of Geologists*, p. 51–59.
- Ridgley, J.L., 1977, Stratigraphy and depositional environments of Jurassic–Cretaceous sedimentary rocks in the southwest part of the Chama Basin, New Mexico, *in* Fassett, J.E., ed., San Juan Basin III: New Mexico Geological Society Guidebook, p. 153–158.
- Ridgley, J.L., 1989, Contrasting styles of fault control on position of pre-Dakota unconformity and on depositional environments of Dakota Sandstone, northern San Juan Basin, Colorado [abs.]: *American Association of Petroleum Geologists Bulletin*, v. 73, no. 9, p. 1172.
- Ridgley, J.L., 1990, Genetic lithofacies in the Dakota Sandstone, a major oil- and gas-producing formation, northern San Juan Basin, Colorado and New Mexico, *in* Carter, L.M.H., ed., USGS research on energy resources, 1990: U.S. Geological Survey Circular 1060, p. 67–68.
- Ridgley, J.L., 1992, Reconstruction of paleoshorelines and sandstone geometry of Dakota Sandstone, northern San Juan Basin, Colorado and New Mexico [abs.]: *Society for Sedimentary Geology (SEPM) 1992 theme meeting, Mesozoic of the Western Interior*, p. 55–56.
- Ridgley, J.L., 1995, Impact of small-scale structure on stratigraphy, sedimentation, and hydrocarbon reservoir compartments in the San Juan Basin: examples from the Cretaceous Dakota Sandstone [abs.]: *Geological Society of America, Annual Meeting*, v. 27, no. 6, p. 230.
- Ridgley, J.L., 2001a, Sequence stratigraphic analysis and facies architecture of the Cretaceous Mancos Shale on and near the Jicarilla Apache Indian Reservation, New Mexico—Their relation to sites of oil accumulation: U.S. Department of Energy Report DE-AI26-98BC15026R11 (CD-ROM).
- Ridgley, J.L., 2001b, Subsurface analysis of the Mesaverde Group on and near the Jicarilla Apache Indian Reservation, New Mexico—Its implication on sites of oil and gas accumulation: Department of Energy Report DE-AI26-98BC15026R14, 40 p.
- Ross, L.M., 1980, Geochemical correlation of San Juan Basin oils—A study: *Oil and Gas Journal*, v. 78, no. 44, p. 102–110.
- Saucier, A.E., 1974, Stratigraphy and uranium potential of the Burro Canyon Formation in the southern Chama Basin, *in* Siemers, C.T., ed., Ghost Ranch, north-central New Mexico: *New Mexico Geological Society Guidebook*, p. 211–217.
- Schmoker, J.W., 1996, Methodology for assessing continuous-type (unconventional) hydrocarbon accumulations, *in* Gautier, D.L., Dolton, G.L., Takahashi, K.I., and Varnes, K.L., eds., 1995 National assessment of United States oil and gas resources—Results, methodology, and supporting data: U.S. Geological Survey Digital Data Series 30, release 2.

- Schmoker, J.W., 2003, U.S. Geological Survey assessment concepts for continuous petroleum accumulations, *in* USGS Uinta-Piceance Assessment Team, Petroleum systems and geologic assessment of oil and gas in the Uinta-Piceance Province, Utah and Colorado: U.S. Geological Survey Digital Data Series 69–B, chap. 17, 7 p. [<http://pubs.usgs.gov/dds/dds-069/dds-069-b/chapters.html>, last accessed 04/2008].
- Schmoker, J.W., and Klett, T.R., 2003, U.S. Geological Survey assessment concepts for conventional petroleum accumulations, *in* USGS Uinta-Piceance Assessment Team, Petroleum systems and geologic assessment of oil and gas in the Uinta-Piceance Province, Utah and Colorado: U.S. Geological Survey Digital Data Series 69–B, chap. 19, 6 p. [<http://pubs.usgs.gov/dds/dds-069/dds-069-b/chapters.html>, last accessed 04/2008].
- Scott, A.R., Kaiser, W.R., and Ayers, W.B., Jr., 1991, Composition, distribution, and origin of Fruitland Formation and Pictured Cliffs Sandstone gases, San Juan Basin, Colorado and New Mexico, *in* Schwochow, S.D., Murray D.K., and Fahy, M.F., eds., Coalbed methane of Western North America: Rocky Mountain Association of Geologists, p. 93–108.
- Sears, J.D., 1934, Geology and fuel resources of the southern part of the San Juan Basin, New Mexico; Part 1. The coal field from Gallup eastward toward Mount Taylor: U.S. Geological Survey Bulletin 860–A, p. 1–29.
- Siemers, C.T., and Wadell, J.S., 1977, Humate deposits of the Menefee Formation (Upper Cretaceous), northwestern New Mexico, *in* Fassett, J.E., ed., San Juan Basin III (Supplement): New Mexico Geological Society Guidebook, p. 1–21.
- Shomaker, J.W., and Hiss, W.L., 1974, Humate mining in northwestern New Mexico, *in* Siemers, C.T., ed., Ghost Ranch, north-central New Mexico: New Mexico Geological Society Guidebook, p. 333–336.
- Stone, W.J., 1981, Hydrogeology of the Gallup Sandstone, San Juan Basin, northwest New Mexico: Groundwater, v. 19, no. 1, p. 4–11.
- Struna, S.M., and Poettmann, F.H., 1988, In-situ combustion in the lower Hospah formation, McKinley County, New Mexico: Society of Petroleum Engineers Reservoir Engineering, v. 3, no. 2, p. 440–448.
- Taylor, D.J., and Huffman, Jr., A.C., 1998, Map showing inferred and mapped basement faults, San Juan Basin and vicinity, New Mexico and Colorado: U.S. Geological Survey Geological Investigations Series 2641, scale 1:500,000.
- Taylor, D.J., and Huffman, Jr., A.C., 2001, Seismic evaluation study report—Jicarilla Apache Indian Reservation: U.S. Department of Energy Report DE-AI26-98BC15026R10 (CD-ROM).
- Teufel, L., and Herrin, J.M., 2003, Optimization of infill drilling in naturally fractured tight-gas reservoirs in the San Juan Basin: American Association of Petroleum Geologists 2003 Annual Convention, May 11–14, Salt Lake City, Utah, Abstracts of Program, CD-ROM.
- Thaden, R.E., and Zech, R.S., 1984, Preliminary structure contour map on the base of the Cretaceous Dakota Sandstone in the San Juan Basin and vicinity, New Mexico, Arizona, Colorado, and Utah: U.S. Geological Survey Miscellaneous Field Studies Map 1673, scale 1:500,000.
- Tillman, R.W., 1985, The Tocito and Gallup Sandstones, New Mexico, a comparison, *in* Tillman, R.W., Swift, D.W.J., and Walker, R.G., eds., Shelf sands and sandstone reservoirs: Society for Sedimentary Geology Short Course Notes 13, p. 403–464.
- Tissot, B.P., and Welte, D.H., 1978, Petroleum formation and occurrence—A new approach to oil and gas exploration: Berlin, Springer-Verlag, 521 p.
- Valasek, David, 1995, The Tocito sandstone in a sequence stratigraphic framework—An example of landward stepping small-scale genetic sequences, *in* Van Wagoner, J.C., and Bertram, G.T., eds., Sequence stratigraphy of foreland basin deposits: American Association of Petroleum Geologists Memoir 64, p. 349–369.
- Van Delinder, D.G., 1986, Crude-oil analyses of samples from the Hospah (Dakota, Gallup), Media-Entrada, Chaco Wash (Menefee), and two undesignated (Gallup) fields, McKinley County, New Mexico: New Mexico Bureau of Mines and Mineral Resources Open-File Report 271, 24 p.
- Whyte, M.R., and Shomaker, J.W., 1977, A geological appraisal of the deep coals of the Menefee Formation of the San Juan Basin, New Mexico, *in* Fassett, J.E., ed., San Juan Basin III (Supplement): New Mexico Geological Society Guidebook 28th Field Conference, p. 41–48.
- Wright Dunbar, R., 2001, Outcrop analysis of the Cretaceous Mesaverde Group: Jicarilla Apache Indian Reservation, New Mexico: U.S. Department of Energy Report DE-AI26-98BC15026R9 (CD-ROM).
- Wright-Dunbar, R., Zech, R.S., Crandall, G.A., and Katzman, D., 1992, Strandplain and deltaic depositional models for the Point Lookout Sandstone, San Juan Basin and Four Corners Platform, New Mexico and Colorado, *in* Lucas, S.G., Kues, B.S., Williamson, T.E., and Hunt, A.P., eds., San Juan Basin IV: New Mexico Geological Society Guidebook, p. 199–206.
- Zapp, A.D., 1949, Geology and coal resources of the Durango area, La Plata and Montezuma Counties, Colorado: U.S. Geological Survey Oil and Gas Investigations Preliminary Map 109, scale 1:31,680.

Appendix A. Assessment results summary for the Mancos-Menefee Composite Total Petroleum System, San Juan Basin Province, New Mexico and Colorado.

[MMBO, million barrels of oil; BCFG, billion cubic feet of gas; MMBNGL, million barrels of natural gas liquids. Results shown are fully risked estimates. For gas fields, all liquids are included under the NGL (natural gas liquids) category. F95 denotes a 95 percent chance of at least the amount tabulated. Other fractiles are defined similarly. Fractiles are additive only under the assumption of perfect positive correlation. CBG, coalbed gas. Gray cells indicate not assessed or applicable.]

Assessment Units (AU)	Field Type	Total Undiscovered Resources											
		Oil (MMBO)				Gas (BCFG)				NGL (MMBNGL)			
		F95	F50	F5	Mean	F95	F50	F5	Mean	F95	F50	F5	Mean
Conventional Oil and Gas Resources													
Gallup Sandstone Conventional Oil and Gas AU	Oil	0.00	1.98	6.29	2.34	0.00	0.29	0.98	0.35	0.00	0.00	0.01	0.00
Mancos Sandstones Conventional Oil AU	Oil	5.41	11.33	20.72	11.99	23.34	53.28	106.75	57.57	0.84	2.07	4.52	2.3
Dakota-Greenhorn Conventional Oil and Gas AU	Oil	0.78	2.26	4.73	2.45	2.53	7.49	17.1	8.34	0.02	0.07	0.16	0.08
	Gas					5.59	12.63	22.4	13.35	0.22	0.50	0.96	0.53
Total		6.19	15.57	31.74	16.78	31.46	73.69	147.23	79.61	1.08	2.64	5.65	2.91
Continuous Gas Resources													
Menefee Coalbed Gas AU	CBG					228.3	569.08	1,418.55	663.94	0.00	0.00	0.00	0.00
Mesaverde Central-Basin Continuous Gas AU	Gas					1,053.32	1,305.62	1,618.35	1,316.79	3.44	5.12	7.6	5.27
Mancos Sandstones Continuous Gas AU	Gas					3,980.80	5,062.07	6,437.03	5,116.37	50.64	73.97	108.04	75.96
Dakota-Greenhorn Continuous Gas AU	Gas					3,148.66	3,896.17	4,821.14	3,928.98	10.29	15.27	22.66	15.72
Total						8,411.08	10,832.94	14,295.07	11,026.08	64.37	94.36	138.3	96.95

Appendix B. Input data form used in evaluating the Mancos-Menefee Composite Total Petroleum System, Dakota-Greenhorn Conventional Oil and Gas Assessment Unit (50220304), San Juan Basin Province.

Appendix B. Input data form used in evaluating the Mancos-Menefee Composite Total Petroleum System, Dakota-Greenhorn Conventional Oil and Gas Assessment Unit (50220304), San Juan Basin Province.

**SEVENTH APPROXIMATION
DATA FORM FOR CONVENTIONAL ASSESSMENT UNITS (NOGA, Version 5, 6-30-01)**

IDENTIFICATION INFORMATION

Assessment Geologist:.....	J.L. Ridgley	Date:	9/25/2002
Region:.....	North America	Number:	5
Province:.....	San Juan Basin	Number:	5022
Total Petroleum System:.....	Mancos-Menefee Composite	Number:	502203
Assessment Unit:.....	Dakota-Greenhorn Conventional Oil and Gas	Number:	50220304
Based on Data as of:.....	PI/Dwights 2001, NRG 2001 (data current through 1999)		
Notes from Assessor:.....	_____		

CHARACTERISTICS OF ASSESSMENT UNIT

Oil (<20,000 cfg/bo overall) or Gas (≥20,000 cfg/bo overall):... Oil

What is the minimum accumulation size?..... 0.5 mmmboe grown
(the smallest accumulation that has potential to be added to reserves in the next 30 years)

No. of discovered accumulations exceeding minimum size:..... Oil: 7 Gas: 3
Established (>13 accums.) _____ Frontier (1-13 accums.) X Hypothetical (no accums.) _____

Median size (grown) of discovered oil accumulation (mmbo):
1st 3rd 5.98 2nd 3rd 1.69 3rd 3rd _____
Median size (grown) of discovered gas accumulations (bcfg):
1st 3rd _____ 2nd 3rd _____ 3rd 3rd _____

Assessment-Unit Probabilities:

<u>Attribute</u>	<u>Probability of occurrence (0-1.0)</u>
1. CHARGE: Adequate petroleum charge for an undiscovered accum. ≥ minimum size.....	<u>1.0</u>
2. ROCKS: Adequate reservoirs, traps, and seals for an undiscovered accum. ≥ minimum size.....	<u>1.0</u>
3. TIMING OF GEOLOGIC EVENTS: Favorable timing for an undiscovered accum. ≥ minimum size.....	<u>1.0</u>

Assessment-Unit GEOLOGIC Probability (Product of 1, 2, and 3):..... 1.0

4. **ACCESSIBILITY:** Adequate location to allow exploration for an undiscovered accumulation ≥ minimum size..... 1.0

UNDISCOVERED ACCUMULATIONS

No. of Undiscovered Accumulations: How many undiscovered accums. exist that are ≥ min. size?:
(uncertainty of fixed but unknown values)

Oil Accumulations:.....min. no. (>0)	<u>1</u>	median no.	<u>2</u>	max no.	<u>4</u>
Gas Accumulations:.....min. no. (>0)	<u>1</u>	median no.	<u>2</u>	max no.	<u>3</u>

Sizes of Undiscovered Accumulations: What are the sizes (**grown**) of the above accums?:
(variations in the sizes of undiscovered accumulations)

Oil in Oil Accumulations (mmbo):.....min. size	<u>0.5</u>	median size	<u>1</u>	max. size	<u>6</u>
Gas in Gas Accumulations (bcfg):.....min. size	<u>3</u>	median size	<u>6</u>	max. size	<u>25</u>

AVERAGE RATIOS FOR UNDISCOVERED ACCUMS., TO ASSESS COPRODUCTS

(uncertainty of fixed but unknown values)

<u>Oil Accumulations:</u>	minimum	median	maximum
Gas/oil ratio (cfg/bo).....	<u>1700</u>	<u>3400</u>	<u>5100</u>
NGL/gas ratio (bnl/mmcf).....	<u>4</u>	<u>9</u>	<u>14</u>
<u>Gas Accumulations:</u>	minimum	median	maximum
Liquids/gas ratio (bliq/mmcf).....	<u>20</u>	<u>40</u>	<u>60</u>
Oil/gas ratio (bo/mmcf).....	<u> </u>	<u> </u>	<u> </u>

SELECTED ANCILLARY DATA FOR UNDISCOVERED ACCUMULATIONS

(variations in the properties of undiscovered accumulations)

<u>Oil Accumulations:</u>	minimum	median	maximum
API gravity (degrees).....	<u>30</u>	<u>50</u>	<u>55</u>
Sulfur content of oil (%).....	<u>0.01</u>	<u>0.1</u>	<u>0.2</u>
Drilling Depth (m)	<u>300</u>	<u>1100</u>	<u>2400</u>
Depth (m) of water (if applicable).....	<u> </u>	<u> </u>	<u> </u>
<u>Gas Accumulations:</u>	minimum	median	maximum
Inert gas content (%).....	<u>0.1</u>	<u>0.5</u>	<u>1</u>
CO ₂ content (%).....	<u>0.1</u>	<u>0.2</u>	<u>0.5</u>
Hydrogen-sulfide content (%).....	<u>0</u>	<u>0</u>	<u>0</u>
Drilling Depth (m).....	<u>560</u>	<u>1250</u>	<u>2200</u>
Depth (m) of water (if applicable).....	<u> </u>	<u> </u>	<u> </u>

Appendix C. Input data form used in evaluating the Mancos-Menefee Composite Total Petroleum System, Dakota-Greenhorn Continuous Gas Assessment Unit (50220363), San Juan Basin Province.

Appendix C. Input data form used in evaluating the Mancos-Menefee Composite Total Petroleum System, Dakota-Greenhorn Continuous Gas Assessment Unit (50220363), San Juan Basin Province.

FORSPAN ASSESSMENT MODEL FOR CONTINUOUS ACCUMULATIONS--BASIC INPUT DATA FORM (NOGA, Version 8, 8-16-02)

IDENTIFICATION INFORMATION

Assessment Geologist:...	<u>J.L. Ridgley</u>	Date:	<u>9/25/2002</u>
Region:.....	<u>North America</u>	Number:	<u>5</u>
Province:.....	<u>San Juan Basin</u>	Number:	<u>5022</u>
Total Petroleum System:..	<u>Mancos-Menefee Composite</u>	Number:	<u>502203</u>
Assessment Unit:.....	<u>Dakota-Greenhorn Continuous Gas</u>	Number:	<u>50220363</u>
Based on Data as of:.....	<u>PI/Dwights 2001</u>		
Notes from Assessor:....	<u></u>		

CHARACTERISTICS OF ASSESSMENT UNIT

Assessment-Unit type: Oil (<20,000 cfg/bo) or Gas (≥20,000 cfg/bo) Gas

What is the minimum total recovery per cell?... 0.02 (mmbo for oil A.U.; bcfg for gas A.U.)

Number of tested cells:..... 5823

Number of tested cells with total recovery per cell ≥ minimum: 5262

Established (>24 cells ≥ min.) X Frontier (1-24 cells) Hypothetical (no cells)

Median total recovery per cell (for cells ≥ min.): (mmbo for oil A.U.; bcfg for gas A.U.)

1st 3rd discovered	<u>1.4</u>	2nd 3rd	<u>0.9</u>	3rd 3rd	<u>0.45</u>
--------------------	------------	---------	------------	---------	-------------

Assessment-Unit Probabilities:

<u>Attribute</u>	<u>Probability of occurrence (0-1.0)</u>
1. CHARGE: Adequate petroleum charge for an untested cell with total recovery ≥ minimum	<u>1.0</u>
2. ROCKS: Adequate reservoirs, traps, seals for an untested cell with total recovery ≥ minimum.	<u>1.0</u>
3. TIMING: Favorable geologic timing for an untested cell with total recovery ≥ minimum.....	<u>1.0</u>

Assessment-Unit GEOLOGIC Probability (Product of 1, 2, and 3):..... 1.0

4. **ACCESS:** Adequate location for necessary petroleum-related activities for an untested cell with total recovery ≥ minimum 1.0

NO. OF UNTESTED CELLS WITH POTENTIAL FOR ADDITIONS TO RESERVES IN THE NEXT 30 YEARS

- Total assessment-unit area (acres): (uncertainty of a fixed value)
 minimum 2,412,000 median 2,513,000 maximum 2,563,000
- Area per cell of untested cells having potential for additions to reserves in next 30 years (acres):
 (values are inherently variable)
 calculated mean 148 minimum 40 median 135 maximum 360
- Percentage of total assessment-unit area that is untested (%): (uncertainty of a fixed value)
 minimum 60 median 66 maximum 70
- Percentage of untested assessment-unit area that has potential for additions to reserves in next 30 years (%): (a necessary criterion is that total recovery per cell ≥ minimum)
 (uncertainty of a fixed value) minimum 46 median 55 maximum 76

TOTAL RECOVERY PER CELL

Total recovery per cell for untested cells having potential for additions to reserves in next 30 years:

(values are inherently variable)

(mmbo for oil A.U.; bcfg for gas A.U.) minimum 0.02 median 0.4 maximum 8

AVERAGE COPRODUCT RATIOS FOR UNTESTED CELLS, TO ASSESS COPRODUCTS

(uncertainty of fixed but unknown values)

<u>Oil assessment unit:</u>	minimum	median	maximum
Gas/oil ratio (cfg/bo).....	<u> </u>	<u> </u>	<u> </u>
NGL/gas ratio (bnl/mmcfg).....	<u> </u>	<u> </u>	<u> </u>
<u>Gas assessment unit:</u>			
Liquids/gas ratio (bliq/mmcfg).....	<u>2</u>	<u>4</u>	<u>6</u>

SELECTED ANCILLARY DATA FOR UNTESTED CELLS

(values are inherently variable)

<u>Oil assessment unit:</u>	minimum	median	maximum	
API gravity of oil (degrees).....	<u> </u>	<u> </u>	<u> </u>	
Sulfur content of oil (%).....	<u> </u>	<u> </u>	<u> </u>	
Drilling depth (m)	<u> </u>	<u> </u>	<u> </u>	
Depth (m) of water (if applicable).....	<u> </u>	<u> </u>	<u> </u>	
<u>Gas assessment unit:</u>				
Inert-gas content (%).....	<u>0.00</u>	<u>1.20</u>	<u>2.80</u>	
CO ₂ content (%).....	<u>0.00</u>	<u>1.10</u>	<u>6.60</u>	
Hydrogen-sulfide content (%).....	<u>0.00</u>	<u>0.00</u>	<u>0.00</u>	
Drilling depth (m).....	<u>2000</u>	<u>2200</u>	<u>3000</u>	
Depth (m) of water (if applicable).....	<u> </u>	<u> </u>	<u> </u>	
<u>Success ratios:</u>	calculated mean	minimum	median	maximum
Future success ratio (%).....	<u>85</u>	<u>80</u>	<u>85</u>	<u>90</u>
Historic success ratio, tested cells (%).....	<u>90</u>			

Appendix D. Input data form used in evaluating the Mancos-Menefee Composite Total Petroleum System, Gallup Sandstone Conventional Oil and Gas Assessment Unit (50220302), San Juan Basin Province.

Appendix D. Input data form used in evaluating the Mancos-Menefee Composite Total Petroleum System, Gallup Sandstone Conventional Oil and Gas Assessment Unit (50220302), San Juan Basin Province.

**SEVENTH APPROXIMATION
DATA FORM FOR CONVENTIONAL ASSESSMENT UNITS (NOGA, Version 5, 6-30-01)**

IDENTIFICATION INFORMATION

Assessment Geologist:.....	<u>J.L. Ridgley</u>	Date:	<u>9/25/2002</u>
Region:.....	<u>North America</u>	Number:	<u>5</u>
Province:.....	<u>San Juan Basin</u>	Number:	<u>5022</u>
Total Petroleum System:.....	<u>Mancos-Menefee Composite</u>	Number:	<u>502203</u>
Assessment Unit:.....	<u>Gallup Sandstone Conventional Oil and Gas</u>	Number:	<u>50220302</u>
Based on Data as of:.....	<u>PI/Dwights 2001, NRG 2001 (data current through 1999)</u>		
Notes from Assessor:.....	_____		

CHARACTERISTICS OF ASSESSMENT UNIT

Oil (<20,000 cfg/bo overall) **or** Gas (≥20,000 cfg/bo overall):... Oil

What is the minimum accumulation size?..... 0.5 mmbone grown
(the smallest accumulation that has potential to be added to reserves in the next 30 years)

No. of discovered accumulations exceeding minimum size:..... Oil: 2 Gas: 0
Established (>13 accums.) _____ Frontier (1-13 accums.) X Hypothetical (no accums.) _____

Median size (grown) of discovered oil accumulation (mmbone):
1st 3rd _____ 2nd 3rd _____ 3rd 3rd _____
Median size (grown) of discovered gas accumulations (bcfg):
1st 3rd _____ 2nd 3rd _____ 3rd 3rd _____

Assessment-Unit Probabilities:

<u>Attribute</u>	<u>Probability of occurrence (0-1.0)</u>
1. CHARGE: Adequate petroleum charge for an undiscovered accum. ≥ minimum size.....	<u>0.8</u>
2. ROCKS: Adequate reservoirs, traps, and seals for an undiscovered accum. ≥ minimum size.....	<u>1.0</u>
3. TIMING OF GEOLOGIC EVENTS: Favorable timing for an undiscovered accum. ≥ minimum size.....	<u>1.0</u>

Assessment-Unit GEOLOGIC Probability (Product of 1, 2, and 3):..... 0.8

4. **ACCESSIBILITY:** Adequate location to allow exploration for an undiscovered accumulation ≥ minimum size..... 1.0

UNDISCOVERED ACCUMULATIONS

No. of Undiscovered Accumulations: How many undiscovered accums. exist that are ≥ min. size?:
(uncertainty of fixed but unknown values)

Oil Accumulations:.....min. no. (>0)	<u>1</u>	median no. <u>2</u>	max no. <u>4</u>
Gas Accumulations:.....min. no. (>0)	<u>0</u>	median no. <u>0</u>	max no. <u>0</u>

Sizes of Undiscovered Accumulations: What are the sizes (**grown**) of the above accums?:
(variations in the sizes of undiscovered accumulations)

Oil in Oil Accumulations (mmbone):.....min. size	<u>0.5</u>	median size <u>1</u>	max. size <u>15</u>
Gas in Gas Accumulations (bcfg):.....min. size	_____	median size _____	max. size _____

AVERAGE RATIOS FOR UNDISCOVERED ACCUMS., TO ASSESS COPRODUCTS

(uncertainty of fixed but unknown values)

<u>Oil Accumulations:</u>	minimum	median	maximum
Gas/oil ratio (cfg/bo).....	75	150	225
NGL/gas ratio (bnl/mmcf).....	5	10	15
<u>Gas Accumulations:</u>	minimum	median	maximum
Liquids/gas ratio (bliq/mmcf).....	_____	_____	_____
Oil/gas ratio (bo/mmcf).....	_____	_____	_____

SELECTED ANCILLARY DATA FOR UNDISCOVERED ACCUMULATIONS

(variations in the properties of undiscovered accumulations)

<u>Oil Accumulations:</u>	minimum	median	maximum
API gravity (degrees).....	20	28	32
Sulfur content of oil (%).....	0.2	0.25	0.5
Drilling Depth (m)	121	487	945
Depth (m) of water (if applicable).....	_____	_____	_____
<u>Gas Accumulations:</u>	minimum	median	maximum
Inert gas content (%).....	_____	_____	_____
CO ₂ content (%).....	_____	_____	_____
Hydrogen-sulfide content (%).....	_____	_____	_____
Drilling Depth (m).....	_____	_____	_____
Depth (m) of water (if applicable).....	_____	_____	_____

Appendix E. Input data form used in evaluating the Mancos-Menefee Composite Total Petroleum System, Mancos Sandstones Conventional Oil Assessment Unit (50220303), San Juan Basin Province.

Appendix E. Input data form used in evaluating the Mancos-Menefee Composite Total Petroleum System, Mancos Sandstones Conventional Oil Assessment Unit (503220303), San Juan Basin Province.

**SEVENTH APPROXIMATION
DATA FORM FOR CONVENTIONAL ASSESSMENT UNITS (NOGA, Version 5, 6-30-01)**

IDENTIFICATION INFORMATION

Assessment Geologist:.....	J.L. Ridgley	Date:	9/25/2002
Region:.....	North America	Number:	5
Province:.....	San Juan Basin	Number:	5022
Total Petroleum System:.....	Mancos-Menefee Composite	Number:	502203
Assessment Unit:.....	Mancos Sandstones Conventional Oil	Number:	50220303
Based on Data as of:.....	PI/Dwights 2001, NRG 2001 (data current through 1999)		
Notes from Assessor:.....	_____		

CHARACTERISTICS OF ASSESSMENT UNIT

Oil (<20,000 cfg/bo overall) or Gas (≥20,000 cfg/bo overall):... Oil

What is the minimum accumulation size?..... 0.5 mboe grown
(the smallest accumulation that has potential to be added to reserves in the next 30 years)

No. of discovered accumulations exceeding minimum size:..... Oil: 29 Gas: 2
Established (>13 accums.) X Frontier (1-13 accums.) _____ Hypothetical (no accums.) _____

Median size (grown) of discovered oil accumulation (mbo):
1st 3rd 5.84 2nd 3rd 1.84 3rd 3rd 2.9
Median size (grown) of discovered gas accumulations (bcfg):
1st 3rd _____ 2nd 3rd _____ 3rd 3rd _____

Assessment-Unit Probabilities:

<u>Attribute</u>	<u>Probability of occurrence (0-1.0)</u>
1. CHARGE: Adequate petroleum charge for an undiscovered accum. ≥ minimum size.....	<u>1.0</u>
2. ROCKS: Adequate reservoirs, traps, and seals for an undiscovered accum. ≥ minimum size.....	<u>1.0</u>
3. TIMING OF GEOLOGIC EVENTS: Favorable timing for an undiscovered accum. ≥ minimum size.....	<u>1.0</u>

Assessment-Unit GEOLOGIC Probability (Product of 1, 2, and 3):..... 1.0

4. **ACCESSIBILITY:** Adequate location to allow exploration for an undiscovered accumulation ≥ minimum size..... 1.0

UNDISCOVERED ACCUMULATIONS

No. of Undiscovered Accumulations: How many undiscovered accums. exist that are ≥ min. size?:
(uncertainty of fixed but unknown values)

Oil Accumulations:.....min. no. (>0)	<u>2</u>	median no.	<u>5</u>	max no.	<u>10</u>
Gas Accumulations:.....min. no. (>0)	<u>0</u>	median no.	<u>0</u>	max no.	<u>0</u>

Sizes of Undiscovered Accumulations: What are the sizes (**grown**) of the above accums?:
(variations in the sizes of undiscovered accumulations)

Oil in Oil Accumulations (mbo):.....min. size	<u>0.5</u>	median size	<u>2</u>	max. size	<u>10</u>
Gas in Gas Accumulations (bcfg):.....min. size	_____	median size	_____	max. size	_____

AVERAGE RATIOS FOR UNDISCOVERED ACCUMS., TO ASSESS COPRODUCTS

(uncertainty of fixed but unknown values)

<u>Oil Accumulations:</u>	minimum	median	maximum
Gas/oil ratio (cfg/bo).....	2400	4800	7200
NGL/gas ratio (bngl/mmcf).....	20	40	60
<u>Gas Accumulations:</u>	minimum	median	maximum
Liquids/gas ratio (bliq/mmcf).....	_____	_____	_____
Oil/gas ratio (bo/mmcf).....	_____	_____	_____

SELECTED ANCILLARY DATA FOR UNDISCOVERED ACCUMULATIONS

(variations in the properties of undiscovered accumulations)

<u>Oil Accumulations:</u>	minimum	median	maximum
API gravity (degrees).....	33	40	45
Sulfur content of oil (%).....	0	0.1	0.3
Drilling Depth (m)	60	1760	2300
Depth (m) of water (if applicable).....	_____	_____	_____
<u>Gas Accumulations:</u>	minimum	median	maximum
Inert gas content (%).....	_____	_____	_____
CO ₂ content (%).....	_____	_____	_____
Hydrogen-sulfide content (%).....	_____	_____	_____
Drilling Depth (m).....	_____	_____	_____
Depth (m) of water (if applicable).....	_____	_____	_____

Appendix F. Input data form used in evaluating the Mancos-Menefee Composite Total Petroleum System, Mancos Sandstones Continuous Gas Assessment Unit (50220362), San Juan Basin Province.

**FORSPAN ASSESSMENT MODEL FOR CONTINUOUS
ACCUMULATIONS--BASIC INPUT DATA FORM (NOGA, Version 8, 8-16-02)**

IDENTIFICATION INFORMATION

Assessment Geologist:...	<u>J.L. Ridgley</u>	Date:	<u>9/25/2002</u>
Region:.....	<u>North America</u>	Number:	<u>5</u>
Province:.....	<u>San Juan Basin</u>	Number:	<u>5022</u>
Total Petroleum System:..	<u>Mancos-Menefee Composite</u>	Number:	<u>502203</u>
Assessment Unit:.....	<u>Mancos Sandstones Continuous Gas</u>	Number:	<u>50220362</u>
Based on Data as of:.....	<u>PI/Dwights 2001</u>		
Notes from Assessor:.....	<u> </u>		

CHARACTERISTICS OF ASSESSMENT UNIT

Assessment-Unit type: Oil (<20,000 cfg/bo) **or** Gas (≥20,000 cfg/bo) Gas

What is the minimum total recovery per cell?... 0.02 (mmbo for oil A.U.; bcfg for gas A.U.)

Number of tested cells:..... 513

Number of tested cells with total recovery per cell ≥ minimum: 460

Established (>24 cells ≥ min.) X Frontier (1-24 cells) Hypothetical (no cells)

Median total recovery per cell (for cells ≥ min.): (mmbo for oil A.U.; bcfg for gas A.U.)

1st 3rd discovered	<u>0.53</u>	2nd 3rd	<u>0.31</u>	3rd 3rd	<u>0.14</u>
--------------------	-------------	---------	-------------	---------	-------------

Assessment-Unit Probabilities:

<u>Attribute</u>	<u>Probability of occurrence (0-1.0)</u>
1. CHARGE: Adequate petroleum charge for an untested cell with total recovery ≥ minimum	<u>1.0</u>
2. ROCKS: Adequate reservoirs, traps, seals for an untested cell with total recovery ≥ minimum.	<u>1.0</u>
3. TIMING: Favorable geologic timing for an untested cell with total recovery ≥ minimum.....	<u>1.0</u>

Assessment-Unit GEOLOGIC Probability (Product of 1, 2, and 3):..... 1.0

4. **ACCESS:** Adequate location for necessary petroleum-related activities for an untested cell with total recovery ≥ minimum 1.0

NO. OF UNTESTED CELLS WITH POTENTIAL FOR ADDITIONS TO RESERVES IN THE NEXT 30 YEARS

1. Total assessment-unit area (acres): (uncertainty of a fixed value)

minimum	<u>1,845,000</u>	median	<u>1,884,000</u>	maximum	<u>1,942,000</u>
---------	------------------	--------	------------------	---------	------------------

2. Area per cell of untested cells having potential for additions to reserves in next 30 years (acres):
(values are inherently variable)

calculated mean	<u>105</u>	minimum	<u>40</u>	median	<u>100</u>	maximum	<u>200</u>
-----------------	------------	---------	-----------	--------	------------	---------	------------

3. Percentage of total assessment-unit area that is untested (%): (uncertainty of a fixed value)

minimum	<u>96</u>	median	<u>97.1</u>	maximum	<u>98</u>
---------	-----------	--------	-------------	---------	-----------

4. Percentage of untested assessment-unit area that has potential for additions to reserves in next 30 years (%): (a necessary criterion is that total recovery per cell ≥ minimum)
(uncertainty of a fixed value)

minimum	<u>35</u>	median	<u>60</u>	maximum	<u>75</u>
---------	-----------	--------	-----------	---------	-----------

TOTAL RECOVERY PER CELL

Total recovery per cell for untested cells having potential for additions to reserves in next 30 years:

(values are inherently variable)

(mmbo for oil A.U.; bcfg for gas A.U.) minimum 0.02 median 0.35 maximum 5

AVERAGE COPRODUCT RATIOS FOR UNTESTED CELLS, TO ASSESS COPRODUCTS

(uncertainty of fixed but unknown values)

<u>Oil assessment unit:</u>	minimum	median	maximum
Gas/oil ratio (cfg/bo).....	<u> </u>	<u> </u>	<u> </u>
NGL/gas ratio (bnl/mmcfg).....	<u> </u>	<u> </u>	<u> </u>
<u>Gas assessment unit:</u>			
Liquids/gas ratio (bliq/mmcfg).....	<u>8</u>	<u>15</u>	<u>21</u>

SELECTED ANCILLARY DATA FOR UNTESTED CELLS

(values are inherently variable)

<u>Oil assessment unit:</u>	minimum	median	maximum	
API gravity of oil (degrees).....	<u> </u>	<u> </u>	<u> </u>	
Sulfur content of oil (%).....	<u> </u>	<u> </u>	<u> </u>	
Drilling depth (m)	<u> </u>	<u> </u>	<u> </u>	
Depth (m) of water (if applicable).....	<u> </u>	<u> </u>	<u> </u>	
<u>Gas assessment unit:</u>				
Inert-gas content (%).....	<u>0.10</u>	<u>0.20</u>	<u>0.40</u>	
CO ₂ content (%).....	<u>0.50</u>	<u>1.40</u>	<u>1.80</u>	
Hydrogen-sulfide content (%).....	<u>0.00</u>	<u>0.00</u>	<u>0.00</u>	
Drilling depth (m).....	<u>1280</u>	<u>2195</u>	<u>2439</u>	
Depth (m) of water (if applicable).....	<u> </u>	<u> </u>	<u> </u>	
<u>Success ratios:</u>	calculated mean	minimum	median	maximum
Future success ratio (%).....	<u>83</u>	<u>75</u>	<u>83</u>	<u>90</u>
Historic success ratio, tested cells (%).....	<u>90</u>			

Appendix G. Input data form used in evaluating the Mancos-Menefee Composite Total Petroleum System, Mesa Verde Central-Basin Continuous Gas Assessment Unit (50220361), San Juan Basin Province.

**FORSPAN ASSESSMENT MODEL FOR CONTINUOUS
ACCUMULATIONS--BASIC INPUT DATA FORM (NOGA, Version 8, 8-16-02)**

IDENTIFICATION INFORMATION

Assessment Geologist:...	S.M. Condon	Date:	9/24/2002
Region:.....	North America	Number:	5
Province:.....	San Juan Basin	Number:	5022
Total Petroleum System:..	Mancos-Menefee Composite	Number:	502203
Assessment Unit:.....	Mesaverde Central-Basin Continuous Gas	Number:	50220361
Based on Data as of:.....	PI/Dwights 2001		
Notes from Assessor:.....			

CHARACTERISTICS OF ASSESSMENT UNIT

Assessment-Unit type: Oil (<20,000 cfg/bo) or Gas (≥20,000 cfg/bo) Gas

What is the minimum total recovery per cell?... 0.02 (mmbo for oil A.U.; bcfg for gas A.U.)

Number of tested cells:..... 6667

Number of tested cells with total recovery per cell ≥ minimum: 6478

Established (>24 cells ≥ min.) X Frontier (1-24 cells) Hypothetical (no cells)

Median total recovery per cell (for cells ≥ min.): (mmbo for oil A.U.; bcfg for gas A.U.)

1st 3rd discovered	<u>2.1</u>	2nd 3rd	<u>1.6</u>	3rd 3rd	<u>0.5</u>
--------------------	------------	---------	------------	---------	------------

Assessment-Unit Probabilities:

<u>Attribute</u>	<u>Probability of occurrence (0-1.0)</u>	
1. CHARGE: Adequate petroleum charge for an untested cell with total recovery ≥ minimum		<u>1.0</u>
2. ROCKS: Adequate reservoirs, traps, seals for an untested cell with total recovery ≥ minimum.		<u>1.0</u>
3. TIMING: Favorable geologic timing for an untested cell with total recovery ≥ minimum.....		<u>1.0</u>

Assessment-Unit GEOLOGIC Probability (Product of 1, 2, and 3):..... 1.0

4. ACCESS: Adequate location for necessary petroleum-related activities for an untested cell with total recovery ≥ minimum	<u>1.0</u>
---	------------

NO. OF UNTESTED CELLS WITH POTENTIAL FOR ADDITIONS TO RESERVES IN THE NEXT 30 YEARS

1. Total assessment-unit area (acres): (uncertainty of a fixed value)				
	minimum	<u>2,231,000</u>	median	<u>2,348,000</u>
			maximum	<u>2,583,000</u>
2. Area per cell of untested cells having potential for additions to reserves in next 30 years (acres): (values are inherently variable)				
	calculated mean	<u>150</u>	minimum	<u>40</u>
			median	<u>140</u>
			maximum	<u>320</u>
3. Percentage of total assessment-unit area that is untested (%): (uncertainty of a fixed value)				
	minimum	<u>47</u>	median	<u>57</u>
			maximum	<u>62</u>
4. Percentage of untested assessment-unit area that has potential for additions to reserves in next 30 years (%): (a necessary criterion is that total recovery per cell ≥ minimum) (uncertainty of a fixed value)				
	minimum	<u>15</u>	median	<u>22</u>
			maximum	<u>26</u>

TOTAL RECOVERY PER CELL

Total recovery per cell for untested cells having potential for additions to reserves in next 30 years:
(values are inherently variable)

(mmbo for oil A.U.; bcfg for gas A.U.) minimum 0.02 median 0.5 maximum 6

AVERAGE COPRODUCT RATIOS FOR UNTESTED CELLS, TO ASSESS COPRODUCTS

(uncertainty of fixed but unknown values)

<u>Oil assessment unit:</u>	minimum	median	maximum
Gas/oil ratio (cfg/bo).....	<u> </u>	<u> </u>	<u> </u>
NGL/gas ratio (bnl/mmcfg).....	<u> </u>	<u> </u>	<u> </u>
<u>Gas assessment unit:</u>			
Liquids/gas ratio (bliq/mmcfg).....	<u>2</u>	<u>4</u>	<u>6</u>

SELECTED ANCILLARY DATA FOR UNTESTED CELLS

(values are inherently variable)

<u>Oil assessment unit:</u>	minimum	median	maximum	
API gravity of oil (degrees).....	<u> </u>	<u> </u>	<u> </u>	
Sulfur content of oil (%).....	<u> </u>	<u> </u>	<u> </u>	
Drilling depth (m)	<u> </u>	<u> </u>	<u> </u>	
Depth (m) of water (if applicable).....	<u> </u>	<u> </u>	<u> </u>	
<u>Gas assessment unit:</u>				
Inert-gas content (%).....	<u>0.01</u>	<u>0.25</u>	<u>0.50</u>	
CO ₂ content (%).....	<u>0.50</u>	<u>1.00</u>	<u>3.00</u>	
Hydrogen-sulfide content (%).....	<u>0.00</u>	<u>0.00</u>	<u>0.00</u>	
Drilling depth (m).....	<u>500</u>	<u>1485</u>	<u>2275</u>	
Depth (m) of water (if applicable).....	<u> </u>	<u> </u>	<u> </u>	
<u>Success ratios:</u>	calculated mean	minimum	median	maximum
Future success ratio (%).....	<u>94</u>	<u>90</u>	<u>94</u>	<u>97</u>
Historic success ratio, tested cells (%).....	<u>97</u>			

Appendix H. Input data form used in evaluating the Mancos-Menefee Composite Total Petroleum System, Menefee Coalbed Gas Assessment Unit (50220381), San Juan Basin Province.

**FORSPAN ASSESSMENT MODEL FOR CONTINUOUS
ACCUMULATIONS--BASIC INPUT DATA FORM (NOGA, Version 8, 8-16-02)**

IDENTIFICATION INFORMATION

Assessment Geologist:...	<u>S.M. Condon</u>	Date:	<u>9/24/2002</u>
Region:.....	<u>North America</u>	Number:	<u>5</u>
Province:.....	<u>San Juan Basin</u>	Number:	<u>5022</u>
Total Petroleum System:..	<u>Mancos-Menefee Composite</u>	Number:	<u>502203</u>
Assessment Unit:.....	<u>Menefee Coalbed Gas</u>	Number:	<u>50220381</u>
Based on Data as of:.....	<u>PI/Dwights 2001</u>		
Notes from Assessor:.....	<u>Analog: Uinta-Piceance Mesaverde Coalbed Gas Assessment Unit (50200282)</u>		

CHARACTERISTICS OF ASSESSMENT UNIT

Assessment-Unit type: Oil (<20,000 cfg/bo) or Gas (≥20,000 cfg/bo) Gas

What is the minimum total recovery per cell?... 0.02 (mmbo for oil A.U.; bcfg for gas A.U.)

Number of tested cells:..... 3

Number of tested cells with total recovery per cell ≥ minimum: 0

Established (>24 cells ≥ min.) Frontier (1-24 cells) Hypothetical (no cells) X

Median total recovery per cell (for cells ≥ min.): (mmbo for oil A.U.; bcfg for gas A.U.)

1st 3rd discovered	<u> </u>	2nd 3rd	<u> </u>	3rd 3rd	<u> </u>
--------------------	-----------------------------	---------	-----------------------------	---------	-----------------------------

Assessment-Unit Probabilities:

<u>Attribute</u>	<u>Probability of occurrence (0-1.0)</u>
1. CHARGE: Adequate petroleum charge for an untested cell with total recovery ≥ minimum	<u>1.0</u>
2. ROCKS: Adequate reservoirs, traps, seals for an untested cell with total recovery ≥ minimum.	<u>1.0</u>
3. TIMING: Favorable geologic timing for an untested cell with total recovery ≥ minimum.....	<u>1.0</u>

Assessment-Unit GEOLOGIC Probability (Product of 1, 2, and 3):..... 1.0

4. **ACCESS:** Adequate location for necessary petroleum-related activities for an untested cell with total recovery ≥ minimum 1.0

NO. OF UNTESTED CELLS WITH POTENTIAL FOR ADDITIONS TO RESERVES IN THE NEXT 30 YEARS

1. Total assessment-unit area (acres): (uncertainty of a fixed value)

minimum	<u>4,317,000</u>	median	<u>4,797,000</u>	maximum	<u>5,037,000</u>
---------	------------------	--------	------------------	---------	------------------

2. Area per cell of untested cells having potential for additions to reserves in next 30 years (acres): (values are inherently variable)

calculated mean	<u>129</u>	minimum	<u>40</u>	median	<u>120</u>	maximum	<u>280</u>
-----------------	------------	---------	-----------	--------	------------	---------	------------

3. Percentage of total assessment-unit area that is untested (%): (uncertainty of a fixed value)

minimum	<u>100</u>	median	<u>100</u>	maximum	<u>100</u>
---------	------------	--------	------------	---------	------------

4. Percentage of untested assessment-unit area that has potential for additions to reserves in next 30 years (%): (a necessary criterion is that total recovery per cell ≥ minimum) (uncertainty of a fixed value)

minimum	<u>1</u>	median	<u>9</u>	maximum	<u>27</u>
---------	----------	--------	----------	---------	-----------

TOTAL RECOVERY PER CELL

Total recovery per cell for untested cells having potential for additions to reserves in next 30 years:
(values are inherently variable)

(mmbo for oil A.U.; bcfg for gas A.U.) minimum 0.02 median 0.08 maximum 5

AVERAGE COPRODUCT RATIOS FOR UNTESTED CELLS, TO ASSESS COPRODUCTS

(uncertainty of fixed but unknown values)

<u>Oil assessment unit:</u>	minimum	median	maximum
Gas/oil ratio (cfg/bo).....	<u> </u>	<u> </u>	<u> </u>
NGL/gas ratio (bnl/mmcfg).....	<u> </u>	<u> </u>	<u> </u>

<u>Gas assessment unit:</u>	minimum	median	maximum
Liquids/gas ratio (bliq/mmcfg).....	<u> 0 </u>	<u> 0 </u>	<u> 0 </u>

SELECTED ANCILLARY DATA FOR UNTESTED CELLS

(values are inherently variable)

<u>Oil assessment unit:</u>	minimum	median	maximum
API gravity of oil (degrees).....	<u> </u>	<u> </u>	<u> </u>
Sulfur content of oil (%).....	<u> </u>	<u> </u>	<u> </u>
Drilling depth (m)	<u> </u>	<u> </u>	<u> </u>
Depth (m) of water (if applicable).....	<u> </u>	<u> </u>	<u> </u>

<u>Gas assessment unit:</u>	minimum	median	maximum
Inert-gas content (%).....	<u> 0.10 </u>	<u> 0.30 </u>	<u> 1.00 </u>
CO ₂ content (%).....	<u> 0.20 </u>	<u> 4.00 </u>	<u> 15.00 </u>
Hydrogen-sulfide content (%).....	<u> 0.00 </u>	<u> 0.00 </u>	<u> 0.00 </u>
Drilling depth (m).....	<u> 90 </u>	<u> 900 </u>	<u> 1400 </u>
Depth (m) of water (if applicable).....	<u> </u>	<u> </u>	<u> </u>

<u>Success ratios:</u>	calculated mean	minimum	median	maximum
Future success ratio (%).....	<u> 70 </u>	<u> 50 </u>	<u> 70 </u>	<u> 90 </u>

Historic success ratio, tested cells (%)..



Click here to return to
Volume Title Page

Geology, Sequence Stratigraphy, and Oil and Gas Assessment of the Lewis Shale Total Petroleum System, San Juan Basin, New Mexico and Colorado



Click here to return to
[Volume Title Page](#)

By R.F. Dubiel

Chapter 5 of 7

Total Petroleum Systems and Geologic Assessment of Undiscovered Oil and Gas Resources in the San Juan Basin Province, Exclusive of Paleozoic Rocks, New Mexico and Colorado

Compiled by U.S. Geological Survey San Juan Basin Assessment Team

Digital Data Series 69–F

U.S. Department of the Interior
U.S. Geological Survey

U.S. Department of the Interior
KEN SALAZAR, Secretary

U.S. Geological Survey
Marcia K. McNutt, Director

U.S. Geological Survey, Reston, Virginia 2013

For product and ordering information:

World Wide Web: <http://www.usgs.gov/pubprod>

Telephone: 1-888-ASK-USGS

For more information on the USGS—the Federal source for science about the Earth, its natural and living resources, natural hazards, and the environment:

World Wide Web: <http://www.usgs.gov>

Telephone: 1-888-ASK-USGS

Suggested citation:

Dubiel, R.F., 2013, Geology, sequence stratigraphy, and oil and gas assessment of the Lewis Shale Total Petroleum System, San Juan Basin, New Mexico and Colorado, chap. 5 of U.S. Geological Survey San Juan Basin Assessment Team, Total petroleum systems and geologic assessment of undiscovered oil and gas resources in the San Juan Basin Province, exclusive of Paleozoic rocks, New Mexico and Colorado: U.S. Geological Survey Digital Data Series 69-F, p. 1–45.

Any use of trade, product, or firm names is for descriptive purposes only and does not imply endorsement by the U.S. Government.

Although this report is in the public domain, permission must be secured from the individual copyright owners to reproduce any copyrighted material contained within this report.

Contents

Abstract.....	1
Introduction.....	1
Geologic Setting.....	2
Stratigraphy	2
Sequence Stratigraphy.....	8
The Lewis Shale Total Petroleum System.....	11
Hydrocarbon Source Rock.....	16
Source Rock Maturation.....	17
Hydrocarbon Migration Summary	21
Hydrocarbon Reservoir Rocks.....	21
Hydrocarbon Traps and Seals	22
Assessment of Oil and Gas Resources	22
Lewis Continuous Gas Assessment Unit (AU 50220261)	23
Assessment Results	23
Acknowledgments	26
References Cited.....	26
Appendixes	
A. Data form for the Lewis Continuous Gas Assessment Unit (AU 50220261).....	30
B. Summary of assessment results for the Lewis Continuous Gas Assessment Unit (AU 50220261).....	45

Figures

1. Location map of the San Juan Basin Province.....	3
2. Cross sections of the San Juan Basin	4
3. Maps showing geology of the San Juan Basin Province, Lewis Shale isopach, and Lewis Shale Total Petroleum System, and cross sections of San Juan Basin	12
4. Burial history curves for the Lewis Shale Total Petroleum System	18
5. Petroleum system events chart for the Lewis Shale Total Petroleum System.....	20
6. Map of the Lewis Continuous Gas Assessment Unit.....	24

Geology, Sequence Stratigraphy, and Oil and Gas Assessment of the Lewis Shale Total Petroleum System, San Juan Basin, New Mexico and Colorado

By R.F. Dubiel

Abstract

The Lewis Shale Total Petroleum System (TPS) in the San Juan Basin Province contains a continuous gas accumulation in three distinct stratigraphic units deposited in genetically related depositional environments: offshore-marine shales, mudstones, siltstones, and sandstones of the Lewis Shale, and marginal-marine shoreface sandstones and siltstones of both the La Ventana Tongue and the Chacra Tongue of the Cliff House Sandstone. The Lewis Shale was not a completion target in the San Juan Basin (SJB) in early drilling from about the 1950s through 1990. During that time, only 16 wells were completed in the Lewis from natural fracture systems encountered while drilling for deeper reservoir objectives. In 1991, existing wells that penetrated the Lewis Shale were re-entered by petroleum industry operators in order to fracture-stimulate the Lewis and to add Lewis gas production onto preexisting, and presumably often declining, Mesaverde Group production stratigraphically lower in the section. By 1997, approximately 101 Lewis completions had been made, both as re-entries into existing wells and as add-ons to Mesaverde production in new wells. Based on recent industry drilling and completion practices leading to successful gas production from the Lewis and because new geologic models indicate that the Lewis Shale contains both source rocks and reservoir rocks, the Lewis Shale TPS was defined and evaluated as part of this U.S. Geological Survey oil and gas assessment of the San Juan Basin.

Gas in the Lewis Shale Total Petroleum System is produced from shoreface sandstones and siltstones in the La Ventana and Chacra Tongues and from distal facies of these prograding clastic units that extend into marine rocks of the Lewis Shale in the central part of the San Juan Basin. Reservoirs are in shoreface sandstone parasequences of the La Ventana and Chacra and their correlative distal parasequences in the Lewis Shale where both natural and artificially enhanced fractures produce gas. The Lewis Continuous Gas Assessment Unit (AU 50220261) is thought to be self-sourced from and self-sealed by marine shales and mudstones deposited within the Lewis Shale that enclose clastic parasequences in the La Ventana and Chacra Tongues. The gas resource is thought to be a continuous accumulation sourced from the Lewis Shale

throughout the depositional basin. In the Lewis Continuous Gas Assessment Unit (AU 50220261), for continuous gas resources, there is an F95 of 8,315.22 billion cubic feet of gas (BCFG) and an F5 of 12,282.31 BCFG, with a mean value of 10,177.24 BCFG. There is an F95 of 18.08 million barrels of natural gas liquids (MMBNGL) and an F5 of 47.32 MMBNGL, with a mean of 30.53 MMBNGL.

Introduction

This report presents the results of a geologic assessment of the undiscovered oil and gas resources of the Lewis Shale Total Petroleum System (TPS) within the San Juan Basin (SJB) Province of northwestern New Mexico and southwestern Colorado (fig. 1). The Cretaceous Lewis Shale TPS represents one of the four total petroleum systems defined for this project to assess the undiscovered hydrocarbon resources of the San Juan Basin (see chap. 1, this CD-ROM; fig. 3). The four total petroleum systems are, in ascending stratigraphic order, the Todilto TPS, Mancos-Menefee Composite TPS, Lewis Shale TPS, and Fruitland TPS.

The Lewis Shale TPS contains three distinct stratigraphic units deposited in genetically related depositional environments:

1. offshore-marine shales, mudstones, siltstones, and sandstones of the Lewis Shale, and marginal-marine shoreface to turbidite sandstones and siltstones of both
2. the La Ventana Tongue, and
3. the Chacra Tongue of the Cliff House Sandstone.

Although the La Ventana and Chacra Tongues had produced gas for many years prior to, and were included in, the 1995 USGS assessment of oil and gas resources in the San Juan Basin (Huffman, 1996), the Lewis Shale was not assessed as part of that effort. The Lewis Shale was not a completion target in the San Juan Basin in early drilling from about the 1950s through 1990. During that time, only 16 wells were completed in the Lewis where natural fracture systems were

encountered while drilling for deeper objectives (Jennings and others, 1997a,b). Burlington Resources operates approximately 6,500 of more than 18,000 existing wells in the SJB (Dube and others, 2000). The Lewis Shale was drilled through but not tested, and thus is “behind pipe” in about 3,500 wells operated by Burlington Resources. Many of these wells extend down to the Mesaverde Group and older stratigraphic units (Jennings and others, 1997a,b; Dube and others, 2000; Bereskin, 2001a,b, 2003). In 1991, Burlington Resources began a program to recomplete existing wells that penetrated the Lewis Shale in order to fracture-stimulate the Lewis (Jennings and others, 1997; Dube and others, 2000) and to add Lewis production to preexisting, and presumably often declining, Mesaverde production. By 1997, Burlington Resources reported that approximately 101 Lewis completions had been made, both as re-entries into existing wells and as add-ons to Mesaverde production in new wells (Jennings and others, 1997; Dube and others, 2000). Burlington Resources had described a trend in the SJB that includes both the 16 Lewis completions from naturally fractured wells and successful new fracture-stimulated completions (Jennings and others, 1997; Dube and others, 2000; Shirley, 2001). This trend contains more than 3,500 existing wells operated by Burlington Resources that penetrate the Lewis (Dube and others, 2000). In addition, several recent publications have indicated that commercial gas production currently exists from the Lewis Shale (Jennings and others, 1997a,b; Dube and others, 2000; Shirley, 2001). For these reasons, and because new geologic models indicate that the Lewis Shale contains both source rocks and reservoir rocks, the Lewis Shale TPS was defined and evaluated as part of this U.S. Geological Survey (USGS) oil and gas assessment in the San Juan Basin. This report assesses the undiscovered gas resources within the Lewis Shale TPS in the San Juan Basin.

Geologic Setting

The Lewis Shale Total Petroleum System lies within the San Juan Basin in northwestern New Mexico and southwestern Colorado (fig. 1). The San Juan Basin is an asymmetric structural depression of Laramide age (fig. 2A) that contains strata ranging in age from Cambrian to Quaternary (Fassett and Hinds, 1971). Upper Cretaceous sediments in the SJB (fig. 2B) were deposited in the Cretaceous Western Interior Seaway, and, similar to most other Cretaceous strata in the SJB that were deposited in response to alternating marine transgressions and regressions, they form a series of interfingered continental, marginal-marine, and marine units. Continental fluvial and coal deposits on the southwestern margin of the SJB grade to the northeast into marginal-marine, estuarine, and shoreface strata. All of these strata continue to grade northeastward into offshore-marine rocks that originally were deposited in the depositional basin that extended eastward into Kansas and adjoining states (see for example, Molenaar, 1977; Roberts and Kirschbaum, 1995).

Stratigraphy

Strata within the Lewis Shale TPS include the Lewis Shale and rocks that are within or are correlative to the Mesaverde Group (fig. 2B). The Mesaverde Group was first described by Holmes (1877), but Collier (1919) later named the unit for exposures at the type locality in what is now Mesaverde National Park in southwestern Colorado. Numerous studies describe the stratigraphy in and around the San Juan Basin (Sears and others, 1941; Pike, 1947; Beaumont and others, 1956; Hollenshead and Pritchard, 1961; and many others). Many other regional studies related to economic coal and petroleum resources in the San Juan Basin have also addressed stratigraphic issues (for example, Fassett, 1977, 2000; Molenaar, 1983; Molenaar and others, 2002; and many others). Holmes (1877) also named the overlying Pictured Cliffs Sandstone, which interfingers with and progrades over the Lewis Shale to the northeast in the SJB (fig. 2B).

The Mesaverde Group in the San Juan Basin was deposited on the western shelf of the epicontinental Cretaceous Western Interior Seaway. The SJB lies south of a major subsiding Cretaceous foreland basin that was bounded on the west by the Sevier fold and thrust belt (Weimer, 1960; Molenaar, 1983). The SJB during the Cretaceous was bounded to the west by the Mogollon rim in central Arizona. During deposition of rocks forming the Lewis Shale TPS, the western shoreline of the Cretaceous Western Interior Seaway passed through the southwest part of the SJB with the seaway extending eastward through Kansas (Roberts and Kirschbaum, 1995). The Mesaverde Group comprises several stratigraphic units and facies, in ascending order: shoreface sandstones of the Point Lookout Sandstone, marginal-marine to continental deposits of the Menefee Formation, and shoreface sandstones of the Cliff House Sandstone. The marine strata of the Lewis Shale interfinger with and grade southwestward into shoreface sandstones of both the Cliff House Sandstone and the Pictured Cliffs Sandstone (fig. 2B).

Although the general stratigraphy of the Mesaverde Group was established long ago, more recent studies employing well-log cross sections and modern sedimentologic concepts have led to a greater understanding of the surface and subsurface marine shales and shoreface deposits, especially in the Cliff House Sandstone. The Cliff House comprises three units:

1. the basal Cliff House Sandstone,
2. the La Ventana Tongue, and
3. a unit designated by several names but most often called the Chacra Tongue (fig. 2B).

There has been much discussion in the literature as to the naming and designation of the “Chacra.”

Dane (1936) named the Chacra sandstone member (lower case convention in use at that time) of the Mesaverde Formation, based on outcrops at Chacra Mesa in the southeastern SJB. This paralleled his designation of the La Ventana sandstone member of the Mesaverde Formation in the same

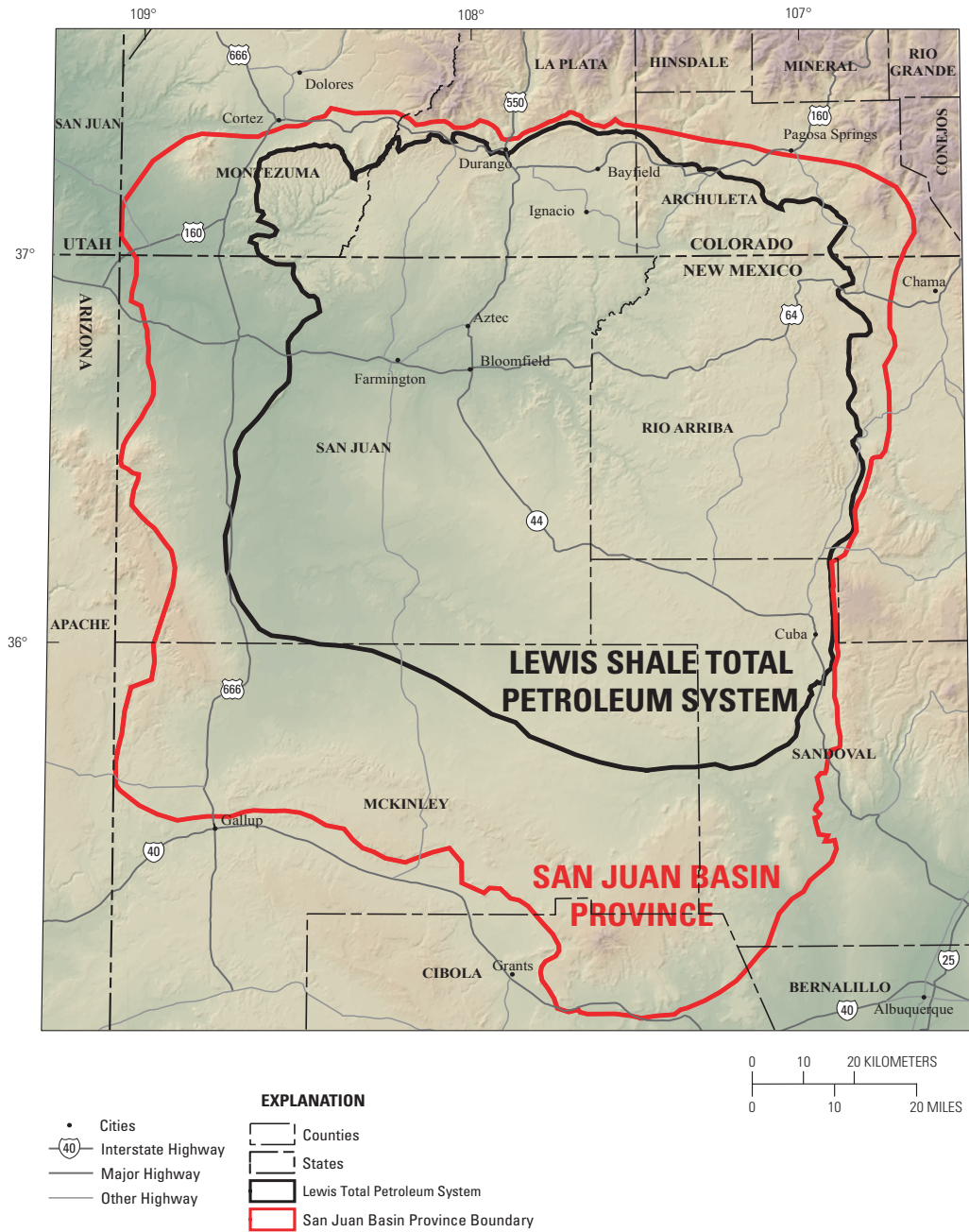


Figure 1. Index map of the San Juan Basin Province showing the outline of the Lewis Shale Total Petroleum System and the boundary of the San Juan Basin Province.

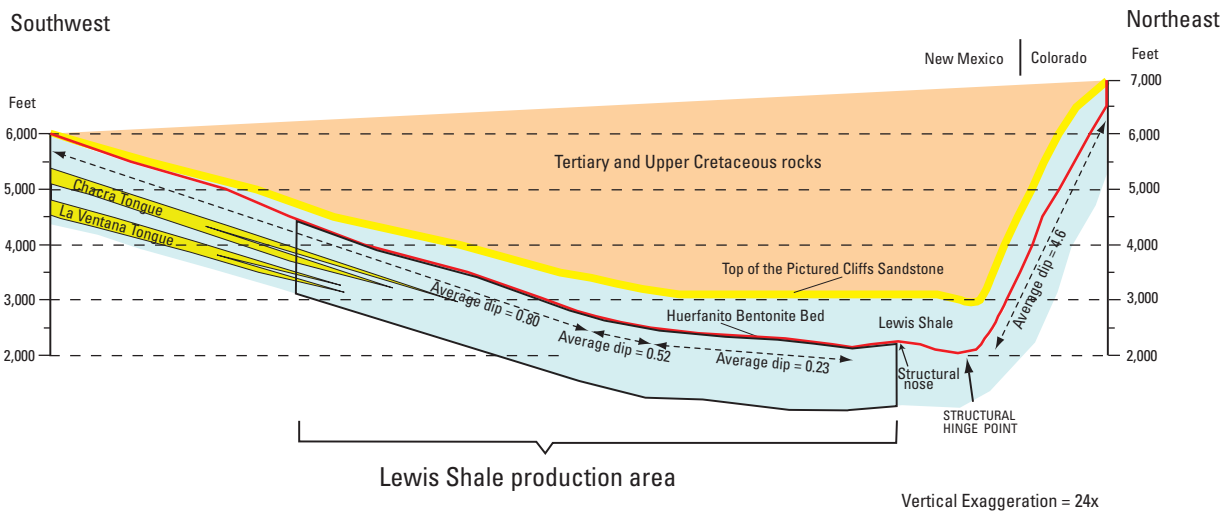
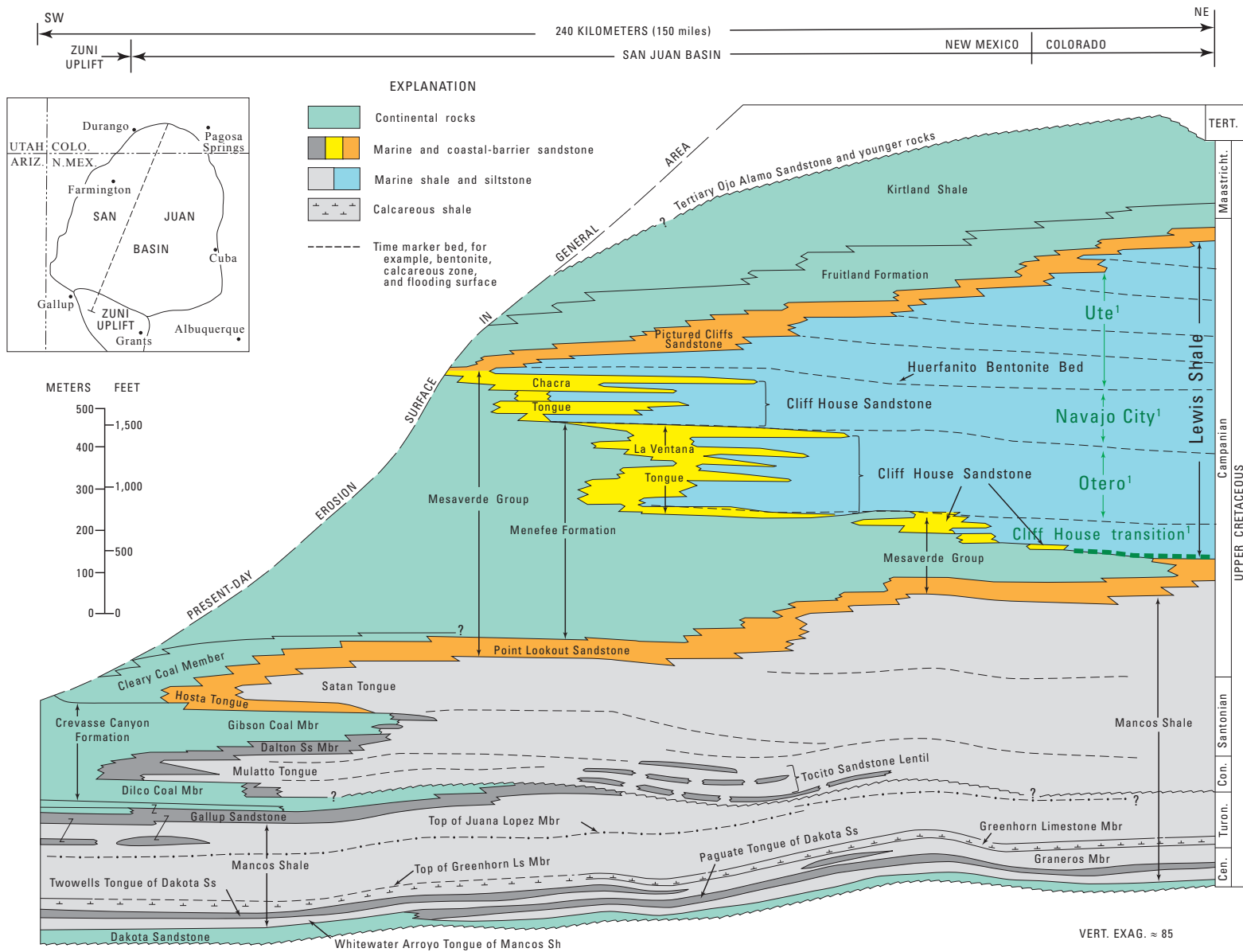


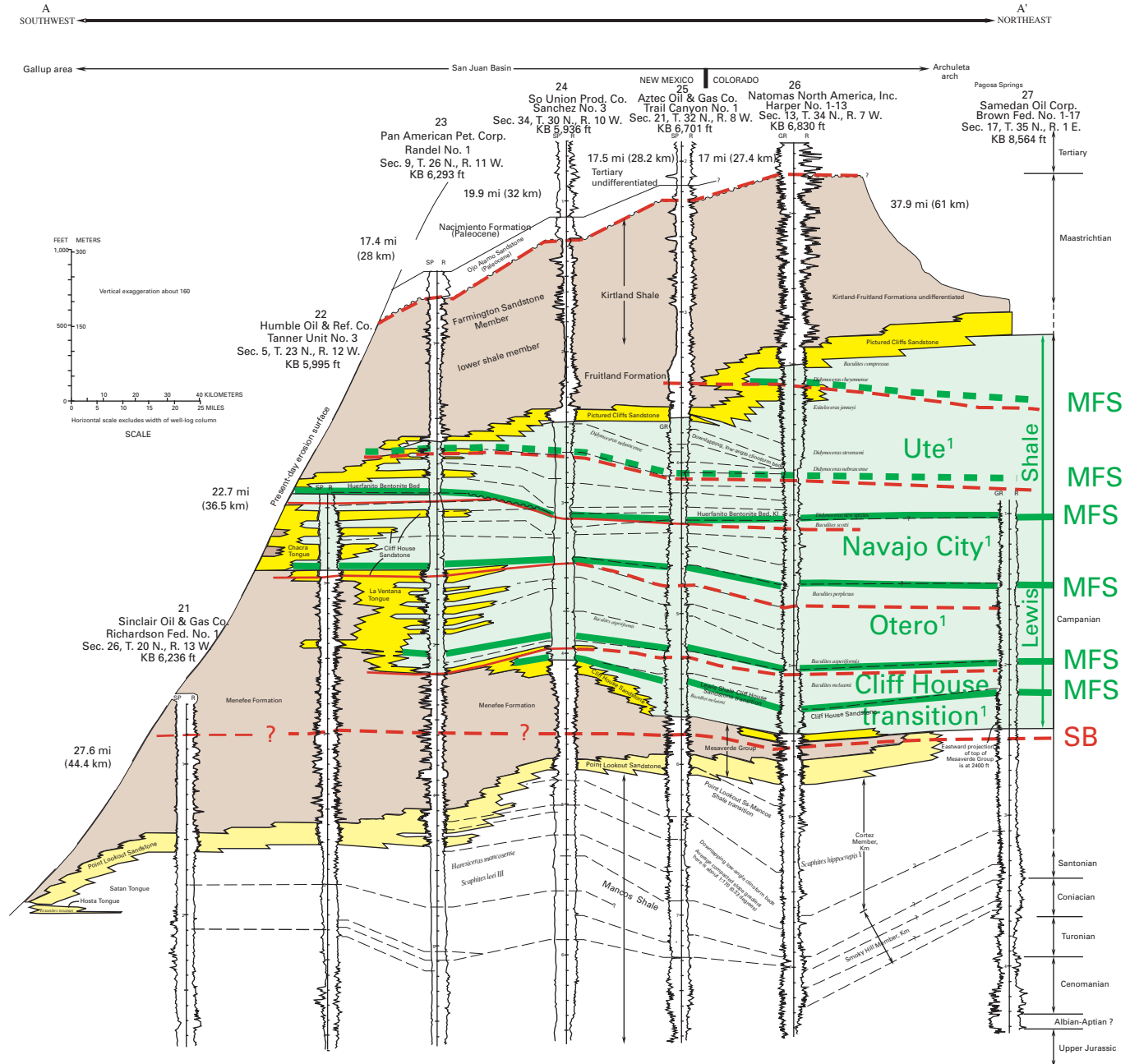
Figure 2A. Structural profile oriented southwest–northeast across the central part of the San Juan Basin, showing the Lewis Shale, La Ventana and Chacra Tongues of the Cliff House Sandstone, and overlying rocks. Top of profile is shown as flat because Tertiary and Cretaceous rocks are incompletely shown. Area of Lewis Shale production is shown with blue line. The San Juan Basin is shown at a vertical exaggeration of 24x. Modified from Fassett (2000, his fig. 23).



¹Informal interval within Lewis Shale.

Figure 2B. Stratigraphic cross section of the San Juan Basin, highlighting depositional facies and units in the Lewis Shale Total Petroleum System. Modified from Molenaar (1977). Cen., Cenomanian; Turon., Turonian; Con., Coniacian; Maastricht., Maastrichtian; Tert., Tertiary; Ss, Sandstone; Ls, Limestone; Mbr, Member.

6 Total Petroleum Systems and Geologic Assessment of Undiscovered Oil and Gas Resources in the San Juan Basin Province



¹Informal interval within Lewis Shale.

Figure 2C. Well-log cross section showing stratigraphic units and sequence stratigraphic units and surfaces used to analyze the Lewis Shale. Modified from Molenaar and others (2002). Kl, Lewis Shale; Km, Mancos Shale; Ss, Sandstone; MFS, maximum flooding surface; SB, sequence boundary.

EXPLANATION

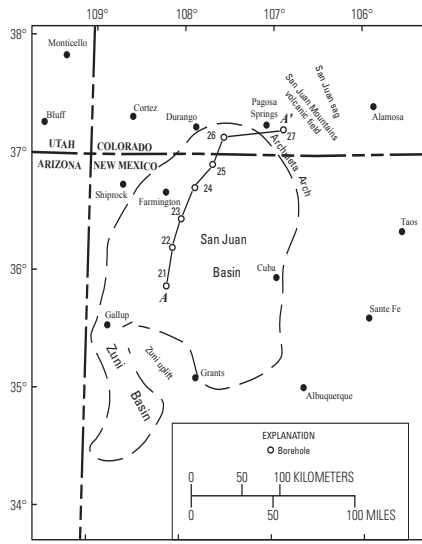
- Formation or member contact
- /?—— Contact that rises (uniformly or abruptly) in stratigraphic position. Queried where uncertain
- - - - Contact, position is uncertain
- ~~~~/?~~~ Unconformity. Queried where uncertain.
- SP Spontaneous-potential curve
- GR Gamma-ray curve
- R Resistivity curve
- KB Kelly bushing

Borehole depths shown are in thousands of feet below elevation of Kelly bushing. Also note that only partial logs of boreholes are shown; upper and lower parts of logs are omitted where they are not applicable to this study.

CRETACEOUS ROCKS

- Nonmarine rocks (various formations)
- Marginal-marine and shoreface sandstone (various formations)
- Dominantly marine shale, mudstone, and siltstone (Lewis Shale)
- Dominantly marine shale and siltstone (Mancos Shale)

- Marine flooding surface (MFS) (dashed where inferred)
- Sequence boundary (SB) (dashed where inferred)



INDEX MAP SHOWING LOCATION OF CROSS SECTION

Figure 2C. Well-log cross section showing stratigraphic units and sequence stratigraphic units and surfaces used to analyze the Lewis Shale. Modified from Molenaar and others (2002). Kl, Lewis Shale; Km, Mancos Shale; Ss, Sandstone; MFS, maximum flooding surface; SB, sequence boundary; Ute¹, Navajo City¹, Otero¹, Cliff House transition¹, informal terms used by drillers and geologists in the basin.—Continued

publication for outcrops near the town of La Ventana. At that time, neither Dane nor other workers had yet correlated sandstones from their study area in the southeast around the southern part of the San Juan Basin to the type section of the Cliff House Sandstone on the northwestern flank of the SJB. Beaumont and others (1956) abandoned Dane's original name "Chacra" in favor of the Cliff House Sandstone during their mapping around the southern SJB. However, they retained the name La Ventana Tongue of the Cliff House in the southeast SJB. Apparently they thought at the time that all of the La Ventana (and Danes's Chacra) was equivalent to the entire section of the Cliff House at the type section and on the northwest margin of the SJB. On a subsurface cross section of well logs, Fassett (1977) relabeled the "Chacra" as the unnamed tongue, despite indicating in the text that this unit correlated on outcrop to Dane's (1936) original "Chacra." He also suggested that the name Tsaya Canyon sandstone tongue of the Cliff House Sandstone be considered for the unit, but he did not formally rename it, because the publication was a guidebook. Fassett (1977) referred to sandstones below the La Ventana as basal Cliff House Sandstone. Fassett (1977) also indicated reasons against resurrecting the name Chacra, citing the recently proposed adoption of a similar name, "Chacra producing interval," by the New Mexico Oil Conservation Commission. The proposed "Chacra producing interval" would contain sandstones within both the Chacra and La Ventana. Additionally, Fassett (1977) indicated that some geologists working in the subsurface of the SJB had incorrectly identified the uppermost two sandstones of the La Ventana as Chacra, adding to the stratigraphic confusion.

Subsequently, Beaumont and Hoffman (1992) proposed the informal name Chacra Mesa tongue for the unit, again based on outcrops on Chacra Mesa. This proposal introduced yet another name for the same unit originally designated by Dane (1936). The fact that the La Ventana extends northward in the subsurface from outcrops near the town of La Ventana to the outcrop belt of the Cliff House south of its type section (Fassett, 1977) indicates that Dane's (1936) original stratigraphic interpretation of the La Ventana and Chacra was probably correct. Fassett (1977) stated that he and others had earlier suggested that Dane's (1936) original definition be restored, as did Beaumont and Hoffman (1992). Apparently, no outcrop studies document that the three stratigraphic subdivisions recognized within the Cliff House on the southeast margin of the SJB (basal Cliff House, La Ventana, and Chacra) can be correlated to similar subdivisions within the Cliff House on the northwest flank of the SJB. However, well-log cross sections (Molenaar and Baird, 1992; Molenaar and others, 2002) and subsurface correlation of well logs for this assessment study enable correlation of these units. A sequence stratigraphic study of the Cliff House Sandstone in Mancos Canyon in the northwest SJB near the type section of the Mesaverde identified complex packaging of shoreface sandbodies within the Cliff House (Olsen and others, 1999). Further studies of this kind have the potential for elucidating

more detailed relations between the internal geometry of the Cliff House at the type section and the stratigraphic units designated by Dane (1936) in the southeast SJB. From the previously published regional well-log cross sections and those done for the present assessment study, Dane's (1936) original interpretation of major recognizable units within the Cliff House appears correct, and these units can be recognized and correlated in the subsurface cross sections used in this assessment. For these reasons, the present report refers to the unit in question as the Chacra Tongue of the Cliff House Sandstone to parallel Dane's (1936) original formal designation of the La Ventana Tongue and his original interpretation and designation of the stratigraphic relations of the "Chacra."

The Huerfanito Bentonite Bed is a laterally extensive unit within the Lewis Shale formed from altered volcanic ash that can be traced in well logs and on the outcrop throughout the San Juan Basin (fig. 2A) (Fassett, 2000). The Huerfanito Bentonite Bed extends across the deeper part of the original depositional basin and overlies the Chacra Tongue in the southwest part of the San Juan Basin (fig. 2B). The Huerfanito can be identified in well logs and used as a subsurface stratigraphic marker. It demarcates the Lewis Shale into two parts (Fassett and Hinds, 1971; Manfrino, 1984). The Lewis Shale has been subdivided in industry reports since the 1990s into three informal intervals, the Ute, Navajo City, and Otero intervals (fig. 2B) (see for example, Bereskin, 2001a; Jennings and others, 2001). However, the names "Navajo City Chacra interval" and "Otero Chacra interval" were used at least as early as 1983 (Meibos, 1983). In addition, more recent studies also refer to a fourth interval within the basal part of the Lewis Shale as the upper Cliff House (Bereskin, 2001a, 2003) or the Cliff House transition interval (Jennings and others, 1997a,b; Dube and others, 2000; Molenaar and others, 2002; Mavor and others, 2003). In this assessment report, the Lewis Shale comprises, in ascending order, the Cliff House transition, Otero, and Navajo City intervals below the Huerfanito Bentonite Bed and the Ute interval above the Huerfanito (fig. 2B).

Sequence Stratigraphy

In basins or fields with extensive well-log control, the application of sequence stratigraphic concepts can result in a high-resolution stratigraphic framework for subsurface correlation and for analyzing reservoir, source, and seal distribution (Van Wagoner and others, 1990). The application of sequence stratigraphic concepts and designation of sequence stratigraphic units and surfaces is particularly enlightening in terms of reservoir and source rocks. A sequence stratigraphic interpretation of the Lewis Shale TPS allows depositional units to be evaluated in light of the processes that formed them, processes that are also germane to the designation of components of the TPS such as reservoirs and source rocks, and the processes of generation, migration, and accumulation of hydrocarbons.

The marine rocks of the Lewis Shale TPS were deposited first during the youngest major transgression of the Cretaceous sea in the early part of the Campanian (fig. 2B) and subsequently during the last Cretaceous marine regression in the latter part of the Campanian (see for example, Weimer, 1960; Peterson and Kirk, 1977; Haq and others, 1988). The Cliff House transition, Otero, and Navajo City intervals of the offshore Lewis Shale that were deposited during the Campanian transgression are laterally equivalent to associated marginal-marine and shoreface deposits of the basal Cliff House Sandstone and to the La Ventana and Chacra Tongues of the Cliff House Sandstone. The Huerfanito Bentonite Bed (Fassett and Hinds, 1971) was deposited during the maximum Campanian marine transgression and represents altered volcanic ash that accumulated along the maximum flooding surface of this probable second-order sea-level cycle. The Ute interval of the offshore Lewis Shale above the Huerfanito Bentonite Bed was deposited during the major marine regression in the latter part of the Campanian. In this upper part of the section, the Lewis Shale grades to the southwest into progradational shoreface sandstones of the Pictured Cliffs Sandstone.

The Campanian transgression and regression within the Lewis Shale and associated shoreface sandstones likely represents a second-order relative sea-level cycle. Well-log cross sections and correlation of ammonite-bearing zones within the Lewis Shale (Molenaar and others, 2002) indicate down-lap of strata within the Ute interval onto the Huerfanito Bentonite Bed and associated shales, both of which extend to the southwest over the Chacra Tongue. The Huerfanito and associated marine shales represent the condensed section associated with the maximum marine flooding surface (MFS) during the Campanian (fig. 2C), corresponding to the farthest southwestward transgression of the Campanian Western Interior Seaway in the SJB. The maximum marine flooding surface separates strata of the second-order transgressive system tract (TST) below the Huerfanito and MFS, comprising the Lewis Shale, Cliff House Sandstone, and La Ventana and Chacra Tongues, from progradational strata of the highstand system tract (HST) above, including the Lewis Shale and laterally equivalent part of the Pictured Cliffs Sandstone. Additionally, the transgressive nature of the TST in the lower part of the Lewis Shale is indicated by the back-stepping pattern of shoreface sandstones in the Cliff House transition that are successively overlain to the southwest by the La Ventana Tongue and subsequently by the Chacra Tongue (fig. 2C). A second-order sequence boundary likely exists near the top of the uppermost sandstone of the progradational Point Lookout Sandstone and within the laterally equivalent part of the Menefee Formation, but below the stratigraphically lowest sandstones of the Cliff House. This sequence boundary is expected here because the large basinward shift in shoreface facies demonstrated by the strongly prograding Point Lookout Sandstone and the laterally equivalent continental facies of the Menefee were most likely deposited in response to a slowing of relative sea-level rise and/or lowering of sea level prior to the major transgression represented by the back-stepping pattern of the shoreface sandstones and marine rocks of the overlying Cliff House Sandstone and Lewis Shale, respectively. The

corresponding candidate for a second-order sequence boundary at the top of the Lewis Shale perhaps lies at the unconformity separating the Kirtland-Fruitland Formations (undifferentiated) from the overlying Tertiary Ojo Alamo Sandstone. These two sequence boundaries define a second-order sequence encompassing the Lewis Shale and correlative units (Haq and others, 1988).

One previous report (Dube and others, 2000) refers to the intervals within the Lewis Shale as four informal members, each capped by a regional flooding surface. Within the Campanian second-order sequence, the present assessment study recognizes five, and possibly a sixth, third-order sequences within the Lewis, each replete with third-order sequence boundaries and maximum flooding surfaces (fig. 2C). Three of the third-order sequences are within the lower part of the Lewis Shale, and the fourth, fifth, and the possible sixth third-order sequences lie within the Lewis Shale above the Huerfanito Bentonite Bed. Each MFS is identified on well logs as a shale-rich interval that extends across the basin and overlies a parasequence set of shoreface sandstones to the southwest. Two third-order maximum flooding surfaces that extend from the central part of the SJB to the southwest can be identified in Lewis Shale well logs and cross sections below the Huerfanito (fig. 2C). The first maximum flooding surface (MFS) overlies the Cliff House Sandstone and the corresponding Cliff House transition interval of the Lewis. The second maximum flooding surface (MFS) overlies the La Ventana Tongue and the laterally equivalent Otero interval of the Lewis. The overlying Chacra Tongue and laterally equivalent Navajo City interval are overlain by the maximum marine flooding surface associated with the Huerfanito Bentonite. Here, the second-order and the third-order maximum flooding surfaces coincide. Each of these three maximum flooding surfaces can be traced basinward on well logs throughout the Lewis Shale in the SJB. Within the upper part of the Lewis Shale, in the thick Ute interval, there are two additional shale-rich intervals that extend westward over slightly back-stepping parasequence sets of the correlative Pictured Cliffs Sandstone. The lower of the two shale intervals extends southwestward over a slightly backstepping parasequence set of shoreface sandstones in the Pictured Cliffs. In addition, the lower shale interval is overlain by a downlapping clinofform pattern of time lines based on ammonite correlations in the well-log cross section (fig. 2C) (Molenaar and others, 2002). The uppermost shale interval is associated with an aggradational parasequence set of shoreface sandstones in the Pictured Cliffs Sandstone. This aggradational pattern was investigated by Roberts and McCabe (1992) and attributed by them to a slight pause in shoreline progradation. This aggradational pattern is interpreted here to be associated with the third-order MFS at this position. These two additional shale breaks in the Ute interval appear to delineate the fourth and fifth, and the possible sixth, third-order sequences within the Lewis Shale.

In addition to serving as sequence-stratigraphic markers for well-log correlation, the third-order maximum flooding surfaces form the natural breaks in the Lewis Shale that have

been historically used to divide the Lewis into four informal intervals, which are, in ascending order,

1. the Cliff House transition,
2. Otero,
3. Navajo City, and
4. Ute intervals (figs. 2B and 2C).

Although sequences are typically defined as lying between sequence boundaries (Van Wagoner and others, 1990), the Cliff House transition, Otero, and Navajo City intervals of the Lewis Shale as previously defined lie between the third-order maximum flooding surfaces and not the associated sequence boundaries. Additionally, previous reports have not recognized the additional third-order sequences in the Ute interval described in this assessment report.

In addition to the maximum flooding surfaces, third-order sequence boundaries can also be recognized on the figure 2C cross section. The third-order sequence boundaries associated with the maximum flooding surfaces are inferred from the stacking pattern of the shoreface parasequence sets within the Cliff House transition, La Ventana, Chacra, and Pictured Cliffs discernable in electric logs and by the landward shift in facies and the subsequent deepening events indicated by the marine shale intervals. The critical observations of basinward shift in actual facies associated with the sequence boundaries are not possible without direct observations of the facies from core or outcrops, which were not made in the present study. Despite this limitation, sequence stratigraphic concepts require a sequence boundary between maximum flooding surfaces (Van Wagoner and others, 1990). At the top of each of the third-order backstepping parasequence sets of the Cliff House transition, Otero, and Navajo City intervals there is a marked progradation of the sandbody at the top of the parasequence set. The sequence boundary is thus placed just below this sandbody, on the presumption that it represents a slight basinward shift in facies due to a relative sea-level drop or stillstand.

The shoreface sandstones recognized on the cross section (fig. 2C) within the basal Cliff House and La Ventana and Chacra Tongues represent third-order parasequences in sequence-stratigraphic terms. Within the basal Cliff House Sandstone, the shoreface parasequences form a back-stepping pattern except for the uppermost sandstone, which builds out slightly basinward. The subtle progradation of this uppermost sandstone may be due to it overlying the third-order sequence boundary and thus being part of the HST in this third-order sequence. Alternatively, it may be part of a thin low-stand systems tract overlying the sequence boundary. The sandstone parasequence set of the basal Cliff House is then overlain by the marine flooding surface separating the Cliff House transition from the overlying Otero interval (fig. 2C). The backstepping pattern results in a vertical well-log pattern in which successively higher coarsening-upward units are slightly more distal in facies than those immediately underlying.

This backstepping accounts for the observed slight “fining-upward” character of the Cliff House transition interval of the Lewis (Mavor and others, 2003), despite its generally coarser grain size compared to the overlying intervals in the Lewis Shale. In a detailed study of basal Cliff House sandbodies on the northwest side of the SJB, Olsen and others (1999) documented high-order prograding parasequence sets within the generally backstepping basal Cliff House sandbody. These prograding sandbodies probably represent fourth-order parasequence sets.

The La Ventana Tongue of the Cliff House Sandstone, located stratigraphically above and farther to the southwest than the basal Cliff House Sandstone, internally displays a more vertical aggradational pattern of shoreface parasequences, with a slight progradational parasequence at the top. The subtle progradation of this uppermost parasequence again may be due to its deposition as the uppermost part of the third-order HST, or it may be a small remnant of the lowstand systems tract above the third-order sequence boundary. The La Ventana shoreface parasequences extend into the Otero interval of the Lewis Shale where they form the siltstones and mudstones that produce gas from this part of the section in the central SJB. The La Ventana is also overlain by a third-order marine flooding surface as demonstrated by the marine shale signature in the well logs, extending to the southwest from the Lewis Shale over the top of the La Ventana shoreface parasequence set. The Chacra Tongue of the Cliff House Sandstone, again located stratigraphically higher and farther to the southwest than the underlying La Ventana, internally forms a slightly forward-stepping package of shoreface parasequences. These progradational parasequences and their distal equivalents extend into the Lewis Shale and form the sandy to silty mudstone beds in the Navajo City interval that commonly produce gas. Again, the uppermost parasequence builds out basinward, suggesting it overlies the third-order sequence boundary near the top of the Navajo City interval. The Chacra Tongue is also overlain by a marine flooding surface—this one coincident with the second-order maximum marine flooding surface in the basin represented by the shale interval that contains the Huerfanito Bentonite Bed.

Similar to the designated internal intervals within the Lewis Shale below the Huerfanito Bentonite Bed, the Ute interval above the Huerfanito contains several third-order maximum flooding surfaces and sequence boundaries. The strongly prograding shoreface sandstones within the Pictured Cliffs Sandstone are punctuated by at least two backstepping intervals (fig. 2C). Each of these intervals likely contains both a third-order sequence boundary and a maximum flooding surface similar to those described for the lower part of the Lewis Shale below the Huerfanito. The three resulting intervals in the Ute are thus of the same order of magnitude in thickness and duration as the three intervals in the lower part of the Lewis. The duration of each of the six intervals is approximately 1 to 1.5 million years based on the ammonite zonations (Obradovich, 1993; Roberts and Kirschbaum, 1995; Molenaar and others, 2002). This duration of 1 to 1.5 million

years compares favorably with the duration of third-order relative sea-level cycles on the global sea-level chart (Haq and others, 1988).

Recognition of the third-order sequence boundaries and marine flooding surfaces allows subsurface correlation between the La Ventana and Chacra Tongues shoreface sandstones and the equivalent distal sandstones and siltstones within the corresponding informal intervals designated in the Lewis Shale. In addition, it suggests that cycles similar in magnitude to those within the Cliff House transition, Otero, and Navajo City intervals of the lower part of the Lewis Shale are also present within the much thicker Ute interval in the upper part of the Lewis Shale. Application of these sequence stratigraphic concepts allows an interpretation not only of the stratigraphic and sedimentologic relations between the units but also of the genetic relation of depositional units and significant surfaces as potential reservoirs, source rocks, and migration pathways for hydrocarbons within the Lewis Shale Total Petroleum System. In addition, the sequence stratigraphic interpretations indicate that concepts applied to exploration for and production of gas from the lower part of the Lewis Shale may also be applicable to the Ute interval of the Lewis Shale above the Huerfanito Bentonite Bed, and to similar Cretaceous third-order sequences in other basins. Recognition of third-order cycles in the Ute interval on the scale of those previously recognized in the Cliff House transition, Otero, and Navajo City intervals suggests that additional similar reservoirs and source rocks may be present in the upper part of the Lewis Shale associated with the third-order sequence boundaries and maximum flooding surfaces.

The Lewis Shale Total Petroleum System

The Lewis Shale Total Petroleum System includes all major outcrops and subsurface deposits of the Lewis Shale and laterally equivalent rocks of the La Ventana and Chacra Tongues of the Cliff House Sandstone of the Mesaverde Group (fig. 3A). The Lewis Shale is thought to be the source rock for the Lewis Shale TPS (see following section on Hydrocarbon Source Rocks). The Lewis Shale and the laterally equivalent La Ventana and Chacra Tongues of the Cliff House Sandstone are the reservoir rocks for a continuous gas accumulation in the Lewis Shale TPS. The Lewis Shale TPS normally also would include rocks assigned to the basal part of the Cliff House Sandstone (those sandstones of the Cliff House Sandstone that interfinger with the Cliff House transition zone of the Lewis Shale; figs. 2B and 2C) because they are genetically related to the Chacra and La Ventana, they similarly interfinger basinward with the Lewis Shale, and they may have been charged with gas generated from the Lewis. However, for this study the basal Cliff House Sandstone of that interval is included in and assessed as part of the Mancos-Menefee Composite TPS (see chap. 4, this CD-ROM)

because the database used for this assessment often included and designated wells producing from sandstones within the basal Cliff House as Mesaverde production. Thus, those sandstones are assessed as part of the Mancos-Menefee Composite TPS, which includes all the other Mesaverde units. This separation of basal Cliff House from La Ventana and Chacra production is in part an artifact of pool definitions by the New Mexico Oil Conservation Division (NMOCD).

In 1977, the NMOCD defined a “Chacra line” running northwest to southeast across the SJB. This line delineates the down-dip limit of production from progradational shoreface sandstones of the La Ventana and Chacra Tongues, known collectively in industry terms as the “Chacra” sandstones or “Chacra producing interval.” North and east of the “Chacra line,” where the majority of Mesaverde production exists, the lower part of the Lewis Shale up to the Huerfanito Bentonite Bed was originally included in leases of the Mesaverde Group production in the Mesaverde pool definition (Dube and others, 2000). Since that original definition, the NMDOC revised the upper limit of the Mesaverde pool to include an additional 250 ft of Lewis Shale above the Huerfanito Bentonite Bed. Currently, completion or recompletion of the Lewis Shale producing interval in what are or were primarily Mesaverde wells is dealt with administratively as a pay-add; that is, the production of gas from the Lewis is commingled with and added to Mesaverde production from the same well, which also simplifies the regulatory approval process. It also maximizes Lewis economics because the Lewis can be completed with Mesaverde and/or Dakota Group production and does not require a separate well bore or production string. However, it complicates the assessment of gas produced solely from the Lewis Shale because that gas is co-mingled both as actual gas production and as reported in the IHS database used in this assessment (IHS, 2000a,b).

It was not possible to separate the Cliff House Sandstone (basal Cliff House interval) production from overall Mesaverde production simply by examining the production data as reported for Cliff House or Mesaverde wells in the IHS database (IHS, 2000a,b). Lewis gas is similarly commingled and produced with Mesaverde gas. It was possible to distinguish some of the Lewis Shale gas production from Mesaverde production using Estimated Ultimate Recovery (EUR) curves generated from the production database (IHS, 2000a) by isolating EUR curves that showed a significant spike in increased gas production since about 1990. This is the general onset date for the recent industry trend to establish Lewis gas production from recompletions in preexisting Mesaverde wells. In addition, all Mesaverde records in the IHS database (IHS, 2000a,b) for the SJB were individually checked, and those well records that reported a perforated interval for the Lewis Shale were used in the assessment of the Lewis TPS.

The stratigraphically younger shoreface deposits of the Pictured Cliffs Sandstone, although laterally equivalent to the Lewis Shale, are included in the overlying Fruitland TPS for the SJB assessment (see chap. 6, this CD-ROM). These

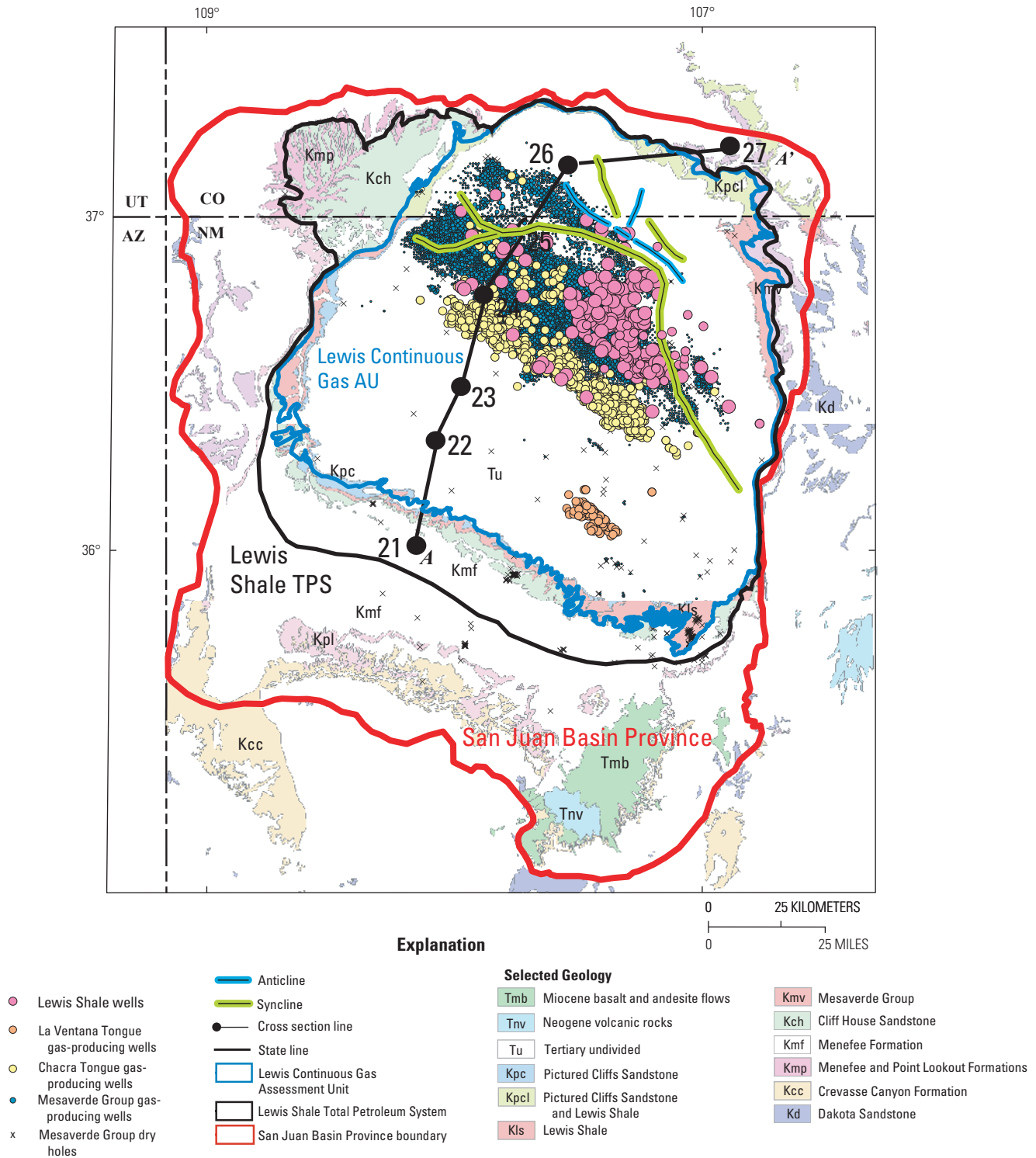


Figure 3A. Map showing geology of the San Juan Basin Province, Lewis Shale Total Petroleum System boundary, line of stratigraphic cross section shown on fig. 2C, structural elements, and oil and gas wells. Geology from Green (1997).

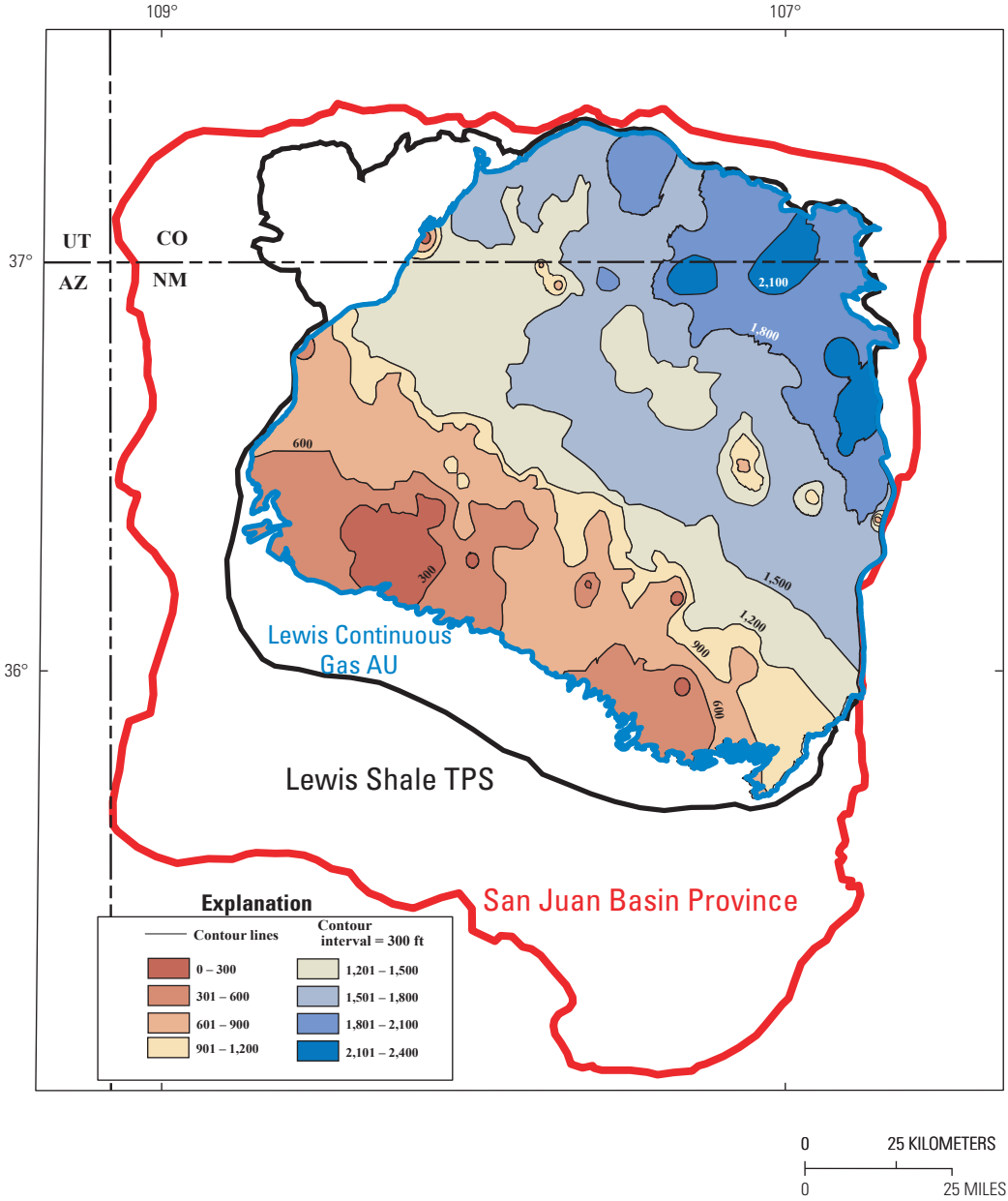


Figure 3B. Isopach map of the Lewis Shale constructed from IHS database (IHS, 2000b).

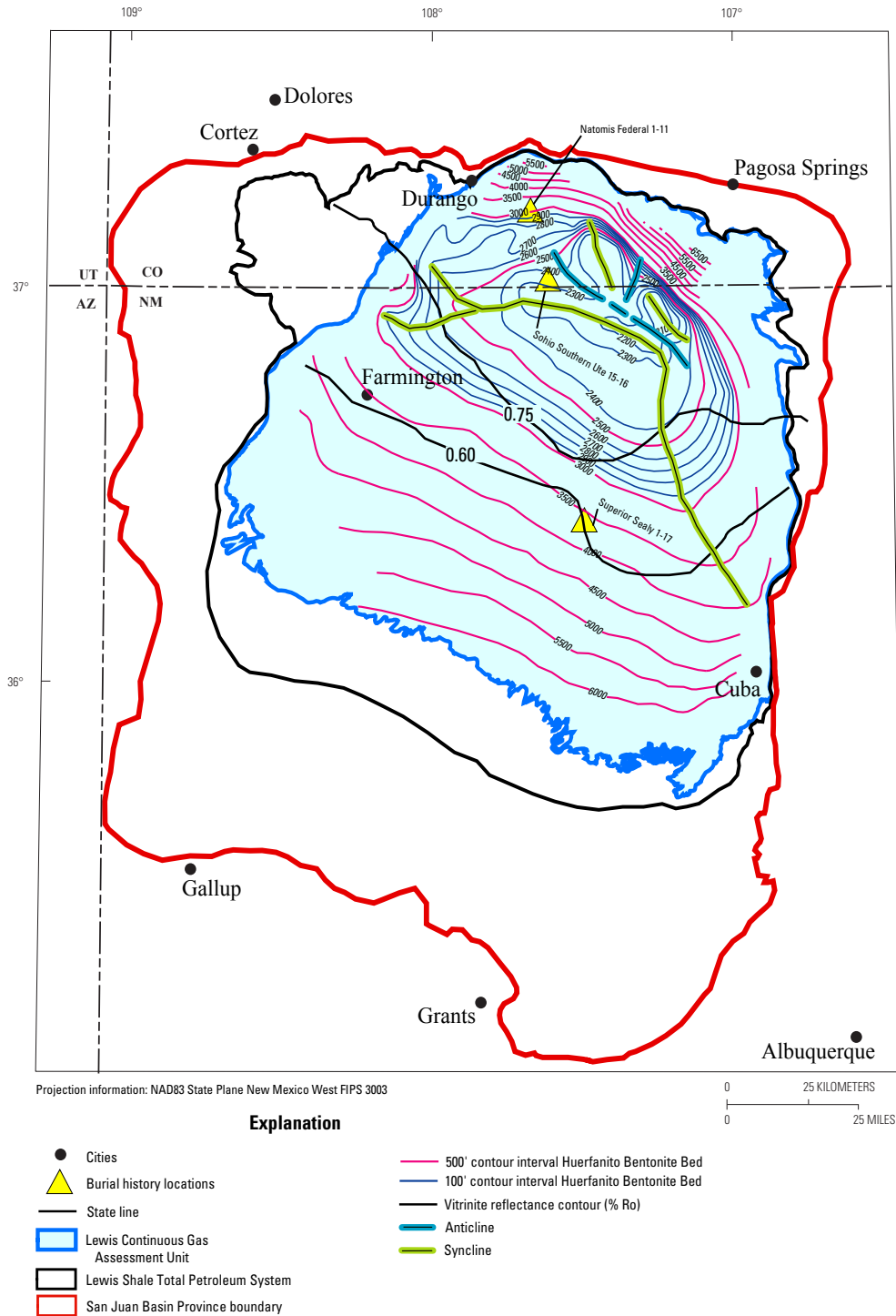


Figure 3C. Map of the Lewis Shale Total Petroleum System showing structure contours on the Huerfanito Bentonite Bed (from Fassett, 2000), structural elements, location of wells used in burial history curves, and vitrinite reflection contours. Vitrinite reflectance (R₀) values contoured (in percent) from data in Fassett and Nuccio (1990), Law (1992), and Fassett (2000).

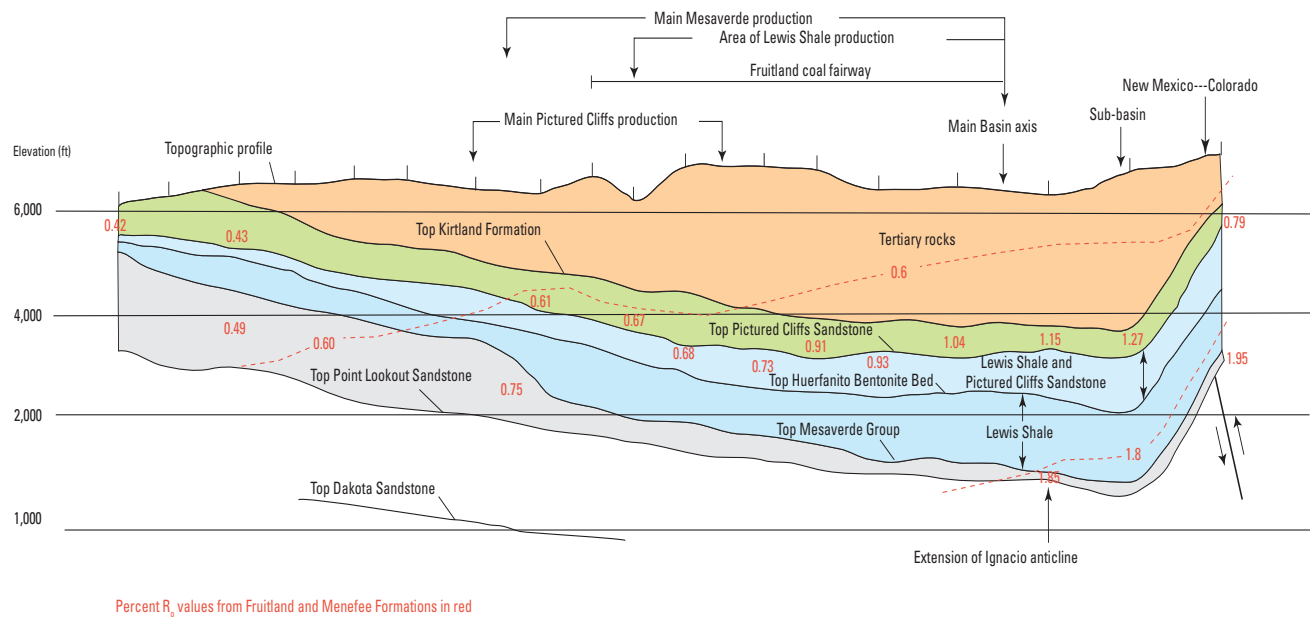
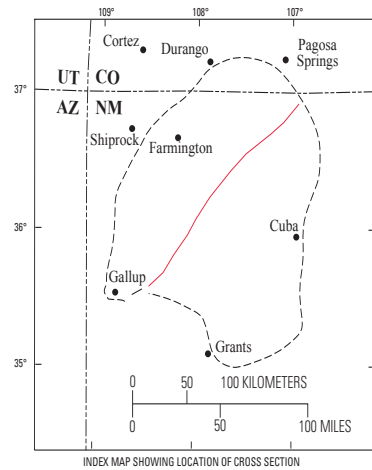
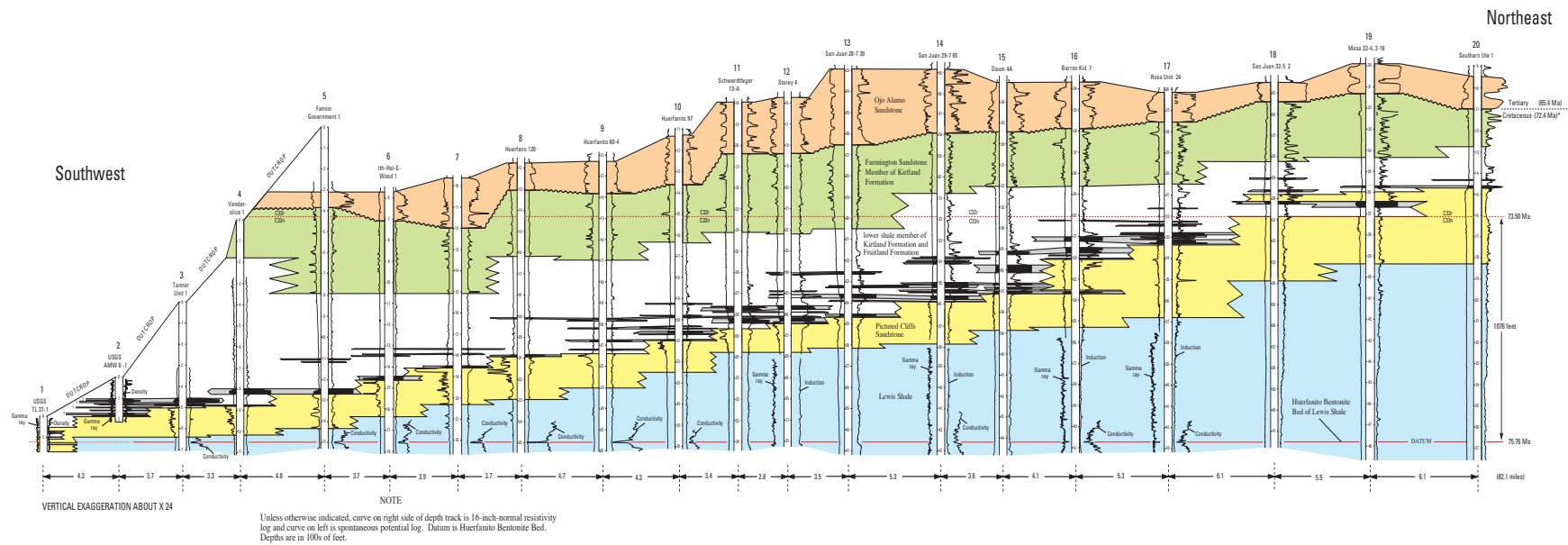


Figure 3D. Cross sections of the San Juan Basin showing vitrinite reflectance values (below) and stratigraphic units bounding the Lewis Shale (above). (Modified from Fassett, 2000, plate 1).

Pictured Cliffs progradational shoreface sandstones interfinger with and grade distally into offshore marine strata of the Lewis Shale (fig. 2C), but the gas produced from Pictured Cliffs reservoirs geochemically appears to have been sourced primarily from coals of the Fruitland Formation (J.R. Hatch, USGS, written commun., 2003). Based on the gas production that could be assigned to Lewis Shale source rocks and reservoirs, the Lewis Shale TPS boundary was drawn to include the subsurface and outcrop extent of the Lewis Shale and the La Ventana and Chacra Tongues of the Cliff House Sandstone (fig. 3A). The TPS boundary does not include small isolated outcrops of any of these units outside the main contiguous outcrop belt. The boundary extends to the southwest and to the northeast a short distance into the outcrop belt of the Menefee Formation because the well-log cross section indicates that several of the shoreface sandstones of the La Ventana Tongue may extend into the main body of the Menefee. The TPS boundary was drawn to include any of these minor sandstones or associated fluvial sandstones in the Menefee that might have been charged with gas from the Lewis Shale.

The Lewis Shale TPS has been interpreted as a continuous gas accumulation (Masters, 1979). The Lewis Shale is thought to be the source rock for the continuous gas accumulation based on modest levels of total organic carbon (TOC) and as much as 2,400 ft of formation thickness (Mavor and others, 2003). Reservoirs are thin sandstones and siltstones within the Lewis Shale itself and sandstones and siltstones of the adjacent La Ventana and Chacra Tongues, producing from natural and artificially stimulated fractures and charged from the Lewis Shale. EUR curves from La Ventana and Chacra wells are similar to EUR curves from other continuous gas reservoirs in that they show declining water and gas production curves (Troy Cook, USGS, oral commun., 2000). There are only minor associated liquid hydrocarbons in the TPS in the form of condensate produced with the gas. Solid bitumen has been observed in sandstone pores and fractures (Parris and others, 2002). These two observations are evidence for present and past liquid hydrocarbons in the Lewis Shale despite very low oil yields from Lewis reservoirs (Parris and others, 2003; Fishman and others, 2004).

The La Ventana and Chacra Tongues and their distal equivalents in the Lewis Shale are typical of low-porosity and low-permeability “tight” gas sandstones. Presumably, in more proximal settings, the La Ventana and Chacra sandstones have slightly greater porosity and permeability resulting from deposition in slightly higher energy shoreface depositional environments. A map plot of water production from wells in the La Ventana and Chacra shows increased water production to the southwest with the highest water production at the up-dip southwest margin of the gas-producing trend (IHS, 2000a,b). The marine Lewis is transitional in lithology from the proximal shoreface sandstones and siltstones of the La Ventana and Chacra Tongues to more distal thin-bedded marine siltstones, shales, and mudstones in the central part of the SJB. Gas production in the Lewis Shale is from natural fractures and fracture-stimulated clastic-rich zones in the

primarily mudstone-dominated parts of the wells (Frantz and others 1999; Dube and others, 2000). These clastic-rich zones contain numerous interbeds of brittle siltstones and thin sandstones that are susceptible to fracturing (Jennings and others, 1997a; Mavor and others, 2003).

Hydrocarbon Source Rock

The organic-carbon-rich marine rocks of the Lewis Shale (figs. 2C and 3A–D) are thought to be the source for the continuous gas accumulation in the Lewis Shale TPS; however, there is little definitive data in the published literature on Lewis gas analyses or composition. The Lewis Shale is as much as 2,400 ft thick (fig. 3B); the thickest section being in the deepest northeastern part of the structural basin. This increased thickness is due both to greater accommodation space in the original depositional basin in that area and to facies changes because to the southwest, shoreface strata are assigned to the La Ventana and Chacra Tongues and the Pictured Cliffs Sandstone. Structure contours on the Huerfanito Bentonite Bed (fig. 3C) within the Lewis Shale depict both the present structure in the Lewis and the general structure of the San Juan Basin. Rocks dip to the northeast on the Chaco slope in the southwestern part of the basin, and they dip less steeply into the central part of the San Juan Basin (fig. 3C). In the structurally deeper distal part of the basin, essentially flat-lying Lewis Shale near the SJB axis is disrupted by a small anticline (fig. 3C). North of that, two small synclines displace the Lewis Shale to its greatest depth in the basin. The beds dip steeply up to the outcrop on the northeast margin of the basin.

The depositional environment of the Lewis Shale in part dictated its role as a hydrocarbon source rock in the SJB. The Lewis Shale was deposited under marine conditions during both the early Campanian relative sea-level rise and the subsequent relative sea-level fall in the latter part of the Campanian. The Lewis Shale is predominantly sandy siltstone and silty to sandy mudstone, with minor thin sandstones and organic-carbon-rich shale, all of which interfinger and grade to the southwest into the fine- to coarse-grained sandstones and siltstones of the basal Cliff House, La Ventana and Chacra Tongues, and the Pictured Cliffs Sandstone. All of these marginal-marine and shoreface clastics were supplied by depositional systems prograding into the SJB from the southwest. The Lewis Shale was deposited primarily in offshore marine settings, with clastic material derived from the fluvial and deltaic systems to the southwest. These deltas supplied terrestrial organic carbon (type-III kerogen) to the Lewis depositional basin in addition to the clastic material. Marine organisms living in the water column in the Cretaceous Western Interior Sea provided type-II kerogen to the Lewis Shale. Below the Huerfanito Bentonite Bed, the lower part of the Lewis Shale that was deposited under an overall marine transgression would be expected to have a predominance of marine organic matter (type-II kerogen) because clastics were being preferentially deposited in

more proximal nearshore settings. In contrast, the upper part of the Lewis Shale above the Huerfanito was deposited under regressive marine conditions with progradation of nearshore and continental systems that would have deposited a proportionally larger component of terrestrial organic matter (type-III kerogen) mixed with marine organic matter and a relatively higher component of clastic material. Similar relations have been documented by at least one other detailed study between transgressive and regressive shales above and below the Tocito Sandstone Lentil within the Mancos Shale of the San Juan Basin (Pasley and others, 1993). In those units, the distribution of petroleum source rocks was based on analysis of the architecture of the depositional sequence. For the Mancos Shale, the transgressive shale above the Tocito Sandstone Lentil contained predominantly marine organic matter, whereas the shale below the Tocito contained a larger proportion of terrestrial organic material (Pasley and others, 1993). This relation documents the variable distribution of marine dominated organic material in transgressive shales versus the abundance of terrestrial organic matter in regressive marine shales that is predicted from sequence stratigraphic concepts. The sequence stratigraphic analysis and the recognition of the third-order maximum flooding surfaces in the Lewis Shale TPS allow similar predictions for the richest organic source beds within the Lewis Shale. These third-order marine flooding surfaces represent times of maximum transgression of the Lewis seaway, and thus, would also represent times of minimum clastic input into the deeper part of the basin, corresponding to times of potentially maximum marine organic-matter accumulation. These marine-dominated organic-carbon-rich shale intervals at the third-order maximum marine flooding surfaces are postulated here to represent the richest source beds within the Lewis Shale. The marine flooding surfaces that delineate the Cliff House transition, Otero, and Navajo City intervals in the lower part of the Lewis Shale were deposited in an overall transgressive system of the second-order TST. Thus, they would be expected to contain a proportionally greater component of marine organic matter than the third-order maximum flooding surfaces identified in the Ute interval of the Lewis Shale. This parallels the expectation that, in general, the Lewis Shale deposited as part of the second-order TST below the Huerfanito Bentonite Bed should contain a greater proportion of marine organic matter than the Lewis Shale that is part of the second-order HST above the Huerfanito. The marine shales deposited adjacent to the Huerfanito Bentonite Bed correspond to both the second-order and the third-order maximum flooding surfaces, and they should contain the highest percentage of marine organic matter and represent the best hydrocarbon source rock in the Lewis Shale TPS.

This link between the maximum flooding surfaces and organic-rich shale beds has not necessarily been recognized in previous sampling of the Lewis Shale for organic-carbon analyses. Reported geochemical analyses generally do not refer to the specific stratigraphic interval or the corresponding sequence stratigraphic unit from which the samples were collected. Thus, previously collected samples may not represent

the richest source rocks present in the Lewis. The marine rocks of the Lewis Shale are reported to have total organic carbon (TOC) contents that range from 0.45 to 2.5 percent and average about 1.0 percent (Dube and others, 2000). Mavor and others (2003) report TOC varies from 0.5 to 2.5 percent with an average TOC of 1.3 percent. The hydrogen index (HI) varies from 150 to 270 mg/g, values expected to produce wet and/or dry gas (J.R. Hatch, written commun., 2002), although Mavor and others (2003) report a HI from 25 to 49 mg/g, and an OI (oxygen index) from 2 to 16 mg/g. Organic matter was primarily marine in origin in the offshore part of the depositional basin, with a southwest-sourced terrestrial organic matter component contributed from the continental clastic-source depositional systems. It is thus likely that the organic matter in the Lewis contains a mixture of type-II and type-III kerogen. Based on the distribution of vitrinite reflectance values bracketing the Lewis Shale (see next section on Source Rock Maturity), its known gas production (Jennings and others, 1997; Dube and others, 2000), EUR curves for Lewis wells that respond similarly to wells in other known continuous gas fields (Troy Cook, USGS, oral commun., 2000), and recent distribution of and production from wells recompleted in the Lewis (Jennings and others, 1997; Dube and others, 2000), the Lewis Shale in this assessment is considered to host a self-sourced continuous gas accumulation, as previously indicated by Masters (1979).

Despite the fact that wells in the Lewis TPS primarily produce gas, it is apparent from petrographic studies that at least some oil probably was generated early in the maturation history of the Lewis Shale (Parris and others, 2003; Fishman and others, 2004). The overall low organic content of the rocks based on TOC values, the mixture of type-II and type-III organic matter present, and the extent of time the rocks have been in the dry gas generation window probably limited the volume of oil generated. There is only minimal condensate reported from Lewis production (IHS, 2000a,b).

Source Rock Maturation

Thermal maturation contours in the Lewis (fig. 3C) are drawn primarily from previous work and analyses on organic-carbon-rich rocks above and below the Lewis Shale (Rice, 1983; Law, 1992). A stratigraphic cross section (fig. 3D) (see chaps. 4 and 6, this CD-ROM; adapted from Fassett, 2000) illustrates the distribution of vitrinite reflectance (R_o) values from the Fruitland and Menefee Formations, which stratigraphically bracket the Lewis Shale in the SJB (fig. 3C). Mavor and others (2003) reports vitrinite reflectance (R_o) from 1.79 to 1.88 percent in the Lewis Shale. In the structurally deepest part of the SJB, the Lewis has attained a thermal maturity sufficient to generate wet and/or dry gas (figs. 3C and 3D). Recent petrographic work on Lewis cores suggests that some parts of the Lewis Shale may have contained an oil precursor (Parris and others, 2003).

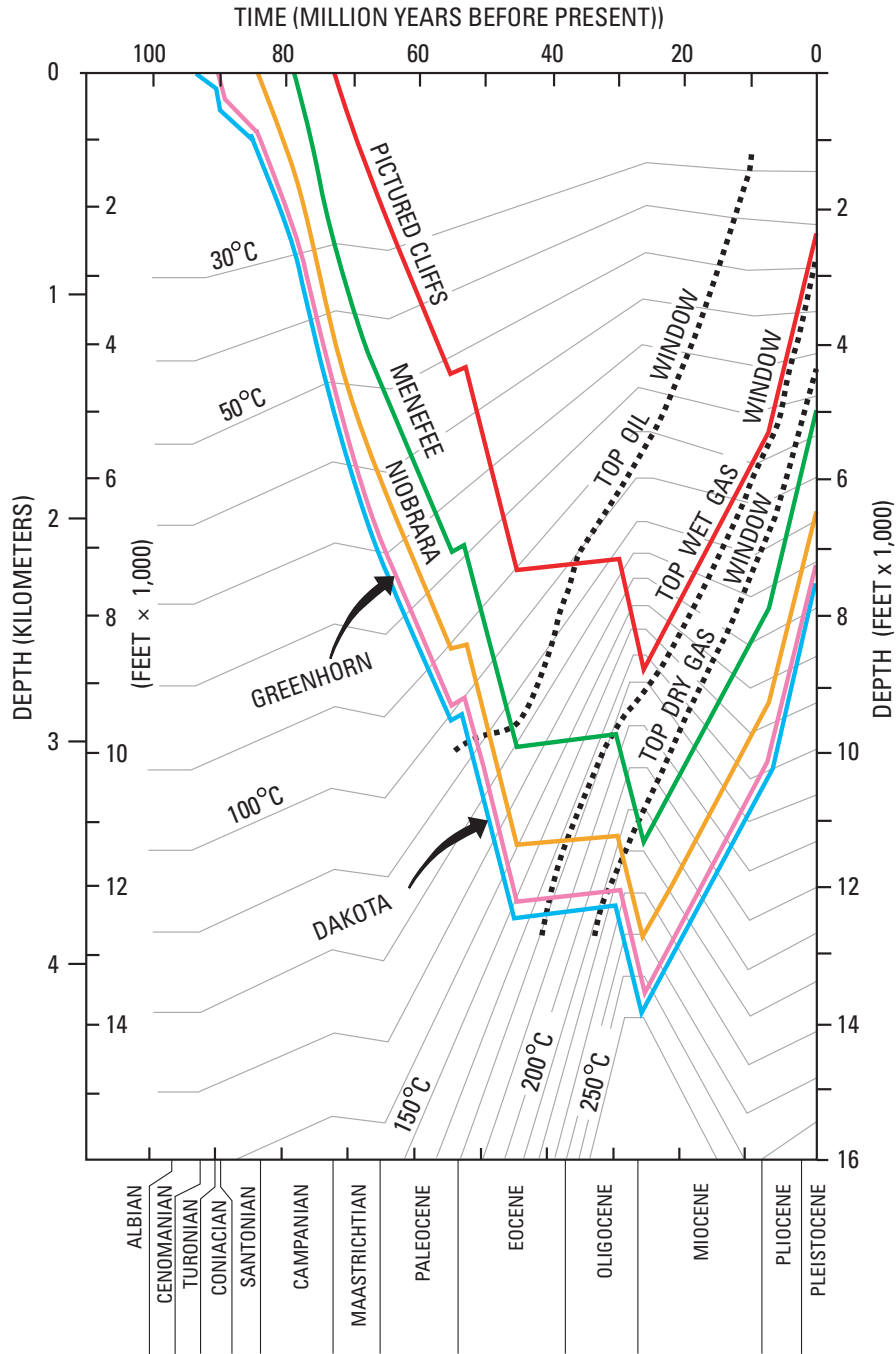


Figure 4A. Burial history curves from Natomas 1-11 Federal well in the Lewis Shale Total Petroleum System. Well is located on figure 3C. Modified from Bond (1984). See Bond (1984) for additional discussion.

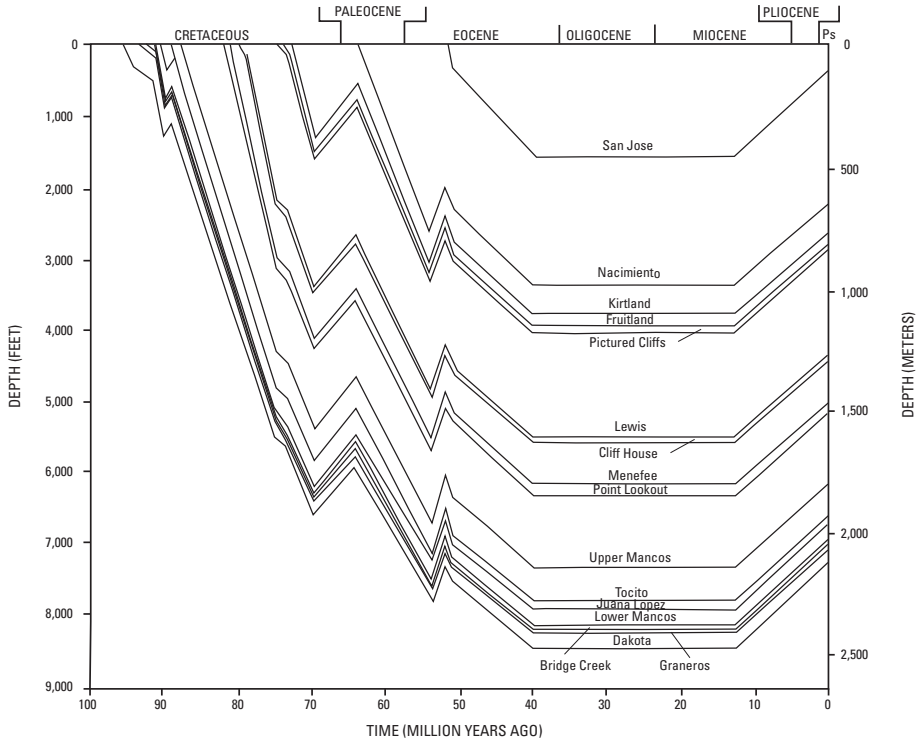


Figure 4B. Burial history curve from Superior Sealy 1-17 well in the Lewis Shale Total Petroleum System. Well is located on figure 3C. Modified from Law (1992)

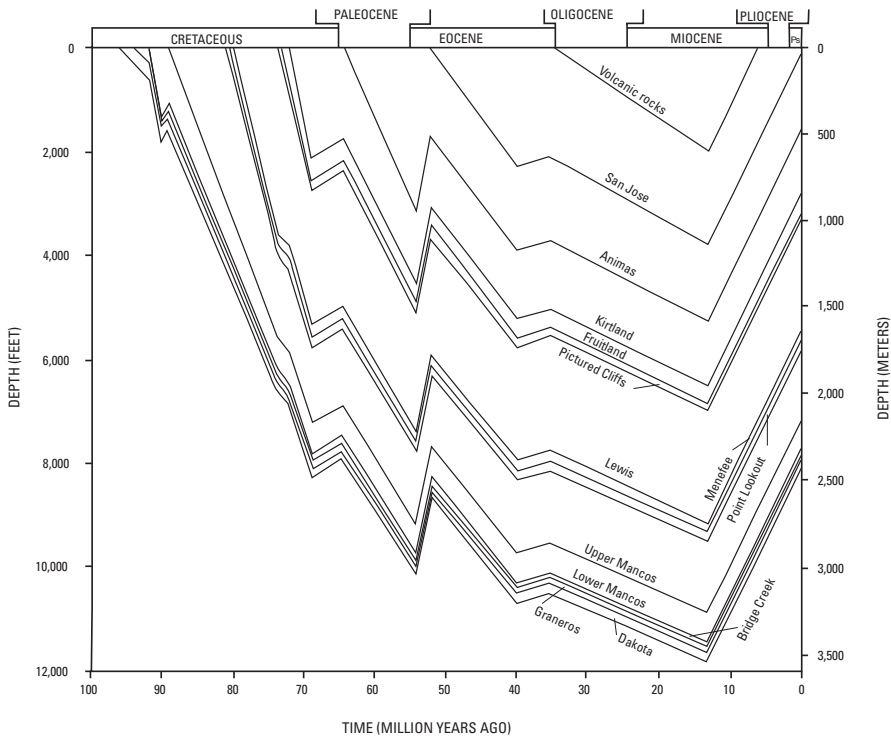


Figure 4C. Burial history curve from Sohio Southern Ute 15-16 well in the Lewis Shale Total Petroleum System. Well is located on figure 3C. See Law (1992) for additional discussion. Modified from Law (1992).

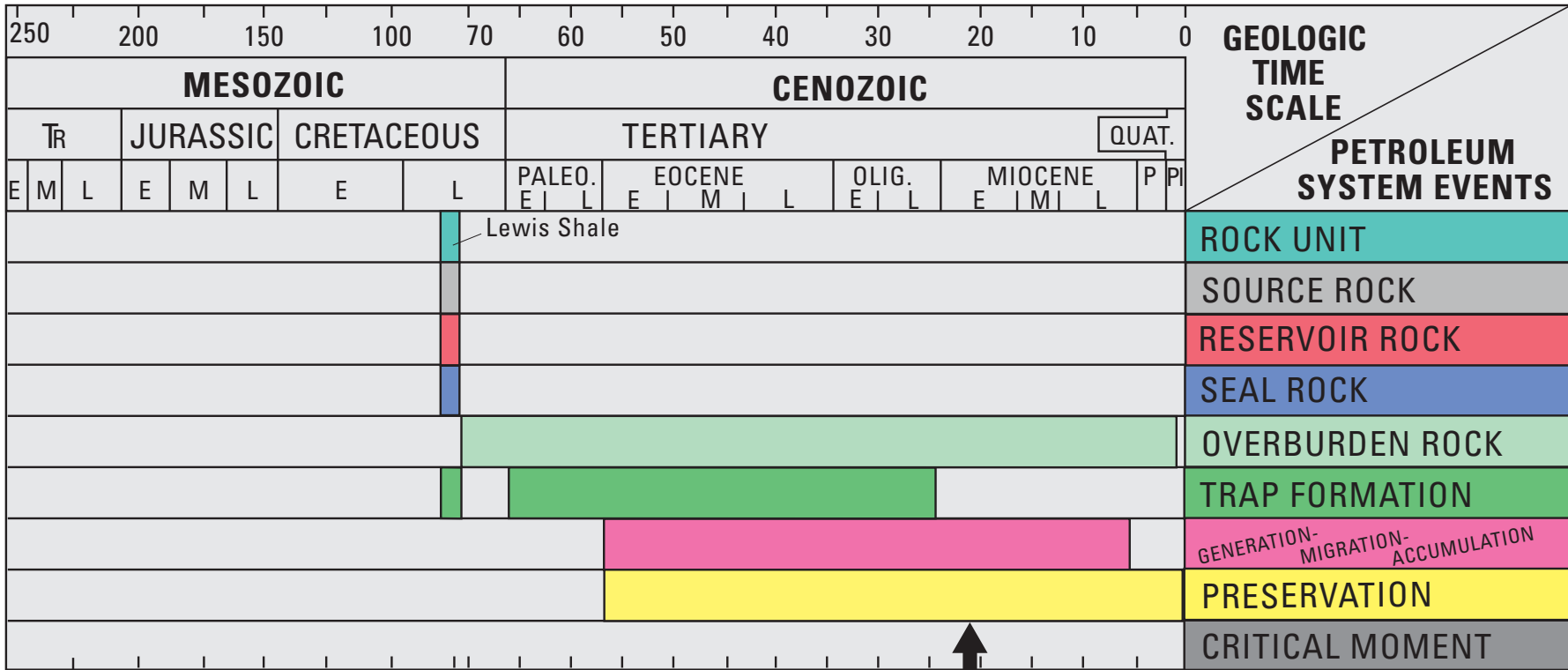


Figure 5. Petroleum system events chart for the Lewis Shale Total Petroleum System in the San Juan Basin. Tr, Triassic; Paleo., Paleocene; Olig., Oligocene; P, Pliocene; PI, Pleistocene; Quat., Quaternary; E, early; M, middle; L, late.

The maturation history of the Lewis Shale can be summarized from burial history curves (figs. 4A–C) (Bond, 1984; Law, 1992). The Lewis Shale and adjacent La Ventana and Chacra Tongues were deposited during the Campanian on the western edge of the Cretaceous Western Interior Seaway (Molenaar, 1977). Accommodation space generated both by subsidence related to basin development and by relative sea-level fluctuations resulted in the deposition and preservation of Cretaceous sediments (Roberts and Kirschbaum, 1995). During the Laramide orogeny at the end of the Cretaceous, the San Juan Basin underwent significant relatively rapid structural deformation and subsidence. Tertiary strata were deposited over the Cretaceous rocks from the Paleocene to the Miocene. Maximum burial of Campanian strata, including the Lewis Shale source rock, occurred at about the Oligocene-Miocene boundary, the critical moment for the Lewis Shale source rock (fig. 5). From the Miocene to the present, there has been uplift and erosion. The Lewis Shale entered the top of the oil generation window toward the middle of the Eocene, and it entered the gas generation window at about the end of the Oligocene. Mavor and others (2003) also report a T_{max} of 424° to 493° C for the Lewis Shale. This source rock maturation and burial history suggests that the organic-carbon-rich rocks of the Lewis Shale primarily generated dry gas from the middle Eocene onward. Recent petrographic studies (Parris and others, 2003; Fishman and others, 2004) suggest evidence for present and past minor liquid hydrocarbons in the Lewis despite very low oil yields from Lewis reservoirs.

Hydrocarbon Migration Summary

The Lewis Shale TPS contains a continuous gas accumulation in the Lewis Shale and the interfingering La Ventana and Chacra Tongues in a deep-basin gas trap (Masters, 1979). Despite little geochemical evidence to type the gas generated from the Lewis, and the fact that Lewis gas production is comingled with Mesaverde gas production, the gas in the Lewis is thought to be self-sourced, and it has not undergone significant migration, based on sequence stratigraphic analysis in this assessment and previously reported low but consistent TOC values over a stratigraphic thickness of as much as 2,400 ft (Dube and others, 2000). However, some local migration must have occurred to charge the laterally adjacent shoreface sandstones of the La Ventana and Chacra Tongues and the more distal equivalents of these sandstones and siltstones that extend basinward into the Lewis Shale. These sandstones and siltstones extend far into the basin where they interfinger with and are in direct contact with Lewis Shale source rock. Both distally in the basin and proximally in the southwest part of the SJB, gas-producing intervals are immediately adjacent to the third-order marine maximum flooding surfaces that delineate the four informal intervals in the Lewis and to other shale-rich intervals. The juxtaposition of organic-rich shales at these marine flooding surfaces to potential clastic reservoir

facies provides the most likely mechanism and pathway for hydrocarbon migration into the clastic-rich units that are the principal gas reservoirs in the Lewis. The organic-carbon-rich mudstones deposited along the maximum flooding surfaces and other minor mudstone-rich intervals may also have acted as internal baffles and barriers to significant hydrocarbon migration as a result of their low porosity and permeability.

Hydrocarbon Reservoir Rocks

Reservoir rocks in the Lewis Shale Total Petroleum System include the Lewis Shale itself, and the La Ventana and Chacra Tongues of the Cliff House Sandstone that interfinger with the Lewis (figs. 2B and 2C). The Lewis Shale is predominantly sandy siltstone and silty mudstone with minor thin sandstones and organic-rich shales all deposited in a marine setting, as indicated by the fine-grained lithology, dark-gray to black color, organic content, sedimentary structures, and inclusion of marine organisms such as ammonite fossils and numerous marine trace fossils. These fine-grained rocks were deposited as offshore marine strata in the deeper parts of the depositional basin. The Lewis thin-bedded fine-grained sandstones and siltstones are distal facies of, interfinger with, and grade into sandstones and siltstones of more proximal marginal-marine deposits of the Cliff House Sandstone, including the La Ventana and Chacra Tongues. These sandstones and siltstones were derived from clastic systems with a source area located southwest of the San Juan Basin. The Cliff House Sandstone forms a series of stacked shoreline deposits that grade basinward to the northeast into finer-grained offshore deposits (Fassett, 1977, 1983; Molenaar, 1977; Molenaar and others, 2002). The shoreface deposits are identified by an array of features including the stacking pattern of parasequences recognized on well logs, sedimentary structures observed in outcrop and in core, facies associations on outcrop, and stacked coarsening-upward parasequence patterns on well logs (Palmer and Scott, 1984; Beaumont and Hoffman, 1992). The depositional strike of the shoreface sandstones is NW.–SE., generally parallel to the structure contours in the Lewis Shale. The shoreface strata grade distally into thin-bedded, fine-grained sandstones and siltstones that interfinger with the marine shale and mudstones of the Lewis. These distal thin-bedded clastics were probably deposited by longshore currents and as sediment gravity flows and turbidites.

The Lewis Shale is predominantly sandy siltstone and silty mudstone, with thin beds of silty sandstone and organic-carbon-rich shale. It has porosity ranging from 2 to 8 percent, with matrix permeability averaging about 0.01 md (millidarcies). Mavor and others (2003) report porosity ranging from 2.9 to 5.44 percent and gas permeability from 0.2 to 215 md. Water saturation ranges from 20 to 100 percent, averaging about 70 percent (Dube and others, 2000). The continuous gas accumulation extends from the Lewis Shale into the La Ventana and Chacra Tongues. These units appear to produce

from typical “tight” gas sandstones having low porosity and permeability. Sandstones have porosity of 8 to 14 percent, permeabilities of 0.15 to 0.3 md, and water saturation of about 30 to 45 percent (Hoppe, 1978a,b,c,d,e). Most of the wells that produce gas are underpressured at about 0.22 psi/ft (Dube and others, 2000).

Gas production from the main body of the Lewis Shale is reported to be due to the development of natural or artificially induced fractures in thin-bedded clastic units that are cemented and brittle compared to the adjoining shales and mudstones (Jennings and others, 1997; Frantz and others, 1999). Sandstones and siltstones in the La Ventana and Chacra Tongues are reservoirs that produce gas as typical “tight” gas sandstones, whereas intervals of interbedded shale, mudstone, siltstone, and sandstone in the Lewis Shale require natural fractures or fracture stimulation to produce gas (Jennings and others, 1997a). The self-sourced and self-sealing gas accumulation is underpressured at present at about 0.22 psi/ft. The underpressured reservoirs may indicate that gas has migrated up-dip into the water-saturated zone on the southwest margin of the basin. Adsorption isotherms generated for the quantification of the amount of adsorbed gas-in-place on organic matter in the Lewis Shale (Dubiel and others, 2000) indicate that with reservoirs underpressured at about 0.22 psi/ft, the pressure can not be reduced sufficiently in the present production wells to release the adsorbed gas.

Hydrocarbon Traps and Seals

The Lewis Shale TPS is thought to be self-sourced regarding hydrocarbon generation. The fine-grain size and low permeability of Lewis shales and mudstones likely resulted in a thick stratigraphic section of rocks that is essentially self-sealing with regard to hydrocarbon migration. The fine-grained mudrocks and shales of the Lewis Shale interfinger on a small scale with the interbedded and fractured fine-grained sandstones and siltstones. Many of these beds can be traced to the southwest where they grade into distal sandstones and siltstones of the basal Cliff House Sandstone, La Ventana Tongue, or Chacra Tongue. The back-stepping nature of the parasequence sets that form the basal Cliff House Sandstone, La Ventana, and Chacra Tongues resulted in shoreface parasequences and parasequence sets that are overlain by successively finer-grained rocks, allowing for trapping of gas in the shoreface and distal clastic strata by the shales and mudstones, which also form the seals or serve as impediments to gas migration.

In the Lewis Shale and the La Ventana and Chacra Tongues, the gas-producing intervals are within either the sandy shoreface parasequences or the correlative sandy or silty distal extensions of those parasequences that extend into the Lewis Shale. The producing intervals are in the sandy and silty strata in the Lewis presumably because they are more cemented, brittle, and therefore more susceptible to either

natural or artificially induced fractures that produce gas. In addition, the sandy and silty upper parts of the parasequences commonly are overlain by organic-carbon-rich shale to mudstone that are associated with marine flooding surfaces. Thus the reservoir strata are immediately overlain and underlain by likely hydrocarbon-rich source rocks that also served as seals or impediments to gas migration. These facies relations indicate that the Lewis Shale itself is the primary intraformational seal for the continuous gas accumulation in siltstones and sandstones in the Lewis Shale TPS. The facies relations indicate that the trap and seal thus formed concomitantly with deposition of the strata. Presumably gas is trapped by a process that is diffusion dependent, whereby gas cannot effectively migrate through the fine-grained mudrocks and/or is trapped in the central part of the basin by infiltration and pore-space saturation by meteoric or migrating formation waters around the basin margins. Masters (1979) felt that the gas was in part trapped by the up-dip water in rocks at the margins of the San Juan Basin, a mechanism proposed for other basin-centered gas accumulations in Rocky Mountain basins (Brown and others, 1986).

Significant gas migration through and within the Lewis Shale TPS is dependent upon lateral continuity or juxtaposition of porous and permeable, thin clastic units and/or a natural fracture network. Gas production is enhanced by intercepting natural fractures in the well bore or by inducing fractures through artificial stimulation (Frantz and others, 1999).

Assessment of Oil and Gas Resources

The geologic events chart (fig. 5) summarizes the important elements and timing of processes that contributed to generation and accumulation of hydrocarbons in the Lewis Shale Total Petroleum System. Deposition of the Lewis Shale and laterally equivalent La Ventana and Chacra Tongues of the Cliff House Sandstone during the Campanian Stage of the Upper Cretaceous formed the source rocks, reservoir rocks, and seals for the hydrocarbons. The overburden rocks required to bury and to bring the Lewis Shale marine source rocks to thermal maturity include the Upper Cretaceous Pictured Cliffs Sandstone, Kirtland Shale, and Fruitland Formation, the Upper Cretaceous to Paleocene Ojo Alamo Sandstone and Animas Formation, and the Paleocene Nacimiento Formation. Deposition of the Eocene San Jose Formation and Oligocene to Miocene volcanic rocks further buried the Lewis Shale to a maximum depth of about 9,000 ft by the middle Miocene. Deposition of Paleocene to Miocene rocks was concomitant with structural downwarping of the San Juan Basin as part of the Laramide orogeny. Regional uplift of the San Juan Basin began about 13 million years ago resulting in erosion that exposed rocks as old as Cretaceous around the margins of the basin. Based on the burial history curves (figs. 4A–C), hydrocarbon generation began in the Eocene. Based on the distribution of producing gas wells, dry holes, water production, and

the distribution of favorable reservoir- and source-rock facies, one assessment unit was defined, mapped and assessed for the Lewis Shale Total Petroleum System—the Lewis Continuous Gas Assessment Unit. The methodology employed for assessment of continuous gas accumulations is described by Schmoker (1996).

Lewis Continuous Gas Assessment Unit (AU 50220261)

The Lewis Continuous Gas Assessment Unit (AU 50220261) is defined by a combination of factors including the occurrence of known underpressured gas production in the Lewis Shale and La Ventana and Chacra Tongues of the Cliff House Sandstone, as well as known reservoir and source rocks, natural or artificially stimulated fractures in these rocks that enable gas production, and the extensive subsurface distribution of the Lewis Shale in the SJB. Production to date from the Lewis Shale is primarily from recompletions in preexisting Mesaverde wells that already penetrate the Lewis. However, the reservoir facies that produce gas from the Lewis in recompleted Mesaverde wells occur throughout the subsurface extent of the Lewis in the SJB, as do the presumed source rocks within the Lewis. In addition, the Lewis Shale throughout a large portion of the basin was buried deeply enough by Eocene time to generate hydrocarbons. Because the Lewis Shale is thought to be both self-sourced and self-sealed, trap formation and hydrocarbon accumulation likely occurred throughout a large area of the subsurface. The distribution of natural fractures is unknown, but artificially induced fractures are a successful completion and production practice in many Lewis recompletions. Thus, the Lewis Shale is potentially capable of producing gas in a large area of the SJB whether or not preexisting Mesaverde wells or natural fractures exist.

Known production in the Lewis is primarily from silty or sandy intervals that are susceptible to natural or artificially induced fractures. These intervals in the Lewis Shale represent the distal equivalents of parasequences that can be traced into more proximal facies in the La Ventana and Chacra Tongues. The proximal shoreface facies of the La Ventana and Chacra Tongues are present only in the southwest part of the San Juan Basin; however, the distal parasequences and the source rocks in the Lewis Shale extend virtually to the outcrop throughout the rest of the SJB. Examination of EUR curves from the IHS production database (Troy Cook, USGS, written commun., 2002) indicate that the La Ventana and Chacra wells behave in a manner consistent with a continuous gas accumulation. That is, they exhibit gas production curves that decline at rates consistent with wells in other known continuous gas accumulations.

Designation of the nature of the gas accumulation and the production curves for the Lewis Shale itself is more problematic due to the Lewis being produced from preexisting Mesaverde wells and co-mingling of the gas being produced

and reported. No wells exist in the database that report solely Lewis gas production to evaluate whether the Lewis presents production EUR curves consistent with a continuous gas accumulation. However, wells that were recompleted in the Lewis were identified in the database, and EUR curves from those wells were examined.

Because the La Ventana and Chacra are producing from a continuous gas accumulation sourced from the Lewis Shale, and because EUR curves for those units display a “typical” production curve for a continuous gas accumulation (Troy Cook, USGS, written commun., 2000), it was plausible to include those two units in the Lewis Continuous Gas Assessment Unit. Thus, the Lewis Continuous Gas Assessment Unit (AU 50220261) is defined to include both the La Ventana and the Chacra Tongues and the Lewis Shale over the entire subsurface extent of the units.

Assessment Results

Data retrieval from the IHS well file identified over 5,000 Mesaverde wells in the San Juan Basin. By identifying which wells were recompleted since about 1990, and individually examining the well reports for perforated intervals, 1,144 tested cells were attributed to the Lewis Shale. To obtain EUR curves for these Lewis wells, it was necessary to examine individual Mesaverde EUR curves and identify those with production increase “spikes” within the last ten years, presumably due to Lewis recompletions. The presumed increased contribution to the gradually declining production curve was interpreted as Lewis Shale production. Based on the EUR curves, a minimum total recovery per cell was established at 0.02 BCF gas (appendix A). Wells with gas production below this minimum value were not included, because they have production too small to be representative of the assessment unit. This left 1,087 tested cells with EURs greater than or equal to the minimum EUR. The total number of producing wells was divided by three, separating the production data into three thirds. The EURs for the producing wells were plotted separately for the first third of the wells, the second third, and the third third. The median EUR is 0.5 BCFG for the first third of the producing wells, 0.25 BCFG for the second third, and 0.22 BCFG for the third third. There is adequate access, charge, reservoir, trap, seal, and timing and generation of hydrocarbons, indicating a geologic probability of 1.0 for finding at least one additional untested cell with total recovery greater than the stated minimum of 0.02 BCFG.

GIS techniques were applied to geographic coverages for the assessment unit to determine the total assessment-unit area, the area per cell of untested cells, and the untested area (appendix A). The median area of the assessment unit is 4,804,000 acres. The uncertainty of the location of the line defining the assessment unit is about 10 percent, so that the maximum area is 5,284,000 acres and the minimum area is 4,324,000 acres.

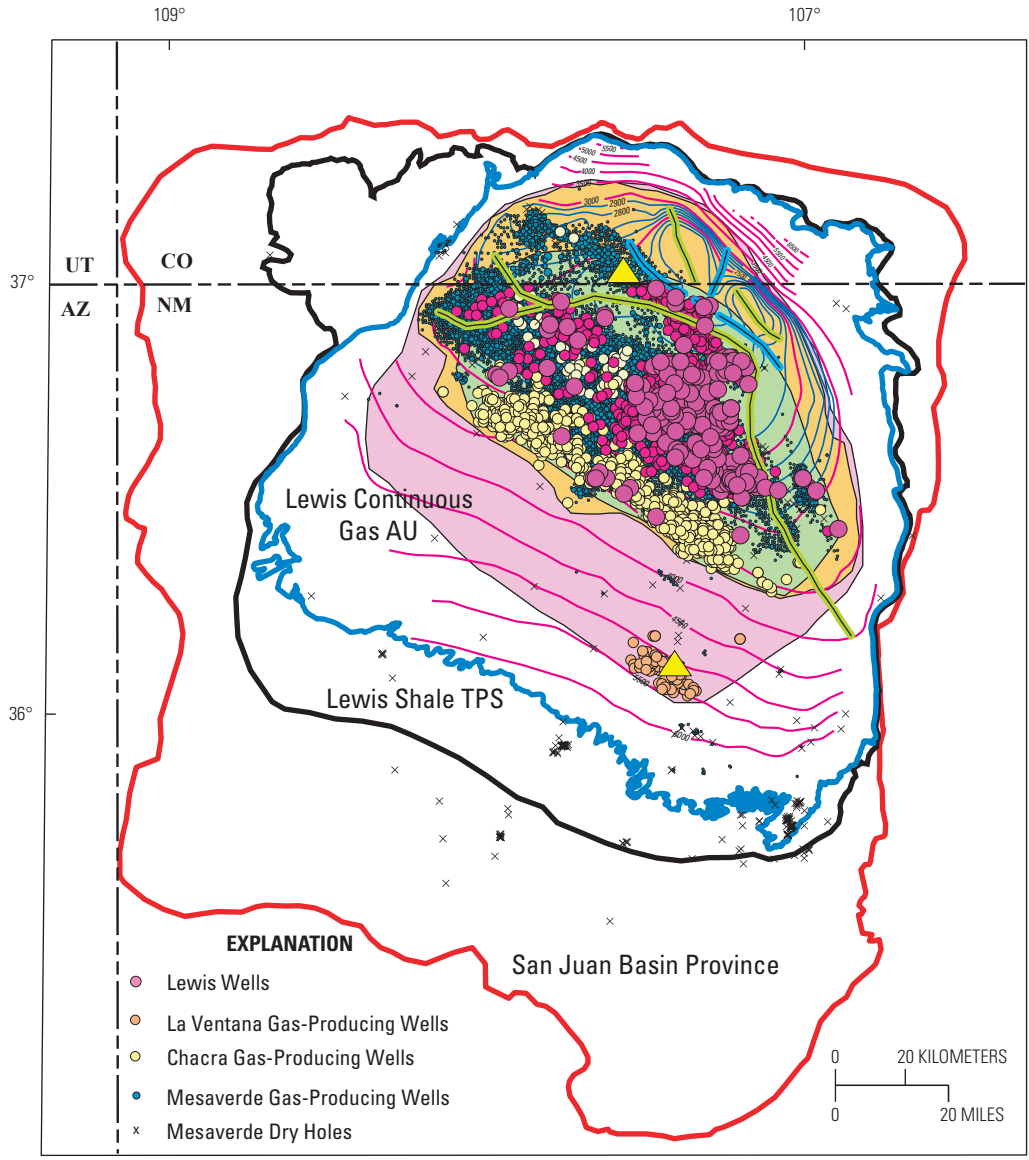


Figure 6. Map of the Lewis Continuous Gas Assessment Unit (AU 50220261) showing producing wells in the Chacra and La Ventana Tongues of the Cliff House Sandstone (yellow and orange circles, respectively) and Lewis Shale (pink circles), Mesaverde Group dry holes (x), and maximum (pink), median (orange), and minimum (green) assessment unit areas (see text for discussion).

The area per cell of untested cells is related to the drainage area of a well. The closest drilling of Mesaverde wells in the basin at present is 40 acres, and this is the presumed minimum size of cells for Lewis wells. The median is 100 acres, and the maximum is 200 acres. At the median, the untested area of the assessment unit is 97.5 percent, with a minimum of 97 percent and a maximum of 98 percent.

The Lewis Continuous Gas Assessment Unit (AU 50220261) includes strata of the Lewis Shale and the La Ventana and Chacra Tongues of the Cliff House Sandstone. The distribution of existing producing wells in the Lewis Shale TPS in the San Juan Basin is related to two factors:

1. the distribution of subsurface shoreface parasequences and distal equivalents in the La Ventana and Chacra Tongues and the four informal intervals of the Lewis Shale and
2. the preexisting wells completed in the Mesaverde below the Lewis Shale.

The sandstones of the La Ventana Tongue produce gas in a small area in the southeast part of the SJB and from more distal equivalents of the uppermost parasequences in the central part of the SJB. The small area is part of a northwest-trending belt on the southwest side of the SJB (fig. 6) where the La Ventana occurs in the subsurface (see for example, Fassett, 1977). The Chacra produces gas from shoreface sands that exist in a northwest-trending belt in the subsurface. In contrast, the present distribution of producing wells in the Lewis Shale is, at least for the time being, related to the distribution of preexisting Mesaverde wells that are being recompleted in the Lewis, primarily by Burlington Resources. Similar productive facies in the Lewis Shale probably exist anywhere in the Lewis where sandy and silty interbeds were deposited that are susceptible to either natural or artificially induced fracturing and where they are adjacent to hydrocarbon source rocks. In the farthest northeast portion of the SJB, no production is presently known from the Lewis Shale north of the small anticline in the deepest part of the SJB. Limited data from individual wells and an examination of cumulative water production from wells in the database (IHS, 2000a,b) indicate that distal very fine grained sandstones and siltstones within the Lewis Shale may be too "tight," that is they lack sufficient permeability to produce gas in that area. In addition, previous publications indicate that gas-bearing sandstones in the SJB are water saturated updip on the basin margins, forming part of the trapping mechanism for the basin-centered gas (Masters, 1979). Examination of the cumulative water production from wells producing gas from the Chacra sandstones, for example, indicate that water production within individual wells increases to the southwest of the Chacra producing trend, corroborating the interpretation that water saturation of those sandstones increases toward the southwest basin margin. Thus, production of gas from the La Ventana and Chacra Tongues and the Lewis Shale appears to be limited to the southwest by water saturation of the updip sandstones. Toward the other margins of the basin, production

appears to be limited by a combination of water saturation in the sandstones and lack of permeability and porosity in the finer-grained distal sandstones and siltstones within the Lewis Shale.

Coupled with this understanding of the geologic controls on the distribution of known production in the assessment unit, GIS techniques again were used to define the minimum, median, and maximum untested areas of the assessment unit that have potential for additions to reserves in the next 30 years. The maximum untested area (fig. 6) was determined to include the area of La Ventana production farthest to the southwest and follows the depositional strike of the shoreface sandstones of the La Ventana to the northwest. In the northwest, northeast, and southwest margins of the basin, the maximum area was determined based on the presumed updip limit of water saturation that limits gas production in the underlying Mesaverde rocks on the basin margin, based on the distribution of Mesaverde producing wells. The maximum percentage of the untested assessment unit area that has potential for addition to reserves is 40 percent. The median area was determined to include all wells to the southwest that produced from the Chacra, including those wells that have smaller total gas production and higher water production than most wells in the northwest-trending depositional facies trend of shoreface sandstones in the Chacra Tongue (fig. 6). To the northwest, northeast, and southeast the median area was determined along the structural contour on the Huerfanito Bentonite Bed that marks the presumed limit of the majority of producing wells in the Chacra. This line was determined on the premise that Chacra gas production is in part limited by depositional facies and updip water saturation in the Chacra Tongue. The median percentage of the untested area that has potential for addition to reserves is 34 percent. The minimum area (fig. 6) was determined to encircle the tight distribution of Chacra production on the southwest basin margin that appears to be controlled by the depositional strike of the shoreface sandstones and the updip limit of significant gas production imposed by water saturation within the updip rocks. To the northeast, the minimum area line was determined along the axis of the small anticline that also marks the northeast limit of significant gas production in Mesaverde wells (fig. 3A). Presumably the lack of porosity and permeability coupled with updip water saturation limits Mesaverde production in this direction and would limit Lewis Shale production as well. On the southeast and northeast basin margins, the minimum area line was determined to include all known Lewis and Mesaverde producing wells because Mesaverde exploration over the last few decades has apparently delimited the extent of productive rocks in these areas based on water saturation in the updip basin margins. The minimum percentage of the untested area that has potential for addition to reserves is 23 percent.

The results of the assessment of undiscovered gas resources in the Lewis Continuous Gas Assessment Unit (AU 50220261) are presented in appendix B. Allocations of those resources to State and various Federal lands are

in appendix A. The Monte Carlo simulations, verified by the analytical probability method, provide the following results for the assessment unit. In the Lewis Continuous Gas Assessment Unit (AU 50220261), for continuous gas resources, there is an F95 of 8,315.22 BCFG and an F5 of 12,282.31 BCFG, with a mean value of 10,177.24 BCFG. There is an F95 of 18.08 MMBNGL and an F5 of 47.32 MMBNGL, with a mean of 30.53 MMBNGL.

Acknowledgments

Many people contributed to my understanding of the Lewis Shale TPS for this assessment. Al Merewether (USGS, retired) graciously provided digital copies of his and C.M. Molenaar's (USGS, deceased) cross section of well logs in the San Juan Basin (Molenaar and others, 2002). Troy Cook (USGS) generated and analyzed Estimated Ultimate Recovery (EUR) data curves of Lewis gas production and assisted in deciphering those wells that were recompleted in the Lewis. Joe Hatch (USGS) provided compilations and interpretations of the limited geochemical analyses available for the Lewis Shale in the USGS database. Neil Fishman (USGS) and Ron Hill (USGS) engaged in discussions on the organic facies of the Lewis and potential gas generation. Mark Kirschbaum (USGS) aided with insightful discussions on Cretaceous stratigraphy and sedimentology. Steve Condon (USGS) provided critical manipulations of the stratigraphic database. Sargent McDonald (USGS contractor) compiled the GIS data and coverages for this report. I thank all of these colleagues for their assistance.

References Cited

- Beaumont, E.C., Dane, C.H., and Sears, J.D., 1956, Revised nomenclature of Mesaverde Group in San Juan Basin, New Mexico: American Association of Petroleum Geologists Bulletin, v. 40, p. 2149–2162.
- Beaumont, E.C., and Hoffman, G.K., 1992, Relationships between the Upper Coal Member of the Menefee Formation, the La Ventana Tongue, and the Lewis Shale in the southeastern San Juan Basin, *in* Lucas, S.G., Kues, B.S., Williamson, T.E., and Hunt, A.P., eds., San Juan Basin IV: New Mexico Geological Society, 43rd Field Conference Guidebook, p. 207–216.
- Bereskin, B., 2003, Geological and production attributes of “shale” reservoirs, San Juan Basin, U.S.A., *in* Bereskin, B., and Mavor, M., eds., Shale gas geology and engineering—An overview: American Association of Petroleum Geologists Short Course Notes, Annual Meeting, Salt Lake City Utah, May 2003, 44 p. (section 1).
- Bereskin, S.R., 2001a, Geological and production characteristics of the Lewis Shale, San Juan Basin, *in* The Lewis Shale, San Juan Basin—Approaches to Rocky Mountain tight shale gas plays: Petroleum Technology Transfer Council Conference, Southwest Region, Albuquerque, New Mexico, February 21, 2001, unpaginated.
- Bereskin, S.R., 2001b, Geologic and production characteristics of the Lewis Shale (San Juan Basin) as results apply to other Cretaceous “shales” of the Western Interior—The next “CBM Play” of the Rocky Mountains, USA and Canada (abs.): Outcrop (Newsletter of the Rocky Mountain Association of Geologists), v. 50, no. 10, p. 5.
- Bereskin, S.R., Christiansen, G.E., and Jennings, G.L., 2003, The application of horizontal and deviated wellbores as a means of increasing gas productivity from Cretaceous shales along the Western Interior Seaway: Example from the Lewis Shale, San Juan Basin, Colorado and New Mexico, U.S.A.: American Association of Petroleum Geologists, 2003 Annual Meeting, Salt Lake City, 1 p.
- Bond, W.A., 1984, Application of Lopatin's method to determine burial history, evolution of the geothermal gradient, and timing of hydrocarbon generation in Cretaceous source rocks in the San Juan Basin, northwestern New Mexico and southwestern Colorado, *in* Woodward, J., Meissner, F.F., and Clayton, J.L., eds., Hydrocarbon source rocks of the greater Rocky Mountain Region: Rocky Mountain Association of Geologists, p. 433–447.
- Brown, C.A., Smagala, T.M., and Haeefe, G.R., 1986, Southern Piceance Basin model—Cozette, Corcoran and Rollins sandstones, *in* Spencer, C.W., and Mast, R.F., eds., Geology of tight gas reservoirs: American Association of Petroleum Geologists, Studies in Geology 24, p. 207–219.
- Christiansen, Glen, and Olszewski, Adam, 2001, Lewis Shale reservoir characterization and log model development, *in* The Lewis Shale, San Juan Basin—Approaches to Rocky Mountain tight shale gas plays: Petroleum Technology Transfer Council Conference, Southwest Region, Albuquerque, New Mexico, February 21, 2001, unpaginated.
- Collier, A.J., 1919, Coal south of Mancos, Montezuma County, Colorado: U.S. Geological Survey Bulletin 691–K, p. 293–310.
- Dane, C.H., 1936, Geology and fuel resources of the southern part of the San Juan Basin, New Mexico, Part 3—The La Ventana-Chacra Mesa coalfield: U.S. Geological Survey Bulletin 860–C, 166 p.
- Dube, H.G., Christiansen, G.E., Frantz, J.H., Jr., Fairchild, N.R., Olszewski, A.J., Sawyer, W.K., and Williamson, J.R., 2000, The Lewis Shale, San Juan Basin—What we now know: Society of Petroleum Engineers, SPE paper 63091, presented at the 2000 SPE Annual Technical Conference and Exhibition, Dallas, Tex., October 1–4, 2000, 24 p.

- Fassett, J.E., 1977, Geology of the Point Lookout, Cliff House, and Pictured Cliffs Sandstones of the San Juan Basin, New Mexico and Colorado, *in* Fassett, J.E., ed., San Juan Basin III: New Mexico Geological Society 28th Field Conference Guidebook, p. 193–197.
- Fassett, J.E., 1983, Stratigraphy and oil and gas production of northwest New Mexico updated through 1983, *in* Fassett, J.E., ed., Oil and Gas Fields of the Four Corners Area, vol. III: Four Corners Geological Society, p. 849–865.
- Fassett, J.E., 2000, Geology and coal resources of the Upper Cretaceous Fruitland Formation, San Juan Basin, New Mexico and Colorado, chap. Q *in* Kirschbaum, M.A., Roberts, L.N.R., and Biewick, L.R.H., eds., Geologic assessment of coal in the Colorado Plateau—Arizona, Colorado, New Mexico, and Utah: U.S. Geological Survey Professional Paper 1625–B, 131 p.
- Fassett, J.E., and Hinds, J.S., 1971, Geology and fuel resources of the Fruitland Formation and Kirkland Shale of the San Juan Basin, New Mexico and Colorado: U.S. Geological Survey Professional Paper 676, 76 p.
- Fassett, J.E., and Nuccio, V.F., 1990, Vitrinite reflectance values of coal from drill-hole cuttings from the Fruitland and Menefee Formations, San Juan Basin, New Mexico: U.S. Geological Survey Open-File Report 90–290, 21 p.
- Fishman, N.S., Parris, T.M., Hall, D.L., Pawlewicz, M.J., and Burruss, R.C., 2004, Just how many episodes of petroleum generation took place in the Upper Cretaceous Lewis Shale, San Juan Basin, New Mexico and Colorado?: Four Corners Geological Society, Monthly Newsletter, May 2004, 2 p.
- Frantz, J.H., Fairchild, N.R., Jr., Dube, H.G., Campbell, S.M., Christiansen, G.E., and Olszewski, A.J., 1999, Evaluating reservoir production mechanisms and hydraulic fracture geometry in the Lewis Shale, San Juan Basin: SPE paper 56552, presented at the 1999 SPE Annual Technical Conference and Exhibition, Houston, Tex., October 3–6, 1999, p. 121–128.
- Green, G.N., 1997, The digital geologic map of New Mexico in ARC/INFO format, version 1.0: U.S. Geological Survey Open-File Report 97–0052, <http://greenwood.cr.usgs.gov/open-file-reports/ofr-97-0052>.
- Haq, B.U., Hardenbol, Jan, and Vail, P.R., 1988, Mesozoic and Cenozoic chronostratigraphy and cycles of sea-level change, *in* Wilgus, C.K., Hastings, B.S., Posamentier, Henry, Van Wagoner, John, Ross, C.A., and Kendall, C.G., eds., Sea-level changes—An integrated approach: Society of Economic Paleontologists and Mineralogists, Special Publication, no. 42, p. 71–108.
- Hollenshead, C.T., and Pritchard, R.L., 1961, Geometry of producing Mesaverde sandstones, San Juan Basin, *in* Peterson, J.A., and Osmund, J.C., eds., Geometry of sandstone bodies: American Association of Petroleum Geologists, Research Committee Symposium, p. 98–118.
- Holmes, H.W., 1877, Report (on the San Juan district, Colorado): U.S. Geological Survey Territorial 9th Annual Report, p. 237–276.
- Hoppe, W.F., 1978a, Animas Chacra, *in* Fassett, J.E., Thomaidis, N.D., Matheny, M.L., and Ullrich, R.A., eds., Oil and gas fields of the Four Corners area, vol. I: Four Corners Geological Society, p. 184–185.
- Hoppe, W.F., 1978b, Bloomfield Chacra, *in* Fassett, J.E., Thomaidis, N.D., Matheny, M.L., and Ullrich, R.A., eds., Oil and gas fields of the Four Corners area, vol. I: Four Corners Geological Society, p. 241–242.
- Hoppe, W.F., 1978c, Harris Mesa Chacra, *in* Fassett, J.E., Thomaidis, N.D., Matheny, M.L., and Ullrich, R.A., eds., Oil and gas fields of the Four Corners area, vol. I: Four Corners Geological Society, p. 329–330.
- Hoppe, W.F., 1978d, Largo Chacra, *in* Fassett, J.E., Thomaidis, N.D., Matheny, M.L., and Ullrich, R.A., eds., Oil and gas fields of the Four Corners area, vol. II: Four Corners Geological Society, p. 442–443.
- Hoppe, W.F., 1978e, Otero Chacra, *in* Fassett, J.E., Thomaidis, N.D., Matheny, M.L., and Ullrich, R.A., eds., Oil and gas fields of the Four Corners area, vol. II: Four Corners Geological Society, p. 374–375.
- Huffman, A.C., Jr., 1996, San Juan Basin Province (022), *in* Gautier, D.L., Dolton, G.L., Takahashi, K.I., and Varnes, K.L., eds., 1995 National assessment of United States oil and gas resources—Results, methodology, and supporting data: U.S. Geological Survey Digital Data Series 30, Release 2, 1996.
- IHS Energy Group, 2000a [includes data current as of December 1999], PI/Dwights plus U.S. production data: IHS Energy Group, 15 Inverness Way East, D205, Englewood, CO 80112, U.S.A.
- IHS Energy Group, 2000b [includes data current as of December 1999], PI/Dwights plus U.S. well data: IHS Energy Group, 15 Inverness Way East, D205, Englewood, CO, 80112, U.S.A.
- Jennings, G.L., Greaves, K.H., and Bereskin, S.R., 1997a, Natural gas resource potential of the Lewis Shale, San Juan Basin, New Mexico and Colorado: Tuscaloosa, University of Alabama, National Coalbed Methane Symposium, paper 9766, p. 557–564.

- Jennings, G.L., Greaves, K.H., and Bereskin, S.R., 1997b, Natural gas resource potential of the Lewis Shale, San Juan Basin, New Mexico and Colorado [abs.], in Close, J.C., and Casey, T.A., eds., Natural fracture systems in the southern Rockies: Four Corners Geological Society, p. 131.
- Law, B.E., 1992, Thermal maturity patterns of Cretaceous and Tertiary rocks, San Juan Basin, Colorado and New Mexico: Geological Society of America Bulletin, v. 104, p. 192–207.
- Manfrino, Carrie, 1984, Stratigraphy and palynology of the upper Lewis Shale, Pictured Cliffs Sandstone, and lower Fruitland Formation (Upper Cretaceous) near Durango, Colorado: Mountain Geologist, v. 21, no. 4, p. 115–132.
- Masters, J.A., 1979, Deep basin gas trap, western Canada: American Association of Petroleum Geologists Bulletin, v. 63, p. 152–181.
- Mavor, M.J., Bereskin, S.R., Robinson, J.R., and Pratt, T.J., 2003, Lewis Shale gas resource and production potential: Gas Research Institute Report GRI-03/0037, 281 p.
- Meibos, L.C., 1983, Navajo City Chacra, in Fassett, J.E., Hamilton, W., Marton, G.W., and Middleman, A.A., eds., Oil and gas fields of the Four Corners area, vol. III: Four Corners Geological Society Guidebook, p. 989–991.
- Molenaar, C.M., 1977, Stratigraphy and depositional history of Upper Cretaceous rocks of the San Juan Basin area, New Mexico and Colorado, with a note on economic resources, in Fassett, J.E., James, H.L., and Hodgson, H.E., eds., San Juan Basin III—Guidebook of northwestern New Mexico: New Mexico Geological Society, 28th Field Conference Guidebook, p. 159–166.
- Molenaar, C.M., 1983, Major depositional cycles and regional correlations of Upper Cretaceous rocks, southern Colorado Plateau and adjacent areas, in Reynolds, M.W., and Dolly, E.D., eds., Mesozoic paleogeography of the west-central United States: Rocky Mountain Section, SEPM, p. 201–224.
- Molenaar, C.K., and Baird, J.M., 1992, Regional stratigraphic cross sections of Upper Cretaceous rocks across the San Juan Basin, northwestern New Mexico and southwestern Colorado: U.S. Geological Survey Open-File Report 92–257, 3 sheets.
- Molenaar, C.M., Cobban, W.A., Merewether, E.A., Pillmore, C.A., Wolfe, D.G., and Holbrook, J.M., 2002, Regional stratigraphic cross sections of Cretaceous rocks from east-central Arizona to the Oklahoma panhandle: U.S. Geological Survey Miscellaneous Field Studies Map 2382.
- NRG Associates, 1999 [includes data current as of December 1998], The significant oil and gas fields of the United States: NRG Associates, Inc., P.O. Box 1655, Colorado Springs, CO 80901, U.S.A.
- Obradovich, J.D., 1993, A Cretaceous time scale, in Caldwell, W.G.E., and Kauffman, E.G., eds., Evolution of the Western Interior basin: Geological Association of Canada, Special Paper 39, p. 379–396.
- Olsen, T.R., Mellere, D.A., and Olsen, T., 1999, Facies architecture and geometry of landward-stepping shoreface tongues—The Upper Cretaceous Cliff House Sandstone (Mancos Canyon, southwest Colorado): Sedimentology, v. 46, p. 603–625.
- Palmer, J.J., and Scott, A.J., 1984, Stacked shoreline and shelf sandstone of La Ventana Tongue (Campanian), northwest New Mexico: American Association of Petroleum Geologists Bulletin, v. 68, p. 74–91.
- Parris, T. M., Fishman, N.S., Pawlewicz, M.J., and Christian, G.E., 2003, Origin, conditions, and timing of gas generation in the Lewis Shale, San Juan Basin, New Mexico: American Association of Petroleum Geologists, 2003 Annual Meeting, Salt Lake City, Utah, p. A133.
- Pasley, M.A., Riley, G.W., and Nummedal, Dag, 1993, Sequence stratigraphic significance of organic matter variations—Example from the Upper Cretaceous Mancos Shale of the San Juan Basin, New Mexico, in Katz, B.J., and Pratt, L.M., eds.: American Association of Petroleum Geologists, Studies in Geology no. 37, p. 221–241.
- Peterson, Fred, and Kirk, A.R., 1977, Correlation of the Cretaceous rocks in the San Juan, Black Mesa, Kaiparowits, and Henry Basins, southern Colorado Plateau, in Fassett, J.E., James, H.L., and Hodgson, H.E., eds., San Juan Basin III—Guidebook of northwestern New Mexico: New Mexico Geological Society, 28th Field Conference Guidebook, p. 167–178.
- Pike, W.S., Jr., 1947, Intertonguing marine and non-marine Upper Cretaceous deposits of New Mexico, Arizona and south-west Colorado: Geological Society of America Memoir 24, 103 p.
- Rice, D.D., 1983, Relation of natural gas composition to thermal maturity and source rock type in San Juan Basin, northwestern new Mexico and southwestern Colorado: American Association of Petroleum Geologists Bulletin, v. 67, p. 1199–1218.
- Roberts, L.N.R., and Kirschbaum, M.A., 1995, Paleogeography of the Late Cretaceous of the Western Interior of middle North America—Coal distribution and sediment accumulation: U.S. Geological Survey Professional Paper 1561, 115 p.
- Roberts, L.N.R., and McCabe, P.J., 1992, Peat accumulation in coastal-plain mires: A model for coals of the Fruitland Formation (Upper Cretaceous) of southern Colorado, U.S.A.: International Journal of Coal Geology, v. 21, p. 115–138.

- Sears, J.D., Hunt, C.B., and Hendricks, T.A., 1941, Transgressive and regressive Cretaceous deposits in the southern San Juan Basin, New Mexico: U.S. Geological Survey Professional Paper 193-F, p. 101–121.
- Schmoker, J.W., 1996, Methodology for assessing continuous-type (unconventional) hydrocarbon accumulations, *in* Gautier, D.L., Dolton, G.L., Takahashi, K.I., and Varnes, K.L., eds., 1995 National assessment of United States oil and gas resources—Results, methodology, and supporting data: U.S. Geological Survey Digital Data Series 30, release 2.
- Shirley, K., 2001, Lewis not overlooked anymore: American Association of Petroleum Geologists Explorer, March 2001, p. 26–27.
- Van Wagoner, J.C., Mitchum, R.M., Campion, K.M., and Rahmanian, V.D., 1990, Siliciclastic sequence stratigraphy in well logs, cores, and outcrops: Concepts for high-resolution correlations of time and facies: American Association of Petroleum Geologists, Methods in Exploration Series, no. 7, 55 p.
- Weimer, R.J., 1960, Upper Cretaceous stratigraphy, Rocky Mountain area: American Association of Petroleum Geologists Bulletin, v. 44, p. 1–20.

Appendix A. Data form for the Lewis Continuous Gas Assessment Unit (AU 50220261).

FORSPAN ASSESSMENT MODEL FOR CONTINUOUS ACCUMULATIONS--BASIC INPUT DATA FORM (NOGA, Version 8, 8-16-02)

IDENTIFICATION INFORMATION

Assessment Geologist:...	<u>R.F. Dubiel</u>	Date:	<u>9/24/2002</u>
Region:.....	<u>North America</u>	Number:	<u>5</u>
Province:.....	<u>San Juan Basin</u>	Number:	<u>5022</u>
Total Petroleum System:..	<u>Lewis Shale</u>	Number:	<u>502202</u>
Assessment Unit:.....	<u>Lewis Continuous Gas</u>	Number:	<u>50220261</u>
Based on Data as of:.....	<u>PI/Dwights 2001</u>		
Notes from Assessor:.....	<u></u>		

CHARACTERISTICS OF ASSESSMENT UNIT

Assessment-Unit type: Oil (<20,000 cfg/bo) or Gas (≥20,000 cfg/bo) Gas

What is the minimum total recovery per cell?... 0.02 (mmbo for oil A.U.; bcfg for gas A.U.)

Number of tested cells:..... 1144

Number of tested cells with total recovery per cell ≥ minimum: 1087

Established (>24 cells ≥ min.) X Frontier (1-24 cells) Hypothetical (no cells)

Median total recovery per cell (for cells ≥ min.): (mmbo for oil A.U.; bcfg for gas A.U.)

1st 3rd discovered	<u>0.5</u>	2nd 3rd	<u>0.25</u>	3rd 3rd	<u>0.22</u>
--------------------	------------	---------	-------------	---------	-------------

Assessment-Unit Probabilities:

<u>Attribute</u>	<u>Probability of occurrence (0-1.0)</u>	
1. CHARGE: Adequate petroleum charge for an untested cell with total recovery ≥ minimum	<u>1.0</u>	<u>1.0</u>
2. ROCKS: Adequate reservoirs, traps, seals for an untested cell with total recovery ≥ minimum.	<u>1.0</u>	<u>1.0</u>
3. TIMING: Favorable geologic timing for an untested cell with total recovery ≥ minimum.....	<u>1.0</u>	<u>1.0</u>

Assessment-Unit GEOLOGIC Probability (Product of 1, 2, and 3):..... 1.0

4. **ACCESS:** Adequate location for necessary petroleum-related activities for an untested cell with total recovery ≥ minimum 1.0

NO. OF UNTESTED CELLS WITH POTENTIAL FOR ADDITIONS TO RESERVES IN THE NEXT 30 YEARS

- Total assessment-unit area (acres): (uncertainty of a fixed value)
 minimum 4,324,000 median 4,804,000 maximum 5,284,000
- Area per cell of untested cells having potential for additions to reserves in next 30 years (acres):
 (values are inherently variable)
 calculated mean 105 minimum 40 median 100 maximum 200
- Percentage of total assessment-unit area that is untested (%): (uncertainty of a fixed value)
 minimum 97 median 97.5 maximum 98
- Percentage of untested assessment-unit area that has potential for additions to reserves in next 30 years (%): (a necessary criterion is that total recovery per cell ≥ minimum)
 (uncertainty of a fixed value) minimum 23 median 34 maximum 40

Assessment Unit (name, no.)
 Lewis Continuous Gas, 50220261

TOTAL RECOVERY PER CELL

Total recovery per cell for untested cells having potential for additions to reserves in next 30 years:
 (values are inherently variable)
 (mmbo for oil A.U.; bcfg for gas A.U.) minimum 0.02 median 0.5 maximum 6

AVERAGE COPRODUCT RATIOS FOR UNTESTED CELLS, TO ASSESS COPRODUCTS

(uncertainty of fixed but unknown values)

<u>Oil assessment unit:</u>	minimum	median	maximum
Gas/oil ratio (cfg/bo).....	<u> </u>	<u> </u>	<u> </u>
NGL/gas ratio (bngl/mmcf).....	<u> </u>	<u> </u>	<u> </u>
<u>Gas assessment unit:</u>			
Liquids/gas ratio (bliq/mmcf).....	<u>1</u>	<u>3</u>	<u>5</u>

SELECTED ANCILLARY DATA FOR UNTESTED CELLS

(values are inherently variable)

<u>Oil assessment unit:</u>	minimum	median	maximum
API gravity of oil (degrees).....	<u> </u>	<u> </u>	<u> </u>
Sulfur content of oil (%).....	<u> </u>	<u> </u>	<u> </u>
Drilling depth (m)	<u> </u>	<u> </u>	<u> </u>
Depth (m) of water (if applicable).....	<u> </u>	<u> </u>	<u> </u>
<u>Gas assessment unit:</u>			
Inert-gas content (%).....	<u>0.00</u>	<u>1.50</u>	<u>10.00</u>
CO ₂ content (%).....	<u>0.00</u>	<u>1.00</u>	<u>3.00</u>
Hydrogen-sulfide content (%).....	<u>0.00</u>	<u>0.00</u>	<u>0.00</u>
Drilling depth (m).....	<u>500</u>	<u>1200</u>	<u>2500</u>
Depth (m) of water (if applicable).....	<u> </u>	<u> </u>	<u> </u>
<u>Success ratios:</u>	calculated mean	minimum	median
Future success ratio (%).....	<u> </u>	<u>60</u>	<u>90</u>
Historic success ratio, tested cells (%)	<u>95</u>		

Assessment Unit (name, no.)
 Lewis Continuous Gas, 50220261

ALLOCATIONS OF POTENTIAL ADDITIONS TO RESERVES TO STATES
Surface Allocations (uncertainty of a fixed value)

1. <u>Colorado</u>	represents	<u>14.63</u>	areal % of the assessment unit
<u>Oil in oil assessment unit:</u>			
	minimum	median	maximum
Volume % in entity.....	_____	_____	_____
Portion of volume % that is offshore (0-100%)..	_____	_____	_____
<u>Gas in gas assessment unit:</u>			
Volume % in entity.....	_____	<u>15</u>	_____
Portion of volume % that is offshore (0-100%)..	_____	<u>0</u>	_____
2. <u>New Mexico</u>	represents	<u>85.37</u>	areal % of the assessment unit
<u>Oil in oil assessment unit:</u>			
	minimum	median	maximum
Volume % in entity.....	_____	_____	_____
Portion of volume % that is offshore (0-100%)..	_____	_____	_____
<u>Gas in gas assessment unit:</u>			
Volume % in entity.....	_____	<u>85</u>	_____
Portion of volume % that is offshore (0-100%)..	_____	<u>0</u>	_____
3. _____	represents	_____	areal % of the assessment unit
<u>Oil in oil assessment unit:</u>			
	minimum	median	maximum
Volume % in entity.....	_____	_____	_____
Portion of volume % that is offshore (0-100%)..	_____	_____	_____
<u>Gas in gas assessment unit:</u>			
Volume % in entity.....	_____	_____	_____
Portion of volume % that is offshore (0-100%)..	_____	_____	_____
4. _____	represents	_____	areal % of the assessment unit
<u>Oil in oil assessment unit:</u>			
	minimum	median	maximum
Volume % in entity.....	_____	_____	_____
Portion of volume % that is offshore (0-100%)..	_____	_____	_____
<u>Gas in gas assessment unit:</u>			
Volume % in entity.....	_____	_____	_____
Portion of volume % that is offshore (0-100%)..	_____	_____	_____

Assessment Unit (name, no.)
Lewis Continuous Gas, 50220261

5.	_____	represents	_____	areal % of the assessment unit
<u>Oil in oil assessment unit:</u>				
		minimum	median	maximum
	Volume % in entity.....	_____	_____	_____
	Portion of volume % that is offshore (0-100%)..	_____	_____	_____
<u>Gas in gas assessment unit:</u>				
	Volume % in entity.....	_____	_____	_____
	Portion of volume % that is offshore (0-100%)..	_____	_____	_____
6.	_____	represents	_____	areal % of the assessment unit
<u>Oil in oil assessment unit:</u>				
		minimum	median	maximum
	Volume % in entity.....	_____	_____	_____
	Portion of volume % that is offshore (0-100%)..	_____	_____	_____
<u>Gas in gas assessment unit:</u>				
	Volume % in entity.....	_____	_____	_____
	Portion of volume % that is offshore (0-100%)..	_____	_____	_____
7.	_____	represents	_____	areal % of the assessment unit
<u>Oil in oil assessment unit:</u>				
		minimum	median	maximum
	Volume % in entity.....	_____	_____	_____
	Portion of volume % that is offshore (0-100%)..	_____	_____	_____
<u>Gas in gas assessment unit:</u>				
	Volume % in entity.....	_____	_____	_____
	Portion of volume % that is offshore (0-100%)..	_____	_____	_____
8.	_____	represents	_____	areal % of the assessment unit
<u>Oil in oil assessment unit:</u>				
		minimum	median	maximum
	Volume % in entity.....	_____	_____	_____
	Portion of volume % that is offshore (0-100%)..	_____	_____	_____
<u>Gas in gas assessment unit:</u>				
	Volume % in entity.....	_____	_____	_____
	Portion of volume % that is offshore (0-100%)..	_____	_____	_____

Assessment Unit (name, no.)
 Lewis Continuous Gas, 50220261

ALLOCATIONS OF POTENTIAL ADDITIONS TO RESERVES TO LAND ENTITIES
Surface Allocations (uncertainty of a fixed value)

1. <u>Federal Lands</u>	represents	<u>37.81</u>	areal % of the assessment unit
<u>Oil in oil assessment unit:</u>	minimum	median	maximum
Volume % in entity.....	_____	_____	_____
Portion of volume % that is offshore (0-100%)..	_____	_____	_____
<u>Gas in gas assessment unit:</u>			
Volume % in entity.....	_____	<u>38</u>	_____
Portion of volume % that is offshore (0-100%)..	_____	<u>0</u>	_____
2. <u>Private Lands</u>	represents	<u>17.33</u>	areal % of the assessment unit
<u>Oil in oil assessment unit:</u>	minimum	median	maximum
Volume % in entity.....	_____	_____	_____
Portion of volume % that is offshore (0-100%)..	_____	_____	_____
<u>Gas in gas assessment unit:</u>			
Volume % in entity.....	_____	<u>17</u>	_____
Portion of volume % that is offshore (0-100%)..	_____	<u>0</u>	_____
3. <u>Tribal Lands</u>	represents	<u>40.73</u>	areal % of the assessment unit
<u>Oil in oil assessment unit:</u>	minimum	median	maximum
Volume % in entity.....	_____	_____	_____
Portion of volume % that is offshore (0-100%)..	_____	_____	_____
<u>Gas in gas assessment unit:</u>			
Volume % in entity.....	_____	<u>41</u>	_____
Portion of volume % that is offshore (0-100%)..	_____	<u>0</u>	_____
4. <u>Other Lands</u>	represents	_____	areal % of the assessment unit
<u>Oil in oil assessment unit:</u>	minimum	median	maximum
Volume % in entity.....	_____	_____	_____
Portion of volume % that is offshore (0-100%)..	_____	_____	_____
<u>Gas in gas assessment unit:</u>			
Volume % in entity.....	_____	_____	_____
Portion of volume % that is offshore (0-100%)..	_____	_____	_____

Assessment Unit (name, no.)
Lewis Continuous Gas, 50220261

5. <u>CO State Lands</u>	represents	<u>0.28</u>	areal % of the assessment unit
<u>Oil in oil assessment unit:</u>	minimum	median	maximum
Volume % in entity.....	_____	_____	_____
Portion of volume % that is offshore (0-100%)..	_____	_____	_____
<u>Gas in gas assessment unit:</u>			
Volume % in entity.....	_____	<u>0</u>	_____
Portion of volume % that is offshore (0-100%)..	_____	<u>0</u>	_____
6. <u>NM State Lands</u>	represents	<u>3.86</u>	areal % of the assessment unit
<u>Oil in oil assessment unit:</u>	minimum	median	maximum
Volume % in entity.....	_____	_____	_____
Portion of volume % that is offshore (0-100%)..	_____	_____	_____
<u>Gas in gas assessment unit:</u>			
Volume % in entity.....	_____	<u>4</u>	_____
Portion of volume % that is offshore (0-100%)..	_____	<u>0</u>	_____
7. _____	represents	_____	areal % of the assessment unit
<u>Oil in oil assessment unit:</u>	minimum	median	maximum
Volume % in entity.....	_____	_____	_____
Portion of volume % that is offshore (0-100%)..	_____	_____	_____
<u>Gas in gas assessment unit:</u>			
Volume % in entity.....	_____	_____	_____
Portion of volume % that is offshore (0-100%)..	_____	_____	_____
8. _____	represents	_____	areal % of the assessment unit
<u>Oil in oil assessment unit:</u>	minimum	median	maximum
Volume % in entity.....	_____	_____	_____
Portion of volume % that is offshore (0-100%)..	_____	_____	_____
<u>Gas in gas assessment unit:</u>			
Volume % in entity.....	_____	_____	_____
Portion of volume % that is offshore (0-100%)..	_____	_____	_____

Assessment Unit (name, no.)
 Lewis Continuous Gas, 50220261

ALLOCATIONS OF POTENTIAL ADDITIONS TO RESERVES TO FEDERAL LAND SUBDIVISIONS
Surface Allocations (uncertainty of a fixed value)

1. <u>Bureau of Land Management (BLM)</u>	represents	<u>30.75</u>	areal % of the assessment unit
<u>Oil in oil assessment unit:</u>			
Volume % in entity.....	minimum	median	maximum
Portion of volume % that is offshore (0-100%)..	_____	_____	_____
<u>Gas in gas assessment unit:</u>			
Volume % in entity.....	_____	<u>31</u>	_____
Portion of volume % that is offshore (0-100%)..	_____	<u>0</u>	_____
2. <u>BLM Wilderness Areas (BLMW)</u>	represents	_____	areal % of the assessment unit
<u>Oil in oil assessment unit:</u>			
Volume % in entity.....	minimum	median	maximum
Portion of volume % that is offshore (0-100%)..	_____	_____	_____
<u>Gas in gas assessment unit:</u>			
Volume % in entity.....	_____	_____	_____
Portion of volume % that is offshore (0-100%)..	_____	_____	_____
3. <u>BLM Roadless Areas (BLMR)</u>	represents	_____	areal % of the assessment unit
<u>Oil in oil assessment unit:</u>			
Volume % in entity.....	minimum	median	maximum
Portion of volume % that is offshore (0-100%)..	_____	_____	_____
<u>Gas in gas assessment unit:</u>			
Volume % in entity.....	_____	_____	_____
Portion of volume % that is offshore (0-100%)..	_____	_____	_____
4. <u>National Park Service (NPS)</u>	represents	<u>0.05</u>	areal % of the assessment unit
<u>Oil in oil assessment unit:</u>			
Volume % in entity.....	minimum	median	maximum
Portion of volume % that is offshore (0-100%)..	_____	_____	_____
<u>Gas in gas assessment unit:</u>			
Volume % in entity.....	_____	<u>0</u>	_____
Portion of volume % that is offshore (0-100%)..	_____	<u>0</u>	_____

Assessment Unit (name, no.)
Lewis Continuous Gas, 50220261

5. <u>NPS Wilderness Areas (NPSW)</u>	represents	_____	areal % of the assessment unit
<u>Oil in oil assessment unit:</u>	minimum	_____	median
Volume % in entity.....	_____	_____	maximum
Portion of volume % that is offshore (0-100%)..	_____	_____	_____
<u>Gas in gas assessment unit:</u>			
Volume % in entity.....	_____	_____	_____
Portion of volume % that is offshore (0-100%)..	_____	_____	_____
6. <u>NPS Protected Withdrawals (NPSP)</u>	represents	_____	areal % of the assessment unit
<u>Oil in oil assessment unit:</u>	minimum	_____	median
Volume % in entity.....	_____	_____	maximum
Portion of volume % that is offshore (0-100%)..	_____	_____	_____
<u>Gas in gas assessment unit:</u>			
Volume % in entity.....	_____	_____	_____
Portion of volume % that is offshore (0-100%)..	_____	_____	_____
7. <u>US Forest Service (USFS)</u>	represents	6.67	areal % of the assessment unit
<u>Oil in oil assessment unit:</u>	minimum	_____	median
Volume % in entity.....	_____	_____	maximum
Portion of volume % that is offshore (0-100%)..	_____	_____	_____
<u>Gas in gas assessment unit:</u>			
Volume % in entity.....	_____	7	_____
Portion of volume % that is offshore (0-100%)..	_____	0	_____
8. <u>USFS Wilderness Areas (USFSW)</u>	represents	_____	areal % of the assessment unit
<u>Oil in oil assessment unit:</u>	minimum	_____	median
Volume % in entity.....	_____	_____	maximum
Portion of volume % that is offshore (0-100%)..	_____	_____	_____
<u>Gas in gas assessment unit:</u>			
Volume % in entity.....	_____	_____	_____
Portion of volume % that is offshore (0-100%)..	_____	_____	_____

Assessment Unit (name, no.)
 Lewis Continuous Gas, 50220261

9. <u>USFS Roadless Areas (USFSR)</u>	represents _____	areal % of the assessment unit	
<u>Oil in oil assessment unit:</u>	minimum	median	maximum
Volume % in entity.....	_____	_____	_____
Portion of volume % that is offshore (0-100%)..	_____	_____	_____
<u>Gas in gas assessment unit:</u>			
Volume % in entity.....	_____	_____	_____
Portion of volume % that is offshore (0-100%)..	_____	_____	_____
10. <u>USFS Protected Withdrawals (USFSP)</u>	represents _____	areal % of the assessment unit	
<u>Oil in oil assessment unit:</u>	minimum	median	maximum
Volume % in entity.....	_____	_____	_____
Portion of volume % that is offshore (0-100%)..	_____	_____	_____
<u>Gas in gas assessment unit:</u>			
Volume % in entity.....	_____	_____	_____
Portion of volume % that is offshore (0-100%)..	_____	_____	_____
11. <u>US Fish and Wildlife Service (USFWS)</u>	represents _____	areal % of the assessment unit	
<u>Oil in oil assessment unit:</u>	minimum	median	maximum
Volume % in entity.....	_____	_____	_____
Portion of volume % that is offshore (0-100%)..	_____	_____	_____
<u>Gas in gas assessment unit:</u>			
Volume % in entity.....	_____	_____	_____
Portion of volume % that is offshore (0-100%)..	_____	_____	_____
12. <u>USFWS Wilderness Areas (USFWSW)</u>	represents _____	areal % of the assessment unit	
<u>Oil in oil assessment unit:</u>	minimum	median	maximum
Volume % in entity.....	_____	_____	_____
Portion of volume % that is offshore (0-100%)..	_____	_____	_____
<u>Gas in gas assessment unit:</u>			
Volume % in entity.....	_____	_____	_____
Portion of volume % that is offshore (0-100%)..	_____	_____	_____

Assessment Unit (name, no.)
Lewis Continuous Gas, 50220261

13. <u>USFWS Protected Withdrawals (USFWSP)</u>	represents	_____	areal % of the assessment unit
<u>Oil in oil assessment unit:</u>	minimum	_____	median
Volume % in entity.....	_____	_____	maximum
Portion of volume % that is offshore (0-100%)..	_____	_____	_____
<u>Gas in gas assessment unit:</u>			
Volume % in entity.....	_____	_____	_____
Portion of volume % that is offshore (0-100%)..	_____	_____	_____
14. <u>Wilderness Study Areas (WS)</u>	represents	_____	areal % of the assessment unit
<u>Oil in oil assessment unit:</u>	minimum	_____	median
Volume % in entity.....	_____	_____	maximum
Portion of volume % that is offshore (0-100%)..	_____	_____	_____
<u>Gas in gas assessment unit:</u>			
Volume % in entity.....	_____	_____	_____
Portion of volume % that is offshore (0-100%)..	_____	_____	_____
15. <u>Department of Energy (DOE)</u>	represents	_____	areal % of the assessment unit
<u>Oil in oil assessment unit:</u>	minimum	_____	median
Volume % in entity.....	_____	_____	maximum
Portion of volume % that is offshore (0-100%)..	_____	_____	_____
<u>Gas in gas assessment unit:</u>			
Volume % in entity.....	_____	_____	_____
Portion of volume % that is offshore (0-100%)..	_____	_____	_____
16. <u>Department of Defense (DOD)</u>	represents	_____	areal % of the assessment unit
<u>Oil in oil assessment unit:</u>	minimum	_____	median
Volume % in entity.....	_____	_____	maximum
Portion of volume % that is offshore (0-100%)..	_____	_____	_____
<u>Gas in gas assessment unit:</u>			
Volume % in entity.....	_____	_____	_____
Portion of volume % that is offshore (0-100%)..	_____	_____	_____

Assessment Unit (name, no.)
 Lewis Continuous Gas, 50220261

17. Bureau of Reclamation (BOR)	represents	0.34	areal % of the assessment unit	
<u>Oil in oil assessment unit:</u>				
Volume % in entity.....	minimum		median	maximum
Portion of volume % that is offshore (0-100%)..	_____		_____	_____
<u>Gas in gas assessment unit:</u>				
Volume % in entity.....			0	
Portion of volume % that is offshore (0-100%)..	_____		0	_____
18. Tennessee Valley Authority (TVA)	represents		areal % of the assessment unit	
<u>Oil in oil assessment unit:</u>				
Volume % in entity.....	minimum		median	maximum
Portion of volume % that is offshore (0-100%)..	_____		_____	_____
<u>Gas in gas assessment unit:</u>				
Volume % in entity.....				
Portion of volume % that is offshore (0-100%)..	_____		_____	_____
19. Other Federal	represents		areal % of the assessment unit	
<u>Oil in oil assessment unit:</u>				
Volume % in entity.....	minimum		median	maximum
Portion of volume % that is offshore (0-100%)..	_____		_____	_____
<u>Gas in gas assessment unit:</u>				
Volume % in entity.....				
Portion of volume % that is offshore (0-100%)..	_____		_____	_____
20. _____	represents		areal % of the assessment unit	
<u>Oil in oil assessment unit:</u>				
Volume % in entity.....	minimum		median	maximum
Portion of volume % that is offshore (0-100%)..	_____		_____	_____
<u>Gas in gas assessment unit:</u>				
Volume % in entity.....				
Portion of volume % that is offshore (0-100%)..	_____		_____	_____

Assessment Unit (name, no.)
 Lewis Continuous Gas, 50220261

ALLOCATIONS OF POTENTIAL ADDITIONS TO RESERVES TO ECOSYSTEMS
Surface Allocations (uncertainty of a fixed value)

1. <u>Grand Canyon Lands (GDCL)</u>	represents	<u>3.13</u>	areal % of the assessment unit
<u>Oil in oil assessment unit:</u>	minimum	median	maximum
Volume % in entity.....	_____	_____	_____
Portion of volume % that is offshore (0-100%)..	_____	_____	_____
<u>Gas in gas assessment unit:</u>			
Volume % in entity.....	_____	<u>5</u>	_____
Portion of volume % that is offshore (0-100%)..	_____	<u>0</u>	_____
2. <u>Navajo Canyonlands (NVCL)</u>	represents	<u>72.31</u>	areal % of the assessment unit
<u>Oil in oil assessment unit:</u>	minimum	median	maximum
Volume % in entity.....	_____	_____	_____
Portion of volume % that is offshore (0-100%)..	_____	_____	_____
<u>Gas in gas assessment unit:</u>			
Volume % in entity.....	_____	<u>80</u>	_____
Portion of volume % that is offshore (0-100%)..	_____	<u>0</u>	_____
3. <u>South-Central Highlands (SCHL)</u>	represents	<u>9.53</u>	areal % of the assessment unit
<u>Oil in oil assessment unit:</u>	minimum	median	maximum
Volume % in entity.....	_____	_____	_____
Portion of volume % that is offshore (0-100%)..	_____	_____	_____
<u>Gas in gas assessment unit:</u>			
Volume % in entity.....	_____	<u>5</u>	_____
Portion of volume % that is offshore (0-100%)..	_____	<u>0</u>	_____
4. <u>White Mountain-San Francisco Peaks (WMSF)</u>	represents	<u>15.03</u>	areal % of the assessment unit
<u>Oil in oil assessment unit:</u>	minimum	median	maximum
Volume % in entity.....	_____	_____	_____
Portion of volume % that is offshore (0-100%)..	_____	_____	_____
<u>Gas in gas assessment unit:</u>			
Volume % in entity.....	_____	<u>10</u>	_____
Portion of volume % that is offshore (0-100%)..	_____	<u>0</u>	_____

Assessment Unit (name, no.)
 Lewis Continuous Gas, 50220261

5.	_____	represents	_____	areal % of the assessment unit
<u>Oil in oil assessment unit:</u>				
		minimum	median	maximum
	Volume % in entity.....	_____	_____	_____
	Portion of volume % that is offshore (0-100%)..	_____	_____	_____
<u>Gas in gas assessment unit:</u>				
	Volume % in entity.....	_____	_____	_____
	Portion of volume % that is offshore (0-100%)..	_____	_____	_____
6.	_____	represents	_____	areal % of the assessment unit
<u>Oil in oil assessment unit:</u>				
		minimum	median	maximum
	Volume % in entity.....	_____	_____	_____
	Portion of volume % that is offshore (0-100%)..	_____	_____	_____
<u>Gas in gas assessment unit:</u>				
	Volume % in entity.....	_____	_____	_____
	Portion of volume % that is offshore (0-100%)..	_____	_____	_____
7.	_____	represents	_____	areal % of the assessment unit
<u>Oil in oil assessment unit:</u>				
		minimum	median	maximum
	Volume % in entity.....	_____	_____	_____
	Portion of volume % that is offshore (0-100%)..	_____	_____	_____
<u>Gas in gas assessment unit:</u>				
	Volume % in entity.....	_____	_____	_____
	Portion of volume % that is offshore (0-100%)..	_____	_____	_____
8.	_____	represents	_____	areal % of the assessment unit
<u>Oil in oil assessment unit:</u>				
		minimum	median	maximum
	Volume % in entity.....	_____	_____	_____
	Portion of volume % that is offshore (0-100%)..	_____	_____	_____
<u>Gas in gas assessment unit:</u>				
	Volume % in entity.....	_____	_____	_____
	Portion of volume % that is offshore (0-100%)..	_____	_____	_____

Assessment Unit (name, no.)
Lewis Continuous Gas, 50220261

9.	_____	represents _____	areal % of the assessment unit	
<u>Oil in oil assessment unit:</u>				
		minimum	median	maximum
	Volume % in entity.....	_____	_____	_____
	Portion of volume % that is offshore (0-100%)..	_____	_____	_____
<u>Gas in gas assessment unit:</u>				
	Volume % in entity.....	_____	_____	_____
	Portion of volume % that is offshore (0-100%)..	_____	_____	_____
10.	_____	represents _____	areal % of the assessment unit	
<u>Oil in oil assessment unit:</u>				
		minimum	median	maximum
	Volume % in entity.....	_____	_____	_____
	Portion of volume % that is offshore (0-100%)..	_____	_____	_____
<u>Gas in gas assessment unit:</u>				
	Volume % in entity.....	_____	_____	_____
	Portion of volume % that is offshore (0-100%)..	_____	_____	_____
11.	_____	represents _____	areal % of the assessment unit	
<u>Oil in oil assessment unit:</u>				
		minimum	median	maximum
	Volume % in entity.....	_____	_____	_____
	Portion of volume % that is offshore (0-100%)..	_____	_____	_____
<u>Gas in gas assessment unit:</u>				
	Volume % in entity.....	_____	_____	_____
	Portion of volume % that is offshore (0-100%)..	_____	_____	_____
12.	_____	represents _____	areal % of the assessment unit	
<u>Oil in oil assessment unit:</u>				
		minimum	median	maximum
	Volume % in entity.....	_____	_____	_____
	Portion of volume % that is offshore (0-100%)..	_____	_____	_____
<u>Gas in gas assessment unit:</u>				
	Volume % in entity.....	_____	_____	_____
	Portion of volume % that is offshore (0-100%)..	_____	_____	_____

Assessment Unit (name, no.)
Lewis Continuous Gas, 50220261

ALLOCATIONS OF POTENTIAL ADDITIONS TO RESERVES TO LAND ENTITIES
Subsurface Allocations (uncertainty of a fixed value)

Based on Data as of: _____

1. <u>All Federal Subsurface</u>	_____	represents	_____	areal % of the assessment unit
<u>Oil in oil assessment unit:</u>		minimum	median	maximum
Volume % in entity.....	_____	_____	_____	_____
Portion of volume % that is offshore (0-100%)..	_____	_____	_____	_____
<u>Gas in gas assessment unit:</u>				
Volume % in entity.....	_____	_____	_____	_____
Portion of volume % that is offshore (0-100%)..	_____	_____	_____	_____
2. <u>Other Subsurface</u>	_____	represents	_____	areal % of the assessment unit
<u>Oil in oil assessment unit:</u>		minimum	median	maximum
Volume % in entity.....	_____	_____	_____	_____
Portion of volume % that is offshore (0-100%)..	_____	_____	_____	_____
<u>Gas in gas assessment unit:</u>				
Volume % in entity.....	_____	_____	_____	_____
Portion of volume % that is offshore (0-100%)..	_____	_____	_____	_____

Appendix B. Summary of assessment results for the Lewis Continuous Gas Assessment Unit (AU 50220261).

[MMBO, million barrels of oil. BCFG, billion cubic feet of gas. MMBNGL, million barrels of natural gas liquids. Minimum, for conventional resources this is the minimum field size assessed (MMBO or BCFG); for continuous-type resources this is the minimum cell estimated ultimate recovery assessed. Prob., probability (including both geologic and accessibility probabilities) of at least one field (or for continuous-type resources, cell) equal to or greater than the minimum. Results shown are fully risked estimates. For gas fields, all liquids are included under the NGL (natural gas liquids) category. F95 represents a 95 percent chance of at least the amount tabulated. Other fractiles are defined similarly. Fractiles are additive under the assumption of perfect positive correlation. Shading indicates not applicable]

Undiscovered Resources												
Field	Oil (MMBO)				Gas (BCFG)				NGL (MMBNGL)			
Type	F95	F50	F5	Mean	F95	F50	F5	Mean	F95	F50	F5	Mean
Lewis Continuous Gas												
Oil	0.00	0.00	0.00	0.00	0.00	0.00	0.00	0.00	0.00	0.00	0.00	0.00
Gas					8,315.22	10,105.95	12,282.31	10,177.24	18.08	29.25	47.32	30.53
Total	0.00	0.00	0.00	0.00	8,315.22	10,105.95	12,282.31	10,177.24	18.08	29.25	47.32	30.53



Click here to return to
Volume Title Page

Geology and Oil and Gas Assessment of the Fruitland Total Petroleum System, San Juan Basin, New Mexico and Colorado



Click here to return to
[Volume Title Page](#)

By J.L. Ridgley, S.M. Condon, and J.R. Hatch

Chapter 6 of 7

Total Petroleum Systems and Geologic Assessment of Undiscovered Oil and Gas Resources in the San Juan Basin Province, Exclusive of Paleozoic Rocks, New Mexico and Colorado

Compiled by U.S. Geological Survey San Juan Basin Assessment Team

Digital Data Series 69–F

U.S. Department of the Interior
U.S. Geological Survey

U.S. Department of the Interior
KEN SALAZAR, Secretary

U.S. Geological Survey
Marcia K. McNutt, Director

U.S. Geological Survey, Reston, Virginia 2013

For product and ordering information:

World Wide Web: <http://www.usgs.gov/pubprod>

Telephone: 1-888-ASK-USGS

For more information on the USGS—the Federal source for science about the Earth, its natural and living resources, natural hazards, and the environment:

World Wide Web: <http://www.usgs.gov>

Telephone: 1-888-ASK-USGS

Suggested citation:

Ridgley, J.L., Condon, S.M., and Hatch, J.R., 2013, Geology and oil and gas assessment of the Fruitland Total Petroleum System, San Juan Basin, New Mexico and Colorado, chap. 6 of U.S. Geological Survey San Juan Basin Assessment Team, Total petroleum systems and geologic assessment of undiscovered oil and gas resources in the San Juan Basin Province, exclusive of Paleozoic rocks, New Mexico and Colorado: U.S. Geological Survey Digital Data Series 69–F, p. 1–100.

Any use of trade, product, or firm names is for descriptive purposes only and does not imply endorsement by the U.S. Government.

Although this report is in the public domain, permission must be secured from the individual copyright owners to reproduce any copyrighted material contained within this report.

Contents

Abstract.....	1
Introduction	1
Fruitland Total Petroleum System	5
Hydrocarbon Reservoir Rocks.....	5
Pictured Cliffs Sandstone.....	5
Fruitland Formation.....	6
Cretaceous and Tertiary Formations	7
Hydrocarbon Source Rock.....	12
Fruitland Formation Source Rock Characterization.....	12
Vitrinite Reflectance.....	12
Geochemical Characteristics	13
Source Rock Maturation and Thermal History	18
Fruitland Formation Hydrology	22
Pressure Regimes in the Fruitland Formation.....	22
Meteoric Water Incursion.....	22
Relation of Groundwater Flow to Thermal History.....	23
Water Inorganic Compositions.....	25
Water Dating.....	25
Carbon Isotopes of Dissolved Inorganic Carbon in Produced Waters.....	28
Fruitland Formation Gas	28
Gas Chemistry.....	28
Distribution of Gas Wetness	28
Distribution of Methane Isotopes	31
Carbon Dioxide Content.....	35
Gas Generation Processes	45
Microbial	45
Thermogenic.....	48
Gas Origin.....	48
Hydrocarbon Migration Summary	50
Hydrocarbon Traps and Seals	51
Assessment Unit Definitions.....	51
Pictured Cliffs Continuous Gas Assessment Unit (50220161)	51
Introduction.....	51
Source.....	54
Maturation.....	54
Migration	54
Reservoirs	54
Traps/Seals	54
Geologic Model.....	54
Assessment Results	54

Basin Fruitland Coalbed Gas Assessment Unit (50220182) and Fruitland Fairway Coalbed Gas Assessment Unit (50220181)	55
Introduction.....	55
Production Characteristics of the Basin Fruitland Coalbed Gas and Fruitland Fairway Coalbed Gas Assessment Units.....	58
Water Production.....	58
Cumulative Gas Production	58
Normalized Gas Production	65
Relations Among Gas, Water Production, Groundwater Flow, and Microbial-Gas Generation	65
Basin Fruitland Coalbed Gas Assessment Unit (50220182).....	70
Introduction.....	70
Source.....	70
Maturation.....	70
Migration	70
Reservoirs	73
Traps/Seals	73
Geologic Model	73
Assessment Results	73
Fruitland Fairway Coalbed Gas Assessment Unit (50220181).....	74
Introduction.....	74
Source.....	78
Maturation.....	78
Migration	78
Reservoirs	78
Traps/Seals	80
Geologic Model	80
Assessment Results	80
Tertiary Conventional Gas Assessment Unit (50220101).....	81
Introduction.....	81
Source.....	84
Maturation.....	84
Migration	84
Reservoirs	84
Traps/Seals	84
Geologic Model	84
Assessment Results	84
Summary.....	86
Acknowledgments	86
References Cited.....	86

Appendixes

A.	Assessment results summary for the Fruitland Total Petroleum System, San Juan Basin Province, New Mexico and Colorado.....	92
B–E.	Input data form used in evaluating the Fruitland Total Petroleum System.....	
B.	Pictured Cliffs Continuous Gas Assessment Unit (50220181), San Juan Basin Province	93
C.	Basin Fruitland Coalbed Gas Assessment Unit (50220182), San Juan Basin Province	95
D.	Basin Fruitland Fairway Coalbed Gas Assessment Unit (50220181), San Juan Basin Province.....	97
E.	Tertiary Conventional Gas Assessment Unit (50220101), San Juan Basin Province	99

Figures

1.	Map showing structural elements in the San Juan Basin and the location of inferred basement structural blocks	2
2.	Map showing boundary of the Fruitland Total Petroleum System	3
3.	Chart showing regional chronostratigraphic correlations in the San Juan Basin to the base of the Jurassic, and the extent of the total petroleum systems and assessment units defined in the 2002 National Oil and Gas Assessment of the San Juan Basin Province	4
4.	Cross section extending from southwest to northeast across the central San Juan Basin	8
5.	Isopach map of net coal in the Fruitland Formation	10
6.	Structure contour map drawn on top of the Pictured Cliffs Sandstone	11
7–9.	Crossplots showing relations between.....	
7.	Gas methane $\delta^{13}\text{C}$ and gas wetness	15
8.	Gas methane $\delta^{13}\text{C}$, CO_2 content, and gas wetness.....	16
9.	Gas wetness	17
10.	Burial history curves	19
11–18.	Maps showing.....	
11.	Distribution of $\delta^{18}\text{O}$ ‰ in produced Fruitland Formation waters.....	24
12.	Pressure regimes in the Fruitland Formation and inferred directions of groundwater flow	26
13.	Relation between minimum $^{129}\text{I}/\text{I}$ ages and distribution of $\delta^{18}\text{O}$ ‰ in produced Fruitland Formation waters.....	29
14.	Relation between pressure gradients and methane carbon ($\delta^{18}\text{C}$) isotope of dissolved inorganic carbon in Fruitland Formation produced waters.....	30
15.	Distribution of gas wetness in Fruitland Formation gases	32
16.	Distribution of CO_2 concentration in Fruitland Formation gases	33
17.	Distribution of $\delta^{13}\text{C}$ of methane to gas wetness in Fruitland Formation gases	34
18.	Relation between $\delta^{18}\text{O}$ of produced Fruitland Formation waters and methane carbon isotope ($\delta^{13}\text{C}$) in Fruitland Formation gas	36

19.	Crossplot showing relation between $\delta^{13}\text{C}_{\text{CO}_2}$ and $\delta^{13}\text{C}$ methane of gas in the Fruitland Formation	37
20.	Crossplot showing relation between $\delta^{13}\text{C}$ CO_2 and the CO_2 content of gas in the Fruitland Formation.....	37
21–29.	Maps showing.....	
21.	Relation between pressure gradient and CO_2 concentration in Fruitland Formation gas.....	38
22.	Relation between net coal in the Fruitland Formation and distribution of CO_2 concentration in Fruitland Formation gases	39
23.	Distribution of CO_2 concentration in Fruitland Formation gases	41
24.	Relation between shorelines in Pictured Cliffs Sandstone and the isopach thickness of the interval between Huerfanito Bentonite Bed of Lewis Shale and top of Pictured Cliffs Sandstone	43
25.	Distribution of CO_2 concentration in Fruitland Formation gases with respect to Pictured Cliffs Sandstone shorelines.....	44
26.	Relation between net coal in the Fruitland Formation and shorelines in the Pictured Cliffs Sandstone.....	46
27.	Relation between $\delta^{18}\text{O}$ of produced Fruitland Formation waters and carbon dioxide concentration in Fruitland Formation gas	47
28.	Distribution of $\delta^{13}\text{C}$ of dissolved inorganic carbon in Fruitland Formation produced waters in relationship to $\delta^{18}\text{O}$ of produced waters.....	49
29.	Boundary of the Pictured Cliffs Continuous Gas Assessment Unit and Pictured Cliffs Sandstone gas fields.....	52
30.	Events chart showing key geologic events for the Pictured Cliffs Continuous Gas Assessment Unit.....	53
31.	Graph showing estimated ultimate recoveries of Pictured Cliffs Continuous Gas Assessment Unit gas wells divided by time of completion.....	56
32.	Graph showing distribution of estimated ultimate recoveries of Pictured Cliffs Continuous Gas Assessment Unit gas wells.....	56
33.	Map showing assessment unit boundaries for the Basin Fruitland Coalbed Gas and Fruitland Fairway Coalbed Gas Assessment Units and major gas fields Blanco and Ignacio-Blanco in Fruitland Formation.....	57
34.	Map showing distribution of cumulative produced water in Fruitland Formation with respect to the Basin Fruitland Coalbed Gas and Fruitland Fairway Coalbed Gas Assessment Units	59
35.	Graphs showing relation between cumulative water production and length of production.....	60
36.	Map showing distribution of length of production time of Fruitland Formation wells with respect to the Basin Fruitland Coalbed Gas and Fruitland Fairway Coalbed Gas Assessment Units	62
37.	Graphs showing relation between cumulative gas production and length of production.....	63
38.	Map showing distribution of cumulative gas production of Fruitland Formation wells with respect to the Basin Fruitland Coalbed Gas and Fruitland Fairway Coalbed Gas Assessment Units	64

39. Map showing distribution of normalized gas production of Fruitland Formation wells with respect to the Basin Fruitland Coalbed Gas and Fruitland Fairway Coalbed Gas Assessment Units	66
40. Graphs showing relation between normalized gas production and length of production.....	67
41. Graphs showing relation between cumulative gas production and normalized gas production for production time.....	68
42. Map showing relation between basin structure and the Fruitland Fairway Coalbed Gas Assessment Unit.....	69
43. Map showing the assessment unit boundaries for the Basin Fruitland Coalbed Gas AU and the Basin Fruitland gas fields	71
44. Events chart showing key geologic events for the Basin Fruitland Coalbed Gas Assessment Unit.....	72
45. Graph showing estimated ultimate recoveries of Basin Fruitland Coalbed Gas Assessment Unit gas wells divided by time of completion.....	75
46. Graph showing distribution of estimated ultimate recoveries of Basin Fruitland Coalbed Gas Assessment Unit gas wells	75
47. Map showing assessment unit boundary for the Fruitland Fairway Coalbed Gas Assessment Unit and the location of the Fruitland Fairway gas fields.....	76
48. Map showing relation between cumulative gas production in the Fruitland Fairway Coalbed Gas Assessment Unit and distribution of $\delta^{18}\text{O}$ in produced Fruitland Formation waters	77
49. Events chart showing key geologic events for the Fruitland Fairway Coalbed Gas Assessment Unit.....	79
50. Graph showing estimated ultimate recoveries of Fruitland Fairway Coalbed Gas Assessment Unit gas wells divided by time of completion.....	82
51. Graph showing distribution of estimated ultimate recoveries of Fruitland Fairway Coalbed Gas Assessment Unit gas wells	82
52. Map showing assessment unit boundary for the Tertiary Conventional Gas Assessment Unit and Tertiary gas fields	83
53. Events chart showing key geologic events for the Tertiary Conventional Gas Assessment Unit.....	85

Tables

1. Some Pictured Cliffs Sandstone and Tertiary reservoir rocks characteristics and oil and gas compositions in the Fruitland Total Petroleum System	6
2. Means, standard deviations, ranges, and number of determinations for total organic carbon contents and hydrogen indices of the Fruitland Formation source rocks in the Fruitland Total Petroleum System	13
3. Means, standard deviations, and number of chemical analyses of produced natural gases from the Fruitland Formation and Pictured Cliffs Sandstone in the Fruitland Total Petroleum System	14

Geology and Oil and Gas Assessment of the Fruitland Total Petroleum System, San Juan Basin, New Mexico and Colorado

By J.L. Ridgley, S.M. Condon, and J.R. Hatch

Abstract

The Fruitland Total Petroleum System (TPS) of the San Juan Basin Province includes all genetically related hydrocarbons generated from coal beds and organic-rich shales in the Cretaceous Fruitland Formation. Coal beds are considered to be the primary source of the hydrocarbons. Potential reservoir rocks in the Fruitland TPS consist of the Upper Cretaceous Pictured Cliffs Sandstone, Fruitland Formation (both sandstone and coal beds), and the Farmington Sandstone Member of the Kirtland Formation, and the Tertiary Ojo Alamo Sandstone, and Animas, Nacimiento, and San Jose Formations.

Analysis of the geochemistry of Fruitland coal-bed gas and co-produced water suggests that hydrocarbons in Fruitland coal beds began to form early in the depositional history of the Fruitland Formation with the generation of early microbial gas. Source rocks in the Fruitland entered the oil generation zone in the late Eocene and continued to generate minor oil and large quantities of thermogenic gas into middle Miocene time. Near the end of the Miocene, thermogenic hydrocarbon generation and subsidence in the San Juan Basin ceased, and the basin was uplifted and differentially eroded. Late-stage (secondary) microbial gas has been documented in Fruitland coal-bed reservoirs and was formed by microbial reduction of carbon dioxide during introduction of groundwater in the late Pliocene and Pleistocene. Most of this late-stage microbial gas is found just downdip from the northern, western, and southern Fruitland outcrops. The northern part of the Fruitland Formation is overpressured as a result of artesian conditions established in the Pliocene or Pleistocene. South and east of the overpressured area, the Fruitland is either normally pressured or underpressured.

Four assessment units (AU) were defined in the Fruitland TPS. Of the four AUs, one consists of conventional gas accumulations and the other three are continuous-type gas accumulations: Tertiary Conventional Gas AU, Pictured Cliffs Continuous Gas AU, Basin Fruitland Coalbed Gas (CBG) AU, and Fruitland Fairway CBG AU. No oil resources that have the potential for additions to reserves in the next 30 years were estimated for this TPS. Gas resources that have the potential for additions to reserves in the next 30 years are estimated at a mean of 29.3 trillion cubic feet of gas (TCFG). Of this

amount, 23.58 TCFG will come from coal-bed gas accumulations and 83.1 percent of this total is estimated to come from the Basin Fruitland CBG AU. The remaining 5.72 TCFG is allocated to continuous-type gas accumulations (5.64 TCFG) and conventional gas accumulations (0.08 TCFG). Although the Fruitland Fairway CBG AU has produced the most significant amount of coal-bed gas to date, the area of the AU is limited. New potentially productive wells will come from infill drilling, and the number of these wells will be limited by effective drainage area. Total natural gas liquids (NGL) that have the potential for additions to reserves in the next 30 years are estimated at a mean of 17.76 million barrels. Of this amount, 16.92 million barrels will come from the Pictured Cliffs Continuous Gas AU and the remainder from the Tertiary Conventional Gas AU.

Introduction

The Fruitland Total Petroleum System (TPS) encompasses the central basin structural element of the San Juan Basin Province (figs. 1 and 2). The boundary of the TPS has been defined as the area enclosed by outcrops of the base of the Pictured Cliffs Sandstone. In Colorado, the Pictured Cliffs and Lewis Shale were grouped together on the digital geologic map used for this study (Green, 1992), and the TPS boundary is drawn at the base of the combined unit. This TPS is the youngest assessed in the San Juan Basin Province (fig. 3) and has been divided into four assessment units (AU), in ascending order:

1. Pictured Cliffs Continuous,
2. Basin Fruitland Coalbed Gas (CBG),
3. Fruitland Fairway CBG, and
4. Tertiary Conventional Gas.

The four AUs in the TPS produce mostly gas and limited small amounts of natural gas liquids (NGL) sourced from coals and carbonaceous shale; their stratigraphic extents are shown in figure 3.

2 Total Petroleum Systems and Geologic Assessment of Undiscovered Oil and Gas Resources in the San Juan Basin Province

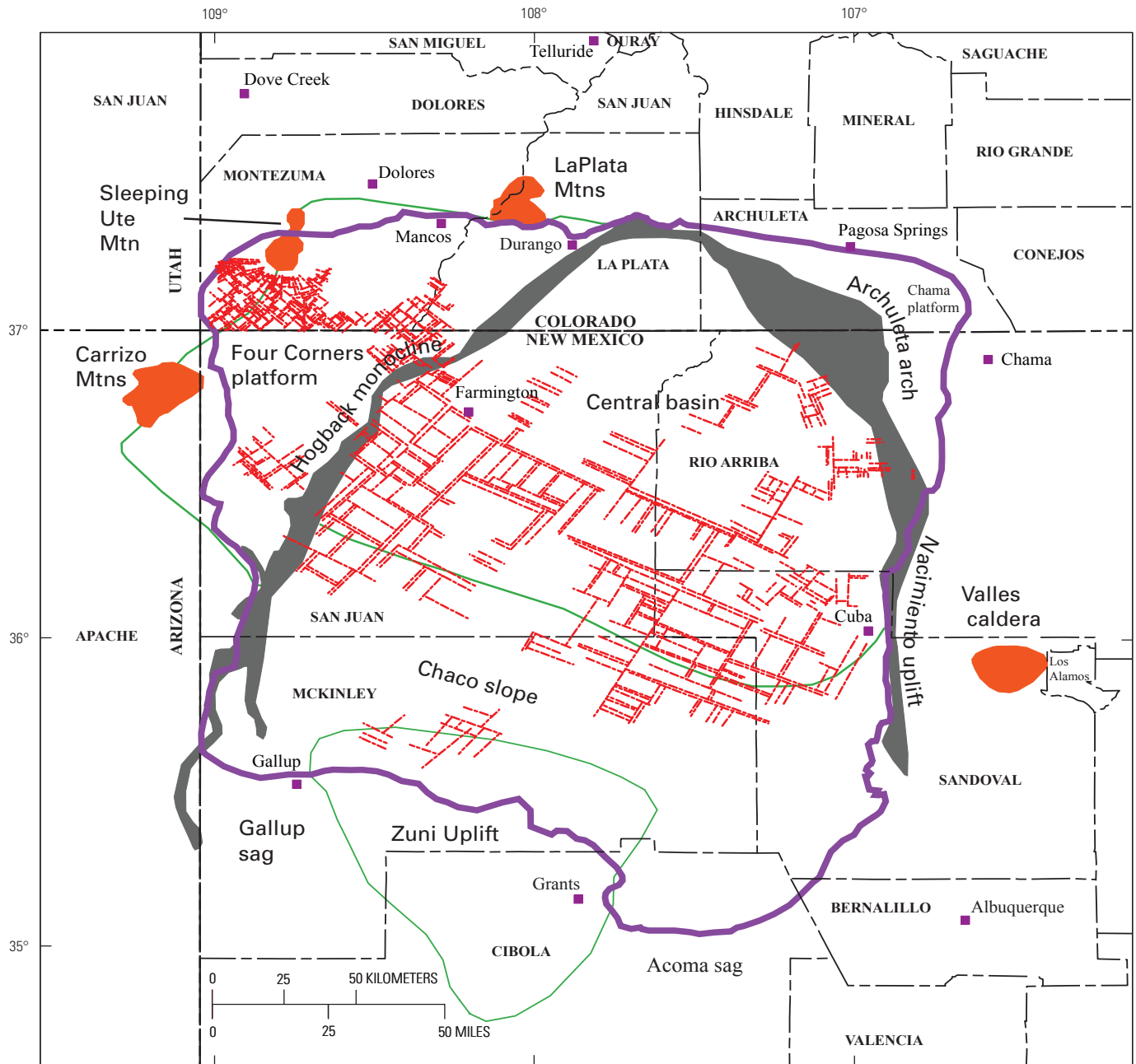


Figure 1. Map showing structural elements in the San Juan Basin and the location of inferred basement structural blocks (dashed red lines). Modified from Taylor and Huffman (1998, 2001), Fassett (2000), and Huffman and Taylor (2002). San Juan Basin Province (5022) boundary (purple line). Orange polygons are Late Cretaceous and Tertiary intrusive and extrusive igneous centers; gray polygons are areas of steep dip along monoclines; green lines outline some of the main structural elements.

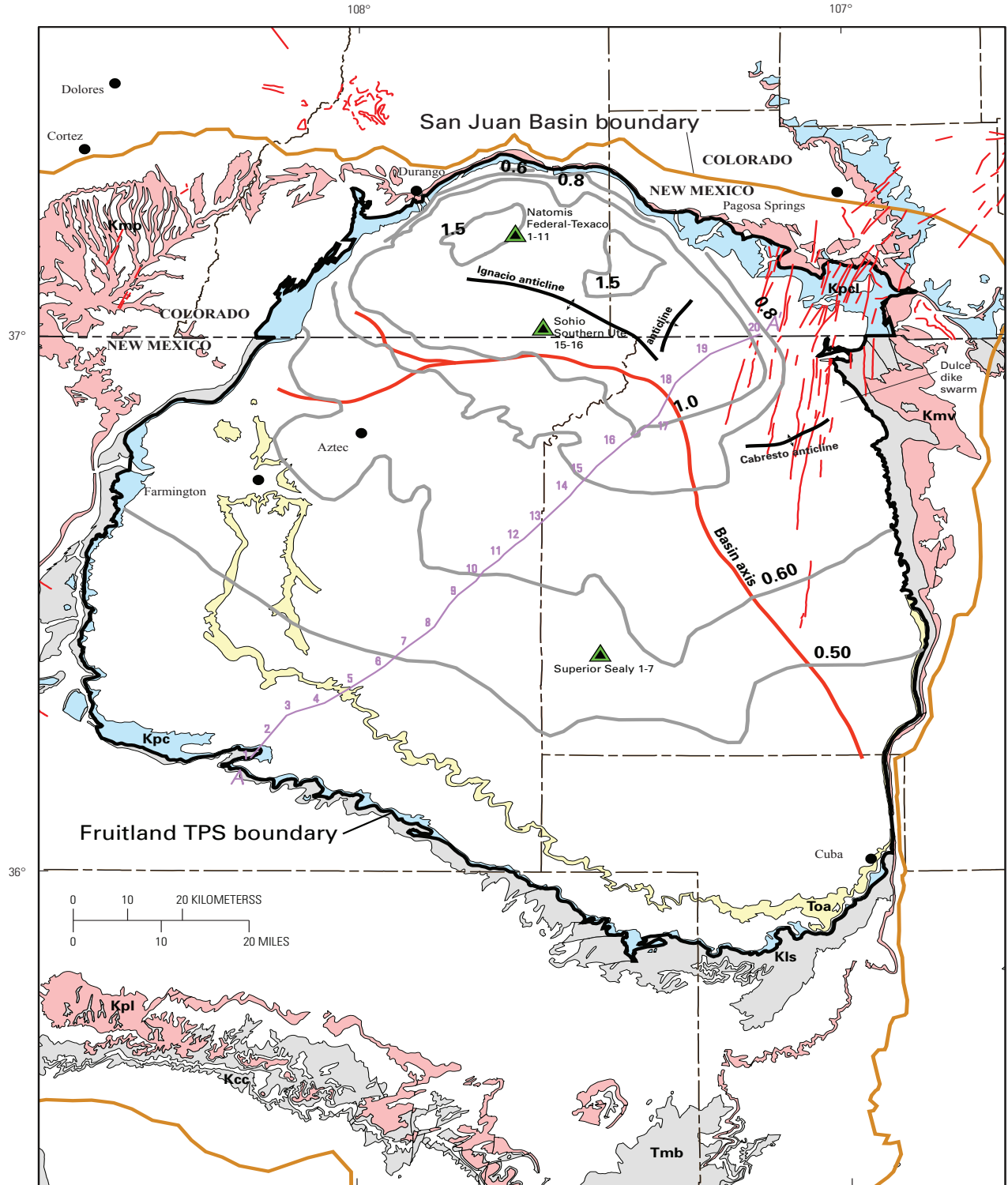


Figure 2. Map showing boundary of the Fruitland Total Petroleum System (TPS). Symbols for geologic map units: Toa, Tertiary Ojo Alamo Sandstone; Tmb, Tertiary Miocene volcanics; Kpc, Pictured Cliffs Sandstone; Kpl, Pictured Cliffs Sandstone and Lewis Shale; Kls, Lewis Shale; Kcc, Crevasse Canyon Formation; Kmp, Menefee Formation and Point Lookout Sandstone; Kmv, Mesaverde Group; Kpl, Point Lookout Sandstone; thin red vertical lines and patches, dikes (Green, 1992; Green and Jones, 1997). Contours (gray) show vitrinite reflectance (R_m) values, in percent, from data in Fassett and Nuccio (1990), Law (1992), and Fassett (2000). Also shown are the locations of regional cross section A–A' (in fig. 4), principal folds in the basin, and wells (green and black triangles) used to make the burial history curves in this report (figs. 10A–C).

Cretaceous rocks, beginning with the Dakota Sandstone, comprise wedges of marine-to-continental transgressive and regressive strata that occupy the San Juan Basin (Baltz, 1967; Fassett, 1974, 1977, 2000; Molenaar, 1977b; Owen and Siemers, 1977; Posamentier and others, 1992; Nummedal and Molenaar, 1995; Wright Dunbar, 2001). Within these wedges of strata, various shorelines generally have a northwest–southeast orientation that may be controlled by basement structural blocks (fig. 1) (Taylor and Huffman, 1998, 2001; Huffman and Taylor, 2002). The configuration of the San Juan Basin, as observed today, was not present during the Cretaceous. Instead, deposition in the basin was continuous to the northeast in the direction of deeper marine sedimentation. The Fruitland TPS consists of the last major regressive wedge of strata (Pictured Cliffs Sandstone-Fruitland Formation-Kirtland Shale) and all Tertiary strata (fig. 3). A regional unconformity separates Cretaceous and Tertiary rocks (Baltz, 1967; Sikkink, 1987). Tertiary rocks were deposited solely in continental depositional environments. Their present-day extent is confined to the northern part of the San Juan Basin Province, except for the Chuska Sandstone, which is on the west margin of the basin.

Originally, the Fruitland depositional system covered an area greater than its extent today. The source of sediment was from the south and southwest, and streams generally flowed to the northeast. Thus groundwater movement would have been in this direction at least through the Cretaceous, about 10 m.y. after deposition of the Fruitland. Uplift of the central basin margins and erosion of the Fruitland outside the central basin may have begun in the latest Cretaceous or earliest Paleocene, but the timing of this event is not everywhere well constrained, and erosion of the Fruitland in some areas could be late Miocene and younger. The Cretaceous-Tertiary unconformity in the northern part of the San Juan Basin separates the Paleocene Ojo Alamo Sandstone from the underlying Kirtland Shale, and in places along the east side of the San Juan Basin, the Fruitland is absent by erosion (Fassett, 1985, 2000). Prior to deposition of the Ojo Alamo, the basin was uplifted and tilted to the northwest (Fassett, 1985). This tectonic tilt would have resulted in erosion of the Fruitland along the southeast part of the central basin (fig. 1). If the Fruitland was still present elsewhere outside the central basin, then groundwater flow may have been to the northeast, north, or northwest (reflecting tectonic tilt).

From Paleocene through Eocene time, most of the sediments were derived from the north and northwest and deposited by south and southeastward flowing streams (Fassett, 1985). Northward groundwater flow through the Fruitland probably ceased at this time. Southward groundwater flow through the Fruitland may have been initiated in the latter part of the Paleocene as a result of uplift of the area north of the San Juan Basin and local erosion of the Ojo Alamo Sandstone prior to deposition of the Paleocene Animas and Nacimiento Formations (Fassett, 1985). Erosion also occurred between deposition of the Paleocene Nacimiento Formation and the Eocene San Jose Formation (Fassett, 1985) along the

northern, eastern, and southern margins of the basin. However, deposition continued to be from the northwest, north, and northeast as evidenced by stratigraphic relations between the Animas and Nacimiento Formations, which are stratigraphic time equivalents. Deposition of the San Jose may have been principally from the north, although a southeast source in the Nacimiento Mountains has also been suggested (Baltz, 1967). On the northwest rim of the basin, the San Jose rests with angular unconformity on the Fruitland Formation (see discussion in Fassett, 1985). This configuration may have allowed for incursion of Eocene and younger meteoric waters into the Fruitland from the northwest as the basin continued to subside to the south.

Key elements that define the Fruitland TPS are

1. source rocks of sufficient thermal maturity to generate hydrocarbons,
2. reservoir rocks to host the accumulations,
3. migration pathways that allow the hydrocarbons to move into reservoirs,
4. structural or stratigraphic traps in which hydrocarbons could accumulate, and
5. seals to contain the accumulations.

These key elements are described more fully below and in each assessment unit discussion. Methodologies for assessing continuous-type and conventional accumulations are discussed in Schmoker (2003) and Schmoker and Klett (2003).

Fruitland Total Petroleum System

Hydrocarbon Reservoir Rocks

Potential reservoir rocks in the Fruitland TPS consist of the Upper Cretaceous Pictured Cliffs Sandstone, Fruitland Formation (both sandstone and coal beds), and the Farmington Sandstone Member of the Kirtland Shale and the Tertiary Ojo Alamo Sandstone, and Animas, Nacimiento, and San Jose Formations (fig. 3).

Pictured Cliffs Sandstone

The Pictured Cliffs Sandstone is a marginal-marine deposit that prograded northeastward across the San Juan Basin (fig. 4A) (Fassett and Hinds, 1971). It gradationally overlies the Lewis Shale, and sandstone beds increase in thickness upward through a transition zone from the Lewis to the Pictured Cliffs. The Pictured Cliffs crops out around the perimeter of the central San Juan Basin. It ranges in thickness from 0 to about 400 ft (Fassett and Hinds, 1971) and is thickest in the north-central part of the basin (fig. 4). It consists of very fine to medium-grained, well-sorted sandstone and siltstone and mudrock interbeds. Sandstone beds are elongated in a northwest–southeast direction, wedge out gradually to the northeast, and terminate abruptly to the southwest (Arnold,

1974). See table 1 for description of reservoir properties, API gravities, and inert gas composition of Pictured Cliffs reservoir rocks and gases.

The Pictured Cliffs can be divided into three general production areas (Cumella, 1981; Goberdhan, 1996):

1. the northeast area, where sandstones have low permeability and are gas saturated, and production is dependant on fractures;
2. the central producing area, where production is dependant on primary porosity and permeability, and fractures enhance production; and
3. the southwest area, where sandstones are composed of permeable sandstones, which are mostly water saturated.

Tight sandstones in the northeast result from precipitation of authigenic illite and/or mixed-layer smectite clays and dolomite (Hoppe, 1992). Arnold (1974) also noted low permeabilities in the Pictured Cliffs in the eastern part of the basin. The Fruitland Formation throughout most of the basin gradationally overlies the Pictured Cliffs Sandstone.

Fruitland Formation

Deposition of the Fruitland Formation is closely related to and interfingers with the underlying Pictured Cliffs Sandstone and overlying Kirtland Shale (fig. 4). The formation consists of coal, carbonaceous shale, siltstone, and sandstone deposited in fluvial channels and nearshore paludal environments (Fassett and Hinds, 1971). The basal contact with the underlying Pictured Cliffs is gradational to sharp and intertonguing in some places, and the contact with the overlying Kirtland Shale is gradational. There is no break in deposition between the Fruitland and Kirtland; the two formations represent different sequences of facies related to the final withdrawal of the sea from the San Juan Basin. Both formations

are time transgressive and rise stratigraphically to the northeast (fig. 4). Various workers have picked the contact between the Fruitland and Kirtland at the base of different discontinuous sandstone beds; however, Fassett and Hinds (1971) suggested that the contact between the two formations be placed at the top of the highest coal bed or very carbonaceous shale. Shale in the overlying Kirtland appears to be less organic rich than that in the Fruitland (Fassett and Hinds, 1971, p. 25).

Remnants of the original Fruitland Formation depositional system are confined primarily to the central basin part of the San Juan Basin (figs. 1 and 2) and coincide with the extent of the Fruitland TPS (fig. 2). The Fruitland ranges in thickness from 0 to 500 ft but is absent in areas along the east side of the San Juan Basin where it has been eroded below the unconformity at the base of the Paleocene Ojo Alamo Sandstone (Fassett and Hinds, 1971). The various lithostratigraphic units that compose the Fruitland are laterally discontinuous, reflecting the heterogeneous nature of the depositional environments (Ambrose and Ayers, 1994; Ayers and others, 1994; Fassett, 2000; Wray, 2001). This heterogeneous character of the depositional system and lateral discontinuity of coal beds has pronounced implications for fluid flow both prior to thermal maturation and subsequent to coal maturation. Reservoir rocks in the Fruitland consist of coal and sandstone. Net coal in the Fruitland ranges from a few feet to as much as 100 ft (fig. 5); the thickest areas of net coal are located in the central and northwestern part of the TPS. Overall trends in net coal thickness are northeast–southwest, except in the Fruitland Fairway area (Fruitland Fairway CBG AU) where the trend is northwest–southeast and in the southern part of the TPS where the trends are east–northeast (fig. 5). Thickness of overburden, defined as the interval from the land surface to the top of the Pictured Cliffs Sandstone, varies from 0 to as much as 4,000 ft in places on the east side of the basin (Ayers and others, 1994, and their fig. 2.14).

Table 1. Some Pictured Cliffs Sandstone and Tertiary reservoir rocks characteristics and oil and gas compositions (compiled from Brown, 1973, and from field descriptions in Fassett, 1978a,b, 1983a) in the Fruitland Total Petroleum System. Reported minimums and maximums are shown; calculated averages are not shown when there were fewer than five values reported. Fluid pressure gradients were calculated from bottom-hole pressures and bottom-perforated depth. No data were available from the Cabresto Canyon field (Tertiary production).

[ND, No data; --, not applicable; min., minimum; max., maximum; avg., average]

		Porosity (%)	Permeability (millidarcies)	Water saturation (%)	Fluid pressure gradient (psi/ft)	Oil API gravity (degrees)	Nitrogen (%)	CO ₂ (%)	Net pay (ft)
Pictured Cliffs Sandstone	min.	1	0.0	30	0.15	47	0.26	0.08	5
	max.	24	150	90	0.47	60	0.4	2.3	150
	avg.	14	12.5	51	0.28	--	0.85	0.98	44
Tertiary rocks	min.	14	ND	40	0.15	ND	0.17	0.19	7
	max.	15	8	50	0.43	47	3.95	0.88	20

The coals in the Fruitland consist mostly of vitrinite and lesser amounts of liptinite and inertinite. The coal structure itself is not permeable and has virtually no porosity (Scott, 1994). The permeability in coals occurs in sets of orthogonal cleats (fractures) (Kaiser and Ayers, 1994; Tremain and others, 1994); this permeability can be quite high and various values have been reported. Permeability in the cleats can vary depending on whether the cleats are open or closed. Cleat development appears also to be related to coal rank, maceral composition, and tectonic compression (Scott and others, 1994a; Tremain and others, 1994).

The importance of understanding the role of permeability in cleats to gas production and ultimate gas recovery has been demonstrated in a 3-D seismic study of the cleats in the Cedar Hill field (Shuck and others, 1996). In their study, Shuck and others (1996) determined that the face-cleat direction, which trended northeast over a portion of the field, was not open. Instead the butt-cleat direction, which coincided with the northwest direction of maximum stress, was open. The preferential closing of one direction of cleats to permeability was related to tectonic stress. The field is located in the overpressured portion of the Fruitland Formation, and it was initially assumed that both directions of the cleats would be open to fluid movement because overpressuring would keep the cleats open. This was not the case. The loss of permeability in one direction, coupled with local faulting, enhanced compartmentalization and resulted in local heterogeneity in gas production.

Sandstones in the Fruitland are minor reservoirs for gas; most gas production is from the Fruitland coal beds. The sandstones consist primarily of quartz and lesser amounts of feldspar and clay minerals. Calcite is the primary cement, and concretion zones have been documented (see summary in Fassett and Hinds, 1971). Little has been reported on lithologic characteristics of producing sandstones. Most of the descriptions of Fruitland reservoirs have focused on the coals. However, gas is produced from sandstone beds of the Fruitland in the Glades field, San Juan County, New Mexico. Sandstones in this field have 8- to 15-percent porosity; net pay was reported as 20 ft (see discussion in Fassett, 1983). No water saturation or permeability values were reported.

Cretaceous and Tertiary Formations

The Kirtland Formation gradationally overlies the Fruitland and has been divided into a lower shale member, the Farmington Sandstone Member, and an upper unnamed shale member by Bauer (1916). Others (Fassett and Hinds, 1971; Fassett, 2000) combined the Farmington Sandstone Member and upper member into one unit. Gas and high-gravity oil have been recovered from the Farmington Sandstone Member in the northwestern part of the San Juan Basin near the towns of Aztec, Bloomfield, and Farmington (fig. 6) (Fassett, 1978a,b, 1983). The Farmington consists of isolated and stacked fluvial channels and mudrock interbeds. Sandstone beds consist of fine- to medium-grained, poorly sorted arkose (Fassett and Hinds, 1971). Typical channel dimensions are 3 ft thick and

30 ft wide, with undetermined lengths (Fassett, 1983). The Farmington is approximately 400 ft thick in areas where it produces oil or gas (Riggs, 1978). The Farmington was not quantitatively assessed in this assessment of the San Juan Basin, because it has not produced oil or gas in fields greater than the minimum sizes of 0.5 million barrels of oil or 3.0 billion cubic feet of gas.

The Paleocene Ojo Alamo Sandstone unconformably overlies the Kirtland Shale in much of the basin; in places erosion at the unconformity has removed the Fruitland Formation and Pictured Cliffs Sandstone, and the Ojo Alamo overlies the Lewis Shale (Fassett, 1974). On the west side of the basin, the Ojo Alamo pinches out depositionally just south of the New Mexico-Colorado State line, and on the east side it extends northward to a point near the San Juan River (Fassett and Hinds, 1971). The Ojo Alamo is a fluvial sequence of coarse clastic rocks interbedded with thin mudstone beds that had its source to the north of the San Juan Basin (Fassett and Hinds, 1971; Sikkink, 1987). The unit is conglomeratic on the west side of the basin, but pebbles are rare in outcrops on the east side (Sikkink, 1987). Over the years, there have been many different interpretations of what strata should be included in the Ojo Alamo leading to different estimates of its thickness. Reported thicknesses vary from 70 to 400 ft (Craig, 2001). Sandstones of the Ojo Alamo have produced some gas in both the western and eastern parts of the TPS.

Basal Tertiary units in much of the Colorado part of the San Juan Basin include the upper part of the Animas Formation and the correlative Nacimiento Formation. The Animas can be divided into a lower conglomeratic and an upper sandstone and shale sequence (Baltz, 1953). The lower part is composed mainly of andesitic debris derived from source areas to the north of the basin and also contains metamorphic and igneous rock fragments. Thin beds of carbonaceous shale and coaly shale are also present locally (Aubrey, 1991). The upper part of the Animas is composed of sandy tuffaceous shale and coarse-grained tuffaceous sandstone, including some conglomerate. The thickness of the upper member of the Animas ranges from 1,100 ft at the Animas River near Durango, Colo., to 2,670 ft in the eastern part of La Plata County, Colo. (Reeside, 1924).

The Paleocene Nacimiento Formation overlies and inter-fingers laterally with the upper member of the Animas Formation in Colorado, and gradationally overlies the Ojo Alamo Sandstone in New Mexico. Most outcrops of the Nacimiento are along the west side of the central basin in New Mexico; the Animas extends farther south along the eastern outcrops. The Nacimiento has a higher proportion of sandstone at its northern outcrops and a greater proportion of mudrocks in southern exposures. Williamson and Lucas (1992) recognized several divisions of the Nacimiento along the southern rim of the central basin. The lower part consists of drab-colored sandstone, mudrocks, and thin coal or lignite beds. The middle part is mainly variegated purple, gray, and green mudrocks and less abundant sandstone. The upper part is dominantly sandstone, although mudrocks, some very carbonaceous, are

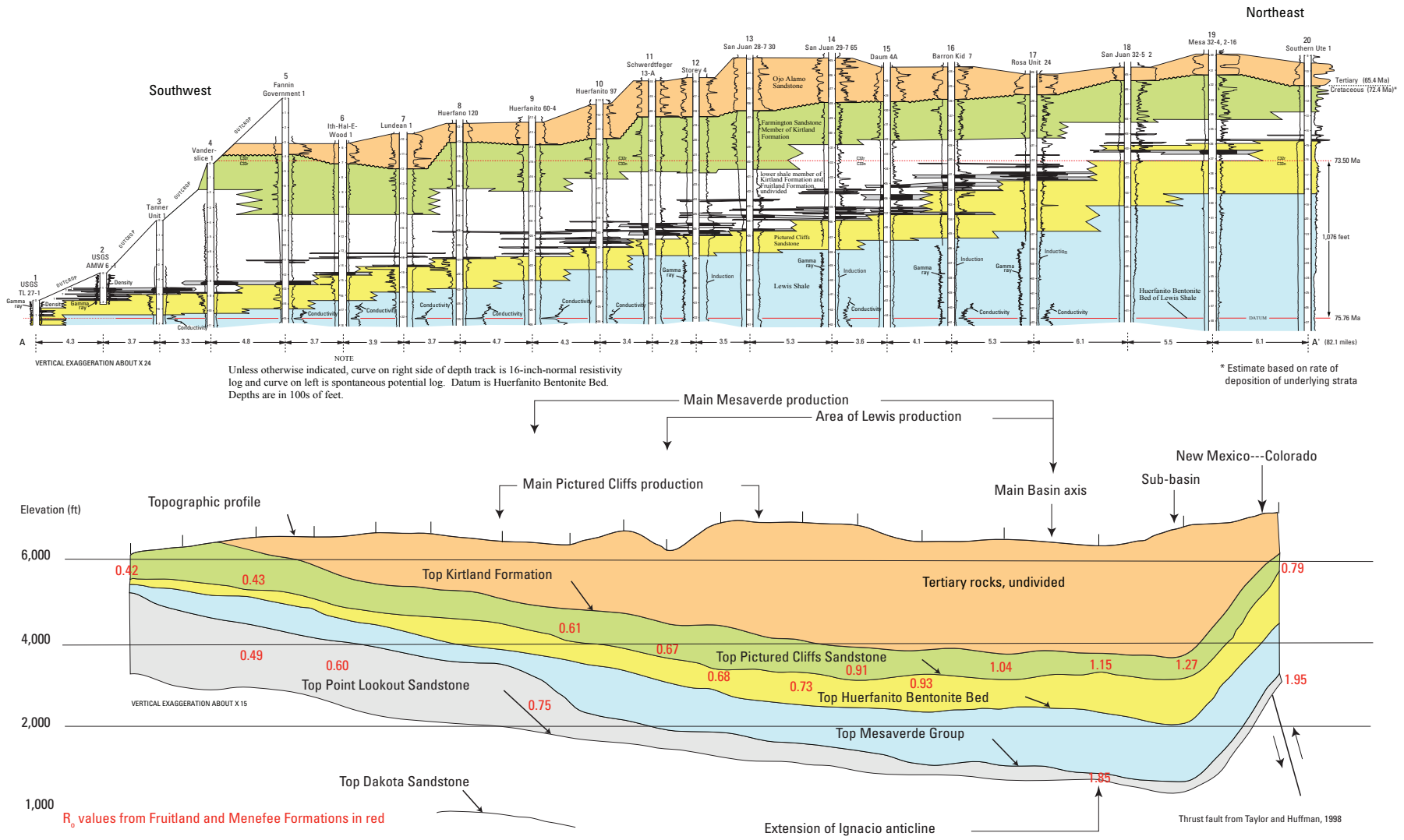


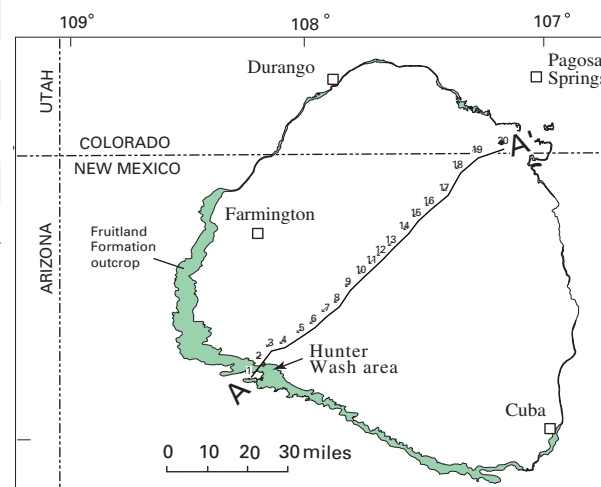
Figure 4. Cross section extending from southwest to northeast across the central San Juan Basin (modified from Fassett, 2000). Structure section at bottom of figure was produced from data from IHS Energy Group (2002). R_m values (in red) were compiled from Fassett and Nuccio (1990) and Law (1992).

List of drill holes on cross section A-A'

Hole number	Company	Drill hole name	Location				Longitude	Latitude
			T.N.	R.W.	Sec.	Quarter		
1	U.S.Geological Survey	Tanner Lake 27-1	23	13	27	NE	-108.20863	36.20174
2	U.S.Geological Survey	Alamo Mesa West 6-1	23	12	6	SW	-108.16351	36.25208
3	Humble Oil & Refining	Tanner Unit 1	24	12	21	SW	-108.12527	36.29552
4	H. L. Fanning	Vanderslice 1	24	12	13	SW	-108.0684	36.30875
5	Davis Oil	Fannin Government 1	24	11	3	NW	-107.99737	36.34906
6	Sun Oil	Heirs Ith-Hal-E-Wood 1	25	10	19	SW	-107.94365	36.38110
7	El Paso Natural Gas	Lundean 1	25	10	9	NE	-107.90435	36.42016
8	El Paso Natural Gas	Huerfano 120	26	10	25	NW	-107.84311	36.45483
9	Turner & Webb	Huerfanito 60-4	26	9	4	SW	-107.79830	36.51276
10	El Paso Natural Gas	Huerfanito 97	27	9	24	SW	-107.74418	36.55835
11	El Paso Natural Gas	Schwerdtfeger 13	27	8	8	NE	-107.70009	36.59342
12	El Paso Natural Gas	Storey 4	28	8	34	NE	-107.66434	36.62203
13	El Paso Natural Gas	San Juan 28-7 30	28	7	18	SW	-107.61931	36.65882
14	El Paso Natural Gas	San Juan 29-7 65	29	7	22	NE	-107.55481	36.71582
15	El Paso Natural Gas	Daum 4-A	29	7	1	NE	-107.51615	36.75915
16	El Paso Natural Gas	Barron Kid 7	30	6	21	NE	-107.46263	36.80087
17	El Paso Natural Gas	Rosa Unit 24	31	5	32	SW	-107.39026	36.85170
18	Stanolind Oil and Gas	San Juan 32-5 Unit	32	5	35	SW	-107.33902	36.93009
19	Phillips Petroleum	Mesa Unit 32-4 2-16	32	4	16	SW	-107.26464	36.98390
20	Stanolind Oil and Gas	Southern Ute 1	32	3	22	NE	-107.15853	37.00997

EXPLANATION

-  Unconformity at Cretaceous-Tertiary boundary; 7-8 m.y. hiatus
-  Position of magnetic-polarity reversal: chron C33n is normal polarity, chron C32r is reversed polarity
-  Black areas within resistivity log curve are coal beds; gray areas show correlations of coal beds between holes
-  Datum: Huerfanito Bentonite Bed; dotted where projected
-  Conglomeratic sandstone (High-energy, braided streams; northerly source area)
-  Fine- to medium-grained sandstones (Low-gradient intermittent small streams; southwest source area)
-  Fine- to medium-grained sandstones, siltstones, mudstones, carbonaceous shales and mudstones and coals (Back shore to lower alluvial plain)
-  Fine- to medium-grained sandstone (Shoreface)
-  Mudstone, limestone concretions, rare thin fine-grained sandstone or siltstone layers (Offshore marine)



MAP SHOWING LINE OF SECTION

Figure 4. Cross section extending from southwest to northeast across the central San Juan Basin (modified from Fassett, 2000). Structure section at bottom of figure was produced from data from IHS Energy Group (2002). R_m values (in red) were compiled from Fassett and Nuccio (1990) and Law (1992).—Continued

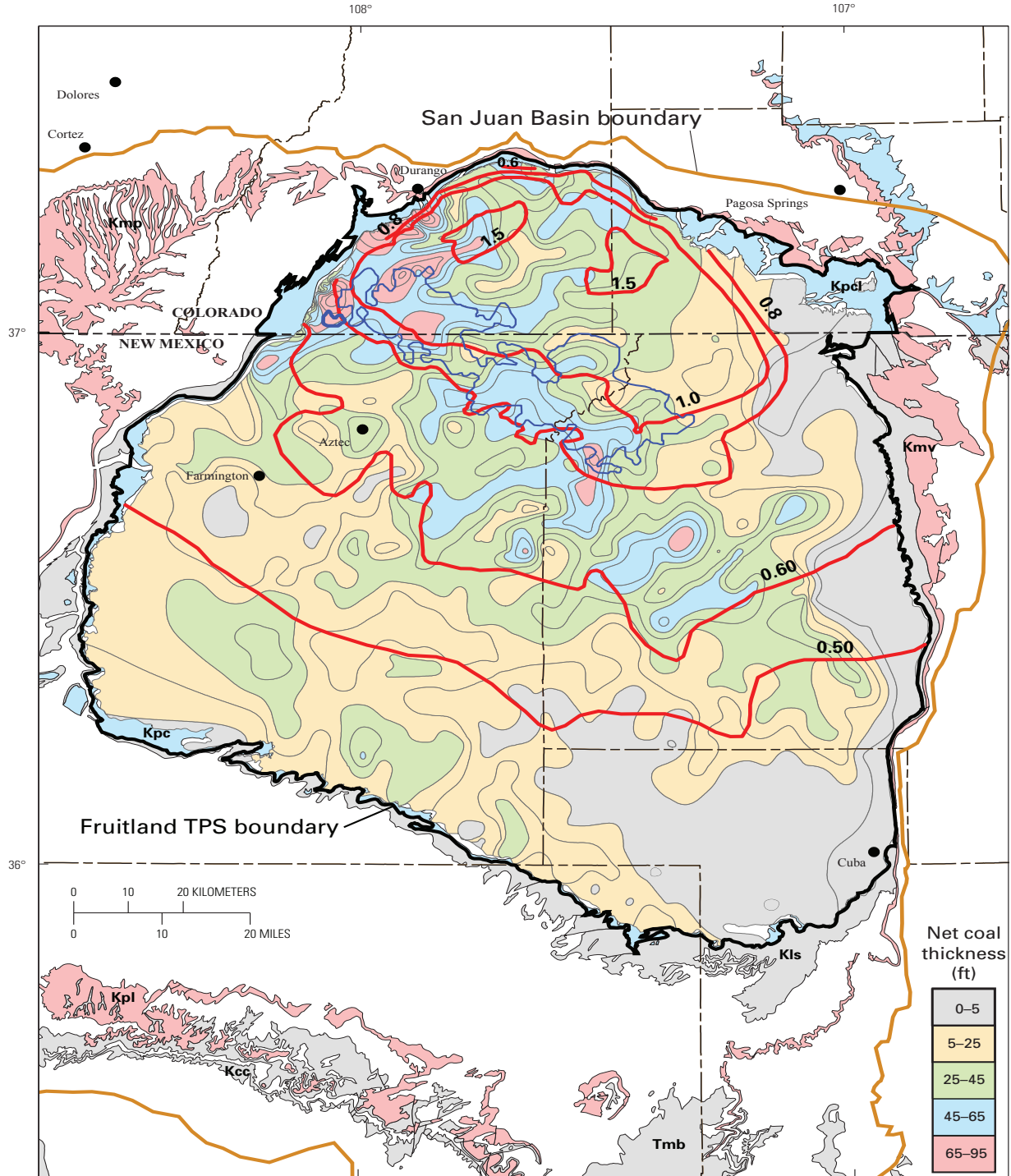


Figure 5. Isopach map of net coal in the Fruitland Formation (modified from Fassett, 2000). Shown are the boundaries of the Fruitland Total Petroleum System (TPS) (black) and Fruitland Fairway Coalbed Gas Assessment Unit (AU) (dark blue). Symbols for geologic map units: Toa, Tertiary Ojo Alamo Sandstone; Tmb, Tertiary Miocene volcanics; Kpc, Pictured Cliffs Sandstone; Kpcl, Pictured Cliffs Sandstone and Lewis Shale; Kls, Lewis Shale; Kcc, Crevasse Canyon Formation; Kmp, Menefee Formation and Point Lookout Sandstone; Kmv, Mesaverde Group; Kpl, Point Lookout Sandstone (Green, 1992; Green and Jones, 1997). Contours (red) show vitrinite reflectance (R_m) values, in percent, from data in Fassett and Nuccio (1990), Law (1992), and Fassett (2000).

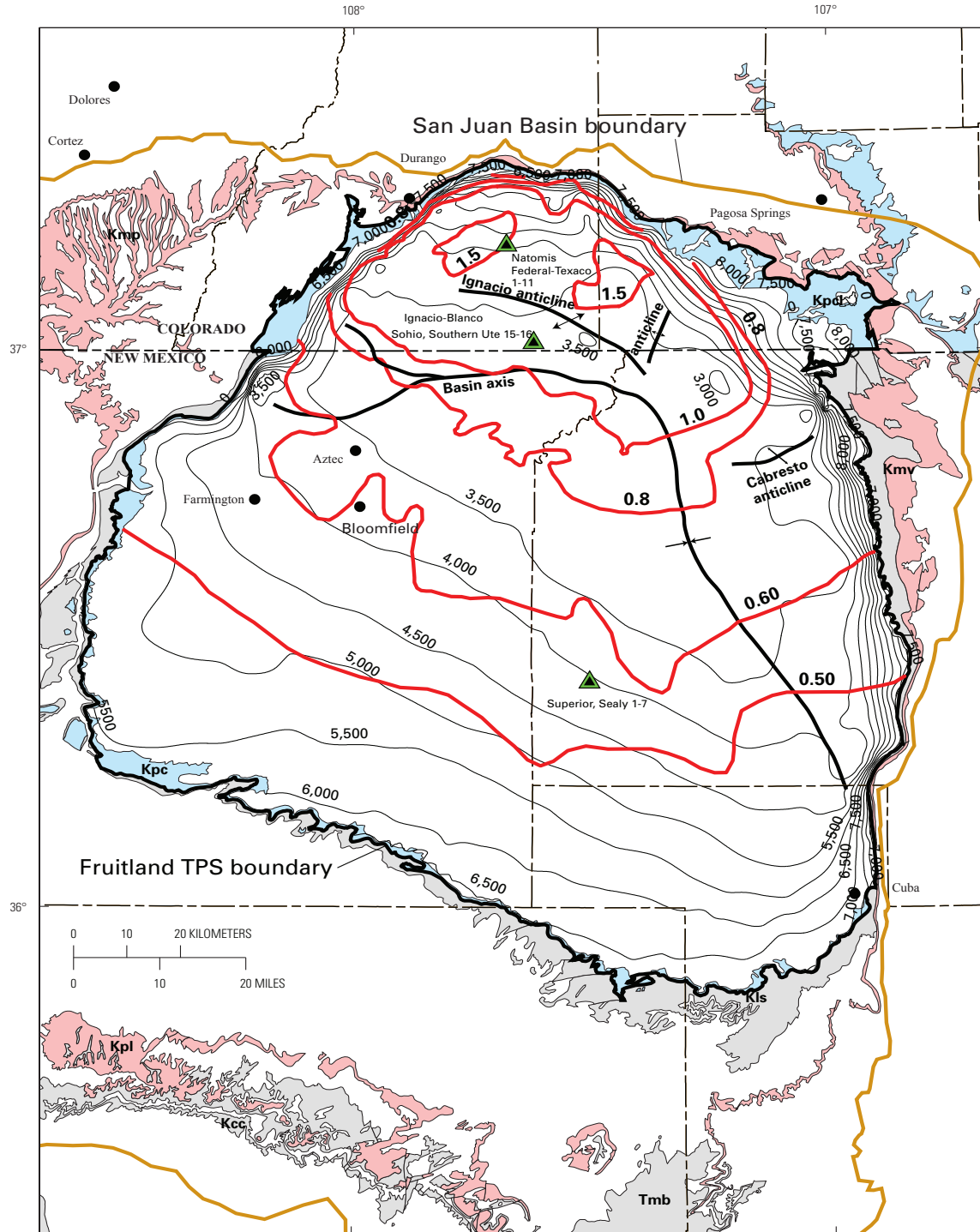


Figure 6. Structure contour map (black lines) drawn on top of the Pictured Cliffs Sandstone (modified from Fassett, 2000). Contour interval 500 ft; datum is mean sea level. Map showing the boundary of the Fruitland Total Petroleum System (heavy black line). Symbols for geologic map units: Toa, Tertiary Ojo Alamo Sandstone; Tmb, Tertiary Miocene volcanics; Kpc, Pictured Cliffs Sandstone; Kpcl, Pictured Cliffs Sandstone and Lewis Shale; Kls, Lewis Shale; Kcc, Crevasse Canyon Formation; Kmp, Menefee Formation and Point Lookout Sandstone; Kmv, Mesaverde Group; Kpl, Point Lookout Sandstone (Green, 1992; Green and Jones, 1997). Contours (red) show vitrinite reflectance (R_m) values, in percent, from data in Fassett and Nuccio (1990), Law (1992), and Fassett (2000). Also shown are the locations of principal folds in the basin and wells (green and black triangles) used to make the burial history curves in this report (figs. 10A–C).

also common. Overall, the Nacimiento ranges from about 500 to 1,800 ft thick (Baltz, 1967; Craigg, 2001) with thicker strata located in the center of the basin. The thick, mudrock-rich central basin strata are thought to have a lacustrine origin (Fassett, 1974). Small quantities of gas are produced from sandstone in the Nacimiento in both the eastern and western parts of the TPS.

The Eocene San Jose Formation is a thick, heterogeneous, terrestrial unit that crops out over the northern and east-central parts of the basin. In Colorado, the San Jose commonly overlies the Animas Formation, and in New Mexico it overlies the Nacimiento Formation. The San Jose has been divided into various formal and informal members in studies including those by Baltz (1967), Brimhall (1973), and Smith (1992). In general, the lower part consists of stacked fluvial sandstone channels assigned to the Cuba Mesa Member. The middle part consists of the sandstone-rich Ditch Canyon and Llaves Members and the mudrock-dominated Regina Member (Baltz, 1967; Smith, 1992). The upper part of the San Jose consists of the siltstone-dominated Tapicitos Member. These members are not all present in the same areas; the sequence of sandstone- and mudrock-dominated intervals changes depending on where the San Jose is examined. Carbonaceous shale or coal/lignite beds have not been reported from any part of the San Jose. The San Jose is the uppermost rock unit in this part of the San Juan Basin, and its original thickness is unknown because of erosion. Thicknesses of less than 200 ft to more than 2,700 ft have been reported. In the area of the Cabresto Canyon gas field (see fig. 52) and the Cabresto anticline (fig. 6), the San Jose is about 2,100 ft thick.

The relatively shallow depth and high porosity of most Tertiary rocks in the basin contribute to their being water saturated in many areas, which may limit their potential for oil and gas production. According to Craigg (2001), the Ojo Alamo Sandstone is a dependable aquifer and produces water from wells and springs. The Animas and Nacimiento Formations have similar water-yielding capacity—only used locally as aquifers in areas where thin, fine-grained sandstone beds predominate (mainly in the central and southern parts of the basin), but increasing in quality in the north and northeast where sandstone beds are more abundant (Craigg, 2001). The San Jose is an aquifer in many parts of the basin, decreasing its potential as a gas-bearing unit (Anonymous, 1998).

Hydrocarbon Source Rock

The Fruitland TPS has two principal sources of hydrocarbons: coal beds and carbonaceous shale in the Fruitland Formation. The coal beds are thought to be the principal source of hydrocarbons in the Pictured Cliffs Sandstone and Fruitland Formation (Rice, 1983). The Kirtland Shale contains a high percentage of shale beds; however, little is known about the hydrocarbon generative capability of these beds. One sample from the Kirtland had a total organic carbon (TOC) value of 0.17 (Threlkeld, written commun., 2001). Because of

the possible low TOC content, the shales are not considered to be a major source of hydrocarbons in sandstone beds of the Kirtland, such as the Farmington Sandstone Member, which locally has produced gas and condensate.

The Paleocene Ojo Alamo Sandstone contains local concentrations of gas on the northeast side of the basin. However, few interbedded shale beds occur in the Ojo Alamo (Fassett and Hinds, 1971; Sikkink, 1987), so the gas must have been generated in some other formation. Shale beds in the Paleocene Nacimiento Formation are of nonmarine origin and probably contain low TOC content, although a few scattered lignite and carbonaceous shale beds have been documented (Baltz, 1967). Two shale samples from the Nacimiento had TOC values less than 0.5 (Threlkeld, written commun., 2001). Shale beds in the Nacimiento are not thought to be the source of gas found in small accumulations in the Nacimiento or the overlying Eocene San Jose Formation.

Because Tertiary strata do not appear to contain shale beds capable of producing hydrocarbons in any measurable quantity, hydrocarbons found in them must have been generated elsewhere. The most likely source of these hydrocarbons is the coal in the underlying Fruitland Formation. Therefore, because the Fruitland coal beds are considered to be the principal source of hydrocarbons in strata above the Lewis Shale, all strata above the Lewis and all hydrocarbons, discovered or not, in these strata have been placed in the Fruitland TPS.

Fruitland Formation Source Rock Characterization

Vitrinite Reflectance

Coal beds are present throughout the Fruitland Formation; they are thickest in the central and northern part and thinnest in the east and southeast part of the TPS (fig. 5). Vitrinite reflectance values from coal samples increase from less than 0.5 percent in the southwest to over 1.5 percent in the north (fig. 5) (Rice, 1983; Fassett, 2000). The increase in reflectance values corresponds to an increase in coal rank from subbituminous to medium and low volatile bituminous (Rice, 1983). It has been suggested that coal will produce thermal methane at vitrinite reflectance values of 0.5 percent and greater and microbial gas at values less than this (Scott, 1994). Using this vitrinite reflectance value as a cutoff for thermal-gas generation, most of the coals in the Fruitland Formation are considered capable of producing thermogenic methane.

The vitrinite isorefectance lines are subparallel to structure contours drawn on top of the Pictured Cliffs Sandstone (fig. 6) and on the underlying Huerfano Bentonite Bed (Fassett, 2000). The dominant northwest–southeast orientation of the isorefectance lines and structure contours reflect present-day structure in the basin. Because the rank of coal generally parallels the structural configuration of the basin, the pattern of thermal maturity of the coals is primarily related to past depth of burial. Overburden above the coals is thickest in the northern part of the TPS and thins gradually to the

southwest where the Fruitland is exposed at the outcrop, as well as toward outcrops at the other basin margins (Fassett and Hinds, 1971; Scott and others, 1994b; Fassett, 2000). The most mature coal does not everywhere coincide with the area of greatest past basin subsidence or with present overburden in the basin. It has been suggested that the isolated areas of greatest thermal maturity have been influenced by emplacement of batholiths in the San Juan Mountains during the Oligocene (Rice, 1983) by a deep-seated heat source underlying the northern part of the San Juan Basin, or by a thermal convective cell that channeled heated fluids vertically upward in this area (Law, 1992). Isoreflectance contours in some areas are subparallel to thick trends in net coal, whereas in other areas they crosscut net coal trends (fig. 5) (Scott and others, 1994b; Fassett, 2000).

Geochemical Characteristics

Table 2 is a summary of the principal geochemical parameters of Fruitland coal beds. Geochemical analyses of Fruitland coal beds show they have a high total organic carbon (TOC) as compared to the average carbonaceous shale, which generally has less than 10 percent TOC. The hydrogen index range, which is often used to identify source rock type, suggests a mixture of type-II and type-III organic matter. Based on the maceral composition and the hydrogen index range of 23–380 mg/g for the Fruitland coals, it is expected that the bulk of the hydrocarbons produced will be wet or dry gas (Jones, 1987) (table 2), although small quantities of oil and condensate have also been reported from reservoirs in the Fruitland TPS (Clayton and others, 1991).

The composition of gas produced from coals is dependent, in part, on the maceral composition of the coal. Coals are composed of type-III terrestrial organic matter and generally consist of various proportions of vitrinite, liptinite (exinite), and inertinite macerals. Vitrinite is derived from lignin and cellulose walls of plant matter, and liptinite is derived from pollens, resins, waxes, and fats and is hydrogen rich (Stach and others, 1982). Vitrinites are composed of structured humic material and matrix gels; the humic material tends to produce chemically dry gas, whereas, the matrix gels, because they are more hydrogen rich, tend to produce chemically wetter gas (Tissot and Welte, 1987; Rice and others, 1989, 1992;

Clayton and others, 1991; Rice, 1993). Coals from the Fruitland Formation have been documented to contain greater than 80-percent vitrinite, composed mostly of humic material (Rice and others, 1989; Mavor and Nelson, 1997). However, matrix gels and liptinite macerals make up as much as 30 percent of some coal samples; thus, these coals are capable of producing some oil and wet gas (samples that contain more than 1–2 percent ethane and higher molecular weight hydrocarbons) (Rice and others, 1989; Rice, 1993).

The composition of gas produced from the coal beds is not just a function of organic matter composition but is also related to the thermal maturity of the coals in addition to any microbial-gas generation. A number of studies have discussed the variation in composition of the coal-bed gases and related these to thermal maturity patterns in the basin (Rice, 1983; Rice and others, 1989; Scott and others, 1991; Scott, 1994; Scott and others, 1994a). Fruitland coal-produced gases can be separated into two general groups:

1. overpressured and
2. underpressured to normally pressured (table 3), which are coincident with the present-day pressure distribution in the Fruitland Formation (Scott, 1994).

Generally, gas from the overpressured area is drier and contains more carbon dioxide (table 3). The overpressured area lies approximately between the 0.8- and 1.6-percent R_m vitrinite isorefectance contours (fig. 5). Wet Fruitland gases (those with 1 percent or more of high molecular weight hydrocarbons) generally occur between the 0.49- and 0.75-percent R_m vitrinite reflectance contours (Scott, 1994). However, dry gas may occur outside the overpressured area, and wet gas has been found within the overpressured area. It has been suggested that the regional distribution in composition of the coal-derived gas is not just dependent on coal rank and coal composition, but basin hydrology is also a contributing factor because the gas wetness correlates better with pressure regimes in the Fruitland (Scott and Kaiser, 1991; Scott, 1994).

The range of gas wetness, CO_2 concentration, and isotopes of methane and carbon dioxide reported from Fruitland TPS reservoirs are summarized in table 3. An understanding of the probable distribution of wet gas, which determines the expectation of NGLs, and the distribution of CO_2 concentrations, which affects British Thermal Unit (BTU) values, can

Table 2. Means, standard deviations, ranges, and number of determinations for total organic carbon contents and hydrogen indices of the Fruitland Formation source rocks in the Fruitland Total Petroleum System, San Juan Basin, Colorado and New Mexico. Total organic carbon contents and hydrogen indices are summarized from samples with $T_{max} \leq 450^\circ C$. Data from Rice and others (1989), Clayton and others (1991), Pasley and others (1991), Michael and others (1993), Gries and others (1997), and Threlkeld (written commun., 2001).

Interval	Total organic carbon (%)	Hydrogen index (mg/g) (Rock-Eval)	Expected types of HC
Fruitland Formation coal	58 ± 15 range = 24–72 (n = 24)	225 ± 90 range = 23–380 (n = 24)	Wet and/or dry gas

be used in economic analysis of Fruitland gas. Most Fruitland wells that produce wet gas produce lower volumes of gas when compared to wells that produce dry gas. Gas wetness values and CO₂ concentration in gases from underpressured and normally pressured Fruitland Formation reservoirs and the Pictured Cliffs Sandstone reservoirs are similar (table 3) (figs. 7A, 7B, 8A, and 8B). Gases from the overpressured Fruitland coal are drier (Scott, 1994) and tend to have higher CO₂ contents—although these contents vary throughout the overpressured area (Scott, 1994)—compared to the underpressured and normally pressured Fruitland and Pictured Cliffs reservoirs. The distribution of gas wetness in the Pictured Cliffs Sandstone and Fruitland Formation appears to be independent of present depth of burial (figs. 9A and 9B). Gas wetness values in Pictured Cliffs and Fruitland generally appear to be independent of methane δ¹³C (figs. 7A and 7B). However, gases in the Pictured Cliffs tend to be wet (wetness values >1 percent), whereas those in the Fruitland are either wet or dry (figs. 8A and 8B). Data used in figures 7 and 8 may not be equivalent, because carbon-isotope values of methane were not available for all samples (Threlkeld, written commun., 2001).

Because microbial processes are important in many coal-bed-methane gas systems, methane δ¹³C can provide information on the thermal history of the source beds and on the relative contribution of thermogenic and microbial processes to gas generation. The relative contribution of thermogenic and microbial processes is important to understand in the Fruitland TPS because it has been suggested that as much as 25–50 percent of the gas is microbially generated in Fruitland reservoirs in the Fruitland Fairway Coalbed Gas AU (Scott and others, 1991). Methane δ¹³C varies little in either the Fruitland Formation or the Pictured Cliffs Sandstone gases, although a few samples have values as much as 10 per mil greater or less than the average value (figs. 7A and 7B). The similarity in average methane δ¹³C values for Fruitland and Pictured

Cliffs gases suggests a common source for the gas. Late-stage (secondary) microbial methane has been reported from the northern, southern, and northwestern part of the TPS in areas influenced by meteoric recharge. Evidence for microbial activity in the recent geologic past is based on heavy δ¹³C isotopes of dissolved inorganic carbon in the waters co-produced with the coal-bed gas and from heavy δ¹³C isotopes of carbon in carbon dioxide and lighter than expected δ¹³C of the methane in the gas (Scott and others, 1991; Scott, 1994).

Oils (condensates) are produced from some of the Fruitland coals (Clayton and others, 1991). These oils can be distinguished from other Cretaceous, Pennsylvanian, and Jurassic oils in the basin by their isoprenoid ratios and carbon-isotope compositions. Oils produced from Fruitland coals and Pictured Cliffs Sandstone reservoirs differ in their pristane/phytane (Pr/Py) ratios. Pr/Py in condensates from the Pictured Cliffs are roughly half (0.5) that found in the Fruitland samples, which is greater than 1 (Rice and others, 1989; Clayton and others, 1991). Other differences in the characteristics of Fruitland Formation and Pictured Cliffs Sandstone oils suggest that the Pictured Cliffs Sandstone oils may have been partially sourced from the underlying Lewis Shale (Clayton and others, 1991); this represents an exception to our earlier statement that all hydrocarbons in the Fruitland TPS were sourced from the Fruitland. Gas wetness in the Pictured Cliffs Sandstone gases has been documented to increase in the east and southeast part of the TPS. In this area, the net Fruitland coal thickness decreases (fig. 5). This inverse relation suggests a contribution of gas to the Pictured Cliffs from the Lewis Shale in the eastern part of the Fruitland TPS. The relative contribution of Lewis-sourced gas and oil cannot be estimated, and for the purpose of this assessment, the gas resources are treated as having been mostly derived from Fruitland source rocks. Oil in the Pictured Cliffs Continuous Gas AU is minor and values are too low to be assessed. A discussion of the Lewis TPS is found in chapter 5.

Table 3. Means, standard deviations, and number of chemical analyses of produced natural gases from the Fruitland Formation and Pictured Cliffs Sandstone, San Juan Basin, New Mexico and Colorado in the Fruitland Total Petroleum System. The Fruitland gases have been differentiated between the overpressured and normally to underpressured areas of production, because their composition differs between the two pressure regimes. Data from Rice (1983), Moore and Sigler (1987), Rice and others (1988), Scott and others (1991).

[Wetness percent = 100 x (1-[mol%C₂/Σmol%C₁-C₃]). n, number of samples; avg., average; Fm, Formation]

Producing interval	Wetness (%)	CO ₂ (mole percent)	δ ¹³ C _{CH₄} (per mil)	δ ¹³ C _{CO₂} (per mil)
Fruitland Fm. coal, overpressured,	3 ± 3 (n = 157)	6.4 ± 3.7 (n = 157)	-39.8 ± 6.9 (n = 73)	12.8 ± 4.2 (n = 8)
Fruitland Fm. coal, underpressured and normal pressured	8 ± 4 (n = 111)	1.4 ± 1.5 (n = 111)	avg = -42.5	
Pictured Cliffs Sandstone	10.5 ± 3.9 (n = 95)	0.7 ± 0.9 (n = 95)	-43.5 ± 4.5 (n = 52) avg = -42.5	6.9 ± 14.0 (n = 5)

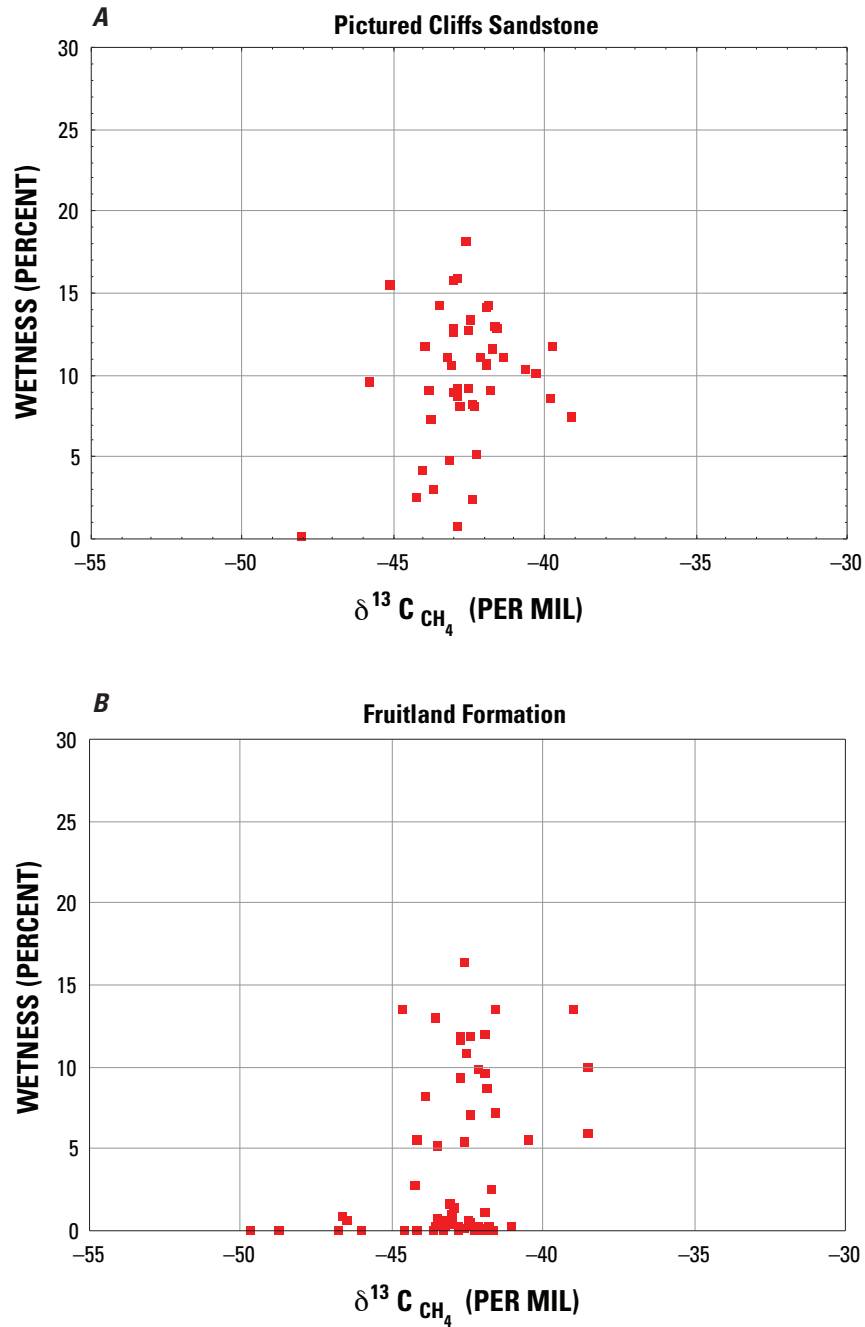


Figure 7. Crossplot showing relation between gas methane $\delta^{13}\text{C}$ and gas wetness, where wetness percent = $100 \times (1 - [\text{mol}\% \text{C}_7 / \sum \text{mol}\% \text{C}_1 - \text{C}_5])$. (A) Pictured Cliffs Sandstone, N= 45 samples; (B) Fruitland Formation, N= 68 samples. Data are from Threlkeld (written commun., 2001).

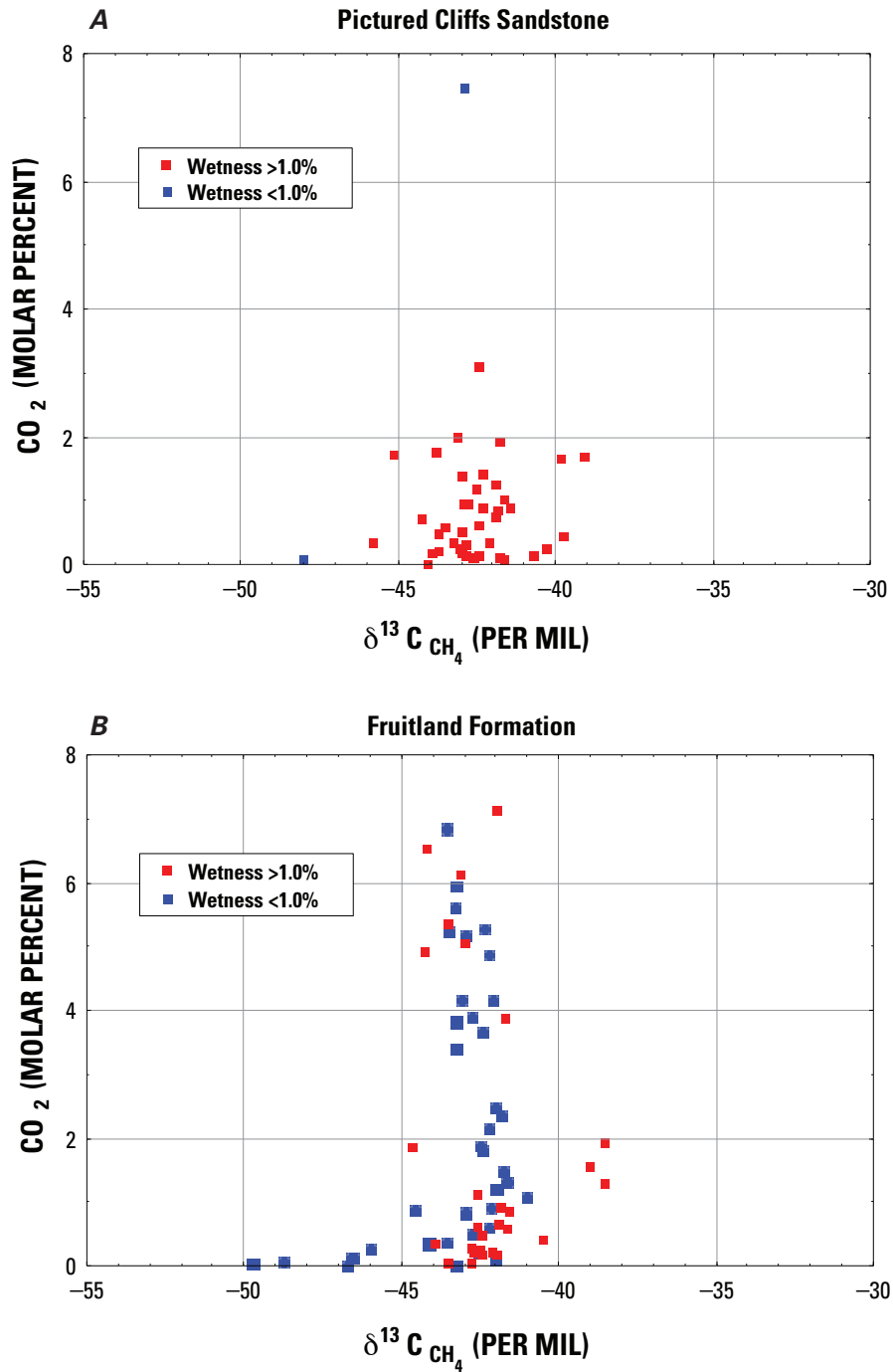


Figure 8. Crossplot showing relation between gas methane $\delta^{13}\text{C}$, CO_2 content, and gas wetness, where wetness percent = $100 \times (1 - [\text{mol}\% \text{C}_1 / \sum \text{mol}\% \text{C}_1 - \text{C}_5])$. Data are from Threlkeld (written commun., 2001). (A) Pictured Cliffs Sandstone; N= 45 samples. (B) Fruitland Formation; N= 68 samples.

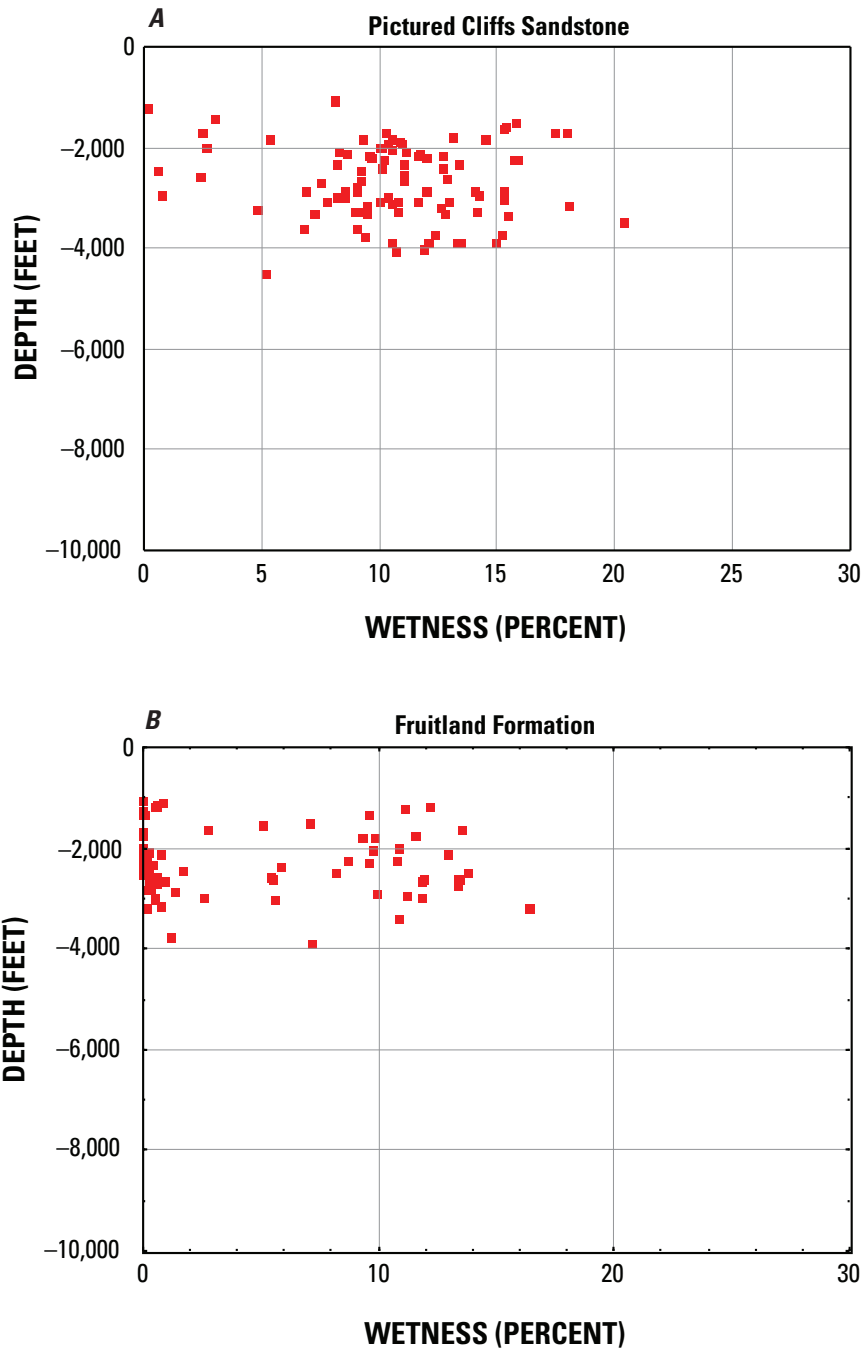


Figure 9. Crossplot showing relation between gas wetness, where wetness percent = $100 \times (1 - [\text{mol}\%C_1 / \sum \text{mol}\%C_1 - C_5])$ and present reservoir depth. Data are from Threlkeld (written commun., 2001). (A) Pictured Cliffs Sandstone; N= 95 samples. (B) Fruitland Formation; N= 85 samples.

Source Rock Maturation and Thermal History

The thermal history of the Fruitland coal beds is closely linked to the structural evolution of the basin. During the Late Cretaceous, about 90 Ma (million years before present), the central part of the San Juan Basin began to subside slowly. The Fruitland Formation was deposited in a span of about 1 million years, roughly from 75.5 to 74.5 Ma (Fassett, 2000), during the early stage of basin subsidence. Maximum subsidence in the deepest part of the basin, north of the Colorado-New Mexico State line, occurred during the late Oligocene. During the Miocene, the basin axis shifted to the area south of the Colorado-New Mexico State line. Differential uplift, erosion, and thermal cooling throughout the basin followed basin subsidence. Rocks in the San Juan Basin are generally underpressured. The exception to this is an area of overpressuring in the Fruitland Formation, which extends southeastward from the outcrops along the northern rim of the basin. The overpressuring has been attributed to artesian conditions (Scott and Kaiser, 1991; Scott, 1994).

Burial history curves can be used to examine the relation between structural evolution of the basin and thermal maturation of coals for different parts of the basin. Thermal maturation studies (Bond, 1984; Law, 1992) indicate changes in the geothermal gradient in the basin at different periods of geologic time. These changes may occur at different times for different parts of the basin. The highest geothermal gradient was reached in the Oligocene (Bond, 1984). The southernmost burial curve is for the Superior Sealy 1-7 well located in the southern part of the central basin, north of the Chaco slope (figs. 1, 2, and 10A) (Law, 1992) and is peripheral to the deep part of the central basin. In this area, vitrinite reflectance values in the Fruitland are between 0.5- and 0.6-percent R_m ; these values are within the early stage of thermal-methane generation from coals (Scott and others, 1994b). Gas produced would likely be wet, containing several percent or more ethane and higher hydrocarbons, in addition to methane, and a gas index (C_1/C_{1-5}) less than 0.94 (Rice and others, 1992; Scott and others, 1994b). The burial reconstruction indicates that the Fruitland in this area was buried to a depth of about 4,000 ft, and it stayed at this depth for about 27 m.y. (from 40 to 13 Ma).

Two burial history curves (figs. 2, 10B, and 10C) (Bond, 1984; Law, 1992) from the northern part of the basin (and TPS) show slightly different profiles and hence, structural evolution for the deep part of the basin. The composite curve for the Bakke Southern Ute 2 and Sohio Southern Ute 15-16 wells (fig. 10B) indicates that the area near the present-day axis of the basin continued to subside until the late Miocene. Maximum burial in this area was in the late Miocene (~13 Ma). Although temperature profiles through this well have not been constructed, maximum temperature in the Fruitland, based on mean vitrinite reflectance values between 1.2- and 1.3-percent R_m , would only have been slightly less than those for the northern burial reconstruction. The duration of maximum temperature would have been less than for the northern well because maximum burial occurred about 12 million years later. The

Fruitland in this area was at one time buried to depths greater than 6,000 ft; following post-Miocene uplift and erosion, the formation is now found at about 3,000 ft. Vitrinite reflectance values in the area of this well are bounded by the 1.0- and 1.5-percent R_m isoreflectance contours.

Coal beds in this area are within the medium to low volatile bituminous rank and are expected to produce both wet and dry gas. The zone of oil generation is commonly taken to extend from 0.5- to 1.3-percent R_m (Tissot and Welte, 1987), and thus, there is an expectation that most Fruitland gas from this area would be wet. However, the degree of gas wetness might be different for coal-derived gases when compared to gas derived from typical marine organic matter. Scott and others (1994b) suggested that maximum wet-gas generation in coals ceases by a vitrinite reflectance value of 0.8-percent R_m , and secondary cracking of condensate occurs between vitrinite reflectance values of 1.0- to 1.35-percent R_m . This well is within the area of overpressuring as defined above, and gas from the overpressured area tends to be dry. The dry nature of the gas in this area can be attributed to two factors:

1. organic matter type, and
2. length of time of high heat history or time-temperature factors.

Fruitland coals are dominantly composed of humic material, which primarily produces dry rather than wet gas. It has been well documented that thermal gases become progressively drier with increased temperature and thermal maturity of organic matter (Scott, 1994). Any wet gas originally produced in this area may have thermally cracked during prolonged heating through the Miocene, cumulatively producing overall dry gas. Alternatively, Bond (1984) suggested that the high temperatures reached in Cretaceous rocks from late Eocene through late Oligocene (10- to 15-m.y. duration) were more important to thermal maturation of organic matter than the duration of the heat event in the Miocene, which was geologically short. Bond's model does not specifically address gas composition changes in coals with temperature or time.

The northernmost burial history curve for the Natomas North America Federal-Texaco 1-11 well (figs. 1 and 10C) (Bond, 1984) indicates that subsidence of the basin in this area ceased in the late Oligocene and that uplift and erosion followed. The top of the Pictured Cliffs can be used as a proxy for the base of the Fruitland in this well. The burial reconstruction indicates that the top of the Pictured Cliffs may have been buried more than 8,000 ft. Assuming the reconstruction is accurate, it suggests that the deep part of the San Juan Basin was at one time north of the present-day basin axis and that the axis of the basin shifted to the south as the northern part of the basin was uplifted. This shift may partially explain the high vitrinite reflectance values (>1.5-percent R_m) in the area of this well.

The area of the Natomas North America Federal-Texaco 1-11 well also coincides with a northwest-southeast trend of high R_m values in the Fruitland (fig. 1) (Law, 1992; Fassett, 2000). The localized higher R_m values along this trend are indicative of locally higher heat flow. Magnetic data does not indicate the presence of buried intrusions in the

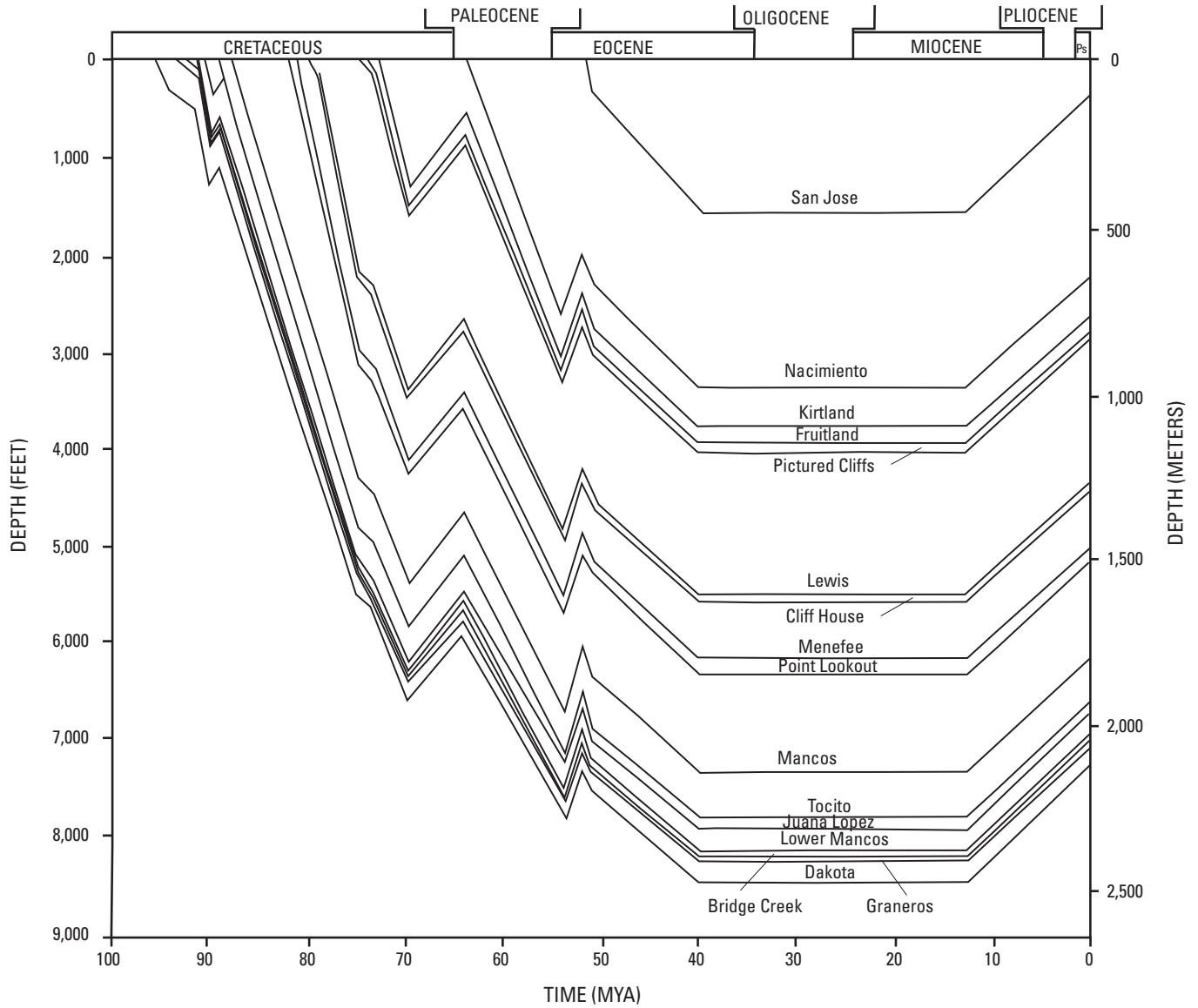


Figure 10A. Burial history curve for the Superior Sealy 1-7 well in the southern part of the central San Juan Basin (modified from Law, 1992). Geologic time scale is from the Geological Society of America web page <http://www.geosociety.org/science/timescale/timescl.htm>, last accessed 2/1/2008. Ps, Pleistocene; MYA, million years ago.

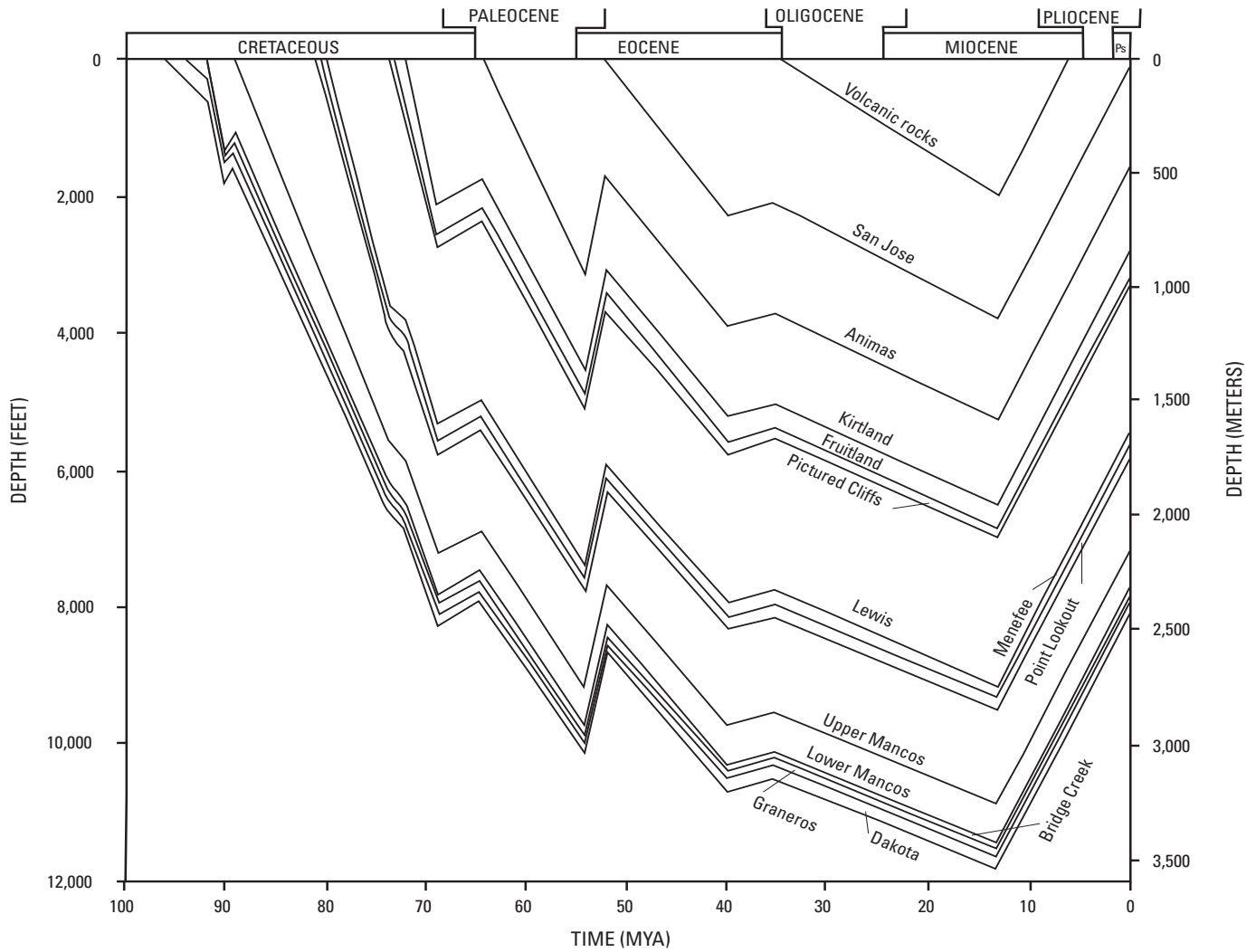


Figure 10B. Composite burial history curve for the Bakke Southern Ute 2-Sohio Southern Ute 15-16 well in the northern part of the central San Juan Basin (modified from Law, 1992). Geologic time scale is from the Geological Society of America web page <http://www.geosociety.org/science/timescale/timescl.htm>, last accessed 2/1/2008. Ps, Pleistocene; MYA, million years ago.

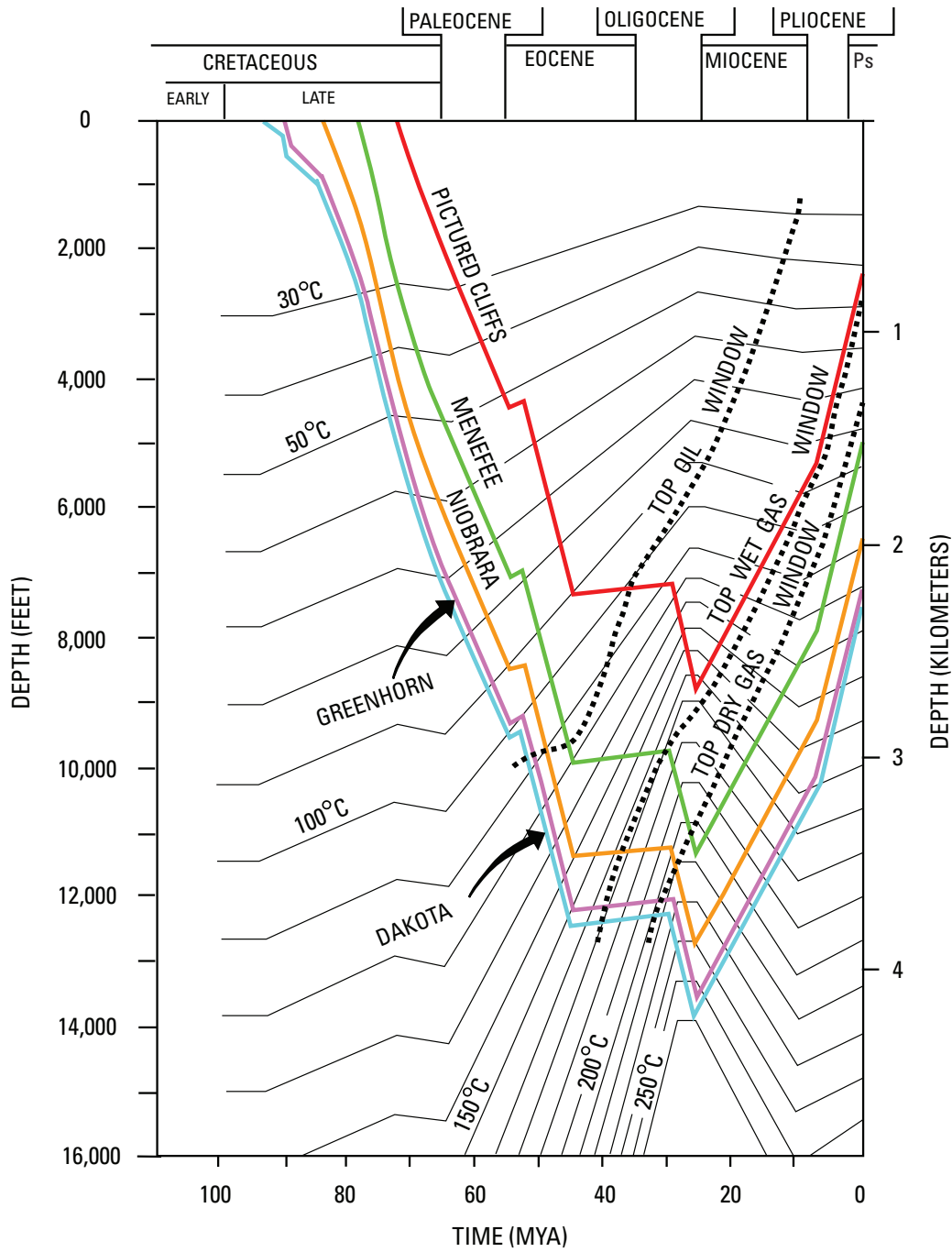


Figure 10C. Burial history curve for the Natomas North America 1-11 Federal-Texaco 1-11 well in the northern part of the San Juan Basin (modified from Bond, 1984). Geologic time scale is from the Geological Society of America web page <http://www.geosociety.org/science/timescale/timescl.htm>, last accessed 2/1/2008. Ps, Pleistocene; MYA, million years ago.

area (Fassett, 2000); thus, the higher heat flow is not related to intrusive activity but is most likely a reflection of depth of burial accompanied by a higher geothermal gradient. The northwest–southeast trend of high R_m values may reflect the former position of the axis of the basin (Fassett, 2000) before it shifted to the south in the Miocene as the northern part of the basin was uplifted. The area of the present-day structural axis of the basin (fig. 6) is determined from structure contours drawn on the top of the Huerfano Bentonite Bed (Fassett, 2000) and represents the deepest part of the San Juan Basin during the Miocene (see burial history curve, fig. 10B).

Fruitland Formation Hydrology

Pressure Regimes in the Fruitland Formation

The area of overpressure in the Fruitland Formation is found throughout most of Colorado and extreme northern New Mexico where the Fruitland is preserved (Kaiser and others, 1994; Scott and others, 1994b, their fig. 4). The overpressure is considered to be a result of artesian conditions (piston flow) that developed from the Pliocene to the present (Oldacker, 1991; Scott and others, 1994b; Cox and others, 2001). Overpressuring under artesian conditions results when pressure in a formation, as a consequence of downward confined flow of water, rises above hydrostatic pressure for the formation at any given location (Scott and others, 1994b). When this happens, the hydraulic head rises above the land surface. It is important to determine when initial overpressure conditions were established because once these conditions (assuming no overpressure is a remnant of thermal-gas generation) were established along the southern part of the overpressure boundary, the younger water can displace older water efficiently only if there is leakage of pressure. The system acts like a giant piston. When pushing more water in at the updip end, this water can only migrate downdip if there are pressure leaks in the system.

If there are no leaks or if leakage is slow in the southern part of the overpressured system, the updip water cannot migrate very far or fast. If there are few pressure leaks, the waters can only mix slowly by diffusion. Understanding this scenario is important when evaluating the model of timing of generation of late-stage microbial gas and hence its contribution to Fruitland gas production.

The overpressure conditions observed today are superimposed on past geologic conditions, such as basin subsidence and tectonism, thermal maturity, coal composition, and geohydrology that initially influenced the generation and composition of coal-bed gas. The overpressuring is apparently unrelated to thermal-gas production (Scott and others, 1994b). In the geologic model presented herein and by others, most of the thermally derived coal-bed gas probably ceased forming after the early late Miocene. Generation of thermal gas may have ceased somewhat earlier north and south of the area of the present-day basin structural axis, which achieved its current configuration in the Miocene.

Meteoric Water Incursion

Water produced from the Fruitland Formation probably is of various ages. Concepts of fluid flow and distribution of stable isotopes of water in sedimentary basins suggests that the oldest post-depositional meteoric water would reside at the distal ends of the flow paths (Fritz and Fontes, 1980; Criss, 1999; Cox and others, 2001). Mixing of connate water and younger water has occurred along the flow paths. It has been proposed that meteoric waters entering the Fruitland would be younger than the period of maximum thermal-gas generation (Kaiser and Ayers, 1994; Kaiser and others, 1994; Scott and others, 1994b). The principal role of groundwater flow would be to

1. redistribute any gas that might be carried in solution;
2. affect the amount of water produced at any particular well;
3. permit the generation of younger microbial gas by CO_2 reduction, as a consequence of the introduction of methane-producing bacteria; and
4. possibly destroy existing gas because of oxidation of methane by certain bacteria.

The rate of groundwater flow through the now overpressured area would be influenced by

1. the distribution of facies (that is geometry of coal, shale, and sandstone at any depth);
2. the development and direction of cleats and faults, which serve as the principal conduits for fluid movement;
3. the rate of pressure leakage as a consequence of discharge of water or vertical migration of fluids through faults; and
4. the regional distribution of Fruitland outcrops, throughout geologic time, as younger formations were eroded from the area of the northern part of the San Juan Basin.

In the latter case, the outcrop area that has received meteoric water recharge has been reduced through erosion to its present-day configuration.

The areal extent of the Fruitland Formation affected by the post-deposition introduction of meteoric water can be partly observed in the regional distribution of $\delta^{18}\text{O}$ (fig. 11) and δD (deuterium) of produced waters (Cox and others, 2001; Snyder and others, 2003). The area studied corresponds approximately, but not entirely, with the area of artesian overpressure (fig. 12). Note that the inferred direction of meteoric flow, based on $\delta^{18}\text{O}$ isotopes of -16 to -13 per mil in the produced water (fig. 11), and the areal distribution of overpressure and underpressure (fig. 12) have different orientations. The overpressure area has a dominant southeast orientation in the northeastern part of the TPS, whereas in the same area, meteoric water flow is north–south, coincident with the modern drainage of the Los Pinos River (fig. 11). The maps showing $\delta^{18}\text{O}$ and δD distribution (Cox and others, 2001; Snyder and others, 2003) are not contoured on a single

horizon and therefore only provide a general picture of relative groundwater movement in the Fruitland (an important point when considering rates and times of fluid movement, timing of overpressure, and generation of late-stage microbial gas). Cox and others (2001) suggested that the distribution of the $\delta^{18}\text{O}$ isotope (fig. 11) in the produced water is related to incursion of meteoric water and that little rock-water interaction, which would alter the $\delta^{18}\text{O}$ values, has occurred. The distribution and shifts in the corresponding δD values were also considered to reflect the incursion of meteoric water, except that some sample values reflect the exchange in deuterium isotopes between the water and the coal-derived methane (Kaiser and others, 1994; Cox and others, 2001).

In the northern part of the San Juan Basin, the regional distribution of the $\delta^{18}\text{O}$ in waters produced from the Fruitland Formation (fig. 11) indicates three areas of southerly, southeasterly, and southwesterly directed flow paths of isotopically light water (-16 to -13 per mil $\delta^{18}\text{O}$) (Cox and others, 2001). The eastern path is elongate north-south and is subparallel in part to

1. the Spring Creek anticline, a south to southeasterly plunging anticline (Harr, 1988, his fig. 3), and
2. the unnamed southeast plunging syncline that separates Spring Creek and Ignacio anticlines and the course of Los Pinos River (fig. 11).

The distribution of $\delta^{18}\text{O}$ isotopes of the middle flow path, which trends east to southeast, appears to be influenced, at least in part, by the position of the Ignacio anticline, an east- to southeast-trending structure in Colorado, and in part by the Bondad anticline (fig. 11), an east- to southwest-trending anticline (Harr, 1988, his fig. 3). The distribution of $\delta^{18}\text{O}$ isotopes of the western flow path has a general south to southwest trend and tends to be subparallel to the courses of the Animas and Florida Rivers (fig. 11) and also to a south-plunging structural low on top of the Mancos Shale (Harr, 1988, his fig. 3). Although it has been suggested that the flow of water in the Fruitland Formation corresponds to the presently defined potentiometric surfaces (fig. 12), it appears that the flow paths, as defined by $\delta^{18}\text{O}$ isotopes of Fruitland produced waters, may be influenced by the position of major subsurface folds in the Fruitland and by the position of several rivers, which may also be controlled by subsurface folds and faults.

The distribution of $\delta^{18}\text{O}$ in produced waters does not reflect the thermal maturation of the Fruitland or the present-day structural configuration of the basin, except superficially in the area of northern New Mexico, just south of the Colorado-New Mexico State line. In this area, the trend of $\delta^{18}\text{O}$ values are subparallel to the vitrinite reflectance isotherms and structure contours and coincide with part of the present-day basin axis (fig. 11). Fruitland waters, in this area, have $\delta^{18}\text{O}$ values between -8 and -5 per mil (Cox and others, 2001), and one Fruitland well south of the water-isotope study area has a $\delta^{18}\text{O}$ value of -5.7 per mil (Ridgley, unpub. data, 2001), thus indicating that some Fruitland waters are isotopically heavier south of the Colorado-New Mexico State line. These isotopically heavier waters are probably older than the isotopically

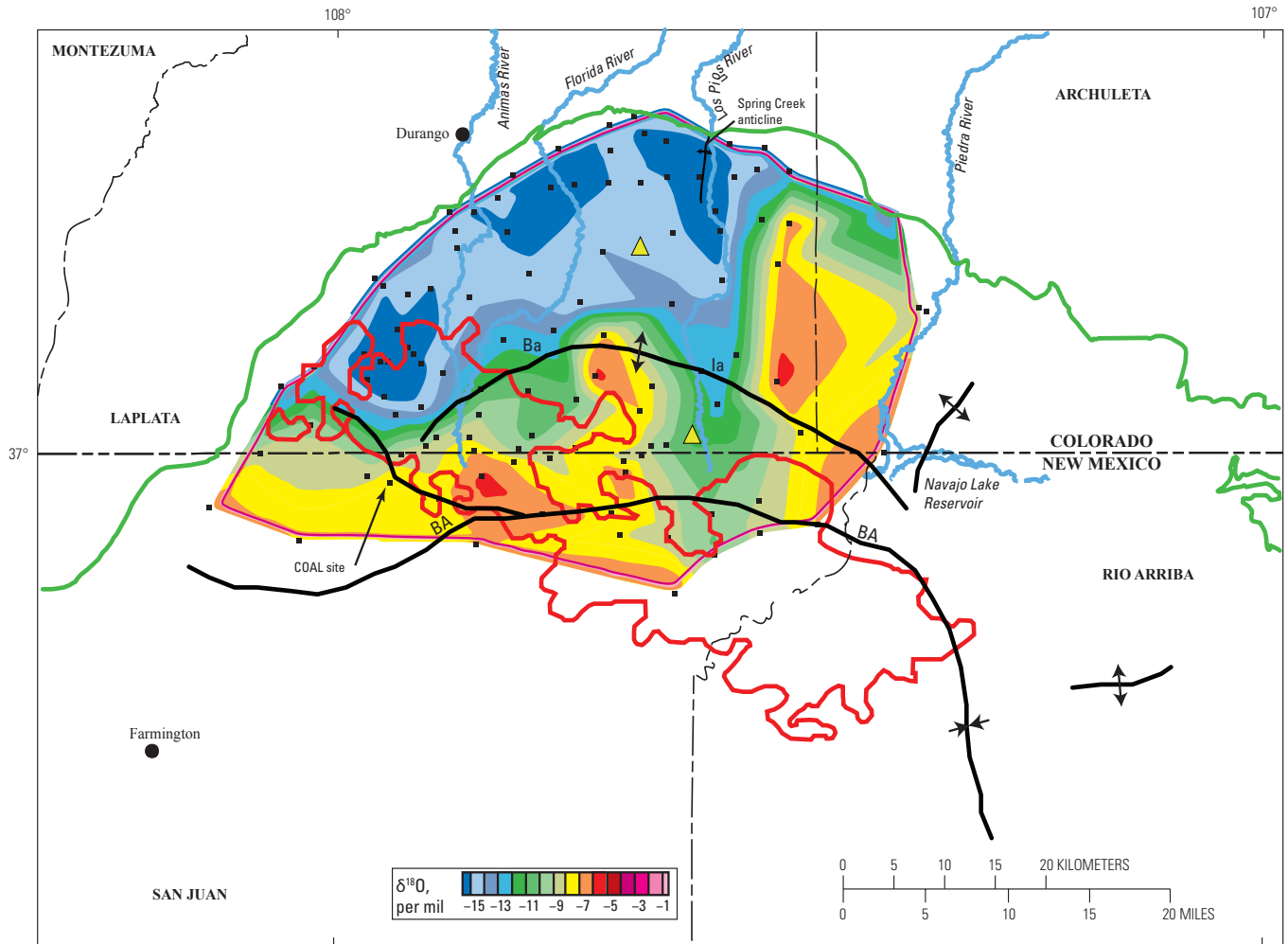
lighter waters to the north, although the relative age difference between these waters is unknown (Cox and others, 2001). The pattern of isotopically heavier waters (-8 per mil $\delta^{18}\text{O}$ and heavier) may be closer to the original distribution of $\delta^{18}\text{O}$ in the Fruitland and therefore represent "relict" connate formation waters. This interpretation is based on the pattern of waters lighter than -8 per mil to waters heavier than this. Isotopically light waters appear to "cut into" or overlap isotopically heavy waters (fig. 11), especially in the eastern part of the TPS.

Isotopically light waters (lighter than -8 per mil $\delta^{18}\text{O}$) represent meteoric and mixed meteoric and connate formation water. The isotopic distribution of the water reflects multiple periods of incursion of meteoric water (Kaiser and others, 1994) related to erosion of the Fruitland and younger formations both coincident with and outside the present boundary of the Fruitland outcrop and the present-day San Juan Basin. These multiple incursions, which are interpreted from the overlapping or superimposed $\delta^{18}\text{O}$ distributions, have obscured the original distribution of $\delta^{18}\text{O}$ in Fruitland Formation waters, leaving behind, in some areas, "lenses" of older formation waters. Although piston flow may have been important early in the history of the influx of meteoric water, the present isotopic pattern suggests that diffusion and mixing may be more important today because water cannot escape rapidly downdip from the basin margin.

Relation of Groundwater Flow to Thermal History

With deepening of the basin during the Oligocene and Miocene, it is possible that groundwater flow through the Fruitland could have been from both the north and south or may have ceased in the northern part of the basin due to deeper burial and extensive overburden. Reconstruction of the timing of erosion of the Fruitland to its present configuration is important because it constrains fluid movement in the Fruitland and bears on the issue of timing of microbial-gas generation (whether pre- or post-thermal-gas generation). Because most strata younger than the Mesaverde Group are absent from the area south of the central basin (figs. 1 and 2), reconstruction of the potentiometric surfaces throughout geologic time has uncertainty.

From the late Oligocene to the present, the basin has been differentially uplifted and eroded, and thermal cooling has occurred. Present temperatures in the Fruitland are generally below 60°C based on bottom-hole temperatures of wells completed in the Fruitland. Erosion of sediments overlying the Fruitland around the northern and western margins of the basin in Colorado and New Mexico allowed the introduction of meteoric water, which has southerly, southwesterly, and southeasterly flow paths as determined by the potentiometric map of the area (fig. 12) (Oldaker, 1991; Scott and others, 1994b; Kaiser and others, 1994) and by the regional distribution of $\delta^{18}\text{O}$ of waters produced from the Fruitland Formation (fig. 11) (Cox and others, 2001).



EXPLANATION

- Anticline
- Syncline
- Fruitland Fairway Coalbed Gas AU boundary
- Basin Fruitland Coalbed Gas AU boundary
- Sampled well
- Burial history location

Figure 11. Map showing distribution of $\delta^{18}O$ ‰ in produced Fruitland Formation waters in Colorado and northern New Mexico with respect to the northern part of the Basin Fruitland Coalbed Gas and Fruitland Fairway Coalbed Gas Assessment Units (AU). Base from Cox and others (2001). Ba, Bondad anticline; Ia, Ignacio anticline; BA, basin axis.

The present structural axis of the basin (fig. 6) in New Mexico crosses isorefectance contours ranging from 0.9-percent R_m on the west to 1.2-percent R_m on the east. In this area, the Fruitland presently is found at depths ranging from 2,500–3,500 ft and is most deeply buried in the western part. Uncorrected bottom-hole temperatures for wells completed in the Fruitland Formation or underlying Pictured Cliffs Sandstone range from 36° to 50°C. This temperature range is irregularly distributed throughout the area of the structural axis of the basin. Stable isotopes of produced water are not available along the complete length of the basin axis in New Mexico, but where available, the $\delta^{18}O$ values range from –10 to –7 per mil (fig. 11). The isotopically heavier water is found along the western and extreme eastern parts of the basin axis. An area of isotopically lighter water, $\delta^{18}O$ values of –10 to –9 per mil, is found in between where it occurs at the southern terminus of north to south overlapping flow paths of younger water. These flow paths appear to be controlled, at least in part, by the position of the Los Pinos River (fig. 11).

North of the structural axis of the basin, uncorrected bottom-hole temperatures for wells completed in the Fruitland range from 35°–60°C. Temperatures vary throughout the area and may be related to local structures. The highest temperatures are found just north of the Bondad anticline (fig. 11) and in the vicinity of a southeast-plunging syncline, which is mapped at the top of the Mancos Shale (Harr, 1988, his fig. 3). The western part of this syncline is associated with an east- to southeast-plunging plume of water whose oxygen isotopes are depleted to the west ($\delta^{18}O$ values of –14.9 per mil) and become more enriched to the south and southeast ($\delta^{18}O$ values of –6.5 to –8.0 per mil) (fig. 11) (Colorado Oil and Gas Commission, 1999a). There does not appear to be a good correlation between temperature and $\delta^{18}O$ values along this trend, implying that the temperatures are residual from earlier geologic thermal events and are not influenced by the introduction of post-depositional meteoric water.

Chloride concentrations and total dissolved solids (tds) content of the produced water within this plume vary directly with the enrichment of $\delta^{18}O$ values in the water and both become enriched to the south and southeast (Colorado Oil and Gas Commission, 1999a), although they only reach a maximum of 1940 mg/L. The highest tds concentration in the waters (10,261–10,864 mg/L) occurs along the east and southeast margins of the plume. The high tds content and relatively low chloride content implies that the waters are not sodium chloride type. Rather, like most of the Fruitland waters, the waters are probably sodium-bicarbonate waters with some percent of chloride.

Water Inorganic Compositions

Further evidence for incursion of meteoric water and mixed meteoric-connate water is the distribution of cation and anion concentrations, principally sodium, chloride, and bicarbonate. Only a few analyses of Fruitland water chemical composition have been published (Kaiser and others, 1994). In the northern part of the basin, in the overpressured area,

sodium, chloride, and bicarbonate concentrations increase from north to south along inferred flow paths (Kaiser and others, 1994, their fig. 8.13). The highest concentrations of sodium, chloride, and bicarbonate occur south of the Fruitland Fairway AU in the transition zone between overpressured (greater than 0.433 psi/ft) and underpressured areas (fig. 12) (Kaiser and others, 1994; Scott, 1994). Analyses of water samples from the southern part of the Basin Fruitland CBG AU (Kaiser and others, 1994; Threlkeld, written commun., 2001) indicate an increase in sodium, chloride, and bicarbonate concentrations from south to north toward the transition zone. The transition zone is a hydrogeochemical boundary (Kaiser and others, 1994) and is also an area of regional facies changes in coal that coincides with a change in potentiometric surface and pressure.

Although the data set of published chemical analyses of Fruitland Formation waters is small, the fact that the waters with the highest sodium, chloride, and bicarbonate concentrations are found in the transition zone between overpressured and underpressured areas and in the northern part of the underpressured area suggests that Fruitland waters over a broader area may have at one time been characterized by high sodium and bicarbonate concentrations and relatively high chloride concentrations and that these concentrations have been modified by post-depositional influx of meteoric waters from the north and south. The time of these influxes is unknown. Thus, the transition zone may be viewed either as a zone of convergent waters that have migrated from south to north and from north to south, or as a zone of preservation of nearly connate waters.

Water Dating

It is not possible to date waters using $\delta^{18}O$ and δD values. It is only possible to discuss relative age difference between water masses using these data. A crossplot of $\delta^{18}O$ and δD values from Fruitland waters (Kaiser and others, 1994; Cox and others, 2001; Snyder and others, 2003) shows that the data points cluster around the global meteoric line, implying that the waters are dominantly of meteoric origin. This would be expected because original depositional environments of the Fruitland were dominantly fluvial; coals were deposited in swamps located landward of the coast in the alluvial plain, lower and upper delta plain, and coastal plain environments (Fassett and Hinds, 1971; Ambrose and Ayers, 1994; Ayers and Zellers, 1994; Fassett, 2000). Although a truly marine water signature of these waters would not be expected, a brackish water signature might be expected for coals deposited in proximity to the coast. Shifts in deuterium values were attributed to hydrogen exchange between methane and water. Slight shifts from the global meteoric water line in the oxygen values were attributed to influx of slightly evaporated meteoric water. Two data points from a limited data set of oxygen and deuterium stable-isotope analysis (Kaiser and others, 1994) are isotopically similar to those in waters from the Paleocene Ojo Alamo Sandstone

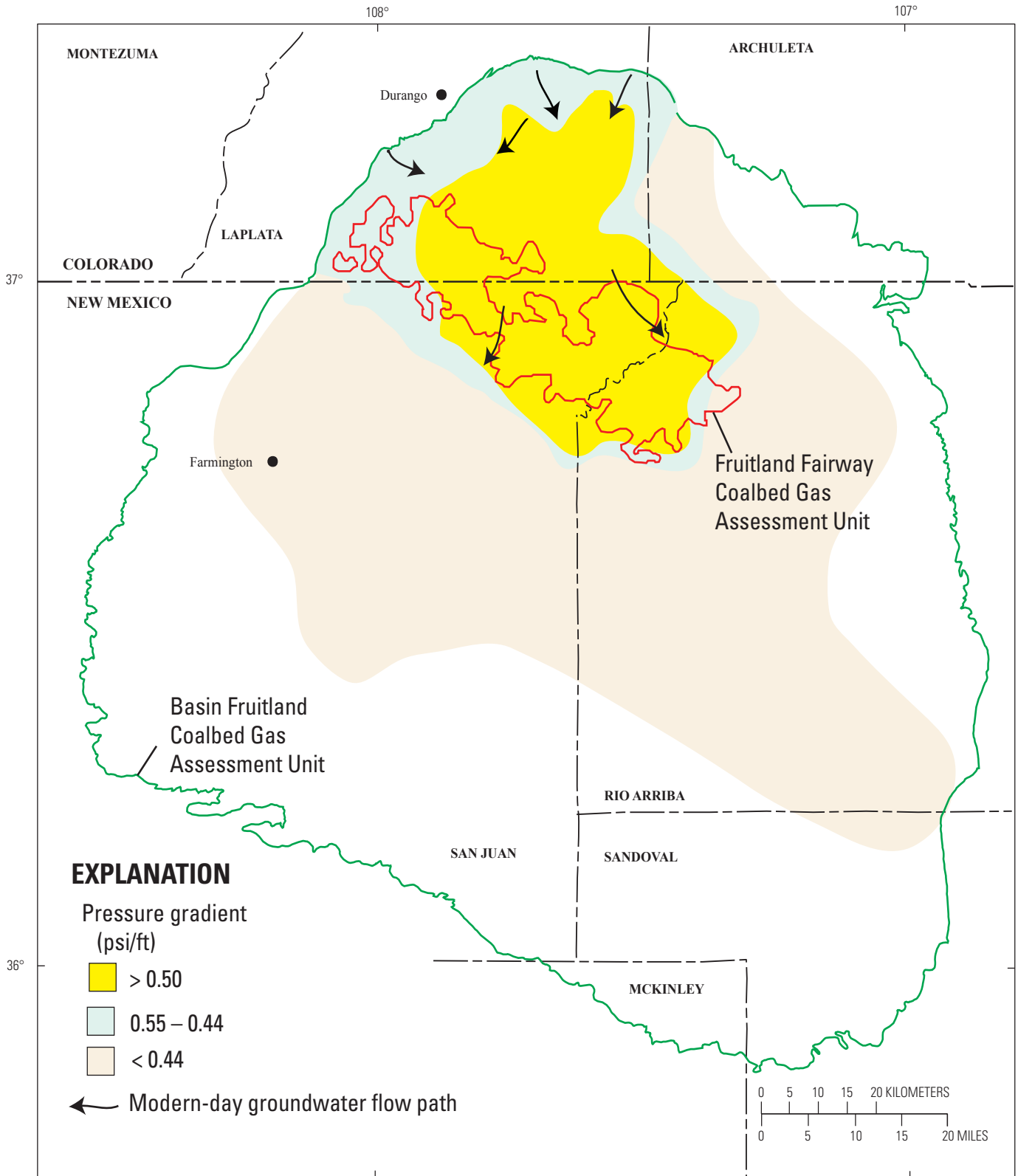


Figure 12. Map showing pressure regimes in the Fruitland Formation and inferred directions of groundwater flow based on potentiometric surfaces. Yellow, significant overpressure; light blue, normal to slight overpressure; light tan, underpressure. Modified from Scott and others (1994b).

and Nacimiento Formation (Phillips and others, 1986); it has been suggested that these waters are Holocene age. The two Fruitland data points are from the southern part of the basin. Otherwise, dates of the Fruitland waters are conjectural (Cox and others, 2001) and are based on the erosional history of the Fruitland and the time periods when meteoric water could have been introduced.

The best ways to date Fruitland waters is with ^{36}Cl isotope and $^{129}\text{I}/\text{I}$ isotope, although ^{14}C may be used if the waters are less than about 50,000 years old (Martini and others, 1998). ^{36}Cl has a half-life of 300,000 years (Nolte and others, 1991) and thus can be used to date waters to about 2 million years in age (about the beginning of the Pleistocene). $^{129}\text{I}/\text{I}$ isotope has a half-life of 15.7 million years and can possibly date waters between 80 and 100 million years old. Although these dating techniques have been used to date formation waters with varying success, a question remains on how reliable this technique is in dating waters in active groundwater flow systems and where multiple mixing events have occurred in the geologic past. Dating waters using the ratio $^{129}\text{I}/\text{I}$ is reviewed in Fabryka-Martin and others (1985), Fehn and others (1992), Moran and others (1995), Moran (1996), and Moran and others (1998).

The only published date for Fruitland waters is a ^{14}C age of 33,176 years (late Pleistocene) for carbon as dissolved bicarbonate in formation water (Mavor and others, 1991 as cited in Kaiser and others, 1994) at the COAL (Completion Optimization and Assessment Laboratory) site (fig. 11). This age is much younger than an uncorrected $4 \pm \text{Ma}$ age (amount of error not stated) implied by $^{129}\text{I}/\text{I}$ isotopes in a well to the northwest (in more $\delta^{18}\text{O}$ -depleted water of -14 per mil) or an uncorrected $20 \pm \text{Ma}$ age (amount of error not stated) implied by $^{129}\text{I}/\text{I}$ isotopes in a well to the northeast (in more $\delta^{18}\text{O}$ -enriched water of -9 per mil) (Colorado Oil and Gas Commission, 1999b). The oxygen isotope of this water is unknown, but it appears to lie near the -9 per mil value (fig. 11). In a limited study, uncorrected $^{129}\text{I}/\text{I}$ isotope ages of Fruitland waters in Colorado ranged from $4\text{--}45 \text{ Ma}$ (plus or minus some error that was not stated) (Colorado Oil and Gas Commission, 1999b). With the exception of two points, which were thought to be in an area of faulting, the uncorrected $^{129}\text{I}/\text{I}$ isotope ages varied directly with the $\delta^{18}\text{O}$ values; the older ages were associated with isotopically enriched waters. In an active groundwater flow system, this scenario would be expected, that is $\delta^{18}\text{O}$ -depleted water, which occurs updip and closer to the outcrop and present and past recharge areas, should be relatively younger than water found downdip.

In a recent comprehensive study designed to date Fruitland Formation waters in Colorado using ^{36}Cl and ^{129}I , geologically young water was found in close proximity to the outcrop and older water was found in the central part of the coal-gas producing area (Snyder and others, 2003). Three sets of water ages were determined including:

1. those with an anthropogenic (modern) signature,

2. those showing various ages reflecting different degrees of iodine enrichment and water mixing (dilution), and
3. those with an apparent modern signature due to increased levels of fissogenic ^{129}I , but whose minimum age is much older.

Samples that fall in the latter category are mostly found in the area along the Colorado-New Mexico State line.

When corrected for the addition of fissiogenic ^{129}I , some of the waters in the central part of the study area yield corrected ages between 70 and 75 Ma, which is near the age of deposition of the Fruitland. Waters dated using ^{36}Cl showed two distributions:

1. those with ages less than 2 million years, which were found within 5 km of the outcrop, and
2. those in the central part of the gas-producing area that were below the detection limit of the accelerator mass spectrometer ($^{36}\text{Cl}/\text{Cl}$ of 1×10^{-15}) (Snyder and others, 2003).

Minimum ages of Fruitland waters, using $^{129}\text{I}/\text{I}$, ranged from $5\text{--}57 \text{ Ma}$, with the oldest ages occurring in the basin center (Snyder and others, 2003). Uncertainties of minimum $^{129}\text{I}/\text{I}$ ages ranged from $1\text{--}10 \text{ m.y.}$; however, most analyses have an error range of $1\text{--}5 \text{ m.y.}$ When the $^{129}\text{I}/\text{I}$ minimum dates (Snyder and others, 2003, their table 1) are plotted on a map showing the regional distribution of $\delta^{18}\text{O}$ in produced Fruitland waters, the resulting pattern is not what would be expected if the $\delta^{18}\text{O}$ was related to Pliocene and younger flow (fig. 13). Instead, except for very young water (post-nuclear testing, which produces an anthropogenic signature), the youngest dated water in the northern part of the basin is Oligocene. Most of the data points in this part of the basin have Eocene or Paleocene ages. The youngest dated waters, exclusive of those that have apparent modern ages, are found throughout the areas of the Fruitland Fairway where the coal beds are thicker. Several waters in this latter area yield minimum ^{129}I ages of Miocene, Oligocene, and Pliocene (1 data point). This pattern of apparently young waters occurring south of apparently older waters can be interpreted in several ways:

1. water migrated from south to north in Oligocene and later time and was trapped in the area of thick coal where the orientation of coal beds changed from northeast–southwest to northwest–southeast;
2. water flow may have been focused upward in the area of the Fruitland Fairway in the Oligocene and Miocene, thus possibly enriching gas resources there (Scott and others, 1994b); and
3. the apparent young waters may be geologically older if ages are corrected for an increased fissiogenic iodine component (Snyder and others, 2003).

If the distribution of minimum ^{129}I ages is valid, then the $\delta^{18}\text{O}$ distribution in the produced water might actually reflect Miocene and older hydrologic events, except near the northern and western basin margins. These data have important

implications for hydrologic modeling of the Fruitland and are not in agreement with hydrologic models that propose basin-wide migration of younger water through the Fruitland (Kaiser and others, 1994; Cox and others, 2001). Some of the apparent differences may simply reflect differences in scale, regional flow modeling versus point location of geochemical data (which could represent areas by-passed by regional flow), as well as differences in depth for observed or inferred parameters.

The age discrepancy of the Fruitland waters points to the uncertainty in determining the timing of influx meteoric water, and hence to the generation of late-stage microbial gas and its ultimate contribution to gas resources. If recharge waters infiltrated the Fruitland during the late Miocene and Pliocene as the basin was uplifted and eroded, as has been suggested (Scott and others, 1994b), they would have been cool (lighter stable isotopes). These cool waters would have mixed with hot formation waters of 70°–100°C (heavier stable isotopes). Any methane-producing bacteria introduced with these recharge waters probably could survive at these temperatures, but they might not generate much bacterial gas until the formation temperature cooled to less than 50°–60°C in the Pleistocene. Optimal temperatures for bacterial gas generation of about 45°C were achieved relatively recently based on one burial history reconstruction (fig. 10C), and thus help constrain the length of time for late-stage microbial-gas generation.

Carbon Isotopes of Dissolved Inorganic Carbon in Produced Waters

Published $\delta^{13}\text{C}$ analyses for carbon of total dissolved carbon (DIC) in produced waters are too few to determine regional trends (fig. 14) (Scott and others, 1994b). Heavy $\delta^{13}\text{C}$ values of DIC are found in the underpressured, transitional pressured, and overpressured parts of the Fruitland Formation and are usually associated with microbial-gas generation. The lighter values are found closer to the outcrop, and it has been suggested (Kaiser and others, 1994) that these values represent a greater mixture of isotopically light thermogenic CO_2 or CO formed in soils with isotopically heavier CO_2 formed as a result of degradation of organic acids and reduction of CO_2 by methanogenic bacteria. These values could also be interpreted as a mixture of microbial gas and thermogenic CO_2 that formed at various stages of carbon fractionation. All the reported $\delta^{13}\text{C}$ values of the DIC are heavy and suggest present or past contribution from microbial-gas generation, by the CO_2 -reduction pathway. The $\delta^{13}\text{C}$ values of the DIC may have formed at different times depending whether the chemical system has been open or closed as well as on the past and present formation hydrodynamics.

Fruitland Formation Gas

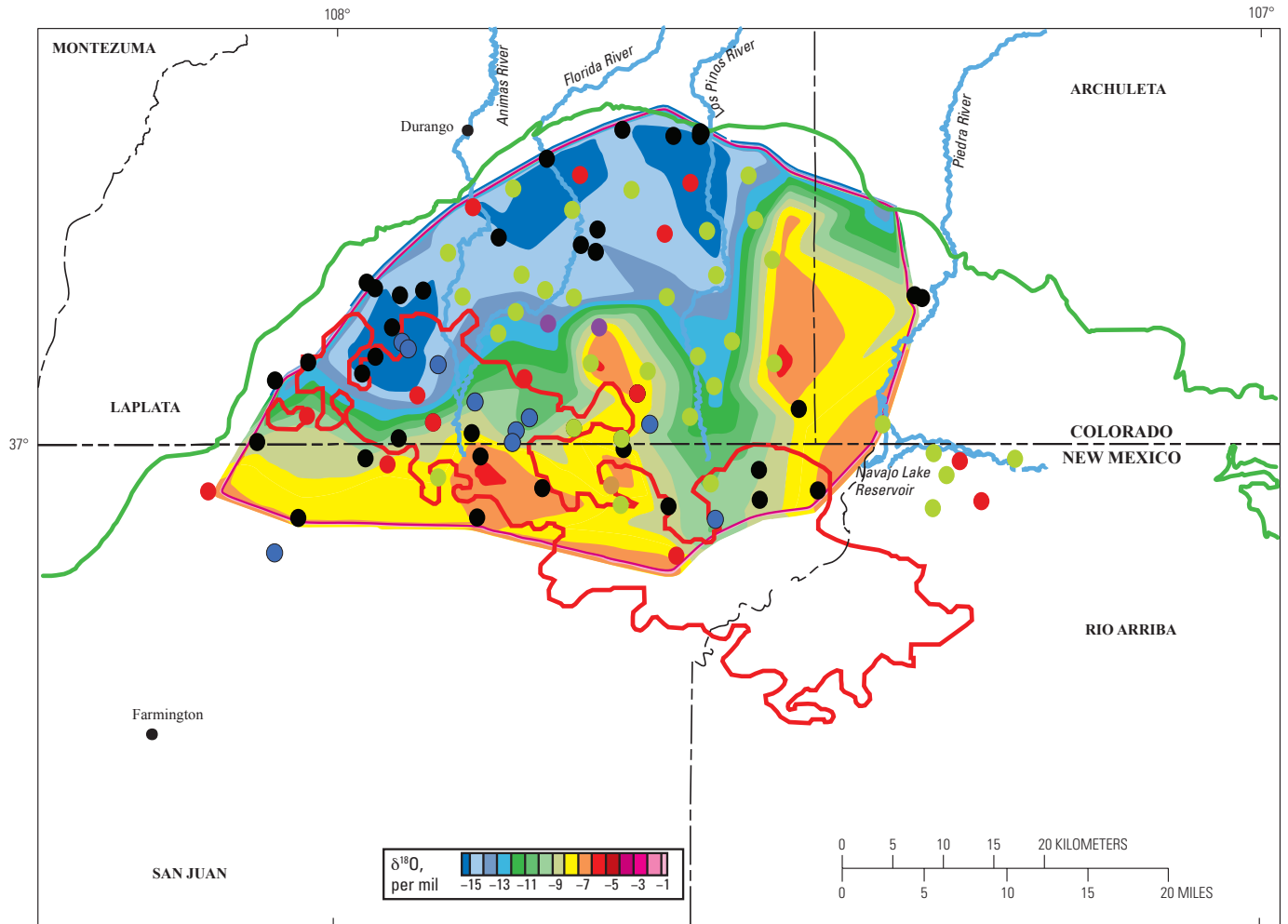
Gas Chemistry

Can a knowledge of the past groundwater and thermal histories be used to evaluate the present distribution of gas and produced-water compositions and to evaluate the relative contribution of microbial gas and thermal gas to total gas produced? Can these data be used more effectively to determine the relative gas richness of an area, which ultimately affects the potential resources assigned to an area? As discussed below, these data can lead to interpretations that are modifications of the prevailing models, and they support the current assessment divisions of the Fruitland used in this study.

Comprehensive studies of the gas chemistry of the Fruitland Formation indicate major compositional differences between the overpressured, transitional pressured, and underpressured areas (table 3) (Rice, 1983; Scott, 1994; Scott and others, 1994a,b). Gases from the Fruitland in the overpressured area are generally dry ($C_1/\Sigma C_{1-5} > 0.97$) and contain up to 26.4-percent (mean of 6.5) CO_2 and various amounts of nitrogen (Scott and others, 1994b). In the underpressured areas, gases are generally wet ($C_1/\Sigma C_{1-5} < 0.94$), contain less than 2-percent (mean of 0.9) CO_2 , and contain various amounts of nitrogen (Scott and others, 1994b). Gases from the transition zone have chemical analyses that fall between the two end members. There are exceptions (high and low values) to the general gas composition for each area (Scott, 1994).

Distribution of Gas Wetness

Gas produced from the region of the Fruitland that is bounded by the >0.8 -percent R_m isoreflectance contours is dry, except for a few areas where $C_1/\Sigma C_{1-5} < 0.94$ (fig. 15) (Scott, 1994, his pl. 1). The onset of intense thermogenic gas generation is considered to occur between vitrinite reflectance values 0.8–1.0 percent R_m and wet-gas generation between 0.5–0.8 percent R_m (Tissot and Welte, 1987; Scott, 1994, his table 2). Cracking of condensate to methane occurs between vitrinite reflectance values 1.0–1.35 percent R_m and maximum generation of thermogenic methane between 1.20–2.0 percent R_m (Tissot and Welte, 1987; Scott, 1994, his table 2). Maximum measured vitrinite values in the Fruitland are less than 1.7 (Fassett, 2000, his fig. 37). Thus, the overall pattern of gas composition (in terms of dryness) in the Fruitland (Scott, 1994, his pl. 1) can be explained by the thermal maturity (perhaps coupled with change in organic matter type) of the Fruitland Formation, given sufficient geologic time at these temperature conditions. Scott and others (1994b) suggested that a compositional gas gradient would be expected from 0.8- to 1.35-percent R_m , and the lack of this gradient was evidence of the gas being a mixture of thermogenic and late-stage microbial gas. However, the original gas wetness ($C_1/\Sigma C_{1-5}$) data was contoured at 0.9, 0.94, and 0.97 intervals (Scott, 1994), and thus the broad intervals chosen may actually have obscured any finer regional trends to the compositional data.



EXPLANATION

- | | | | |
|---|------------------------------------|-------------------------------|-----------------------------|
| — Fruitland Fairway Coalbed Gas AU boundary | (Modern–Pleistocene)
● 0–1.8 Ma | (Miocene)
● 5.3–23.8 Ma | (Eocene)
● 33.7–55.5 Ma |
| — Basin Fruitland Coalbed Gas AU boundary | (Pliocene)
● 1.8–5.3 Ma | (Oligocene)
● 23.8–33.7 Ma | (Paleocene)
● 55.5–65 Ma |

Figure 13. Map showing relation between minimum ¹²⁹I/I ages and distribution of δ¹⁸O ‰ in produced Fruitland Formation waters in Colorado and northern New Mexico in the San Juan Basin. Iodine ages from Snyder and others (2003). Base from Cox and others (2001). AU, Assessment Unit; Ma, million years before present.

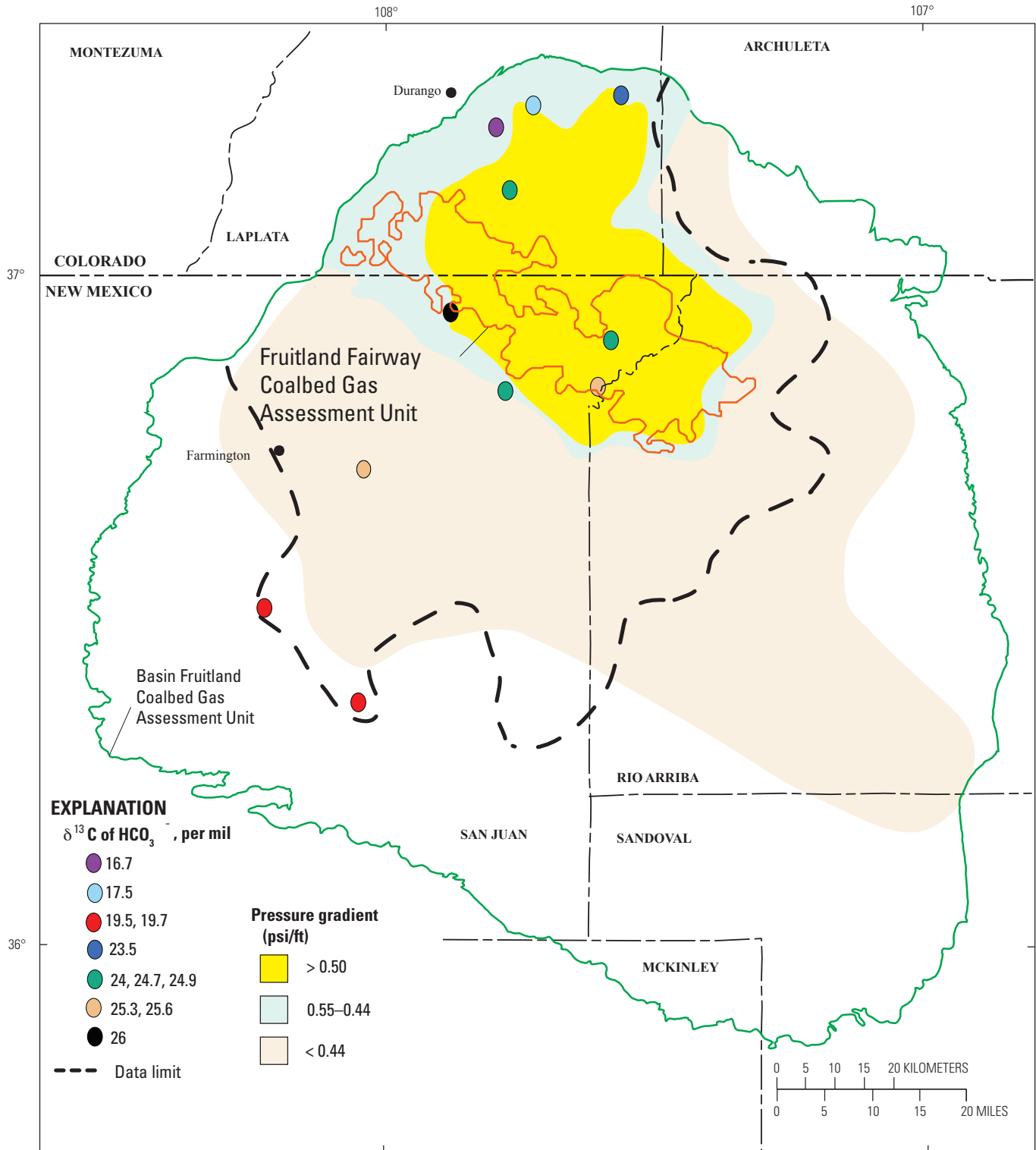


Figure 14. Map showing relation between pressure gradients (Scott and others, 1994b) and carbon ($\delta^{13}\text{C}$) isotope of dissolved inorganic carbon in Fruitland Formation produced waters. $\delta^{13}\text{C}$ ‰ of dissolved inorganic carbon from Scott and others (1994b) and Threlkeld (written commun., 2001). Yellow, significant overpressure; light blue, normal to slight overpressure; light tan, underpressure.

Although there has probably been some mixing of thermogenic gas with late-stage microbial gas, the pattern of gas composition may simply reflect changes in thermal maturity of the organic matter over geologic time, or it might also reflect mixing of early microbial gas with a later thermal gas.

One exception to the regional pattern of gas composition is an area of dry gas in the southwestern part of the Basin Fruitland CBG AU (fig. 15). In this area, the Fruitland gas is considered to be a mixture of microbial and thermogenic gas (Rice, 1983; Scott and others, 1994b). Another exception is an area along the east side of the Basin Fruitland CBG AU in northwestern Rio Arriba County (figs. 12 and 15) where intermediate and wet gases characteristic of the transition and underpressured areas have been documented. In this area, the gas composition does not appear to be related to the thermal maturity of the Fruitland (Scott, 1994, his pl. 1; Scott and others, 1994b) in that the compositions do not appear to conform to vitrinite isoreflectance contours. However, there are no vitrinite data reported for this area that would determine the actual shape of the isoreflectance contours. Isoreflectance contours just to the north appear to reflect the position of the southeast extension of the Ignacio anticline as well as the position of the axis of the San Juan Basin (Scott, 1994; Fassett, 2000) before it shifted to the south in the Miocene. In Colorado, on the east side of the overpressured area, there are too few gas and vitrinite analyses to determine the position of isoreflectance contours or the position of the dry-wet gas boundary (Scott, 1994; Scott and others, 1994b; Fassett, 2000).

The pattern of chemically wet and dry gas in the Fruitland is not only affected by thermal maturity of the Fruitland but also by maceral type and possibly basin hydrology (Scott, 1994; Scott and other, 1994b). Wet gas, which is now confined primarily to the southern part of the Basin Fruitland CBG AU, is produced primarily from older Fruitland coal beds, whereas in the northern part of the Basin Fruitland CBG AU gas is produced from coals stratigraphically younger in the formation. This relative change in stratigraphic age might be accompanied by slight differences in maceral type, and hence, this could influence the type of hydrocarbons produced. Too few studies have been conducted on Fruitland maceral composition to determine whether maceral type changes significantly areally within the Fruitland (Fassett, 2000). A change in maceral composition accompanied by variable thermal history might account for some of the observed pattern of gas wetness. The area of dry gas was interpreted to represent a mixture of thermogenic gas and late-stage microbial gas (Scott, 1994; Scott and others, 1994a,b). Based on the presence of very heavy ^{13}C values of the dissolved inorganic carbon (fig. 14) (Scott and others, 1994b), some microbial gas (methane) has been produced, contributing to the overall dryness of the gas.

It has been suggested that the distribution of wet and dry gas corresponds more closely to regional overpressure than to coal rank (Scott and others, 1994b) and is closely tied to basin hydrodynamics. However, as discussed above, thermal maturity, time, maceral composition, and degree of mixing of thermogenic and microbial gas can explain some aspects of the regional distribution of gas composition. Basin hydrodynamics

is important, especially in the northern part of the overpressure area, but its control on gas composition may be overestimated. Between vitrinite reflectance values 0.7–0.8 percent R_m , tongues of dry gas extend south from the main area of dry gas (fig. 15) and can be interpreted to represent

1. original distribution of dry/wet gas that occurred within these vitrinite values, or
2. areas into which dry gas has migrated during pressure readjustment between the overpressured and underpressured areas.

These areas might be controlled by faults, although the detailed studies to demonstrate this control have not been conducted. The convoluted pattern of wet- and dry-gas composition may reflect pinchout of coal beds and/or their offset by faulting (Scott 1994; Scott and others, 1994b). Coals south of the overpressured area tend to be elongate parallel to the southwest to northeast regional dip, whereas coals in the southern part of the overpressured area tend to be oriented northwest–southeast parallel to Pictured Cliffs Sandstone shorelines. The convoluted pattern of wet- and dry-gas composition (0.94 and 0.97 contours) also approximately corresponds to the southern boundary of the 3-percent CO_2 contour (figs. 15 and 16).

Distribution of Methane Isotopes

Some studies (Scott and others, 1991; Scott and others, 1994a,b) have indicated that the various carbon isotopes of methane, carbon dioxide, and dissolved inorganic carbon in produced waters throughout the overpressured area are a result of a mixture of older thermogenic gas and younger late-stage microbial gas generated during influx of Pliocene and younger meteoric water. The carbon isotope of methane ranges from -46.7 to -34.1 per mil (table 3) (fig. 17) (Jones and others, 1985; Rice and others, 1989; Scott and others, 1991; Threlkeld, written commun., 2001). The lightest values are found in the southern part of the underpressured Basin Fruitland CBG AU as well as in a small area on the northern rim of the San Juan Basin in the overpressured area of the Basin Fruitland CBG AU (fig. 17). Between these areas the distribution of carbon isotopes varies, but in a narrow range. The heaviest values, less than -41 per mil, are mostly found in the overpressured area, both in the Fruitland Fairway and Basin Fruitland CBG AUs (fig. 17).

When overlain on the regional map of $\delta^{18}\text{O}$ of produced water, $\delta^{13}\text{C}$ of methane trends from lighter to heavier values along broad groundwater flow paths as defined by the changes in the regional $\delta^{18}\text{O}$ -isotope values (fig. 18). In the area of isotopically light water (-16 to -13 per mil $\delta^{18}\text{O}$), the $\delta^{13}\text{C}$ values of the methane are highly variable and probably represent various degrees of gas mixing or original signatures. Heavy $\delta^{13}\text{C}$ values of the methane (-41.0 to -39 per mil) are irregularly distributed but, in general, tend to occur where produced water has $\delta^{18}\text{O}$ isotopes >-10 per mil. The regional distribution of $\delta^{13}\text{C}$ of methane can be explained by mixing of various amounts of thermogenic and microbial gas (pre- or

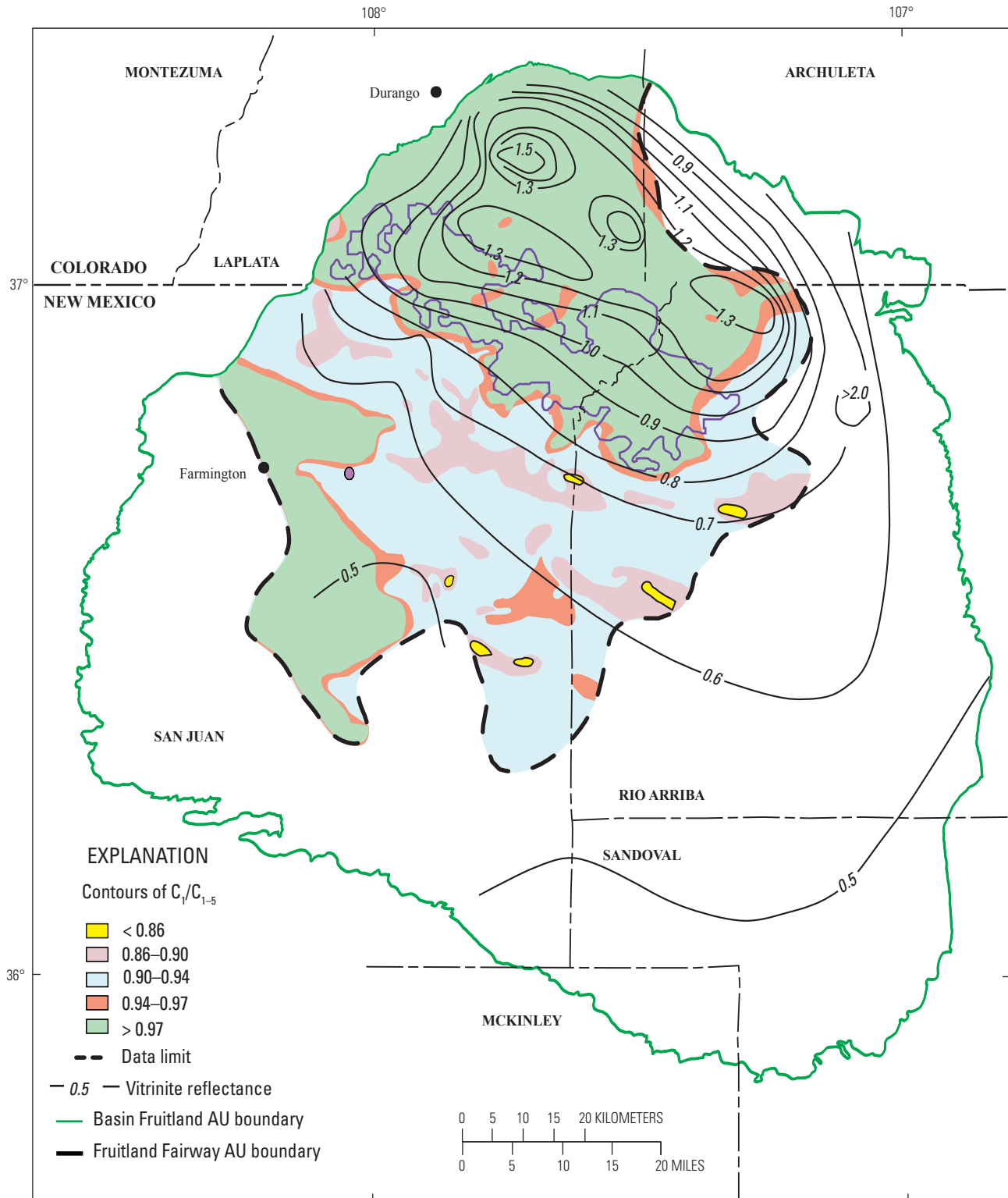
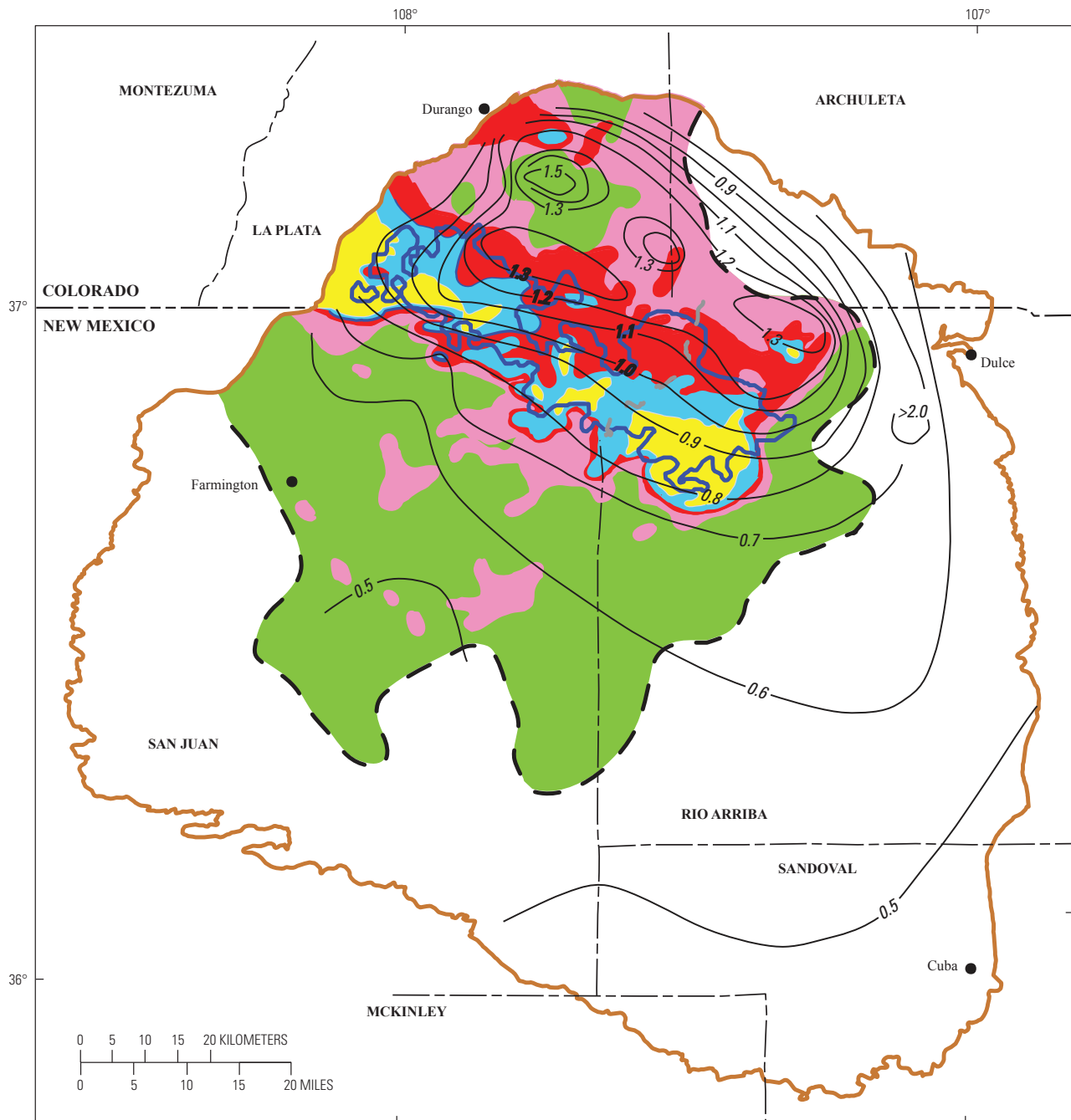


Figure 15. Map showing distribution of gas wetness (defined by $C_1/\Sigma C_{1-5}$) in Fruitland Formation gases with respect to the Basin Fruitland Coalbed Gas and Fruitland Fairway Coalbed Gas Assessment Units and vitrinite reflectance. Gas wetness contour data from Scott (1994). Vitrinite reflectance data from Law (1992). Dry gas (>0.97 gas wetness) that was thermally generated is associated with the area of greater thermal maturity (vitrinite reflectance >0.8% R_m); dry gas (>0.97 gas wetness) that is associated with lower thermal maturity (vitrinite reflectance <0.6% R_m) may have a higher microbial-gas component.



EXPLANATION

CO₂ concentration (percent)

- < 1
- 1-3
- 3-6
- 6-10
- > 10

- Data limit
- Vitrinite reflectance
- Basin Fruitland Coalbed Gas AU boundary
- Fruitland Fairway Coalbed Gas AU boundary

Figure 16. Map showing distribution of CO₂ concentration in Fruitland Formation gases with respect to the Basin Fruitland Coalbed Gas and Fruitland Fairway Coalbed Gas Assessment Units and vitrinite reflectance. The highest concentration of CO₂ (>6 percent) is roughly coincident with the Fruitland Fairway Coalbed Gas Assessment Unit (AU) and with areas of moderate thermal maturity (vitrinite reflectance 0.8–1.2 percent R_m). CO₂ contour data from Scott (1994). Vitrinite reflectance data from Law (1992).

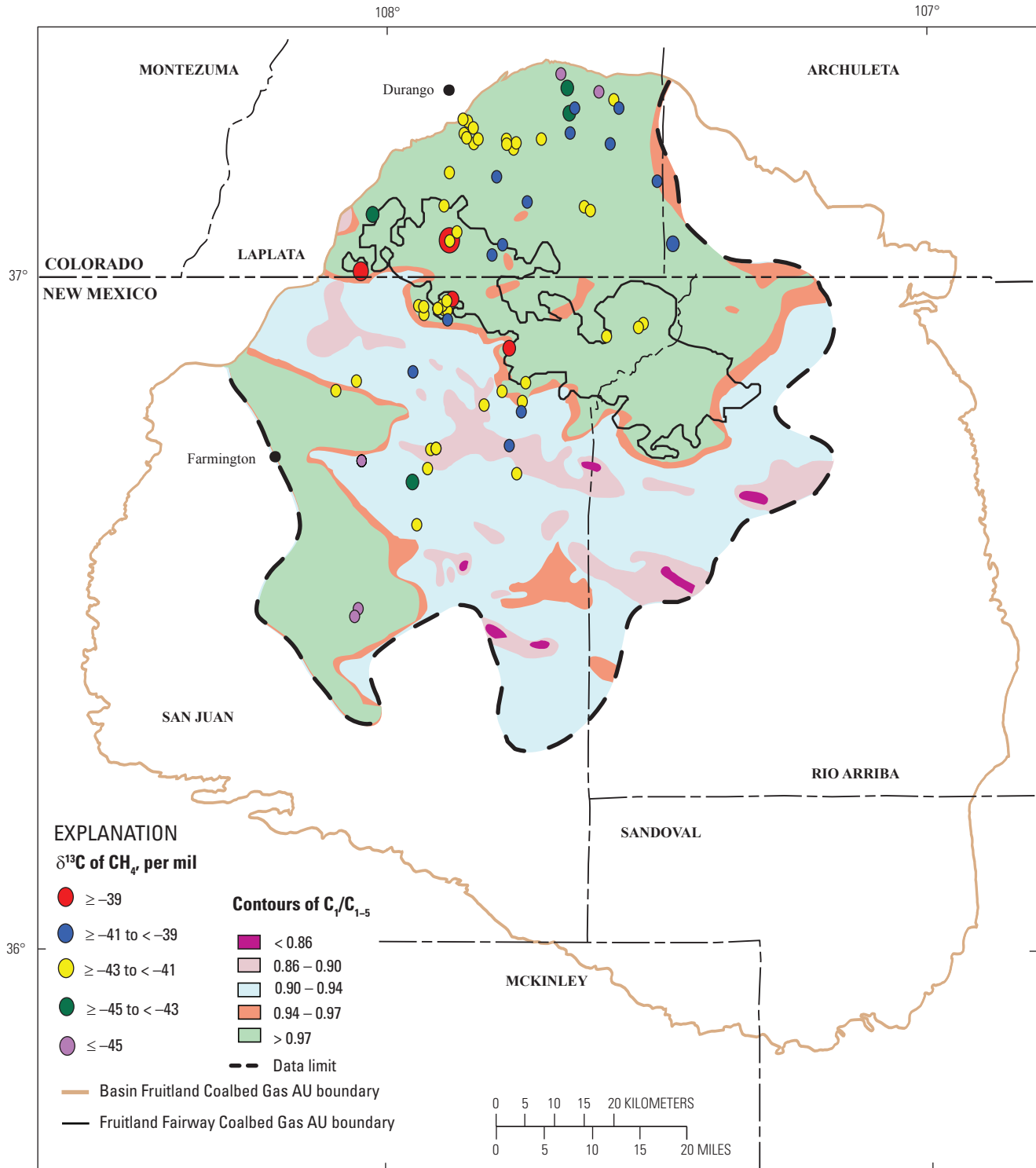


Figure 17. Map showing the distribution of $\delta^{13}\text{C}$ of methane to gas wetness (defined by $\text{C}_1/\Sigma\text{C}_{1-5}$) in Fruitland Formation gases. Isotopically light methane ($< -45 \delta^{13}\text{C}_{\text{CH}_4}$) is found in both the extreme northern and southern areas of the Basin Fruitland Coalbed Gas Assessment Unit (AU); the light isotope reflects a greater contribution of microbial methane. Contours of gas wetness from Scott (1994). Carbon-isotope data of methane from Scott and others (1994b) and Threlkeld (written commun., 2001).

post-thermal-gas generation) as well as isolated areas of what may be interpreted as original thermogenic gas and shows a more complex pattern than previously published (Scott and others, 1994b). The original distribution of carbon isotopes of thermal methane is unknown.

Carbon Dioxide Content

There is little publicly available concentration and carbon-isotope data for CO₂ in Fruitland gas, although this data is important in economic resource analysis of Fruitland gas and in production practices. High content of CO₂ affects the heating value of the gas and the CO₂ must be disposed of, thereby increasing production costs. Available analyses indicate the $\delta^{13}\text{C}$ is 12.8 ± 4.2 per mil (table 3). The heavy isotope suggests at least a partial microbial origin. A crossplot of the $\delta^{13}\text{C}_{\text{CO}_2}$ versus $\delta^{13}\text{C}$ methane (n=8) does not show any definite relation between the two, but rather suggests mixing of various amounts of microbial and thermogenic CO₂ (fig. 19). However, this observation is based on a small sample set and may not be representative of the broader population. There appears to be a correlation between the $\delta^{13}\text{C}$ CO₂ and the CO₂ content of the gas, based on a small sample set (n=7) (fig. 20). As the CO₂ content in the gas increases, the carbon isotope becomes heavier, which suggests a greater fraction of microbially derived gas with increased CO₂ content. This is not the trend that would be expected if the CO₂ content was fixed prior to generation of late-stage microbial gas via CO₂ reduction (during which CO₂ is consumed) and if little or no additional CO₂ was generated by other microbes. A crossplot of $\delta^{13}\text{C}$ methane versus CO₂ content shows no correlation (n=68) between the two (fig. 8B). This reflects the narrow range of $\delta^{13}\text{C}$ -isotope values in the methane.

The distribution of CO₂ content in Fruitland gas shows significant differences between the overpressured and underpressured areas of the Basin Fruitland CBG AU as well as differences between these two areas and the overpressured Fruitland Fairway CBG AU (fig. 21) (Scott, 1994, his pl. 2; Scott and others, 1994b). In some areas, the data points are abundant, and the contours of CO₂ content are well constrained. In other areas, data points are sparse, and the contours should be considered as approximately located and alternative patterns should be considered. On a regional scale, the broad area of the Fruitland Fairway CBG AU is circumscribed by the 3- to 6-percent CO₂ contour.

In the underpressured part of the Basin Fruitland CBG AU, CO₂ content of gases is mostly less than 1 percent, except in areas in closer proximity to the southern Fruitland Fairway CBG AU boundary (fig. 21) (Scott, 1994, his pl. 2; Scott and others 1994b). In a narrow to broad convolute area bordering the southern boundary of the Fruitland Fairway CBG AU, gases contain between 1–3 percent CO₂. This area crosscuts the underpressured, transition pressured, and the overpressured area (fig. 21). There are several ways to interpret the pattern of this convolute area:

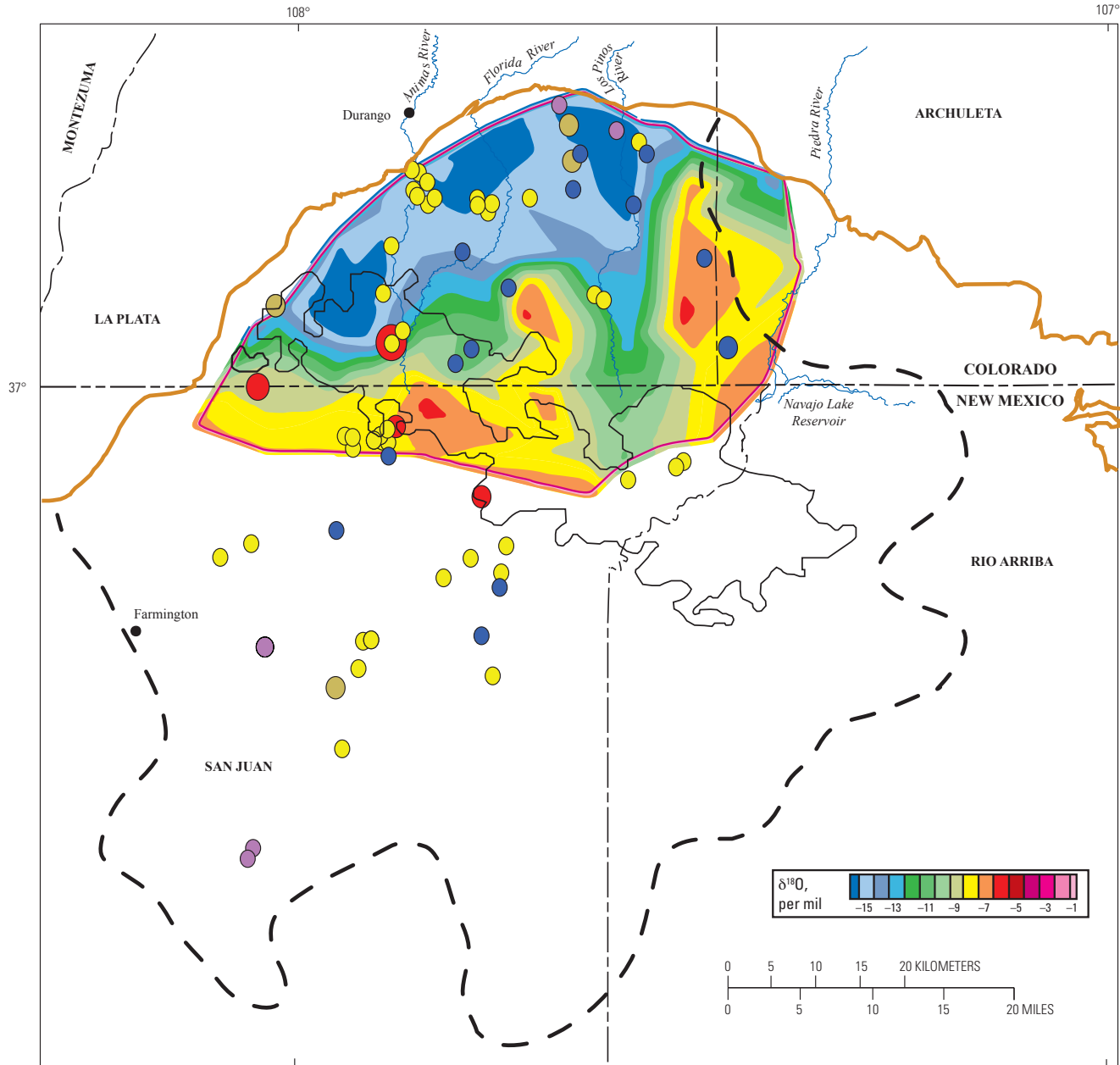
1. the area represents southward projecting tongues of gas (with 1–3 percent CO₂) that migrated into this area during pressure readjustment between the overpressured and underpressured areas,
2. the area represents gases (with 1–3 percent CO₂) trapped along the leading edge of older flow paths of waters (ages unknown) that flowed northward (in the geologic past prior to the present potentiometric distribution and present-day topography) perhaps from the time of deposition through the Miocene as the basin was being downwarped,
3. the area reflects changes in thickness and trends of net coal, or
4. some combination of the above.

If the first hypothesis is valid, there is uncertainty why simple north to south migration would produce the observed narrow band of gas that contains 1–3 percent CO₂ throughout a broad regional area. The 1–3 percent CO₂ contours in the southern part of the Basin Fruitland CBG AU loosely correlate with locally thicker coal (fig. 22).

Most of the overpressured area of the Basin Fruitland CBG AU contains from 1–3 percent CO₂ except for areas along the northern margin where greater and less CO₂ content has been reported (fig. 21) (Scott and others, 1994b). A broad area of less than 1-percent CO₂ content is found in the central-northern part of the overpressured Basin Fruitland CBG AU. This area coincides with a more thermally mature area of the Fruitland (fig. 15) and the probable location of the axis of the basin during the Oligocene. It also approximately coincides with an area of thin net coal (fig. 22). Although more data points are needed to better define this area of low CO₂ content, the coincidence of low content with high thermal maturity, and hence low CO₂ production, may reflect the original CO₂ content of Fruitland gas and thermal maturation conditions in this area. Today, this area is where Fruitland groundwater flow has $\delta^{18}\text{O}$ values around –15 to –13 per mil (fig. 11). Despite these light $\delta^{18}\text{O}$ values, here and elsewhere in the overpressured part of the Basin Fruitland CBG AU (figs. 11 and 12), it appears little CO₂ is being produced by microbial activity.

Gases from most Fruitland Fairway CBG AU wells have CO₂ contents greater than 6 percent and are found in two broad and nearly contiguous areas (fig. 16). Both areas have steep CO₂-concentration gradients to the south and broader concentration gradients to the north. In the east half of the Fruitland Fairway CBG AU, this gradient is broader. Within the 6-percent CO₂ contour, there are isolated pods where the CO₂ content of the gas exceeds 10 percent (fig. 16) (Scott and others, 1994b, their fig 8). The area occupied by the wells having gases with at least 6-percent CO₂ is significantly greater in the eastern part of the Fruitland Fairway AU than in the west.

The irregular northern and southern boundary of the 6-percent contour approximates regional trends in net coal thickness, and the area bounded by the six-percent CO₂ contour also approximates the area of thickest coal (fig. 22). The Fruitland depositional system extended far beyond the



EXPLANATION

- | | | |
|-----|----------------------------------|---|
| --- | Data limit | δ¹³C of CH₄, per mil |
| — | Basin Fruitland Coalbed Gas AU | ● ≥ -39 |
| — | Fruitland Fairway Coalbed Gas AU | ● ≥ -41 to < -39 |
| | | ● ≥ -43 to < -41 |
| | | ● ≥ -45 to < -43 |
| | | ● ≤ -45 |

Figure 18. Map showing relation between $\delta^{18}\text{O}$ of produced Fruitland Formation waters and methane carbon isotope ($\delta^{13}\text{C}$) in Fruitland Formation gas. Carbon-isotope data in methane from Scott and others (1994b) and Threlkeld (written commun., 2001). Oxygen-isotope base map from Cox and others (2001). AU, Assessment Unit.

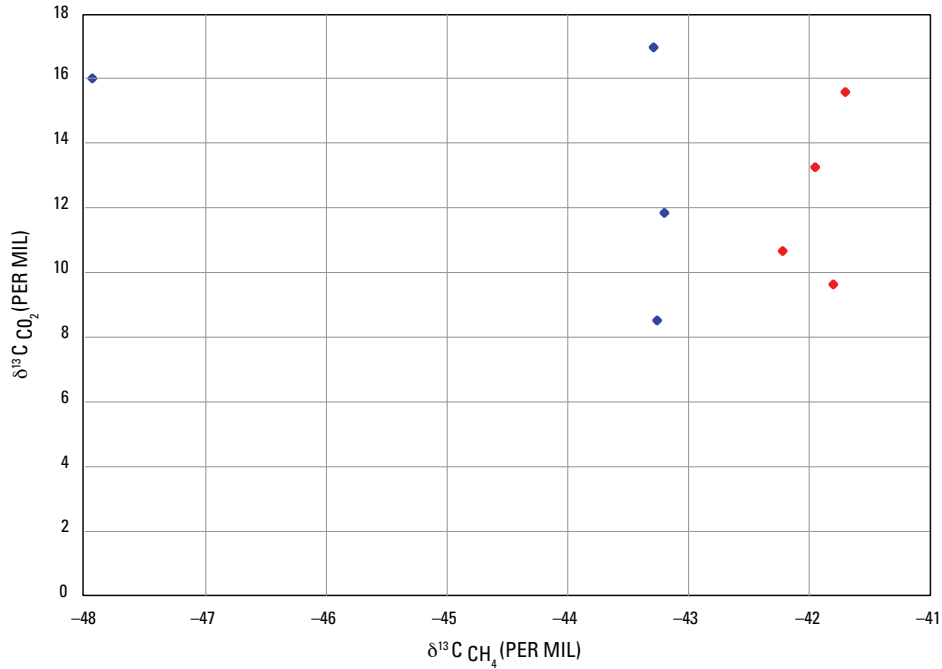


Figure 19. Crossplot showing relation between $\delta^{13}\text{C CO}_2$ and $\delta^{13}\text{C}$ methane of gas (n=8) in the Fruitland Formation. Data from Colorado (red) and New Mexico (blue) are from Threlkeld (written commun., 2001).

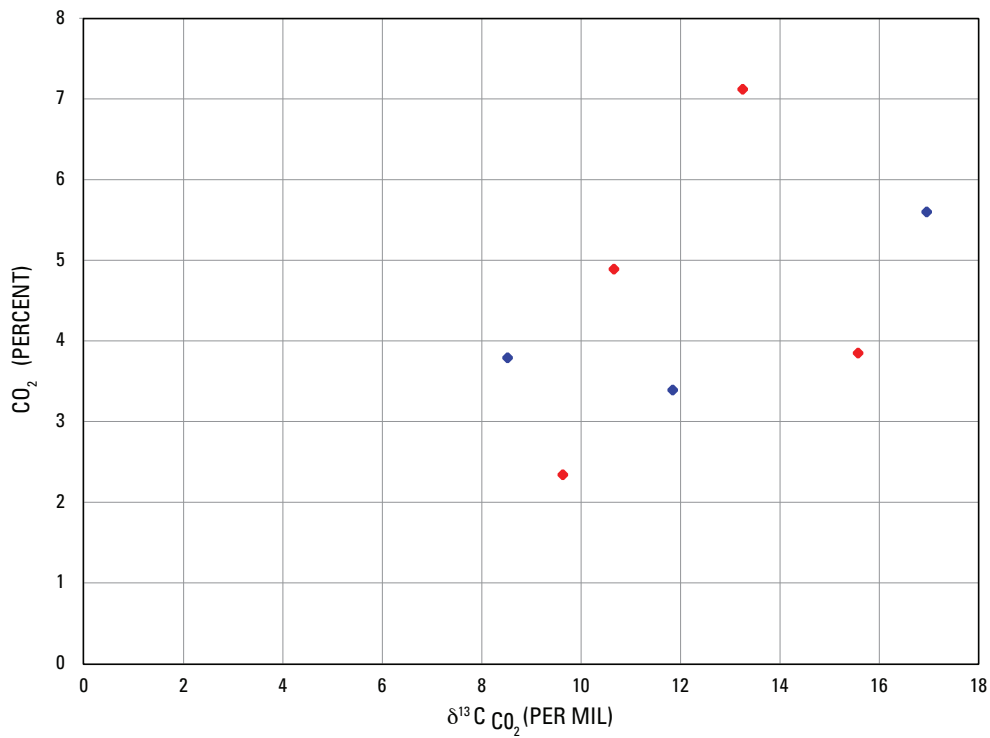


Figure 20. Crossplot showing relation between $\delta^{13}\text{C CO}_2$ and the CO₂ content of gas (n=7) in the Fruitland Formation. Data from Colorado (red) and New Mexico (blue) are from Threlkeld, (written commun., 2001).

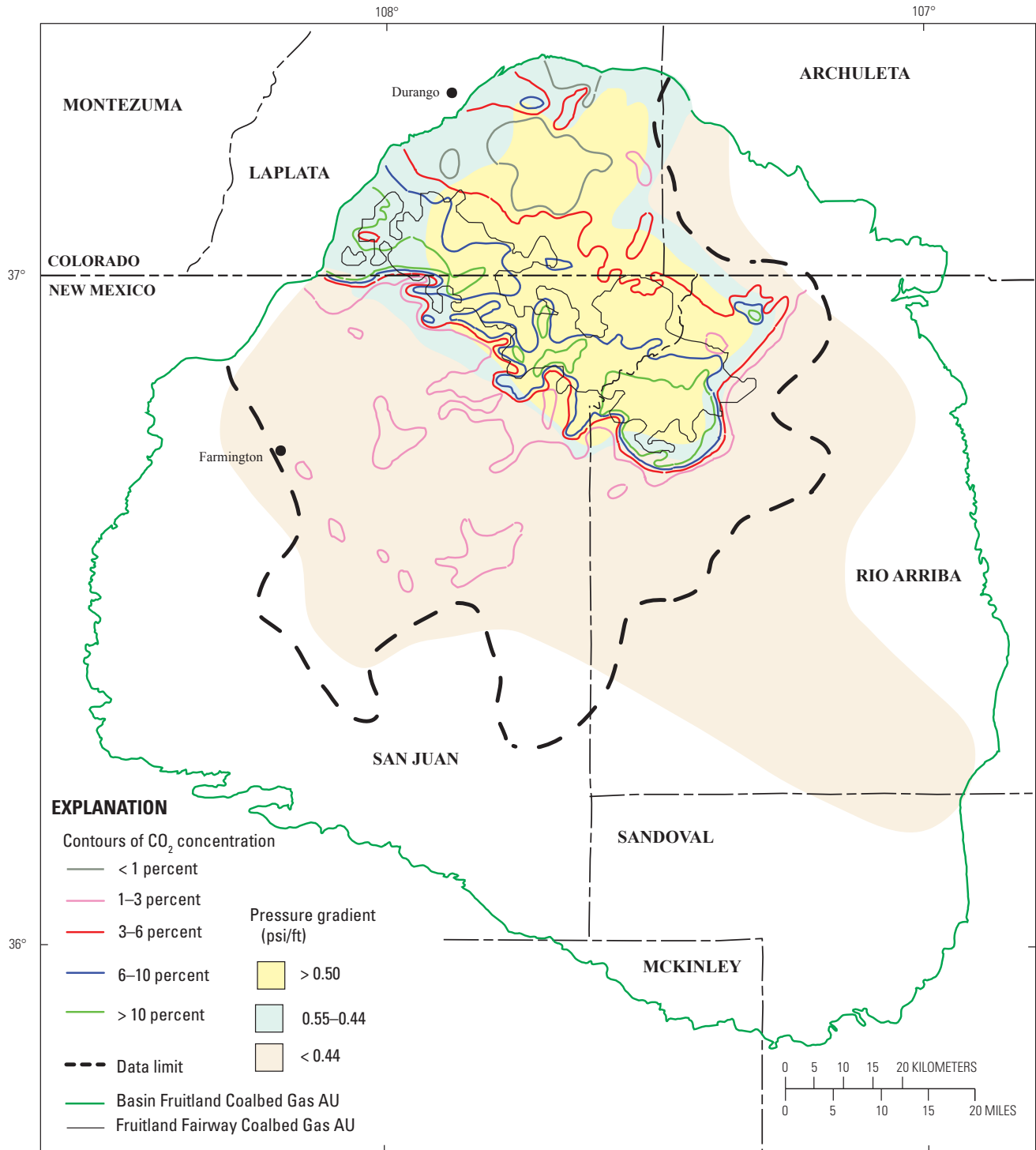


Figure 21. Map showing the relation between pressure gradient (Scott and others, 1994b) and CO₂ concentration in Fruitland Formation gas. CO₂ contour data from Scott (1994). Yellow, significant overpressure; light blue, normal to slight overpressure; light tan, underpressure. AU, assessment unit.

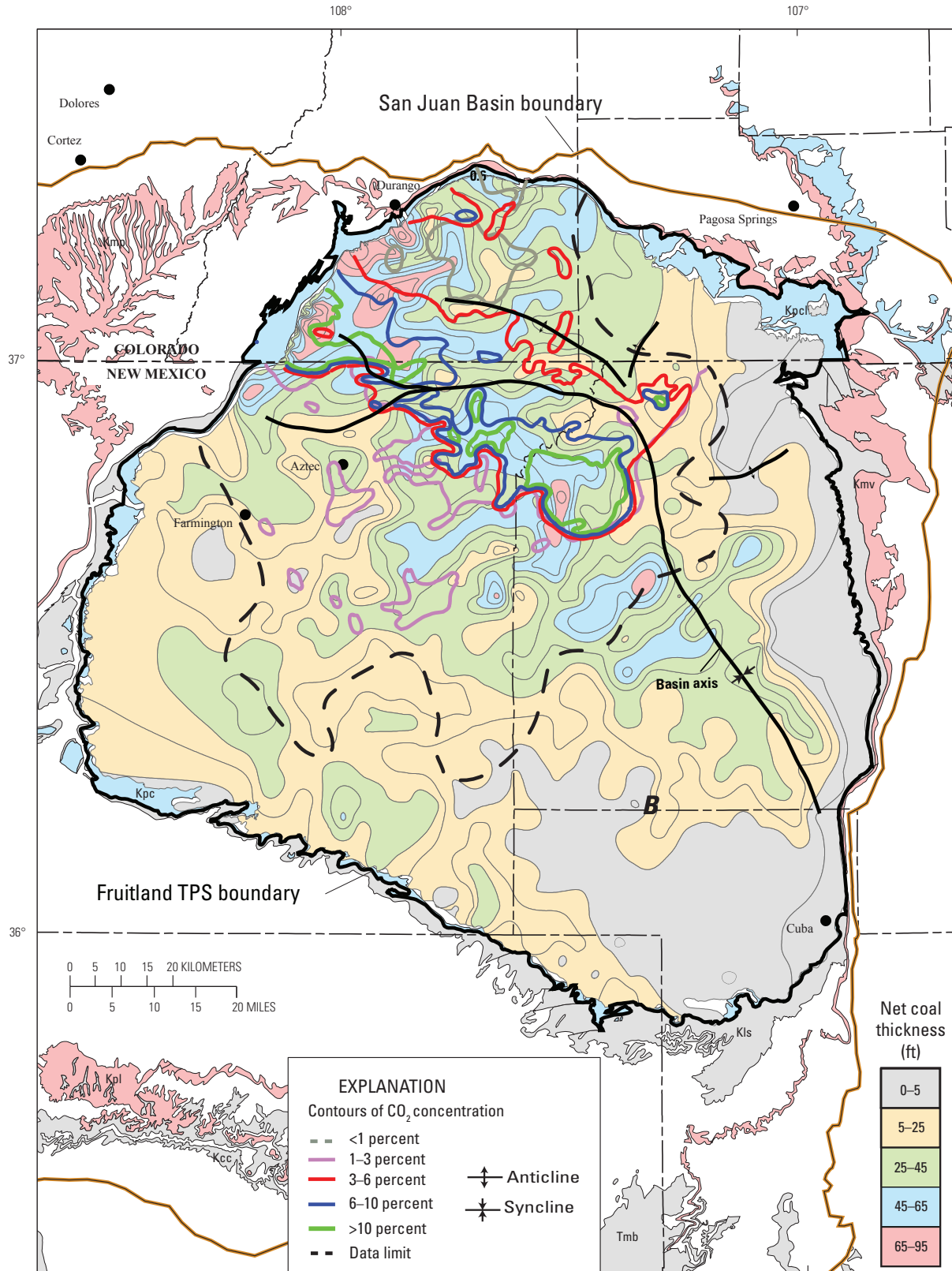


Figure 22. Map showing the relation between net coal in the Fruitland Formation (modified from Fassett, 2000) and distribution of CO₂ concentration in Fruitland Formation gases. Contour data from Scott (1994). Symbols for geologic map units: Toa, Tertiary Ojo Alamo Sandstone; Tmb, Tertiary Miocene volcanics; Kpc, Pictured Cliffs Sandstone; Kpcl, Pictured Cliffs Sandstone and Lewis Shale; Kls, Lewis Shale; Kcc, Crevasse Canyon Formation; Kmp, Menefee Formation and Point Lookout Sandstone; Kmv, Mesaverde Group; Kpl, Point Lookout Sandstone (Green, 1992; Green and Jones, 1997). TPS, Total Petroleum System.

present basin boundary, and thus the present western configuration represents a truncation of the original geometry of the coal in the area of the outcrop. The configuration of the 6- and 10-percent contours seem to follow the net coal isopach trends and probably extended beyond the present western margin of the Fruitland Formation. Because the thick coal area bounded by the 6-percent CO₂ concentration has been folded, it might be assumed that the distribution of CO₂ in this area would be a result of post-deposition meteoric redistribution of CO₂ down structural dip. However, the general positions of these contours appear to be controlled more by original depositional conditions (coal geometry) than by subsequent incursion of meteoric waters and structural orientation (figs. 11 and 22). This does not mean that incursion of younger meteoric waters have not had some effect in redistributing the CO₂, but it may not be as important as suggested by Scott and others (1994b) in controlling the spatial distribution of high CO₂ content.

In places the CO₂ contours cut across structure contours drawn on top of the Huerfanito Bentonite Bed, especially along the northern and western basin margins, and the area of greater than 3-percent CO₂ generally now lies within the deepest part of the present-day basin (fig. 23A). CO₂ contours also crosscut vitrinite isorefectance contours (fig. 16) in places. The irregularity of the CO₂ contours implies that controls other than basin structure or thermal maturity are responsible for irregular CO₂ distribution. Differential adsorption of CO₂ by coal may be one control on the irregular pattern of CO₂ distribution. Carbon dioxide has been found to adsorb more tightly to coal matrix, compared to methane. Another control would be microbial generation of methane by CO₂ reduction. This process could operate both pre- and post-thermogenic gas generation and generally results in lowering CO₂ concentration because CO₂ is consumed in the process of methane generation. Groundwater flow can also alter the spatial distribution of CO₂ either through redistribution or as part of the microbial-gas-generation process. If generation of late-stage microbial gas by CO₂ reduction (post-thermogenic gas generation) is an important component of gas resources, as suggested, it might be expected that CO₂ content would reflect geologically recent basin groundwater flow patterns. These groundwater patterns would be younger than the structural configuration of the basin (Scott and others, 1994b).

In the area south of the Fruitland Fairway CBG AU, the apparent lack of strong correspondence between CO₂ concentration and thermal maturity and structure contours, and the convolute nature of the CO₂-concentration contours suggests some element of groundwater (or gas) flow from south to north in the geologic past. The convolute position of the 3–6 percent CO₂ contour circumscribes the Fruitland Fairway CBG AU as well as the southern boundary of the northwest–southeast trend of thick net coal (figs. 22). The convolute pattern implies that groundwater flow events may have modified the original CO₂ distribution, and the original CO₂ content in this area was influenced by coal thickness and geometry, reservoir pressure, and thermal history. Likewise, the northern boundary of the convolute pattern of the 3–6 and 6–10 percent

CO₂ contours in the Fruitland Fairway CBG AU and overpressured part of the Basin Fruitland CBG AU might also reflect modification of original CO₂ concentration by groundwater flow from the north. It should be considered that the flow events are not time equivalent.

Although the CO₂ contours do not appear to conform strongly to current basin structure or thermal maturity trends, they do show a correlation with trends in isopach thickness between the Huerfanito Bentonite Bed and the top of the Pictured Cliffs Sandstone (fig. 23B), the position of major shoreline trends as inferred from ammonite zones (figs. 24 and 25), and net coal thickness isopachs (fig. 22) (Fassett, 2000). All these features as well as the pattern of CO₂ content have a strong northwest–southeast orientation, subparallel to the regional structural grain at the time of deposition. The correlation of broad regional patterns of CO₂ content with these features suggests that geologic rather than hydrodynamic controls, which are more southerly or northerly directed, may be more important in controlling the distribution of CO₂ content in Fruitland gas.

Regional trends in the isopach thickness of the interval between the top of the Huerfanito Bentonite Bed and the top of the Pictured Cliffs Sandstone appear to coincide with the major shorelines established for the Pictured Cliffs Sandstone (fig. 24) (Fassett, 2000). The spacing of the isopach contours reflects the rate of deposition and regression relative to the rate of subsidence. Where the contours are farther apart, regression was more rapid, and where they are more closely spaced, regression was slower (Fassett, 2000). The close spacing of the 750- to 1,000-ft contours is interpreted to coincide with major buildups of sandstones of the Pictured Cliffs (see wells 16–18 on fig. 4). The Pictured Cliffs shoreline defined by the *Didymoceras cheyennense* ammonite zone approximately parallels the 750-ft-isopach contour (fig. 24) and is located between wells 16 and 17 (fig. 4). The Pictured Cliffs shoreline defined by the *Baculites compressus* ammonite zone roughly parallels the 950-ft-isopach contour (fig. 24) and is located between wells 17 and 18 (fig. 4). Thick net coal accumulated behind these sandstone buildups (see wells 15–17 on fig. 4).

The northern boundary of the 3–6 percent CO₂ contour lies approximately south of the Pictured Cliffs shoreline defined by the *Baculites compressus* ammonite zone, and the northern boundary of the 6–10 percent CO₂ contour lies roughly south of the Pictured Cliffs shoreline defined by the *Didymoceras cheyennense* ammonite zone (fig. 25) (Fassett, 2000). The ammonite zones were defined in the Lewis Shale, which intertongues with the overlying Pictured Cliffs Sandstone. The zones have been used in determining major shoreline positions in the Pictured Cliffs Sandstone (Fassett, 2000), as well as for defining the position and regional extent of stratigraphic rise of Pictured Cliffs shorelines from southwest to northeast across the basin. On a regional scale, shifts in shoreline position influence the geometry and thickness of coal and influence the pathways of subsequent groundwater movement. Major CO₂ content changes that are coincident with defined shifts in shorelines suggest that geologic rather

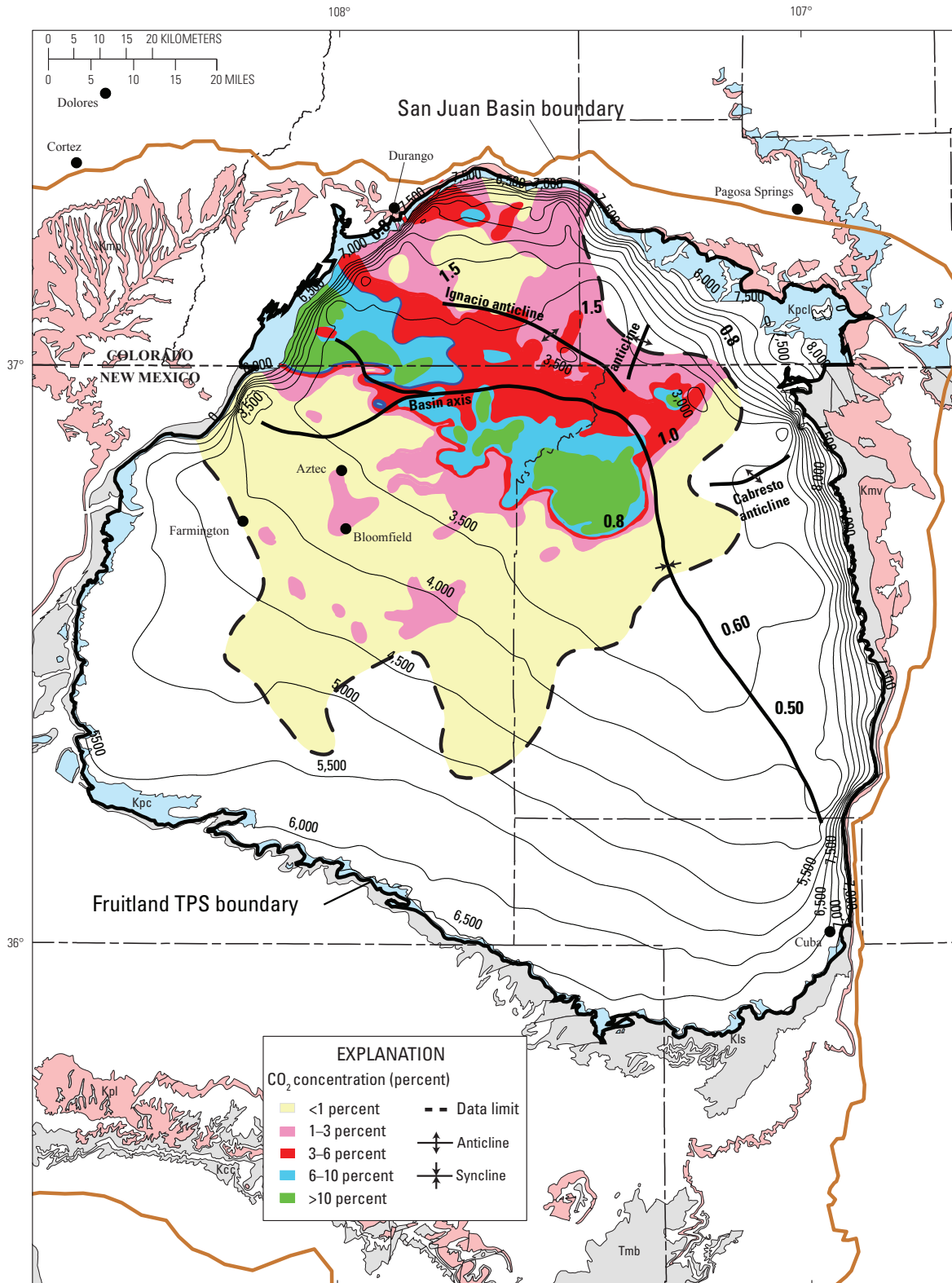
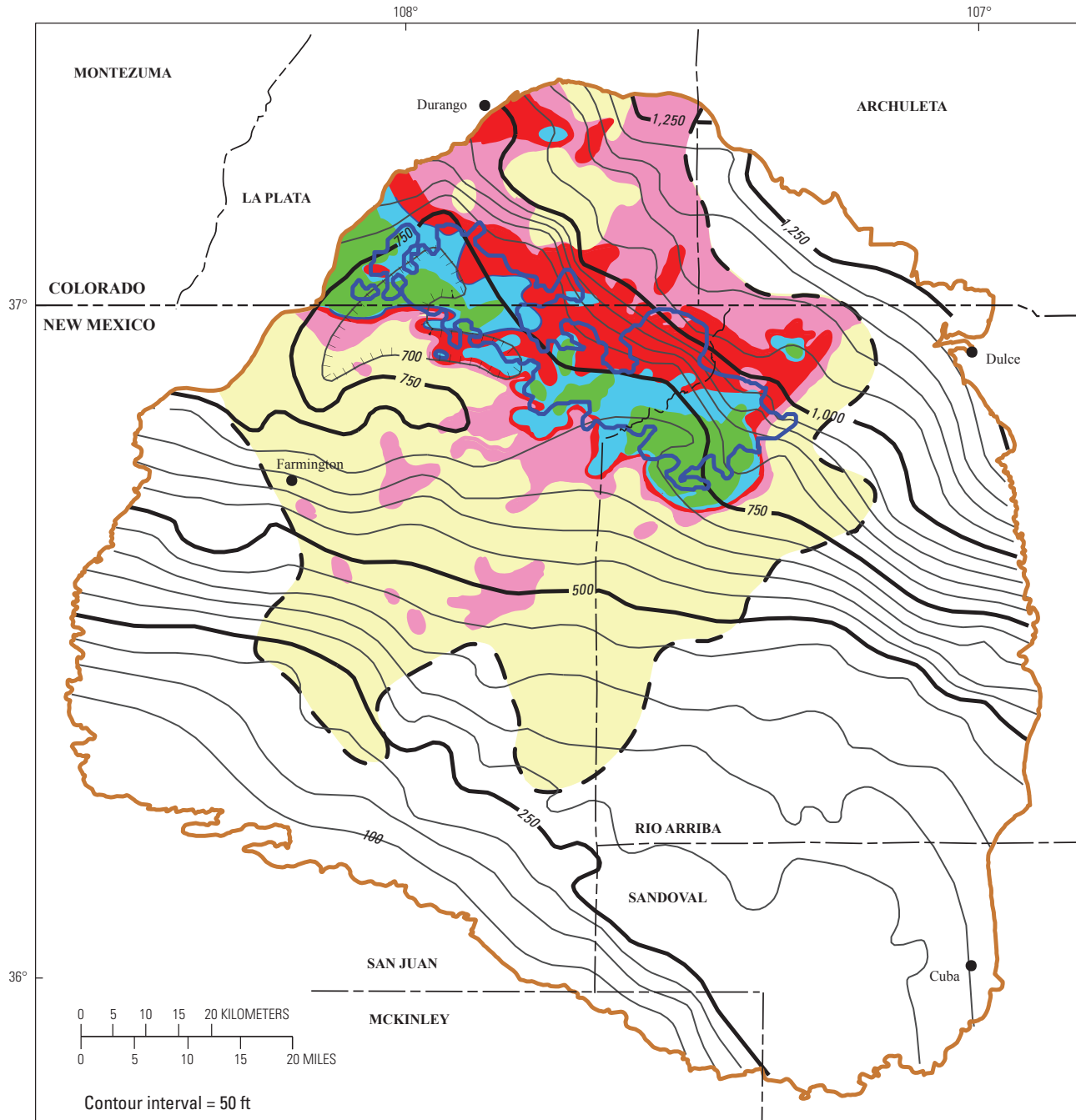


Figure 23A. Map showing distribution of CO₂ concentration in Fruitland Formation gases and relation to structure contours drawn on top of Pictured Cliffs Sandstone. Contour data from Scott (1994). TPS, Total Petroleum System. Symbols for geologic map units: Toa, Tertiary Ojo Alamo Sandstone; Tmb, Tertiary Miocene volcanics; Kpc, Pictured Cliffs Sandstone; Kpcl, Pictured Cliffs Sandstone and Lewis Shale; Kls, Lewis Shale; Kcc, Crevasse Canyon Formation; Kmp, Menefee Formation and Point Lookout Sandstone; Kmv, Mesaverde Group; Kpl, Point Lookout Sandstone (Green, 1992; Green and Jones, 1997). TPS, Total Petroleum System.



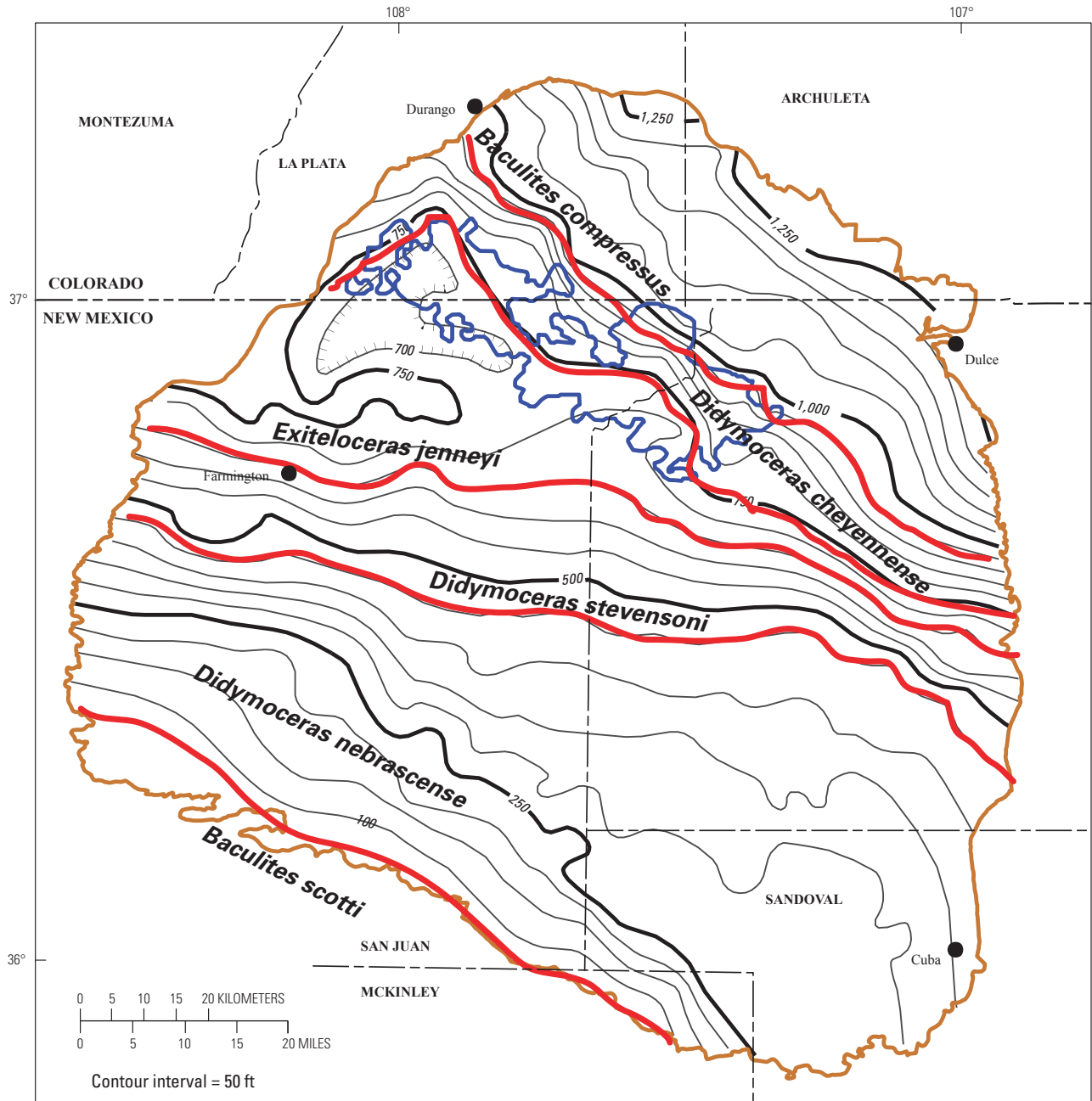
EXPLANATION

CO₂ concentration (percent)

- < 1
- 1-3
- 3-6
- 6-10
- >10

- Data limit
- Basin Fruitland Coalbed Gas AU boundary
- Fruitland Fairway Coalbed Gas AU boundary
- 200 — Thickness of isopach interval (Huerfanito Bentonite Bed to top of Pictured Cliffs Sandstone)

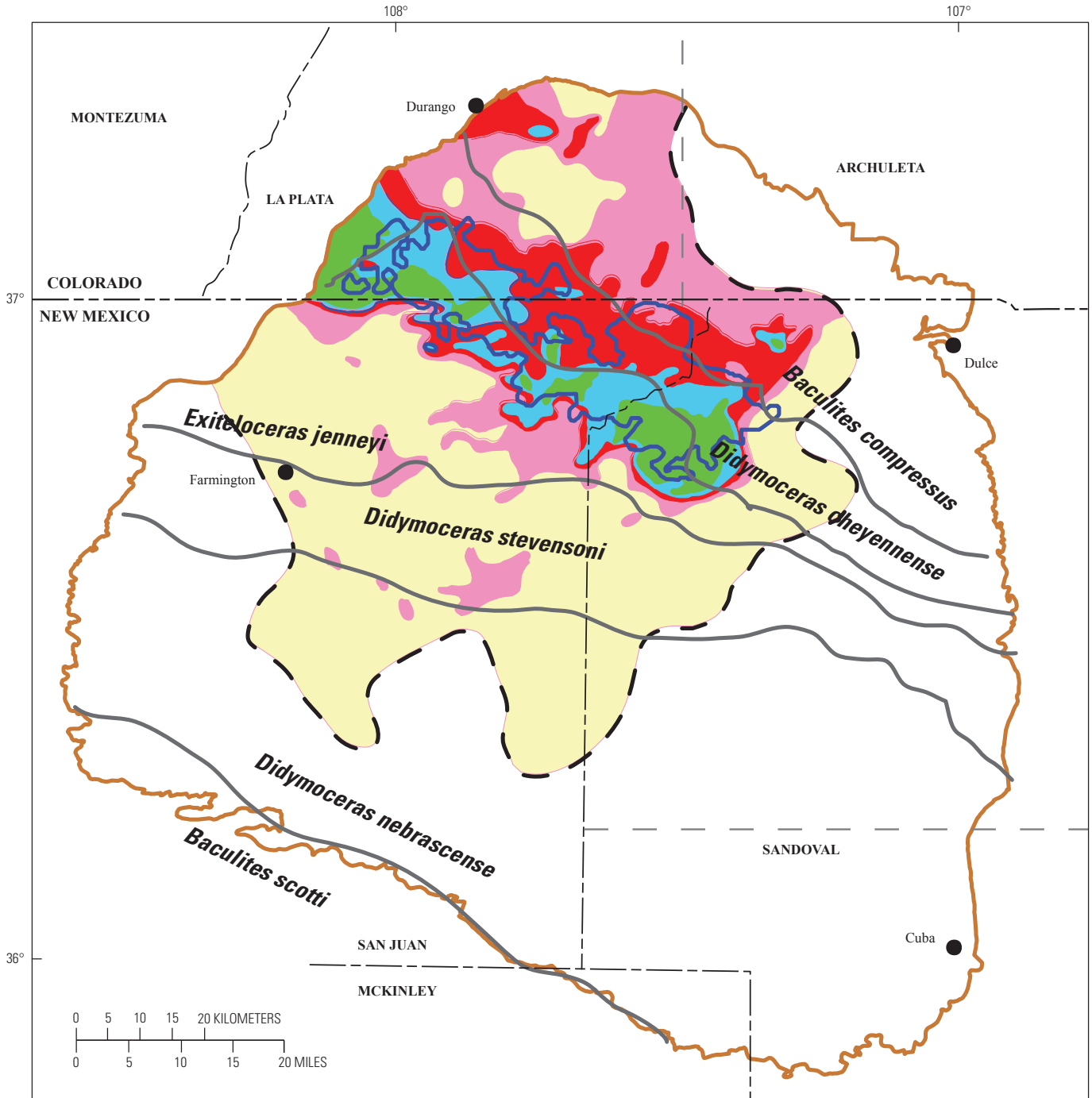
Figure 23B. Map showing distribution of CO₂ concentration in Fruitland Formation gases and relation to the isopach thickness of the interval between Huerfanito Bentonite Bed of Lewis Shale and top of the Pictured Cliffs Sandstone (modified from Fassett, 2000). Contour data from Scott (1994). AU, assessment unit.



EXPLANATION

- Basin Fruitland Coalbed Gas AU boundary
- Fruitland Fairway Coalbed Gas AU boundary
- 200 — Thickness of isopached interval (Huerfanito Bentonite Bed to top of Pictured Cliffs Sandstone)

Figure 24. Map showing relation between shorelines (red), defined by labeled ammonite zones, in Pictured Cliffs Sandstone and the isopach thickness of the interval between Huerfanito Bentonite Bed of Lewis Shale and top of Pictured Cliffs Sandstone (modified from Fassett, 2000). AU, Assessment Unit.



EXPLANATION

CO₂ concentration (percent)

- < 1
- 1-3
- 3-6
- 6-10
- >10

- Data limit
- Pictured Cliffs Sandstone shorelines
- Basin Fruitland Coalbed Gas AU boundary
- Fruitland Fairway Coalbed Gas AU boundary

Figure 25. Map showing distribution of CO₂ concentration in Fruitland Formation gases with respect to Pictured Cliffs Sandstone shorelines, defined by labeled ammonite zones, (gray) (modified from Fassett, 2000). CO₂ contour data from Scott (1994). AU, Assessment Unit.

than present-day hydrodynamic controls are more important in controlling the spatial distribution of CO₂ content, especially in the area of the Fruitland Fairway CBG AU.

Superposition of the major shoreline trends, defined by ammonite zones, on net coal isopachs (fig. 26) (Fassett, 2000) shows some relation between the two, although in some areas the relation does not hold. This is probably because the coal thickness was summed over some thickness interval, and the coal was not entirely deposited in areas related to a particular shoreline. The thickest net coal lies landward of the shoreline defined by the ammonite *Didymoceras cheyennense*, and thick net coal is found landward of the western part of the shoreline defined by the ammonite *Baculites compressus* (fig. 26) (Fassett, 2000). These two shoreline positions were developed over periods of relatively slow sea level rise, resulting in stacking of shoreface sandstones and greater thickness of accumulation of coal in coastal and lower alluvial plain settings. These coals might have greater lateral continuity than coals deposited during periods of more rapid progradation, a factor that ultimately will influence later groundwater flow.

Superposition of CO₂ contours on net coal isopachs indicates a relation between CO₂ concentration and net coal thickness and trends in coal thickness (fig. 22). There are two areas of greater than 6-percent CO₂ concentration that are separated by an area of greater than 3-percent but less than 6-percent CO₂ that is coincident with a northeasterly trend of thin net coal (25–45 ft). This northeasterly trend in thin net coal separates two areas of thicker net coal that on a regional scale may not be in effective hydraulic communication with each other. Gases from wells in the southeast lobe of thick net coal, where the coal is thickest, have CO₂ concentrations of 6 percent or higher. The northern and eastern boundaries to the 10-percent concentration in this lobe appear to be constrained by areas of thin net coal (fig. 22) and sandstone (Scott and others, 1994b). This area of high CO₂ concentration also corresponds to an area where wells have very high bottom-hole pressures (Scott and others, 1994b). The high pressures in these wells have some influence on the amount of CO₂ concentration because of sorption conditions. The present structural axis of the basin generally follows the same easterly and southeasterly trend of thin coal isopach (fig. 22) and further helps to isolate this area of thick net coal from later incursion of meteoric waters from the north and west, primarily because of the difference in orientation of the regional dip. This relation will be shown to be important in controlling the regional distribution of gas resources in the Fruitland Fairway CBG AU.

In the Fruitland Fairway CBG and Basin Fruitland CBG AUs, regional pressure gradients, considered by many to reflect later hydrodynamic repressuring of the Fruitland, crosscut CO₂ contours, and thus it appears that repressuring events have had only minor influence on redistributing CO₂ concentration (fig. 21). CO₂ concentrations (greater than 6 percent) similar to those found in the overpressured (>0.50 psi/ft) area of the southeastern part of the Fruitland Fairway occur in less pressured (0.44–0.50 psi/ft) strata, implying that geologic factors other than pressure gradients are also important in controlling the CO₂ concentration in the gases. Superposition of

the CO₂ contours on the regional δ¹⁸O-isotope pattern (fig. 27) shows little modification to the position of the contours by subsequent groundwater flow. The only exception to this is an area of recent recharge in the northern part of the basin where high CO₂ in the gas might be related to active microbial action. The relations discussed above have been used in evaluating controls on the spatial distribution of gas resources in the Basin Fruitland and Fruitland Fairway CBG AUs.

Gas Generation Processes

Microbial

An understanding of past and ongoing methanogenic activity is important because of the contribution of late-stage microbial gas to the total gas resources (Scott and others, 1994b). Only in areas where methanogenesis is ongoing could potential resources be increased by some factor due to the generation of microbial gas. In areas where methanogenic activity has ceased, the total in-place gas resources would be fixed. Formation and retention of early formed microbial gas has probably been overlooked as a component of Fruitland gas. Scott and others (1994b) suggested that any early formed microbial gas would have been lost or not retained due to the high water content of the peat and limited sorption sites. However for at least the first 10 m.y. after deposition, groundwater flow in the Fruitland was to the north. During this time the lignite was being compacted and dewatered and over time thermally transformed from lignite to subbituminous coal.

Methane produced today in the Powder River Basin comes from thermally immature to subbituminous coals where cleats are not well developed. The gas is formed by microbial activity as groundwater encountered the coals (Gorody, 1999). The time of gas generation is unknown. It has been estimated to be from 35 to 10 Ma, when uplift and erosion of the basin began, or to have formed since the Pleistocene (Gorody, 1999). If extensive quantities of microbial gas can form in subbituminous coals under the right hydrodynamic conditions, then a similar model could be applied to the Fruitland during the first 10 m.y. after deposition. Thus, some portion of gas produced today may have early microbial origin. Mixture of early microbial gas with later thermally generated gas might account for the small range of carbon isotopes of the methane and for heavy carbon isotopes of the dissolved inorganic carbon in produced waters throughout the production area. During thermogenic gas generation, the dissolved bicarbonate would not be used in the creation of methane, and if it was not removed in extensive mineral diagenesis (isotopically heavy carbonate could be indicative of early microbial processes), it will remain if the system was closed to future groundwater flow.

The most thermally mature part of the Fruitland, as determined by vitrinite reflectance values, reached a maximum temperature of about 165°C in the Oligocene (~25 Ma) in the northern part of the Basin Fruitland CBG AU (fig. 10C). The Fruitland in this area may have been buried up to as much as

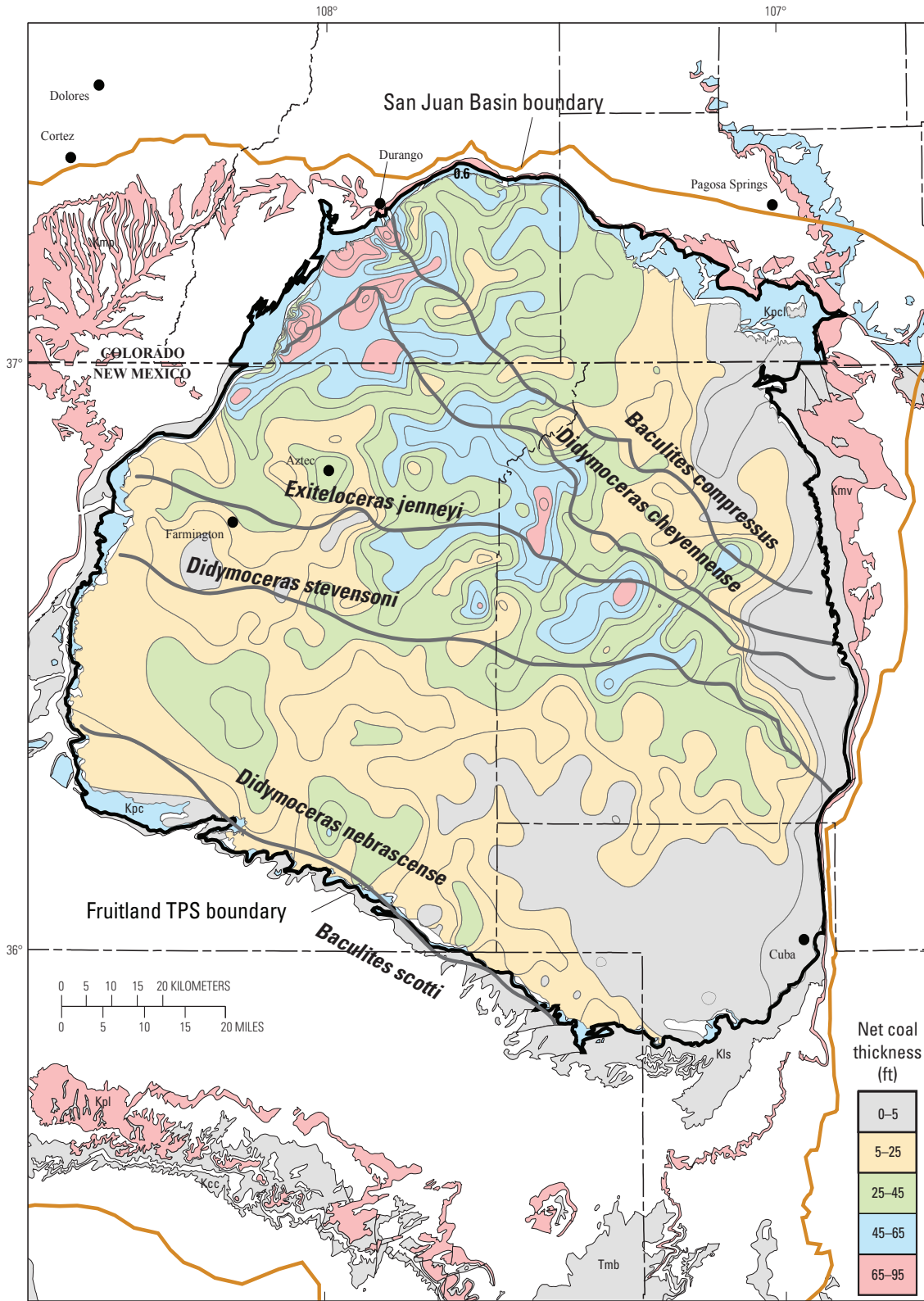
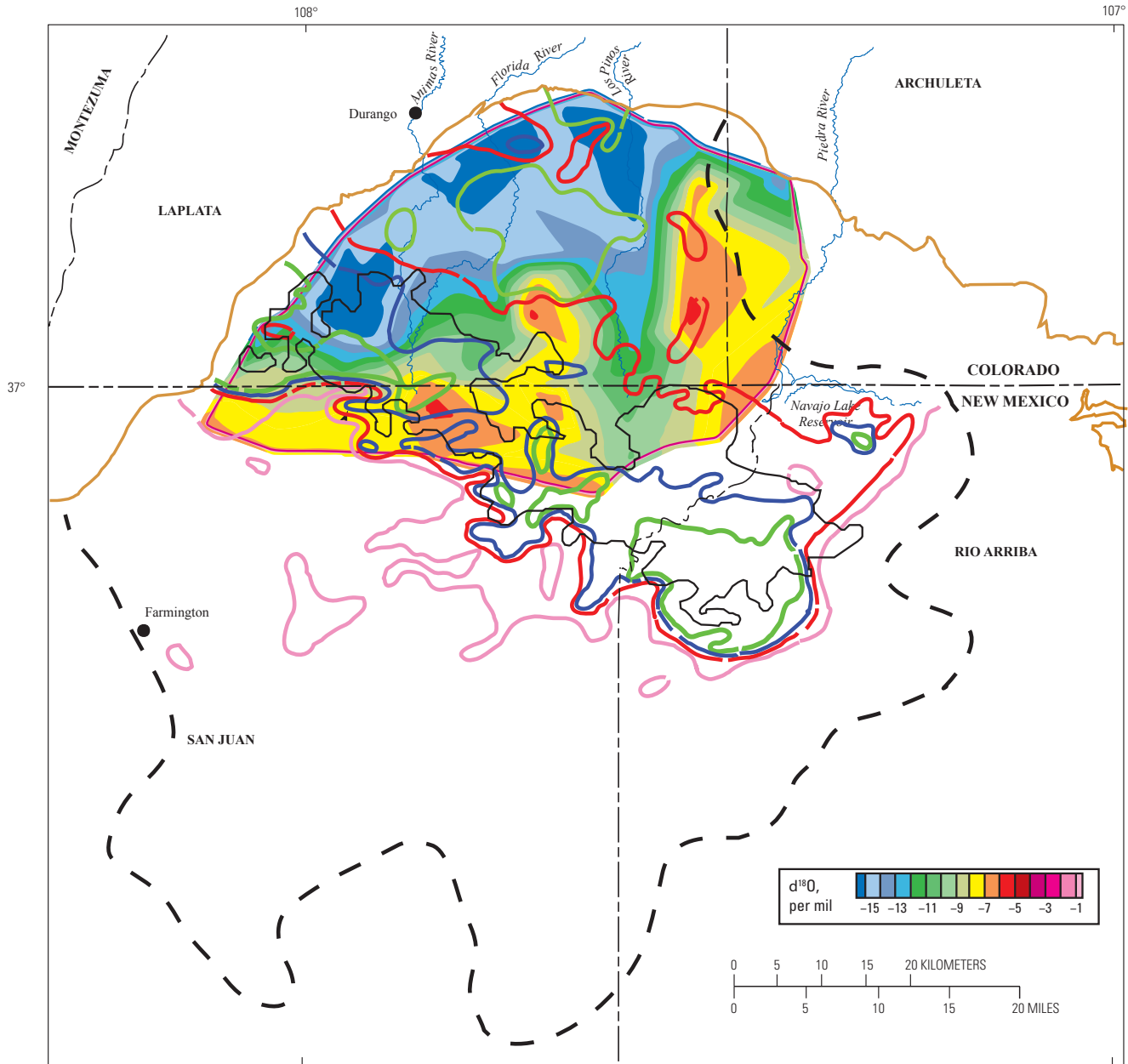


Figure 26. Map showing the relation between net coal in the Fruitland Formation (modified from Fassett, 2000) and shorelines in the Pictured Cliffs Sandstone, defined by labeled ammonite zones (black). Symbols for geologic map units: Toa, Tertiary Ojo Alamo Sandstone; Tmb, Tertiary Miocene volcanics; Kpc, Pictured Cliffs Sandstone; Kpcl, Pictured Cliffs Sandstone and Lewis Shale; Kls, Lewis Shale; Kcc, Crevasse Canyon Formation; Kmp, Menefee Formation and Point Lookout Sandstone; Kmv, Mesaverde Group; Kpl, Point Lookout Sandstone (Green, 1992; Green and Jones, 1997). TPS, Total Petroleum System.



EXPLANATION

- | | | |
|---|----------------|------------------------------------|
| Contours of CO ₂ concentration | | Basin Fruitland Coalbed Gas AU |
| — < 1 percent | — 6–10 percent | |
| — 1–3 percent | — > 10 percent | — Fruitland Fairway Coalbed Gas AU |
| — 3–6 percent | --- Data limit | |

Figure 27. Map showing relation between $\delta^{18}\text{O}$ of produced Fruitland Formation waters and carbon dioxide concentration in Fruitland Formation gas. CO₂ contours from Scott (1994). Oxygen-isotope base map from Cox and others (2001). AU, Assessment Unit.

9,000 ft (fig. 10C); although present depths of burial are about 2,200 ft. This area now falls within water flow paths having $\delta^{18}\text{O}$ values of -15 per mil (fig. 11) and present-day temperatures of the Fruitland in this area are near 45°C , using uncorrected bottom-hole temperatures from wells that are completed in the Fruitland. This latter temperature is well within the temperature range of $30^\circ\text{--}80^\circ\text{C}$ for microbial-gas generation (see discussion in Gorody, 1999). The Fruitland in this area cooled to a temperature of 80°C near the Miocene–Pliocene boundary (5 Ma) (fig. 10C). Thus from the middle Eocene, when temperatures in the Fruitland exceeded 80°C , to the Pliocene, generation of any significant volume of microbial gas would have been inhibited by formation temperatures exceeding 80°C .

Optimal temperature conditions for microbial-gas generation range from $35^\circ\text{--}45^\circ\text{C}$ (Zeikus and Winfrey, 1976), but may range as high as 60°C (Fishman and others, 2001). In the TPS, these temperatures were not reached (post-thermal-gas generation) until the onset of the Pleistocene (1.8 Ma) (fig. 10C). Thus, optimal temperature conditions for generation of microbial gas throughout the Fruitland (post-thermal-gas generation) have existed only since the onset of the Pleistocene (fig. 10C). However, thermal conditions suitable for early (pre-thermal gas) microbial-gas generation (fig. 10C) existed at least through the Paleocene and possibly into the early Eocene, a time spanning 10–25 m.y. from the time of deposition.

Thermogenic

Because there is more gas present in Fruitland Fairway coals than can be accounted for by standard coal volume calculations, it has been suggested that 25–50 percent of the gas produced in the Fruitland Fairway was generated in place during coalification and that the remainder migrated there in the Oligocene or was generated in place as late-stage microbial gas from the middle Pliocene to Holocene as a consequence of introduction of meteoric water (Scott and others, 1994b). The model (Scott and others, 1994b) that has been proposed to explain the high gas content in the Fruitland Fairway coals is

1. thermally generated gas that exceeded coal storage capacity migrated in the Oligocene from north to south (from the deep part of the basin toward the south into somewhat lower rank coals); this thermal gas was then trapped in coals just north of a possible structural hingeline, where the coal geometry changed;
2. in the middle Pliocene, after uplift, erosion, and thermal cooling, meteoric waters entered the basin from the north, bringing bacteria that produced late-stage microbial gas and carbon dioxide (and heavy carbon in bicarbonate in water due to CO_2 reduction);
3. as this evolved groundwater moves southward down dip it “sweeps” or dissolves methane that later fills cleats or is resorbed by coals, which are now undersaturated due to uplift and erosion; and

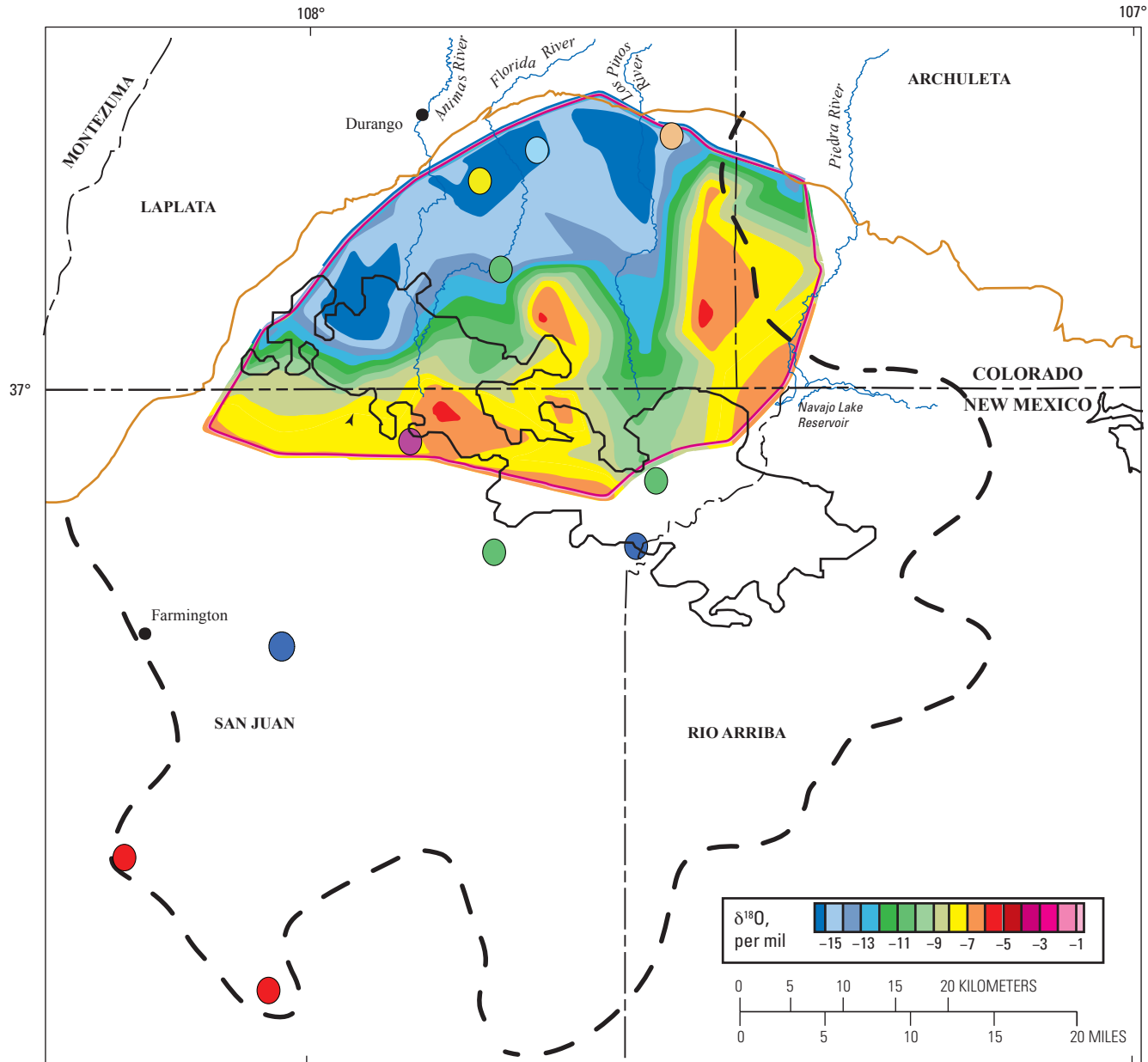
4. water flows vertically upward in the area just north of the hingeline and further augments the gas content of the coals.

Gas Origin

Considering some of the data and spatial relations previously presented, there are some problems with the above model. Fruitland gas is undoubtedly a mixture of variable proportions of thermogenic and microbial gas, based on the carbon isotopes of the methane, carbon dioxide, and dissolved bicarbonate. The principal question concerning the microbial part is the age of generation and the percent contribution to total gas resources. Is it all post-thermogenic as a result of introduction of microbes with meteoric water of Pliocene and younger age or generated in place by microbial communities that came back to life after dormancy? Was some or much of the microbial component generated prior to thermal-gas generation? How does resolving these questions affect the evaluation of potential and future gas resources in the Fruitland?

Groundwater flow may be important in modifying Fruitland gas production and has been instrumental in generation of late-stage microbial gas in some areas. However, the role of Pliocene and younger groundwater might not be constructive in all areas and in generating large quantities of late-stage microbial gas. In some areas, it can be a destructive process resulting in oxidation of methane (Gorody, 2001). The distribution of $\delta^{13}\text{C}$ of DIC, distribution of $^{129}\text{I}/\text{I}$ minimum ages, $\delta^{13}\text{C}$ of methane, and CO_2 content do not correspond with trends (taken to represent direction of more recent groundwater flow) in $\delta^{18}\text{O}$ content of produced water (figs. 13–16, 18, 27, and 28). These distributions also do not correspond with trends in pressure gradient. On the contrary, the distribution of $\delta^{13}\text{C}$ of DIC and $\delta^{13}\text{C}$ of methane is rather uniform (within a narrow range of values) except along the northern and southwest margins of the Fruitland. CO_2 content seems to more closely correspond with thicker and less mature coal. In addition, limited data indicates no linear mixing relation between CO_2 concentration and the $\delta^{13}\text{C}$ of methane (fig. 8B) or between the $\delta^{13}\text{C}$ of CO_2 and $\delta^{13}\text{C}$ of methane (fig. 19). Some data show a slight linear relation between $\delta^{13}\text{C}$ CO_2 and CO_2 concentration, and this relation seems to be different for gas in Colorado and New Mexico (fig. 20).

Isotopically heavy bicarbonate waters (figs. 14 and 28) (Scott and others, 1991) are found in the overpressured northern part of the Basin Fruitland CBG AU, in the very southwestern underpressured part of the Basin Fruitland CBG AU, and in the overpressured Fruitland Fairway CBG AU, and have been used in arguments for late-stage microbial-gas generation in these areas. However, isotopically heavy carbon as dissolved bicarbonate has been found in one Pictured Cliffs Sandstone well (18.52 per mil) and one Fruitland Formation well (25.29 per mil) south of the Fruitland Fairway and northeast of Farmington, N. Mex., in the underpressured part of the Fruitland Formation (Ridgley, unpub. data, 2001). These data suggest that generation of microbial gas in the Fruitland



EXPLANATION

- - - Data limit
 - Basin Fruitland Coalbed Gas AU
 - Fruitland Fairway Coalbed Gas AU
- | $\delta^{18}\text{O}$ of dissolved inorganic carbon species | | |
|---|------------------|--------------|
| ● 16.7 | ● 23.5 | ● 25.3, 25.6 |
| ● 17.5 | ● 24, 24.7, 24.9 | ● 26 |
| ● 19.5, 19.7 | | |

Figure 28. Map showing the distribution of $\delta^{13}\text{C}$ of dissolved inorganic carbon in Fruitland Formation produced waters in relation to $\delta^{18}\text{O}$ of produced waters. Oxygen-isotope base map from Cox and others (2001). $\delta^{13}\text{C}$ of dissolved inorganic carbon from Scott and others (1994b) and Threlkeld (written commun., 2001). AU, Assessment Unit.

is a much more common phenomena and is not a process confined to the overpressured area or to the southwest margin of the Fruitland. The time of formation, as discussed above, could vary.

Minimum $^{129}\text{I}/\text{I}$ ages for the produced waters from these two wells are Eocene (Pictured Cliffs) and earliest Miocene (Fruitland) (Ridgley, unpub. data, 2001). If these ages are valid, then the heavy bicarbonate signatures of the water should be this age or older, unless microbial communities that produced microbial methane by the CO_2 -reduction pathway go dormant and survive high heat only to become active once the temperatures cool to an optimal range. If this is the case, there is no connection between heavy bicarbonate signatures, the age of the formation water, or later inferred flow paths.

If some produced waters in the underpressured part of the Fruitland are Miocene or older and if they originated from a part of the basin that was less thermally mature and hence in a temperature range where CO_2 content might have been higher, then it is possible that (based on solubility conditions) the waters may have transported both methane and CO_2 in solution. This water may also have been enriched in bicarbonate content if bacterial methanogenesis had occurred in the geologic past. This hypothesis is supported, in part, by the $^{129}\text{I}/\text{I}$ minimum age of the water and the heavy $\delta^{13}\text{C}$ of the dissolved inorganic carbon of the previously mentioned well. In this scenario, northward flowing waters may have been trapped near the area of the Fruitland Fairway as the basin was slowly being downwarped. Trapping would have been aided by permeability barriers, such as:

1. changes in coal and sandstone geometry in the area of thick net coal, which is one characteristic of the Fruitland Fairway CBG AU (fig. 5), or
2. faults that formed during Laramide tectonism.

In the area of thick net coal, contours of net coal thickness are mostly oriented northwest–southeast in contrast to the dominantly northeast-trending net coal isopachs to the south. Here waters (and higher bicarbonate content) and gases would have been trapped and mixed with in-place water and in-place generated gas as the basin continued to subside to the north. Subsequently, when the basin axis shifted south to its present position, these waters and gases would be unable to migrate from the area, because of later artesian pressuring from the north coupled with the change in coal-bed geometry and structural dip of the Fruitland coal beds (structural hinge-line of Scott, 1994; Fassett, 2000) to the south. The waters and gases would be isolated from later groundwater influx, and the chemical system in this area would be closed. The gas composition would reflect a mixture of early microbial and later thermogenic gas. Therefore, the southern boundary of the overpressured area may in fact reflect overpressuring of these older waters trapped between younger artesian conditions to the north and a structural/geologic setting that does not permit rapid loss of water to the south that would relieve overpressuring.

Eocene, Oligocene, and Miocene minimum ages based on $^{129}\text{I}/\text{I}$ ratios have been documented in Fruitland waters from

the northern part of the Fruitland Formation (fig. 13) (Colorado Oil and Gas Commission, 1999b; Snyder and others, 2003). The preponderance of Oligocene and Miocene minimum ages in the area of the southern part of the overpressured zone (Fruitland Fairway) could support

1. the migration of gas in the Oligocene from north to south (from the deep part of the basin toward the south into somewhat lower rank coals) and
2. vertically upward flow of water in the area just north of the hingeline as has been suggested by Scott and others (1994b).

However, these waters would have to somehow bypass a large area containing older waters (Paleocene and Eocene). Alternatively, these waters could be related to northward flow in the Fruitland during the Oligocene and Miocene as the basin was being downwarped. The absence of dated waters of Pliocene and younger age over most of the Fruitland in the northern part of the TPS suggests that the hydrologic model proposed (Kaiser and others, 1994; Cox and others, 2001) for the Fruitland needs to be reevaluated.

Hydrocarbon Migration Summary

Hydrocarbons migrated laterally and downward from the Fruitland Formation into the Pictured Cliffs Sandstone by way of faults, fractures (cleats) in the Fruitland coals, or by diffusion. Pressure differences between the Fruitland and Pictured Cliffs have been proposed as the cause of diffusion from one formation to the other (Rice and others, 1988; Scott and others, 1991). Hydrocarbons have migrated upsection from the Fruitland to the Farmington Sandstone Member of the Kirtland Shale and to Tertiary rocks in the northwestern and northeastern parts of the San Juan Basin. Migration paths have not been positively identified for the Farmington accumulations. Fractures and dike-margin discontinuities associated with the late Oligocene Dulce dike swarm (Ruf and Erslev, 2005) are thought to be the main migration pathways for gas accumulations in Tertiary rocks in the Cabresto Canyon producing area (see fig. 52).

The principal reservoirs in the Fruitland Formation are the coals, although sandstone channels are also reservoirs. Coals (exclusive of their cleats) have low porosity and virtually no permeability, and thus, the gases are sorbed onto the coal matrix (Scott, 1994). Migration of gas from the coal, by way of cleats, into other reservoirs, such as the interbedded sandstones, can occur when pressure is decreased below the sorptive capacity of the coal at a given temperature. Pressure decreases usually occur during production but may also have occurred in the geologic past during periods of uplift and erosion. Migration of coal-derived gas may also occur by diffusion (Scott, 1994), and if it enters the hydrologic regime, the gas may dissolve in the water and be transported to other sites of accumulation. The regional changes in composition of Fruitland gas suggest that some migration of gases has occurred (Scott, 1994).

Permeability in coals is much higher than that of the interbedded sandstones; the permeability is confined to cleats (Scott, 1994; Cox and others, 2001). Extensive cleat development in the coals is the principal permeability pathway required for production from these reservoirs (Tremain and others, 1994; Shuck and others, 1996), but also serves as a pathway for gas to migrate away from the coals as the pressure changes in the reservoir. Local faults in the Fruitland also serve as conduits for gas migration as well as provide better deliverability of gas to the wellbore (Tremain and others, 1994; Shuck and others, 1996).

Hydrocarbon Traps and Seals

Stratigraphic traps are the principal trapping mechanism for gas in the Pictured Cliffs Sandstone. These traps form when sandstone lenses in the Pictured Cliffs pinch out updip into coal or mudrocks in the lower part of the Fruitland Formation. Seals for the Pictured Cliffs are complex—a combination of mudrocks in the overlying Fruitland and Kirtland Formations, coal beds into which sandstone lenses pinch out, and cementation of the reservoir rocks (Cumella, 1981; Goberdhan, 1996). Water saturation on the south margin of the basin acts as a relative permeability barrier to migration, whereas diagenesis of reservoir rocks is a sealing mechanism on the north margin (Cumella, 1981; Goberdhan, 1996).

Several types of traps can be found in Fruitland Formation reservoirs; each varies in size or areal extent. At the smallest scale, the coals in the Fruitland serve not only as the source of the produced gas in the Fruitland, but also the trap and reservoir. Permeabilities in coals (exclusive of cleats) are virtually nonexistent, and the gases are sorbed onto the coal matrix (Scott, 1994). At larger scales, the heterogeneous character of coal-bed reservoirs tends to divide the reservoir into compartments. The compartments may form when one or possibly both cleat directions are closed or nearly closed as a result of tectonic stress (Shuck and others, 1996). The degree of development of the cleat system and direction of cleat development are primarily controlled by directions of tectonic stress; however, coal rank and coal matrix composition (maceral type) also have been shown to be important in forming compartments (Tremain and others, 1994). Other compartments may form as a result of intersecting faults or lateral pinchout of coal. Folds do not appear to be a major control on coal-gas accumulation, but fractures and faults associated with development of folds do affect permeability (Kaiser and Ayers, 1994). Seals in Fruitland reservoirs may be

1. closed cleats due to tectonic stress,
2. cemented faults,
3. interbedded tightly cemented sandstone reservoirs that are not fractured, and
4. carbonaceous shale or mudstone interbeds.

Stratigraphic traps (pinchouts of fluvial channels into overbank mudrocks) are also the primary trap type in the

Farmington Sandstone Member of the Kirtland Formation. Combination stratigraphic traps in fluvial channels and a structural trap on the crest of an anticline are trapping mechanisms in Tertiary formations at the Cabresto Canyon field (see fig. 52). Seals in both cases are fluvial overbank mudrocks.

Assessment Unit Definitions

Pictured Cliffs Continuous Gas Assessment Unit (50220161)

Introduction

The Pictured Cliffs Continuous Gas AU boundary was drawn to include all known and undiscovered gas accumulations in the Pictured Cliffs Sandstone in the San Juan Basin (fig. 29). The digital geologic maps of Colorado (Green, 1992) and New Mexico (Green and Jones, 1997) were used to draw the boundary, which was the upper contact of the Pictured Cliffs outcrop in most places (fig. 29). Along part of the eastern side of the basin, the Pictured Cliffs is absent at the surface, and in that area the top of the Lewis Shale was used as the boundary. In the 1995 National Assessment Play 2211 (Huffman, 1996), the Pictured Cliffs Sandstone Gas Play, was assessed. This same unit was assessed as the Pictured Cliffs Continuous Gas AU in this report.

Production from the Pictured Cliffs Sandstone started in 1927 with discoveries in the Blanco and Fulcher Kutz fields in New Mexico (fig. 29). The initial phase of widespread development drilling was from 1950 to 1959, but exploration slowed throughout the 1960s (IHS Energy Group, 2002). Another phase of drilling lasted from 1971 to 1980, with another slowdown from 1981 to about 1995. Drilling increased somewhat from 1995 to the present, with the exception of 1998, which saw little development drilling. Major gas fields producing from the Pictured Cliffs Sandstone are shown on figure 29. Production from this assessment unit as of January 2003 is about 1.1 million barrels of oil (MMBO) and 4.0 trillion cubic feet of natural gas (TCFG) (IHS Energy Group, 2003).

Currently, drilling is permitted on 160-acre spacing, and the potential for future additions to reserves may depend on decreasing the well spacing. The outer margins of the major gas fields have been fairly well defined, especially along the southwest side of the AU, where increased water saturation has resulted in a number of dry holes. Water saturation also increases along the northeast side of the gas-producing area in the AU, but some of the most recent drilling has been in this area, in the deepest part of the basin.

Areas where the reservoir rock is tightly cemented would possibly benefit by decreasing the well spacing because the possibility of interference between wells is less in those areas. Key parameters of the Pictured Cliffs Continuous Gas AU are listed below and are summarized on figure 30.

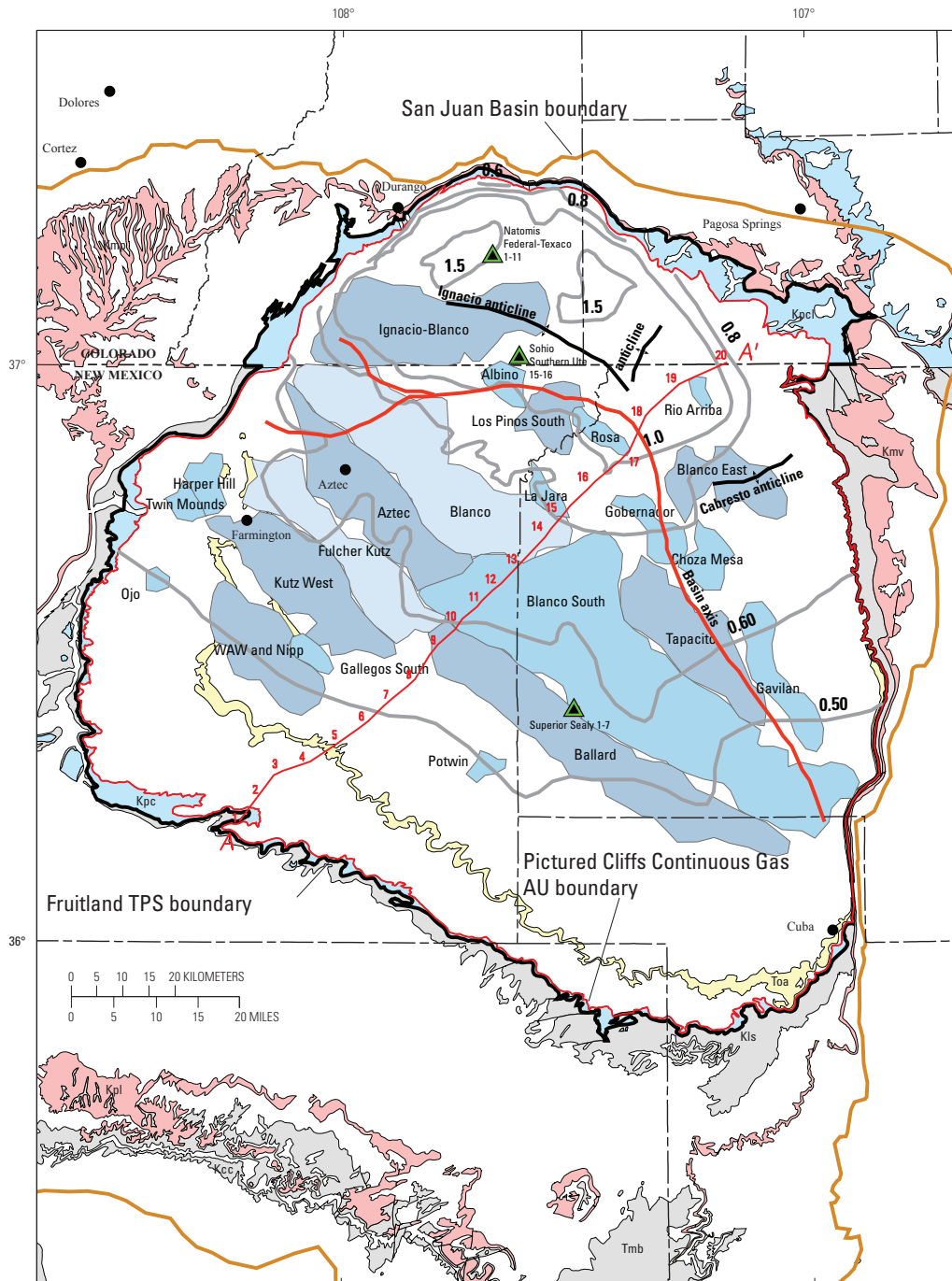
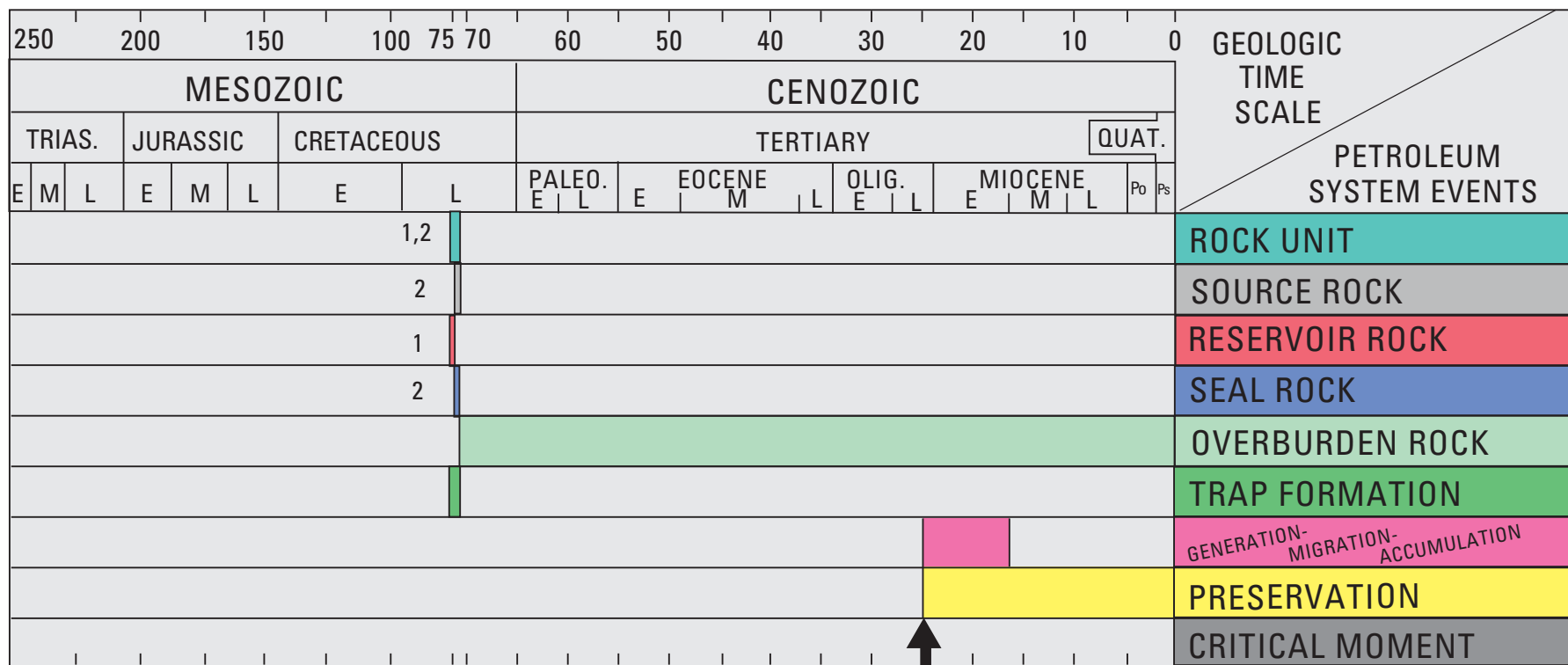


Figure 29. Map showing the boundary of the Pictured Cliffs Continuous Gas Assessment Unit (AU) (red polygon) and Pictured Cliffs Sandstone gas fields (shades of blue). Also shown are the locations of the regional cross section A–A' (see fig. 4), principal folds in the basin, and wells (green and black triangles) used to make the burial history curves in this report (figs. 10A–C). Symbols for geologic map units: Toa, Tertiary Ojo Alamo Sandstone; Tmb, Tertiary Miocene volcanics; Kpc, Pictured Cliffs Sandstone; Kpcl, Pictured Cliffs Sandstone and Lewis Shale; Kls, Lewis Shale; Kcc, Crevasse Canyon Formation; Kmp, Menefee Formation and Point Lookout Sandstone; Kmv, Mesaverde Group; Kpl, Point Lookout Sandstone (Green, 1992; Green and Jones, 1997). Contours (gray) show vitrinite reflectance (R_m) values, in percent, from data in Fassett and Nuccio (1990), Law (1992), and Fassett (2000). TPS, Total Petroleum System.



Rock units:
 Late Cretaceous—
 1. Pictured Cliffs Sandstone
 2. Fruitland Formation

Figure 30. Events chart that shows key geologic events for the Pictured Cliffs Continuous Gas Assessment Unit. Black arrow, critical moment (Magoon and Dow, 1994) for gas generation. TRIAS., Triassic; PALEO., Paleocene; OLIG., Oligocene; QUAT., Quaternary; Po, Pliocene; Ps, Pleistocene; E, early; M, middle; L, late. Geologic time scale is from the Geological Society of America web page <http://www.geosociety.org/science/timescale/timescl.htm>, last accessed 2/1/2008, and from Berggren and others, (1995).

Source

The major source rocks are overlying Fruitland Formation coal beds and carbonaceous shales. Shale beds in the underlying Lewis Shale may locally be source rocks, especially on the east side of the TPS. However, it is not possible to quantify the relative contribution of Lewis-sourced gas. The Lewis is discussed more fully in Chapter 5.

Maturation

Thermal maturation is interpreted to range from late Oligocene to early Miocene time.

Migration

Migration of gas was lateral and downward from Fruitland coal into the Pictured Cliffs. In some areas, migration was upward from the underlying Lewis Shale. Migration is thought to have been diffuse, over a wide area, and not constrained to specific routes along faults or structures. Natural fractures probably supplemented migration in some areas. Scott and others (1991) stated that gas in the Pictured Cliffs probably has a mixed source—from the Lewis and Fruitland. They suggested that higher reservoir pressures in the Fruitland during generation and/or pressure decline in the Pictured Cliffs during production resulted in downward migration of gas from the Fruitland into the Pictured Cliffs.

Reservoirs

Shoreface and foreshore sandstones provide the reservoirs, which are lenticular along depositional dip and elongated along depositional strike. Although the Pictured Cliffs accumulation is regarded as “continuous,” the distribution of producing wells shows a strong correlation with shoreline trends (IHS Energy Group, 2002). Wells with higher production are not associated with thicker sandstone beds of the Pictured Cliffs; rather, production is greater along trends of higher porosity and permeability, probably enhanced by natural or induced fractures.

Traps/Seals

Stratigraphy is the main trapping mechanism and is due to the landward pinchout of marginal-marine sandstones into paludal shales and coals. These traps are augmented by the northward structural dip of the basin in the areas of greatest production; most gas is recovered south of the basin axis (fig. 29) as well as along the south (updip) side of sandstone lenses. Paludal shales in the lower part of the Fruitland and fluvial overbank mudrocks in the upper part of the Fruitland and in the Kirtland Formation act as seals. Overall, the Pictured Cliffs is relatively low in permeability, due to cementa-

tion, which reduces the potential for long-distance migration of gas into or out of the formation.

Geologic Model

Gas was generated from Fruitland coal in the late Oligocene to early Miocene (fig. 10C) and migrated laterally and downward into shoreface sandstones of the Pictured Cliffs Sandstone. The areas of greater gas production are where Fruitland coal is thickest. The top of the Lewis Shale (base of Pictured Cliffs) entered the zone of generation of wet gas in the late Oligocene and never was thermally mature to enter the zone of generation of dry gas (fig. 10C) in the northern part of the TPS; the Lewis also contributed gas to the Pictured Cliffs. Overlying shales in the Fruitland and Kirtland Formations act as seals, and the gas was trapped in overlapping, lenticular sandstones in the Pictured Cliffs. Gas is also prevented from migrating out of the Pictured Cliffs by updip water to the north and south of the main producing area. Cementation of the Pictured Cliffs prevents long-distance migration of gas. Production is greatest along northwest- to southeast-oriented trends of higher porosity and permeability, commonly along the updip sides of sandstone lenses of the Pictured Cliffs.

Assessment Results

The Pictured Cliffs Continuous Gas Assessment Unit (50220161) was assessed to have potential additions to reserves of 5,640.25 billion cubic feet of gas (BCFG) and 16.92 million barrels of natural gas liquids (MMBNGL) at the mean. The volumes of undiscovered oil, gas, and natural gas liquids estimated in 2002 for the Pictured Cliffs Continuous Gas AU are shown in appendix A. These values are higher for both gas and natural gas liquids compared to the 1995 USGS assessment (Huffman, 1996), for which the estimates were 3,264.04 BCFG and 0.10 MMBNGL at the mean. These numbers are not directly comparable, because of differences in cell size, area assessed, and projected success ratio. A summary of the input data of the AU is presented on the data form in appendix B.

This AU encompasses an area of 4,206,000 acres at the median, 4,041,000 acres at the minimum, and 4,297,000 acres at the maximum. There were 6,809 tested cells (wells that have produced or had some other production test, such as initial production test, drill stem test, or core analysis). A 0.02 BCFG recovery cutoff was used per cell. Applying this cutoff, 6,352 tested cells equaled or exceeded this cutoff. There is adequate charge; favorable reservoirs, traps, and seals over most of the area; and favorable timing for charging the reservoirs with greater than the minimum recovery of 0.02 BCFG. If the production history of the Pictured Cliffs Continuous Gas AU is divided into nearly three equal discovery time periods, plots of the estimated ultimate recoveries (EUR) indicate that the first third of discovery history had the highest median recovery per cell (0.66 BCFG) (fig. 31).

The second third had slightly lower recovery, at 0.56 BCFG per cell, and for the third period of time, recovery dropped to 0.33 BCFG per cell. Higher EUR recoveries for the first-third time period likely reflects discovery of the best sandstone reservoirs compared to sandstones discovered in the subsequent time periods. The EUR distribution for all producing wells in the AU (fig. 32) shows a median total recovery per cell of 0.5 BCFG. The EUR distributions were factored into the calculation of potential undiscovered resources.

Even with a large part of the AU assigned to established fields, the median untested area is 84 percent of the total median AU area. The untested areas are mainly

1. south of the producing fields to the Pictured Cliffs outcrops where the Pictured Cliffs is largely water saturated and has high water/gas ratios,
2. northeast of established producing areas where the Pictured Cliffs is tightly cemented and also displays high water/gas ratios, and
3. areas within producing fields that remain undrilled.

Consequently, part of the untested area was considered unfavorable for adding potential reserves in the next 30 years. At the minimum we estimate 14 percent of the untested area to have potential additions to reserves in the next 30 years. At the median this value is 37 percent of the untested area, and at the maximum this value is 47 percent. These values were calculated by multiplying the various percentages of untested area deemed favorable by different success ratios. New discoveries will consist of infill drilling on closer spacing, step-out drilling from existing fields, and new field discoveries from wildcat drilling—probably in the area northeast of current production. The minimum cutoff of 0.02 BCFG would apply to the percentage of untested cells considered to have potential additions to reserves. Total gas recovery per cell of these untested cells is estimated at 0.02 BCFG at the minimum, 0.25 BCFG at the median, and 7.0 BCFG at the maximum. The maximum of 7.0 BCFG was based on the isolated occurrences of high producing wells (fig 32).

Basin Fruitland Coalbed Gas Assessment Unit (50220182) and Fruitland Fairway Coalbed Gas Assessment Unit (50220181)

Introduction

The Fruitland Formation is divided into two assessment units because of different cumulative gas production:

1. Basin Fruitland CBG AU, which consists of overpressured and underpressured areas, and
2. Fruitland Fairway CBG AU, which consists of an overpressured area (fig. 33).

Coal-bed-gas exploration in the Fruitland is discussed in Mathney and Ulrich (1983) and summarized below. Gas was first identified in the Fruitland Formation in 1951 with a discovery in the Ignacio Blanco Fruitland field (fig. 33). The discovery was a

combined structural-stratigraphic trap; gas in the Fruitland was produced from sandstone beds. In 1952, gas was discovered in sandstone beds in the Fruitland Formation in the Aztec, Gallegos, and Kutz West fields. The Los Pinos North and South fields were discovered in 1953 within the Fruitland Fairway CBG AU. In 1956, coal-bed gas was discovered in the Fruitland in the Flora Vista and Kutz fields in New Mexico, and in the Bondad field (now part of the Ignacio Blanco field) on the Bondad anticline in Colorado. Gas was discovered in the Fruitland at the Crouch Mesa field in 1959. No new Fruitland coal-bed-gas production was added until 1966 when the Pinion North and South fields were discovered. In 1968, Fruitland production was added from the Blanco (fig. 33) and Gallegos South fields and in 1969 coal-bed gas was discovered at the Pump Mesa field. Gas was discovered in the Fruitland in the Mt. Nebo field in 1972 and in the Sedro Canyon field in 1973. Gas production was added from the Fruitland at the Connor and Jasis fields in 1976. Most of the smaller Fruitland fields now are found within the broader area assigned to the Blanco or Ignacio-Blanco fields (fig. 33) and are not shown, because there are little data to define the old field boundaries. A review of the field descriptions (Fassett, 1978a,b) shows that most of the above fields are small, consisting of one to several wells; some of these fields no longer produce. The initial reservoir targets for production appear to have been channel sandstone and not coal, which today is the principal exploration target and producer of coal-bed gas.

This pattern of early development suggests that the initial exploration philosophy was targeted at the sandstone reservoirs and that coal as both source and reservoir of gas was not fully appreciated. An early geochemical study of gas composition in the Fruitland Formation and underlying Pictured Cliffs Sandstone reservoirs indicated that the coals and coaly beds were the likely source of the gas (Rice, 1983); however, the Fruitland coal beds, as reservoirs, were not a major target of gas exploration at this time. In the 1980s, additional wells were completed in the Fruitland in various fields within both the Basin Fruitland CBG AU and the Fruitland Fairway CBG AU. It was not until the 1990s (IHS Energy, 2002) that the number of yearly well completions in the Fruitland increased to where the Fruitland Formation has become the single largest producer of natural gas in the basin.

Beginning in the late 1980s and continuing into the early 1990s, the number of geologic, geochemical, and hydrologic studies of the Fruitland increased; the results of these studies provided invaluable information on the distribution and nature of the coal-bed-gas resource. Coal resources have been estimated to exceed 200 billion tons and to contain at least 50 TCFG (Kelso and other, 1987; Kelso and Wicks, 1988; Ayers and others, 1994; Rice and Finn, 1996). To date, over 4,000 wells have produced more than 8.4 TCFG from Fruitland reservoirs only (IHS Energy, 2002). This is more coal-bed gas than has been produced from any other coal-bearing formation in the nation (IHS Energy, 2002).

Coal-bed-gas production appears to be controlled by several factors that include:

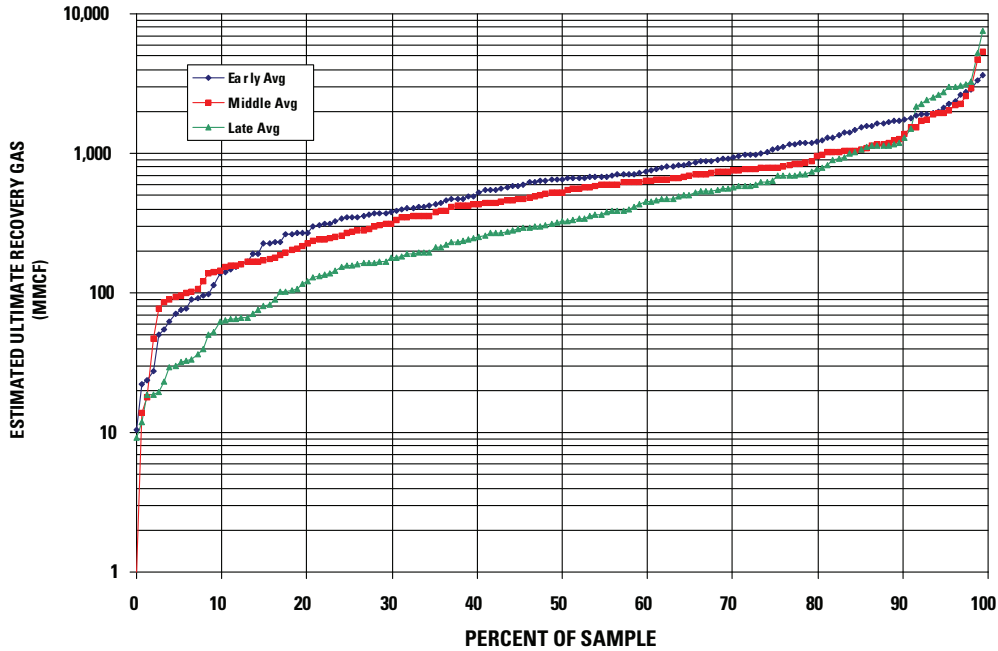


Figure 31. Graph showing estimated ultimate recoveries (EUR) of Pictured Cliffs Continuous Gas Assessment Unit gas wells divided by time of completion into three nearly equal blocks of time. EUR data calculated using data from IHS Energy (2002). Data provided by T. Cook (written commun., 2002). MMCF, million cubic feet.

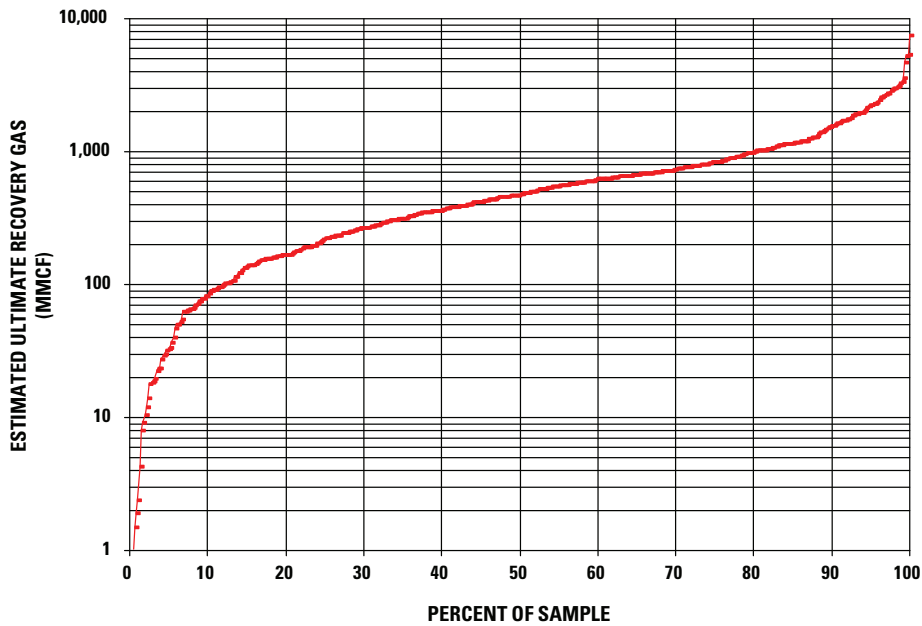


Figure 32. Graph showing distribution of estimated ultimate recoveries (EUR) of Pictured Cliffs Continuous Gas Assessment Unit gas wells. EUR data calculated using data from IHS Energy (2002). Data provided by T. Cook (written commun., 2002). MMCF, million cubic feet.

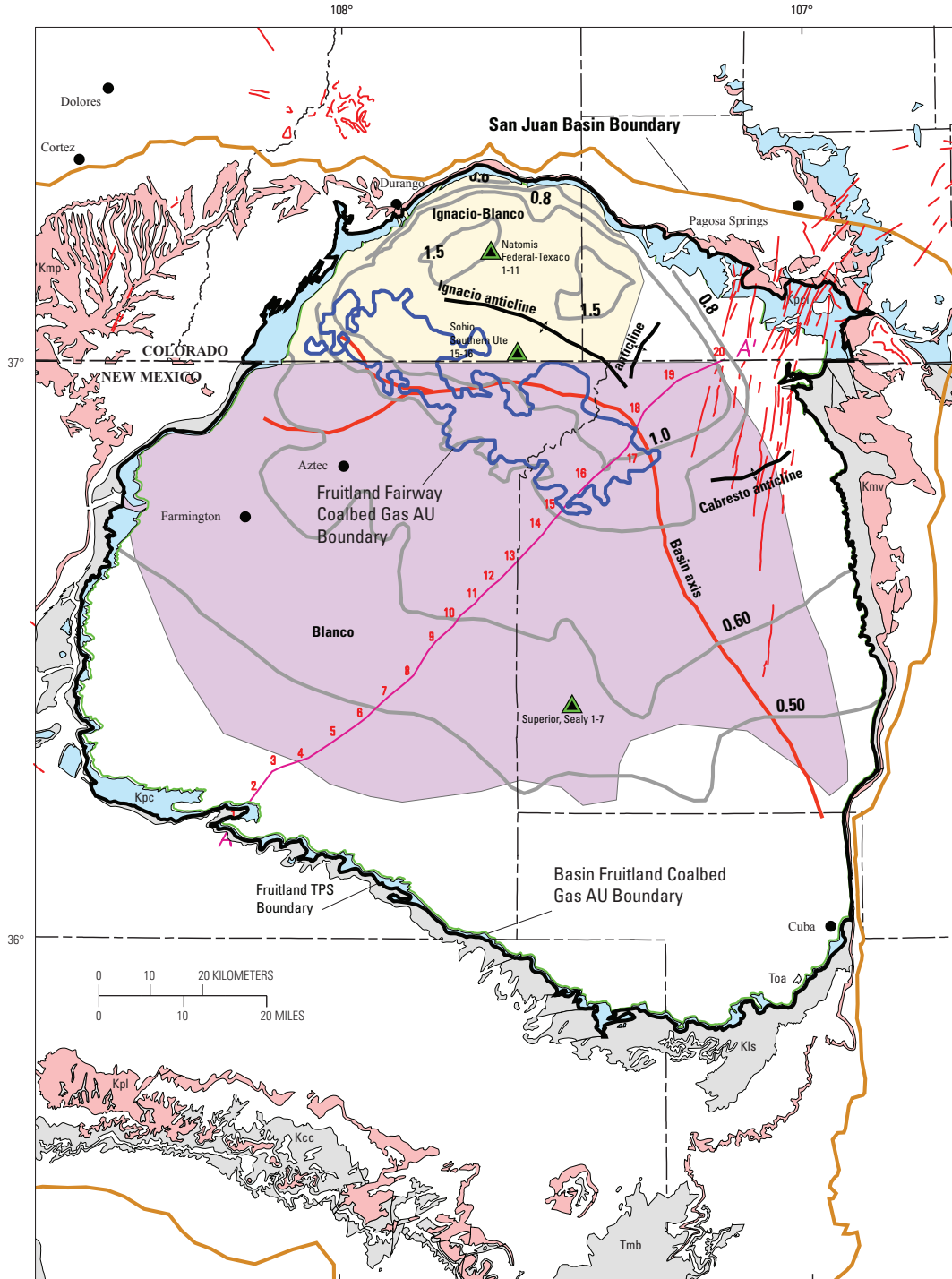


Figure 33. Map showing the assessment unit (AU) boundaries for the Basin Fruitland Coalbed Gas (green line) and Fruitland Fairway Coalbed Gas (blue line) Assessment Units and major gas fields Blanco (purple) and Ignacio-Blanco (yellow) in the Fruitland Formation. Also shown are the locations of the regional cross section (see fig. 4), principal folds in the basin, and wells (green and black triangles) used to make the burial history curves in this report (figs. 10). Symbols for geologic map units: Toa, Tertiary Ojo Alamo Sandstone; Tmb, Tertiary Miocene volcanics; Kpc, Pictured Cliffs Sandstone; Kpl, Pictured Cliffs Sandstone and Lewis Shale; Kls, Lewis Shale; Kcc, Crevasse Canyon Formation; Kmp, Menefee Formation and Point Lookout Sandstone; Kmv, Mesaverde Group; Kpl, Point Lookout Sandstone; thin red vertical lines and patches, dikes (Green, 1992; Green and Jones, 1997). Contours (gray) show vitrinite reflectance (R_m) values, in percent, from data in Fassett and Nuccio (1990), Law (1992), and Fassett (2000). TPS, Total Petroleum System.

1. coal-bed thickness, which is controlled by the depositional history;
2. coal maturation;
3. structural history, which affects the degree of fracturing and cleat development;
4. composition or maceral type; and
5. hydrologic history.

These controls were previously discussed. Although natural fractures or cleats are found in all the coals, the cleat density appears to increase in areas where tectonic features such as faults, folds, or lineaments are better developed (Fassett, 1991). Wells are completed using either hydraulic fracturing or open-hole cavity techniques.

The area of overpressure is not equally gas rich throughout its extent. The most gas-rich area does, in fact, lie within the Fruitland Fairway CBG AU, and there are geologic reasons why the overpressured area north of the Fruitland Fairway is not as gas rich as the Fruitland Fairway. Thus, had the overpressured area been treated as a single assessment unit, as was done in the 1995 USGS assessment (Rice and Finn, 1996), the current methodology, which uses a cell approach for continuous-type resources (Schmoker, 1996), would have probably overestimated the relative gas richness because production data from the gas-rich Fruitland Fairway would have skewed the resource model.

Production Characteristics of the Basin Fruitland Coalbed Gas and Fruitland Fairway Coalbed Gas Assessment Units

Water Production

Coal-bed-gas production and economics is affected by the quantity of water produced with the gas. The distribution of cumulative water production shows marked differences between the Basin Fruitland CBG and Fruitland Fairway CBG AUs (fig. 34), and within the Basin Fruitland CBG AU there are marked differences between the overpressured area north of the Fruitland Fairway and the underpressured and transitional pressured areas south and east of the Fruitland Fairway (fig. 34). Plots of cumulative water production versus total production time for both the Basin Fruitland CBG and Fruitland Fairway CBG AUs show three populations of cumulative water production (figs. 35A and 35B). Similar population distributions are observed in plots (not shown) where water production was normalized to production time. The first population is from 0 to 60 months of production, usually the time of greatest dewatering. In the Fruitland Fairway CBG AU, cumulative water production for this population is generally less than 100,000 barrels, whereas in the Basin Fruitland CBG AU, it is generally less than 200,000 barrels. In the Basin Fruitland CBG AU, wells with higher cumulative water production in the same population are from the overpressured area.

The greatest amount of cumulative produced water is from wells that have been on production between 85 and

220 months in the Basin Fruitland CBG and between 85 and 180 months in the Fruitland Fairway CBG AUs (figs. 35A and 35B). This is to be expected because of the longer production history. In the Basin Fruitland CBG AU, cumulative water production for this population is generally less than 1,000,000 barrels for most wells. A small number of wells have produced between 1,000,000 and 2,000,000 barrels of water; all but four of these occur in the overpressured area north of the Fruitland Fairway CBG AU (figs. 34 and 35A). Nine wells have produced in excess of 3,000,000 barrels of water; these wells lie close to the northern margin of the Basin Fruitland CBG AU (figs. 34 and 35A) within groundwater flow paths, defined by water $\delta^{18}\text{O}$ values between -16 and -15 per mil, that are most geologically recent.

In the Fruitland Fairway CBG AU, cumulative water production for the population of wells producing between 85 and 180 months is generally less than 500,000 barrels (fig. 35B). A small number of wells have cumulative water production between 500,000 and 1,000,000 barrels. These wells are scattered throughout the western, central, and southeastern parts of the AU. Five wells have cumulative water production greater than 1,000,000 and less than 3,000,000 barrels; four of these are clustered in the southeast part of the AU, at the southeast end of defined overpressure (fig. 12), and one is found in the northwest part of the AU (figs. 34 and 35B).

Except for several wells in the Basin Fruitland CBG AU, wells that have been in production more than 220 months in the Basin Fruitland CBG AU and more than 180 months in the Fruitland Fairway CBG AU have cumulative water production less than 100,000 barrels (figs. 35A and 35B). Many wells in the Basin Fruitland CBG AU for this population have reported zero produced water. Whether this is real or an artifact of reporting or past-required reporting practices for these wells is unknown. Most of these wells are located in the Aztec field, which is the oldest producing Fruitland field (fig. 34).

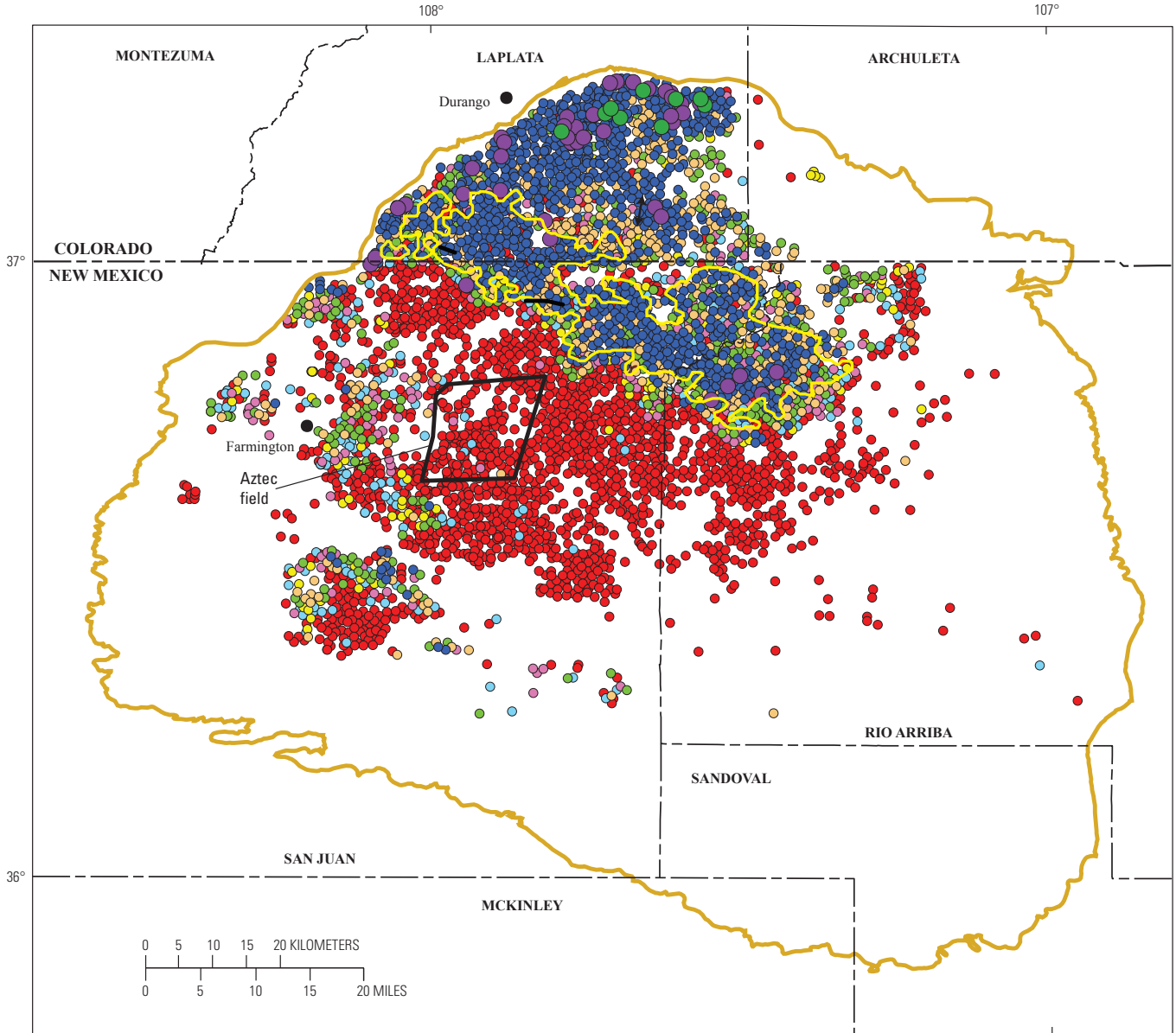
Cumulative Gas Production

Fruitland gas production data were examined in order to evaluate the regional variability as a function of

1. length of production time,
2. position in the Fruitland depositional system,
3. thermal maturity of the coals,
4. past and present structural position in the basin, and
5. post-depositional hydrodynamic processes.

Both cumulative and normalized (cumulative production/total months of production) data were evaluated as were the lengths of time the wells had been producing. The data were then examined within the context of

1. geographic position within the depositional system (fluvial or coastal),
2. net thickness of coal,



EXPLANATION

- | | |
|---|--|
| <ul style="list-style-type: none"> — Fruitland Fairway Coalbed Gas AU boundary — Basin Fruitland Coalbed Gas AU boundary | <p>Cummulative water production, barrels</p> <ul style="list-style-type: none"> ● 0–5,000 ● 5,001–10,000 ● 10,001–15,000 ● 15,001–25,000 ● 25,001–50,000 ● 50,001–100,000 ● 100,001–1,000,000 ● 1,000,001–3,000,000 ● 3,000,001–10,000,000 |
|---|--|

Figure 34. Map showing distribution of cumulative produced water in the Fruitland Formation with respect to the Basin Fruitland Coalbed Gas and Fruitland Fairway Coalbed Gas Assessment Units (AU). Production data from IHS Energy Group (2002).

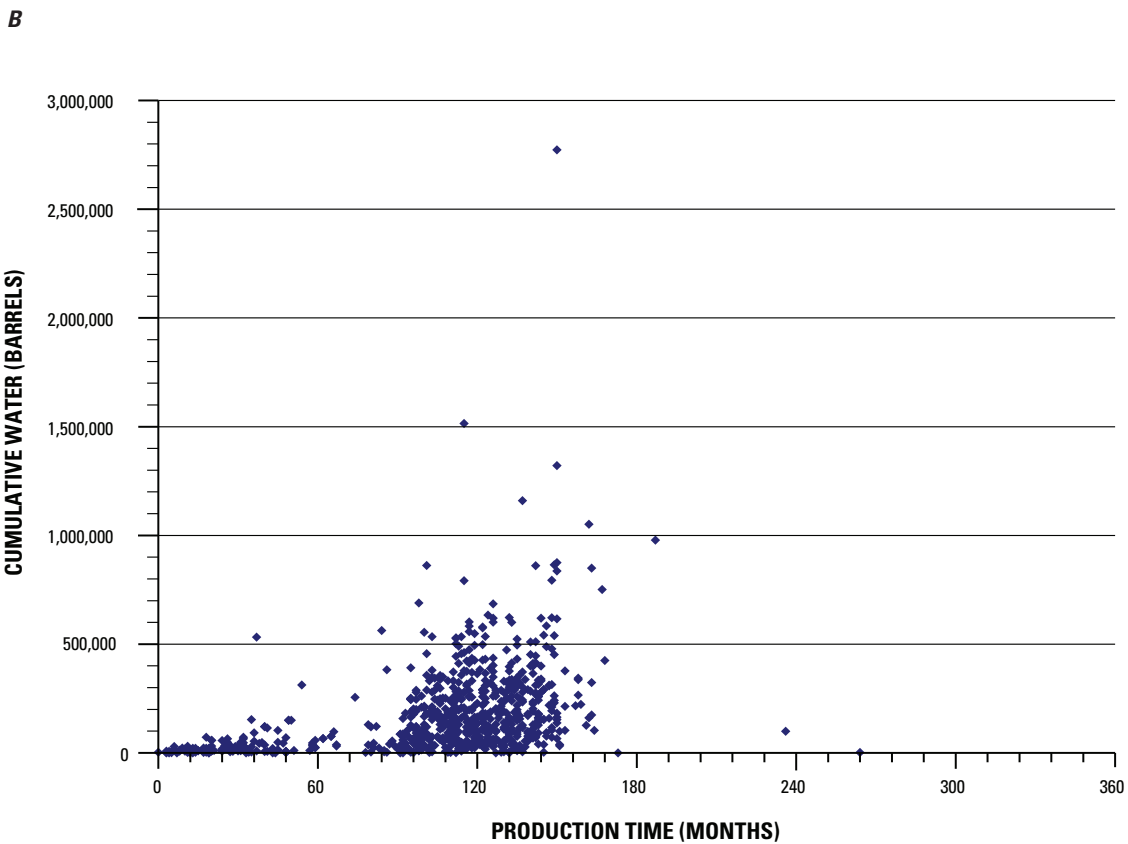
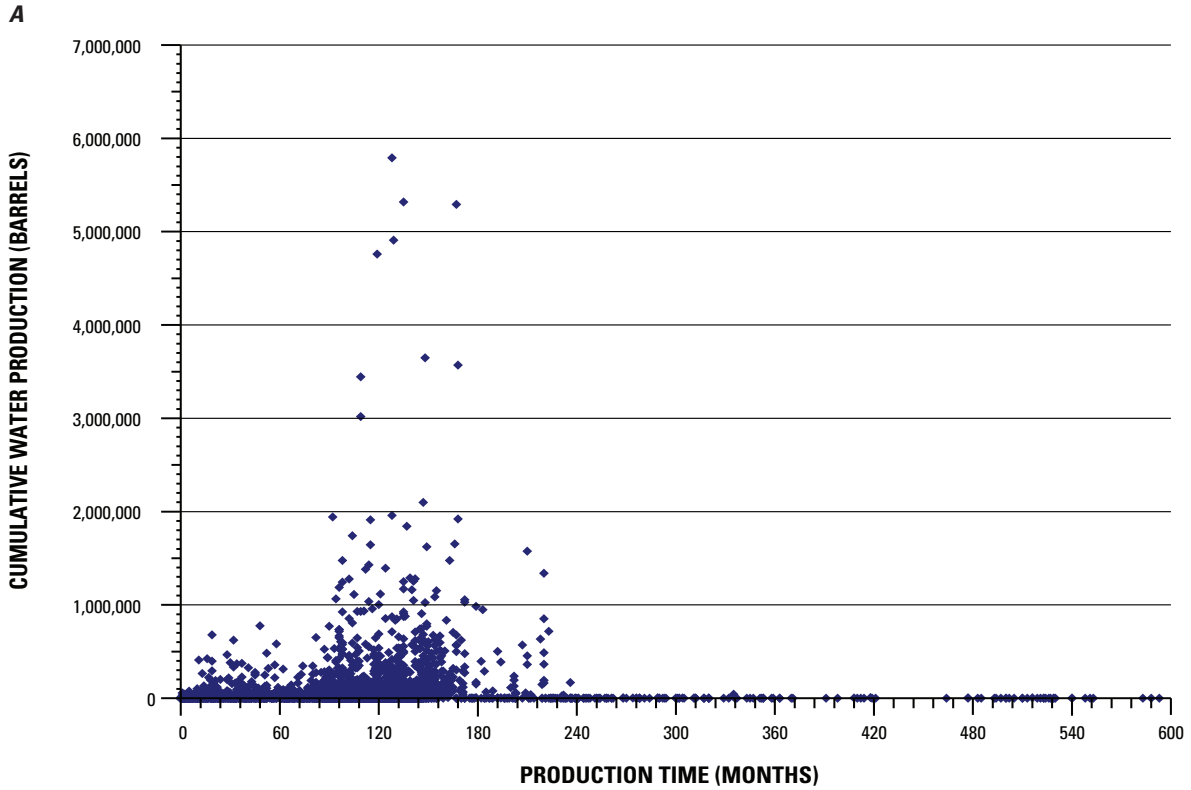


Figure 35. Graphs showing relation between cumulative water production and length of production. Production data from IHS Energy Group (2002). (A) Basin Fruitland Coalbed Gas Assessment Unit. (B) Fruitland Fairway Coalbed Gas Assessment Unit.

3. time as related to position of the various Pictured Cliffs shorelines, and
4. geographic position with respect to the regional $\delta^{18}\text{O}$ - and δD -isotope patterns in co-produced waters.

The various relations among gas and water production (cumulative, normalized, and production time) and the regional patterns of

1. oxygen and deuterium isotopes in produced waters,
2. $\delta^{13}\text{C}$ of methane and carbon dioxide in the gases, and
3. gas wetness ($C_1/\Sigma C_1-C_5$) were analyzed in order to evaluate the model (Scott, 1994; Scott and others, 1994a,b) of late-stage microbial-gas generation and its contribution to overall gas resources.

Most Fruitland wells have produced gas from 61 to 180 months (fig. 36). A comparison of cumulative gas production versus length of production shows some interesting differences between the Basin Fruitland CBG AU and the Fruitland Fairway CBG AU (figs. 37A and 37B). In both AUs, the greatest production is from wells that have been on production from 84 to 168 months. Wells that have produced for longer than 168 months are mainly in the Basin Fruitland CBG AU (fig. 37A) and do not show significant increased gas production with time. These older wells tend to be low volume gas producers, suggesting that the areas of production may not be as rich in gas resources as elsewhere in the Fruitland or that early wells were not completed as well as later wells. Although cumulative gas production does show an overall increase up to 168 months, there is no linear correlation between length of production and cumulative production. The lack of correlation reflects the variability of the coal reservoirs and their adsorbed gas content. This variability is the ultimate control on potential gas resources and is more likely related to local geologic factors. Post-depositional hydrodynamic conditions may actually be a detriment to gas production for some wells in the overpressured part of the Basin Fruitland CBG AU because the increased volume of produced water may not allow for effective dewatering.

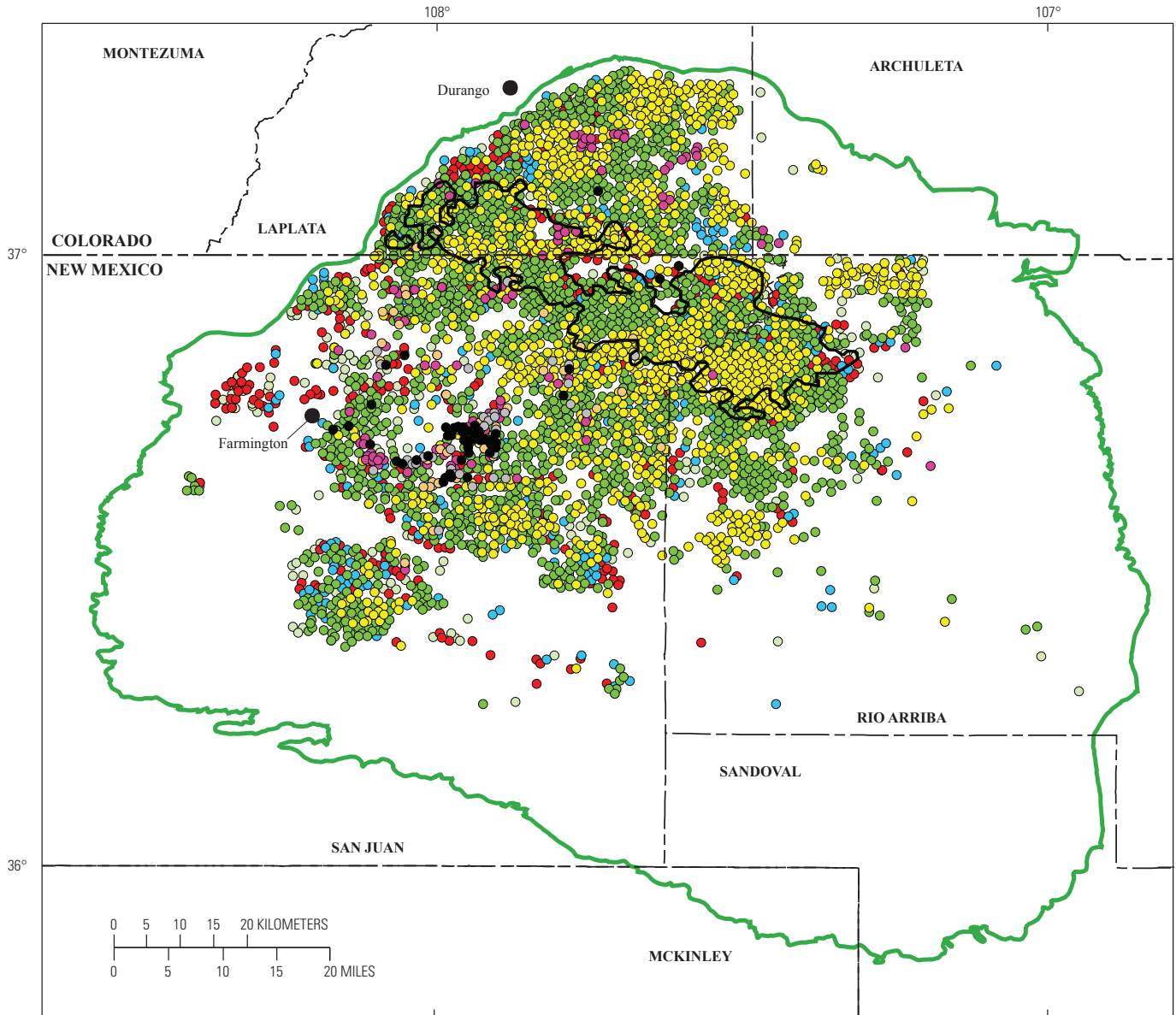
A map of cumulative gas production (independent of length of production) for the Basin Fruitland CBG and Fruitland Fairway CBG AUs shows that, overall, the best producing wells (greater than 1 BCFG cumulative production) are within the Fruitland Fairway AU (fig. 38). However within the Basin Fruitland CBG AU, there are several areas where production exceeds one BCFG per well (fig. 38). Some of these wells are located adjacent to the northern, southern, and western margins of the Fruitland Fairway CBG AU and probably should have been included in that AU. However, there are several areas in the overpressured area well north of the Fruitland Fairway CBG AU in Colorado, notably along and near parts of the Animas, Florida, and Los Pinos Rivers (see fig. 11 for location) that have cumulative production exceeding 1 BCFG. The latter observation suggests that gas might be carried in groundwater that eventually discharges to these rivers in the subsurface (Cox and others, 2001). Wells along these flow paths could be producing thermal gas that is desorption from coal or dissolved in groundwater, or mixed with late-stage microbial gas. These wells are

also associated with northeast trends in thick net coal (fig. 5) and most have produced for more than 120 months (figs. 36 and 38). In the Basin Fruitland CBG AU, south of the Fruitland Fairway CBG AU, there are three areas with greater than 1 BCFG cumulative production. These areas are along the La Plata River, in the Kutz field and southeast of Farmington, N. Mex. (fig. 38). The latter areas are associated with the older Fruitland fields, such as Aztec and Kutz (IHS Energy Group, 2002).

Visual comparison of cumulative gas production between the overpressured part of the Basin Fruitland CBG AU and the Fruitland Fairway CBG AU for similar lengths of production time (figs. 36 and 38) demonstrates the enhanced gas richness of the Fruitland Fairway AU. Except for a few areas in the overpressured part of the Basin Fruitland AU, both the Fruitland Fairway CBG AU and the overpressured part of the Basin Fruitland CBG AU have similar ranges in cumulative produced water (independent of time) (fig. 34). Areas of high cumulative gas production in the overpressured part of the Fruitland are associated with thick coal trends, although net coal thickness tends to be greater overall in the Fruitland Fairway AU. During gas generation in the Oligocene and Miocene, gas generated from coals in the overpressured part of the Basin Fruitland CBG AU would have been dry, and based on coal rank, more gas per equivalent volume of coal should have been generated compared to gas from slightly lower rank coals in the Fruitland Fairway CBG AU.

The rate of methane production from coals has been documented to increase with coal rank (Das and others, 1991). Factors that affect the amount of gas that can be stored, as adsorbed or free gas, in a coal seam include surface area, pore volume, and cleat and fracture development. Although high rank coals have less surface area to adsorb gas compared to low rank coals because more gas is generated at higher rank, the high rank coals are better reservoirs (Das and others, 1991). High rank coals tend to be more brittle and to develop better cleats and fractures for a given maceral composition than low rank coals, and thus, have greater area to store free gas. Moreover, carbon contents are above 91 percent and pore volume (capacity to store gas) increases in high rank coals (Das and others, 1991). Given these factors and assuming no significant change in maceral composition throughout the entire overpressured area, the northern part of the Basin Fruitland CBG AU should have been as rich or richer in initial gas resources as the Fruitland Fairway CBG AU in areas of similar net coal thickness. If the Fruitland Fairway CBG AU gas production has been augmented by methane carried in solution by south-flowing waters (Scott and others, 1994b), then one might expect to see a north to south gradient in cumulative gas production for equivalent periods of production time. Maps of cumulative gas production and production time do not appear to support this general hypothesis (figs. 36 and 38).

The underpressured part of the Basin Fruitland CBG AU is found mainly in New Mexico. Except as mentioned above, most wells in the underpressured part of this AU have produced 1 BCFG or less, and of these, the majority has produced less than 0.5 BCFG (fig. 38). Production from this part of the Fruitland occurs in low rank coals (less than 0.75-percent R_m), and



EXPLANATION

- | | | | | | |
|---|---|---|---------|---|---------|
| — | Fruitland Fairway Coalbed Gas AU boundary | ○ | 0-12 | ● | 181-240 |
| — | Basin Fruitland Coalbed Gas AU boundary | ● | 13-36 | ● | 241-300 |
| | | ● | 37-60 | ● | 301-360 |
| | | ● | 61-120 | ● | 361-615 |
| | | ● | 121-180 | | |

Figure 36. Map showing distribution of length of production time of Fruitland Formation wells with respect to the Basin Fruitland Coalbed Gas and Fruitland Fairway Coalbed Gas Assessment Units (AU). Production data from IHS Energy Group (2002).

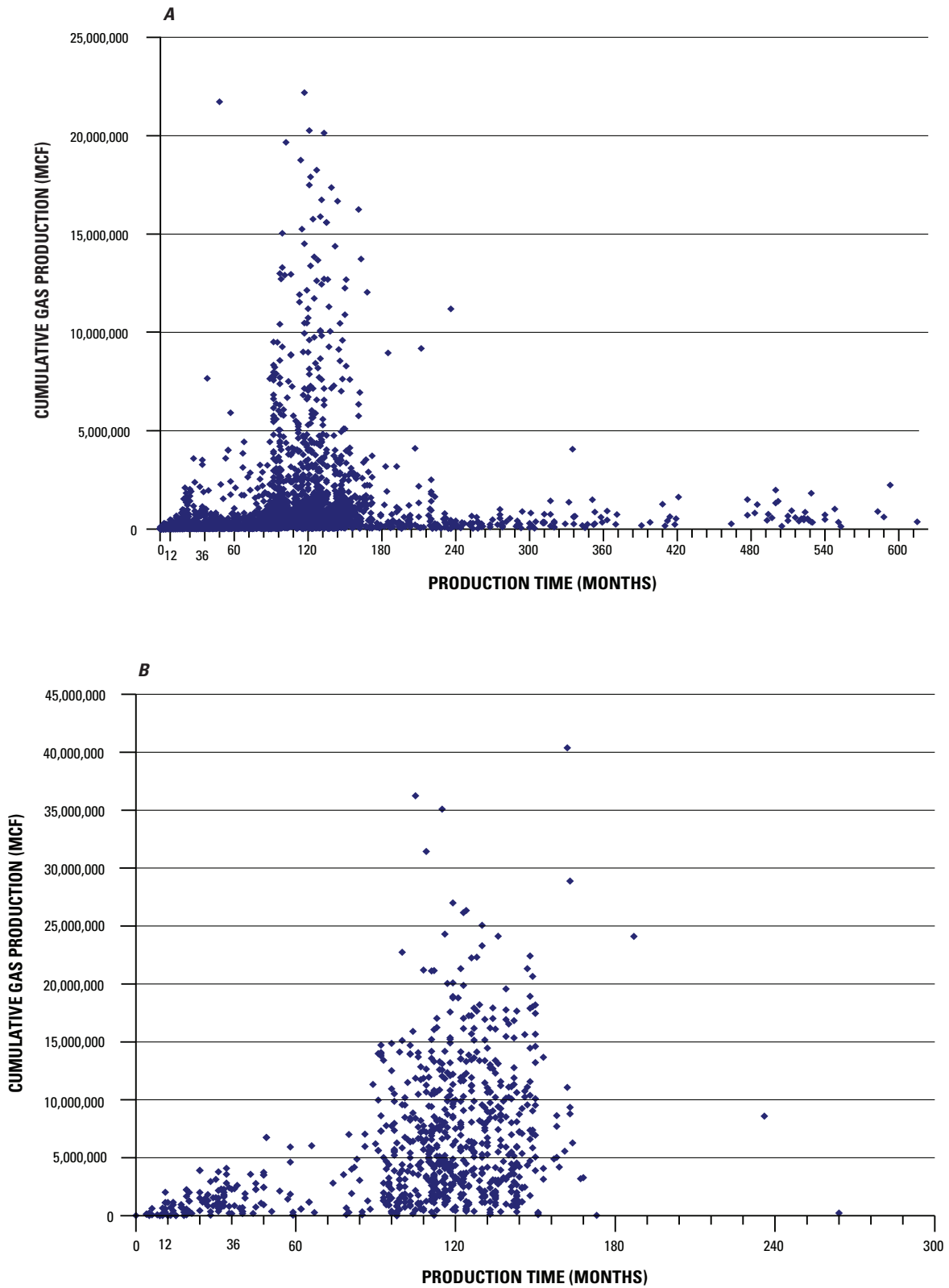
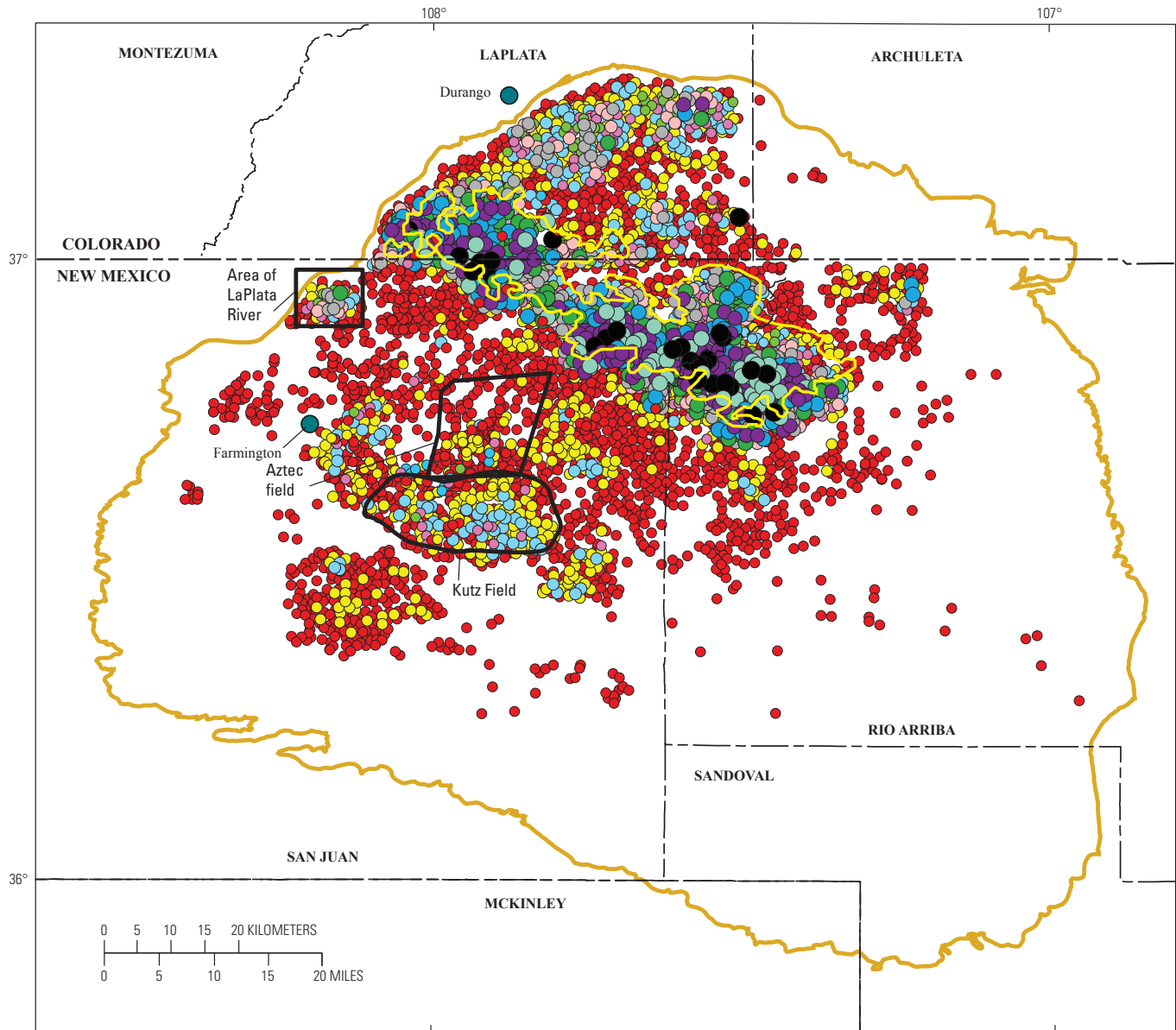


Figure 37. Graphs showing relation between cumulative gas production and length of production. Production data from IHS Energy Group (2002). MCF, thousand cubic feet. (A) Basin Fruitland Coalbed Gas Assessment Unit. (B) Fruitland Fairway Coalbed Gas Assessment Unit.



EXPLANATION

- Fruitland Fairway Coalbed Gas AU boundary
- Basin Fruitland Coalbed Gas AU boundary

Cummulative gas values, BCF

- | | | |
|--|--|---|
| ● 0-0.5 | ● 2.0-2.5 | ● 7.0-9.0 |
| ● 0.5-1.0 | ● 2.5-3.0 | ● 9.0-15.0 |
| ● 1.0-1.5 | ● 3.0-5.0 | ● 15.0-20.0 |
| ● 1.5-2.0 | ● 5.0-7.0 | ● >20.0 |

Figure 38. Map showing distribution of cumulative gas production (independent of length of production time) of Fruitland Formation wells with respect to the Basin Fruitland Coalbed Gas and Fruitland Fairway Coalbed Gas Assessment Units (AU). Production data from IHS Energy Group (2002). BCF, billion cubic feet.

overall net coal thickness is lower. The coals in this part of the Fruitland would be expected to contain less gas resources than higher rank coal beds to the north. In contrast, cumulative gas production from the overpressured part of the Basin Fruitland CBG AU is regionally more variable. Areas immediately north and northeast of the Fruitland Fairway CBG AU and along the west and north margins of the Basin Fruitland CBG AU are characterized by wells that have produced 1 BCFG or less. As in the underpressured area south of the Fruitland Fairway CBG AU, the majority of these wells have produced 0.5 BCFG or less to date. The low production may reflect length of production; most of the wells have been producing from 13 to 120 months (fig. 36). On the east side of the AU, low production may also be related to thin net coal (fig. 5).

Normalized Gas Production

Cumulative gas production data are independent of the length of time of production. In order to deal with the variability of production time, production data were normalized over the entire range of production time. This allows for a more realistic evaluation of the potential gas richness of an area. It was not possible to compute normalized monthly data for all wells, because in some cases the first production date was missing from the IHS Energy database (IHS Energy Group, 2002); therefore, the distribution of cumulative and normalized production data analyzed is not the same. The normalized monthly gas production data range from less than 1 MMCFG per month to nearly 0.5 BCFG per month (fig. 39). Crossplots of normalized monthly gas production versus length of production for the Basin Fruitland CBG and Fruitland Fairway CBG AUs show two distinct populations (figs. 40A and 40B), similar to the crossplots of cumulative gas production versus production time. These distinct populations correspond to 0 to 60 months and greater than 84 months of production. There is no linear correlation between normalized monthly gas production and length of production time. The lack of correlation reflects the variability of the coal reservoirs and their adsorbed gas content and water production. This variability is the ultimate control on potential gas resources and is related to local geologic factors.

In the Basin Fruitland CBG AU, normalized monthly gas production is commonly less than 10 MMCF, except for a few areas, mostly in the overpressured part of the AU (fig. 39). These latter areas are associated with courses of the Los Pinos, Animas, and Florida Rivers (see fig. 11 for location), and wells in this area have produced for longer periods of time. Within past groundwater flow paths as defined by $\delta^{18}\text{O}$ values, there is a tendency for normalized monthly production (and cumulative gas production) to decrease from north to south in the direction of isotopically heavier water (figs. 10, 38, and 39). An exception is the area immediately north of the west part of the Fruitland Fairway CBG AU. In this area, one well with high normalized monthly production data is in the Basin Fruitland CBG AU (but perhaps should have been included in the Fruitland Fairway AU); it has produced for 48 months.

Although there is no linear correlation between cumulative or normalized gas production and length of production, there is a linear correlation between cumulative gas and normalized gas production. This should be expected. However, rather than a single linear correlation, the data for both the Basin Fruitland AU and Fruitland Fairway AU show two distinct linear correlations (figs. 41A and 41B). These correlations correspond to the 0–60 months and greater than 84 months of production. The difference in slope of the data may reflect the time of major dewatering, which generally occurs in the first 60 months of a well's production history. During the period of major dewatering, cumulative gas production and correspondingly normalized monthly production should grow at a rate slower than later in the life of a well.

Relations Among Gas, Water Production, Groundwater Flow, and Microbial-Gas Generation

Cumulative and normalized gas production for wells differ significantly between the overpressured Basin Fruitland and Fruitland Fairway CBG AUs and do not show strong gradients that are coincident with groundwater flow, and hence augmentation of gas content by late-stage microbial gas, except close to the northern and western basin margins near major rivers. Ayers and others (1994) have suggested that the southern boundary of the Fruitland Fairway is bounded by a structural hingeline, which controls the southern extent of overpressure, and high water and high gas production. Water production in the overpressured part of the Basin Fruitland and Fruitland Fairway AUs is similar and quite dissimilar to the underpressured part of the Basin Fruitland CBG AU (fig. 34). This change in water production appears to correspond with a change in coal geometry (fig. 5) and is probably influenced more by paleoshoreline position in the Pictured Cliffs Sandstone rather than being influenced by any structural hingeline. The southern boundary of the Fruitland Fairway CBG AU in some areas approximates the position of the 2,400-ft contour of the Huerfanito Bentonite Bed (fig. 42) (Fassett, 2000), and thus is north of the proposed structural hingeline that subparallels the 2,600-ft contour (Ayers and others, 1994). Steepening of the Huerfanito contours occurs from 3,000 to 2,500 ft, south of the Fruitland Fairway, and might actually represent a mid-Paleocene to late Eocene Laramide tectonic event (Fassett, 2000). Between structure contour 2,400 and 2,150 ft (interpolated) (fig. 42), the present dip of the Huerfanito flattens in the eastern part of the TPS. The flattening of the gradient in this area, coupled with a significant change in sandstone and coal geometry in the Fruitland, may make it more difficult to move fluids up and out of the basin to the south. However, this argument does not hold for the western half of the Fruitland Fairway, which climbs structurally higher to the southwest. The lack of strong correspondence of the Fruitland Fairway CBG AU high gas production area to structure, as well as to later groundwater

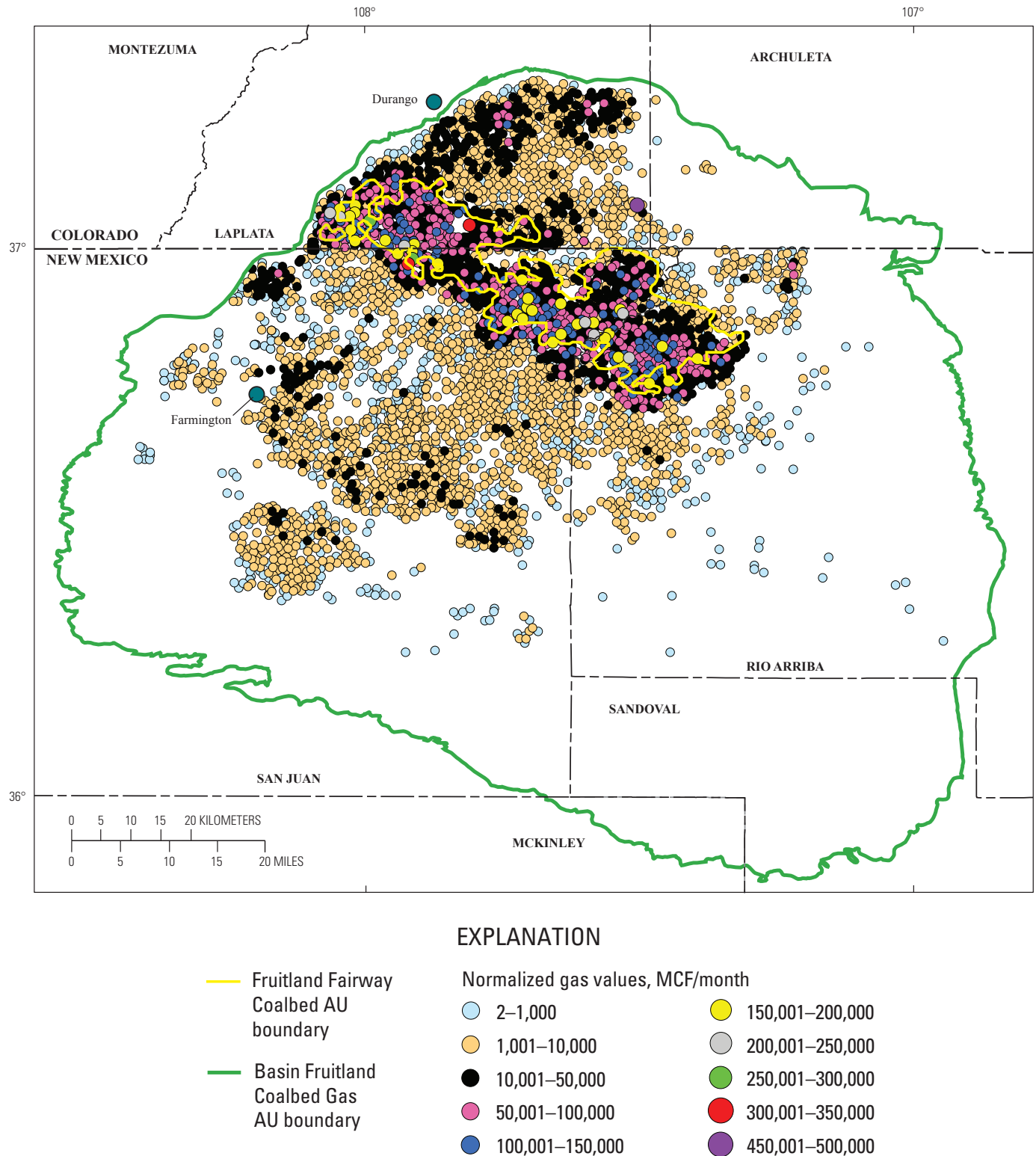


Figure 39. Map showing distribution of normalized (cumulative gas/number of months of production) gas production of Fruitland Formation wells with respect to the Basin Fruitland Coalbed Gas and Fruitland Fairway Coalbed Gas Assessment Units (AU). Production data from IHS Energy Group (2002). MCF, thousand cubic feet.

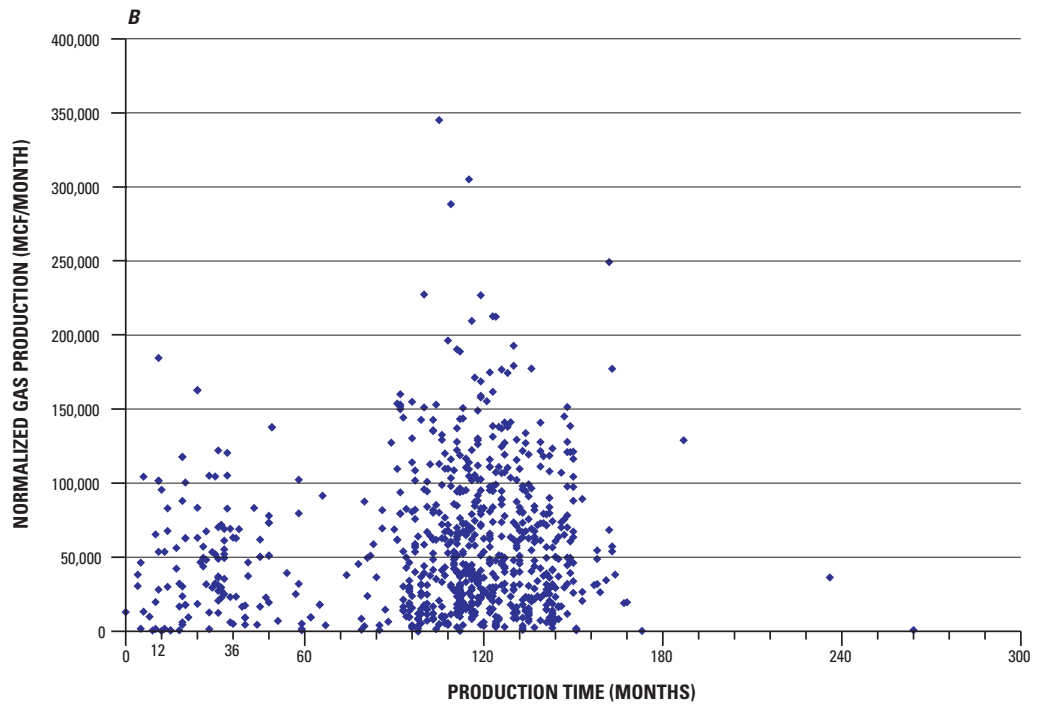
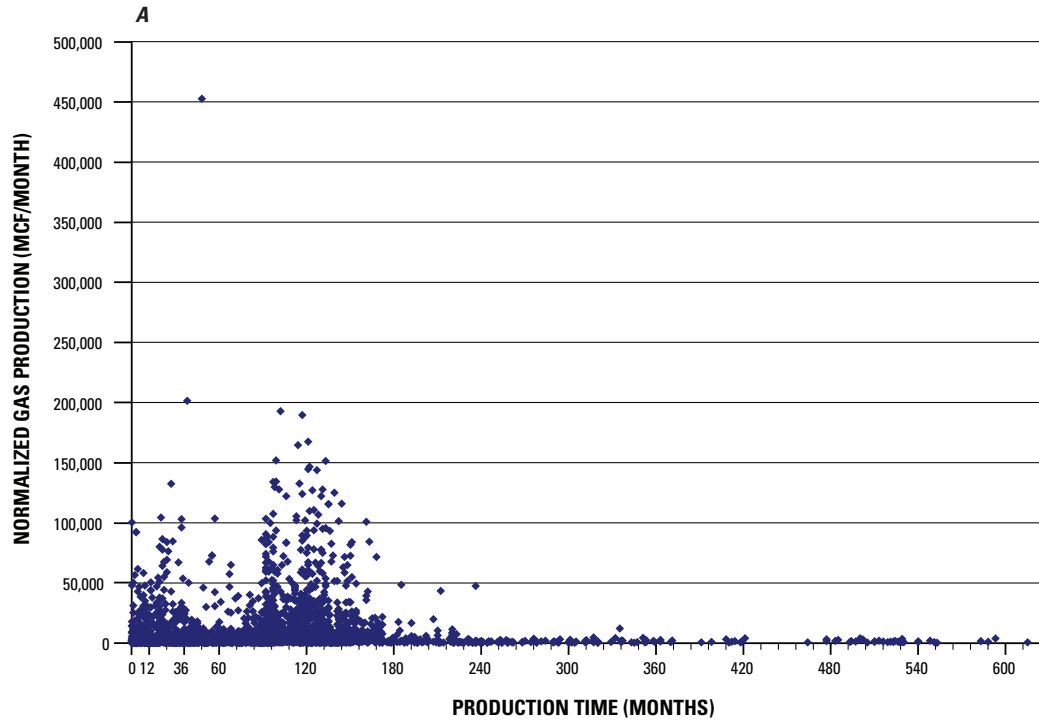


Figure 40. Graphs showing relation between normalized (cumulative gas/number of months of production) gas production and length of production. Production data from IHS Energy Group (2002). MCF, thousand cubic feet. (A) Basin Fruitland Coalbed Gas Assessment Unit. (B) Fruitland Fairway Coalbed Gas Assessment Unit.

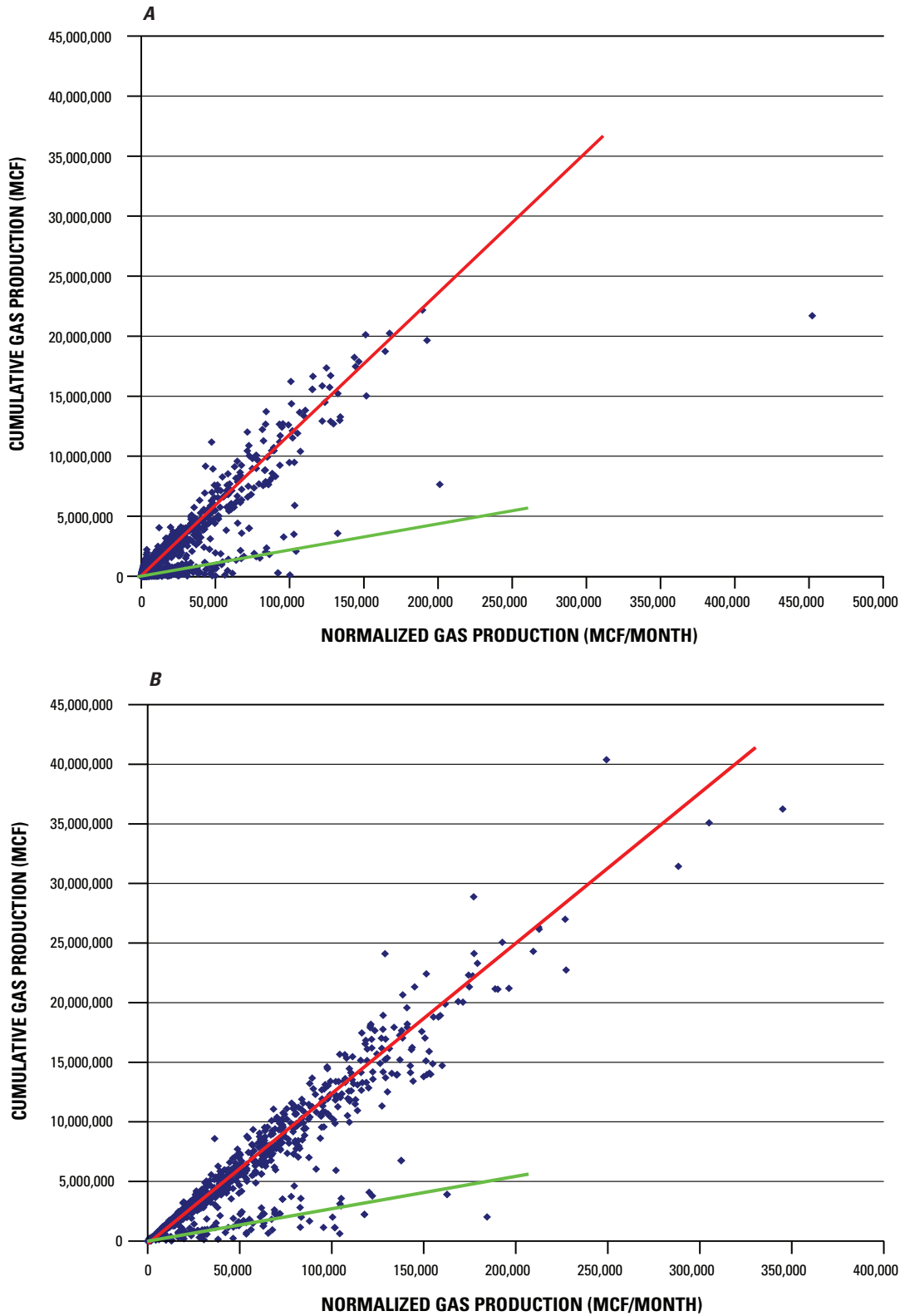
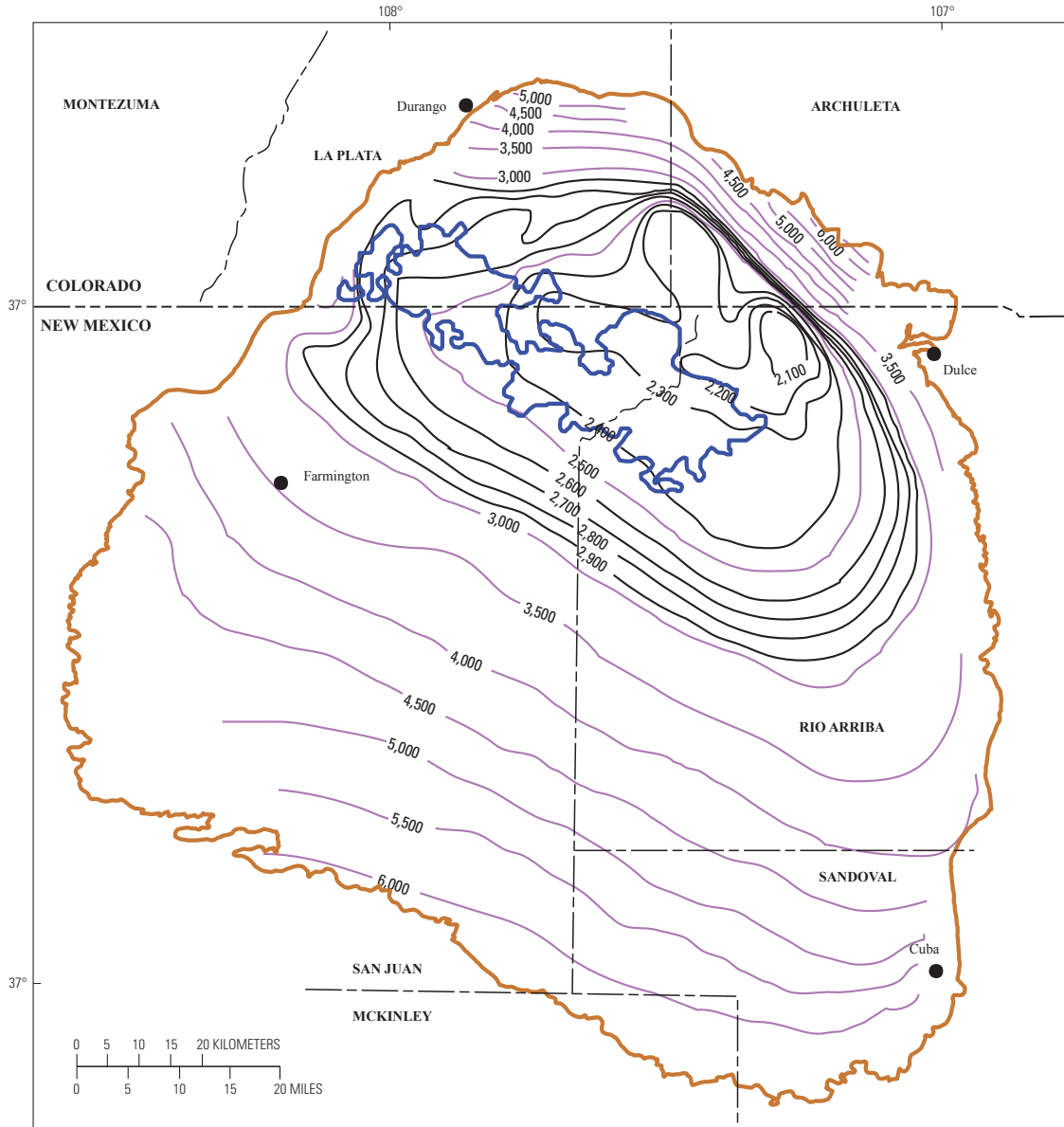


Figure 41. Graphs showing relation between cumulative gas production and normalized (cumulative gas/number of months of production) gas production for production time 0–60 months (green line) and >83 months (red line). Production data from IHS Energy Group (2002). MCF, thousand cubic feet. (A) Basin Fruitland Coalbed Gas Assessment Unit. (B) Fruitland Fairway Coalbed Gas Assessment Unit.



EXPLANATION

- Basin Fruitland Coalbed Gas AU boundary
- Fruitland Fairway Coalbed Gas AU boundary
- 5,000 — Structure contour on top of Huerfanito Bentonite Bed
- Contour interval = 500 ft, light purple lines
- Contour interval = 100 ft, black lines

Figure 42. Map showing relation between basin structure, contoured on top of the Huerfanito Bentonite Bed of Lewis Shale, and the Fruitland Fairway Coalbed Gas Assessment Unit (AU) (purple). Modified from Fassett (2000).

flow patterns, suggests that the overall gas content in the Fruitland Fairway CBG AU is controlled by factors associated with the depositional environments. Factors such as migration of gas or generation of late-stage microbial gas, or oxidation of methane (Gorody, 2001), while important in some areas of the overpressured Basin Fruitland CBG AU, might actually be less important in the Fruitland Fairway CBG AU, except along the extreme western part.

It was suggested, herein, that some of the evidence of microbial-gas generation (for example, heavy bicarbonate waters and small range in $\delta^{13}\text{C}$ of methane) could be related to an early (pre-thermal gas) stage of microbial-gas generation. These observations, based on $^{129}\text{I}/\text{I}$ ages and $\delta^{18}\text{O}$ isotopes of the produced water, are especially pertinent to areas south of the Fruitland Fairway CBG AU in the transition and underpressured areas as well as to areas in part of the Fruitland Fairway CBG AU. An early stage of microbial gas, formed under the right hydrodynamic and trapping conditions and mixed with later thermal-generated gas, will look similar to a late-generated microbial gas that mixed with an earlier thermal-generated gas. However, the two processes would not be time equivalent. Thus, it is possible that the late-stage microbial gas observed closer to the northern and western outcrop is unrelated to microbial-gas processes observed elsewhere in the Basin Fruitland and Fruitland Fairway CBG AUs.

Basin Fruitland Coalbed Gas Assessment Unit (50220182)

Introduction

In previous studies, the Fruitland Formation was divided into two areas:

1. overpressured and
2. transitional pressured to underpressured (Kaiser and others, 1994; Rice and Finn, 1996).

Past studies have examined production histories and changes in gas composition between the overpressured and underpressured transition areas (Scott, 1994; Scott and others, 1994b; Rice and Finn, 1996) and have documented real differences. For this assessment, the boundary between the Basin Fruitland and the Fruitland Fairway was drawn using gas production characteristics, as discussed above, rather than using the area of overpressure. The Basin Fruitland CBG AU was drawn to include the area basinward of the Fruitland Formation outcrops and includes all of the transitional pressured and underpressured reservoirs in addition to that portion of the overpressured area not included in the Fruitland Fairway CBG AU (fig. 43). This AU differs from any single Fruitland coal-bed gas play in the 1995 USGS National Oil and Gas Assessment (Rice and Finn, 1996) in that it combines the San Juan Basin-Underpressured Discharge Play, San Juan Basin-Underpressured Play, and the northern part of the San Juan Basin-Overpressured Play into one AU. Current well spacing is at 160 acres.

Production is mostly controlled by net coal thickness, degree of cleat development, thermal history, and, in the overpressured area, by the volume of water produced. Cumulative gas production is generally higher in the overpressured area compared to the underpressured area for wells producing for the same length of time, but in both areas it is much less than that observed in the Fruitland Fairway CBG AU (fig. 38). Normalized gas production is generally less than 10,000 thousand cubic feet (MCF) per month in the AU, except in that part of the overpressured area that is associated with thick net coal (fig. 39). Cumulative water production is significantly higher in the overpressured part of the AU compared to the underpressured part and is similar to that produced from the Fruitland Fairway (fig. 34). Wells with the highest cumulative water production in the overpressured area are located closer to the outcrop or courses of rivers. This high water production might have an effect on cumulative and normalized gas production value because the coals cannot be dewatered as rapidly under artesian conditions. The pattern of high water production in the overpressured area tends to correspond to areas with thicker net coal rather than to directions of inferred post-depositional groundwater flow (figs. 5, 11, and 33). Those areas with less water production correspond to areas with thinner net coal and are similar to values observed in wells in the underpressured area, which is also characterized by net coal generally <45 ft thick. Key parameters of the Basin Fruitland Continuous Gas AU are listed below and are summarized on figure 44.

Source

Fruitland coal beds

Maturation

Late Eocene to middle Miocene for thermal gas. Late Cretaceous to early middle Eocene for possible early microbial gas. Pliocene to Holocene for late-stage microbial gas (fig. 44).

Migration

The principal reservoirs in the Fruitland Formation are the coals, although production also occurs in sandstone channels. Coals (exclusive of cleats) have low porosity and virtually no permeability, and thus the gases are sorbed onto the coal structure (Scott, 1994). This means that initially most of the coal-bed gas is essentially generated in place and has not migrated. However, migration of gas from the coal into other reservoirs, such as the interbedded sandstones, has occurred when pressure decreased below the sorptive capacity of the coal at a given temperature. Usually this occurs during production but may also have occurred in the geologic past during periods of uplift and erosion. Migration of coal-derived gas may also occur by diffusion, and if it enters the

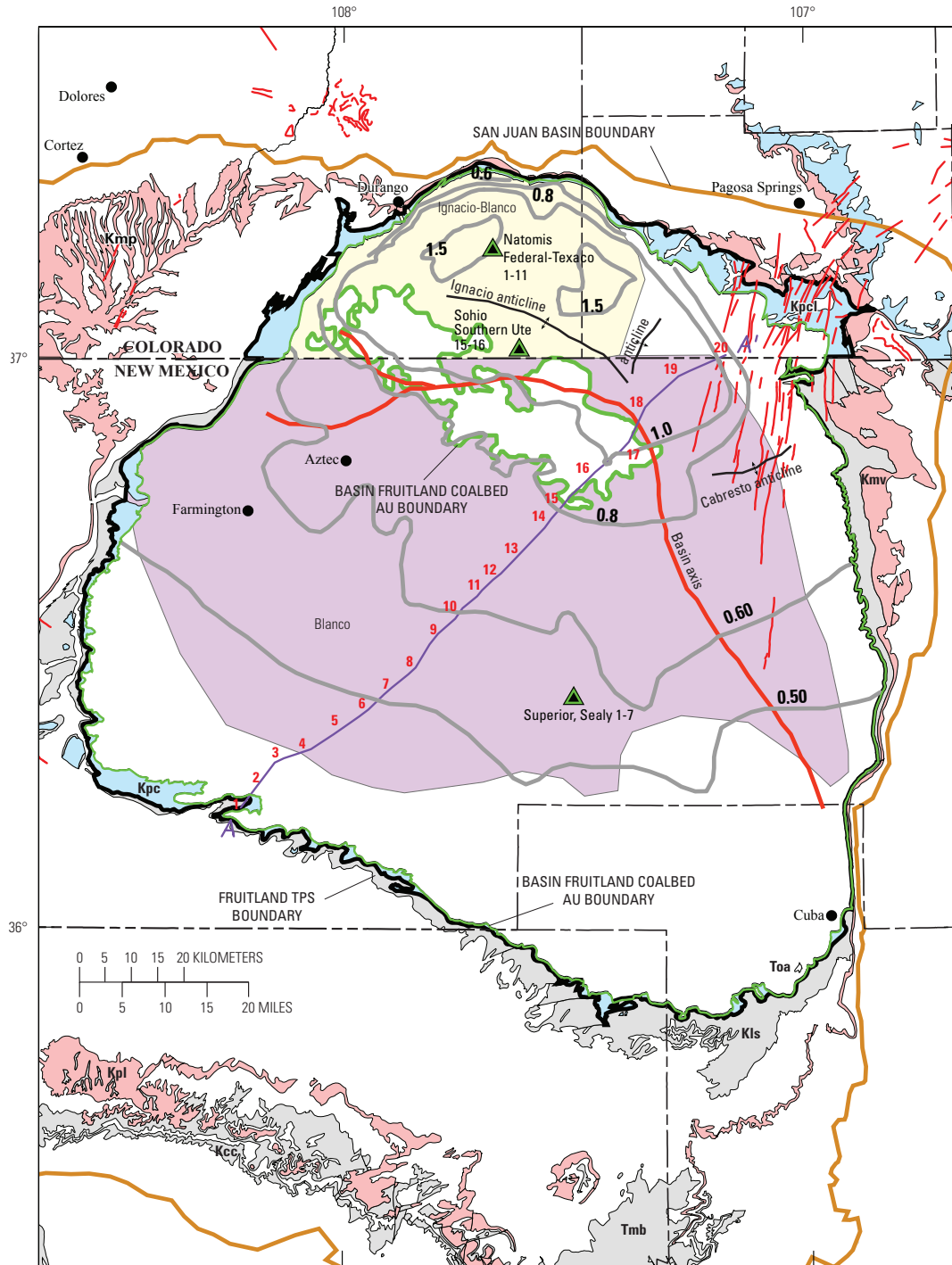


Figure 43. Map showing the assessment unit (AU) boundaries for the Basin Fruitland Coalbed Gas AU (green) and the Basin Fruitland gas fields. Ignacio Blanco gas field (yellow). Blanco gas field (lavender). Symbols for geologic map units: Toa, Tertiary Ojo Alamo Sandstone; Tmb, Tertiary Miocene volcanics; Kpc, Pictured Cliffs Sandstone; Kpcl, Pictured Cliffs Sandstone and Lewis Shale; Kls, Lewis Shale; Kcc, Crevasse Canyon Formation; Kmp, Menefee Formation and Point Lookout Sandstone; Kmv, Mesaverde Group; Kpl, Point Lookout Sandstone; thin red vertical lines and patches, dikes (Green, 1992; Green and Jones, 1997). Thermal maturity contours (gray) show vitrinite reflectance (R_m) values contoured from data in Fassett and Nuccio (1990), Law (1992), and Fassett (2000). Also shown are the locations of the regional cross section A–A' (see fig. 4), principal folds in the basin, and location of wells (green and black triangles) used to make the burial history curves in this report (figs. 10A–C). TPS, Total Petroleum System.

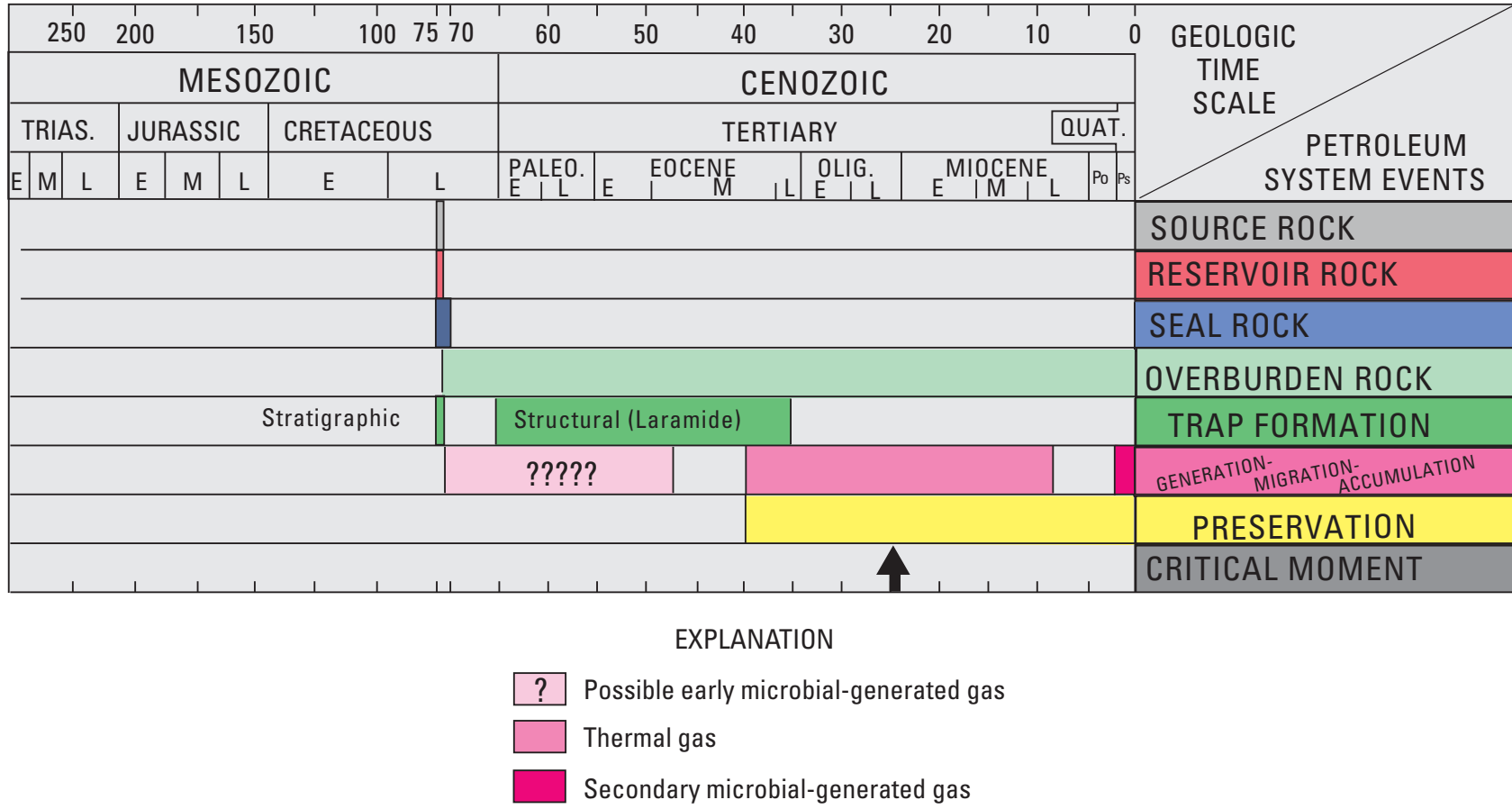


Figure 44. Events chart that shows key geologic events for the Basin Fruitland Coalbed Gas Assessment Unit. Black arrow, critical moment (Magoon and Dow, 1994) for gas generation. TRIAS., Triassic; PALEO., Paleocene; OLIG., Oligocene; QUAT., Quaternary; Po, Pliocene; Ps, Pleistocene; E, early; M, middle; L, late. Geologic time scale is from the Geological Society of America web page <http://www.geosociety.org/science/timescale/timescl.htm>, last accessed 2/1/2008, and from Berggren and others (1995).

hydrologic regime, the gas may dissolve in the water and thus be transported to other sites of accumulation. The regional changes in composition of Fruitland gas suggest some migration of gases has occurred (Scott, 1994). It has been proposed that this migrated gas might also be sorbed onto the coal matrix, under the right reservoir pressure and temperature conditions (Scott and others, 1994b).

Reservoirs

The principal reservoirs in the Fruitland Formation are the coal beds, although production may be from interbedded sandstone channel beds.

Traps/Seals

Several types of traps form in Fruitland reservoirs; each trap varies in magnitude or areal extent. At the smallest scale, the coals in the Fruitland serve not only as the source of the produced gas in the Fruitland but also as the trap and reservoir. At larger scales, the heterogeneous character of coal-bed reservoirs tends to form compartments. The compartments may form when one or possibly both cleat directions are closed or nearly closed as a result of tectonic stress (Shuck and others, 1996). Directions of tectonic stress primarily control the degree of development of the cleat system and direction of cleat development; however, coal rank and coal matrix composition (maceral type) also have been shown to be important (Tremain and others, 1994). Other compartments may form as a result of intersecting faults or lateral pinchout of coal beds. Folds do not appear to control coal-gas accumulation, but fractures and faults associated with development of folds do affect permeability (Kaiser and Ayers, 1994). Seals in Fruitland reservoirs may be

1. closed cleats due to tectonic stress,
2. cemented faults,
3. interbedded tightly cemented sandstone reservoirs that are not fractured, and
4. interbedded low permeability shale or mudstone beds.

Geologic Model

The Basin Fruitland Assessment Unit includes large areas that are overpressured or underpressured and some areas that are of normal pressure. The overpressured area generally is of higher thermal maturity compared to other areas. Both wet and dry gases are found in underpressured to normally pressured areas. Isotopically lighter methane gases are confined to the northern and southern basin margins. Lower CO₂ content is found in both the overpressured and underpressured areas of the AU. Gas in the Basin Fruitland was generated essentially in place, although in some areas gas resources may contain a

component that is related to migration of gas in groundwater during various stages of gas generation.

Volumetrically most of the gas produced from the Basin Fruitland CBG AU is probably of thermogenic origin and mostly generated in place, with maximum generation in the late Oligocene when the basin axis was north of its present location. The period of thermal-gas generation ranged from late Eocene through middle Miocene. Gas throughout the AU, in all three pressure regimes, is a variable mixture of thermogenic and microbial (early or late; fig. 44) as evidenced by the $\delta^{13}\text{C}$ values of methane, carbon dioxide, and bicarbonate. Early microbial-gas generation (fig. 44) is conjectural but is supported by some geochemical evidence previously presented. There appears to be some component of northward flow in the Fruitland at least into the Paleocene and possibly as late as the Miocene and a southward flow in the overpressured area in the Paleocene or early Eocene. Late-stage microbial-gas generation (fig. 44) may be confined to the near-outcrop areas along the northern and western rims of the basin. The presence of isotopically heavy bicarbonate produced water and mixed-isotope signatures of methane and carbon dioxide appears to be ubiquitous throughout the Fruitland. These observations don't necessarily require a young (more recent) age for occurrence.

Assessment Results

The Basin Fruitland Coalbed Gas AU was assessed to have undiscovered resources of 19,594.74 billion cubic feet of gas (BCFG) and 0 million barrels of natural gas liquids (MMBNGL) at the mean. The volumes of undiscovered oil, gas, and natural gas liquids estimated in 2002 for the Basin Fruitland CBG AU are shown in appendix A. The Basin Fruitland Assessment Unit encompasses an area of 3,926,000 acres at the median, 3,825,000 acres at the minimum, and 4,027,000 acres at the maximum extent of the AU. There is adequate charge; favorable reservoirs, traps, and seals at least over most of the area; and favorable timing for charging the reservoirs with greater than the minimum recovery of 0.02 BCFG. A summary of the input data of the AU is presented on the data form in appendix C.

There were 4,102 tested cells (wells that have produced or had some other production test, such as initial production test, drill stem test, or core analysis). A 0.02 BCFG recovery cutoff was used per cell. Applying this cutoff, 3,690 tested cells equaled or exceeded this cutoff. If the production history of the Basin Fruitland CBG AU is divided into nearly three equal discovery time periods, plots of the estimated ultimate recoveries (EUR) indicate that the middle time period has the best EUR distribution, overall, and the best median total recovery (1.1 BCFG) per cell (fig. 45). This may reflect a better understanding of how to explore for and develop coal-bed gas resources, compared to the first time period. Recoveries have declined in the last-third time period, perhaps reflecting that the best overall producing areas have been found. The

EUR distribution for the Basin Fruitland CBG AU (fig. 46) shows a median total recovery per cell of 0.6 BCFG.

The untested part of the AU was evaluated geologically. In the eastern and southern part of the AU, there are areas of thin net coal (fig. 5), low permeability coals, and less well-developed cleat and fracture systems. A poorly developed cleat and fracture network coupled with thin net coal could make some areas less favorable for development because of the greater difficulty in producing the gas. Wells in this area might also produce lower volumes of gas compared to other parts of the AU. Although there are some isolated areas of gas production from coals on the east side of the AU (fig. 38), much of that area remains open for exploration. A similar case can be made in the southern part of the AU where large tracts of land have yet to be tested. Some of these areas are associated with thin net coal (fig. 5). However, as with the east side of the AU, some recent exploration and production has taken place outside of existing fields, indicating that additional gas can potentially be found in the underpressured part of the formation.

Taking these geologic constraints as well as distribution of gas production volumes into consideration, we did not consider the entire untested area as favorable for having potential additions to reserves in the next 30 years. At the minimum we estimate 45 percent of the untested area to have potential additions to reserves in the next 30 years. At the median this value is 55 percent, and at the maximum, 60 percent. These values were obtained by multiplying the various percentages of untested area deemed favorable by different success ratios. These values are lower than those estimated for the Fruitland Fairway CBG AU (appendix A), reflecting different geologic conditions. New discoveries will come from infill drilling on closer spacing, step-out drilling from existing fields, and new field discoveries from wildcat drilling in less explored areas of the AU. The minimum cutoff of 0.02 BCFG would apply to the percentage of untested cells considered to have potential additions to reserves. Total gas recovery per cell for these untested cells is estimated at 0.02 BCFG at the minimum, 0.6 BCFG at the median, and 20 BCFG at the maximum. These values are based on the EUR distributions (fig. 46) and are significantly lower than for the Fruitland Fairway CBG AU (appendix A). The maximum value of 20 BCFG was based on isolated occurrences of high producing wells, one of which has produced 40 BCFG (fig. 46).

Fruitland Fairway Coalbed Gas Assessment Unit (50220181)

Introduction

The Fruitland Fairway Coalbed Gas AU was drawn to include the area basinward of the Fruitland outcrops, exclusive of the area assigned to the Basin Fruitland Coalbed Gas AU, that is characterized by

1. overpressure and

2. wells that have both high cumulative gas production and average daily production exceeding 1,000 cubic feet gas per day (Palmer and others, 1992) (fig. 47).

The boundary between high and low cumulative producing wells generally occurs between 0.5 and 1.0 BCFG (fig. 38). Within this AU, most, but not all, wells have produced at least 1 BCFG. In the Basin Fruitland CBG AU, most, but not all, wells have produced 0.5 BCFG or less. Generally wells in the latter AU that produced 0.5 BCFG or greater are isolated wells or small fields, not contiguous with the Fruitland Fairway CBG AU. The southern and eastern boundaries of the Fruitland Fairway CBG AU were drawn between the area of very high gas and water production and areas of low gas and water production (figs. 34 and 38). Although the AU boundary is irregular, the AU roughly corresponds to the northwest–southeast trend of greatest net coal thickness (fig. 5). The eastern boundary also coincides with low net coal. Well spacing until recently was at 320 acres; this has been reduced to 160 acres. This AU differs from any single Fruitland coal-bed gas play in the 1995 USGS National Oil and Gas Assessment (Rice and Finn, 1996) in that it includes only part of the San Juan Basin-Overpressured Play.

Cumulative gas production from the Fruitland Fairway CBG AU can be divided into three areas, based on the relation between overall production (independent of time) and $\delta^{18}\text{O}$ values of the produced water (fig. 48). These areas also roughly coincide with changes in net coal thickness. The northwest area (area 1 on fig. 48) includes water with $\delta^{18}\text{O}$ values that range between -16 and -8 per mil from north to south and that are defined by a series of south-plunging water masses ($\delta^{18}\text{O}$ between -16 and -13 per mil as seen in fig. 11). These water masses appear to impinge on more easterly oriented water masses with $\delta^{18}\text{O}$ values between -12 and -8 per mil (fig. 11). Net coal thickness of this area generally exceeds 45 ft (fig. 5).

Most of the wells in area 1 of the Fruitland Fairway CBG AU have cumulative gas production that exceeds 3 BCFG (fig. 48). Several wells exceed 20 BCFG cumulative production. There is a slight gradient of increasing cumulative gas production, from north to south; wells with the highest cumulative production tend to cluster along the southern boundary in this part of the AU. This suggests a slight local modification of gas production by groundwater flow, with the best wells producing from older water flow paths. Part of this apparent gradient may also be due to changes in coal thickness. Thinner coal is found along the southeast boundary of this area (fig. 5). However despite this slight production gradient, cumulative production here is uniformly high, implying that this area was probably already enriched in gas resources prior to the introduction of any later water. The contribution of late-stage microbial-generated methane (Scott, 1994; Scott and others, 1994b) is not easily determined but may actually be less than previously proposed for this area if the concept of early generation of microbial gas is considered. The carbon isotopes of the methane, carbon dioxide, and dissolved inorganic carbon

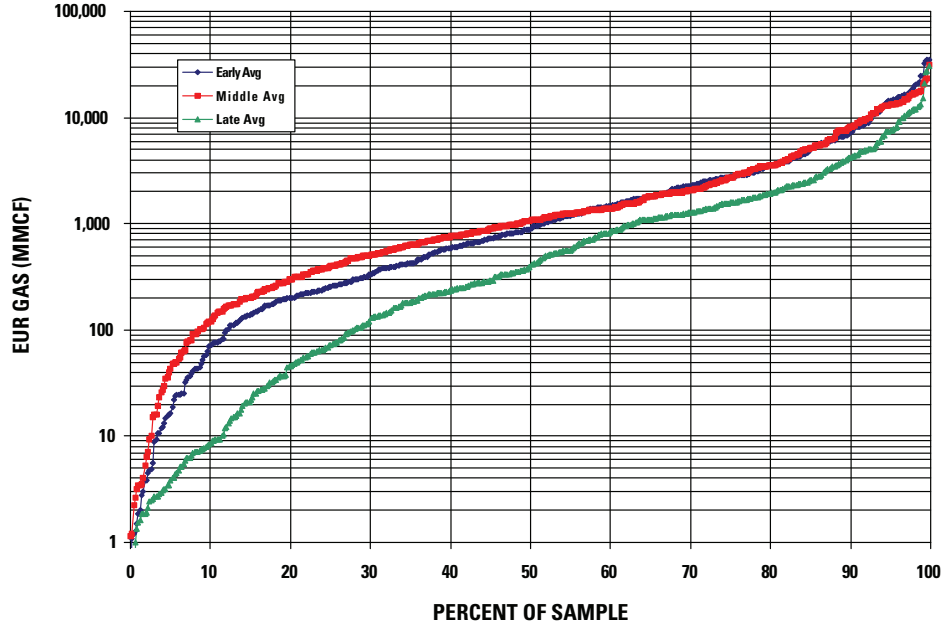


Figure 45. Graph showing estimated ultimate recoveries (EUR) of Basin Fruitland Coalbed Gas Assessment Unit (AU) gas wells divided by time of completion into three nearly equal blocks. EUR data calculated using data from IHS Energy (2002). Data provided by T. Cook (written commun., 2002). MMCF, million cubic feet.

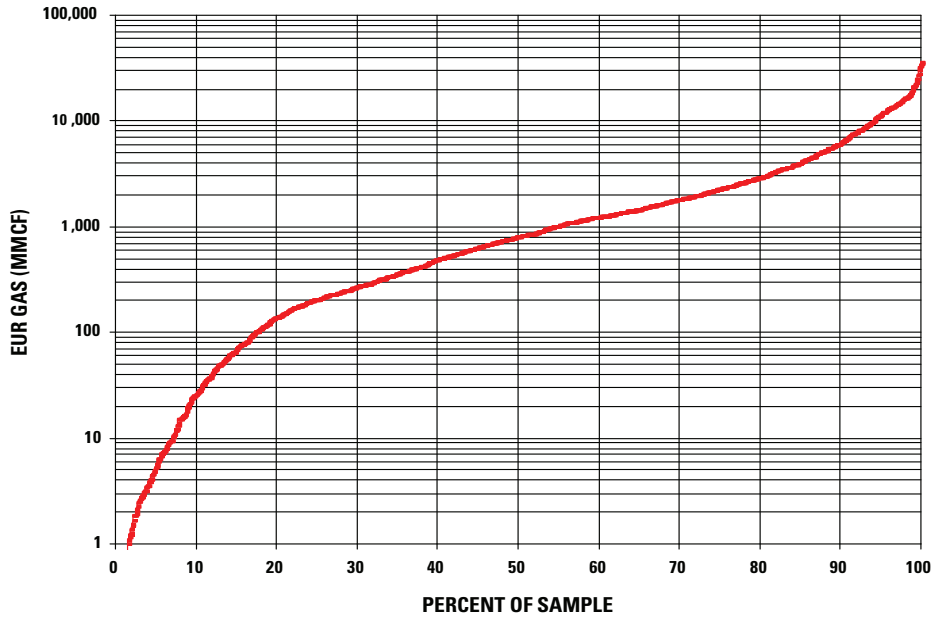


Figure 46. Graph showing distribution of estimated ultimate recoveries (EUR) of Basin Fruitland Coalbed Gas Assessment Unit gas wells. EUR data calculated using data from IHS Energy (2002). Data provided by T. Cook (written commun., 2002). MMCF, million cubic feet.

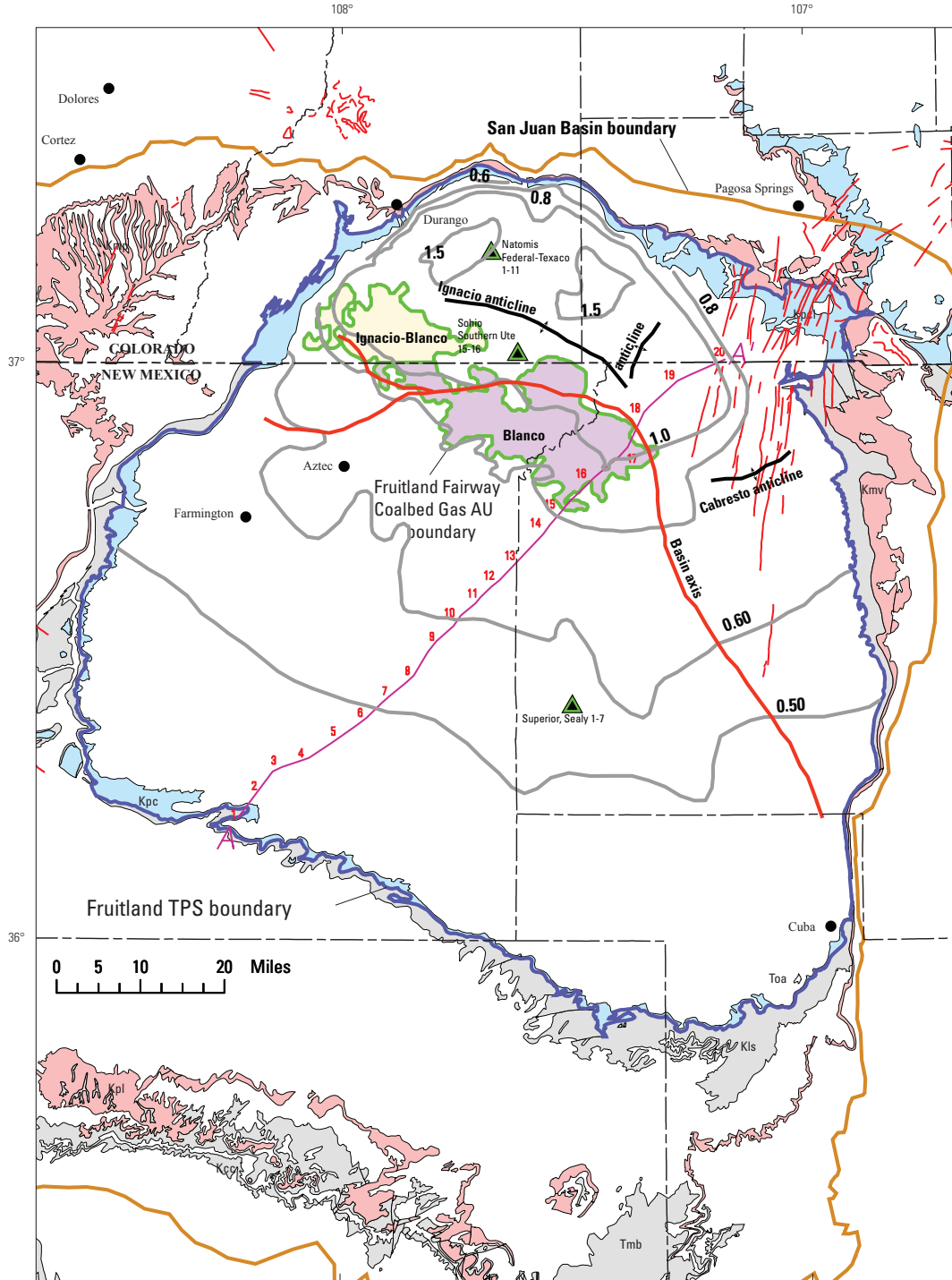
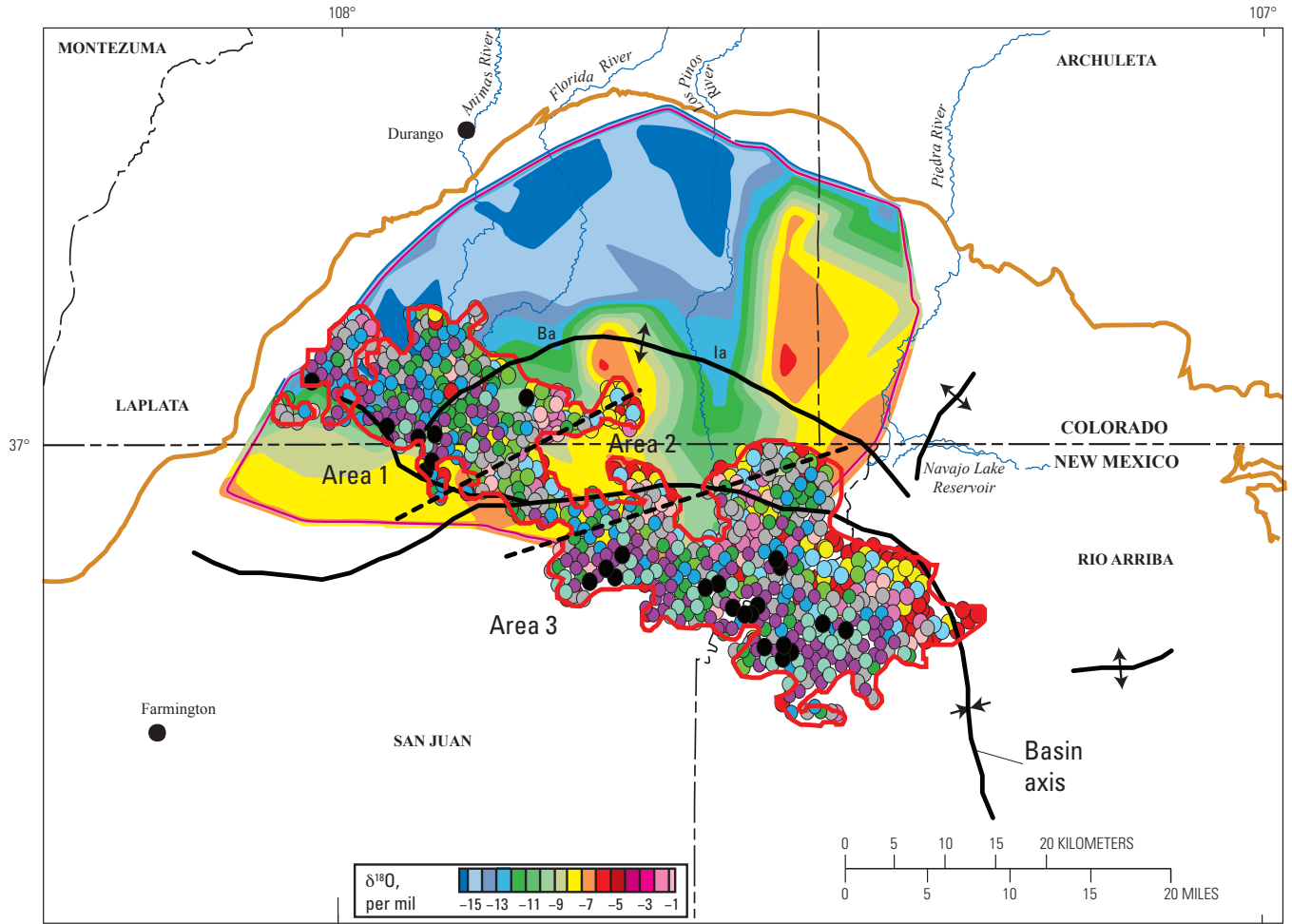


Figure 47. Map showing the assessment unit (AU) boundary for the Fruitland Fairway Coalbed Gas Assessment Unit (green line) and the location of the Fruitland Fairway gas fields. Ignacio Blanco gas field (yellow). Blanco gas field (purple). Also shown are the locations of the regional cross section A–A' (see fig. 4), principal folds in the basin, and wells (green and black triangles) used to make the burial history curves in this report (figs. 10A–C). Symbols for geologic map units: Toa, Tertiary Ojo Alamo Sandstone; Tmb, Tertiary Miocene volcanics; Kpc, Pictured Cliffs Sandstone; Kpcl, Pictured Cliffs Sandstone and Lewis Shale; Kls, Lewis Shale; Kcc, Crevasse Canyon Formation; Kmp, Menefee Formation and Point Lookout Sandstone; Kmv, Mesaverde Group; Kpl, Point Lookout Sandstone; thin red vertical lines and patches, dikes (Green, 1992; Green and Jones, 1997). Contours (gray) show vitrinite reflectance (R_m) values, in percent, from data in Fassett and Nuccio (1990), Law (1992), and Fassett (2000). TPS, Total Petroleum System.



EXPLANATION

- | | | | |
|---|---|--------------------------------|-------------|
| ↕ | Anticline | Cumulative gas production, BCF | |
| ↘ | Syncline | ● 0-0.5 | ● 3.0-5.0 |
| — | Fruitland Fairway Coalbed Gas AU boundary | ● 0.5-1.0 | ● 5.0-7.0 |
| — | Basin Fruitland Coalbed Gas AU boundary | ● 1.0-1.5 | ● 7.0-9.0 |
| | | ● 1.5-2.0 | ● 9.0-15.0 |
| | | ● 2.0-2.5 | ● 15.0-20.0 |
| | | ● 2.5-3.0 | ● >20.0 |

Figure 48. Map showing relation between cumulative gas production (independent of length of production time) in the Fruitland Fairway Coalbed Gas Assessment Unit (AU) and distribution of $\delta^{18}\text{O}$ in produced Fruitland Formation waters. Production data from IHS Energy Group (2002). Oxygen-isotope base map from Cox and others (2001). Ba, Bondad anticline; Ia, Ignacio anticline; BCF, billion cubic feet.

certainly indicate some microbial contribution to the gas, but the isotopes are not indicative of time of genesis (early or late) or of the proportion of thermal component. North of the Fruitland Fairway CBG AU boundary, cumulative gas production drops dramatically in similar or more $\delta^{18}\text{O}$ -depleted waters except in areas along the northern margin of the Basin Fruitland CBG AU and along the courses of several rivers (figs. 11 and 38).

The middle part of the Fruitland Fairway CBG AU (area 2 on fig. 48) includes water with $\delta^{18}\text{O}$ values that range between -10 and -6 per mil and is defined by a series of east-to southeast-oriented water masses (fig. 11). Generally, wells in area 2 (fig. 48) have produced less than 3 BCFG, even though, based on $\delta^{18}\text{O}$ values, the waters would be relatively older than in area 1 of the Fruitland Fairway CBG AU to the west. This area is characterized by generally thinner net coal (less than 45 ft) (fig. 5), and the decrease in production may reflect the decrease in net coal thickness. This area of thin net coal also coincides with the position of a part of the present-day basin axis (figs. 22 and 48), an area where fluid flow rates would be slower because of the lower structural gradient. As documented in the west area of the Fruitland Fairway AU, there is a slight increase in cumulative gas production from north to south in the direction of isotopically heavier water. Overall, wells with the highest cumulative production are found along the southern boundary of this part of the AU.

The eastern part of the Fruitland Fairway CBG AU (area 3 on fig. 48) is characterized by overall high cumulative gas production; the majority of the wells have produced more than 5 BCFG. Net coal thickness in this area generally exceeds 45 ft. Water-isotope chemistry is lacking for most of this part of the AU, except along the northern part where $\delta^{18}\text{O}$ values range between -10 and -7 per mil (fig. 11). However, based on regional trends, most of this part of the Fruitland Fairway should be at least this heavy and could have $\delta^{18}\text{O}$ values as heavy as -5 or -4 per mil. There is a slight gradient of increasing cumulative gas production from north to south; wells with the highest cumulative production tend to cluster along the southern boundary of this part of the AU. Part of this apparent gradient may be due to change in net coal thickness. Thicker coal is found along the southern boundary of the AU in this area (fig. 5). Similar to area 1 of the Fruitland Fairway, the pattern of cumulative gas production implies that area 3 was probably already enriched in gas resources prior to the introduction of younger water or to the addition of any late-stage microbial gas. North and east of area 3 of the Fruitland Fairway CBG AU boundary, cumulative gas production drops dramatically suggesting that some geologic controls, other than groundwater flow, are more important in localizing higher cumulative production in the Fruitland Fairway AU (fig. 38). The northeast and east boundaries of the AU appear to be controlled by thin net coal (fig. 5) and higher sandstone content (Scott and others, 1994b).

Normalized (monthly) gas production is significantly higher in the Fruitland Fairway CBG AU than in either the northern or southern part of the Basin Fruitland CBG AU (fig. 39). In the Fruitland Fairway CBG AU, normalized

monthly gas production is commonly between 50 and 150 MMCF. The same three area divisions of the Fruitland Fairway CBG AU are observed for normalized production (fig. 39). The western and eastern parts of the AU are more enriched than the central part, which has uniformly lower normalized gas volumes. In the western and eastern parts of the Fruitland Fairway AU, there is a slight tendency for normalized gas production to increase from north to south in the direction of isotopically heavier produced waters (figs. 11 and 39). Wells with the highest normalized gas production tend to occur in the southern half of the western and eastern parts of this AU, where net coal is thicker. Net coal thickness may be a more important control on production than any post-deposition groundwater flow. Key parameters of the Fruitland Fairway Continuous Gas AU are listed below and are summarized on figure 49.

Source

The primary petroleum source rock for this assessment unit is interpreted to be coals of the Fruitland Formation.

Maturation

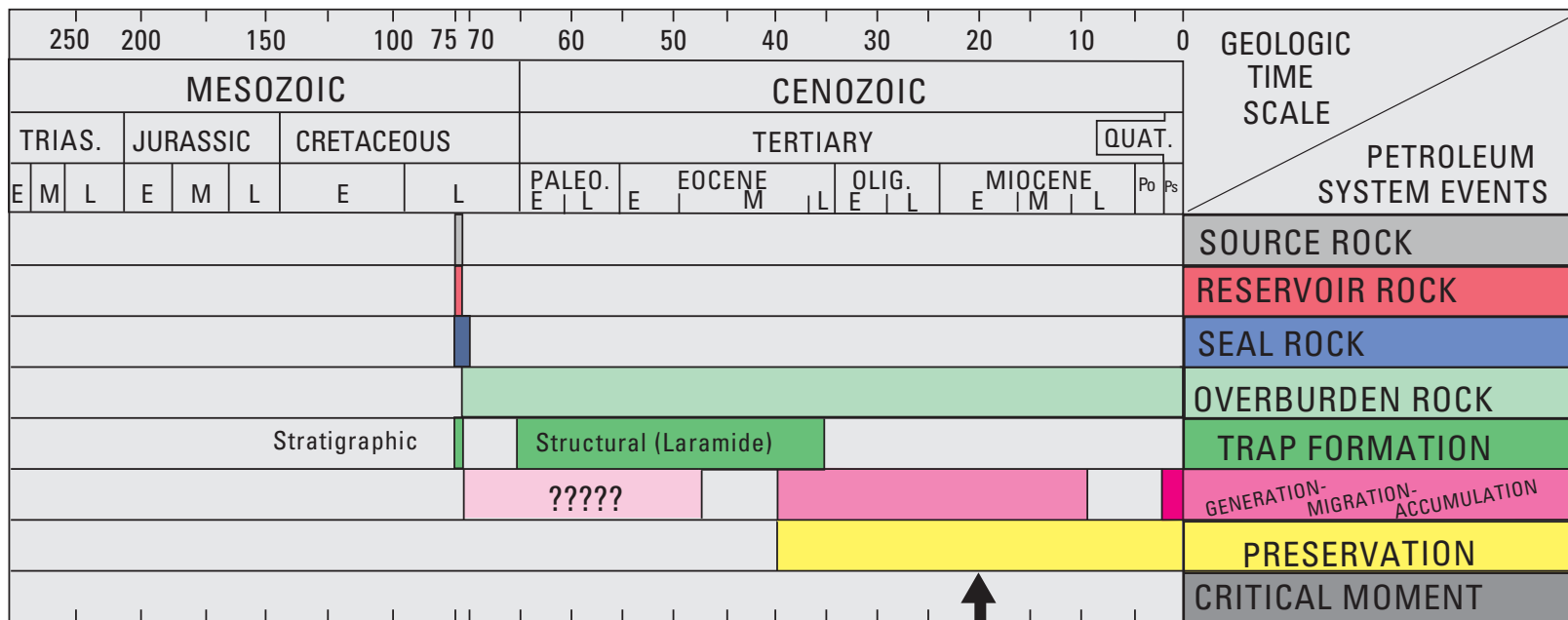
Late Eocene to late Miocene maturation for thermal gas, Late Cretaceous to early middle Eocene for possible early microbial gas, and Pliocene to Holocene for late-stage microbial gas (fig. 49).

Migration

The principal reservoirs in the Fruitland Formation are the coals, although production also occurs in sandstone channel beds. Coals (exclusive of cleats) have low porosity and virtually no permeability, and thus the gases are sorbed onto the coal matrix (Scott, 1994). This means that most of the coal-bed gas is essentially generated in place and has not migrated. However, migration of gas from the coal into other reservoirs, such as the interbedded sandstones, has occurred when pressure decreased below the sorptive capacity of the coal at a given temperature. Usually, this occurs during production but may also have occurred during the geologic past during periods of uplift and erosion. Migration of coal-derived gas may also occur by diffusion, and, if it enters the hydrologic regime, the gas may dissolve in the water and thus be transported to other sites of accumulation. The regional changes in composition of Fruitland gas suggest some migration of gases has occurred (Scott, 1994).

Reservoirs

The principal reservoirs in the Fruitland Formation are the coals, although production may also be from interbedded sandstone channels.



- ? Possible early microbial-generated gas
- Thermal gas
- Secondary microbial-generated gas

Figure 49. Events chart that shows key geologic events for the Fruitland Fairway Coalbed Gas Assessment Unit. Black arrow, critical moment (Magoon and Dow, 1994) for gas generation. TRIAS., Triassic; PALEO., Paleocene; OLIG., Oligocene; QUAT., Quaternary; Po, Pliocene; Ps, Pleistocene; E, early; M, middle; L, late. Geologic time scale is from the Geological Society of America web page <http://www.geosociety.org/science/timescale/timescl.htm>, last accessed 2/1/2008, and from Berggren and others (1995).

Traps/Seals

Several types of traps form in Fruitland reservoirs; each varies in magnitude or areal extent. At the smallest scale, the coals in the Fruitland serve not only as the source of the produced gas in the Fruitland but are also the trap and reservoir. At larger scales, the heterogeneous character of coal-bed reservoirs tends to form compartments. The compartments may form when one or possibly both cleat directions are closed or nearly closed as a result of tectonic stress (Shuck and others, 1996). Directions of tectonic stress primarily control the degree and direction of cleat development; however, coal rank and coal matrix composition (maceral type) also have been shown to be important (Tremain and others, 1994). Other compartments may form as a result of intersecting faults. Folds do not appear to control coal-gas accumulation, but fractures and faults associated with development of folds do affect permeability (Kaiser and Ayers, 1994). Seals in Fruitland reservoirs may be

1. closed cleats, due to tectonic stress,
2. cemented faults,
3. interbedded sandstone reservoirs that are not fractured, and
4. interbedded low-permeability shale or mudstone beds.

Geologic Model

There are several underlying geologic controls for the position of the Fruitland Fairway CBG AU, most of which have been previously discussed, but the principal controls on gas resources appear to be net coal thickness and location of these coals near the structural axis of the basin, the position of which inhibits groundwater flow out of the deepest part of the basin. The Fruitland Fairway AU is located in the southern part of the overpressured part of the Fruitland. The thick coals in the AU were deposited behind two shorelines in the Pictured Cliffs that were associated with stillstand conditions and slower rates of progradation. Isopachs of these coals have a northwest–southeast orientation compared to the northeast–southwest orientation of net coal isopachs to the north and south. These differences in orientation of coal geometry may have affected groundwater flow from the south and north throughout geologic time. The present Fruitland Fairway CBG AU may be viewed either as an area of groundwater convergence or as a remnant of an originally broader area rich in gas resources.

The Fruitland Fairway CBG AU is located entirely within the overpressured part of the Fruitland in an area of higher thermal maturity compared to the underpressured to normally pressured area to the south. Both wet and dry gases are found in the AU, but most gas is dry (fig. 15). The highest CO₂ content (>5.9 percent) is confined to the Fruitland Fairway CBG. Gas in the Fruitland Fairway CBG AU was generated essentially in place, although in some areas gas resources may contain a

component that is related to migration of gas in groundwater during various stages of gas generation.

Volumetrically most of the gas produced from the Fruitland Fairway CBG AU is probably of thermogenic gas origin, and the gas was mostly generated in place. The period of thermal-gas generation ranged from late Eocene through late Miocene (fig. 49), with the maximum gas generation in early Miocene, coincident with deepening of the basin in this area. Gas throughout the AU is a variable mixture of thermogenic and microbial (early or late) as evidenced by the $\delta^{13}\text{C}$ values of methane, carbon dioxide, and bicarbonate. Early microbial-gas generation (fig. 49) is conjectural but is supported by some geochemical evidence previously presented. Significant late-stage microbial-gas generation (fig. 49) as a result of post-Miocene groundwater flow is difficult to support based on ¹²⁹I/I dates of the formation water (Snyder and others, 2003), unless the microbial communities could have survived the high heat (up to 165°C) in the Oligocene and Miocene. The presence of isotopically heavy bicarbonate produced water and mixed-isotope signatures of methane and carbon dioxide appears to be ubiquitous throughout the Fruitland. These observations don't necessarily require a young (more recent) age for occurrence.

Assessment Results

The Fruitland Fairway CBG AU was assessed to have undiscovered resources of 3,981.14 billion cubic feet of gas (BCFG) at the mean. The volumes of undiscovered oil, gas, and natural gas liquids estimated in 2002 for the Fruitland Fairway CBG AU are shown in appendix A. The Fruitland Fairway Assessment Unit encompasses an area of 227,000 acres and because this area is completely surrounded by the Basin Fruitland CBG AU, its size remained the same when estimating the minimum, median, and maximum area of the assessment unit. There is adequate charge; favorable reservoirs, traps, and seals; and favorable timing for charging the reservoirs with greater than the minimum recovery of 0.02 BCFG. A summary of the input data of the AU is presented on the data form in appendix D.

There were 934 tested cells (wells that have produced or had some other production test, such as initial production test, drill stem test, or core analysis). A 0.02 BCFG recovery cutoff was used per cell, and applying this cutoff, 890 tested cells equaled or exceeded this cutoff. If the production history of the Fruitland Fairway CBG AU is divided into nearly three equal discovery time periods, plots of the estimated ultimate recoveries (EUR) indicate that the middle time period has a slightly better EUR distribution than the first time period and the best median total recovery (13 BCFG) per cell (fig. 50). This may reflect a better understanding of how to explore for and develop coal-bed gas resources, compared to the first time period. Recoveries have declined in the last-third time period, perhaps reflecting that the best overall producing areas have been found. The EUR distribution for the Fruitland Fairway AU (fig. 50) shows a median total recovery per

cell of 9.5 BCFG. The EUR distributions were factored into calculation of potential additions to reserves.

The Fruitland Fairway CBG AU has been extensively drilled. At the minimum we estimate 93 percent of the untested area (areas not drilled) to have potential additions to reserves in the next 30 years. At the median, this value is 95 percent, and at the maximum, this value is 97 percent. The high percentage of the untested area considered to have potential additions to reserves in the next 30 years reflects a circumscribed area that has been geologically well defined, and the average production is well known based on drilling. No unfavorable areas in the AU were identified. New discoveries will essentially be infill drilling on closer-acre spacing, testing for smaller compartments that are not in communication with each other. New Mexico recently adopted a 160-acre spacing. The minimum cutoff of 0.02 BCFG would apply to the percentage of untested cells considered to have potential additions to reserves. Total gas recovery per cell for these untested cells is estimated at 0.02 BCFG at the minimum, 9.5 BCFG at the median, and 40 BCFG at the maximum. These values are based on the EUR distributions (fig. 51).

Tertiary Conventional Gas Assessment Unit (50220101)

Introduction

The Tertiary Conventional Gas Assessment Unit boundary was drawn to include all possible gas accumulations in Tertiary rocks in the San Juan Basin. The digital geologic maps of Colorado (Green, 1992) and New Mexico (Green and Jones, 1997) were used to draw the boundary, which was the basal contact of the Animas Formation in the north and the Ojo Alamo Sandstone in the south (fig. 52). The AU thus consists of the geographic area encompassing the Animas Formation, Ojo Alamo Sandstone, Nacimiento Formation, and San Jose Formation. Significant Tertiary conventional gas had not yet been developed in 1995, so this assessed unit is new for this report.

A few gas and oil shows have been discovered in Tertiary rocks in the basin since the late 1950s. The Lee M. Crane, Martin No. 1 well in San Juan County, New Mexico (fig. 52), was spudded in 1957 and has produced over 4,000 bbl oil and nearly 90,000 MCF gas. Well data from PI/Dwights (IHS Energy Group, 2002) indicates that the well was originally tested for the Farmington Sandstone Member of the Kirtland Shale at a depth of 901 to 1,130 ft. All oil and gas production has been from the Ojo Alamo Sandstone whose base is at 887 ft. This well doesn't appear to be associated with any obvious structural high, but is just updip from an area where the Mesaverde Formation produces gas and condensate.

Gas was produced for 25 years from one well in the Nacimiento in the Arch field (fig. 52), west of Cabresto Canyon field. This discovery was made in 1975 by accident while drilling a Pictured Cliffs development well (Emmendorfer, 1983). Production was from a channel sandstone complex in the Nacimiento on the northeast flank of a small anticline.

Emmendorfer (1983) speculated that the source of the gas in this well could have come from either a casing failure of a nearby Pictured Cliffs well or from coal within the Nacimiento adjacent to the producing sandstone bed. Casing failure was eliminated as a source of the gas by testing the nearby wells. No coal was actually identified in the Nacimiento at this location. The Animas/Nacimiento has R_m values between about 0.7 percent and 1.0 percent in this general area (Law, 1992), and the possibility exists that thin coal, carbonaceous shale, or lacustrine rocks within the Tertiary section generated the more than 60,000 MCF gas recovered from this well. Gas migration from deeper in the basin also cannot be ruled out.

Kiffen field (fig. 52) is near the Arch field, and it produced over 12,000 MCF gas from 1977 to 1986 from one well in the Nacimiento. The producing interval in this well was also shallow, less than 800 ft. (Riggs, 1983). Production was thought to be from either a thin, fractured sandy interval or a porous and permeable sandstone in the Nacimiento (Riggs, 1983). The producing well is on the north side of a small anticline. Riggs (1983) did not speculate as to the source of the gas in this well, but tests on all adjacent wells eliminated casing failure as a source. Migration upsection from the Fruitland to a combination trap in the Nacimiento, coal or lacustrine rocks in the Nacimiento, or updip migration from older units are possibilities.

A Nacimiento well in the Ignacio-Blanco field (fig. 52) in southern Colorado produced over 43,000 MCFG from 1986 to 1988. This well currently produces from the Dakota Sandstone and the Menefee Formation, and is on a small anticline trending southeastward into the deepest part of the basin. The depth of Nacimiento production is not known, but the top of the Ojo Alamo here is at 2,170 ft (IHS Energy Group, 2002), and the Nacimiento is above that.

The Gavilan field (fig. 52), southeast of the Cabresto Canyon field, had minor production from the Nacimiento from the early 1980s to as late as 1997, but these wells are now inactive. This production was also on the east flank of a small anticline. Production at Gavilan is mainly from the Pictured Cliffs Sandstone, but sandstones of the Fruitland and Kirtland Formations also have gas shows in this area (Conyers, 1978).

Just southeast of the Gavilan field, a few wells formerly produced from the Ojo Alamo Sandstone in what was known as the Schmitz Torreón-Puerco field (Needham, 1978). This area is now included in the Blanco South field (fig. 29), and production is attributed to the Pictured Cliffs Sandstone. Production was from some lenticular sandstones in the middle of the Ojo Alamo Sandstone and from the lower part of the Ojo Alamo.

The Synergy Operating LLC, 29-4 Carson 20 well, located southwest of Cabresto Canyon field (fig. 52), has produced over 24,000 MCFG from the Nacimiento from 1997 through August 2001. This wildcat well is a workover of a Fruitland well that no longer produces from the Fruitland.

Nearly all of the gas produced from Tertiary rocks in the San Juan Basin has been from the Cabresto Canyon field (fig. 52) and surrounding area (IHS Energy Group, 2002). Limited data is published on this accumulation, key reports being Hoppe (1992) and Anonymous (1998). The field has been

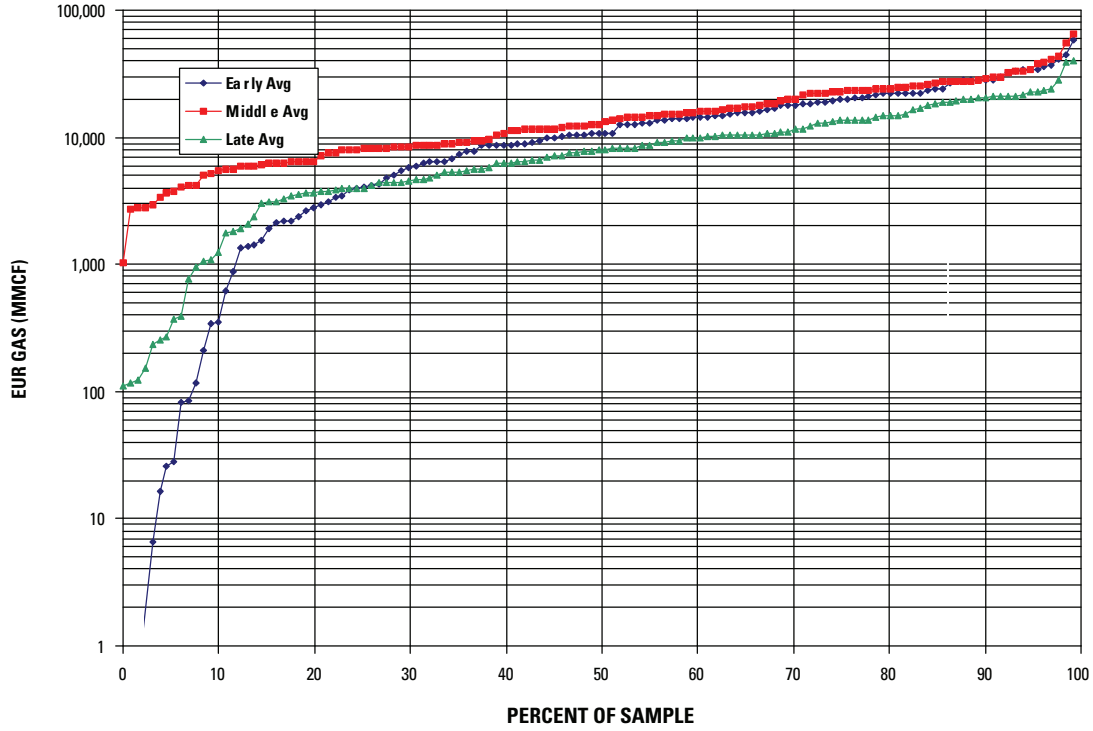


Figure 50. Graph showing estimated ultimate recoveries (EUR) of Fruitland Fairway Coalbed Gas Assessment Unit (AU) gas wells divided by time of completion into three nearly equal blocks. EUR data calculated using data from IHS Energy (2002). Data provided by T. Cook (written commun., 2002). MMCF, million cubic feet.

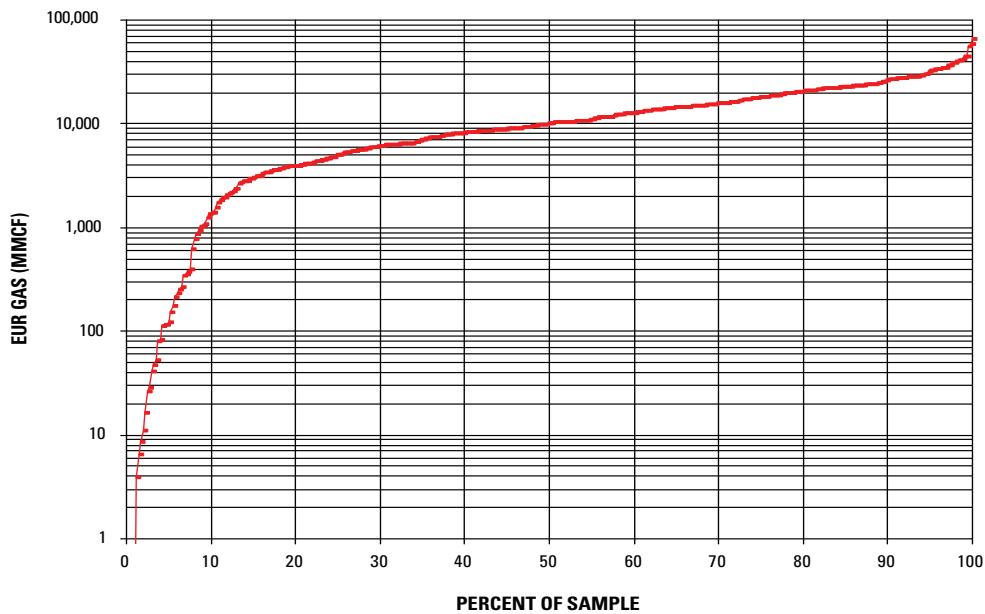


Figure 51. Graph showing distribution of estimated ultimate recoveries (EUR) of Fruitland Fairway Coalbed Gas Assessment Unit (AU) gas wells. EUR data calculated using data from IHS Energy (2002). Data provided by T. Cook (written commun., 2002). MMCF, million cubic feet.

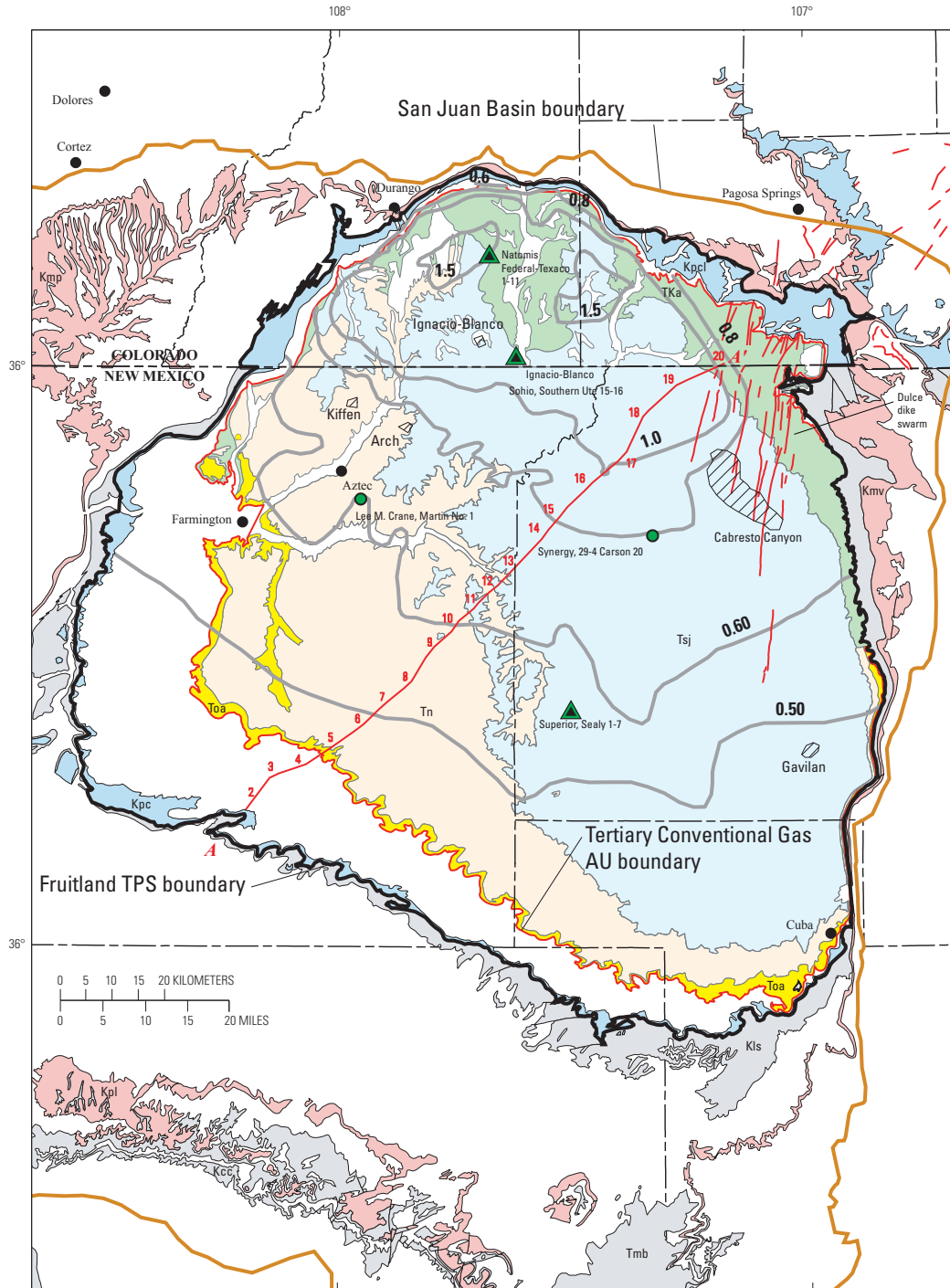


Figure 52. Map showing the assessment unit boundary for the Tertiary Conventional Gas Assessment Unit (AU) (red line) and Tertiary gas fields (cross-hatched pattern). Symbols for geologic map units: Tsj, San Jose Formation; Tn, Nacimiento Formation; Toa, Tertiary Ojo Alamo Sandstone; Tka, Animas Formation; Tmb, Tertiary Miocene volcanics; Kpc, Pictured Cliffs Sandstone; Kpcl, Pictured Cliffs Sandstone and Lewis Shale; Kls, Lewis Shale; Kcc, Crevasse Canyon Formation; Kmp, Menefee Formation and Point Lookout Sandstone; Kmv, Mesaverde Group; Kpl, Point Lookout Sandstone; thin red vertical lines and patches, dikes (Green, 1992; Green and Jones, 1997). Thermal maturity contours (gray) show vitrinite reflectance (R_m) values contoured from data in Fassett and Nuccio (1990), Law (1992), and Fassett (2000). Also shown is the location of the regional cross section A-A' (in fig. 4), principal folds in the basin, location of wells (green and black triangles) used to make the burial history curves in this report (figs. 10A-C), and the general area of the Dulce dike swarm. TPS, Total Petroleum System.

drilled and developed since 1997. As of January, 2003, production from Cabresto Canyon field has been less than 5,000 barrels of oil and about 48.5 billion cubic feet of gas (IHS Energy Group, 2003). Reservoirs are sandstones in the Ojo Alamo Sandstone, and Nacimiento and San Jose Formations.

Tertiary rocks in other areas of the San Juan Basin would also seem to have attributes favorable for gas accumulation; however, there has been very limited production or even shows in other places. Mallon Resources, main operator of the Cabresto Canyon field, noted that the Ojo Alamo is an aquifer in many parts of the San Juan Basin, and does not produce gas on other Mallon properties (Anonymous, 1998). All of the Tertiary rock units are sources of water in the basin, and produce under both water-table and artesian conditions (Brimhall, 1973; Levings and others, 1990; Thorn and others, 1990). Water saturation of Tertiary rocks in most of the San Juan Basin is considered the main reason for the lack of gas accumulations in those rocks. Areas with potential for future discoveries are probably on structures in the region of the Dulce dike swarm (Ruf and Erslev, 2005) (fig. 52) in a setting similar to that at the Cabresto Canyon field. Key parameters of the Tertiary Conventional Gas AU are listed below and are summarized on figure 53.

Source

The primary petroleum source rock for this assessment unit is interpreted to be coals of the Fruitland Formation.

Maturation

Thermal maturation is interpreted to range from late Oligocene to early Miocene time (fig. 53).

Migration

Upward migration occurs along fractures and dike-margin discontinuities associated with dikes that intrude the Tertiary section, then laterally into fluvial sandstones of Tertiary formations.

Reservoirs

Known reservoirs are the Paleocene Ojo Alamo Sandstone and Nacimiento Formation, and Eocene San Jose Formation.

Traps/Seals

Overbank mudstones act as seals; traps are a combination of stratigraphic pinchouts of lenticular fluvial sandstones and an anticline at Cabresto Canyon field (fig. 52). Structure may also play a role at the Gavilan field, south of Cabresto Canyon, and at some small, single-well areas in the northern part of the basin.

Geologic Model

Laramide tectonics in the Late Cretaceous to Eocene caused deepening of the San Juan Basin and uplift of surrounding areas. Tertiary units were sourced from the surrounding uplifted areas and accumulated in the basin. Deposition of Tertiary rocks contributed to maturation of the Fruitland coal source rock; intrusion of the Dulce dike swarm (fig. 52) in the late Oligocene probably also resulted in elevated temperature gradients, at least in local areas. Laramide tectonics also developed a number of small anticlines and synclines on the overall basin structure.

In the late Oligocene to early Miocene, gas generated from the Fruitland could have migrated upward in fracture zones on anticlines, or in the area of the dikes and associated fractures and/or faults. Once gas reached the permeable sandstones of the Ojo Alamo, Nacimiento, and San Jose, it moved laterally into these units. Interbedded mud rocks provide seals, and stratigraphic pinchouts and structural highs on small anticlines, sometimes in combination, form the traps.

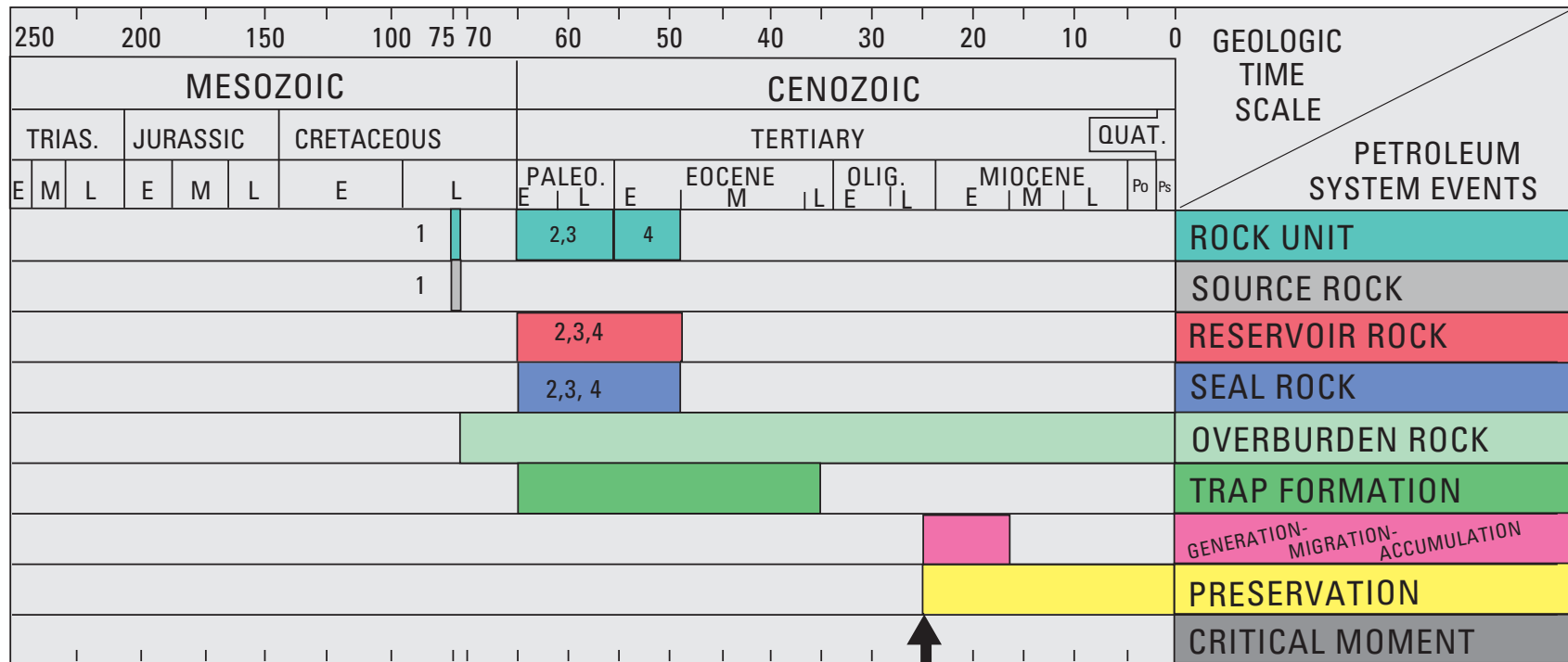
The area of the Dulce dike swarm (in the Cabresto Canyon field) has a number of favorable geologic conditions that led to the accumulation of gas in that region:

1. source rocks of sufficient thickness, quality, and maturity;
2. migration pathways along the dikes and possibly through fractures enhanced by structure;
3. permeable reservoir rocks that are intruded by the dikes; and
4. seals and traps that preserved the gas accumulations.

Assessment Results

The Tertiary Conventional Gas AU (50220101) covers 3,522,254 acres and was estimated to have undiscovered resources of 79.98 BCFG and 0.84 MMBNGL at the mean. The volumes of undiscovered oil, gas, and natural gas liquids estimated in 2002 for the Tertiary Conventional Gas AU are shown in appendix A. A summary of the input data of the AU is presented on the data form in appendix E, which for this AU estimates the numbers and sizes of undiscovered accumulations. There is adequate charge; favorable reservoirs, traps, seals, and access; and favorable timing of generation and migration of hydrocarbons, indicating a geologic probability of 1.0 for finding at least one additional field with a total recovery greater than the stated minimum of 3 BCFG (grown). This unit was not assessed in the 1995 USGS National assessment (Huffman, 1996), because the area of highest production, at Cabresto Canyon, had not yet been developed.

This assessment unit produces mainly gas and minor natural gas liquids (condensate) (IHS Energy Group, 2002), but its production does not appear in the NRG Associates database used for this assessment, because development of the AU occurred largely after the database was published. As of January 2003, gas production from the AU was over 48 BCFG



- Rock units:
- Late Cretaceous—
 1. Fruitland Formation
 - Tertiary—
 2. Ojo Alamo Sandstone (Paleocene)
 3. Nacimiento Formation (Paleocene)
 4. San Jose Formation (Eocene)

Figure 53. Events chart that shows key geologic events for the Tertiary Conventional Gas Assessment Unit. Black arrow, critical moment (Magoon and Dow, 1994) for gas generation. TRIAS., Triassic; PALEO., Paleocene; OLIG., Oligocene; QUAT., Quaternary; Po, Pliocene; Ps, Pleistocene; E, early; M, middle; L, late. Geologic time scale is from the Geological Society of America web page <http://www.geosociety.org/science/timescale/timescl.htm>, last accessed 2/1/2008, and from Berggren and others, (1995).

(IHS Energy Group, 2003), mostly from the Cabresto Canyon field. Dates of first production from the AU were mainly in 1998 to 2001, with a considerable drop-off in wells coming online in 2002 (IHS Energy Group, 2003).

Estimating undiscovered gas resources in the Tertiary Conventional Gas AU is difficult because of the lack of historical production data for the unit and because production has been mainly in one area, to date. A key factor that limits the potential for new gas discoveries is water saturation of the reservoir rocks in much of the AU. The northeast part of the AU was considered to have the best combination of migration pathways and favorable traps, seals, and reservoir rocks for gas accumulations, although this area does not have Fruitland source rocks in the same volume as other parts of the AU. Using these considerations, it was estimated that a minimum of one gas accumulation, above the minimum cutoff of 3 BCFG, could be discovered. It was estimated that a median of five accumulations and a maximum of ten accumulations could be discovered. Sizes of undiscovered accumulations were estimated as 3 BCFG at the minimum, 12 BCFG at the median, and 120 BCFG at the maximum.

Summary

The Fruitland Total Petroleum System includes all genetically related hydrocarbons generated from coal and organic-rich shales in the Cretaceous Fruitland Formation. Four assessment units were defined in the TPS. Of the four assessment units, three were assessed as continuous-type gas accumulations and one as a conventional gas accumulation. The continuous-type assessment units are

1. Pictured Cliffs Continuous Gas AU,
2. Basin Fruitland Coalbed Gas AU, and
3. Fruitland Fairway Coalbed Gas AU.

The conventional accumulation assessment unit is the Tertiary Conventional Gas AU. Total gas resources from this TPS that have the potential for additions to reserves are estimated at a mean of 29.3 TCFG. Of this amount, 23.58 TCFG will come from coal-bed gas accumulations. Total natural gas liquids that have the potential for additions to reserves are estimated at a mean of 17.76 million barrels. Of this amount, 16.92 million barrels will come from the Pictured Cliffs Continuous Gas AU and the remainder from the Tertiary Conventional Gas AU.

Acknowledgments

The authors thank T.S. Collett and A.C. Huffman, Jr., for their thoughtful reviews and T.A. Cook and T.R. Klett for interpretations and graphs of production data. Useful discussions and input were also provided by the U.S Geological Survey (USGS) National Oil and Gas Assessment Team consisting of

R.R. Charpentier, T.A. Cook, R.A. Crovelli, T.R. Klett, and C.J. Schenk.

References Cited

- Ambrose, W.A., and Ayers, W.B., Jr., 1994, Geologic controls on coalbed methane occurrence and production in the Fruitland Formation, Cedar Hill field and the COAL site, *in* Ayers, W.B., Jr., and Kaiser, W.R., eds., Coalbed methane in the Upper Cretaceous Fruitland Formation, San Juan Basin, New Mexico and Colorado: New Mexico Bureau of Mines and Mineral Resources Bulletin 146, p. 41–61.
- Anonymous, 1998, Multiwell Ojo Alamo development advancing in San Juan Basin: *Oil and Gas Journal*, v. 96, no. 17, p. 77.
- Arnold, E.C., 1974, Oil and gas development and production, eastern San Juan Basin, *in* Seimers, C.T., ed., Ghost Ranch—Central-northern New Mexico: New Mexico Geological Society Guidebook, p. 323–328.
- Aubrey, W.M., 1991, Geologic framework of Cretaceous and Tertiary rocks in the Southern Ute Indian Reservation and adjacent areas in the northern San Juan Basin, southwestern Colorado: U.S. Geological Survey Professional Paper 1505–B, p. B1–B24.
- Ayers, W.N., Jr., and Zellers, S.D., 1994, Coalbed methane in the Fruitland Formation, Navajo Lake area; geologic controls on occurrence and producibility, *in* Ayers, W.B., Jr., and Kaiser, W.R., eds., Coalbed methane in the Upper Cretaceous Fruitland Formation San Juan Basin, New Mexico and Colorado: New Mexico Bureau of Mines and Mineral Resources Bulletin 146, p. 63–85.
- Ayers, W.N., Jr., Ambrose, W.A., and Yeh, J.S., 1994, Coalbed methane in the Fruitland Formation, San Juan Basin: depositional and structural controls on occurrence and resources: New Mexico Bureau of Mines and Mineral Resources Bulletin 146, p. 13–40.
- Baltz, E.H., Jr., 1953, Stratigraphic relations of Cretaceous and early Tertiary rocks of a part of northwestern San Juan Basin: U.S. Geological Survey Open-File Report [no number], 80 p.
- Baltz, E.H., Jr., 1967, Stratigraphy and regional tectonic implications of part of Upper Cretaceous and Tertiary rocks, east-central San Juan Basin, New Mexico: U.S. Geological Survey Professional Paper 552, 101 p.
- Bauer, C.M., 1916, Stratigraphy of a part of the Chaco River valley: U.S. Geological Survey Professional Paper 98–P, p. 271–278.

- Berggren, W.A., Kent, D.V., Swisher, C.C., III, and Aubry, M., 1995, A revised Cenozoic geochronology and chronostratigraphy, *in* Berggren, W.A., Kent, D.V., Aubry, M., and Hardenbol, J., eds., *Geochronology, time scales and global stratigraphic correlation*: Society for Sedimentary Geology, SEPM Special Publication No. 54, p. 129–212.
- Bond, W.A., 1984, Application of Lopatin's method to determine burial history, evolution of the geothermal gradient, and timing of hydrocarbon generation in Cretaceous source rocks in the San Juan Basin, northwestern New Mexico and southwestern Colorado, *in* Woodward, J., Meissner, F.F., and Clayton, J.L., eds., *Hydrocarbon source rocks of the greater Rocky Mountain Region*: Rocky Mountain Association of Geologists Guidebook, p. 433–447.
- Brimhall, R.M., 1973, Groundwater hydrology of the San Juan Basin, New Mexico, *in* Fassett, J.E., ed., *Cretaceous and Tertiary rocks of the southern Colorado Plateau: Four Corners Geological Society Guidebook*, p. 197–207.
- Brown, C.F., 1973, A history of the development of the Pictured Cliffs Sandstone in the San Juan Basin of northwestern New Mexico, *in* Fassett, J.E., ed., *Cretaceous and Tertiary rocks of the southern Colorado Plateau: Four Corners Geological Society Guidebook*, p. 178–184.
- Clayton, J.L., Rice, D.D., and Michael, G.E., 1991, Oil-generating coals of the San Juan Basin, New Mexico and Colorado, U.S.A.: *Organic Geochemistry*, v. 17, p. 735–742.
- Colorado Oil and Gas Commission, 1999a, Cause 112, exhibits 11–13.
- Colorado Oil and Gas Commission, 1999b, Cause 112, exhibit 16.
- Conyers, W.P., 1978, Gavilan Pictured Cliffs, *in* Fassett, J.E., ed., *Oil and gas fields of the Four Corners area, volume I: Four Corners Geological Society*, p. 320–322.
- Cox, D., Onsager, P., Thomson, J., Reinke, R., Gianinny, G., Vliss, C., Hugh, J., and Janowiak, M., 2001, San Juan Basin groundwater modeling study: Groundwater-surface water interactions between Fruitland coalbed methane development and rivers: Colorado Oil and Gas Conservation Commission San Juan Basin Study Report, 124 p.
- Craig, S.D., 2001, Geologic framework of the San Juan structural basin of New Mexico, Colorado, Arizona, and Utah, with emphasis on Triassic through Tertiary rocks: U.S. Geological Survey Professional Paper 1420, 70 p.
- Criss, R.E., 1999, *Principals of stable isotope distribution*: New York, Oxford University Press, 254 p.
- Cumella, S.P., 1981, Sedimentary history and diagenesis of the Pictured Cliffs Sandstone, San Juan Basin, New Mexico and Colorado: Texas Petroleum Research Committee, University Division, Austin, Texas, Report UT 81–1, 219 p.
- Das, B.M., Nikols, D.J., Das, Z.U., and Hucka, V.J., 1991, Factors affecting rate and total volume of methane desorption from coalbeds, *in* Schwochow, S.D., Murray, D.K., and Fahy, M.F., eds., *Coalbed methane of western North America*: Rocky Mountain Association of Geologists, p. 69–76.
- Emmendorfer, A.P., 1983, Arch Nacimiento, *in* Fassett, J.E., ed., *Oil and gas fields of the Four Corners area, volume III: Four Corners Geological Society*, p. 931–933.
- Fabryka-Martin, J., Bentley, H., Elmore, D., and Airey, P.L., 1985, Natural iodine-129 as an environmental tracer: *Geochimica et Cosmochimica Acta*, v. 49, p. 337–347.
- Fassett, J.E., 1974, Cretaceous and Tertiary rocks of the eastern San Juan Basin, New Mexico and Colorado, *in* Seimers, C.T., ed., *Ghost Ranch—Central-northern New Mexico*: New Mexico Geological Society Guidebook, p. 225–230.
- Fassett, J.E., 1977, Geology of the Point Lookout, Cliff House and Pictured Cliffs Sandstones of the San Juan Basin, New Mexico and Colorado, *in* Fassett, J.E., ed., *San Juan Basin III: New Mexico Geological Society Guidebook*, p. 193–197.
- Fassett, J.E., ed., 1978a, *Oil and gas fields of the Four Corners area, volume I: Four Corners Geological Society*, 368 p.
- Fassett, J.E., ed., 1978b, *Oil and gas fields of the Four Corners area, volume II: Four Corners Geological Society*, p. 369–727.
- Fassett, J.E., ed., 1983, *Oil and gas fields of the Four Corners area, volume III: Four Corners Geological Society*, p. 729–1143.
- Fassett, J.E., 1985, Early Tertiary paleogeography and paleotectonics of the San Juan Basin area, New Mexico and Colorado, *in* Flores, R.M., and Kaplan, S.S., eds., *Cenozoic paleogeography of west-central United States: Rocky Mountain Section, SEPM (Society for Sedimentary Geology)*, p. 317–334.
- Fassett, J.E., 1991, Oil and gas resources of the San Juan Basin, New Mexico and Colorado, *in* Gluskoter, H.J., Rice, D.D., and Taylor, R.B., eds., *Economic geology: Geological Society of America, The Geology of North America Series*, v. P–2, p. 357–372.
- Fassett, J.E., 2000, Geology and coal resources of the Upper Cretaceous Fruitland Formation, San Juan Basin, New Mexico and Colorado, chap. Q of Kirschbaum, M.A., Roberts, L.N.R., and Biewick, L.R.H., eds., *Geologic assessment of coal in the Colorado Plateau: Arizona, Colorado, New Mexico, and Utah*: U.S. Geological Survey Professional Paper 1625–B, p. Q1–Q132.
- Fassett, J.E., and Hinds, J.S., 1971, Geology and fuel resources of the Fruitland Formation and Kirtland Shale of the San Juan Basin, New Mexico and Colorado: U.S. Geological Survey Professional Paper 676, 76 p.

- Fassett, J.E., and Nuccio, V.F., 1990, Vitrinite reflectance values of coal from drill-hole cuttings from the Fruitland and Menefee Formations, San Juan Basin, New Mexico: U.S. Geological Survey Open-File Report 90-290, 21 p.
- Fehn, U., Peters, E.K., Tullai-Fitzpatrick, S., Kubik, P.W., Sharma, P., Teng, R.T.D., Gove, H.E., and Elmore, D., 1992, ^{129}I and ^{36}Cl concentrations in waters of the eastern Clear Lake area, California: Residence times and sources ages of hydrothermal fluids: *Geochimica et Cosmochimica Acta*, v. 56, p. 2069–2079.
- Fishman, N.S., Ridgley, J.L., and Hall, D.L., 2001, Timing of gas generation in the Cretaceous Milk River Formation, southeastern Alberta and southwestern Saskatchewan—Evidence from authigenic carbonates, *in* Summary of investigations 2001, vol. 1: Saskatchewan Geological Survey, Saskatchewan Energy and Mines, Miscellaneous Report 2001-4.1, p. 125–136.
- Fritz, P., and Fontes, J.C., eds., 1980, Handbook of environmental isotope geochemistry: Amsterdam, Elsevier, 545 p.
- Goberdhan, H.C., 1996, Diagenesis and petrophysics of the Upper Cretaceous Pictured Cliffs Formation of the San Juan Basin, northwest New Mexico and southwest Colorado: College Station, Texas A & M University, M.S. thesis, 143 p.
- Gorody, A.W., 1999, The origin of natural gas in the Tertiary coal-seams on the eastern margin of the Powder River Basin, *in* Coalbed methane and the Tertiary geology of the Powder River Basin, Wyoming and Montana: Wyoming Geological Association Guidebook, 50th Field Conference, p. 89–101.
- Gorody, A.W., 2001, The origin of dissolved gas in shallow aquifers overlying the San Juan Basin's Ignacio Blanco gas field near Bayfield, La Plata County, Colorado, *in* Stilwell, D.P., Wyoming gas resources and technology: Wyoming Geological Association 52nd Field Conference, p. 9–21.
- Green, G.N., 1992, The digital geologic map of Colorado in ARC/INFO format: U.S. Geological Survey Open-File Report 92-507, <http://pubs.er.usgs.gov/usgspubs/ofr/ofr92507A>; last accessed 2/1/2008.
- Green, G.N., and Jones, G.E., 1997, The digital geologic map of New Mexico in ARC/INFO Format: U.S. Geological Survey Open-File Report 97-0052, <http://pubs.er.usgs.gov/usgspubs/ofr/ofr9752>; last accessed 2/1/2008.
- Gries, R.R., Clayton, J.L., and Leonard, China, 1997, Geology, thermal maturation, and source rock geochemistry in a volcanic covered basin: San Juan sag, south central Colorado: American Association of Petroleum Geologists Bulletin, v. 81, p. 1133–1160.
- Harr, C.L., 1988, The Ignacio Blanco gas field, northern San Juan Basin, Colorado, *in* Fassett, J.E., ed., Geology and coal-bed methane resources of the northern San Juan Basin, Colorado and New Mexico: Rocky Mountain Association of Geologists Guidebook, p. 205–219.
- Hoppe, W.F., 1992, Hydrocarbon potential and stratigraphy of the Pictured Cliffs, Fruitland, and Ojo Alamo Formations in the northeastern San Juan Basin, New Mexico, *in* Lucas, S.G., Kues, B.S., Williamson, T.E., and Hunt, A.P., eds., San Juan Basin IV: New Mexico Geological Society Guidebook, p. 359–371.
- Huffman, A.C., Jr., 1996, San Juan Basin Province (22), *in* Gautier, D.L., Dolton, G.L., Takahashi, K.I., and Varnes, K.L., eds., 1995 National Assessment of United States oil and gas resource—Results, methodology, and supporting data: U.S. Geological Survey Digital Data Series 30, release 2.
- Huffman, A.C., Jr., and Taylor, D.J., 2002, Fractured shale reservoirs and basement faulting, San Juan Basin, New Mexico and Colorado: American Association of Petroleum Geologists Rocky Mountain Section Meeting, Laramie, Wyo., p. 30.
- IHS Energy Group, 2002, PI/Dwights Plus US Well Data [data current as of June 2002]: Englewood, Colo., IHS Energy Group; database available from IHS Energy Group, 15 Inverness Way East, D205, Englewood, CO 80112, U.S.A.
- IHS Energy Group, 2003, PI/Dwights Plus US Production Data [data current as of January 2003]: Englewood, Colo., IHS Energy Group; database available from IHS Energy Group, 15 Inverness Way East, D205, Englewood, CO 80112, U.S.A.
- Jones, A.H., Kelkar, S., Bush, D., Hanson, J., Rakop, K., Ahmed, U., Holland, M., Tibbitt, G., Owen, L.B., and Bowman, K.C., 1985, Methane production characteristics of deeply buried coalbed reservoirs: Gas Research Institute Final Report 85/0033, 176 p.
- Jones, R.W., 1987, Organic facies, *in* Brooks, J. and Welte, D., eds., Advances in petroleum geochemistry, v. 2: London, Academic Press, p. 1–90.
- Kaiser, W.R., and Ayers, W.B., Jr., 1994, Coalbed methane production, Fruitland Formation, San Juan Basin: geologic and hydrologic controls: New Mexico Bureau of Mines and Mineral Resources Bulletin 146, p. 187–207.
- Kaiser, W.R., Swartz, T.E., and Hawkins, G.J., 1994, Hydrologic framework of the Fruitland Formation, San Juan Basin: New Mexico Bureau of Mines and Mineral Resources Bulletin 146, p. 133–163.

- Kelso, B.S., Decker, A.D., Wicks, D.E., and Horner, D.M., 1987, GRI geologic and economic appraisal of coal-bed methane in the San Juan Basin, *in* Proceedings, the 1987 coal-bed methane symposium, November 16–19, 1987, The University of Alabama, Tuscaloosa, Alabama: Gas Research Institute, The University of Alabama and the Department of Labor, sponsors, p. 119–130.
- Kelso, B.S., and Wicks, D.E., 1988, A geologic analysis of the Fruitland Formation coal and coal-bed methane resources of the San Juan Basin, southwestern Colorado and northwestern New Mexico, *in* Fassett, J.E., ed., Geology and coal-bed methane resources of the northern San Juan Basin, Colorado and New Mexico: Rocky Mountain Association of Geologists Guidebook, p. 69–79.
- Law, B.E., 1992, Thermal maturity patterns of Cretaceous and Tertiary rocks, San Juan Basin, Colorado and New Mexico: Geological Society of America Bulletin, v. 104, p. 192–207.
- Levings, G.W., Craigg, S.D., Dam, W.L., Kernodle, J.M., and Thorn, C.R., 1990, Hydrogeology of the San Jose, Nacimiento, and Animas Formations in the San Juan structural basin, New Mexico, Colorado, Arizona, and Utah: U.S. Geological Survey Hydrologic Investigations Atlas 720–A.
- Magoon, L.B., and Dow, W.G., 1994, The petroleum system, *in* Magoon, L.B., and Dow, W.G., eds., The petroleum system—from source to trap: American Association of Petroleum Geologists Memoir 60, p. 3–24.
- Martini, A.M., Walter, L.M., Budai, J.M., Ku, T.C.W., Kaiser, C.J., and Schoell, M., 1998, Genetic and temporal relations between formation waters and biogenic methane—Upper Devonian Antrim Shale, Michigan Basin, USA: *Geochimica et Cosmochimica Acta*, v. 62, p. 1699–1720.
- Matheny, M.L., and Ulrich, R.A., 1983, A history of the petroleum industry in the Four Corners area, *in* Fassett, J.E., ed., Oil and gas fields of the Four Corners area, volume III: Four Corners Geological Society, p. 804–810.
- Mavor, M., and Nelson, C.R., 1997, Coalbed reservoir gas-in-place analysis: Chicago, Ill., Gas Research Institute, GRI Report no. GRI-97/0263, 134 p.
- Mavor, M.J., Close, J.C., and Pratt, T.J., 1991, Western Cretaceous coal seam project summary of the Completion Optimization and Assessment Laboratory (COAL) site: Gas Research Institute Topical Report GRI-91/0377, 120 p.
- Michael, G.E., Anders, D.E., and Law, B.E., 1993, Geochemical evaluation of Upper Cretaceous Fruitland Formation coals, San Juan Basin, New Mexico and Colorado: *Organic Geochemistry*, v. 20, p. 475–498.
- Molenaar, C.M., 1977a, San Juan Basin time-stratigraphic nomenclature chart, *in* Fassett, J.E., James, H.L., and Hodgson, H.E., eds., San Juan Basin III: New Mexico Geological Society Guidebook, p. xii.
- Molenaar, C.M., 1977b, Stratigraphy and depositional history of Upper Cretaceous rocks of the San Juan Basin area, New Mexico and Colorado, with a note on economic resources, *in* Fassett, J.E., ed., San Juan Basin III: New Mexico Geological Society Guidebook, p. 159–166.
- Moore, B.J., and Sigler, Stella, 1987, Analyses of natural gases, 1917–85: U. S. Bureau of Mines Information Circular 9129, 1197 p.
- Moran, J., 1996, Origin of iodine in the Anadarko Basin, Oklahoma: An ^{129}I study: American Association of Petroleum Geologists Bulletin, v. 80, p. 685–694.
- Moran, J., Fehn, U., and Hanor, J.S., 1995, Determination of source ages and migration patterns of brines from the U.S. Gulf Coast Basin using ^{129}I : *Geochimica et Cosmochimica Acta*, v. 59, no. 24, p. 5055–5069.
- Moran, J., Fehn, U., and Teng, R.T.D., 1998, Variations in $^{129}\text{I}/^{127}\text{I}$ ratios in recent marine sediment: Evidence for a fossil organic component: *Chemical Geology*, no. 152, p. 193–203.
- Needham, C.N., 1978, Schmitz Torreon-Puerco, *in* Fassett, J.E., ed., Oil and gas fields of the Four Corners area, volume II: Four Corners Geological Society, p. 482–485.
- Nolte, E., Krauthan, P., Korschinek, G., Maloszewski, P., Fritz, P., and Wolf, M., 1991, Measurements and interpretations of ^{36}Cl in groundwater, Milk River aquifer, Alberta, Canada: *Applied Geochemistry*, v. 6, p. 435–447.
- Nummedal, D., and Molenaar, C.M., 1995, Sequence stratigraphy of ramp-setting strand plain successions: the Gallup Sandstone, New Mexico, *in* Van Wagoner, J.C., and Bertram, G.T., eds., Sequence stratigraphy of foreland basin deposits: American Association of Petroleum Geologists Memoir 64, p. 277–310.
- Oldacker, P.R., 1991, Hydrogeology of the Fruitland Formation, San Juan Basin, Colorado and New Mexico, *in* Schwochow, S.D., ed., Coalbed methane of Western North America: Rocky Mountain Association of Geologists, p. 61–66.
- Owen, D.E., and Siemers, C.T., 1977, Lithologic correlation of the Dakota Sandstone and adjacent units along the eastern flank of the San Juan Basin, New Mexico, *in* Fassett, J.E., ed., San Juan Basin III: New Mexico Geological Society Guidebook, p. 179–183.

- Palmer, I.D., Mavor, M.J., Seidle, J.P., Spitler, J.L., and Voltz, R.F., 1992, Open hole cavity completions in coalbed methane wells in the San Juan Basin: Society of Petroleum Engineers Paper SPE 24906, p. 501–516.
- Pasley, M.A., Gregory, W.A., and Hart, G.F., 1991, Organic matter variations in transgressive and regressive shales: *Organic Geochemistry*, v. 17, p. 483–509.
- Phillips, F.M., Peeters, L.A., Tansey, M.K., and Davis, S.N., 1986, Paleoclimatic inferences from an isotopic investigation of groundwater in the central San Juan Basin, New Mexico: *Quaternary Research*, v. 26, p. 179–193.
- Posamentier, H.W., Allen, G.P., James, D.P., and Tesson, M., 1992, Forced regressions in a sequence stratigraphic framework; concepts, examples, and exploration significance: *American Association of Petroleum Geologists Bulletin*, v. 76, p. 1687–1709.
- Reeside, J.B., Jr., 1924, Upper Cretaceous and Tertiary formations of the western part of the San Juan Basin, Colorado and New Mexico: U.S. Geological Survey Professional Paper 134, 117 p.
- Rice, D.D., 1983, Relation of natural gas composition to thermal maturity and source rock type in San Juan Basin, northwestern New Mexico and southwestern Colorado: *American Association of Petroleum Geologist Bulletin*, v. 67, no. 8, p. 1199–1218.
- Rice, D.D., 1993, Composition and origins of coalbed gas: *Proceedings International Coalbed Methane Symposium*, v. 1993, p. 577–588.
- Rice, D.D., Clayton, J.L., Flores, R.M., Law, B.E., and Stanton, R.W., 1992, Some geologic controls of coalbed gas generation, accumulation, and production, Western United States: U.S. Geological Survey Circular 1074, p. 64.
- Rice, D.D., Clayton, J.L., and Pawlewicz, M.J., 1989, Characterization of coal-derived hydrocarbons and source-rock potential of coal beds, San Juan Basin, New Mexico and Colorado, U.S.A.: *International Journal of Coal Geology*, v. 13, p. 597–626.
- Rice, D.D., and Finn, T.M., 1996, Coal-bed gas plays, *in* Gautier, D.L., Dolton, G.L., Takahashi, K.I., and Varnes, K.L., eds., 1995 National assessment of United States oil and gas resources—Results, methodology, and supporting data: U.S. Geological Survey Digital Data Series 30, release 2.
- Rice, D.D., Threlkeld, C.N., Vuletich, A.K., and Pawlewicz, M.J., 1988, Identification and significance of coal-bed gas, San Juan Basin, northwestern New Mexico and southwestern Colorado, *in* Fassett, J.E., ed., *Geology and coal bed methane resources of the northern San Juan Basin, Colorado and New Mexico*: Denver, Colo., Rocky Mountain Association of Geologists, p. 51–59.
- Riggs, E.A., 1978, Bloomfield Farmington, *in* Fassett, J.E., ed., *Oil and gas fields of the Four Corners area, volume I: Four Corners Geological Society*, p. 243–244.
- Riggs, E.A., 1983, Kiffen Nacimiento, *in* Fassett, J.E., ed., *Oil and gas fields of the Four Corners area, volume III: Four Corners Geological Society*, p. 972–974.
- Ruf, J.C., and Erslev, E.A., 2005, Origin of Cretaceous to Holocene fractures in the northern San Juan Basin, Colorado and New Mexico: *Rocky Mountain Geology*, v. 40, no. 1, p. 91–114.
- Schmoker, J.W., 1996, Methodology for assessing continuous-type (unconventional) hydrocarbon accumulations, *in* Gautier, D.L., Dolton, G.L., Takahashi, K.I., and Varnes, K.L., eds., 1995 National assessment of United States oil and gas resources—Results, methodology, and supporting data: U.S. Geological Survey Digital Data Series 30, release 2.
- Schmoker, J.W., 2003, U.S. Geological Survey assessment concepts for continuous petroleum accumulations, chap. 17 *of* USGS Uinta-Piceance Assessment Team, *Petroleum systems and geologic assessment of oil and gas in the Uinta-Piceance Province, Utah and Colorado*: U.S. Geological Survey Digital Data Series 69–B, 7 p. [<http://pubs.usgs.gov/dds/dds-069/dds-069-b/chapters.html>, last accessed 04/2008]
- Schmoker, J.W., and Klett, T.R., 2003, U.S. Geological Survey assessment concepts for conventional petroleum accumulations, chap. 19 *of* USGS Uinta-Piceance Assessment Team, *Petroleum systems and geologic assessment of oil and gas in the Uinta-Piceance Province, Utah and Colorado*: U.S. Geological Survey Digital Data Series 69–B, 6 p. [<http://pubs.usgs.gov/dds/dds-069/dds-069-b/chapters.html>, last accessed 04/2008]
- Scott, A.R., 1994, Coalbed gas composition, Upper Cretaceous Fruitland Formation, San Juan Basin, Colorado and New Mexico: Colorado Geological Survey Open-File Report 94–2, 28 p.
- Scott, A.R., and Kaiser, W.R., 1991, Relation between basin hydrology and Fruitland gas composition, San Juan Basin, Colorado and New Mexico: *Quarterly Review of Methane Coal Seams Technology*, v. 9, no. 1, p. 10–18.

- Scott, A.R., Kaiser, W.R., and Ayers, W.B., Jr., 1991, Composition, distribution, and origin of Fruitland Formation and Pictured Cliffs Sandstone gases, San Juan Basin, Colorado and New Mexico, *in* Schwochow, S.D., Murray, D.K., and Fahy, M.F., eds., *Coalbed methane of western North America*: Denver, Colo., Rocky Mountain Association of Geologists, p. 93–108.
- Scott, A.R., Kaiser, W.R., and Ayers, W.B., Jr., 1994a, Thermal maturity of Fruitland coal and composition of Fruitland Formation and Pictured Cliffs Sandstone gases, *in* Ayers, W.B., Jr., and Kaiser, W.R., eds., *Coalbed methane in the Upper Cretaceous Fruitland Formation San Juan Basin, New Mexico and Colorado*: New Mexico Bureau of Mines and Mineral Resources Bulletin 146, p. 165–186.
- Scott, A.R., Kaiser, W.R., and Ayers, W.B., Jr., 1994b, Thermogenic and secondary biogenic gases, San Juan Basin, Colorado and New Mexico—Implications for coalbed gas producibility: *American Association of Petroleum Geologists Bulletin*, v. 78, no. 8, p. 1186–1209.
- Shuck, E.L., Davis, T.L., and Benson, R.D., 1996, Multicomponent 3-D characterization of a coalbed methane reservoir: *Geophysics*, v. 61, no. 2, p. 315–330.
- Sikkink, P.G.L., 1987, Lithofacies relationships and depositional environment of the Tertiary Ojo Alamo Sandstone and related strata, San Juan Basin, New Mexico and Colorado, *in* Fassett, J.E., and Rigby, J.K., Jr., eds., *The Cretaceous-Tertiary boundary in the San Juan and Raton Basins, New Mexico and Colorado*: Geological Society of America Special Paper 209, p. 81–104.
- Smith, L.N., 1992, Stratigraphy, sediment dispersal, and paleogeography of the lower Eocene San Jose Formation, San Juan Basin, New Mexico and Colorado, *in* Lucas, S.G., Kues, B.S., Williamson, T.E., and Hunt, A.P., eds., *San Juan Basin IV: New Mexico Geological Society Guidebook*, p. 297–309.
- Snyder, G.T., Riese, W.C., Franks, S., Fehn, U., Pelzmann, W.L., Gorody, A.W., and Moran, J.E., 2003, Origin and history of waters associated with coalbed methane:¹²⁹I, ³⁶Cl, and stable isotope results from the Fruitland Formation, Colorado and New Mexico: *Geochimica et Cosmochimica Acta*, v. 67, no. 23, p. 4529–4544.
- Stach, E., Mackowsky, M. T., Teichmuller, M., Taylor, G.H., Chandra, D., and Teichmuller, R., 1982, *Stach's textbook of coal petrology*, 3d revised and enlarged version: Berlin, Gebruder Borntraeger, 569 p.
- Taylor, D.J., and Huffman, A.C., Jr., 1998, Map showing inferred and mapped basement faults, San Juan Basin and vicinity, New Mexico and Colorado: U.S. Geological Survey Geological Investigations Series I-2641, scale 1:500,000.
- Taylor, D.J., and Huffman, A.C., Jr., 2001, Seismic evaluation study report—Jicarilla Apache Indian Reservation: U.S. Department of Energy Report DE-AI26-98BC15026R10 (CD-ROM).
- Thorn, C.R., Levings, G.W., Craig, S.D., Dam, W.L., and Kernodle, J.M., 1990, Hydrogeology of the Ojo Alamo Sandstone in the San Juan structural basin, New Mexico, Colorado, Arizona, and Utah: U.S. Geological Survey Hydrologic Investigations Atlas 720–B.
- Tissot, B., and Welte, D., 1987, *Petroleum formation and occurrence; a new approach to oil and gas exploration*: Berlin, Springer-Verlag, 521 p.
- Tremain, C.M., Laubach, S.E., and Whitehead, N.H., III, 1994, Fracture (cleat) patterns in Upper Cretaceous Fruitland Formation coal seams, San Juan Basin: New Mexico Bureau of Mines and Mineral Resources Bulletin 146, p. 87–118.
- Williamson, T.E., and Lucas, S.G., 1992, Stratigraphy and mammalian biostratigraphy of the Paleocene Nacimiento Formation, southern San Juan Basin, New Mexico, *in* Lucas, S.G., Kues, B.S., Williamson, T.E., and Hunt, A.P., eds., *San Juan Basin IV: New Mexico Geological Society Guidebook*, p. 265–296.
- Wray, L.L., 2001, Geologic mapping and subsurface well log correlations of the Late Cretaceous Fruitland Formation coal beds and carbonaceous shales—The stratigraphic mapping component of the 3M project, San Juan Basin, La Plata County, Colorado: Colorado Oil and Gas Conservation Commission San Juan Basin Study Report, 15 p.
- Wright Dunbar, R., 2001, Outcrop analysis of the Cretaceous Mesaverde Group—Jicarilla Apache Indian Reservation, New Mexico: U.S. Department of Energy Report DE-AI26-98BC15026R9 (CD-ROM).
- Zeikus, J.G., and Winfrey, M.R., 1976, Temperature limitations of methanogenesis in aquatic sediments: *Applied Environmental Microbiology*, v. 31, p. 99–107.

Appendix A. Assessment results summary for the Fruitland Total Petroleum System, San Juan Basin Province, New Mexico and Colorado.

[MMBO, million barrels of oil; BCFG, billion cubic feet of gas; MMBNGL, million barrels of natural gas liquids. Results shown are fully risked estimates. For gas fields, all liquids are included under the NGL (natural gas liquids) category. F95 denotes a 95 percent chance of at least the amount tabulated. Other fractiles are defined similarly. Fractiles are additive only under the assumption of perfect positive correlation. CBG, coalbed gas. Gray column indicates not assessed or applicable]

Assessment Units (AU)	Field Type	Total Undiscovered Resources											
		Oil (MMBO)				Gas (BCFG)				NGL (MMBNGL)			
		F95	F50	F5	Mean	F95	F50	F5	Mean	F95	F50	F5	Mean
Conventional Oil and Gas Resources													
Tertiary Conventional Gas AU	Gas					25.76	74.40	152.91	79.98	0.23	0.73	1.83	0.84
Continuous Gas Resources													
Fruitland Fairway Coal-Bed Gas AU	CBG					3,081.06	3,937.16	5,031.14	3,981.14	0.00	0.00	0.00	0.00
Basin Fruitland Coal-Bed Gas AU	CBG					17,342.26	19,543.12	22,023.27	19,594.74	0.00	0.00	0.00	0.00
Pictured Cliffs Continuous Gas AU	Gas					3,865.41	5,510.68	7,856.23	5,640.25	9.07	15.95	28.06	16.92
Total						24,288.73	28,990.96	34,910.64	29,216.13	9.07	15.95	28.06	16.92

Appendix B. Input data form used in evaluating the Fruitland Total Petroleum System, Pictured Cliffs Continuous Gas Assessment Unit (50220161), San Juan Basin Province.

**FORSPAN ASSESSMENT MODEL FOR CONTINUOUS
ACCUMULATIONS--BASIC INPUT DATA FORM (NOGA, Version 8, 8-16-02)**

IDENTIFICATION INFORMATION

Assessment Geologist:...	<u>S.M. Condon</u>	Date:	<u>9/23/2002</u>
Region:.....	<u>North America</u>	Number:	<u>5</u>
Province:.....	<u>San Juan Basin</u>	Number:	<u>5022</u>
Total Petroleum System:..	<u>Fruitland</u>	Number:	<u>502201</u>
Assessment Unit:.....	<u>Pictured Cliffs Continuous Gas</u>	Number:	<u>50220161</u>
Based on Data as of:.....	<u>PI/Dwights 2001, Four Corners Geological Society</u>		
Notes from Assessor:.....	<u></u>		

CHARACTERISTICS OF ASSESSMENT UNIT

Assessment-Unit type: Oil (<20,000 cfg/bo) or Gas (≥20,000 cfg/bo) Gas

What is the minimum total recovery per cell?... 0.02 (mmbo for oil A.U.; bcfg for gas A.U.)

Number of tested cells:..... 6809

Number of tested cells with total recovery per cell ≥ minimum: 6352

Established (>24 cells ≥ min.) X Frontier (1-24 cells) Hypothetical (no cells)

Median total recovery per cell (for cells ≥ min.): (mmbo for oil A.U.; bcfg for gas A.U.)

1st 3rd discovered	<u>0.66</u>	2nd 3rd	<u>0.56</u>	3rd 3rd	<u>0.33</u>
--------------------	-------------	---------	-------------	---------	-------------

Assessment-Unit Probabilities:

<u>Attribute</u>	<u>Probability of occurrence (0-1.0)</u>
1. CHARGE: Adequate petroleum charge for an untested cell with total recovery ≥ minimum	<u>1.0</u>
2. ROCKS: Adequate reservoirs, traps, seals for an untested cell with total recovery ≥ minimum.	<u>1.0</u>
3. TIMING: Favorable geologic timing for an untested cell with total recovery ≥ minimum.....	<u>1.0</u>

Assessment-Unit GEOLOGIC Probability (Product of 1, 2, and 3):..... 1.0

4. **ACCESS:** Adequate location for necessary petroleum-related activities for an untested cell with total recovery ≥ minimum 1.0

NO. OF UNTESTED CELLS WITH POTENTIAL FOR ADDITIONS TO RESERVES IN THE NEXT 30 YEARS

- Total assessment-unit area (acres): (uncertainty of a fixed value)
 minimum 4,041,000 median 4,206,000 maximum 4,297,000
- Area per cell of untested cells having potential for additions to reserves in next 30 years (acres):
 (values are inherently variable)
 calculated mean 96 minimum 40 median 90 maximum 200
- Percentage of total assessment-unit area that is untested (%): (uncertainty of a fixed value)
 minimum 76 median 84 maximum 88
- Percentage of untested assessment-unit area that has potential for additions to reserves in next 30 years (%): (a necessary criterion is that total recovery per cell ≥ minimum)
 (uncertainty of a fixed value) minimum 14 median 37 maximum 47

TOTAL RECOVERY PER CELL

Total recovery per cell for untested cells having potential for additions to reserves in next 30 years:

(values are inherently variable)

(mmbo for oil A.U.; bcfg for gas A.U.) minimum 0.02 median 0.25 maximum 7

AVERAGE COPRODUCT RATIOS FOR UNTESTED CELLS, TO ASSESS COPRODUCTS

(uncertainty of fixed but unknown values)

<u>Oil assessment unit:</u>	minimum	median	maximum
Gas/oil ratio (cfg/bo).....	<u> </u>	<u> </u>	<u> </u>
NGL/gas ratio (bnl/mmcfg).....	<u> </u>	<u> </u>	<u> </u>
<u>Gas assessment unit:</u>			
Liquids/gas ratio (bliq/mmcfg).....	<u> 1 </u>	<u> 3 </u>	<u> 5 </u>

SELECTED ANCILLARY DATA FOR UNTESTED CELLS

(values are inherently variable)

<u>Oil assessment unit:</u>	minimum	median	maximum
API gravity of oil (degrees).....	<u> </u>	<u> </u>	<u> </u>
Sulfur content of oil (%).....	<u> </u>	<u> </u>	<u> </u>
Drilling depth (m)	<u> </u>	<u> </u>	<u> </u>
Depth (m) of water (if applicable).....	<u> </u>	<u> </u>	<u> </u>
<u>Gas assessment unit:</u>			
Inert-gas content (%).....	<u> 0.20 </u>	<u> 1.00 </u>	<u> 4.00 </u>
CO ₂ content (%).....	<u> 0.05 </u>	<u> 1.00 </u>	<u> 2.50 </u>
Hydrogen-sulfide content (%).....	<u> 0.00 </u>	<u> 0.00 </u>	<u> 0.00 </u>
Drilling depth (m).....	<u> 530 </u>	<u> 650 </u>	<u> 1360 </u>
Depth (m) of water (if applicable).....	<u> </u>	<u> </u>	<u> </u>
<u>Success ratios:</u>	calculated mean	minimum	median
Future success ratio (%).....	<u> 85 </u>	<u> 75 </u>	<u> 85 </u>
Historic success ratio, tested cells (%).....	<u> 93 </u>		

Appendix C. Input data form used in evaluating the Fruitland Total Petroleum System, Basin Fruitland Coalbed Gas Assessment Unit (50220182), San Juan Basin Province.

**FORSPAN ASSESSMENT MODEL FOR CONTINUOUS
ACCUMULATIONS--BASIC INPUT DATA FORM (NOGA, Version 8, 8-16-02)**

IDENTIFICATION INFORMATION

Assessment Geologist:...	<u>J.L. Ridgley</u>	Date:	<u>9/23/2002</u>
Region:.....	<u>North America</u>	Number:	<u>5</u>
Province:.....	<u>San Juan Basin</u>	Number:	<u>5022</u>
Total Petroleum System:..	<u>Fruitland</u>	Number:	<u>502201</u>
Assessment Unit:.....	<u>Basin Fruitland Coalbed Gas</u>	Number:	<u>50220182</u>
Based on Data as of:.....	<u>PI/Dwights 2001</u>		
Notes from Assessor:.....	<u></u>		

CHARACTERISTICS OF ASSESSMENT UNIT

Assessment-Unit type: Oil (<20,000 cfg/bo) or Gas (≥20,000 cfg/bo) Gas

What is the minimum total recovery per cell?... 0.02 (mmbo for oil A.U.; bcfg for gas A.U.)

Number of tested cells:..... 4102

Number of tested cells with total recovery per cell ≥ minimum: 3690

Established (>24 cells ≥ min.) X Frontier (1-24 cells) Hypothetical (no cells)

Median total recovery per cell (for cells ≥ min.): (mmbo for oil A.U.; bcfg for gas A.U.)

1st 3rd discovered	<u>1</u>	2nd 3rd	<u>1.1</u>	3rd 3rd	<u>0.8</u>
--------------------	----------	---------	------------	---------	------------

Assessment-Unit Probabilities:

<u>Attribute</u>	<u>Probability of occurrence (0-1.0)</u>
1. CHARGE: Adequate petroleum charge for an untested cell with total recovery ≥ minimum	<u>1.0</u>
2. ROCKS: Adequate reservoirs, traps, seals for an untested cell with total recovery ≥ minimum.	<u>1.0</u>
3. TIMING: Favorable geologic timing for an untested cell with total recovery ≥ minimum.....	<u>1.0</u>

Assessment-Unit GEOLOGIC Probability (Product of 1, 2, and 3):..... 1.0

4. **ACCESS:** Adequate location for necessary petroleum-related activities for an untested cell with total recovery ≥ minimum 1.0

NO. OF UNTESTED CELLS WITH POTENTIAL FOR ADDITIONS TO RESERVES IN THE NEXT 30 YEARS

- Total assessment-unit area (acres): (uncertainty of a fixed value)
 minimum 3,825,000 median 3,926,000 maximum 4,027,000
- Area per cell of untested cells having potential for additions to reserves in next 30 years (acres):
 (values are inherently variable)
 calculated mean 107 minimum 20 median 100 maximum 240
- Percentage of total assessment-unit area that is untested (%): (uncertainty of a fixed value)
 minimum 80 median 89 maximum 95
- Percentage of untested assessment-unit area that has potential for additions to reserves in next 30 years (%): (a necessary criterion is that total recovery per cell ≥ minimum)
 (uncertainty of a fixed value) minimum 45 median 55 maximum 60

TOTAL RECOVERY PER CELL

Total recovery per cell for untested cells having potential for additions to reserves in next 30 years:

(values are inherently variable)

(mmbo for oil A.U.; bcfg for gas A.U.) minimum 0.02 median 0.6 maximum 20

AVERAGE COPRODUCT RATIOS FOR UNTESTED CELLS, TO ASSESS COPRODUCTS

(uncertainty of fixed but unknown values)

<u>Oil assessment unit:</u>	minimum	median	maximum
Gas/oil ratio (cfg/bo).....	<u> </u>	<u> </u>	<u> </u>
NGL/gas ratio (bnl/mmcfg).....	<u> </u>	<u> </u>	<u> </u>

<u>Gas assessment unit:</u>	minimum	median	maximum
Liquids/gas ratio (bliq/mmcfg).....	<u>0</u>	<u>0</u>	<u>0</u>

SELECTED ANCILLARY DATA FOR UNTESTED CELLS

(values are inherently variable)

<u>Oil assessment unit:</u>	minimum	median	maximum
API gravity of oil (degrees).....	<u> </u>	<u> </u>	<u> </u>
Sulfur content of oil (%).....	<u> </u>	<u> </u>	<u> </u>
Drilling depth (m)	<u> </u>	<u> </u>	<u> </u>
Depth (m) of water (if applicable).....	<u> </u>	<u> </u>	<u> </u>

<u>Gas assessment unit:</u>	minimum	median	maximum
Inert-gas content (%).....	<u>1.00</u>	<u>3.00</u>	<u>18.00</u>
CO ₂ content (%).....	<u>0.00</u>	<u>0.20</u>	<u>3.00</u>
Hydrogen-sulfide content (%).....	<u>0.00</u>	<u>0.00</u>	<u>0.00</u>
Drilling depth (m).....	<u>70</u>	<u>750</u>	<u>1200</u>
Depth (m) of water (if applicable).....	<u> </u>	<u> </u>	<u> </u>

<u>Success ratios:</u>	calculated mean	minimum	median	maximum
Future success ratio (%).....	<u>80</u>	<u>70</u>	<u>80</u>	<u>90</u>

Historic success ratio, tested cells (%). 90

Appendix D. Input data form used in evaluating the Fruitland Total Petroleum System, Basin Fruitland Fairway Coalbed Gas Assessment Unit (50220181), San Juan Basin Province.

FORSPAN ASSESSMENT MODEL FOR CONTINUOUS ACCUMULATIONS--BASIC INPUT DATA FORM (NOGA, Version 8, 8-16-02)

IDENTIFICATION INFORMATION

Assessment Geologist:...	<u>J.L. Ridgley</u>	Date:	<u>9/23/2002</u>
Region:.....	<u>North America</u>	Number:	<u>5</u>
Province:.....	<u>San Juan Basin</u>	Number:	<u>5022</u>
Total Petroleum System:..	<u>Fruitland</u>	Number:	<u>502201</u>
Assessment Unit:.....	<u>Fruitland Fairway Coalbed Gas</u>	Number:	<u>50220181</u>
Based on Data as of:.....	<u>PI/Dwights 2001</u>		
Notes from Assessor:.....	<u></u>		

CHARACTERISTICS OF ASSESSMENT UNIT

Assessment-Unit type: Oil (<20,000 cfg/bo) or Gas (≥20,000 cfg/bo) Gas

What is the minimum total recovery per cell?... 0.02 (mmbo for oil A.U.; bcfg for gas A.U.)

Number of tested cells:..... 934

Number of tested cells with total recovery per cell ≥ minimum: 890

Established (>24 cells ≥ min.) X Frontier (1-24 cells) Hypothetical (no cells)

Median total recovery per cell (for cells ≥ min.): (mmbo for oil A.U.; bcfg for gas A.U.)

1st 3rd discovered	<u>9</u>	2nd 3rd	<u>13</u>	3rd 3rd	<u>8</u>
--------------------	----------	---------	-----------	---------	----------

Assessment-Unit Probabilities:

<u>Attribute</u>	<u>Probability of occurrence (0-1.0)</u>
1. CHARGE: Adequate petroleum charge for an untested cell with total recovery ≥ minimum	<u>1.0</u>
2. ROCKS: Adequate reservoirs, traps, seals for an untested cell with total recovery ≥ minimum.	<u>1.0</u>
3. TIMING: Favorable geologic timing for an untested cell with total recovery ≥ minimum.....	<u>1.0</u>

Assessment-Unit GEOLOGIC Probability (Product of 1, 2, and 3):..... 1.0

4. **ACCESS:** Adequate location for necessary petroleum-related activities for an untested cell with total recovery ≥ minimum 1.0

NO. OF UNTESTED CELLS WITH POTENTIAL FOR ADDITIONS TO RESERVES IN THE NEXT 30 YEARS

- Total assessment-unit area (acres): (uncertainty of a fixed value)

minimum	<u>227,000</u>	median	<u>227,000</u>	maximum	<u>227,000</u>
---------	----------------	--------	----------------	---------	----------------
- Area per cell of untested cells having potential for additions to reserves in next 30 years (acres): (values are inherently variable)

calculated mean	<u>163</u>	minimum	<u>20</u>	median	<u>160</u>	maximum	<u>320</u>
-----------------	------------	---------	-----------	--------	------------	---------	------------
- Percentage of total assessment-unit area that is untested (%): (uncertainty of a fixed value)

minimum	<u>21</u>	median	<u>33</u>	maximum	<u>45</u>
---------	-----------	--------	-----------	---------	-----------
- Percentage of untested assessment-unit area that has potential for additions to reserves in next 30 years (%): (a necessary criterion is that total recovery per cell ≥ minimum) (uncertainty of a fixed value)

minimum	<u>93</u>	median	<u>95</u>	maximum	<u>97</u>
---------	-----------	--------	-----------	---------	-----------

TOTAL RECOVERY PER CELL

Total recovery per cell for untested cells having potential for additions to reserves in next 30 years:

(values are inherently variable)

(mmbbl for oil A.U.; bcfg for gas A.U.) minimum 0.02 median 8 maximum 40

AVERAGE COPRODUCT RATIOS FOR UNTESTED CELLS, TO ASSESS COPRODUCTS

(uncertainty of fixed but unknown values)

<u>Oil assessment unit:</u>	minimum	median	maximum
Gas/oil ratio (cfg/bo).....	<u> </u>	<u> </u>	<u> </u>
NGL/gas ratio (bngl/mmcfg).....	<u> </u>	<u> </u>	<u> </u>
<u>Gas assessment unit:</u>			
Liquids/gas ratio (bliq/mmcfg).....	<u>0</u>	<u>0</u>	<u>0</u>

SELECTED ANCILLARY DATA FOR UNTESTED CELLS

(values are inherently variable)

<u>Oil assessment unit:</u>	minimum	median	maximum
API gravity of oil (degrees).....	<u> </u>	<u> </u>	<u> </u>
Sulfur content of oil (%).....	<u> </u>	<u> </u>	<u> </u>
Drilling depth (m)	<u> </u>	<u> </u>	<u> </u>
Depth (m) of water (if applicable).....	<u> </u>	<u> </u>	<u> </u>
<u>Gas assessment unit:</u>			
Inert-gas content (%).....	<u>0.00</u>	<u>2.40</u>	<u>25.00</u>
CO ₂ content (%).....	<u>0.00</u>	<u>1.00</u>	<u>15.00</u>
Hydrogen-sulfide content (%).....	<u>0.00</u>	<u>0.00</u>	<u>0.00</u>
Drilling depth (m).....	<u>300</u>	<u>750</u>	<u>1200</u>
Depth (m) of water (if applicable).....	<u> </u>	<u> </u>	<u> </u>
<u>Success ratios:</u>			
Future success ratio (%).....	calculated mean <u>95</u>	minimum <u>93</u>	median <u>95</u>
			maximum <u>97</u>
Historic success ratio, tested cells (%) <u>95</u>			

Appendix E. Input data form used in evaluating the Fruitland Total Petroleum System, Tertiary Conventional Gas Assessment Unit (50220101), San Juan Basin Province.

**SEVENTH APPROXIMATION
DATA FORM FOR CONVENTIONAL ASSESSMENT UNITS (NOGA, Version 5, 6-30-01)**

IDENTIFICATION INFORMATION

Assessment Geologist:.....	<u>S.M. Condon</u>	Date:	<u>9/23/2002</u>
Region:.....	<u>North America</u>	Number:	<u>5</u>
Province:.....	<u>San Juan Basin</u>	Number:	<u>5022</u>
Total Petroleum System:.....	<u>Fruitland</u>	Number:	<u>502201</u>
Assessment Unit:.....	<u>Tertiary Conventional Gas</u>	Number:	<u>50220101</u>
Based on Data as of:.....	<u>PI/Dwights 2001, NRG 2001 (data current through 1999)</u>		
Notes from Assessor:.....	<u></u>		

CHARACTERISTICS OF ASSESSMENT UNIT

Oil (<20,000 cfg/bo overall) or Gas (≥20,000 cfg/bo overall):... Gas

What is the minimum accumulation size?..... 0.5 mmmboe grown
(the smallest accumulation that has potential to be added to reserves in the next 30 years)

No. of discovered accumulations exceeding minimum size:..... Oil: 0 Gas: 1
Established (>13 accums.) Frontier (1-13 accums.) X Hypothetical (no accums.)

Median size (grown) of discovered oil accumulation (mmbo):
1st 3rd 2nd 3rd 3rd 3rd

Median size (grown) of discovered gas accumulations (bcfg):
1st 3rd 2nd 3rd 3rd 3rd

Assessment-Unit Probabilities:

<u>Attribute</u>	<u>Probability of occurrence (0-1.0)</u>
1. CHARGE: Adequate petroleum charge for an undiscovered accum. ≥ minimum size.....	<u>1.0</u>
2. ROCKS: Adequate reservoirs, traps, and seals for an undiscovered accum. ≥ minimum size.....	<u>1.0</u>
3. TIMING OF GEOLOGIC EVENTS: Favorable timing for an undiscovered accum. ≥ minimum size	<u>1.0</u>

Assessment-Unit GEOLOGIC Probability (Product of 1, 2, and 3):..... 1.0

4. **ACCESSIBILITY:** Adequate location to allow exploration for an undiscovered accumulation ≥ minimum size..... 1.0

UNDISCOVERED ACCUMULATIONS

No. of Undiscovered Accumulations: How many undiscovered accums. exist that are ≥ min. size?:
(uncertainty of fixed but unknown values)

Oil Accumulations:.....min. no. (>0)	<u>0</u>	median no.	<u>0</u>	max. no.	<u>0</u>
Gas Accumulations:.....min. no. (>0)	<u>1</u>	median no.	<u>5</u>	max. no.	<u>10</u>

Sizes of Undiscovered Accumulations: What are the sizes (**grown**) of the above accums?:
(variations in the sizes of undiscovered accumulations)

Oil in Oil Accumulations (mmbo):.....min. size	<u></u>	median size	<u></u>	max. size	<u></u>
Gas in Gas Accumulations (bcfg):.....min. size	<u>3</u>	median size	<u>12</u>	max. size	<u>120</u>

AVERAGE RATIOS FOR UNDISCOVERED ACCUMS., TO ASSESS COPRODUCTS

(uncertainty of fixed but unknown values)

<u>Oil Accumulations:</u>	minimum	median	maximum
Gas/oil ratio (cfg/bo).....	_____	_____	_____
NGL/gas ratio (bngl/mmcfg).....	_____	_____	_____
<u>Gas Accumulations:</u>	minimum	median	maximum
Liquids/gas ratio (bliq/mmcfg).....	5	10	20
Oil/gas ratio (bo/mmcfg).....	_____	_____	_____

SELECTED ANCILLARY DATA FOR UNDISCOVERED ACCUMULATIONS

(variations in the properties of undiscovered accumulations)

<u>Oil Accumulations:</u>	minimum	median	maximum
API gravity (degrees).....	_____	_____	_____
Sulfur content of oil (%).....	_____	_____	_____
Drilling Depth (m)	_____	_____	_____
Depth (m) of water (if applicable).....	_____	_____	_____
<u>Gas Accumulations:</u>	minimum	median	maximum
Inert gas content (%).....	0.1	2	4
CO ₂ content (%).....	0.1	0.5	1
Hydrogen-sulfide content (%).....	0.1	0.7	2
Drilling Depth (m).....	80	510	1020
Depth (m) of water (if applicable).....	_____	_____	_____



Click here to return to
Volume Title Page

Tabular Data and Graphical Images in Support of the U.S. Geological Survey National Oil and Gas Assessment—San Juan Basin Province (5022)

By T.R. Klett and P.A. Le



Click here to return to
Volume Title Page

Chapter 7 of 7

Total Petroleum Systems and Geologic Assessment of Undiscovered Oil and Gas Resources in the San Juan Basin Province, Exclusive of Paleozoic Rocks, New Mexico and Colorado

Compiled by U.S. Geological Survey San Juan Basin Assessment Team

Digital Data Series 69–F

U.S. Department of the Interior
U.S. Geological Survey

U.S. Department of the Interior
KEN SALAZAR, Secretary

U.S. Geological Survey
Marcia K. McNutt, Director

U.S. Geological Survey, Reston, Virginia 2013

For product and ordering information:

World Wide Web: <http://www.usgs.gov/pubprod>

Telephone: 1-888-ASK-USGS

For more information on the USGS—the Federal source for science about the Earth,
its natural and living resources, natural hazards, and the environment:

World Wide Web: <http://www.usgs.gov>

Telephone: 1-888-ASK-USGS

Suggested citation:

Klett, T.R., and Le, P.A., 2013, Tabular data and graphical images in support of the U.S. Geological Survey National oil and gas assessment—San Juan Basin Province (5022), chap. 7 of U.S. Geological Survey San Juan Basin Assessment Team, Total petroleum systems and geologic assessment of undiscovered oil and gas resources in the San Juan Basin Province, exclusive of Paleozoic rocks, New Mexico and Colorado: U.S. Geological Survey Digital Data Series 69-F, p. 1–17.

Any use of trade, product, or firm names is for descriptive purposes only and does not imply endorsement by the U.S. Government.

Although this report is in the public domain, permission must be secured from the individual copyright owners to reproduce any copyrighted material contained within this report.

Contents

Introduction.....	1
Disclaimers	1
Data Sources.....	1
Data Overview.....	1
Numeric Codes.....	2
Tabular Data.....	3
Summary Tables.....	16
Graphical Data.....	16
File List.....	17
References Cited.....	17

Tabular Data and Graphical Images in Support of the U.S. Geological Survey National Oil and Gas Assessment—San Juan Basin Province (5022)

By T.R. Klett and P.A. Le

Introduction

This chapter describes data used in support of the process being applied by the U.S. Geological Survey (USGS) National Oil and Gas Assessment (NOGA) project. Digital tabular data used in this report and archival data that permit the user to perform further analyses are available elsewhere on this CD-ROM. Computers and software may import the data without transcription from the Portable Document Format files (.pdf files) of the text by the reader. Because of the number and variety of platforms and software available, graphical images are provided as .pdf files and tabular data are provided in a raw form as tab-delimited text files (.tab files).

Disclaimers

This publication was prepared by an agency of the United States Government. Reference therein to any specific commercial product, process, or service by trade name, trademark, manufacturer, or otherwise does not necessarily constitute or imply its endorsement, recommendation, or favoring by the United States Government or any agency thereof. The act of distribution shall not constitute any such warranty, and no responsibility is assumed by the USGS in the use of these data or related materials.

Data Sources

Crude oil and natural gas production data (including all volumetric and descriptive data such as cumulative production, remaining reserves, known recoverable volumes, major producing reservoirs, and petroleum type) and historical data (including field-discovery dates, well-completion dates, exploration objectives, and well depths) for fields, reservoirs, and wells are derived from commercial databases leased and purchased by the USGS, including

- PI/Dwights Plus US Production Data (IHS Energy Group, 2001a),
- PI/Dwights Plus US Well Data (IHS Energy Group, 2001b), and
- NRG Associates, Inc., Significant Oil and Gas Fields of the United States (NRG Associates, 2001).

Data from these databases are subject to proprietary constraints, but derivative representations in the form of graphs and summary statistics are allowed to be published and were prepared for each assessment unit. The USGS, however, cannot verify the accuracy, completeness, or currency of data that are reported in commercial databases. To supplement commercial databases, additional data are obtained, where available, from operators, other Federal and State agencies, or from published geological reports.

The PI/Dwights Plus US Production database provides production data for wells, leases, or production units. The PI/Dwights Plus US Well database provides individual well data (including data for dry holes), including well identification, locations, initial and final classifications, completion dates, and information on penetrated formations. The NRG Associates, Inc., Significant Oil and Gas Fields of the United States database provides volumetric and production data for fields and reservoirs.

Data Overview

This report provides various data files supporting the NOGA project. The files contain data that are the source for the various graphs, data tables, and summary tables used in the assessment process. Tabular data are provided as tab-delimited text files (.tab files), usable in spreadsheet and database software. Graphical and summary data are provided as portable document format files (.pdf files). File name conventions are as follows:

Data tables	Summary tables	Graphs
eco####.tab	c#####.pdf	em#####.pdf
fed####.tab	d#####.pdf	fp#####.pdf
inf####.tab	u#####.pdf	g#####.pdf
ins####.tab		k#####.pdf
kvof####.tab		
own####.tab		
sta####.tab		
vol####.tab		

For identification purposes, the four symbols “####” represent the province code. Files with these numbers contain data for the entire province. Files having the six symbols “#####” (which represents the last six digits of the assessment-unit code) contain data only for that assessment unit.

Numeric Codes

A hierarchical numeric code identifies each region, province, total petroleum system, and assessment unit. The criteria for assigning codes are uniform throughout the NOGA project and throughout all resulting publications. The numeric codes used in this study are listed below.

The assessment-unit portion of the code (*last* two digits) defines the type of assessment unit. Numbers from 01 to 59 represent conventional assessment units, 61 to 79 represent continuous oil or gas assessment units, and 81 to 99 represent coal-bed gas assessment units. No total petroleum system or assessment unit codes end with 0, for example 502200, 50220160, or 50220180.

To maintain the conventional labeling of files (8-character name and 3-character extension), some file names that contain assessment-unit numbers do not include the first two digits. For example, a summary table that contains input data for the Tertiary Conventional Gas Assessment Unit is labeled “c220101.pdf.”

Unit	Name	Code
Region	North America	5
Province	San Juan Basin	5022
Total Petroleum Systems	Fruitland	502201
	Lewis Shale	502202
	Mancos-Menefee Composite	502203
	Todilto	502204
Assessment Units	Tertiary Conventional Gas	50220101
	Pictured Cliffs Continuous Gas	50220161
	Fruitland Fairway Coalbed Gas	50220181
	Basin Fruitland Coalbed Gas	50220182
	Lewis Continuous Gas	50220261
	Mesaverde Updip Oil	50220301
	Gallup Sandstone Conventional Oil and Gas	50220302
	Mancos Sandstones Conventional Oil	50220303
	Dakota-Greenhorn Conventional Oil and Gas	50220304
	Mesaverde Central-Basin Continuous Gas	50220361
	Mancos Sandstones Continuous Gas	50220362
	Dakota-Greenhorn Continuous Gas	50220363
	Menefee Coalbed Gas	50220381
	Entrada Sandstone Conventional Oil	50220401

Tabular Data

The eco####.tab, fed####.tab, own####.tab, and sta####.tab files contain volume-percent data of undiscovered petroleum allocated to ecosystem regions, Federal lands, general land-ownership parcels, and States. Blank cells represent no data.

The eco####.tab table contains 59 columns. The sum of the percentages should equal those for the total area (excluding offshore) in the own####.tab file. Data columns for these files are as follows:

1. Code—assessment-unit code number.
2. Name—assessment-unit name.
3. Area km²—area of the assessment unit in square kilometers.
4. Eco 1—name of first ecosystem that occupies all or part of the assessment-unit area.
5. E1 Area %—percentage of assessment-unit area that is occupied by ecosystem 1.
6. E1 Oil %—estimated percentage of undiscovered oil volume allocated to ecosystem 1.
7. E1 Gas %—estimated percentage of undiscovered gas volume allocated to ecosystem 1.
8. Eco 2—name of second ecosystem that occupies part of the assessment-unit area.
9. E2 Area %—percentage of assessment-unit area that is occupied by ecosystem 2.
10. E2 Oil %—estimated percentage of undiscovered oil volume allocated to ecosystem 2.
11. E2 Gas %—estimated percentage of undiscovered gas volume allocated to ecosystem 2.
12. Eco 3—name of third ecosystem that occupies part of the assessment-unit area.
13. E3 Area %—percentage of assessment-unit area that is occupied by ecosystem 3.
14. E3 Oil %—estimated percentage of undiscovered oil volume allocated to ecosystem 3.
15. E3 Gas %—estimated percentage of undiscovered gas volume allocated to ecosystem 3.
16. Eco 4—name of fourth ecosystem that occupies part of the assessment-unit area.
17. E4 Area %—percentage of assessment-unit area that is occupied by ecosystem 4.
18. E4 Oil %—estimated percentage of undiscovered oil volume allocated to ecosystem 4.
19. E4 Gas %—estimated percentage of undiscovered gas volume allocated to ecosystem 4.
20. Eco 5—name of fifth ecosystem that occupies part of the assessment-unit area.
21. E5 Area %—percentage of assessment-unit area that is occupied by ecosystem 5.
22. E5 Oil %—estimated percentage of undiscovered oil volume allocated to ecosystem 5.
23. E5 Gas %—estimated percentage of undiscovered gas volume allocated to ecosystem 5.
24. Eco 6—name of sixth ecosystem that occupies part of the assessment-unit area.
25. E6 Area %—percentage of assessment-unit area that is occupied by ecosystem 6.
26. E6 Oil %—estimated percentage of undiscovered oil volume allocated to ecosystem 6.
27. E6 Gas %—estimated percentage of undiscovered gas volume allocated to ecosystem 6.
28. Eco 7—name of seventh ecosystem that occupies part of the assessment-unit area.
29. E7 Area %—percentage of assessment-unit area that is occupied by ecosystem 7.
30. E7 Oil %—estimated percentage of undiscovered oil volume allocated to ecosystem 7.
31. E7 Gas %—estimated percentage of undiscovered gas volume allocated to ecosystem 7.
32. Eco 8—name of eighth ecosystem that occupies part of the assessment-unit area.
33. E8 Area %—percentage of assessment-unit area that is occupied by ecosystem 8.
34. E8 Oil %—estimated percentage of undiscovered oil volume allocated to ecosystem 8.
35. E8 Gas %—estimated percentage of undiscovered gas volume allocated to ecosystem 8.
36. Eco 9—name of ninth ecosystem that occupies part of the assessment-unit area.
37. E9 Area %—percentage of assessment-unit area that is occupied by ecosystem 9.
38. E9 Oil %—estimated percentage of undiscovered oil volume allocated to ecosystem 9.
39. E9 Gas %—estimated percentage of undiscovered gas volume allocated to ecosystem 9.
40. Eco 10—name of tenth ecosystem that occupies part of the assessment-unit area.
41. E10 Area %—percentage of assessment-unit area that is occupied by ecosystem 10.
42. E10 Oil %—estimated percentage of undiscovered oil volume allocated to ecosystem 10.
43. E10 Gas %—estimated percentage of undiscovered gas volume allocated to ecosystem 10.
44. Eco 11—name of eleventh ecosystem that occupies part of the assessment-unit area.
45. E11 Area %—percentage of assessment-unit area that is occupied by ecosystem 11.

4 Total Petroleum Systems and Geologic Assessment of Undiscovered Oil and Gas Resources in the San Juan Basin Province

46. E11 Oil %—estimated percentage of undiscovered oil volume allocated to ecosystem 11.
47. E11 Gas %—estimated percentage of undiscovered gas volume allocated to ecosystem 11.
48. Eco 12—name of twelfth ecosystem that occupies part of the assessment-unit area.
49. E12 Area %—percentage of assessment-unit area that is occupied by ecosystem 12.
50. E12 Oil %—estimated percentage of undiscovered oil volume allocated to ecosystem 12.
51. E12 Gas %—estimated percentage of undiscovered gas volume allocated to ecosystem 12.
52. Eco 13—name of thirteenth ecosystem that occupies part of the assessment-unit area.
53. E13 Area %—percentage of assessment-unit area that is occupied by ecosystem 13.
54. E13 Oil %—estimated percentage of undiscovered oil volume allocated to ecosystem 13.
55. E13 Gas %—estimated percentage of undiscovered gas volume allocated to ecosystem 13.
56. Eco 14—name of fourteenth ecosystem that occupies part of the assessment-unit area.
57. E14 Area %—percentage of assessment-unit area that is occupied by ecosystem 14.
58. E14 Oil %—estimated percentage of undiscovered oil volume allocated to ecosystem 14.
59. E14 Gas %—estimated percentage of undiscovered gas volume allocated to ecosystem 14.
10. BLMW Oil %—estimated percentage of undiscovered oil volume allocated to Bureau of Land Management Wilderness Areas.
11. BLMW Gas %—estimated percentage of undiscovered gas volume allocated to Bureau of Land Management Wilderness Areas.
12. BLMR—“BLM Roadless Areas (BLMR),” name of Federal land that occupies all or part of the assessment-unit area.
13. BLMR Area %—percentage of assessment-unit area that is occupied by Bureau of Land Management Roadless Areas.
14. BLMR Oil %—estimated percentage of undiscovered oil volume allocated to Bureau of Land Management Roadless Areas.
15. BLMR Gas %—estimated percentage of undiscovered gas volume allocated to Bureau of Land Management Roadless Areas.
16. NPS—“National Park Service (NPS),” name of Federal land that occupies all or part of the assessment-unit area.
17. NPS Area %—percentage of assessment-unit area that is occupied by National Park Service lands.
18. NPS Oil %—estimated percentage of undiscovered oil volume allocated to National Park Service lands.
19. NPS Gas %—estimated percentage of undiscovered gas volume allocated to National Park Service lands.
20. NPSW—“NPS Wilderness Areas (NPSW),” name of Federal land that occupies all or part of the assessment-unit area.

The fed####.tab table contains 83 columns. The sum of the percentages should equal those for Federal lands in the own####.tab file. Data columns for these files are as follows:

1. Code—assessment-unit code number.
2. Name—assessment-unit name.
3. Area km²—area of the assessment unit in square kilometers.
4. BLM—“Bureau of Land Management (BLM),” name of Federal land that occupies all or part of the assessment-unit area.
5. BLM Area %—percentage of assessment-unit area that is occupied by Bureau of Land Management lands.
6. BLM Oil %—estimated percentage of undiscovered oil volume allocated to Bureau of Land Management lands.
7. BLM Gas %—estimated percentage of undiscovered gas volume allocated to Bureau of Land Management lands.
8. BLMW—“BLM Wilderness Areas (BLMW),” name of Federal land that occupies all or part of the assessment-unit area.
9. BLMW Area %—percentage of assessment-unit area that is occupied by Bureau of Land Management Wilderness Areas.
21. NPSW Area %—percentage of assessment-unit area that is occupied by National Park Service Wilderness Areas.
22. NPSW Oil %—estimated percentage of undiscovered oil volume allocated to National Park Service Wilderness Areas.
23. NPSW Gas %—estimated percentage of undiscovered gas volume allocated to National Park Service Wilderness Areas.
24. NPSP—“NPS Withdrawals (NPSP),” name of Federal land that occupies all or part of the assessment-unit area.
25. NPSP Area %—percentage of assessment-unit area that is occupied by National Park Service Withdrawals.
26. NPSP Oil %—estimated percentage of undiscovered oil volume allocated to National Park Service Withdrawals.
27. NPSP Gas %—estimated percentage of undiscovered gas volume allocated to National Park Service Withdrawals.
28. FS—“Forest Service (FS),” name of Federal land that occupies all or part of the assessment-unit area.
29. FS Area %—percentage of assessment-unit area that is occupied by USDA Forest Service lands.
30. FS Oil %—estimated percentage of undiscovered oil volume allocated to USDA Forest Service lands.

31. FS Gas %—estimated percentage of undiscovered gas volume allocated to USDA Forest Service lands.
32. FSW—“FS Wilderness Areas (FSW),” name of Federal land that occupies all or part of the assessment-unit area.
33. FSW Area %—percentage of assessment-unit area that is occupied by USDA Forest Service Wilderness Areas.
34. FSW Oil %—estimated percentage of undiscovered oil volume allocated to USDA Forest Service Wilderness Areas.
35. FSW Gas %—estimated percentage of undiscovered gas volume allocated to USDA Forest Service Wilderness Areas.
36. FSR—“FS Roadless Areas (FSR),” name of Federal land that occupies all or part of the assessment-unit area.
37. FSR Area %—percentage of assessment-unit area that is occupied by USDA Forest Service Roadless Areas.
38. FSR Oil %—estimated percentage of undiscovered oil volume allocated to USDA Forest Service Roadless Areas.
39. FSR Gas %—estimated percentage of undiscovered gas volume allocated to USDA Forest Service Roadless Areas.
40. FSP—“FS Protected Withdrawals (FSP),” name of Federal land that occupies all or part of the assessment-unit area.
41. FSP Area %—percentage of assessment-unit area that is occupied by USDA Forest Service Protected Withdrawals.
42. FSP Oil %—estimated percentage of undiscovered oil volume allocated to USDA Forest Service Protected Withdrawals.
43. FSP Gas %—estimated percentage of undiscovered gas volume allocated to USDA Forest Service Protected Withdrawals.
44. FWS—“U.S. Fish and Wildlife Service (USFWS),” name of Federal land that occupies all or part of the assessment-unit area.
45. FWS Area %—percentage of assessment-unit area that is occupied by U.S. Fish and Wildlife Service lands.
46. FWS Oil %—estimated percentage of undiscovered oil volume allocated to U.S. Fish and Wildlife Service lands.
47. FWS Gas %—estimated percentage of undiscovered gas volume allocated to U.S. Fish and Wildlife Service lands.
48. FWSW—“USFWS Wilderness Areas (USFWSW),” name of Federal land that occupies all or part of the assessment-unit area.
49. FWSW Area %—percentage of assessment-unit area that is occupied by U.S. Fish and Wildlife Service Wilderness Areas.
50. FWSW Oil %—estimated percentage of undiscovered oil volume allocated to U.S. Fish and Wildlife Service Wilderness Areas.
51. FWSW Gas %—estimated percentage of undiscovered gas volume allocated to U.S. Fish and Wildlife Service Wilderness Areas.
52. FWSP—“USFWS Protected Withdrawals (USFWSP),” name of Federal land that occupies all or part of the assessment-unit area.
53. FWSP Area %—percentage of assessment-unit area that is occupied by U.S. Fish and Wildlife Service Protected Withdrawals.
54. FWSP Oil %—estimated percentage of undiscovered oil volume allocated to U.S. Fish and Wildlife Service Protected Withdrawals.
55. FWSP Gas %—estimated percentage of undiscovered gas volume allocated to U.S. Fish and Wildlife Service Protected Withdrawals.
56. WS—“Wilderness Study Areas (WS),” name of Federal land that occupies all or part of the assessment-unit area.
57. WS Area %—percentage of assessment-unit area that is occupied by Wilderness Study Areas.
58. WS Oil %—estimated percentage of undiscovered oil volume allocated to Wilderness Study Areas.
59. WS Gas %—estimated percentage of undiscovered gas volume allocated to Wilderness Study Areas.
60. DOE—“Department of Energy (DOE),” name of Federal land that occupies all or part of the assessment-unit area.
61. DOE Area %—percentage of assessment-unit area that is occupied by Department of Energy lands.
62. DOE Oil %—estimated percentage of undiscovered oil volume allocated to Department of Energy lands.
63. DOE Gas %—estimated percentage of undiscovered gas volume allocated to Department of Energy lands.
64. DOD—“Department of Defense (DOD),” name of Federal land that occupies all or part of the assessment-unit area.
65. DOD Area %—percentage of assessment-unit area that is occupied by Department of Defense lands.
66. DOD Oil %—estimated percentage of undiscovered oil volume allocated to Department of Defense lands.
67. DOD Gas %—estimated percentage of undiscovered gas volume allocated to Department of Defense lands.
68. BOR—“Bureau of Reclamation (BOR),” name of Federal land that occupies all or part of the assessment-unit area.
69. BOR Area %—percentage of assessment-unit area that is occupied by Bureau of Reclamation lands.
70. BOR Oil %—estimated percentage of undiscovered oil volume allocated to Bureau of Reclamation lands.
71. BOR Gas %—estimated percentage of undiscovered gas volume allocated to Bureau of Reclamation lands.
72. TVA—“Tennessee Valley Authority (TVA),” name of Federal land that occupies all or part of the assessment-unit area.

6 Total Petroleum Systems and Geologic Assessment of Undiscovered Oil and Gas Resources in the San Juan Basin Province

73. TVA Area %—percentage of assessment-unit area that is occupied by Tennessee Valley Authority lands.
74. TVA Oil %—estimated percentage of undiscovered oil volume allocated to Tennessee Valley Authority lands.
75. TVA Gas %—estimated percentage of undiscovered gas volume allocated to Tennessee Valley Authority lands.
76. Other—“Other Federal,” other unspecified Federal lands that occupy all part of the assessment-unit area.
77. Oth Area %—percentage of assessment-unit area that is occupied by other unspecified Federal lands.
78. Oth Oil %—estimated percentage of undiscovered oil volume allocated to other unspecified Federal lands.
79. Oth Gas %—estimated percentage of undiscovered gas volume allocated to other unspecified Federal lands.
80. Fed 20—name of additional specified Federal lands that occupy all or part of the assessment-unit area.
81. F20 Area %—percentage of assessment-unit area that is occupied by additional specified Federal lands.
82. F20 Oil %—estimated percentage of undiscovered oil volume allocated to additional specified Federal lands.
83. F20 Gas %—estimated percentage of undiscovered gas volume allocated to additional specified Federal lands.
14. Tri Oil %—estimated percentage of undiscovered oil volume allocated to tribal lands.
15. Tri Gas %—estimated percentage of undiscovered gas volume allocated to tribal lands.
16. Oth—name of other unspecified lands or offshore areas that occupy all or part of the assessment-unit area.
17. Oth Area %—percentage of assessment-unit area that is occupied by other unspecified lands or offshore areas.
18. Oth Oil %—estimated percentage of undiscovered oil volume allocated to other unspecified lands or offshore areas.
19. Oth Gas %—estimated percentage of undiscovered gas volume allocated to other unspecified lands or offshore areas.
20. State 1—name of first State for which State-owned lands or waters occupy all or part of the assessment-unit area.
21. S1 Area %—percentage of assessment-unit area that is occupied by State 1-owned lands or waters.
22. S1 Oil %—estimated percentage of undiscovered oil volume allocated to State 1-owned lands or waters.
23. S1 Gas %—estimated percentage of undiscovered gas volume allocated to State 1-owned lands or waters.
24. State 2—name of second State for which State-owned lands or waters occupy all or part of the assessment-unit area.

The own####.tab table contains 59 columns. The sum of the percentages should equal 100. Data columns for these files are as follows:

1. Code—assessment-unit code number.
2. Name—assessment-unit name.
3. Area km²—area of the assessment unit in square kilometers.
4. Fed—“Federal Lands,” all Federal lands that occupy all or part of the assessment-unit area.
5. Fed Area %—percentage of assessment-unit area that is occupied by Federal lands.
6. Fed Oil %—estimated percentage of undiscovered oil volume allocated to Federal lands.
7. Fed Gas %—estimated percentage of undiscovered gas volume allocated to Federal lands.
8. Pri—“Private Lands,” all private lands that occupy all or part of the assessment-unit area.
9. Pri Area %—percentage of assessment-unit area that is occupied by private lands.
10. Pri Oil %—estimated percentage of undiscovered oil volume allocated to private lands.
11. Pri Gas %—estimated percentage of undiscovered gas volume allocated to private lands.
12. Tri—“Tribal Lands,” all tribal lands that occupy all or part of the assessment-unit area.
13. Tri Area %—percentage of assessment-unit area that is occupied by tribal lands.
25. S2 Area %—percentage of assessment-unit area that is occupied by State 2-owned lands or waters.
26. S2 Oil %—estimated percentage of undiscovered oil volume allocated to State 2-owned lands or waters.
27. S2 Gas %—estimated percentage of undiscovered gas volume allocated to State 2-owned lands or waters.
28. State 3—name of third State for which State-owned lands or waters occupy all or part of the assessment-unit area.
29. S3 Area %—percentage of assessment-unit area that is occupied by State 3-owned lands or waters.
30. S3 Oil %—estimated percentage of undiscovered oil volume allocated to State 3-owned lands or waters.
31. S3 Gas %—estimated percentage of undiscovered gas volume allocated to State 3-owned lands or waters.
32. State 4—name of fourth State for which State-owned lands or waters occupy all or part of the assessment-unit area.
33. S4 Area %—percentage of assessment-unit area that is occupied by State 4-owned lands or waters.
34. S4 Oil %—estimated percentage of undiscovered oil volume allocated to State 4-owned lands or waters.
35. S4 Gas %—estimated percentage of undiscovered gas volume allocated to State 4-owned lands or waters.
36. State 5—name of fifth State for which State-owned lands or waters occupy all or part of the assessment-unit area.
37. S5 Area %—percentage of assessment-unit area that is occupied by State 5-owned lands or waters.

- 38. S5 Oil %—estimated percentage of undiscovered oil volume allocated to State 5-owned lands or waters.
- 39. S5 Gas %—estimated percentage of undiscovered gas volume allocated to State 5-owned lands or waters.
- 40. State 6—name of sixth State for which State-owned lands or waters occupy all or part of the assessment-unit area.
- 41. S6 Area %—percentage of assessment-unit area that is occupied by State 6-owned lands or waters.
- 42. S6 Oil %—estimated percentage of undiscovered oil volume allocated to State 6-owned lands or waters.
- 43. S6 Gas %—estimated percentage of undiscovered gas volume allocated to State 6-owned lands or waters.
- 44. State 7—name of seventh State for which State-owned lands or waters occupy all or part of the assessment-unit area.
- 45. S7 Area %—percentage of assessment-unit area that is occupied by State 7-owned lands or waters.
- 46. S7 Oil %—estimated percentage of undiscovered oil volume allocated to State 7-owned lands or waters.
- 47. S7 Gas %—estimated percentage of undiscovered gas volume allocated to State 7-owned lands or waters.
- 48. State 8—name of eighth State for which State-owned lands or waters occupy all or part of the assessment-unit area.
- 49. S8 Area %—percentage of assessment-unit area that is occupied by State 8-owned lands or waters.
- 50. S8 Oil %—estimated percentage of undiscovered oil volume allocated to State 8-owned lands or waters.
- 51. S8 Gas %—estimated percentage of undiscovered gas volume allocated to State 8-owned lands or waters.
- 52. State 9—name of ninth State for which State-owned lands or waters occupy all or part of the assessment-unit area.
- 53. S9 Area %—percentage of assessment-unit area that is occupied by State 9-owned lands or waters.
- 54. S9 Oil %—estimated percentage of undiscovered oil volume allocated to State 9-owned lands or waters.
- 55. S9 Gas %—estimated percentage of undiscovered gas volume allocated to State 9-owned lands or waters.
- 56. State 10—name of tenth State for which State-owned lands or waters occupy all or part of the assessment-unit area.
- 57. S10 Area %—percentage of assessment-unit area that is occupied by State 10-owned lands or waters.
- 58. S10 Oil %—estimated percentage of undiscovered oil volume allocated to State 10-owned lands or waters.
- 59. S10 Gas %—estimated percentage of undiscovered gas volume allocated to State 10-owned lands or waters.

The sta####.tab table contains 59 columns. The sum of the percentages should equal 100. Data columns for these files are as follows:

- 1. Code—assessment-unit code number.
- 2. Name—assessment-unit name.
- 3. Area km2—area of the assessment unit in square kilometers.
- 4. State 1—name of first State (onshore and offshore) that occupies all or part of the assessment-unit area.
- 5. S1 Area %—percentage of assessment-unit area that is occupied by State 1.
- 6. S1 Oil %—estimated percentage of undiscovered oil volume allocated to State 1.
- 7. S1 Gas %—estimated percentage of undiscovered gas volume allocated to State 1.
- 8. State 2—name of second State (onshore and offshore) that occupies all or part of the assessment-unit area.
- 9. S2 Area %—percentage of assessment-unit area that is occupied by State 2.
- 10. S2 Oil %—estimated percentage of undiscovered oil volume allocated to State 2.
- 11. S2 Gas %—estimated percentage of undiscovered gas volume allocated to State 2.
- 12. State 3—name of third State (onshore and offshore) that occupies all or part of the assessment-unit area.
- 13. S3 Area %—percentage of assessment-unit area that is occupied by State 3.
- 14. S3 Oil %—estimated percentage of undiscovered oil volume allocated to State 3.
- 15. S3 Gas %—estimated percentage of undiscovered gas volume allocated to State 3.
- 16. State 4—name of fourth State (onshore and offshore) that occupies all or part of the assessment-unit area.
- 17. S4 Area %—percentage of assessment-unit area that is occupied by State 4.
- 18. S4 Oil %—estimated percentage of undiscovered oil volume allocated to State 4.
- 19. S4 Gas %—estimated percentage of undiscovered gas volume allocated to State 4.
- 20. State 5—name of fifth State (onshore and offshore) that occupies all or part of the assessment-unit area.
- 21. S5 Area %—percentage of assessment-unit area that is occupied by State 5.
- 22. S5 Oil %—estimated percentage of undiscovered oil volume allocated to State 5.
- 23. S5 Gas %—estimated percentage of undiscovered gas volume allocated to State 5.
- 24. State 6—name of sixth State (onshore and offshore) that occupies all or part of the assessment-unit area.
- 25. S6 Area %—percentage of assessment-unit area that is occupied by State 6.

8 Total Petroleum Systems and Geologic Assessment of Undiscovered Oil and Gas Resources in the San Juan Basin Province

26. S6 Oil %—estimated percentage of undiscovered oil volume allocated to State 6.
 27. S6 Gas %—estimated percentage of undiscovered gas volume allocated to State 6.
 28. State 7—name of seventh State (onshore and offshore) that occupies all or part of the assessment-unit area.
 29. S7 Area %—percentage of assessment-unit area that is occupied by State 7.
 30. S7 Oil %—estimated percentage of undiscovered oil volume allocated to State 7.
 31. S7 Gas %—estimated percentage of undiscovered gas volume allocated to State 7.
 32. State 8—name of eighth State (onshore and offshore) that occupies all or part of the assessment-unit area.
 33. S8 Gas %—percentage of assessment-unit area that is occupied by State 8.
 34. S8 Oil %—estimated percentage of undiscovered oil volume allocated to State 8.
 35. S8 Gas %—estimated percentage of undiscovered gas volume allocated to State 8.
 36. State 9—name of ninth State (onshore and offshore) that occupies all or part of the assessment-unit area.
 37. S9 Area %—percentage of assessment-unit area that is occupied by State 9.
 38. S9 Oil %—estimated percentage of undiscovered oil volume allocated to State 9.
 39. S9 Gas %—estimated percentage of undiscovered gas volume allocated to State 9.
 40. State 10—name of tenth State (onshore and offshore) that occupies all or part of the assessment-unit area.
 41. S10 Area %—percentage of assessment-unit area that is occupied by State 10.
 42. S10 Oil %—estimated percentage of undiscovered oil volume allocated to State 10.
 43. S10 Gas %—estimated percentage of undiscovered gas volume allocated to State 10.
 44. State 11—name of eleventh State (onshore and offshore) that occupies all or part of the assessment-unit area.
 45. S11 Area %—percentage of assessment-unit area that is occupied by State 11.
 46. S11 Oil %—estimated percentage of undiscovered oil volume allocated to State 11.
 47. S11 Gas %—estimated percentage of undiscovered gas volume allocated to State 11.
 48. State 12—name of twelfth State (onshore and offshore) that occupies all or part of the assessment-unit area.
 49. S12 Area %—percentage of assessment-unit area that is occupied by State 12.
 50. S12 Oil %—estimated percentage of undiscovered oil volume allocated to State 12.
 51. S12 Gas %—estimated percentage of undiscovered gas volume allocated to State 12.
 52. State 13—name of thirteenth State (onshore and offshore) that occupies all or part of the assessment-unit area.
 53. S13 Area %—percentage of assessment-unit area that is occupied by State 13.
 54. S13 Oil %—estimated percentage of undiscovered oil volume allocated to State 13.
 55. S13 Gas %—estimated percentage of undiscovered gas volume allocated to State 13.
 56. State 14—name of fourteenth State (onshore and offshore) that occupies all or part of the assessment-unit area.
 57. S14 Area %—percentage of assessment-unit area that is occupied by State 14.
 58. S14 Oil %—estimated percentage of undiscovered oil volume allocated to State 14.
 59. S14 Gas %—estimated percentage of undiscovered gas volume allocated to State 14.
- The vol####.tab table contains estimates of undiscovered petroleum resources along with parameters that express uncertainty in these estimates. The table contains 40 columns. Blank cells represent no data. Data columns for these files are as follows:**
1. Code—assessment-unit code number.
 2. Name—assessment-unit name.
 3. Type—type of assessment unit, conventional, continuous oil, continuous gas, or coal-bed gas.
 4. Status—remarks indicating that assessment unit was not quantitatively assessed; otherwise blank.
 5. Prob %—geologic probability of the assessment unit.
 6. OILF95 MMB—the estimated value of undiscovered oil (oil in oil accumulations) such that there is a 95-percent probability that this amount or more exists in the assessment unit. The volume is given in millions of barrels of oil (MMBO).
 7. OILF50 MMB—the estimated value of undiscovered oil (oil in oil accumulations) such that there is a 50-percent probability that this amount or more exists in the assessment unit. This is the median value. The volume is given in millions of barrels of oil (MMBO).
 8. OILF5 MMB—the estimated value of undiscovered oil (oil in oil accumulations) such that there is a 5-percent probability that this amount or more exists in the assessment unit. The volume is given in millions of barrels of oil (MMBO).
 9. OILMN MMB—the estimated mean (average) value of undiscovered oil (oil in oil accumulations). The volume is given in millions of barrels of oil (MMBO).
 10. OILSD MMB—the estimated standard deviation value of undiscovered oil (oil in oil accumulations). The volume is given in millions of barrels of oil (MMBO).

11. AGF95 BCF—the estimated value of undiscovered associated/dissolved gas (gas in oil accumulations) such that there is a 95-percent probability that this amount or more exists in the assessment unit. The volume is given in billions of cubic feet of gas (BCFG).
12. AGF50 BCF—the estimated value of undiscovered associated/dissolved gas (gas in oil accumulations) such that there is a 50-percent probability that this amount or more exists in the assessment unit. This is the median value. The volume is given in billions of cubic feet of gas (BCFG).
13. AGF5 BCF—the estimated value of undiscovered associated/dissolved gas (gas in oil accumulations) such that there is a 5-percent probability that this amount or more exists in the assessment unit. The volume is given in billions of cubic feet of gas (BCFG).
14. AGMB BCF—the estimated mean (average) value of undiscovered associated/dissolved gas (gas in oil accumulations). The volume is given in billions of cubic feet of gas (BCFG).
15. AGSD BCF—the estimated standard deviation value of undiscovered associated/dissolved gas (gas in oil accumulations). The volume is given in billions of cubic feet of gas (BCFG).
16. NGLF95 MMB—the estimated value of undiscovered natural gas liquids (NGL in oil accumulations) such that there is a 95-percent probability that this amount or more exists in the assessment unit. The volume is given in millions of barrels of NGL (MMBNGL).
17. NGLF50 MMB—the estimated value of undiscovered natural gas liquids (NGL in oil accumulations) such that there is a 50-percent probability that this amount or more exists in the assessment unit. This is the median value. The volume is given in millions of barrels of NGL (MMBNGL).
18. NGLF5 MMB—the estimated value of undiscovered natural gas liquids (NGL in oil accumulations) such that there is a 5-percent probability that this amount or more exists in the assessment unit. The volume is given in millions of barrels of NGL (MMBNGL).
19. NGLMN MMB—the estimated mean (average) value of undiscovered natural gas liquids (NGL in oil accumulations). The volume is given in millions of barrels of NGL (MMBNGL).
20. NGLSD MMB—the estimated standard deviation value of undiscovered natural gas liquids (NGL in oil accumulations). The volume is given in millions of barrels of NGL (MMBNGL).
21. NGF95 BCF—the estimated value of undiscovered non-associated gas (gas in gas accumulations) such that there is a 95-percent probability that this amount or more exists in the assessment unit. The volume is given in billions of cubic feet of gas (BCFG).
22. NGF50 BCF—the estimated value of undiscovered non-associated gas (gas in gas accumulations) such that there is a 50-percent probability that this amount or more exists in the assessment unit. This is the median value. The volume is given in billions of cubic feet of gas (BCFG).
23. NGF5 BCF—the estimated value of undiscovered non-associated gas (gas in gas accumulations) such that there is a 5-percent probability that this amount or more exists in the assessment unit. The volume is given in billions of cubic feet of gas (BCFG).
24. NGMN BCF—the estimated mean (average) value of undiscovered nonassociated gas (gas in gas accumulations). The volume is given in billions of cubic feet of gas (BCFG).
25. NGSD BCF—the estimated standard deviation value of undiscovered nonassociated gas (gas in gas accumulations). The volume is given in billions of cubic feet of gas (BCFG).
26. LIQF95 MMB—the estimated value of undiscovered liquids (oil and NGL in gas accumulations) such that there is a 95-percent probability that this amount or more exists in the assessment unit. The volume is given in millions of barrels of liquids (MMBL).
27. LIQF50 MMB—the estimated value of undiscovered liquids (oil and NGL in gas accumulations) such that there is a 50-percent probability that this amount or more exists in the assessment unit. This is the median value. The volume is given in millions of barrels of liquids (MMBL).
28. LIQF5 MMB—the estimated value of undiscovered liquids (oil and NGL in gas accumulations) such that there is a 5-percent probability that this amount or more exists in the assessment unit. The volume is given in millions of barrels of liquids (MMBL).
29. LIQMN MMB—the estimated mean (average) value of undiscovered liquids (oil and NGL in gas accumulations). The volume is given in millions of barrels of liquids (MMBL).
30. LIQSD MMB—the estimated standard deviation value of undiscovered liquids (oil and NGL in gas accumulations). The volume is given in millions of barrels of liquids (MMBL).
31. LOF95 MMB—the estimated size of the largest undiscovered conventional oil accumulation such that there is a 95-percent probability of that accumulation being this amount or larger. The volume is given in millions of barrels of oil (MMBO).
32. LOF50 MMB—the estimated size of the largest undiscovered conventional oil accumulation such that there is a 50-percent probability of that accumulation being this amount or larger. This is the median value. The volume is given in millions of barrels of oil (MMBO).
33. LOF5 MMB—the estimated size of the largest undiscovered conventional oil accumulation such that there is a 5-percent probability of that accumulation being this

amount or larger. The volume is given in millions of barrels of oil (MMBO).

34. LOMN MMB—the estimated mean (average) value of the largest undiscovered conventional oil accumulation. The volume is given in millions of barrels of oil (MMBO).
35. LOSD MMB—the estimated standard deviation value of the largest undiscovered conventional oil accumulation. The volume is given in millions of barrels of oil (MMBO).
36. LGF95 BCF—the estimated size of the largest undiscovered conventional gas accumulation such that there is a 95-percent probability of that accumulation being this amount or larger. The volume is given in billions of cubic feet of gas (BCFG).
37. LGF50 BCF—the estimated size of the largest undiscovered conventional gas accumulation such that there is a 50-percent probability of that accumulation being this amount or larger. This is the median value. The volume is given in billions of cubic feet of gas (BCFG).
38. LGF5 BCF—the estimated size of the largest undiscovered conventional gas accumulation such that there is a 5-percent probability of that accumulation being this amount or larger. The volume is given in billions of cubic feet of gas (BCFG).
39. LGMN BCF—the estimated mean (average) value of the largest undiscovered conventional gas accumulation. The volume is given in billions of cubic feet of gas (BCFG).
40. LGSD BCF—the estimated standard deviation value of the largest undiscovered conventional gas accumulation. The volume is given in billions of cubic feet of gas (BCFG).

The inf####.tab table contains input data from the FORSPAN Assessment Model for Continuous Accumulations—Basic Input Data Form used in this assessment and provided in the u#####.pdf files. Blank cells represent no data. This table contains 80 columns. Data columns are:

1. Date—date of assessment.
2. Geol—assessing geologist’s name.
3. Regno—region code number.
4. Reg—region name.
5. Provno—province code number.
6. Prov—province name.
7. TPSno—total petroleum system code number.
8. TPS—total petroleum system name.
9. AUno—assessment-unit code number.
10. AU—assessment-unit name.
11. Data—data sources used to aid in completing the data-input form.
12. Comm—assessment unit type, the primary commodity type in the assessment unit, based on the gas-to-oil ratio of the petroleum endowment, which includes both the discovered and undiscovered petroleum. An assessment unit is characterized as being oil prone if the gas-to-oil ratio is less than 20,000 cubic feet of gas per barrel of oil; otherwise, it is gas prone.
13. RminMMBBCF—minimum total recovery per cell considered for assessment, in million barrels of oil (MMBO) for oil assessment units or billion cubic feet of gas (BCFG) for gas assessment units.
14. Numtest1—number of tested cells in the assessment unit.
15. Numtest2—number of tested cells in the assessment unit that have total recoveries equal to or larger than the specified minimum total recovery per cell.
16. AUM—assessment-unit maturity, the exploration maturity of the assessment unit. Assessment-unit maturity is classified as “established” if more than 24 cells exceed the minimum total recovery, “frontier” if 1 to 24 cells exceed the minimum total recovery, or “hypothetical” if no cells exceed the minimum total recovery.
17. Med1MMBBCF—median total recovery per cell of the set of tested cells equal to or greater than the minimum total recovery that constitute the first one-third of the total number of cells ranked according to date of discovery within the assessment unit, in million barrels of oil (MMBO) for oil assessment units or billion cubic feet of gas (BCFG) for gas assessment units.
18. Med2MMBBCF—median total recovery per cell of the set of tested cells equal to or greater than the minimum total recovery that constitute the second one-third of the total number of cells ranked according to date of discovery within the assessment unit, in million barrels of oil (MMBO) for oil assessment units or billion cubic feet of gas (BCFG) for gas assessment units.
19. Med3MMBBCF—median total recovery per cell of the set of tested cells equal to or greater than the minimum total recovery that constitute the third one-third of the total number of cells ranked according to date of discovery within the assessment unit, in million barrels of oil (MMBO) for oil assessment units or billion cubic feet of gas (BCFG) for gas assessment units.
20. Prob1 %—charge probability, the probability for adequate petroleum charge for at least one untested cell equal to or larger than the minimum total recovery, somewhere in the assessment unit, having the potential to be added to reserves in the next 30 years. Charge probability is given as a fractional value from 0 to 1.0.
21. Prob2 %—rocks probability, the probability for adequate reservoirs, traps, and seals for at least one untested cell equal to or larger than the minimum total recovery, somewhere in the assessment unit, having the potential to be added to reserves in the next 30 years. Rocks probability is given as a fractional value from 0 to 1.0.
22. Prob3 %—timing probability, the probability for favorable geologic timing for at least one untested cell equal to or larger than the minimum total recovery, somewhere

- in the assessment unit, having the potential to be added to reserves in the next 30 years. Timing probability is given as a fractional value from 0 to 1.0.
23. Geoprob %—geologic probability, the product of charge, rocks, and timing probabilities. Geologic probability is given as a fractional value from 0 to 1.0.
 24. Prob4 %—accessibility probability, the probability for adequate location for necessary petroleum-related activities to discover at least one untested cell equal to or larger than the minimum total recovery, somewhere in the assessment unit, having the potential to be added to reserves in the next 30 years. Accessibility probability is given as a fractional value from 0 to 1.0.
 25. TAAmin a—minimum total assessment-unit area, the estimated minimum (F100) area of the assessment unit. The area is given in acres.
 26. TAAmed a—median total assessment-unit area, the estimated median (F50) area of the assessment unit. The area is given in acres.
 27. TAAmax a—maximum total assessment-unit area, the estimated maximum (F0) area of the assessment unit. The area is given in acres.
 28. CAmin a—minimum area per cell of untested cells with potential, the estimated minimum (F100) area per cell of untested cells having the potential for additions to reserves in the specified timeframe for the assessment (30 years for this assessment) in the assessment unit. This area is equivalent to the drainage areas of wells. This area is given in acres.
 29. CAMED a—median area per cell of untested cells with potential, the estimated median (F50) area per cell of untested cells having the potential for additions to reserves in the specified timeframe for the assessment (30 years for this assessment) in the assessment unit. This area is equivalent to the drainage areas of wells. This area is given in acres.
 30. CAmAx a—maximum area per cell of untested cells with potential, the estimated maximum (F0) area per cell of untested cells having the potential for additions to reserves in the specified timeframe for the assessment (30 years for this assessment) in the assessment unit. This area is equivalent to the drainage areas of wells. This area is given in acres.
 31. TAAUmin %—estimated minimum (F100) percentage of the total assessment-unit area that is untested.
 32. TAAUmed %—estimated median (F50) percentage of the total assessment-unit area that is untested.
 33. TAAUmax %—estimated maximum (F0) percentage of the total assessment-unit area that is untested.
 34. UAAPmin %—estimated minimum (F100) percentage of the untested area in the assessment unit having the potential for additions to reserves in the specified timeframe for the assessment (30 years for this assessment).
 35. UAAPmed %—estimated median (F50) percentage of the untested area in the assessment unit having the potential for additions to reserves in the specified timeframe for the assessment (30 years for this assessment).
 36. UAAPmax %—estimated maximum (F0) percentage of the untested area in the assessment unit having the potential for additions to reserves in the specified timeframe for the assessment (30 years for this assessment).
 37. RminMMBBCF—estimated minimum (F100) total recovery per cell for untested cells in the assessment unit having the potential for additions to reserves in the specified timeframe for the assessment (30 years for this assessment). This volume is given as million barrels of oil (MMBO) for oil assessment units and billion cubic feet of gas (BCFG) for gas assessment units.
 38. RmedMMBBCF—estimated median (F50) total recovery per cell for untested cells in the assessment unit having the potential for additions to reserves in the specified timeframe for the assessment (30 years for this assessment). This volume is given as million barrels of oil (MMBO) for oil assessment units and billion cubic feet of gas (BCFG) for gas assessment units.
 39. RmaxMMBBCF—estimated maximum (F0) total recovery per cell for untested cells in the assessment unit having the potential for additions to reserves in the specified timeframe for the assessment (30 years for this assessment). This volume is given as million barrels of oil (MMBO) for oil assessment units and billion cubic feet of gas (BCFG) for gas assessment units.
 40. GminCF/B—estimated minimum (F100) gas-to-oil ratio (GOR), in cubic feet of gas per barrel of oil (CFG/BO), of untested cells equal to or larger than the minimum total recovery in oil assessment units.
 41. GmedCF/B—estimated median (F50) gas-to-oil ratio (GOR), in cubic feet of gas per barrel of oil (CFG/BO), of untested cells equal to or larger than the minimum total recovery in oil assessment units.
 42. GmaxCF/B—estimated maximum (F0) gas-to-oil ratio (GOR), in cubic feet of gas per barrel of oil (CFG/BO), of untested cells equal to or larger than the minimum total recovery in oil assessment units.
 43. NminB/MMCF—estimated minimum (F100) natural gas liquids (NGL) to gas ratio, in barrels of natural gas liquids per million cubic feet of gas (BNGL/MMCFG), of untested cells equal to or larger than the minimum total recovery in oil assessment units.
 44. NmedB/MMCF—estimated median (F50) natural gas liquids (NGL) to gas ratio, in barrels of natural gas liquids per million cubic feet of gas (BNGL/MMCFG), of untested cells equal to or larger than the minimum total recovery in oil assessment units.
 45. NmaxB/MMCF—estimated maximum (F0) natural gas liquids (NGL) to gas ratio, in barrels of natural gas liquids per million cubic feet of gas (BNGL/MMCFG), of

12 Total Petroleum Systems and Geologic Assessment of Undiscovered Oil and Gas Resources in the San Juan Basin Province

- untested cells equal to or larger than the minimum total recovery in oil assessment units.
46. LminB/MMCF—estimated minimum (F100) liquids (oil plus natural gas liquids) to gas ratio (LGR), in barrels of liquids per million cubic feet of gas (BNGL/MMCFG), of untested cells equal to or larger than the minimum total recovery in gas assessment units.
 47. LmedB/MMCF—estimated median (F50) liquids (oil plus natural gas liquids) to gas ratio (LGR), in barrels of liquids per million cubic feet of gas (BNGL/MMCFG), of untested cells equal to or larger than the minimum total recovery in gas assessment units.
 48. LmaxB/MMCF—estimated maximum (F0) liquids (oil plus natural gas liquids) to gas ratio (LGR), in barrels of liquids per million cubic feet of gas (BNGL/MMCFG), of untested cells equal to or larger than the minimum total recovery in gas assessment units.
 49. APImin deg—estimated minimum (F100) API gravity, in degrees, of oil in untested cells in oil assessment units.
 50. APImed deg—estimated median (F50) API gravity, in degrees, of oil in untested cells in oil assessment units.
 51. APImax deg—estimated maximum (F0) API gravity, in degrees, of oil in untested cells in oil assessment units.
 52. Smin %—estimated minimum (F100) sulfur content, in percent, of oil in untested cells in oil assessment units.
 53. Smed %—estimated median (F50) sulfur content, in percent, of oil in untested cells in oil assessment units.
 54. Smax %—estimated maximum (F0) sulfur content, in percent, of oil in untested cells in oil assessment units.
 55. ODmin m—estimated minimum (F100) drilling depth, in meters, of oil in untested cells in oil assessment units.
 56. ODmed m—estimated median (F50) drilling depth, in meters, of oil in untested cells in oil assessment units.
 57. ODmax m—estimated maximum (F0) drilling depth, in meters, of oil in untested cells in oil assessment units.
 58. OWDmin m—estimated minimum (F100) water depth, in meters, of oil in untested cells in oil assessment units (ocean, bays, or lakes; if applicable).
 59. OWDmed m—estimated median (F50) water depth, in meters, of oil in untested cells in oil assessment units (ocean, bays, or lakes; if applicable).
 60. OWDmax m—estimated maximum (F0) water depth, in meters, of oil in untested cells in oil assessment units (ocean, bays, or lakes; if applicable).
 61. IGmin %—estimated minimum (F100) inert gas content, in percent, of gas in untested cells in gas assessment units (nitrogen, and helium, and so forth).
 62. IGmed %—estimated median (F50) inert gas content, in percent, of gas in untested cells in gas assessment units (nitrogen, and helium, and so forth).
 63. IGmax %—estimated maximum (F0) inert gas content, in percent, of gas in untested cells in gas assessment units (nitrogen, and helium, and so forth).
 64. CO2min %—estimated minimum (F100) carbon dioxide content, in percent, of gas in untested cells in gas assessment units.
 65. CO2med %—estimated median (F50) carbon dioxide content, in percent, of gas in untested cells in gas assessment units.
 66. CO2max %—estimated maximum (F0) carbon dioxide content, in percent, of gas in untested cells in gas assessment units.
 67. H2Smin %—estimated minimum (F100) hydrogen sulfide content, in percent, of gas in untested cells in gas assessment units.
 68. H2Smed %—estimated median (F50) hydrogen sulfide content, in percent, of gas in untested cells in gas assessment units.
 69. H2Smax %—estimated maximum (F0) hydrogen sulfide content, in percent, of gas in untested cells in gas assessment units.
 70. GDmin m—estimated minimum (F100) drilling depth, in meters, of gas in untested cells in gas assessment units.
 71. GDmed m—estimated median (F50) drilling depth, in meters, of gas in untested cells in gas assessment units.
 72. GDmax m—estimated maximum (F0) drilling depth, in meters, of gas in untested cells in gas assessment units.
 73. GWDmin m—estimated minimum (F100) water depth, in meters, of gas in untested cells in gas assessment units (ocean, bays, or lakes; if applicable).
 74. GWDmed m—estimated median (F50) water depth, in meters, of gas in untested cells in gas assessment units (ocean, bays, or lakes; if applicable).
 75. GWDmax m—estimated maximum (F0) water depth, in meters, of gas in untested cells in gas assessment units (ocean, bays, or lakes; if applicable).
 76. FSRmean %—estimated mean future success ratio, as percent.
 77. FSRmin %—estimated minimum (F100) future success ratio, as percent.
 78. FSRmed %—estimated median (F50) future success ratio, as percent.
 79. FSRmax %—estimated maximum (F100) future success ratio, as percent.
 80. HSR %—historical success ratio, as percent.

The ins####.tab table contains input data from the Seventh Approximation Data Forms for Conventional Assessment Units used in this assessment and provided in the c#####.pdf files. Blank cells represent no data. This table contains 75 columns. Data columns are as follows:

1. Date—date of assessment.
2. Geol—assessing geologist’s name.
3. Regno—region code number.
4. Reg—region name.
5. Provno—province code number.
6. Prov—province name.
7. TPSno—total petroleum system code number.
8. TPS—total petroleum system name.
9. AUno—assessment-unit code number.
10. AU—assessment-unit name.
11. Data—data sources used to aid in completing the data-input form.
12. Comm—primary commodity type in the assessment unit, based on the gas-to-oil ratio of the petroleum endowment, which includes both the discovered and undiscovered petroleum. An assessment unit is characterized as being oil prone if the gas-to-oil ratio is less than 20,000 cubic feet of gas per barrel of oil; otherwise, it is gas prone.
13. Minsize MMB—minimum accumulation size considered for assessment, in million barrels of oil equivalent (MMBOE).
14. Numoil—number of oil accumulations equal to or larger than the minimum accumulation size discovered in the assessment unit.
15. Numgas—number of gas accumulations equal to or larger than the minimum accumulation size discovered in the assessment unit.
16. AUM—assessment-unit maturity, the exploration maturity of the assessment unit. Assessment-unit maturity is classified as “established” if more than 13 accumulations exceeding minimum size have been discovered, “frontier” if 1 to 13 accumulations exceeding minimum size have been discovered, or “hypothetical” if no accumulations exceeding minimum size have been discovered.
17. MedO1MMB—median size of the set of discovered oil accumulations that constitute the first one-third or one-half of the total number of oil accumulations ranked according to date of discovery within the assessment unit, in million barrels of oil (MMBO). This size is derived from known oil volumes that were adjusted upward to account for estimated future reserve growth. For this assessment, 30 years of reserve growth is considered.
18. MedO2MMB—median size of the set of discovered oil accumulations that constitute the second one-third or one-half of the total number of oil accumulations ranked according to date of discovery within the assessment unit, in million barrels of oil (MMBO). This size is derived from known oil volumes that were adjusted upward to account for estimated future reserve growth. For this assessment, 30 years of reserve growth is considered.
19. MedO3MMB—median size of the set of discovered oil accumulations that constitute the third one-third of the total number of oil accumulations ranked according to date of discovery within the assessment unit, in million barrels of oil (MMBO). This size is derived from known oil volumes that were adjusted upward to account for estimated future reserve growth. For this assessment, 30 years of reserve growth is considered.
20. MedG1BCF—median size of the set of discovered gas accumulations that constitute the first one-third or one-half of the total number of gas accumulations ranked according to date of discovery within the assessment unit, in billion cubic feet of gas (BCFG). This size is derived from known gas volumes that were adjusted upward to account for estimated future reserve growth. For this assessment, 30 years of reserve growth is considered.
21. MedG2BCF—median size of the set of discovered gas accumulations that constitute the second one-third or one-half of the total number of gas accumulations ranked according to date of discovery within the assessment unit, in billion cubic feet of gas (BCFG). This size is derived from known gas volumes that were adjusted upward to account for estimated future reserve growth. For this assessment, 30 years of reserve growth is considered.
22. MedG3BCF—median size of the set of discovered gas accumulations that constitute the third one-third of the total number of gas accumulations ranked according to date of discovery within the assessment unit, in billion cubic feet of gas (BCFG). This size is derived from known gas volumes that were adjusted upward to account for estimated future reserve growth. For this assessment, 30 years of reserve growth is considered.
23. Prob1 %—charge probability, the probability for adequate petroleum charge for at least one undiscovered accumulation equal to or larger than the minimum accumulation size, somewhere in the assessment unit, having the potential to be added to reserves in the next 30 years. Charge probability is given as a fractional value from 0 to 1.0.
24. Prob2 %—rocks probability, the probability for adequate reservoirs, traps, and seals for at least one undiscovered accumulation equal to or larger than the minimum accumulation size, somewhere in the assessment unit, having the potential to be added to reserves in the next 30 years. Rocks probability is given as a fractional value from 0 to 1.0.
25. Prob3 %—timing probability, the probability for favorable geologic timing for at least one undiscovered accumulation equal to or larger than the minimum accumulation size, somewhere in the assessment unit, having the potential to be added to reserves in the next 30 years.

14 Total Petroleum Systems and Geologic Assessment of Undiscovered Oil and Gas Resources in the San Juan Basin Province

- Timing probability is given as a fractional value from 0 to 1.0.
26. Geoprob %—geologic probability, the product of charge, rocks, and timing probabilities. Geologic probability is given as a fractional value from 0 to 1.0.
 27. Prob4 %—accessibility probability, the probability for adequate location for necessary petroleum-related activities to discover at least one undiscovered accumulation equal to or larger than the minimum accumulation size, somewhere in the assessment unit, having the potential to be added to reserves in the next 30 years. Accessibility probability is given as a fractional value from 0 to 1.0.
 28. NOmin—estimated minimum (F100) number of undiscovered oil accumulations equal to or larger than the minimum accumulation size in the assessment unit.
 29. NOmed—estimated median (F50) number of undiscovered oil accumulations equal to or larger than the minimum accumulation size in the assessment unit.
 30. NOmax—estimated maximum (F0) number of undiscovered oil accumulations equal to or larger than the minimum accumulation size in the assessment unit.
 31. NGmin—estimated minimum (F100) number of undiscovered gas accumulations equal to or larger than the minimum accumulation size in the assessment unit.
 32. NGmed—estimated median (F50) number of undiscovered gas accumulations equal to or larger than the minimum accumulation size in the assessment unit.
 33. NGmax—estimated maximum (F0) number of undiscovered gas accumulations equal to or larger than the minimum accumulation size in the assessment unit.
 34. SOminMMB—estimated minimum (F100) size, in million barrels of oil (MMBO), of undiscovered oil accumulations in the assessment unit.
 35. SOmedMMB—estimated median (F50) size, in million barrels of oil (MMBO), of undiscovered oil accumulations in the assessment unit.
 36. SOmaxMMB—estimated maximum (F0) size, in million barrels of oil (MMBO), of undiscovered oil accumulations in the assessment unit.
 37. SGminBCF—estimated minimum (F100) size, in billion cubic feet of gas (BCFG), of undiscovered gas accumulations in the assessment unit.
 38. SGmedBCF—estimated median (F50) size, in billion cubic feet of gas (BCFG), of undiscovered gas accumulations in the assessment unit.
 39. SGmaxBCF—estimated maximum (F0) size, in billion cubic feet of gas (BCFG), of undiscovered gas accumulations in the assessment unit.
 40. GminCF/B—estimated minimum (F100) gas-to-oil ratio (GOR), in cubic feet of gas per barrel of oil (CFG/BO), of undiscovered oil accumulations equal to or larger than the minimum accumulation size in the assessment unit.
 41. GmedCF/B—estimated median (F50) gas-to-oil ratio (GOR), in cubic feet of gas per barrel of oil (CFG/BO), of undiscovered oil accumulations equal to or larger than the minimum accumulation size in the assessment unit.
 42. GmaxCF/B—estimated maximum (F0) gas-to-oil ratio (GOR), in cubic feet of gas per barrel of oil (CFG/BO), of undiscovered oil accumulations equal to or larger than the minimum accumulation size in the assessment unit.
 43. NminB/MMCF—estimated minimum (F100) natural gas liquids (NGL) to gas ratio, in barrels of natural gas liquids per million cubic feet of gas (BNGL/MMCFG), of undiscovered oil accumulations equal to or larger than the minimum accumulation size in the assessment unit.
 44. NmedB/MMCF—estimated median (F50) natural gas liquids (NGL) to gas ratio, in barrels of natural gas liquids per million cubic feet of gas (BNGL/MMCFG), of undiscovered oil accumulations equal to or larger than the minimum accumulation size in the assessment unit.
 45. NmaxB/MMCF—estimated maximum (F0) natural gas liquids (NGL) to gas ratio, in barrels of natural gas liquids per million cubic feet of gas (BNGL/MMCFG), of undiscovered oil accumulations equal to or larger than the minimum accumulation size in the assessment unit.
 46. LminB/MMCF—estimated minimum (F100) liquids (oil plus natural gas liquids) to gas ratio (LGR), in barrels of liquids per million cubic feet of gas (BL/MMCFG), of undiscovered gas accumulations equal to or larger than the minimum accumulation size in the assessment unit.
 47. LmedB/MMCF—estimated median (F50) liquids (oil plus natural gas liquids) to gas ratio (LGR), in barrels of liquids per million cubic feet of gas (BL/MMCFG), of undiscovered gas accumulations equal to or larger than the minimum accumulation size in the assessment unit.
 48. LmaxB/MMCF—estimated maximum (F0) liquids (oil plus natural gas liquids) to gas ratio (LGR), in barrels of liquids per million cubic feet of gas (BL/MMCFG), of undiscovered gas accumulations equal to or larger than the minimum accumulation size in the assessment unit.
 49. APImin deg—estimated minimum (F100) API gravity, in degrees, of oil in undiscovered oil accumulations in the assessment unit.
 50. APImed deg—estimated median (F50) API gravity, in degrees, of oil in undiscovered oil accumulations in the assessment unit.
 51. APImax deg—estimated maximum (F0) API gravity, in degrees, of oil in undiscovered oil accumulations in the assessment unit.
 52. Smin %—estimated minimum (F100) sulfur content, in percent, of oil in undiscovered oil accumulations in the assessment unit.
 53. Smed %—estimated median (F50) sulfur content, in percent, of oil in undiscovered oil accumulations in the assessment unit.

54. Smax %—estimated maximum (F0) sulfur content, in percent, of oil in undiscovered oil accumulations in the assessment unit.
55. ODmin m—estimated minimum (F100) drilling depth, in meters, of undiscovered oil accumulations in the assessment unit.
56. ODmed m—estimated median (F50) drilling depth, in meters, of undiscovered oil accumulations in the assessment unit.
57. ODmax m—estimated maximum (F0) drilling depth, in meters, of undiscovered oil accumulations in the assessment unit.
58. OWDmin m—estimated minimum (F100) water depth, in meters, of undiscovered oil accumulations in the assessment unit (ocean, bays, or lakes; if applicable).
59. OWDmed m—estimated median (F50) water depth, in meters, of undiscovered oil accumulations in the assessment unit (ocean, bays, or lakes; if applicable).
60. OWDmax m—estimated maximum (F0) water depth, in meters, of undiscovered oil accumulations in the assessment unit (ocean, bays, or lakes; if applicable).
61. IGmin %—estimated minimum (F100) inert gas content, in percent, of gas in undiscovered gas accumulations in the assessment unit (nitrogen and helium, and so forth).
62. IGmed %—estimated median (F50) inert gas content, in percent, of gas in undiscovered gas accumulations in the assessment unit (nitrogen and helium, and so forth).
63. IGmax %—estimated maximum (F0) inert gas content, in percent, of gas in undiscovered gas accumulations in the assessment unit (nitrogen and helium, and so forth).
64. CO2min %—estimated minimum (F100) carbon dioxide content, in percent, of gas in undiscovered gas accumulations in the assessment unit.
65. CO2med %—estimated median (F50) carbon dioxide content, in percent, of gas in undiscovered gas accumulations in the assessment unit.
66. CO2max %—estimated maximum (F0) carbon dioxide content, in percent, of gas in undiscovered gas accumulations in the assessment unit.
67. H2Smin %—estimated minimum (F100) hydrogen sulfide content, in percent, of gas in undiscovered gas accumulations in the assessment unit.
68. H2Smed %—estimated median (F50) hydrogen sulfide content, in percent, of gas in undiscovered gas accumulations in the assessment unit.
69. H2Smax %—estimated maximum (F0) hydrogen sulfide content, in percent, of gas in undiscovered gas accumulations in the assessment unit.
70. GDmin m—estimated minimum (F100) drilling depth, in meters, of undiscovered gas accumulations in the assessment unit.
71. GDmed m—estimated median (F50) drilling depth, in meters, of undiscovered gas accumulations in the assessment unit.
72. GDmax m—estimated maximum (F0) drilling depth, in meters, of undiscovered gas accumulations in the assessment unit.
73. GWDmin m—estimated minimum (F100) water depth, in meters, of undiscovered gas accumulations in the assessment unit (ocean, bays, or lakes; if applicable).
74. GWDmed m—estimated median (F50) water depth, in meters, of undiscovered oil accumulations in the assessment unit (ocean, bays, or lakes; if applicable).
75. GWDmax m—estimated maximum (F0) water depth, in meters, of undiscovered oil accumulations in the assessment unit (ocean, bays, or lakes; if applicable).

Data in the kvol####.tab table are derived from a commercially purchased database (NRG Associates, 2001) and are current through 1999. This table contains 15 columns. Blank cells represent no data. Data columns for these files are as follows:

1. Code—assessment-unit code number.
2. Name—assessment-unit name.
3. Numres—number of reported reservoirs in the assessment unit.
4. CUMOIL MMB—cumulative production of oil from the reported reservoirs in the assessment unit. This volume is in million barrels of oil (MMBO).
5. REMOIL MMB—remaining oil reserves in the reported reservoirs in the assessment unit. This volume is in million barrels of oil (MMBO).
6. KROIL MMB—known recoverable oil volume (cumulative production plus remaining reserves) from the reported reservoirs in the assessment unit. This volume is in million barrels of oil (MMBO).
7. CUMGAS BCF—cumulative production of natural gas from the reported reservoirs in the assessment unit. This volume is in billion cubic feet of gas (BCFG).
8. REMGAS BCF—remaining natural gas reserves in the reported reservoirs in the assessment unit. This volume is in billion cubic feet of gas (BCFG).
9. KRGAS BCF—known recoverable natural gas volume (cumulative production plus remaining reserves) from the reported reservoirs in the assessment unit. This volume is in billion cubic feet of gas (BCFG).
10. CUMNGL MMB—cumulative production of natural gas liquids (NGL) from the reported reservoirs in the assessment unit. This volume is in million barrels of natural gas liquids (MMBNGL).
11. REMNGL MMB—remaining natural gas liquids (NGL) reserves in the reported reservoirs in the assessment unit. This volume is in million barrels of natural gas liquids (MMBNGL).

12. KRNL MMB—known recoverable natural gas liquids (NGL) volume (cumulative production plus remaining reserves) from the reported reservoirs in the assessment unit. This volume is in million barrels of natural gas liquids (MMBNGL).
13. CUMPET MMB—cumulative production of petroleum (oil, gas, and NGL) from the reported reservoirs in the assessment unit. This volume is in million barrels of oil equivalent (MMBOE).
14. REMPET MMB—remaining petroleum (oil, gas, and NGL) reserves in the reported reservoirs in the assessment unit. This volume is in million barrels of oil equivalent (MMBOE).
15. KRPET MMB—known recoverable petroleum (oil, gas, and NGL) volume (cumulative production plus remaining reserves) from the reported reservoirs in the assessment unit. This volume is in million barrels of oil equivalent (MMBOE).

Summary Tables

The c#####.pdf and u#####.pdf files are copies of the completed input data forms used in the assessment process. The c#####.pdf files contain the Seventh Approximation Data Forms for Conventional Assessment Units. The u#####.pdf files contain the FORSPAN Assessment Model for Continuous Accumulations—Basic Input Data Form. These data are defined in the inf#####.tab and ins#####.tab sections of this report.

The d#####.pdf files contain three tables of known and grown petroleum volumes in an assessment unit as a whole and in terms of discovery history. Grown field sizes are defined as known accumulation sizes that were adjusted upward to account for estimated future reserve growth. NA means not applicable and shown in place of volumes for which only one field is present to protect the proprietary nature of the data.

Graphical Data

The fp#####.pdf files contain graphs of input data and estimated petroleum resource volumes for continuous assessment units. The data are defined in the inf#####.tab and vol#####.tab sections of this report. The graphs contained in these files were derived from a report generated by a commercial software package. The quality of these preformatted graphs, therefore, does not necessarily meet USGS editorial standards.

The em#####.pdf files contain graphs of input data and estimated petroleum resource volumes for conventional assessment units. The data are defined in the ins#####.tab and vol#####.tab sections of this report. The graphs contained

in these files were derived from a report generated by a commercial software package. The quality of these preformatted graphs, therefore, does not necessarily meet USGS editorial standards.

The g#####.pdf and k#####.pdf files contain graphs of exploration and discovery data for conventional assessment units. The volumetric data are defined in the kvol#####.tab sections of this report. These files are not provided if the total number of accumulations in the assessment unit, greater than or equal to the specified minimum size, is less than four to protect the proprietary nature of the data.

Two sets of exploration-activity and discovery-history graphs are provided for each of the assessment units, one set showing known field sizes (cumulative production plus remaining reserves) and another showing field sizes that were adjusted to compensate for potential reserve growth that may occur in the next 30 years (labeled “grown”). Within each set of graphs, oil fields and gas fields are treated separately. The graphs include:

- Cumulative Number of New-Field Wildcat Wells vs. Drilling-Completion Year
- Number of New-Field Wildcat Wells vs. Drilling-Completion Year
- Oil- or Gas-Field Size (MMBO or BCFG) vs. Oil- or Gas-Field Rank by Size (With Respect to Discovery Halves or Thirds)
- Number of Oil or Gas Fields vs. Oil- or Gas-Field Size Classes (MMBO or BCFG) (With Respect to Discovery Halves or Thirds)
- Volume of Oil or Gas (MMBO or BCFG) vs. Oil- or Gas-Field Size Classes (MMBO or BCFG)
- Oil- or Gas-Field Size (MMBO or BCFG) vs. Field-Discovery Year
- Oil- or Gas-Field Size (MMBO or BCFG) vs. Cumulative Number of New-Field Wildcat Wells
- Cumulative Oil or Gas Volume (MMBO or BCFG) vs. Field-Discovery Year
- Cumulative Oil or Gas Volume (MMBO or BCFG) vs. Cumulative Number of New-Field Wildcat Wells
- Cumulative Number of Oil or Gas Fields vs. Field-Discovery Year
- Cumulative Number of Oil or Gas Fields vs. Cumulative Number of New-Field Wildcat Wells
- Reservoir Depth, Oil or Gas Fields (ft) vs. Field-Discovery Year
- Reservoir Depth, Oil or Gas Fields (ft) vs. Cumulative Number of New-Field Wildcat Wells
- Gas/Oil, Oil Fields (CFG/BO) vs. Mean Reservoir Depth (ft)

- NGL/Gas, Oil Fields (BNGL/MMCFG) vs. Mean Reservoir Depth (ft)
- Liquids/Gas, Gas Fields (BL/MMCFG) vs. Mean Reservoir Depth (ft)
- Number of Reservoirs in Oil Fields vs. API Gravity (Degrees)

If data are insufficient or do not exist, graphs are not provided. Therefore, not all graphs are included in all files.

File List

Data tables
eco5022.tab
fed5022.tab
inf5022.tab
ins5022.tab
kv015022.tab
own5022.tab
sta5022.tab
vol5022.tab

Summary tables	Assessment unit name
c220101.pdf	Tertiary Conventional Gas
c220301.pdf	Mesaverde Updip Oil
c220302.pdf	Gallup Sandstone Conventional Oil and Gas
c220303.pdf	Mancos Sandstones Conventional Oil
c220304.pdf	Dakota-Greenhorn Conventional Oil and Gas
c220401.pdf	Entrada Sandstone Conventional Oil
d220303.pdf	Mancos Sandstones Conventional Oil
d220304.pdf	Dakota-Greenhorn Conventional Oil and Gas
d220401.pdf	Entrada Sandstone Conventional Oil
u220161.pdf	Pictured Cliffs Continuous Gas
u220181.pdf	Fruitland Fairway Coalbed Gas
u220182.pdf	Basin Fruitland Coalbed Gas
u220261.pdf	Lewis Continuous Gas
u220361.pdf	Mesaverde Central-Basin Continuous Gas
u220362.pdf	Mancos Sandstones Continuous Gas
u220363.pdf	Dakota-Greenhorn Continuous Gas
u220381.pdf	Menefee Coalbed Gas

Graphs	Assessment unit name
em220101.pdf	Tertiary Conventional Gas
em220302.pdf	Gallup Sandstone Conventional Oil and Gas
em220303.pdf	Mancos Sandstones Conventional Oil
em220304.pdf	Dakota-Greenhorn Conventional Oil and Gas
em220401.pdf	Entrada Sandstone Conventional Oil
fp220161.pdf	Pictured Cliffs Continuous Gas
fp220181.pdf	Fruitland Fairway Coalbed Gas
fp220182.pdf	Basin Fruitland Coalbed Gas
fp220261.pdf	Lewis Continuous Gas
fp220361.pdf	Mesaverde Central-Basin Continuous Gas
fp220362.pdf	Mancos Sandstones Continuous Gas
fp220363.pdf	Dakota-Greenhorn Continuous Gas
fp220381.pdf	Menefee Coalbed Gas
g220303.pdf	Mancos Sandstones Conventional Oil
g220304.pdf	Dakota-Greenhorn Conventional Oil and Gas
g220401.pdf	Entrada Sandstone Conventional Oil
k220303.pdf	Mancos Sandstones Conventional Oil
k220304.pdf	Dakota-Greenhorn Conventional Oil and Gas
k220401.pdf	Entrada Sandstone Conventional Oil

References Cited

IHS Energy Group, 2001a [includes data current as of December 2000], PI/Dwights Plus US production data: Englewood, Colo., IHS Energy Group; database available from IHS Energy Group, 15 Inverness Way East, D205, Englewood, CO 80112, U.S.A.

IHS Energy Group, 2001b [includes data current as of December 2000], PI/Dwights Plus US well data: Englewood, Colo., IHS Energy Group; database available from IHS Energy Group, 15 Inverness Way East, D205, Englewood, CO 80112, U.S.A.

NRG Associates, 2001 [includes data current as of December 1999], The significant oil and gas fields of the United States: Colorado Springs, Colo., NRG Associates, Inc.; database available from NRG Associates, Inc., P.O. Box 1655, Colorado Springs, CO 80901, U.S.A.



[Click here to return to Volume Title Page](#)

Publishing support provided by:
Denver Publishing Service Center

For more information concerning this publication, contact:
Center Director, USGS Central Energy Resources Science Center
Box 25046, Mail Stop 939
Denver, CO 80225
(303) 236-1647

Or visit the Central Energy Resources Team site at:
<http://energy.usgs.gov/>